

Medical University of South Carolina

MEDICA

MUSC Theses and Dissertations

2017

Investigating the Sub-Lethal Effects of Mercury Exposure Using Environmental Sentinels

Frances M. Nilsen

Medical University of South Carolina

Follow this and additional works at: <https://medica-musc.researchcommons.org/theses>

Recommended Citation

Nilsen, Frances M., "Investigating the Sub-Lethal Effects of Mercury Exposure Using Environmental Sentinels" (2017). *MUSC Theses and Dissertations*. 337.

<https://medica-musc.researchcommons.org/theses/337>

This Dissertation is brought to you for free and open access by MEDICA. It has been accepted for inclusion in MUSC Theses and Dissertations by an authorized administrator of MEDICA. For more information, please contact medica@musc.edu.

Investigating the Sub-lethal Effects of Mercury Exposure
Using Environmental Sentinels

Frances Nilsen

A dissertation submitted to the faculty of the Medical University of South Carolina in
partial fulfillment of the requirements for the degree of Doctor of Philosophy in the
College of Graduate Studies.

Department of Cellular and Molecular Pathobiology

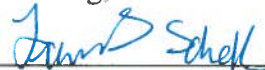
2017

Approved by:

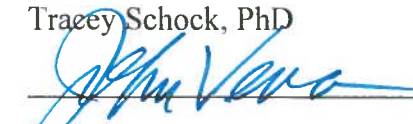
Chairman, Advisory Committee



Stephen Long, PhD



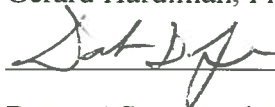
Tracey Schock, PhD



John Vena, PhD



Gerard Hardiman, PhD



Demetri Spyropoulos, PhD

Acknowledgments

I am greatly indebted to many for their guidance, support, and wisdom throughout all stages of this interdisciplinary dissertation. The nature of this project provided the opportunity to combine the biomedical, environmental, and chemical sciences, to better understand the anthropogenic effect on the planet. Without the funding provided by the National Institute of Standards and Technology's Environmental Chemical Sciences Division, and the confidence Dr. Paul Becker, and Dr. John Kucklick had in my ability to translate science to different disciplines, this project would not have been possible.

My advisors, Dr. Tracey Schock, and Dr. Stephen Long, have provided countless hours of guidance in all aspects of this project, but I have learned much more from them over the last four years than what is tangible in this dissertation. Steve instilled a great deal of self confidence in my abilities by being open to my ideas, and flexible to my personal goals for my dissertation. Tracey has given me so much by providing calm, consistent, constructive, yet critical feedback to each piece of my project. I gained so much from her unwavering support, and kindness, particularly her ability to keep her wits about her in stressful situations when I had completely lost mine. Together, my advisors have shaped the scientist that I am becoming, and there is not a day that passes that I am not eternally grateful to them for their guidance.

My committee members, Dr. John Vena, Dr. Gary Hardiman, and Dr. Demetri Spyropoulos, have each played a vital role in this dissertation in becoming truly interdisciplinary, and without each of them this project would have been much more limited in scope. Demetri continually drew my focus back into biomedical science when I strayed too far into other disciplines, and taught me that there are many lenses that science can be seen through, but choosing the appropriate lens is of the utmost importance. This is a lesson that I continually Gary gave so much of his time to help me achieve the milestones of the Marine Biomedicine and Environmental Science program, and without this patience and support, I would not have succeeded at MUSC. His experience in navigating biomedical and environmental science was invaluable in linking all aspects of this dissertation together, as well as guiding me to the next step in my

career. John has been the most kind and supportive mentor since I took his class year ago, but especially after the passing of Dr. Louis J. Guillette Jr. The emotional support he provided not only to me, but to all of Lou's students in our hour of despair was so gracious, and showed me that Lou's legacy was truly in the people he left behind.

Lou instilled in me the desire to show the world what we already knew, that human and environmental health are inextricably linked. Each meeting that I had with Lou filled me with a renewed sense of purpose, and the enthusiasm required to navigate all of the obstacles that would come my way. Whenever I lost my resolve, I would imagine how Lou would have guided me through the murky water with a smile, a cup of tea, and his eternal mantra "What is the question?", which never failed to bring me back on course. This dissertation was done to honor Lou's memory, and continue his legacy, championing the link between environmental and human health. As I go forward into the field of global health, all of the lessons I learned along throughout this project, both scientific and emotional, will be invaluable, and I could never thank each of my mentors enough for their support.

My family has also been so incredibly supportive of my education for the last ten years, and my entire life. I cannot thank my parents enough for instilling in me the desire to learn, and for the many sacrifices they made so that I could excel throughout my education. My siblings have provided a listening ear to the discomfort that comes with growth, and the fear of the unknown. The reprieve they provided meant more to me than I can express in words.

Finally, I must acknowledge my husband, who has endured lonely summer weekends, piles of laundry, and the most stressful, exhausting six months of my life. He has walked this hazardous path with grace and compassion, shown me the power of kindness, the strength that comes from knowing yourself, and that there is no one I would rather spend the rest of my life with.

There is nothing I can say to all of you but, thank you so very much. You have helped me become a scientist, and person, that I am proud to be, and for that I am eternally grateful.

*Investigating the sub-lethal effects of mercury exposure using
environmental sentinels*

By

Frances M. Nilsen

2017

A dissertation submitted to the faculty of the Medical University of South Carolina in
partial fulfillment of the requirements for the degree of Doctor of Philosophy in the
College of Graduate Studies.

Molecular & Cellular Biology & Pathobiology Program
Marine Biomedicine & Environmental Sciences

Abstract

FRANCES NILSEN. Investigating the sub-lethal effects of mercury exposure using environmental sentinels

Mercury (Hg) is a ubiquitous environmental contaminant that is bioaccumulative and toxic. Ecosystems accumulate high mercury concentrations throughout their food web based on their unique environmental characteristics, exposing predators in these environments to mercury concentrations that elicit toxic effects, which are rarely observed outside of the laboratory. These predators provide the opportunity to investigate the sub-lethal effects of chronic mercury exposure that occur prior to the onset of toxic effects.

Here the American alligator is thoroughly assessed for use as a sentinel of human dietary mercury exposure. We find that wild healthy alligators from the southeastern Atlantic coast of the US are exposed to mercury concentrations comparable to human populations with several different diets, and can be used as a sentinel for lifetime mercury exposure. The range of mercury concentrations that alligators are exposed to provide the opportunity to examine biochemical changes as sub-lethal effects, along an increasing mercury gradient. We observe that DNA methylation and mercury concentration are inversely correlated, but may be reversible based on diet. This epigenetic modification provides as assessment tool that can also be used for prevention in humans.

To investigate underlying biochemical changes associated with increasing mercury exposure, a laboratory model of chronic exposure was assessed using an NMR based metabolomics approach. The diamondback terrapin, which is an established

sentinel for mercury exposure, experienced both sub-lethal, and toxic effects, providing the opportunity to examine the onset of toxicity. We observed changes in small molecules involved in oxidative stress management throughout the range of mercury exposures, prior to toxic effects being observed. The terrapins experiencing toxic effects had behavioral changes commonly associated with mercury poisoning, such as neurological and muscular impairment. Many small molecules were altered in these terrapins, but most were related to their impaired foraging abilities.

The Adverse Outcome Pathway (AOP) framework is used to put these data into a greater context that can be used for risk assessment for humans and wildlife. The AOP framework can be used for the prevention of toxicity, and a more complete understanding of the sub-lethal changes associated with this toxic contaminant.

Table of Contents

Chapter One: General Introduction & Literature Review	1
1.1. Mercury exposure	2
1.2. Global & environmental sources of mercury	2
1.3. The biogeochemistry of mercury	3
1.4. Bioaccumulation & biomagnification through the trophic levels.....	7
1.5. Biological mercury hotspots	9
1.6. Effects of mercury in wildlife	13
1.6.1. Effects of mercury in wildlife health	13
1.6.2. Wildlife consumed by humans	15
1.7. Human exposure to mercury	28
1.8. Sentinel/indicators	33
1.9. One health paradigm	36
1.10. The adverse outcome pathway (AOP) framework	37
1.11. Biochemical effect of mercury - molecular mechanism, methylation, & metabolomics	39
1.12. Overall significance & specific aims	51
Chapter Two: American alligators as sentinel species for environmental exposure research	53
2.1. Assessment of the American alligator as a human health sentinel for mercury exposure.....	54
2.2. General methods	58
2.2.1. Sample collection	59
2.2.2. Analytical chemistry methods	62
2.3. Determining the trace elements of concern and their biodistribution in the American alligator in the southeastern United States	69
2.3.1. Introduction	69
2.3.2. Experiment specific methods	71
2.3.2.1. Preliminary scute analysis	77
2.3.2.2. Preliminary organ tissue analysis	84
2.3.2.3. Experimental tissue processing	88
2.3.3. Results & Discussion	97
2.4. Assessing if seasonal changes in mercury concentration exist in alligators	130
2.4.1. Introduction	130
2.4.2. Experiment specific methods	131

2.4.3.	<i>Results & Discussion</i>	140
2.5.	<i>Elucidating the relationship between mercury concentration & body condition</i>	149
2.5.1.	<i>Introduction</i>	149
2.5.2.	<i>Experimental specific methods</i>	151
2.5.3.	<i>Results & Discussion</i>	152
2.6.	<i>Determining if developing alligators are exposed to mercury</i>	160
2.6.1.	<i>Introduction</i>	160
2.6.2.	<i>Experiment specific methods</i>	161
2.6.3.	<i>Results & Discussion</i>	165
2.7.	<i>Investigating maternal transfer of mercury to developing embryos in American alligators</i>	169
2.7.1.	<i>Introduction</i>	169
2.7.2.	<i>Experiment specific methods</i>	169
2.7.3.	<i>Results & Discussion</i>	177
2.8.	<i>Determining the feasibility of mercury dosing for American alligator eggs</i>	188
2.8.1.	<i>Introduction</i>	188
2.8.2.	<i>Experiment specific methods</i>	189
2.8.3.	<i>Results & Discussion</i>	203
2.9.	<i>Chapter Discussion</i>	211
	<i>Chapter Three: Investigating the relationship between mercury exposure & an epigenetic modification</i>	219
3.1.	<i>Determination of DNA methylation changes in response to chronic & acute mercury exposure scenarios in American alligators & diamondback terrapins</i>	220
3.2.	<i>General methods</i>	226
3.2.1.	<i>DNA isolation</i>	226
3.2.2.	<i>Preparation of deoxyribonucleoside solutions for calibration</i>	226
3.2.3.	<i>Hydrolysis of final calibration solutions & experimental DNA extracts</i>	231
3.2.4.	<i>LC-MS/MS method</i>	234
3.2.5.	<i>Global DNA methylation quantification</i>	235
3.3.	<i>Examining the relationship between mercury & DNA methylation in wild American alligators</i>	237
3.3.1.	<i>Introduction</i>	237
3.3.2.	<i>Experiment specific methods</i>	237
3.3.3.	<i>Results</i>	244
3.3.4.	<i>Discussion</i>	272
3.4.	<i>Using captive American alligators to elucidate the relationship between diet & DNA methylation</i>	276
3.4.1.	<i>Introduction</i>	276
3.4.2.	<i>Experiment specific methods</i>	276
3.4.3.	<i>Results & Discussion</i>	278
3.5.	<i>Examining the relationship between DNA methylation & mercury exposure in captive diamondback terrapins</i>	290

3.5.1.	<i>Introduction</i>	290
3.5.2.	<i>Experiment specific methods</i>	291
3.5.3.	<i>Results & Discussion</i>	303
3.6.	<i>Chapter Discussion</i>	317
Chapter Four: Using NMR-based metabolomics to elucidate the biochemical pathways affected by chronic mercury exposure in diamondback terrapins		328
4.1.	<i>Investigating the effect of mercury exposure on the metabolome</i>	329
4.2.	<i>Methods</i>	334
4.2.1.	<i>Experimental design</i>	334
4.2.2.	<i>Methods development</i>	338
4.2.3.	<i>Experimental sample extraction</i>	345
4.2.4.	<i>NMR measurement</i>	347
4.3.	<i>Results</i>	360
4.3.1.	<i>Plasma experimental samples</i>	360
4.3.2.	<i>Liver experimental samples</i>	383
4.3.3.	<i>Cumulative results</i>	401
4.4.	<i>Chapter Discussion</i>	416
Chapter Five: Synopsis, synthesis & final comments		432
5.1.	<i>Major findings of specific aims & experiments</i>	433
5.2.	<i>Ecotoxicology risk assessment</i>	438
5.3.	<i>Human health implications</i>	444
5.4.	<i>Future directions</i>	445
5.5.	<i>Conclusions</i>	447
References		451

Table of Figures

Figure 1.1. The mercury cycle showing Hg ⁰ conversion to CH ₃ Hg and bioaccumulation, taken from Erickson and Lin (1).....	5
Figure 1.2. The Trophic Magnification Slope (TMS) for Hg (THg) and CH ₃ Hg (methylmercury) plotted against latitude for all sites (A) and only freshwater sites (B) reviewed by Lavoie, et al. (36).....	8
Figure 1.3. The sampling sites used in the largemouth bass monitoring effort from 1990-1999, taken from Lange (2).	12
Figure 1.4. A schematic of the Adverse Outcome Framework for Hg exposure including DNA methylation loss.	38
Figure 1.5. Illustration of the three steps of the glutathione (GSH) activity in response to reactive oxygen species (ROS) (209).	41
Figure 1.6. A diagram of the cellular response of glutathione (GSH) to toxic heavy metals (199).	44
Figure 1.7. The GSH pathway, modified from Wu, <i>et al.</i> (210) to highlight the components of GSH synthesis.	49
Figure 1.8. The One-Carbon Metabolism pathways, modified from King, et al. (5) to highlight the small molecules changes in response to Hg exposure in bivalves as demonstrated by Liu, et al. (6).....	50
Figure 2.1. The graphical abstract of the experiments of all Specific Aims discussed within this dissertation.	57
Figure 2.2. Map of all sites used for sample collection in Chapter 2.....	72
Figure 2.3. The posterior section of caudal scute that was used to standardize the total Hg comparisons	79
Figure 2.4. The results for the Hg analysis of three different scutes from three adult American alligators collected in Florida, demonstrating the variation in total Hg between individual scutes, as well as variation within scutes.....	83
Figure 2.5. The Wilcoxon Each Pair Comparison of the total Hg fraction of whole blood from nine sites in the southeastern United States.	106
Figure 2.6. The trace element totals measured in all alligators from all nine sites examined in the survey conducted across the southeastern Atlantic coast of the United States.	107

Figure 2.7. The graphical abstract of the results of Specific Aim1, experiment 1 detailed in this section.	109
Figure 2.8. Scatter plot of the log transformed tissue averages of each trace element measured in American alligator tissue samples.	121
Figure 2.9. Scatter plot of the statistically significant tissue correlations for trace elements in American alligator samples.....	122
Figure 2.10. American alligator tissue correlations (whole blood and scute tissue vs. muscle tissue) for trace elements (Hg, Se, Rb, Zn, Al, Pb), where statistically significant relationships were observed (Table 2.16).....	128
Figure 2.11. The graphical abstract of the results of Specific Aim 1, experiment 2 detailed in this section.	129
Figure 2.12. The average total Hg concentration for all alligators collected in each season from 2007-2014 at Merritt Island National Wildlife Refuge (MINWR) (top). The seasonal comparisons of total Hg concentration in alligators, using Student’s t-Test and Connecting Letters Report (center). The total Hg concentration for all alligators collected in each season from 2007-2014 at Merritt Island National Wildlife Refuge (MINWR), separated by year (bottom).	143
Figure 2.13. The GIS interpolation of the total Hg measurements taken at MINWR from 2007-2014 by season.....	147
Figure 2.14. The graphical abstract of the results of Specific Aim 1, experiment 3 detailed in this section.	148
Figure 2.15. The observable difference in alligators with normal BMI (top) and low BMI (bottom) at MINWR.	150
Figure 2.16. The individual mercury concentrations for each of the alligators in the BMI assessment, separated by group and plotted against their SVL (cm).....	156
Figure 2.17. A boxplot demonstrating the statistically significant difference in total Hg concentration between American alligators with a low ($n = 22$) and normal ($n = 22$) body mass index (BMI) (by season/year of collection, sex and length) at MINWR, FL from 2007-2014 ($p < 0.0087$).	157
Figure 2.18. The amount of change in mercury concentration each BMI group experience between initial and recapture sampling, as indicated by the Wilcoxon Matched Pair analysis... 158	
Figure 2.19. The graphical abstract of the results of Specific Aim 1, experiment 4 which was detailed in this section.....	159

Figure 2.20. The individual mercury measurements from the yolk samples collected at Yawkey, Apopka and Woodruff in 2011.	168
Figure 2.21. The GPS locations of the nests sampled at Yawkey, SC during the summers of 2011, 2013 and 2014. The coordinates are provided in Table 2.28.....	172
Figure 2.22. Embryonic alligator photos.	173
Figure 2.23. The mercury concentrations from the individual nesting female blood samples (filled markers), and the corresponding yolk samples (hollow markers) from Yawkey, SC in 2011, 2013, and 2014.....	184
Figure 2.24. The relationship between putative mother blood samples, egg yolk and embryonic total Hg concentrations.	186
Figure 2.25. The graphical abstract of the results of Specific Aim 1, experiment 5, which was detailed in this section.....	187
Figure 2.26. A map of Lake Woodruff National Wildlife Refuge, FL where alligator eggs for experiment 2.7 were collected.	191
Figure 2.27. The chemical structures, boiling point and molecular weight of Methylmercury-cysteine and Dichlorodiphenyldichloroethylene.....	194
Figure 2.28. The pictorial description of the experimental design for the topical dosing experiment described in section 2.7.2.....	196
Figure 2.29. The pictorial description of the experimental design for the injection dosing experiment described in section 2.7.2.....	200
Figure 2.30. The compartmental analysis of total Hg in American alligator eggs after dosing via the painting method. Carets denote the expected Hg concentration in stage 27 embryos.	209
Figure 2.31. The graphical abstract of the experiments and results of Specific Aim 1, experiment 6 detailed in this section.....	210
Figure 2.32. The graphical abstract of the experiments and results of Specific Aim 1 detailed in this chapter.....	217
Figure 3.1. The oxidation of DNA with hydroxyl adducts to the guanine base residue.	221
Figure 3.2. The graphical abstract of the experiments of Specific Aims 2 detailed in this chapter.	225
Figure 3.3. Confirmation of Hydrolysis Reaction. 15 μ L of five representative genomic DNA samples (labeled A-E) were tested for hydrolysis by agarose gel electrophoresis.	232

Figure 3.4. A map of the six sites used for collection of American alligator blood samples in experiment 3.3.	238
Figure 3.5. The calibration lines created using NIST SRM 3133 (Mercury in Water) for use with the alligator blood samples collected from six sites in Florida in 2012.	242
Figure 3.6. A standard calibration line for calculating global DNA methylation (% 5mdC, 5mdc/dG).	243
Figure 3.7. The mean (\pm SD) total Hg concentrations (ng/g, wet mass) in alligator whole blood partitioned as a function of age class and sampling location in Florida.	248
Figure 3.8. A map of the sampling sites within the connected drainage system flowing south to Florida Bay (A) and sites located in other watersheds. Sites 4 and 5 are part of a connected system that flows north to the Atlantic Ocean, site 6 has isolated drainage to the Gulf of Mexico (B).	251
Figure 3.9. Box and whisker plots showing the difference in % DNA methylation (5mdC/dG) between the two age classes of alligators in experiment 3.3.	258
Figure 3.10. Snout-vent length is plotted against 5mdC/dG for each alligator from experiment 3.3.	259
Figure 3.11. Box-and-whisker plots of global DNA methylation measurements across site and age class from the alligator blood samples used in experiment 3.3.	260
Figure 3.12. The graphical representation of SVL (cm), average mercury concentration, and DNA methylation across all six sites, separated by age class.	261
Figure 3.13. The % DNA methylation data plotted against snout vent length (SVL) for alligators from Lake Lochloosa and St. Johns River (SJR), two low Hg sites.	266
Figure 3.14. The % DNA methylation data plotted against snout vent length (SVL) for alligators from the Lake Kissimmee and Lake Trafford, two moderate Hg sites.	267
Figure 3.15. The % DNA methylation data plotted against snout vent length (SVL) for alligators from the two Everglades sites, WCA2A and WCA3A, two high Hg sites.	268
Figure 3.16. Global measures of DNA methylation are correlated to concentrations of Hg. All individuals ($n = 119$) are plotted together (top), and according to age class (bottom).	269
Figure 3.17. Global measures of DNA methylation are correlated to concentrations of Hg.	270
Figure 3.18. The proportion of global DNA methylation in adults relative to sub-adults from the same site is plotted against the mean concentrations of THg measured for each site.	271

Figure 3.19. The DNA methylation for the erythrocytes and ovary samples from Parrott et al. (3).	286
Figure 3.20. The mercury concentration for the egg yolk and erythrocytes (RBCs) from the 2011 Grow Out study conducted by Parrott et al. (3).	287
Figure 3.21. The comparison between captive juvenile erythrocyte mercury concentration and the erythrocyte (left) and ovary (right) DNA methylation provided by Parrott, <i>et al.</i> (3).	288
Figure 3.22. The relationship between the DNA methylation of captive juvenile alligator tissues, provided by Parrott, <i>et al.</i> (3), and the corresponding nesting females blood mercury concentration.....	289
Figure 3.23. The sampling area where diamondback terrapins were collected along the Ashley River near Charleston, SC in 2004 denoted with yellow bars.	293
Figure 3.24. A schematic for the diamondback terrapin dosing experiment conducted by Schwenter (2007).	302
Figure 3.25. The test DNA methylation calibration curve generated in September 2016 using the LC-MS/MS method. The point at 0 was generated by the lack of any calibration solution in water.	305
Figure 3.26. The hydrolyzed DNA methylation calibration curve generated in September 2016 using the LC-MS/MS method. The error bars represent the standard deviation of all four replicates of each calibrant. The point at 0 was generated by the lack of any calibration solution in water.....	306
Figure 3.27. The proposed AOP design to utilize DNA methylation as an indicator of decreased environmental quality and population level changes to improve wildlife management strategies.	326
Figure 3.28. The graphical abstract of the results of Specific Aims 2 detailed in this chapter....	327
Figure 4.1. The graphical abstract of the goal of the experiments of Specific Aim 3 in this chapter.	333
Figure 4.2. The overlaid sections of the TLCM replicate spectra showing peaks that differ in relative abundance when the wet/dry extraction methods are compared.....	343
Figure 4.3. The overlaid sections of the spectra with peaks that change in relative abundance between the wet/dry extraction methods stability comparison for the terrapin liver control material replicates.	344
Figure 4.4. The Principle Component Analysis (PCA) showing the technical and individual variance between the control materials and experimental samples in the plasma analysis.	351

Figure 4.5. The Principle Component Analysis (PCA) showing the technical and individual variance between the control materials and experimental samples in the liver analysis.	352
Figure 4.6. A representation of uniform (left) and intelligent (right) bucketing techniques.....	355
Figure 4.7. All plasma samples from the Hg dosed terrapin experiment conducted by Schwenter (2007).....	365
Figure 4.8. All plasma samples from the Hg dosed terrapin experiment conducted by Schwenter (2007), excluding the samples from outlier terrapins K11, M20, F3, F10, K9, M11.	366
Figure 4.9. All plasma samples from the Hg dosed terrapin experiment conducted by Schwenter (2007), excluding the samples from outlier terrapins K11, M20, F3, F10, K9, M11 and the initial samples collected before dosing began.	367
Figure 4.10. The significant difference spectra (SDS) for the different groups of plasma samples.	373
Figure 4.11. The average pareto scales PC1 scores for each dose group plotted against the average Hg concentration for each group of the diamondback terrapin Hg dosing experiment, as reported by Schwenter (2007).....	377
Figure 4.12. The average pareto scaled PC1 and PC2 scores for each dose group, separated by year of the diamondback terrapin Hg dosing experiment.	380
Figure 4.13. The PCA scores and loadings plots for all Hg dose terrapin plasma samples.....	381
Figure 4.14. The PCA scores and loadings plots for all Hg dosed terrapin liver samples.....	388
Figure 4.15. The PCA scores and loadings plots for all Hg dosed terrapin liver samples with the three outlying samples removed (M20, F3 and K11).	389
Figure 4.16. The PCA scores and loadings plots for all Hg dosed terrapin liver samples with the three outlying samples removed (M20, F3 and K11), and the three OHD samples removed (M11, F10, K9).	390
Figure 4.17. The significant difference spectra (SDS) for the different groups of liver tissue.	399
Figure 4.18. The chemical shift spectra comparing the differences between the OHD and high dose terrapin liver samples.....	400
Figure 4.19. All biochemical effects of the altered metabolites identified in the Hg dosed diamondback terrapins.	415
Figure 4.20. The biochemical relationships between the altered metabolites and energy metabolism.....	422

Figure 4.21. A diagram of the three components of the tripeptide glutathione (GSH), taken from Eteshola (321). 424

Figure 4.22. The biochemical relationships between the altered metabolites and GSH production. 425

Figure 4.23. The effects of reduced blood glucose levels as a result of decreased feeding observed in the high dose and OHD terrapins within the AOP framework. 430

Figure 4.24. The graphical abstract of all experiments conducted relating to increased Hg exposure. 431

Figure 5.1. The graphical abstract depicting the results from this dissertation and how the results relate back to each other. 437

Figure 5.2. The AOP network devised using the data generated from the Specific Aims of this work. 443

Table of Tables

Table 1.1. Mercury in wildlife from the environment.	17
Table 1.2. The effects of mercury on wildlife, including laboratory studies.	26
Table 1.3. Mercury measurements in human populations.	31
Table 2.1. A list of the SRM Solutions, mass fractions, uncertainties and lot numbers used in the creation of the Calibration Curves.	67
Table 2.2. The capture metadata for all alligator with blood samples used in experiment 2.3.	73
Table 2.4. Total Hg fractions from American alligator tissues collected in Florida in 2014.	86
Table 2.5. American alligator tissue mercury concentration preliminary study ($n = 5$).	87
Table 2.6. The metadata associated with the America alligators used for the tissue comparisons in this study.	91
Table 2.7. The summaries of the total mercury results for the SRM 955c (Toxic Metals in Caprine Blood) used with the alligator blood samples in Experiment 2.2.	93
Table 2.8. The summaries of the total mercury results for the SRM QC03LH3 (Pygmy Sperm Whale Liver) and SRM 1946 (Lake Superior Fish Tissue) used with the alligator tissue samples in Experiment 2.3.	94
Table 2.9. The measured values of Seronorm as a control material throughout the analysis of the Alligator blood samples from Florida and South Carolina.	95
Table 2.10. The measured values of SRM 1577c as a control material throughout the analysis of the Alligator tissue samples using the ICP-MS. Values are presented in ng/g.	96
Table 2.11. The trace element data for the American alligator blood samples analyzed in experiment 2.3.	99
Table 2.12. The mean and standard deviation of variation across samples of all trace metals measured for each location and age class.	105
Table 2.13. The Wilcoxon Each Pair Non-Parametric Multiple Comparison and the p-values associated with the data presented in Figure 2.5 (JMP 11, Cary, NC).	108
Table 2.14. The individual measurements for the 37 American alligator scute, liver tissues analyzed in Experiment 2.3.	114
Table 2.15. The individual measurements for the 37 American alligator blood, samples analyzed in Experiment 2.3.	115

Table 2.16. The individual measurements for the 37 American alligator muscle tissues analyzed in Experiment 2.3.....	116
Table 2.17. The individual measurements for the 37 American alligator liver tissues analyzed in Experiment 2.3.....	117
Table 2.18. The median tissue concentration, minimum and maximum (ng/g, w/w), and average ranking for the six trace elements with statistically significant correlations in American alligator samples.....	120
Table 2.19. The spearman correlation results for significant relationships found for the trace elements measured in whole blood and tissues from the American alligator.	123
Table 2.20. The metadata for all alligators from MINWR used in Experiments 2.4 and 2.5, collected from 2007-2014.	133
Table 2.21. Summary of total mercury results for SRM 955C Levels 2 and 4 (Toxic Metals in Caprine Blood; total mercury $4.95 \pm 0.76 \mu\text{g/kg}$, and $33.9 \pm 2.1 \mu\text{g/kg}$, respectively) used during the analysis of American alligator blood samples in Experiment 2.4.....	137
Table 2.22. The mean mercury concentration for each season/year, followed by the standard deviation and number of alligators in each group.....	142
Table 2.23. The mean mercury concentration of the two BMI statuses identified in this experiment, followed by the standard deviation, mean SVL, and number of alligators in each group.	155
Table 2.24. The metadata associated with the egg yolk samples analyzed in this experiment...	162
Table 2.25. The measurements of the QC04-ERM 1 reference material used in the egg yolk analysis.....	164
Table 2.26. The individual mercury concentrations of the yolk samples collected at Yawkey, Apopka and Woodruff in 2011.	167
Table 2.27. The descriptive statistics for the average mercury concentrations found in the yolk samples at Yawkey, Apopka and Woodruff in 2011.	167
Table 2.28. The metadata associated with the nesting females and their nests from Yawkey, SC during 2011, 2013 and 2014.	174
Table 2.29. Summary of total mercury (Hg) results for QC04-ERM-1, and SRM 955C Levels 2 and 3, used during the analysis of American alligator blood, yolk and embryo samples in Experiment 2.6.....	176
Table 2.30. The total Hg data for the nesting female blood samples and yolk sampled collected at Yawkey, SC in 2011, 2013 and 2014.	182

Table 2.31. The paired nesting female, yolk and embryo total Hg results from Yawkey, SC 2014.	183
Table 2.32. The Hg concentrations used to determine the doses needed to create high Hg eggs in the laboratory.	195
Table 2.33. The total Hg results for the methylmercury-cysteine solutions used in the laboratory dosing of American alligator eggs in experiment 2.7, and the SRM 1641e replicates used as a control material (certified values 101.6 ± 1.7 ng/g Hg).	195
Table 2.34. Summary of total Hg results for SRM 1641e, QC04 ERM-1, and SRM 955c Level 2, used for the analysis of American alligator dosing solutions, egg compartments, and embryonic erythrocyte samples, respectively.	202
Table 2.35. The total Hg results for all embryonic samples collected during experiment 2.7.	207
Table 3.1. The details for the deoxyribonucleoside standards used in the LC-MS/MS DNA methylation analysis.	227
Table 3.2. Initial stock solutions for each deoxyribonucleoside standard for the LC-MS/MS DNA methylation analysis.	227
Table 3.3. Preparation of 20 ng standard/mg stock solutions from initial stock solutions for each deoxyribonucleoside standard for the LC-MS/MS DNA methylation analysis.	228
Table 3.4. Preparation of final calibration solutions (Cal) (1 – 13) for LC-MS/MS DNA methylation analysis.	229
Table 3.5. The final concentrations of each deoxyribonucleoside standard in the final calibration solutions (1 – 13) for the LC-MS/MS DNA methylation analysis.	230
Table 3.6. Preparation of hydrolyzed calibration solutions for the LC-MS/MS DNA methylation analysis.	233
Table 3.7. The multiple reaction monitoring (MRM) transitions and optimized compound-specific MS/MS parameters for each deoxyribonucleoside measured in the LC-MS/MS DNA methylation analysis.	235
Table 3.8. Targeted and experimentally calculated average weight ratio for calibration solutions used in the LC-MS/MS DNA methylation analysis.	236
Table 3.9. Corrected peak area ratios (5mdC/dG) for each calibration solution replicate used in the LC-MS/MS DNA methylation analysis.	236
Table 3.10. Capture and morphometric information for adult alligators examined in experiment 3.3.	239

Table 3.11. Capture and morphometric information for sub-adult alligators examined in experiment 3.3	240
Table 3.12. The summaries of the total Hg results for the SRM 955c used with the alligator blood samples in Experiment 3.3.....	246
Table 3.13. The mean and standard deviation of Hg for each location and age class from experiment 3.3.	247
Table 3.14. The Tukey’s HSD Multiple Comparison results for total Hg concentration compared to location and age class.	249
Table 3.15. The quality control materials used in the LC-MS/MS analysis of the alligator blood sample extracts for DNA methylation.	254
Table 3.16. The alligator DNA methylation data for experiment 3.3.....	255
Table 3.17. The average snout vent length (SVL), % DNA methylation and Hg concentrations for each site and age class of alligators in Florida used in experiment 3.3.	257
Table 3.18. The individual measurements of the NIST SRM 955c Level 2 used in this experiment.	282
Table 3.19. The mercury measurements for all erythrocyte (RBC) and ovary tissue, listed with the corresponding DNA methylation value provided by Parrott, <i>et al.</i> (3).....	282
Table 3.20. The descriptive statistics for the yolk and erythrocyte (RBC) mercury concentrations from the 2011 “grow out” captive juvenile alligator study conducted by Parrott, <i>et al.</i> (3).....	285
Table 3.21. Terrapin morphometric data taken from Schwenter (2007).....	294
Table 3.22. The concentrations of control and Hg soaked shrimp pieces taken from Schwenter (2007).....	295
Table 3.23. Shrimp consumption chart for 2005 taken from Schwenter (2007).....	296
Table 3.24. Shrimp consumption chart for 2006 taken from Schwenter (2007).....	297
Table 3.25. Terrapin Hg concentrations in red blood cells and scutes, reported as ppb (ng/g) taken from Schwenter (2007).	298
Table 3.26. The relative abundances, ratios and descriptive statistics for the calibration solutions used in the terrapin DNA methylation experiment.	307
Table 3.27. The pooled terrapin quality control (QC) material replicates used in the terrapin DNA methylation analysis conducted in September 2016 using the LC-MS/MS method.....	310

Table 3.28. The QC materials from the alligator experiment conducted in 2013, and the terrapin experiment conducted in 2016, used in the DNA methylation analyses using the LC-MS/MS method.	310
Table 3.29. DNA methylation measurements made on the LC-MS/MS in September 2016 of the diamondback terrapin control group samples.	313
Table 3.30. DNA methylation measurements made on the LC-MS/MS in September 2016 of the diamondback terrapin low dose group samples.	314
Table 3.31. DNA methylation measurements made on the LC-MS/MS in September 2016 of the diamondback terrapin high dose group samples.	315
Table 4.1. The total Hg concentration data for liver, kidney, brain and erythrocytes (RB) from the terrapin dosing study taken from Schwenter (2007).	336
Table 4.2. The summary statistics for the relative standard deviation (RSD) calculations of the terrapin plasma control material (TPCM) replicates.	351
Table 4.3. The summary statistics for the relative standard deviation (RSD) calculations of the terrapin liver control material (TLCM) replicates, NIST SRM 1946 replicates, and experimental terrapin liver samples.	352
Table 4.4. The top 20 uniform buckets for each the unscaled and Pareto scaled data, sorted by loadings intensity.	368
Table 4.5. The top 20 intelligent buckets for each the unscaled and Pareto scaled data, sorted by loadings intensity.	369
Table 4.6. The number of significant buckets for each of the plasma dose group t-test comparisons.	371
Table 4.7. The statistically significant buckets identified in AMIX and NMRProcFlow for the comparison of terrapin plasma samples, with the metabolites identified using Chenomx, and verified using the ¹ H and ¹³ C NMR spectra with the HMDB.	375
Table 4.8. The average number of pieces of Freshwater Turtle Gelatin (Mazuri) that each terrapin consumed during the 30-minute feeding period for each month.	391
Table 4.9. The average time (in seconds) each terrapin required to right itself after being paced carapace-down on the ground.	392
Table 4.10. The top 20 uniform buckets for each the mean centered and Pareto scaled liver sample data, sorted by loadings intensity.	393
Table 4.11. The top 20 intelligent buckets for each the mean centered and Pareto scaled data, sorted by loadings intensity.	394

Table 4.12. The number of significant buckets for each of the liver dose group t-test comparisons.	397
Table 4.13. The statistically significant buckets identified in AMIX and NMRProcFlow for the comparison of the OHD and high dose terrapins, with the metabolite identified using Chenomx, and verified using the ¹ H an ¹³ C NMR spectra with the HMDB.	402
Table 4.14. The altered metabolites identified in the Hg dosed terrapins (input compounds), and the other compounds that are effected by the changed metabolite abundances.....	403
Table 4.15. The enzymes that are effected by the altered metabolites identified in the Hg dosed terrapins.	405
Table 4.16. The reactions affected by the sixteen altered metabolites identified in the Hg dosed terrapins.	406
Table 4.17. The gene effected by the sixteen altered metabolites identified in the Hg dosed terrapins.	410

List of Abbreviations

IACUC- the Institutional Animal Care and Use Committee

ASIH- American Society of Ichthyologists and Herpetologists

HML- Hollings Marine Laboratory

NASA- National Aeronautics and Space Administration

IMSS- Integrated Mission Support Systems

FFWCC- Florida Fish and Wildlife Conservation Commission

MINWR- Merritt Island National Wildlife Refuge

NWR- National Wildlife Refuge

ISO- International Organization for Standardization

NIST- National Institute of Standards and Technology

ORM- Office of Reference Materials

EPA- US Environmental Protection Agency

FDA- US Food and Drug Administration

OHC- One Health Commission

GPS- Global Positioning System

SAR- seasonal average rainfall

SVL- snout to vent length

TG-tail girth

BMI- body mass index

TMS- trophic magnification slope

SE US- southeastern United States

WCA2A- water conservation area 2A

WCA3A- water conservation area 3A

ICP-MS- inductively coupled plasma mass spectrometry

LC-MS- liquid chromatography mass spectrometry
LC-MS/MS- liquid chromatography tandem mass spectrometry
Q1-Q3- quadrupole #
AAS- atomic adsorption spectrometry
DMA- direct mercury analyzer
UV-Vis- ultraviolet visible
NMR- nuclear magnetic resonance spectroscopy
MRM- multiple reaction monitoring
RSF- response factor
SRM- standard reference material
QC- quality control
ERM- egg reference material
LOD- limit of detection
Hg- mercury
Hg²⁺- divalent mercury
Hg⁰- elemental mercury
HgS- mercuric sulfide
THg- total mercury
CH₃Hg- methyl mercury
Al- aluminum
V- Vanadium
Cr- chromium
Mn- manganese
Ni- nickel
Co- cobalt
Cu- copper

Zn- zinc
As- arsenic
Se- selenium
Rd- rubidium
Sr- strontium
Mo- molybdenum
Cd- cadmium
Sn- tin
Pb- lead
C- Carbon
S- Sulfur
H- Hydrogen
ANOVA- analysis of variance
ANCOVA- analysis of covariance
SD- standard deviation
CV- coefficient of variance
RSD- relative standard deviation
HSD- honest significant difference
DNA- deoxyribonucleic acid
DNMT- DNA methyl transferase
5mdC- 5' methylated deoxycytosine
dG- deoxyguanine
5mdC/dG- % methylated deoxycytosine
RBC- red blood cells
CAM- chorioallantoic membrane
CNS- central nervous system

NF- κ B- nuclear factor kappa-light-chain-enhancer of activated B cells

ATP- adenosine triphosphate

ADP- adenosine diphosphate

OHD- overt health declines

TCA- tricarboxylic acid

GSH- glutathione

GPX- glutathione peroxidase

ROS- reactive oxygen species

AOP- adverse outcome pathway

CIE- chemical initiating event

MIE- molecular initiating event

KE- key event

KER- key event relationship

AO- adverse outcome

NAFLD- non-alcoholic fatty liver disease

NASH- Nonalcoholic steatohepatitis

Chapter One: General Introduction & Literature Review

Sections of Chapter 1 have been published in the following reference text.

Analysis of Food Toxins and Toxicants: John Wiley & Sons, 2017.

1.1. Mercury exposure

Mercury (Hg) is a naturally occurring, toxic environmental pollutant. It has a ubiquitous distribution across the planet due to its dispersal by atmospheric circulation, after release from the Earth's crust via natural or anthropogenic processes. Once released, it is transformed in the environment and bio-accumulated throughout the food web. The bio-accumulative nature of mercury combined with its ability to cause degenerative diseases that affect the nervous, cardiac and reproductive systems, such as Minamata Disease, make it of particular concern (7). After the effects of exposure were seen in Minamata Japan, the United Nations Environmental Program held the Minamata Convention to convene many nations in the effort to reduce global mercury emissions and prevent future disasters related to mercury exposure (8).

1.2. Global & environmental sources of mercury

Mercury is released into the environment by both natural and anthropogenic activities. It has been recently estimated that over 7,500,000 kg of mercury is released into the atmosphere each year. Natural sources, such as volcanic activity, geothermal sources, soil erosion and meteorological conditions that influence exchange mechanisms of gaseous mercury (Hg^0), account for most, 69%, of the mercury that is released into the atmosphere, including re-emission of previously released mercury by natural and anthropogenic processes (5,207,000 kg / year). Anthropogenic sources such as coal-fired power plants, artisanal gold mining, metals manufacturing, cement production, waste incineration, biomass burning, land use changes and caustic soda production account for much less atmospheric mercury at 2,320,000 kg / year, the remaining 31% (9-12). This

amount of anthropogenically released mercury is projected to increase by as much as 96% by the year 2050, to 4,860,000 kg / year based on the Intergovernmental Panel on Climate Change's (IPCC) development scenarios (13). The projected increase in anthropogenic emissions is due to the increased use of coal-fired power plants in emerging countries, particularly those in Asia (13). Combined with improved mercury sorbent capture technology for power plants, the projected increase will lower the emissions of Hg^0 , but lead to an increased proportion of divalent mercury (Hg^{2+}) in the atmosphere. This will lead to a decrease in long range transport of the lighter, less reactive Hg^0 species, but an increase in local deposition of the heavier, more reactive divalent, Hg^{2+} species into local environments (13).

1.3. The biogeochemistry of mercury

Mercury is predominantly released into the atmosphere as the less reactive form; Hg^0 . Sunlight converts Hg^0 to Hg^{2+} (Figure 1.1). Some of the Hg^{2+} re-converts and goes back into the atmosphere as Hg^0 , while the remaining Hg^{2+} returns to the surface of the Earth by either wet or dry deposition (14). Depending on the concentration of mercury in the air, and the type of ground cover on a particular area of Earth's surface, wet or dry deposition may be of greater environmental importance (14, 15). A location where dry deposition may outweigh the amount of mercury deposited from wet deposition is forested ecosystems (14).

Atmospheric mercury that is deposited onto the surface of leaves in the forest canopy reaches the forest floor by either "through fall" (being washed down by precipitation) or "litter fall" (leaves falling to the forest floor) (16). Wet deposition

requires precipitation to “scavenge” Hg^{2+} particles from the upper atmosphere and bring them to Earth’s surface. This process is dependent on deep convection in the upper atmosphere, and generally brings less Hg^{2+} to the environment than dry deposition (17).

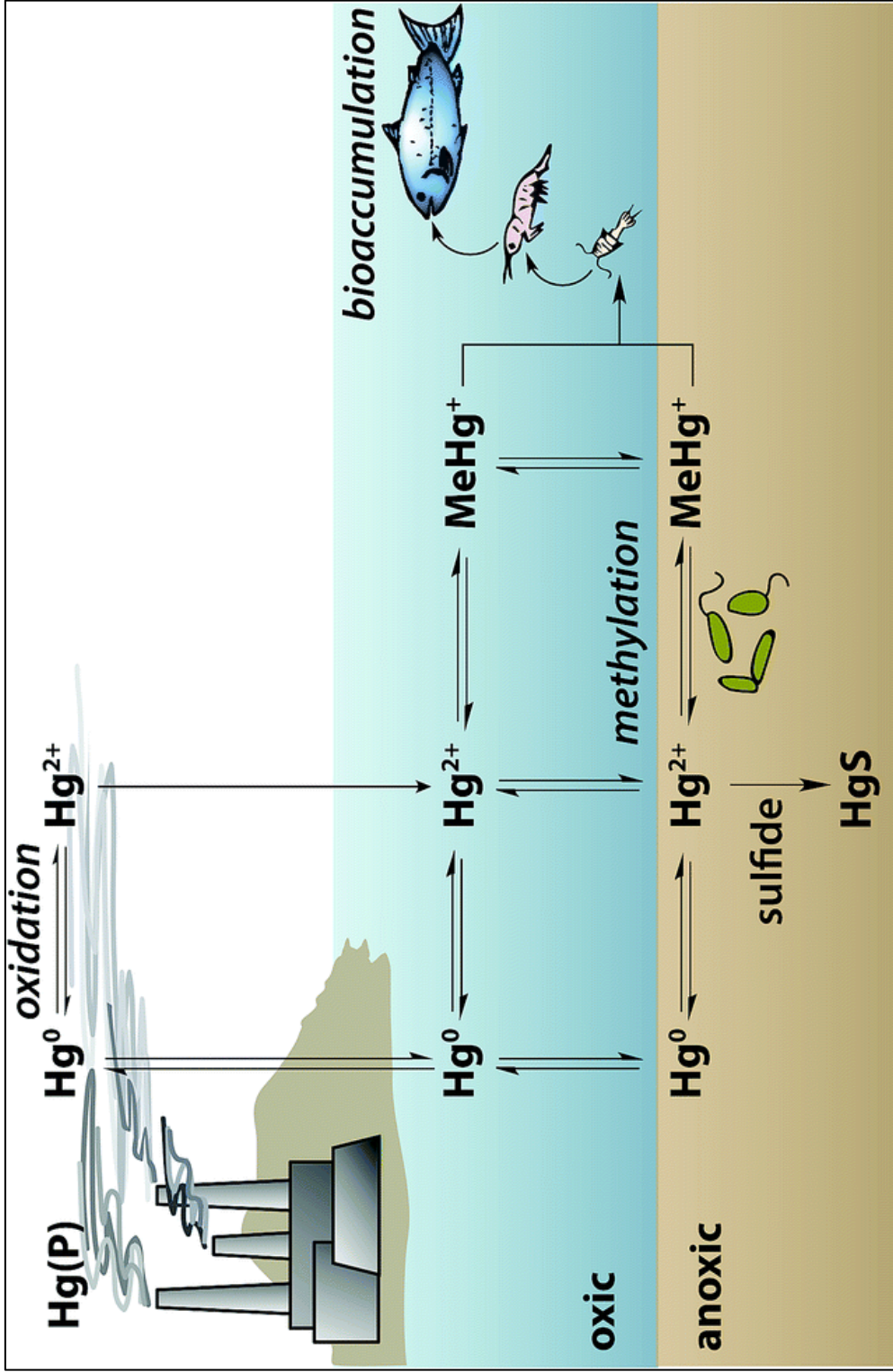


Figure 1.1. The mercury cycle showing Hg^0 conversion to CH_3Hg and bioaccumulation, taken from Erickson and Lin (1).

After the Hg^{2+} is deposited on the foliage, forest floor, or body of water, it eventually reaches the sediment where the environmental biotransformation process to methylmercury (CH_3Hg) begins (18). When Hg^{2+} reaches the sediment, it combines with sulfides released by the bacterial community, forming mercury sulfide, HgS (Figure 1). The HgS can diffuse into bacterial cells, where it becomes subject to the sulfur-reducing reactions of bacterial respiration, a cellular process that is currently not well understood (19, 20). During this transformative process, the sulfide is removed from the Hg^{2+} and a methyl group is added, producing methylmercury, CH_3Hg (14). The production of CH_3Hg happens shortly after the Hg^{2+} reaches the sediment, with rates of production of CH_3Hg being dependent on concentration and composition of bacteria in the soil (4, 21-27). The production of CH_3Hg is optimal at the sediment water interface, which is the oxic-anoxic transition zone in most marine systems. The greatest concentration of CH_3Hg is found at this interface and decreasing with depth as the sediment becomes more anoxic (21, 28). Sulfate-reducing bacteria are responsible for nearly all methylation of mercury in sediment (21). Iron-reducing bacteria also methylate Hg^{2+} , but at a slower rate than sulfate-reducing bacteria, based on laboratory experiments (20, 24, 27-29). The sulfur-reducing bacteria that are responsible for the methylation of Hg^{2+} reach their effective maximum at 12 h after deposition of Hg^{2+} (21).

Different environments and environmental parameters can aid in accumulation of CH_3Hg in the tissues of organisms, as some environments favor the production of CH_3Hg at low levels in the food web (30). In low-sulfide coastal marine sediments, CH_3Hg production is controlled by the partitioning of Hg^{2+} between dissolved and particulate states, which regulates the bioavailability of mercury containing substrates to methylating

bacteria (25). After transforming into CH₃Hg, it diffuses out of the bacterial cells and in the surrounding sediment, where it can be released into the water column, consumed by phytoplankton, and bioaccumulated up the food chain via trophic transfer (19).

1.4. Bioaccumulation & biomagnification through the trophic levels

Methylmercury is subject to both bioaccumulation, in which the concentration increases throughout the organism's lifespan, as well as biomagnification, in which there is a large increase in concentration through the trophic levels. Animals cannot easily detoxify themselves of CH₃Hg, so the longer-lived organisms bioaccumulate concentrations of CH₃Hg that may be toxic both to themselves and their predators (19, 28, 31). The biomagnification of CH₃Hg results in concentrations that more than triple through each succeeding trophic level from the phytoplankton, zooplankton, and small shorter-lived fish to the longer-lived fish and apex predators (30-36). This relationship is modeled using the Trophic Magnification Slope (TMS) derived by Lavoie, *et al.* (36). The TMS is a summary of 205 aquatic food webs worldwide, comparing total mercury (THg) and CH₃Hg concentrations to physiochemical and biological factors that affect biomagnification, including the trophic level, which is identified using stable isotope measurements (Figure 1.2) (36). Lavoie, *et al.* (36) demonstrated that there is variability in the TMS related to the dissolved organic carbon, phosphorous content, and mercury deposition, but the biomagnification of CH₃Hg takes place in all food webs measured.

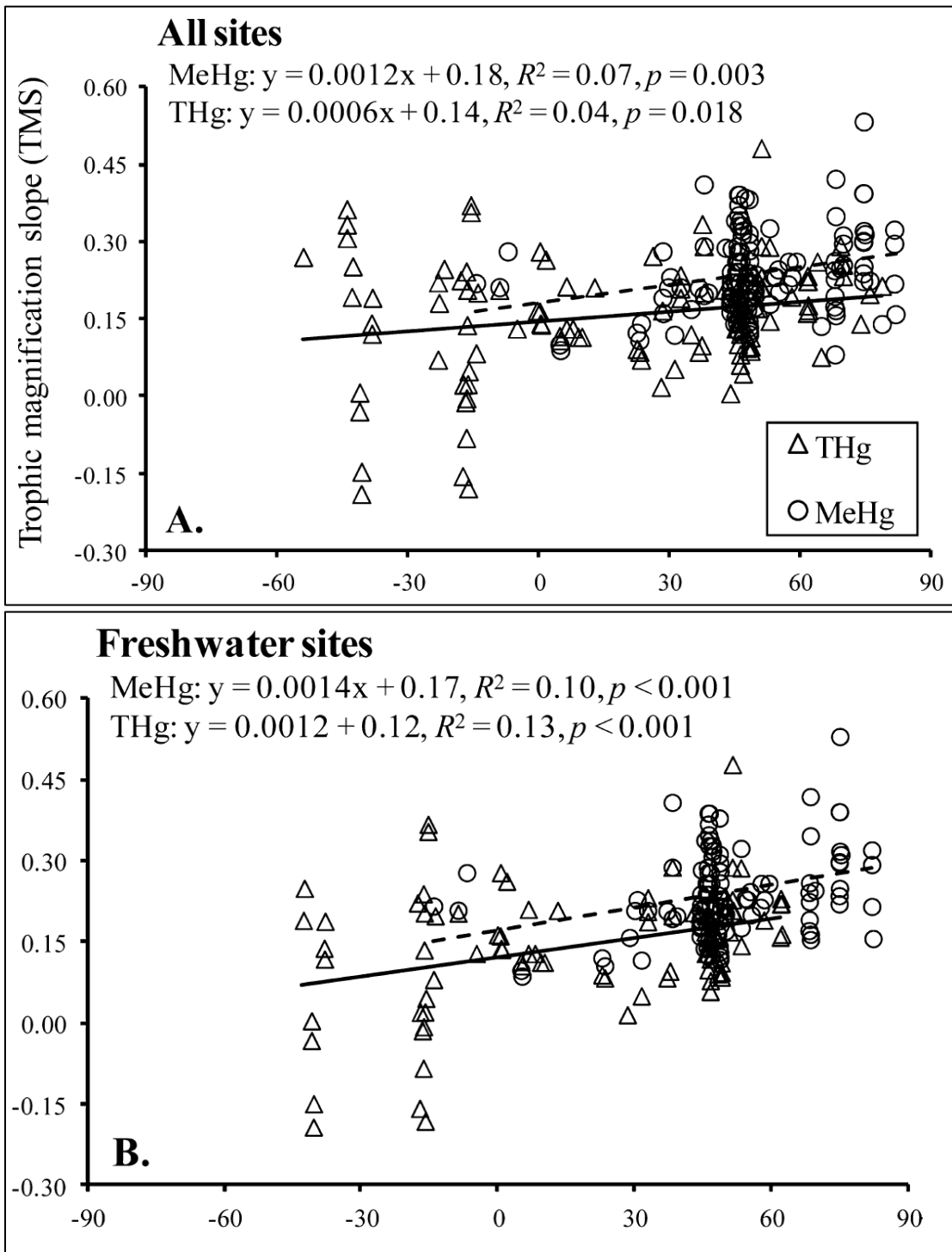


Figure 1.2. The Trophic Magnification Slope (TMS) for Hg (THg) and CH₃Hg (methylmercury) plotted against latitude for all sites (A) and only freshwater sites (B) reviewed by Lavoie, et al. (36). The TMS values represent individual slopes (b) of simple linear regressions between log₁₀ [Hg] and δ¹⁵N for several sites worldwide.

1.5. Biological mercury hotspots

Mercury hotspots have been identified all over the planet based on measurements from fish and human hair samples (37). Despite the measurements being conducted on similar sample types, the mercury hotspots originate from a variety of sources including, but not limited to, chlor-alkali facilities (Czech Republic; Russia), coal-fired power plants (Thailand), artisanal small scale gold mining (Indonesia; Tanzania), mixed use industries (Cameroon; Mexico), dumping-related contamination (Albania; Minamata Bay, Japan), and global deposition (Alaska, USA; Italy; Azores, Portugal, Uruguay; Cook Islands; Japan) (37). However, biological mercury hotspots are not dependent on a local point source of mercury, and are likely the result of globally deposited mercury landing in a sensitive environment (38).

Mercury sensitive areas are generally forested ecosystems that include large wetlands with low water productivity (38, 39). A biological mercury hotspot is characterized by biota that have concentrations of CH_3Hg that are above the concentrations of the surrounding landscape and above the established human health criteria. To classify an area as a biological mercury hotspot, a large amount of scientific investigation as well as significant policy attention is required (39). These criteria remove many mercury hotspots from the biological classification. However, there are several biological mercury hotspots within North America.

The northeastern United States and southeastern Canada are biological mercury hotspots where the largemouth bass (*Micropterus salmoides*) are used as one of the species to monitor human health, as they are pervasive across North America, a sportfish

and secondary consumer, and are commonly consumed by humans (38). Largemouth bass in this area have average mercury concentrations of 0.54 $\mu\text{g/g}$ in their muscle, which is above the critical value for human consumption of 0.3 $\mu\text{g/g}$ set forth by the U.S. Environmental Protection Agency (EPA) (39). Oregon, New Jersey and the Great Lakes areas in the United States all also have mercury concentrations in largemouth bass above the EPA's limit at 0.42, 0.33 and 0.35 $\mu\text{g/g}$, respectively (40-42). In the Florida Everglades, largemouth bass have mercury concentrations that are greater than those of the other hotspots, ranging between 1.0 and 2.0 $\mu\text{g/g}$ in the years measured (43).

The Florida Everglades are one of the most diverse and unique wetland ecosystems on the planet and are home to many endangered species (44). In 1989, a long-term monitoring project was started that used largemouth bass in response to preliminary surveys, demonstrating extremely high levels of mercury in fish from the Everglades region (2). These elevated concentrations were mistakenly attributed to the local point sources of mercury in the area; coal fired power plants, waste incineration and sugar cane farming (43). After these point sources were identified, bioremediation efforts removed them, but elevated concentrations persisted (43). Concentrations of mercury in bass have routinely been higher in the more southern regions of the Everglades, where the biological hotspot has been identified (Figure 1.3) (2, 4). The fast rate at which all available Hg^{2+} is converted to CH_3Hg based on bacterial composition, coupled with the shorter hydroperiod in this region, leads to greater concentrations of CH_3Hg in biota here than in other areas that are known to be hot spots of mercury contamination (4, 45).

Once Hg^{2+} is methylated, the step-wise process up the food chain is less clear in the Everglades than in other ecosystems (31, 32). The CH_3Hg at the bottom of the food

web moves through the water, periphyton, amphipods, hemipterans, shrimp and fish to the apex predators, biomagnifying with each organism, when measured in samples directly from the ecosystem (32). The upper trophic levels and apex predator mercury concentrations have been recorded as high as 0.5 and 11 mg/kg in blood and hair, respectively, for the Florida panther (*Puma concolor*), and 3.88 mg/kg in muscle tissue of the American alligator (*Alligator mississippiensis*) (43). However, the concentration of CH₃Hg is dependent on location in the Everglades, with some regions having greater accumulation potential than others based on fluctuating environmental parameters like hydroperiod and diversity of bacteria in the sediment (4, 32). There is also seasonal variation in the accumulation of CH₃Hg, as the bacteria in soil that convert Hg²⁺ into CH₃Hg rely on the soil being dampened from rainfall, which occurs much more frequently in the summer in Florida than in other seasons (4, 32). The changes in CH₃Hg production that occur seasonally as well as increased eutrophication from rainfall runoff at some sites cause diet shifts in small fish to a more readily available food source, which alters the base of the food web (46). However, it has currently unknown if these seasonal alterations affect the CH₃Hg concentrations observed in apex predators seasonally.

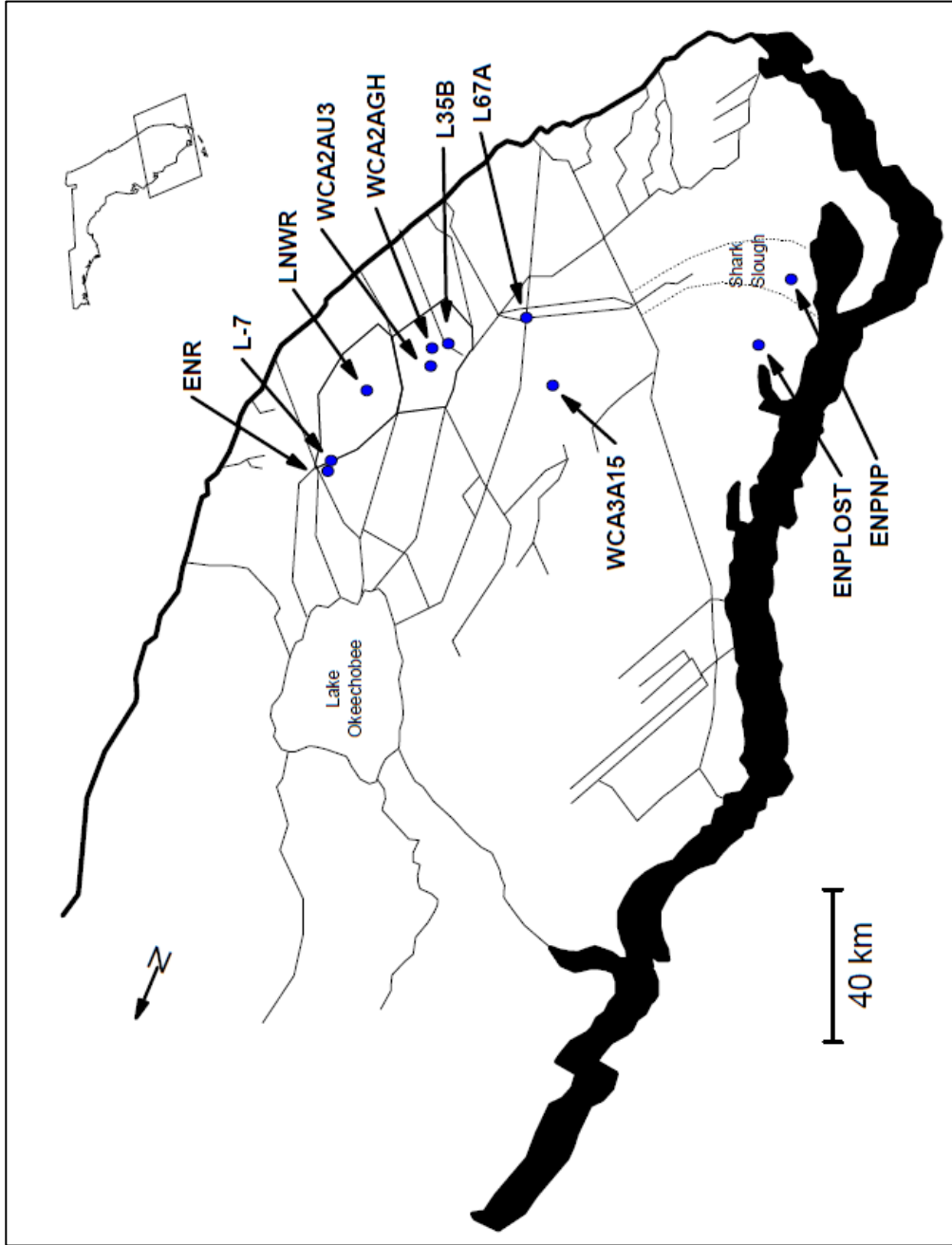


Figure 1.3. The sampling sites used in the largemouth bass monitoring effort from 1990-1999, taken from Lange (2). The Hg hot spot identified by Julian (4) is the area around WCA3A15.

1.6. Effects of mercury in wildlife

Mercury is not just a problem in hotspot locations. A wide variety of animals are exposed to and accumulate mercury at concentrations that can be detrimental to their health and the health of their consumers (Table 1.1) (32, 47-96). Mercury accumulation begins with plants and invertebrates and continues to accumulate through small fish and shellfish, to the larger apex predators, which can have variable concentrations depending on their size and the location where they are collected (48, 54, 67, 97, 98).

1.6.1. Effects of mercury in wildlife health

Free-ranging wildlife.

Observing the effects of mercury in free-ranging wildlife is difficult, as infrequent monitoring/sampling makes identifying changes in behavior/health complicated. The species known to accumulate the highest concentrations of mercury are the apex predators, which elicit the best chance to detect and observe the effects of mercury.

The concentrations of CH₃Hg that are known to accumulate in the tissues of polar bear (*Ursus maritimus*), American alligators, and other apex predators provide an opportunity to study the effects of mercury exposure in wild species (96, 99). Despite the high concentrations of mercury (340 ng/g) found in the medulla oblongata of polar bears from Greenland, it was not high enough to elicit neurotoxic effects (100). However, both the polar bear and the American alligator are subject to epigenetic modifications and genetic polymorphisms due to the high concentrations of CH₃Hg they accumulate over their lifetimes (99, 101, 102). The mechanism of action for these epigenetic changes currently is not well understood.

Laboratory dosed wildlife

Since the effects of high mercury accumulation in free-ranging animals is difficult to observe, laboratory studies have begun to investigate this issue. Several laboratory studies showed that with increasing ambient mercury concentration in the surrounding water, crabs can accumulate approximately 100 ng/g more mercury in their muscle tissue than observed in wild caught animals (Tables 1.1 & 1.2) (103). This finding supports the idea that laboratory studies can facilitate the observation of mercury effects.

In fish, CH₃Hg has been shown to cause an oxidative stress response and cellular apoptosis, as well as reproductive impairment classified by altered hormone profiles, arrested testicular growth, and affected sperm motility (Table 1.2) (99, 101-115). The reproductive impairment observed in white ibises (*Eudocimus albus*) was largely behavioral, resulting in altered pairing behavior with subsequent diminished reproductive success. These behavioral changes were matched to changes in the hormone profiles for estradiol and testosterone in both sexes, and an overall decrease in nests per year (105, 113, 114). Despite the reproductive effects observed, survivorship of exposed animals was unchanged (116). Since survivorship was not affected, it is categorized as a sub-lethal effect of chronic mercury exposure, which is common in wildlife studies. However, two species of mammals, the pig (*Sus spp.*) and rhesus monkey (*Macaca mulatta*), have been shown to have stillbirths and spontaneous abortions, respectively, when exposed to CH₃Hg during pregnancy at a dose of 0.5 mg/kg, which is below the FDA action level of 1.0 mg/kg (115).

1.6.2. Wildlife consumed by humans

For example, the brown crab (*Cancer pagurus*), a large crab from the Azores, has been measured to have between 0.86 and 1.26 mg/kg of mercury in its tissues (Andersen and Depledge, 1997). The Tasmanian giant crab (*Pseudocarcinus gigas*), from Australia, a species that can be double the size and weight of the brown crab, were found to have between 0.6 and 1.2 mg/kg of mercury in the tissues (Table 1.1) (48, 49). This comparison demonstrates that the larger, longer-lived animals do not always have the greatest amounts of mercury in their tissues. Individuals of the same species can also have variable mercury concentrations within their tissues even if the locations are in close proximity (Table 1.1) (50, 117).

Tuna are among the fish known to have the highest mercury concentrations in their muscle tissue, with concentrations ranging from 0.29 – 1.81 µg/g, depending on location (Table 1.1) (54-56). This range of mercury values can elevate the tuna from “safe to consume” to “detrimental to human health” according to the U.S. Food and Drug Administration (FDA), making location vitally important. Swordfish (*Xiphias gladius*) are another open ocean fish that has high concentrations of mercury within its tissues (85). Swordfish from the Azores have less mercury than those from the equatorial region, though both span the range of mercury concentrations that are detrimental for human consumption (0.03-2.4, 0.9-2.2 mg/kg, respectively) (Table 1.1) (85). While oceanic fish accumulate high concentrations of mercury, freshwater fish are also capable of accumulating detrimental concentrations of mercury as well. Freshwater fish throughout Alaska have demonstrated regional mercury increases for a variety of species (Table 1.1) (57).

At the highest trophic level, including the apex predators, the concentrations of mercury continue to increase. Sharks from the southwest Atlantic Ocean have concentrations of mercury up to 2.9 mg/kg in their muscle tissue (86). Aquatic apex predators, like the American alligator, also accumulate high level of mercury, with muscle concentrations being reported from 0.3 up to 5.7 mg/kg (Table 1.1) (95, 96). While most human dietary mercury exposure comes from marine and aquatic sources, low concentrations of mercury have been reported in livestock. Three species of cattle from Spain have been shown to have 40 ng/g total mercury in their muscle tissues (118). Most domestic livestock get exposed to mercury from feed that had been inadvertently contaminated, and levels are lower than the upper level marine predators mentioned above (Table 1.1) (56, 119).

Table 1.1. Mercury in wildlife from the environment.

Common Name	Scientific Name	Location	[Hg] in mg/kg					Source
			Total Organism	Liver	Muscle	Keratin	Blood	
<u>Algae</u>								
Periphyton	<i>various</i>	Everglades (WCA2A), Florida, USA	0.13					(32)
Periphyton	<i>various</i>	Everglades (WCA3A), Florida, USA	0.44					(32)
Kelp (wild)	<i>Ecklonia radiata</i>	Auckland, New Zealand	0.17					(47)
Sea lettuce (wild)	<i>Ulva stenophylla</i>	Auckland, New Zealand	0.1					(47)
Bull Kelp (wild)	<i>Durvillaea antarctica</i>	Auckland, New Zealand	0.04					(47)
Neptune's necklace (wild)	<i>Hormosira banksii</i>	Auckland, New Zealand	0.05					(47)
Red seaweed (wild)	<i>Porphyra spp.</i>	Nelson, New Zealand	0.03					(47)
Wakame (wild)	<i>Undaria pinnatifida</i>	Nelson, New Zealand	0.03					(47)
Kelp (commercial)	<i>Ecklonia radiata</i>	Wairarapa Coast, New Zealand	0.17					(47)
Red seaweed (commercial)	<i>Porphyra spp.</i>	Kaikoura Coast, New Zealand	0.01					(47)
Wakame (commercial)	<i>Undaria pinnatifida</i>	Wellington Harbor, New Zealand	0.05					(47)
Giant Kelp (commercial)	<i>Macrocystis pyrifera</i>	Tory Channel, New Zealand	0.05					(47)
<u>Invertebrates</u>								
Amphipods	<i>Hyaella spp.</i>	Everglades (WCA2A), Florida, USA	3.5					(32) (1995 data)
Amphipods	<i>Hyaella spp.</i>	Everglades (WCA2A), Florida, USA	3					(32) (1996 data)
Hemipterans	<i>Pelocoris spp.;</i> <i>Belastoma spp.</i>	Everglades (WCA2A), Florida, USA	3					(32) (1995 data)
Hemipterans	<i>Pelocoris spp.;</i> <i>Belastoma spp.</i>	Everglades (WCA2A), Florida, USA	62					(32) (1996 data)
Freshwater shrimp	<i>Palaemonetes paludosa</i>	Everglades (WCA2A), Florida, USA	19.5					(32) (1995 data)
Freshwater shrimp	<i>Palaemonetes paludosa</i>	Everglades (WCA2A), Florida, USA	5.8					(32) (1996 data)
Barnacle	<i>Cirripedia spp.</i>	Sao Miguel Island, Portugal			0.07			(48)
Limpet	<i>Patellogastropoda spp.</i>	Sao Miguel Island, Portugal			0.04			(48)
Brown Crab	<i>Cancer pagurus</i>	Sao Miguel Island, Portugal			0.73			(48)
King Crab	<i>Pseudocarcinus gigas</i>	Western Victoria, Australia			1.1			(49)
Blue crab	<i>Cancer sapidus</i>	Quinnipiac Estuary, Canada			0.06			(49)

Common Name	Scientific Name	Location	[Hg] in mg/kg					Source
			Total Organism	Liver	Muscle	Keratin	Blood	
Dungeness crab	<i>Cancer magister</i>	Oregon Coast, USA			0.11			(49)
Purple shore crab	<i>Hemigrapsus nudus</i>	Oregon Coast, USA			0.06			(49)
Heterololigo Squid	<i>Loligo bleekeri</i>	USA			0.03			(56)
Red King Crab	<i>Paralithodes camtschaticus</i>	USA			0.02			(56)
<u>Fish</u>								
Small fish	<i>Gambusai spp.; Heterandia formosa, Lucania goodei</i>	Everglades (WCA2A), Florida, USA	37					(32) (1995 data)
Small fish	<i>Gambusai spp.; Heterandia formosa, Lucania goodei</i>	Everglades (WCA2A), Florida, USA	6					(32) (1996 data)
Bay Anchovy	<i>Anchoa mitchilli</i>	Florida Bay-Marine Area, Florida USA			0.11			(50)
Rainwater Killifish	<i>Lucania parva</i>	Florida Bay-Marine Area, Florida USA			0.06			(50)
Mojarra'	<i>Eucinostomus gula</i>	Florida Bay-Marine Area, Florida USA			0.08			(50)
Bay Anchovy	<i>Anchoa mitchilli</i>	Florida Bay-Estuarine Area, Florida USA			0.21			(50)
Rainwater Killifish	<i>Lucania parva</i>	Florida Bay-Estuarine Area, Florida USA			0.13			(50)
Mojarra	<i>Eucinostomus gula</i>	Florida Bay-Estuarine Area, Florida USA			0.09			(50)
Spotted Seatrout	<i>Cynoscion nebulosus</i>	Florida Bay-Marine Area, Florida USA			0.68			(50)
Red Drum	<i>Sciaenops ocellatus</i>	Florida Bay-Marine Area, Florida USA			0.29			(50)
Gray Snapper	<i>Lutjanus griseus</i>	Florida Bay-Marine Area, Florida USA			0.19			(50)
Spotted Seatrout	<i>Cynoscion nebulosus</i>	Florida Bay-Estuarine Area, Florida USA			1.42			(50)
Red Drum	<i>Sciaenops ocellatus</i>	Florida Bay-Estuarine Area, Florida USA			0.69			(50)
Gray Snapper	<i>Lutjanus griseus</i>	Florida Bay-Estuarine Area, Florida USA			0.41			(50)
Spotted Seatrout	<i>Cynoscion nebulosus</i>	Eastern Florida Bay, Florida, USA			0.96			(53)
Red Drum	<i>Sciaenops ocellatus</i>	Eastern Florida Bay, Florida, USA			0.3			(53)
Gray Snapper	<i>Lutjanus griseus</i>	Eastern Florida Bay, Florida, USA			0.35			(53)

Common Name	Scientific Name	Location	[Hg] in mg/kg					Source
			Total Organism	Liver	Muscle	Keratin	Blood	
Spotted Seatrout	<i>Cynoscion nebulosus</i>	Florida, USA			0.43			(51)
Red Drum	<i>Sciaenops ocellatus</i>	Florida, USA			0.57			(51)
Gray Snapper	<i>Lutjanus griseus</i>	Florida, USA			0.18			(51)
Spotted Seatrout	<i>Cynoscion nebulosus</i>	Gulf of Mexico			0.36			(52)
Red Drum	<i>Sciaenops ocellatus</i>	Gulf of Mexico			0.31			(52)
Gray Snapper	<i>Lutjanus griseus</i>	Gulf of Mexico			0.19			(52)
Albacore Tuna	<i>Thunnus alalunga</i>	Sao Miguel Island, Portugal			0.37			(48)
Bluefin Tuna	<i>Thunnus thynnus</i>	Farm raised, Adriatic Sea		1.17	0.89			(54)
Skipjack Tuna	<i>Katsuwonus pelamis</i>	Sao Miguel Island, Portugal			0.19			(48)
Tuna fish	<i>Thunnus spp.</i>	Misurata, Libya			0.29			(55)
Scabbard fish	<i>Aphanopus carbo</i>	Sao Miguel Island, Portugal			0.28			(48)
Atlantic Bluefin Tuna	<i>Thunnus thynnus</i>	Atlantic Ocean			0.42			(56)
Atlantic Bluefin Tuna	<i>Thunnus thynnus</i>	Pacific Ocean			0.59			(56)
Southern Bluefin Tuna	<i>Thunnus maccoyii</i>	Indian Ocean			0.27			(56)
Bigeye Tuna	<i>Thunnus obesus</i>	Atlantic Ocean			0.27			(56)
Bigeye Tuna	<i>Thunnus obesus</i>	Pacific Ocean			0.98			(56)
Atlantic Blue Marlin	<i>Makaira nigricans</i>	Atlantic Ocean			0.56			(56)
Striped Marlin	<i>Tetrapturus audax</i>	Atlantic Ocean			0.51			(56)
Swordfish	<i>Xiphias gladius</i>	Atlantic Ocean			0.47			(56)
Skipjack Tuna	<i>Katsuwonus pelamis</i>	Philippines			0.05			(56)
Skipjack Tuna	<i>Katsuwonus pelamis</i>	Kiribati			0.04			(56)
Sockeye Salmon	<i>Oncorhynchus nerka</i>	USA			0.03			(56)
Patagonian Toothfish	<i>Dissostichus eleginoides</i>	Chile			0.57			(56)
Southern Bluefin Tuna	<i>Thunnus maccoyii (farmed)</i>	Australia			0.3			(56)
Atlantic Bluefin Tuna	<i>Thunnus thynnus (farmed)</i>	Italy			1.46			(56)
Atlantic Bluefin Tuna	<i>Thunnus thynnus (wild)</i>	Italy			0.97			(56)
Yellowfin Tuna	<i>Thunnus albacares</i>	Marshall Islands			0.04			(56)
Bigeye Tuna	<i>Thunnus obesus</i>	Indonesia			0.47			(56)
Alaska Pollock	<i>Theragra chalcogramma</i>	Russia			0.01			(56)
Forkbeard	<i>Phycis blennoides</i>	Sao Miguel Island, Portugal			0.1			(48)
Rockfish	<i>Sebastes spp.</i>	Sao Miguel Island, Portugal			0.26			(48)
Red Mullet	<i>Mullus spp.</i>	Sao Miguel Island, Portugal			0.12			(48)
Horse Mackerel	<i>Trachurus trachurus</i>	Sao Miguel Island, Portugal			0.04			(48)

Common Name	Scientific Name	Location	[Hg] in mg/kg					Source
			Total Organism	Liver	Muscle	Keratin	Blood	
Grey Mackerel	<i>Scomberomorus semifasciatus</i>	Sao Miguel Island, Portugal			0.2			(48)
Blackspot Seabream	<i>Pagellus bogaraveo</i>	Sao Miguel Island, Portugal			0.26			(48)
Conger Eel	<i>Conger spp.</i>	Sao Miguel Island, Portugal			0.25			(48)
Spotted Moral Eel	<i>Gymnothorax moringa</i>	Sao Miguel Island, Portugal			0.05			(48)
Common Seabream	<i>Pargus pargus</i>	Sao Miguel Island, Portugal			0.48			(48)
Northern pike	<i>Esox Lucius</i>	Yukon River Basin, Alaska, USA	0.51					(58)
Northern pike	<i>Esox Lucius</i>	Yukon River, Alaska, USA			1.51			(59)
Northern pike	<i>Esox Lucius</i>	Yukon River, Alaska, USA			1.07			(60)
Northern pike	<i>Esox Lucius</i>	Yukon River, Alaska, USA			0.73			(60)
Northern pike	<i>Esox Lucius</i>	Kuskokwim River, Alaska, USA			0.63			(59)
Northern pike	<i>Esox Lucius</i>	Kuskokwim River, Alaska, USA			0.74			(60)
Northern pike	<i>Esox Lucius</i>	Innoko NWR, Alaska, USA			0.63			(61)
Northern pike	<i>Esox Lucius</i>	Innoko NWR, Alaska, USA			0.46			(61)
Northern pike	<i>Esox Lucius</i>	Innoko NWR, Alaska, USA			0.44			(66)
Northern pike	<i>Esox Lucius</i>	Innoko NWR, Alaska, USA			0.4			(62)
Northern pike	<i>Esox Lucius</i>	Koyukuk NWR, Alaska, USA			1.0			(62)
Northern pike	<i>Esox Lucius</i>	Nowitna NWR, Alaska, USA			0.49			(62)
Northern pike	<i>Esox Lucius</i>	Nowitna NWR, Alaska, USA			1.05			(64)
Northern pike	<i>Esox Lucius</i>	Selawik NWR, Alaska, USA			0.54			(63)
Northern pike	<i>Esox Lucius</i>	Selawik NWR, Alaska, USA			0.19			(63)
Northern pike	<i>Esox Lucius</i>	Kanuti NWR, Alaska, USA			0.31			(62)
Northern pike	<i>Esox Lucius</i>	Kanuti NWR, Alaska, USA			0.11			(62)
Northern pike	<i>Esox Lucius</i>	Kanuti NWR, Alaska, USA			0.34			(62)
Northern pike	<i>Esox Lucius</i>	Kanuti NWR, Alaska, USA			0.37			(62)
Northern pike	<i>Thymallus arcticus</i>	Yukon River, Alaska, USA			0.37			(62)
Arctic grayling	<i>Thymallus arcticus</i>	Kuskokwim River, Alaska, USA			0.26			(59)
Arctic grayling	<i>Thymallus arcticus</i>	Kuskokwim River, Alaska, USA			0.08			(59)
Arctic grayling	<i>Thymallus arcticus</i>	Kuskokwim River, Alaska, USA			0.1			(60)
Arctic grayling	<i>Thymallus arcticus</i>	Southwestern Alaska, USA			0.19			(65)

Common Name	Scientific Name	Location	[Hg] in mg/kg					Source
			Total Organism	Liver	Muscle	Keratin	Blood	
Arctic grayling	<i>Thymallus arcticus</i>	Innoko NWR, Alaska, USA			0.13			(120)
Arctic grayling	<i>Thymallus arcticus</i>	Innoko NWR, Alaska, USA			0.15			(61)
Arctic grayling	<i>Thymallus arcticus</i>	Selawik NWR, Alaska, USA			0.16			(61)
Arctic grayling	<i>Thymallus arcticus</i>	Selawik NWR, Alaska, USA			0.33			(63)
Arctic grayling	<i>Thymallus arcticus</i>	Nowitna NWR, Alaska, USA			0.11			(63)
Arctic grayling	<i>Thymallus arcticus</i>	Kanuti NWR, Alaska, USA			0.03			(64)
Arctic grayling	<i>Thymallus arcticus</i>	Kanuti NWR, Alaska, USA			0.21			(62)
Arctic grayling	<i>Thymallus arcticus</i>	Kanuti NWR, Alaska, USA			0.13			(62)
Arctic grayling	<i>Thymallus arcticus</i>	Kanuti NWR, Alaska, USA			0.33			(62)
Arctic grayling	<i>Oncorhynchus kisutch</i>	Innoko NWR, Alaska, USA			0.14			(62)
Coho salmon	<i>Oncorhynchus kisutch</i>	Kuskokwim River, Alaska, USA	0.04					(61)
Coho salmon	<i>Oncorhynchus tshawytscha</i>	Innoko NWR, Alaska, USA	0.07					(120)
Chinook salmon	<i>Salvelinus malma</i>	Prince William Sound, Ak USA	0.04					(61)
Dolly varden	<i>Salvelinus malma</i>	Kuskokwim River, Ak, USA			0.16			(57)
Dolly varden	<i>Salvelinus malma</i>	Kuskokwim River, Ak, USA			0.025			{Gray, 1996 #688}
Dolly varden	<i>Salvelinus malma</i>	Innoko NWR, Alaska, USA			0.01			(59)
Dolly varden	<i>Stenodus leucichthys</i>	Kuskokwim River, Ak, USA			0.04			(62)
Inconnu (sheefish)	<i>Stenodus leucichthys</i>	Innoko NWR, Alaska, USA			0.016			(60)
Inconnu (sheefish)	<i>Stenodus leucichthys</i>	Nowitna NWR, Alaska, USA			0.7			(62)
Inconnu (sheefish)	<i>Coregonus sardinela</i>	Seward Peninsula, Alaska, USA			0.15			(64)
Least cisco	<i>Coregonus sardinela</i>	Kanuti NWR, Alaska, USA			0.02			(59)
Least cisco	<i>Coregonus pidschian</i>	Kanuti NWR, Alaska, USA			0.09			(62)
Humpback whitefish	<i>Coregonus spp.</i>	Kuskokwim River, Ak, USA			0.04			(62)
Whitefish	<i>Coregonus spp.</i>	Lower Kuskokwim River, Ak, USA			0.03			(59)
Whitefish	<i>Lota lota</i>	Yukon River Basin, Ak, USA			0.16			(60)
Burbot	<i>Lota lota</i>	Bethel, Ak USA	0.26					(58)
Burbot	<i>Catostomus catostomus</i>	Yukon River Basin, Ak, USA			0.1			(60)
Longnose sucker	<i>Catostomus catostomus</i>	Kanuti NWR, Alaska, USA			0.19			(58)
Longnose sucker	<i>Catostomus catostomus</i>	Kanuti NWR, Alaska, USA			0.11			(62)
Longnose sucker	<i>Cottus cognatus</i>	Innoko NWR, Alaska, USA			0.16			(62)
Slimy sculpin	<i>Cottus cognatus</i>	Kanuti NWR, Alaska, USA	0.07					(61)

Common Name	Scientific Name	Location	[Hg] in mg/kg					Source
			Total Organism	Liver	Muscle	Keratin	Blood	
Slimy sculpin	<i>Cottus cognatus</i>	Kanuti NWR, Alaska, USA	0.07					(62)
Slimy sculpin	<i>Cottus aleuticus</i>	Prince William Sound, Alaska, USA	0.27					(62)
Coastrange sculpin	<i>Cottidae spp.</i>	Kuskokwim River, Alaska, USA			0.16			(59)
Sculpin	<i>Gastrosteus aculeatus</i>	Prince William Sound, Alaska, USA	0.05					(120)
Three-spine stickleback	<i>Dallia pectoralis</i>	Innoko NWR, Alaska, USA			0.14			(59)
Alaska blackfish	<i>Coueseius plumbeus</i>	Kanuti NWR, Alaska, USA	0.05					(62)
Lake chub	<i>Brachyplatystoma filamentosum</i>	Amazon, Brazil	0.08					(62)
Piraiba Catfish	<i>Brachyplatystoma platynemum</i>	Amazon, Brazil			1.97			(67)
Bandeira Catfish	<i>Brachyplatystoma rousseauxii</i>	Amazon, Brazil			2.11			(67)
Gilded Catfish	<i>Brachyplatystoma vaillantii</i>	Amazon, Brazil			0.98			(67)
Laulao Catfish	<i>Phractocephalus hemiliopterus</i>	Amazon, Brazil			0.64			(67)
Redtail Catfish	<i>Pseudoplatystoma punctifer</i>	Amazon, Brazil			0.35			(67)
Spotted tiger shovelnose catfish	<i>Pseudoplatystoma tigrinum</i>	Amazon, Brazil			0.52			(67)
Tiger sorubim	<i>Zungaro</i>	Amazon, Brazil			0.48			(67)
Gilded Catfish	<i>Perca fluviatilis</i>	Slovakia			0.73			(67)
European perch	<i>Somniosus microcephalus</i>	Greenland			1.05			(68)
Greenland shark	<i>Epinephelus itajara</i>	USA			4.1			(69)
Atlantic Goliath Grouper	<i>Pomatomus saltatrix</i>	USA			0.63			(70)
Bluefish	<i>Mugil cephalus</i>	India			0.32			(71)
Flathead grey mullet	<i>Dicentrarchus labrax</i>	Portugal			0.27			(72)
European seabass	<i>Liza aurata</i>	Portugal			96.2			(73)
Golden grey mullet	<i>Sarotherodon melanotheron</i>	Ivory Coast			93.2			(73, 74)
Blackchin tilapia	<i>Mustelus mustelus</i>	Italy			0.17			(74)
Common smooth-hound	<i>Trichiurus lepturus</i>	Brazil			1.77			(75)
Large head hair tail	<i>Carcharhinus limbatus</i>	NG			0.05			(76)
Blacktip shark	<i>Rhizoprionodon terraenovae</i>	NG			3.33			(77)
Atlantic sharp-nosed shark	<i>Roccus saxatilis</i>	Lake Mead, USA			0.76			(77)
Striped bass					0.31			(78)

Common Name	Scientific Name	Location	[Hg] in mg/kg					Source
			Total Organism	Liver	Muscle	Keratin	Blood	
<i>Large Predators</i>								
Beluga Whale (males)	<i>Delphinapterus leucas</i>	Cook Inlet, Alaska, USA		6.14				(79)
Beluga Whale (males)	<i>Delphinapterus leucas</i>	Chucki Sea, Alaska, USA		16.3				(79)
Beluga Whale (females)	<i>Delphinapterus leucas</i>	Cook Inlet, Alaska, USA		4.21				(79)
Beluga Whale (females)	<i>Delphinapterus leucas</i>	Chucki Sea, Alaska, USA		6.07				(79)
Beluga Whale	<i>Delphinapterus leucas</i>	Alaskan Arctic, USA		11.99	1.1	0.51		(80)
Bowhead Whale	<i>Balaena mysticetus</i>	Alaskan Arctic, USA		0.04	0.02	0.01		(80)
Gray Whale	<i>Eschrichtius robustus</i>	Alaskan Arctic, USA		0.02	0.02	0.01		(80)
Black Sea Harbour Porpoise	<i>Phocena phocena relicta</i>	Black Sea, Europe		1.8	0.24			(81)
Black Sea Harbour Porpoise	<i>Phocena phocena relicta</i>	Black Sea, Europe		1.4	0.22			(81)
Black Sea Harbour Porpoise	<i>Phocena phocena relicta</i>	Black Sea, Europe		2.1	0.62			(81)
Black Sea Harbour Porpoise	<i>Phocena phocena relicta</i>	Black Sea, Europe		6.0	0.34			(81)
Black Sea Harbour Porpoise	<i>Phocena phocena relicta</i>	Black Sea, Europe		8.7	0.72			(81)
Black Sea Harbour Porpoise	<i>Phocena phocena relicta</i>	Black Sea, Europe		5.6	0.53			(81)
Black Sea Harbour Porpoise	<i>Phocena phocena relicta</i>	Black Sea, Europe		3.1	0.33			(81)
Black Sea Harbour Porpoise	<i>Phocena phocena relicta</i>	Black Sea, Europe		4.7	0.62			(81)
Ringed Seal	<i>Phoca hispida</i>	Somerset Island, Canada		19.3	0.44			(82)
Ringed Seal	<i>Phoca hispida</i>	Barrow Straight, Canada		16.1	0.91			(82)
Ringed Seal	<i>Phoca hispida</i>	Baffin Island, Canada		0.32	0.08			(82)
Ringed Seal	<i>Phoca hispida</i>	Baffin Island, Canada		3.76	0.31			(82)
Ringed Seal	<i>Phoca hispida</i>	Beaufort Sea, Canada		1	0.23			(82)
Ringed Seal	<i>Phoca hispida</i>	Victoria Island, Canada		27.5	0.72			(82)
Bearded Seal	<i>Erignathus barbatus</i>	Victoria Island, Canada		143	0.53			(82)
Bearded Seal	<i>Erignathus barbatus</i>	Hudson Bay, Canada		26.2	0.09			(82)
Bearded Seal	<i>Erignathus barbatus</i>	Barrow Straight, Canada		79.2	0.2			(82)
Diamondback Terrapin	<i>Malaclemys terrapin</i>	Ashley River, South Carolina, USA				0.34		(83)
Diamondback Terrapin	<i>Malaclemys terrapin</i>	Purvis Creek, South Carolina, USA				3.9		(82)
Diamondback Terrapin	<i>Malaclemys terrapin</i>	Tuckerton, New Jersey, USA		1.1	0.17			(84)
Blue Shark	<i>Prionace glauca</i>	Azores, Portugal	0.96	1.3				(85)
Blue Shark	<i>Prionace glauca</i>	Equatorial Atlantic Ocean	2.2	2.5				(85)
Brazilian Sharp-nosed Shark	<i>Rhizoprionodon lalandei</i>	Southeast Brazilian Coast		0.017				(86)

Common Name	Scientific Name	Location	[Hg] in mg/kg					Source
			Total Organism	Liver	Muscle	Keratin	Blood	
Small eye smooth-hound	<i>Mustelus higmani</i>	Southeast Brazilian Coast		0.009				(86)
Caribbean sharp-nosed shark	<i>Rhizoprionodon porosus</i>	Southeast Brazilian Coast		0.013				(86)
Small nose fanskate	<i>Sympterygia bonapartei</i>	Bahia Blanca, Argentina		0.18				(87)
Southern Eagle Ray	<i>Myliobatis goodei</i>	Bahia Blanca, Argentina		0.43				(87)
Argentine angel shark	<i>Squalina argentina</i>	Bahia Blanca, Argentina		0.48				(87)
Narrow nose smooth-hound	<i>Mustelus schmitti</i>	Bahia Blanca, Argentina		0.89				(88)
Catshark	<i>Halaeulurus bivius</i>	Bahia Blanca, Argentina		2				(88)
Broad nose seven gill shark	<i>Notorhynchus spp.</i>	Bahia Blanca, Argentina		2.51				(88)
Narrow nose smooth-hound	<i>Mustelus schmitti</i>	Buenos Aires, Argentina		0.45				(89)
School shark	<i>Galeorhinus viamenicus</i>	Buenos Aires, Argentina		0.34				(89)
Small nose fanskate	<i>Sympterygia bonapartei</i>	Bahia Blanca estuary, Argentina		0.1				(87)
Argentine angel shark	<i>Squalina argentina</i>	Bahia Blanca estuary, Argentina		0.41				(87)
Swordfish	<i>Xiphias gladius</i>	Azores, Portugal	8.5	2.4				(85)
Swordfish	<i>Xiphias gladius</i>	Equatorial Atlantic Ocean	9.8	2.2				(85)
American alligator	<i>Alligator mississippiensis</i>	Lake Apopka, Florida, USA			0.11			(90)
American alligator	<i>Alligator mississippiensis</i>	Lake Apopka, Florida, USA		0.11	0.057			(91)
American alligator	<i>Alligator mississippiensis</i>	Lake Apopka, Florida, USA		1.76				(121)
American alligator	<i>Alligator mississippiensis</i>	Lake George, Florida, USA			0.04			(90)
American alligator	<i>Alligator mississippiensis</i>	Lake Hancock, Florida, USA			0.1			(90)
American alligator	<i>Alligator mississippiensis</i>	Lake Iamonia, Florida, USA			0.61			(90)
American alligator	<i>Alligator mississippiensis</i>	Lake Kissimmee, Florida, USA					0.417	(93)
American alligator	<i>Alligator mississippiensis</i>	Lake Lochloosa, Florida, USA					0.148	(93)
American alligator	<i>Alligator mississippiensis</i>	Lake Newnans, Florida, USA			0.27			(90)
American alligator	<i>Alligator mississippiensis</i>	Lake Orange, Florida, USA			0.37			(90)
American alligator	<i>Alligator mississippiensis</i>	Lake Rodman, Florida, USA			0.51			(90)
American alligator	<i>Alligator mississippiensis</i>	Lake Trafford, Florida, USA					0.198	(93)
American alligator	<i>Alligator mississippiensis</i>	Lake Trafford, Florida, USA			0.43			(90)
American alligator	<i>Alligator mississippiensis</i>	Lake Woodruff, Florida, USA		7.77				(121)
American alligator	<i>Alligator mississippiensis</i>	Merritt Island NWR, Florida, USA		12.1				(121)

Common Name	Scientific Name	Location	[Hg] in mg/kg					Source
			Total Organism	Liver	Muscle	Keratin	Blood	
American alligator	<i>Alligator mississippiensis</i>	Merritt Island NWR, Florida, USA					0.152	(122)
American alligator	<i>Alligator mississippiensis</i>	Non-Everglades, Florida, USA		2.52	0.33	0.34		{Heaton-Jones, 1997 #277}
American alligator	<i>Alligator mississippiensis</i>	St Johns River, Florida, USA					0.177	(93)
American alligator	<i>Alligator mississippiensis</i>	Everglades (WCA3A), Florida, USA					1.33	(93)
American alligator	<i>Alligator mississippiensis</i>	Everglades (Big Cypress), Florida, USA		3.9	0.4			(95)
American alligator	<i>Alligator mississippiensis</i>	Everglades (National Park), Florida, USA		10.4	1.2			(95)
American alligator	<i>Alligator mississippiensis</i>	Everglades (WCA1), Florida, USA		1.7	0.3			(95)
American alligator	<i>Alligator mississippiensis</i>	Everglades (WCA2A), Florida, USA					1.56	(93)
American alligator	<i>Alligator mississippiensis</i>	Everglades (WCA2A), Florida, USA		4.5	0.75			(95)
American alligator	<i>Alligator mississippiensis</i>	Everglades (WCA3A north), Florida, USA		3.9	0.5			(95)
American alligator	<i>Alligator mississippiensis</i>	Everglades (WCA3A south), Florida, USA		2.3	0.5			(95)
American alligator	<i>Alligator mississippiensis</i>	Everglades (WCA3A), Florida, USA		10.37	1.22	2.23		(96)*
American alligator	<i>Alligator mississippiensis</i>	Everglades, (Holiday Park) Florida, USA		9.97	1.11	1.93		(96)*
American alligator	<i>Alligator mississippiensis</i>	Everglades, (WCA2A & 3A) Florida, USA		39.99	2.61	1.03		(94)
American alligator	<i>Alligator mississippiensis</i>	Par Pond, South Carolina		5.51	1.18	2.37		(96)*

NWR-National Wildlife Refuge

Table 1.2. The effects of mercury on wildlife, including laboratory studies.

Common Name	Scientific Name	Effect	Dosed (Y/N)	[Dose]	Hg Species	Source
<u>[Hg] Outcomes</u>						
Shore crab	<i>Carcinus maenas</i>	Lower [Hg] than Dosed groups (39.7 mg/kg total organism; 78.9 mg/kg in muscle)	N			(103)
Shore crab	<i>Carcinus maenas</i>	Higher [Hg] because of greater [Hg] in water (60 mg/kg total organism; 70 mg/kg in muscle)	Y- 3 days	1 µg/L	CH ₃ Hg	(103)
Shore crab	<i>Carcinus maenas</i>	Higher [Hg] because of greater [Hg] in water (120 mg/kg total organism; 175 mg/kg in muscle)	Y-15 days	2 µg/L	CH ₃ Hg	(103)
<u>Brain Outcomes</u>						
Tilapia	<i>Oreochromis mosambicus</i>	Decreased stimulatory neurotransmitter (5-HT)	Y	0.015 mg/kg	HgCl ₂	(108)
Tilapia	<i>Oreochromis mosambicus</i>	Decreased stimulatory neurotransmitter (5-HT)	Y	0.03 mg/kg	HgCl ₃	(108)
Catfish	<i>Clarias batrachus</i>	Decreased stimulatory neurotransmitter (5-HT)	Y	0.05 mg/L	HgCl ₂	(109)
Catfish	<i>Clarias batrachus</i>	Decreased stimulatory neurotransmitter (5-HT)	Y	0.04 mg/L	CH ₃ HgCl	(109)
Catfish	<i>Clarias batrachus</i>	Increased inhibitory neurotransmitter (DA)	Y	0.05 mg/L	HgCl ₂	(109)
Catfish	<i>Clarias batrachus</i>	Increased inhibitory neurotransmitter (DA)	Y	0.04 mg/L	CH ₃ HgCl	(109)
Catfish	<i>Clarias batrachus</i>	Decreased degradation enzyme (MAO)	Y	0.05 mg/L	HgCl ₂	(109)
Catfish	<i>Clarias batrachus</i>	Decreased degradation enzyme (MAO)	Y	0.04 mg/L	CH ₃ HgCl	(109)
Mummichogs	<i>Fundulus heteroclitus</i>	Elevated degradation enzyme compared to Dosed groups	Y	10 ng/g	CH ₃ Hg	(110)
<u>Reproductive Outcomes</u>						
Guppy	<i>Poecilia reticulata</i>	Impaired spermatogenesis	Y	1.8 µg/L	CH ₃ Hg	(111)
Catfish	<i>Clarias batrachus</i>	decreased testicular phospholipids	Y - 45 days	0.05 mg/L	HgCl ₂	(112)
Catfish	<i>Clarias batrachus</i>	decreased testicular phospholipids	Y - 45 days	0.04 mg/L	CH ₃ HgCl	(112)
Catfish	<i>Clarias batrachus</i>	decreased gonadosomatic index, testicular lipids, phospholipids and cholesterol	Y - 90 days	0.05 mg/L	HgCl ₂	(112)
Catfish	<i>Clarias batrachus</i>	decreased gonadosomatic index, testicular lipids, phospholipids and cholesterol	Y - 90 days	0.04 mg/L	CH ₃ HgCl	(112)
Catfish	<i>Clarias batrachus</i>	decreased gonadosomatic index, testicular lipids, phospholipids and cholesterol	Y - 180 days	0.05 mg/L	HgCl ₂	(112)
Catfish	<i>Clarias batrachus</i>	decreased gonadosomatic index, testicular lipids, phospholipids and cholesterol	Y - 180 days	0.04 mg/L	CH ₃ HgCl	(112)
Spotted Snakehead	<i>Channa punctatus</i>	decreased gonadosomatic index and late stage oocytes	Y - 7-91 days	16 mg/kg	HgCl ₂	(123)
White Ibis	<i>Eudocimus albus</i>	altered pairing behavior, decreased egg productivity, decrease in fledglings	Y	0.05 mg/kg	CH ₃ Hg	(113)
White Ibis	<i>Eudocimus albus</i>	altered pairing behavior, decreased egg productivity, decrease in fledglings	Y	0.1 mg/kg	CH ₃ Hg	(113)
White Ibis	<i>Eudocimus albus</i>	altered pairing behavior, decreased egg productivity, decrease in fledglings	Y	0.3 mg/kg	CH ₃ Hg	(113)

Common Name	Scientific Name	Effect	Dosed (Y/N)	[Dose]	Hg Species	Source
White Ibis	<i>Eudocimus albus</i>	Increased testosterone and decreased nesting effort with increased Hg	N	Environmental		(114)
White Ibis	<i>Eudocimus albus</i>	Increased estradiol during the display stage of breeding in males	Y	0.05 mg/kg	CH ₃ Hg	(105)
White Ibis	<i>Eudocimus albus</i>	decreased estradiol during the laying and incubation stages of breeding in males	Y	0.3 mg/kg	CH ₃ Hg	(105)
White Ibis	<i>Eudocimus albus</i>	Estradiol increased in homosexual males during the display stage of breeding	Y	0.3 mg/kg	CH ₃ Hg	(105)
White Ibis	<i>Eudocimus albus</i>	Estradiol increased in homosexual males during the display stage of breeding	Y	0.1 mg/kg	CH ₃ Hg	(105)
White Ibis	<i>Eudocimus albus</i>	Estradiol decreased in homosexual males during the nest building stage of breeding	Y	0.1 mg/kg	CH ₃ Hg	(105)
White Ibis	<i>Eudocimus albus</i>	Estradiol decreased in homosexual males during the incubation stage of breeding	Y	0.05 mg/kg	CH ₃ Hg	(105)
Rhesus monkey	<i>Macaca mulatta</i>	Abortions, maternal toxicity	Y	0.5 mg/kg	CH ₃ Hg	(115)
Pig	<i>Sus spp.</i>	Stillbirths	Y	0.5 mg/kg	CH ₃ Hg	(115)
<u>Epigenetic Outcomes</u>						
Polar bear	<i>Ursus maritimus</i>	DNA methylation loss	N	Environmental		(99)
Mink	<i>Neovison vison</i>	DNA methylation loss, decreased DNMT1 activity	Y	1.0 mg/kg	CH ₃ Hg	(101)
Chicken	<i>Gallus gallus</i>	DNA methylation loss, increased DNMT1 activity	Y	6.4 µg/g	CH ₃ Hg	(101)
<u>Other Cellular Outcomes</u>						
Tusk	<i>Brosme brosme</i>	GSH Pathway- Changes in oxidative stress markers (FTH1 and GPX1)	N	Environmental		(106)
Zebrafish	<i>Danio rerio</i>	increase in DNA Damage signaling and HIF pathways, Electron transport chain, cell motility	Y	0.2 mg/L	HgCl ₂	(107)

1.7. Human exposure to mercury

The detrimental effects of CH₃Hg exposure in both wildlife and humans include complications in reproduction in water birds, embryonic development in minnows, as well as an increased risk of adult-onset diseases in humans (Tables 1.2 and 1.3) (105, 113, 116, 124-157). People all over the world are exposed to and accumulate CH₃Hg, and humans are suspected to be more susceptible to the effects of mercury at lower concentrations than wildlife (152, 158-160). Dietary consumption of seafood is the dominant route of CH₃Hg exposure for humans; however, low concentrations of mercury have been found in domesticated livestock, making it an additional source of exposure (117, 161-163).

A simple way to identify and compare human populations that are at the greatest risk for mercury exposure is examining the mercury content in hair samples (160). Populations living above latitude 22° N have significantly higher mercury concentrations than those living in regions farther south. This is speculated to be due to a combination of both a largely piscivorous diet and exposure to volatilized mercury from industrialized anthropogenic sources (Table 1.3) (160). The EPA has set a critical value for human consumption of 0.3 mg/kg of mercury, and the FDA level of limited consumption is 1.0 mg/kg of mercury.

In alligators and marine mammals, mercury concentrations have been found to be well above the EPA critical value for human consumption of 0.3 mg/kg and, in many cases, above the FDA action level of 1.0 mg/kg (Tables 1.1 & 1.3) (2, 57). Most members of modernized populations are not likely to encounter such animals as part of their diet except during occasional recreational hunting activities. However, Native Americans as

well as many other populations of native people across the globe participate in the seasonal subsistence hunts of larger predators and are therefore likely to be exposed to hazardous concentrations of mercury from animals that are not part of a normal modernized diet (2, 164, 165). The cultures that participate in marine mammal hunts are particularly susceptible to high mercury concentrations (up to 16.0 mg/kg) that persist throughout their lifetimes (Table 3.1) (57, 79-82, 147, 148, 164).

These ingested high concentrations elicit negative health effects, with the most well-known example being the disaster at Minamata Bay, Japan, where CH₃Hg was released into the bay with industrial wastewater from 1932 to 1968 and CH₃Hg accumulated in seafood. Ill effects of the CH₃Hg laden seafood was seen in the form of neurodegeneration, motor dysfunction, and heart disease throughout the population (7, 8, 149, 150, 166). A similar inadvertent industrial poisoning took place in Iraq in 1971, with similar neurological degeneration seen in the population (167). While both incidents are useful in describing the effects of human exposure to mercury at very high chronic levels, most of the world's population is subject to much lower levels through their diet.

Both adults and children were shown to have multiple organ systems affected by low mercury concentration, including the nervous, motor, renal, cardiovascular, immune, and reproductive systems (150-152, 168, 169). Mercury has been correlated to some specific heart diseases, including coronary heart disease, but no mechanism of action has been identified (153, 154). One study that has received wide acclaim is a birth cohort study of the Faroe Island population, using prenatal mercury concentrations and developmental heart outcomes at 7 years of age; a relationship was found between higher mercury concentrations and cardiovascular risk factors (132). Similar relationships were

found for children of other native populations (155). Native and coastal populations also have greater mercury concentrations in their blood (0.04 mg/kg compared to 0.001 mg/kg), hair (0.01 mg/kg compared to 0.00025 mg/kg), umbilical cord blood of pregnant mothers (0.068 mg/kg compared to 0.0017 mg/kg) than non-coastal populations (156).

Table 1.3. Mercury measurements in human populations.

Age Group	Location	[Hg] in mg/kg				Effect	Source
		Blood	Hair	Urine	Cord Blood		
Children	Greenland (NW)		2-5 µg/g				(126)
Children	Denmark	<1 µg/L					(127)
Children	Poland	<1 µg/L					(127)
Children	Slovakia	<1 µg/L					(127)
Children	Czechia	<1 µg/L					(127)
Children	Slovenia	<1 µg/L					(127)
Children	Morocco	<1 µg/L					(127)
Children	Germany	<1 µg/L					(128)
Children	Belgium		<0.25 µg/g				(129)
Children	Italy	<1 µg/L					(130)
Children	Faroe Islands				12-40 µg/L	deficits in motor, attention and verbal tests	(131)
Children	Greenland				28-777 µg/L	neurobehavioral deficits	(126)
Children	Faroe Islands				10 µg/L	decreased heart rate variability; increased blood pressure	(132)
Children	Germany			0.5-1.0 µg/g			(133)
Children	Germany			1-2 µg/g			(133)
Children	Poland			<0.2 µg/g			(133)
Children	Czechia			<0.2 µg/g			(133)
Children	Czechia			0.2-0.5 µg/g			(133)
Children	Czechia			<0.2 µg/g			(133)
Children	Poland			<0.2 µg/g			(134)
General	Germany	<1 µg/L					(135)
General	Denmark	2-4 µg/g					(157)
General	Norway	4-8 µg/l					(136)
General	Greenland (SW)	8-20 µg/L					(157)
General	Poland		<0.25 µg/g				(137)
General	Belgium		0.25-.5				(129)
General	France		0.5-1 µg/g				(138)
General	Italy		0.5-1 µg/g				(139)
General	Finland		1-2 µg/g			carotid atherosclerotic progression	(140)
General	Greenland (NW)		>10 µg/g				(126)
General	Norway			1-2 µg/g			(136)
General	Poland			<0.2 µg/g			(133)
General	Poland			0.2-0.5 µg/g			(134)
Pregnant	Sweden		.25-.5 µg/g				(141)
Pregnant	France		0.5-1 µg/g				(142)
Pregnant	France		0.5-1 µg/g				(143)
Pregnant	Greenland		15 µg/g			neurobehavioral deficits in their children	(126)
Pregnant	Sweden				<1.7 µg/L		(144)
Post mortem adults	Scandinavia	2.2					(145)
Occupational Exposure (1-20 years)	United States	epidemiological exposure				Parkinson Disease in 2-3% of the population	(146)
Occupational Exposure (20+ years)	United States	epidemiological exposure				Parkinson Disease in 1% of the population	(146)
Subsistence Villagers	Amazon, Brazil		17.4 µg/g				(147)
Subsistence Villagers (Men)	Canadian Arctic	22.7					(148)

Age Group	Location	[Hg] in mg/kg				Effect	Source
		Blood	Hair	Urine	Cord Blood		
Subsistence Villagers (Women)	Canadian Arctic	21.3					(148)
Minamata Bay Population	Japan	epidemiological exposure				Atherosclerotic heart disease	(149)
Shiranui Sea Populations	Japan		2.6			Hypertension	(150)
Shiranui Sea Populations	Japan		12			Hypertension	(150)
Shiranui Sea Populations	Japan		20			Hypertension	(150)
Shiranui Sea Populations	Japan		77			Hypertension	(150)
Tapajos River Populations	Amazon, Brazil		17.8			Increased blood pressure	(151)
Siwaha-Banwol Community	Korea		1.02			Lowered heart rate variability	(168)
Various Populations	Many	low dose epidemiological exposure				Affected motor activity, genome, cardiovascular system and reproduction.	(152, 153)
Finnish Population	Finland		1.9			higher risk of myocardial infarction	(154)
Finnish Population	Finland		1.8			accelerated progression of atherosclerosis	(154)
Finnish Population	Finland		1.9			Cardiovascular effects attenuate the benefits of fish oil	(154)
Finnish Population	Finland		1.9			Increased risk of myocardial infarction, heart disease	(154)
Inuit Children	Nunavik	2.91 nmol/L				Affected heart rate variability	(155)

Age groups were based on those reported in Višnjevec, *et al.* (156)
µg/g unless otherwise noted

1.8. Sentinel/indicators

Physiological effects of mercury exposure are easier to demonstrate in animal species than in humans, since they are also subject to chronic lifetime exposures in their natural environment, but can be replicated in the laboratory. Different animals are indicators of different exposures (83, 101, 170). Small fish can indicate how much mercury is methylated in the environment, and then enters the food web compared to how much mercury is atmospherically deposited. Larger fish can elucidate the intensity of bio-magnification within the specific food web (2). A good model for human exposure are long-lived animals that accumulate high concentrations of mercury in their natural environment (99, 171). Some long-lived free-ranging animals have lifespans comparable to humans and forage at a similar trophic level throughout their lives (171). Apex predators can provide a mechanism to study chronic CH₃Hg exposure at higher accumulation levels than in other species. Several predators have been used to model mercury exposure in human populations, including the polar bear, largemouth bass, tuna, water birds, the diamondback terrapin, and the American alligator (2, 54, 83, 92, 99, 172, 173).

In the Everglades ecosystem, the American alligator is frequently studied as a sentinel species for human dietary exposure to mercury (as the mammalian apex predator, the Florida panther is critically endangered and is subject to strict capture and release laws, in addition to being difficult to find in the wild). There are a variety of reasons the American alligator can be used as a sentinel of ecosystem health, and human exposure to mercury. The American alligator is a long-lived opportunistic predator with a varied aquatic diet, exhibits high site fidelity, has a synchronous reproductive season yielding a

large number of eggs from each nesting female, a stable population, and has the ability to live in close proximity to human populations (i.e. golf courses and recreational parks)(94, 170, 174-177). These characteristics, as well as their classification as “charismatic megafauna, which elicits an exaggerated human response that aids in monitoring, makes the American alligator an excellent proxy for anthropogenic contaminants exposure in coastal ecosystems (178, 179).

The American alligator has been used as a sentinel species for a variety of environmental contaminants, including organic contaminants, pesticides, perfluoroalkyl acids, and hormone profile shifts (90, 170, 175, 180-185). However, there are still several questions to address before the alligator can be used as a model for environmental mercury exposure, which are 1- understand the tissue distribution of mercury; 2- determine if seasonal behaviors and changing body condition alter mercury concentrations; 3-examine the amount of mercury that is transferred to offspring; and 4- determine their utility as a laboratory model.

Many studies focus on the mercury concentration within a single tissue and frequently this same tissue is not routinely used (Table 1.3) (90-92, 94-96, 186-188). To better understand mercury exposure in alligators, the ability to conduct comparisons across previously published data is needed. Understanding the bio-distribution of mercury within all commonly sampled tissues, including whole blood, (which has become the standard for environmental monitoring) would provide tissue accumulation data, thus allowing a more comprehensive analysis of both mercury in the environment and areas that are safe for recreational hunting of alligators (91). It is also important to determine if seasonal behaviors, such as brumation and nesting affect mercury

concentrations in a way that could prevent accurate sampling. As many species are known to off-load large contaminant burdens to their offspring, season as well as changing body condition could play a large role in the mercury concentration measured in wild alligators. Similarly, determining whether mercury is off loaded to offspring like organic contaminants would provide valuable information regarding what mercury concentrations embryonic alligators are exposed to, and if adult females have a similar offloading mechanism observed in other species (189-191). The ability to bring wild caught animals into the lab for close examination cannot be overlooked, as this provides information that cannot be gained from observations in the environment. While adult alligators are not suited for laboratory captivity, their eggs could provide a developmental model for environmental exposures.

All of these questions also provide important human health information, as alligators are recreationally hunted, and consumed by humans within their geographic range. In Florida alone, nearly 8,000 alligators are recreationally hunted each year, and the annual totals continue to rise (192). At least 100 of these alligators come from the Everglades region, and while there are advisories in place due to the high mercury concentrations in the area, there is no way to enforce the regulations to keep people from consuming those alligators.

Since the American alligator has a limited range, it provides a good sentinel for the southeastern Atlantic and Gulf coasts of the United States, but is not suitable as a sentinel for colder habitats along the coast. The diamondback terrapin (*Malaclemys terrapin*) is a mid-level predator with a wider range around both, the Atlantic and Gulf coasts (193). The terrapin has been previously evaluated and identified as a sentinel

species for mercury exposure (83, 84). While this species is a mid-level predator, and provides different level of mercury exposure than an upper-level predator, the terrapin has many of the attractive characteristics that make the alligator a desirable sentinel. The terrapin has a wide geographic range, exhibits high site fidelity, has a synchronous breeding season, but lays less eggs, and eats many of the same food sources as humans, such as crustaceans and fish. The terrapin can provide valuable information regarding the changes predators experience as mercury concentrations increase, and alligators can provide information about the effects of high mercury exposure.

1.9. *One health paradigm*

Environmental sentinels can provide important information about chemical exposure, and ecosystem health, but they can also be used to understand human health issues. In recent years, it has become clear that environmental and human health are not separate areas of study, and influence each other greatly. Without clean water, fertile soil, and diverse food sources, public health will suffer. Anthropogenic activities that impact the environment will also impact the human populations in those areas. This concept is termed “One Health” as discussing human, wildlife and ecosystem issues in isolation doesn’t solve problems – there is *one* health. The one health concept requires collaboration between many disciplines to examine and attain optimal global health. The One Health Commission (OHC) highlights the scope of one health to include the convergence of human, animal, and environmental health, through the human-animal bond to address complex issues (194). To this end, identifying adverse effects in wildlife as a result of a health issue can lead to circumventing those effects in the human population through comprehensive risk assessment tools.

1.10. The adverse outcome pathway (AOP) framework

Advanced risk assessment tools serve to link cause and effect across species, and reduce the use of animals in scientific research (195). The concern for animal welfare combined with the need for predictive toxicology that is relevant to human health has driven the creation of a new tool: the Adverse Outcome Pathway (AOP) framework (195). Within this framework, all of the pieces of toxicological data that have been collected come together to enable predictions regarding health outcomes to be made (195). This framework details a linear cascade of events beginning from a chemical initiation event (CIE) that begins the cascade (Figure 1.4) (195). The CIE is not chemical specific, but is instead an event that takes place as the result of a group of stimulants that interact in the same way (196). The CIE will lead to a molecular initiating event (MIE) that is a measureable change in the biological state or a perturbation as a result of the interaction between the chemical and a biomolecule in the system (195). The MIE then can stimulate many key events (KE) that are independent of each other or interrelated, but connect the molecular initiating event (MIE) to a known adverse outcome (AO) (195). Since the AOP framework is gaining ground in its use for regulatory toxicology, as well as for linking exposure data across species and disciplines, we use it as a guide to link this research with the greater body of work on mercury exposure (Figure 1.4) (196).

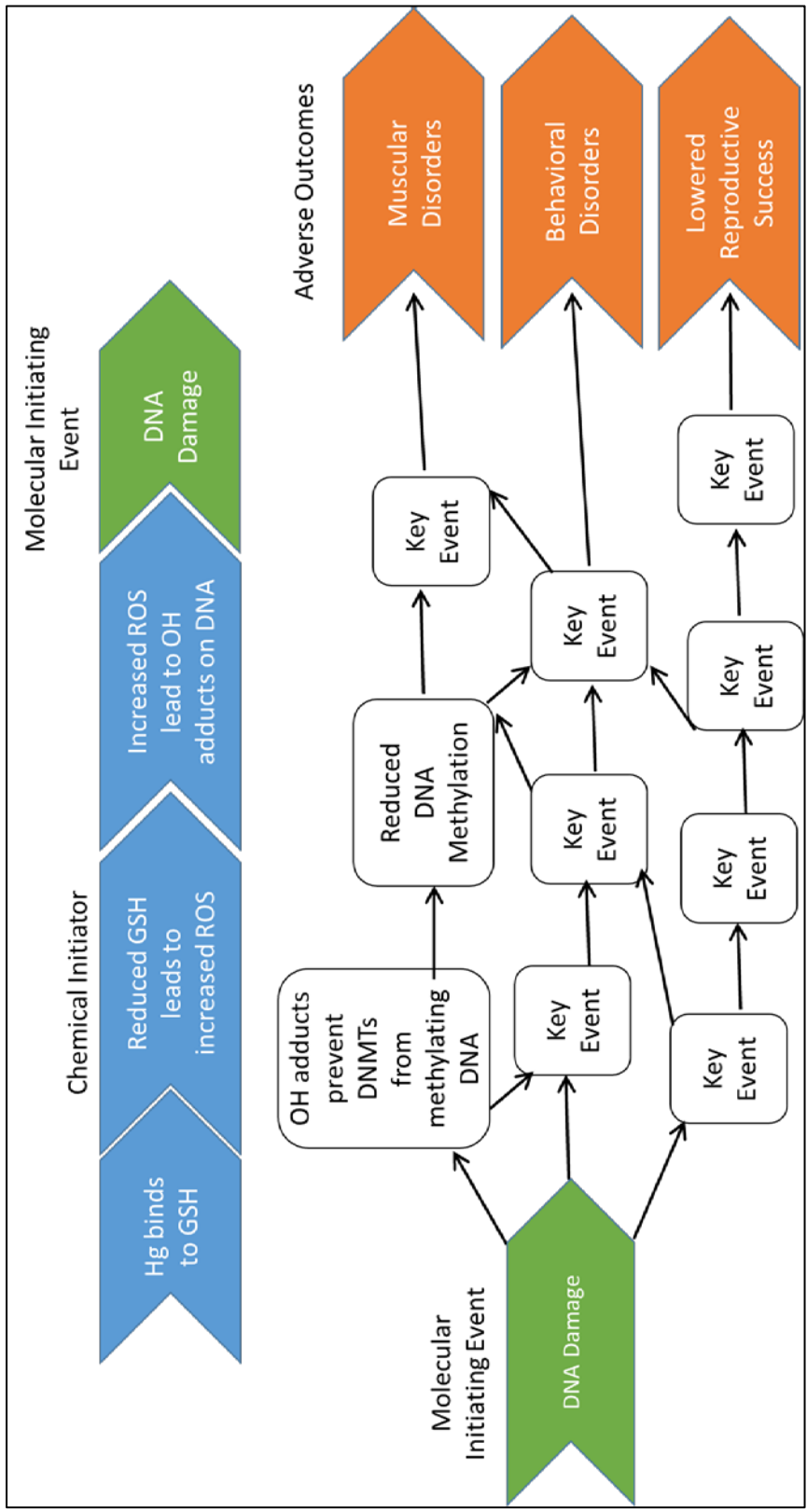


Figure 1.4. A schematic of the Adverse Outcome Framework for Hg exposure including DNA methylation loss.

1.11. Biochemical effect of mercury - molecular mechanism, methylation, & metabolomics

The CH₃Hg that is ingested by consumption of contaminated prey items is digested and absorbed into the body via the intestines (197, 198). Once the CH₃Hg is absorbed by the intestines, intracellular oxidative stress occurs by mercury disassociating with the methyl groups and binding to thiol groups (152). Mercury is a redox-inactive metal, which means that it does not undergo redox cycling like other metals (iron, copper, chromium). Instead, mercury and the other toxic heavy metals (lead, cadmium, and arsenic) deplete the cells' major antioxidant enzymes, particularly those enzymes that contain selenium and those that contain thiol (-SH) groups (199-201). To bind to either of these types of enzymes, the stable C—Hg bond must be broken, which is strong bond, but can be broken due to the strong electron sharing affinities between Hg²⁺ and thiol groups, that result in strong covalent bonds (199, 201). Selenium has been noted as having a protective effect against mercury, since there is a such a high binding affinity between the two, that it effectively removes mercury from being biologically available within the body (201). However, selenium is generally in short supply within the body and is saturated quickly by mercury (201). Thiol containing enzymes are in much greater supply, as they serve to remove reactive oxygen species (ROS) from cells as part of normal cellular function. These thiol containing enzymes also serve to detoxify mercury by binding and removing it from circulation, but depositing it in the excretion organs (199). Bioaccumulation occurs as the body cannot easily remove mercury once it reaches the excretion organs (202-204). In bacteria, detoxification facilitated by two specific

enzymes, organomercurial lyase (MerB) and mercuric ion reductase (MerA) (205). The thiol groups of these two enzymes are critically important to detoxifying the CH₃Hg to the volatile, less reactive form of mercury, Hg⁰, which can be removed from the bacterial cell (205, 206). This process in higher eukaryotes is less clear, but enzymes containing thiol groups likely play a role (206, 207). Since there are no specific enzymes to reduce CH₃Hg to Hg⁰ in higher organisms mercury accumulates (202).

In cells, approximately 90 % of the available thiol groups that are not bound to proteins derive from glutathione (GSH), an antioxidant (199). GSH is synthesized from cysteine, glycine, and serine by the enzyme glutamate-cysteine ligase. The endogenous function of GSH is to remove ROS that accumulate because of normal cellular function, mitochondrial respiration, and any toxic xenobiotic that enters the cell (Figure 1.5) (208, 209). Under normal circumstances, GSH binds to a ROS or xenobiotic, is translocated out of the cell and enters the blood plasma, only to be removed by organs that contain transpeptidase or by the kidney (210). GSH is used and recycled by glutathione S-transferase (GST) once the cell is detoxified, so there is a continual supply of the protective antioxidant (210). GSH metabolism is critical for the detoxification/toxic response of metals in cells, as one mercury molecule can bind two GSH molecules and cause irreversible binding, which removes those molecules from the GSH cycle and they cannot be reused (199). This effectively stops the detoxification process at the first step, and bound Hg—GSH, are translocated out of the cell. The detoxification enzyme, GST, which is critical to the recycling of GSH, has been shown to be inactivated by mercury in dosed animals (Figure 1.5) (211).

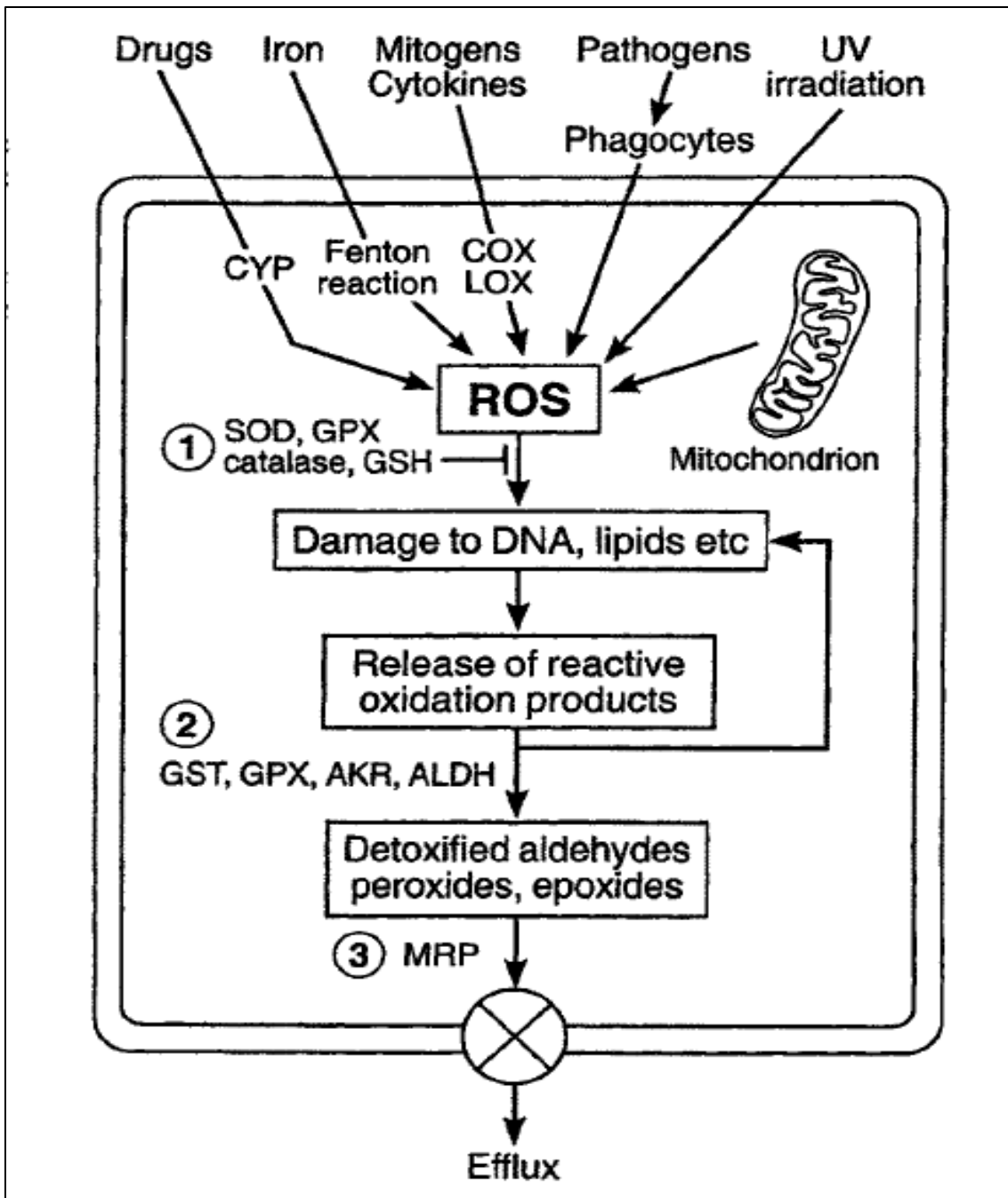


Figure 1.5. Illustration of the three steps of the glutathione (GSH) activity in response to reactive oxygen species (ROS) (209).

The action of Hg^{2+} binding to GSH within the cell initiates the chemical interaction that begins an AOP associated with mercury exposure and increased oxidative stress (Figure 1.4). The removal of GSH function from the cells by binding Hg^{2+} leads to the buildup of ROS within those cells, which can cause increased key events (KEs) such as, lipid peroxidation, protein damage, and DNA damage (Figure 1.6) (199). Both lipid peroxidation (due to disrupted activities of superoxide dismutase and xanthine oxidase), and protein damage, (nephrotic tissue loss) occur as byproducts of the oxidative stress created after Hg^{2+} utilizes all the available GSH (199, 211). Oxidative stress has different effects each organ system, and several different AOs have been identified.

Renal system. The most well understood effects take place in the renal system, as the kidney accumulates the circulating GSH-Hg compounds from the blood plasma at a greater concentration than other organs, since the body cannot easily remove mercury (97, 210, 212, 213). In kidney epithelial cells, Hg^{2+} binds thiol-containing molecules, which impairs NF- κ B activation, DNA binding and transcriptional activity. NF- κ B is a thiol dependent transcription factor, which promotes cell survival and prevents apoptosis; mercury exposure also leads to apoptosis of kidney cells (152, 214). The mechanism of action in the renal system is a direct effect of the ability of Hg^{2+} to covalently bind to thiol groups, removing them from their native function, and causing cellular disturbance. In other tissue and organ systems, the toxic mechanism of mercury exposure has not been directly elucidated. Epidemiological studies have been conducted to determine the effects of mercury on each organ system, rather than distinguish the molecular mechanism.

CNS. Many neurodegenerative disorders are characterized by bound thiol groups that lead to blocked sulfur oxidation, which is also an outcome related to mercury

exposure in this system (152). The effect of mercury on the nervous and neurological systems is believed to be related to the increased production of certain β -amyloids and α -synuclein fibril formation, which are a major component of Lewy bodies (152, 215). Lewy bodies are associated with Parkinson's disease and Lewy body dementia. They could be related to the change in motor activity that is commonly associated with mercury exposure, characterized as reduced grip strength, and increased muscular fatigue (146, 152). Neural cells seem to be the most susceptible to the effects of CH_3Hg , as it has been shown to elicit cell death and apoptosis (124).

Other systems. The effects of mercury exposure on other organ systems require further study, as many of them are epidemiology studies with no direct mechanisms elucidated. Exposures have been linked to adverse reproductive outcomes including, menstrual disorders, lowered fecundity, adverse pregnancy outcomes, less motile sperm and sub-fertility (152). The auto-immune system has also been shown to be negatively impacted by mercury exposure by increased lymphocytes responsiveness and exacerbated lupus-like auto immunity (152). In the cardiovascular system mercury has been shown to disrupt cardiovascular homeostasis in low birth weight children (132, 152). While many biological systems are targets for mercury exposure, with known AOs, the chain of KEs that link the MIE to the AO have not yet been elucidated.

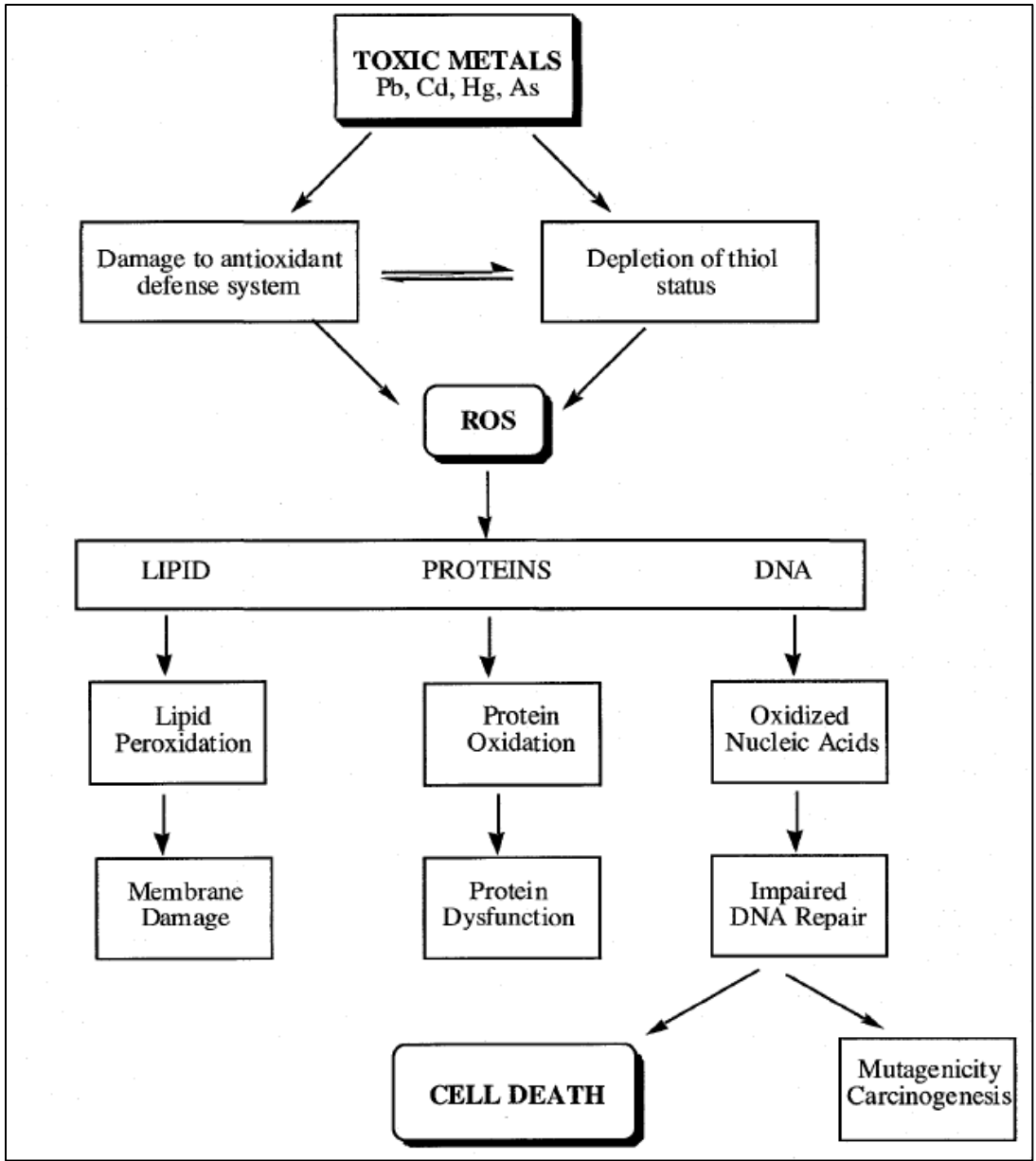


Figure 1.6. A diagram of the cellular response of glutathione (GSH) to toxic heavy metals (199).

Mercury induced DNA damage can affect DNA methylation

Apart from the KEs lipid peroxidation and protein damage, mercury-induced ROS within the cell can also result in DNA damage (Figure 1.6) (199). The damage to the DNA strand occurs by the accumulation of ROS, particularly the hydroxyl ions attach to DNA bases and form “lesions” (216). The attachment of the hydroxyl lesions can cause deletions, strand breakages, and chromosomal rearrangements, and interfere with the ability of DNA to function as a substrate for the DNA methyl transferases (DNMTs), resulting in global DNA hypo methylation (216). The hydroxyl lesions attach to guanine bases changing the shape of the DNA strand, essentially causing a mutation, and affecting methylation on cytosine residues (217, 218). This MIE causes DNA methylation changes. The resulting hypo methylation affects nascent strands more than the parent strands, which suggests that transgenerational epigenetic inheritance may also be an effect of mercury exposure (218).

DNA methylation is a well-studied epigenetic modification, and because DNA methylation is related to oxidative stress, studies have used DNA hypo methylation as a measure of mercury exposure (199, 219). This is not the only mechanism of epigenetic modification, but the others, such as histone modifications and non-coding RNA changes, are less likely to be the direct result of oxidative stress. Histone modifications are regulated by two classes of enzymes, the histone acetylases and the histone deacetylases, which affect how tightly wrapped the DNA is around the histones and allow different promoter regions of the DNA to be read (220, 221). This process can be affected by oxidative stress, but the effects have been shown to be suppressed by inhibitory enzymes that help regulate the acetylation/deacetylation process (220, 221). Long noncoding

RNAs (lncRNA) aid in the regulation of site specific and genome wide epigenetics, as well as histone modification, by serving as scaffolding for the assembly of the acetylation/deacetylation enzymes (222, 223). Both histone modification and lncRNA epigenetic modifications of gene expression are, in some cases, a short-term change (222-224). Changes to the DNA strand itself, through methylation, are more persistent, long-term modifications to the genome that are irreversible (224). The irreversible changes, or mutations, also present a long-term modification for measurement, but since mutations can be related to oxidative stress, aging, evolution, and random recombination, determining the cause of genomic mutations is difficult (225, 226). For these reasons, changes in DNA methylation as a result of lifetime toxic metal exposure are more reliably measured than the other modifications (224).

Global DNA methylation measurements assess methylation across the entire genome, while shorter segment and site-specific analyses provide information only on a section of DNA. DNA heterogeneity, as well as phylogenetic differences in inherent methylation, could present problems when using only a small segment of DNA (227, 228). A global measurement may be a more accurate comparison for organisms without their entire genome sequenced, or for inter-species comparisons. Different segments of DNA are analyzed for methylation depending on the specific goal of each study, which provides results that are difficult to compare across species (99, 101, 229). The longer-lived, larger predators appear to have the greatest potential to have observable DNA methylation changes across their entire genome since they have a greater exposure time, and can accumulate more environmental contaminants during their lifetime. However, differences in DNA methylation have been difficult to observe within a population that

has high contaminant concentrations with little variation in concentration (99). Small variation in contaminant concentrations makes a direct link between the KE, reduced DNA methylation, to a known AO difficult.

Environmental metabolomics and mercury exposure

The biochemical mechanisms related to an AO could be identified by the field of metabolomics, which aims to elucidate the underlying biological mechanisms related to a disease state or phenotype observed in a population (230). Recently, metabolomics has been used to reveal biomarkers of many diseases prevalent in the human population, including various forms of cardiac disease and cancer (231-235). In addition to clinical research, metabolomics is used to address environmental systems, especially those undergoing various types of environmental stress (236, 237). With this approach, the biochemical impacts of environmental stressors can be assessed by analyzing profiles of small molecules associated with many cellular pathways and biological functions (236). This approach could also lend insight to the AOPs that are affected as a result of any MIE. The earthworm (*Eisenia fetida*; *Lumbricus rubellus*) is one of the most noteworthy animal models used for metabolomics studies focused on xenobiotic environmental stress. Earthworms are an optimal model species for laboratory based contaminant research, as they can be easily housed in large numbers, and dosed under identical conditions (238-240). Several studies have used earthworms to investigate the effect different organic contaminants, such as pesticides, have on the metabolic profile (238-241). These studies found small but significant changes in the earthworms' amino acid profiles following contaminant dosing (238-241).

Mercury is transformed in the soil by bacteria, which makes a soil dwelling model species more difficult to examine for mercury specific metabolomic effects. For the study of mercury exposure, an aquatic organism is preferred, so that the mercury species used, CH₃Hg, is not transformed into a different species throughout the course of the study. Plants (*Suaeda salsa*), bivalves (*Ruditapes philippinarum*; *Mytilus galloprovincialis*) and fish (*Liza aurata*) have been used for metabolomic based mercury exposure studies (6, 242-249). These organisms, while diverse, are all found in aquatic environments where mercury has become a problematic contaminant. Rodents have also been used for metabolomic analysis of mercury exposures, as they are a widely accepted proxy for human health (250).

Non-targeted analyses have identified several small molecules that consistently change in response to mercury exposure in a variety of species and lend insight to the affected oxidative stress, glutathione (GSH), and energy metabolism pathways (alanine, arginine, glutamate, aspartate, glycine, ATP and ADP) (6, 242, 245, 246). Glycine is a critical component of GSH synthesis, and changes in glycine concentrations have been observed in all studies examining the metabolomic effects of mercury exposure (6, 242-246, 249). Changes in glycine concentration could lead to drastic changes in the GSH response to oxidative stress and xenobiotic compounds (Figure 1.7) (6, 208, 210). Glycine is also important to the one-carbon metabolism pathway (which includes the folate and methionine cycles, Figure 1.8) that modulates DNA methylation (5, 231). The GSH pathway and the one-carbon metabolism pathway, both, provide cellular targets that could be related to mercury exposure. The metabolic changes seen across multiple

species are more likely to be specific to the exposure rather than the species-specific metabolomics responses observed in some studies (6, 245).

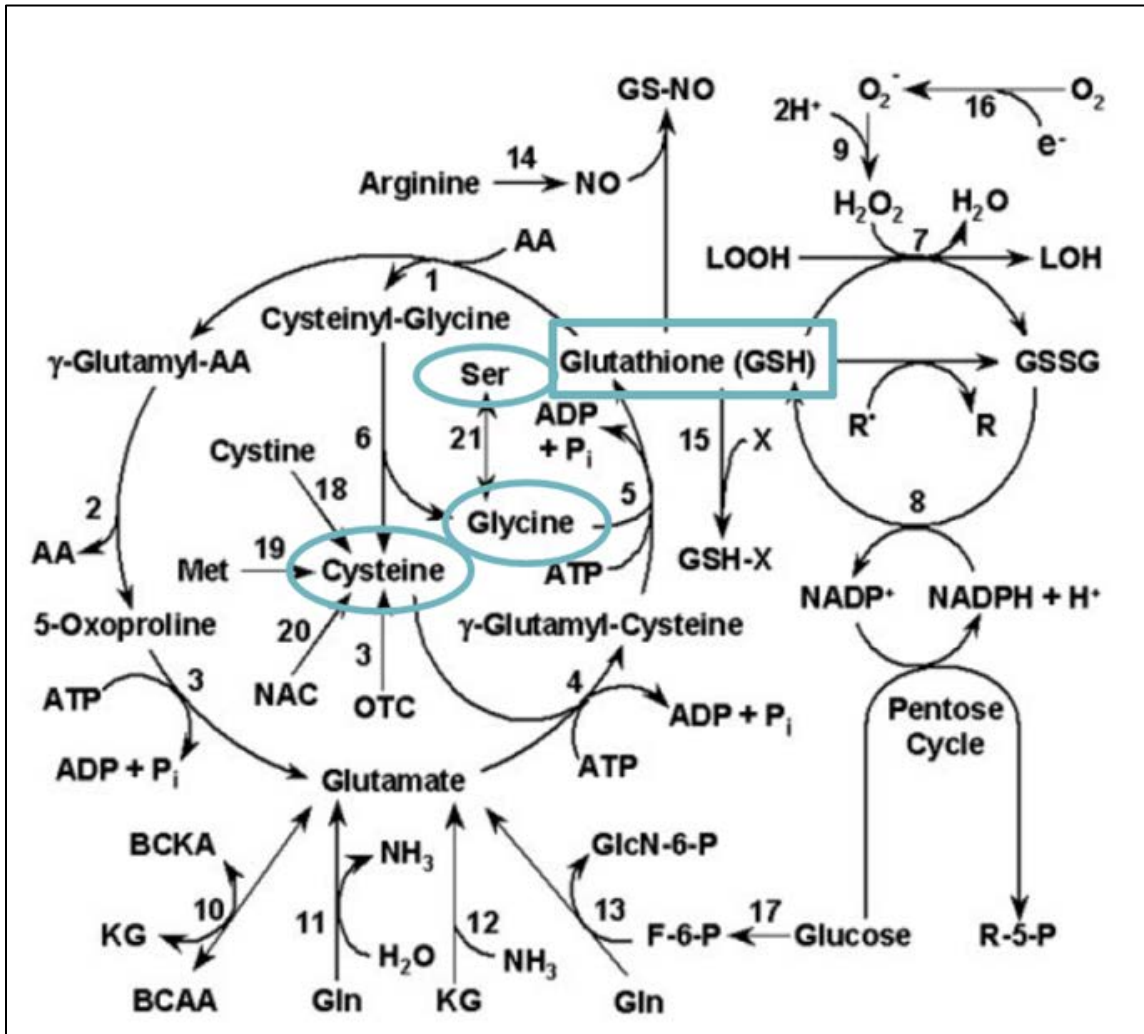


Figure 1.7. The GSH pathway, modified from Wu, *et al.* (210) to highlight the components of GSH synthesis.

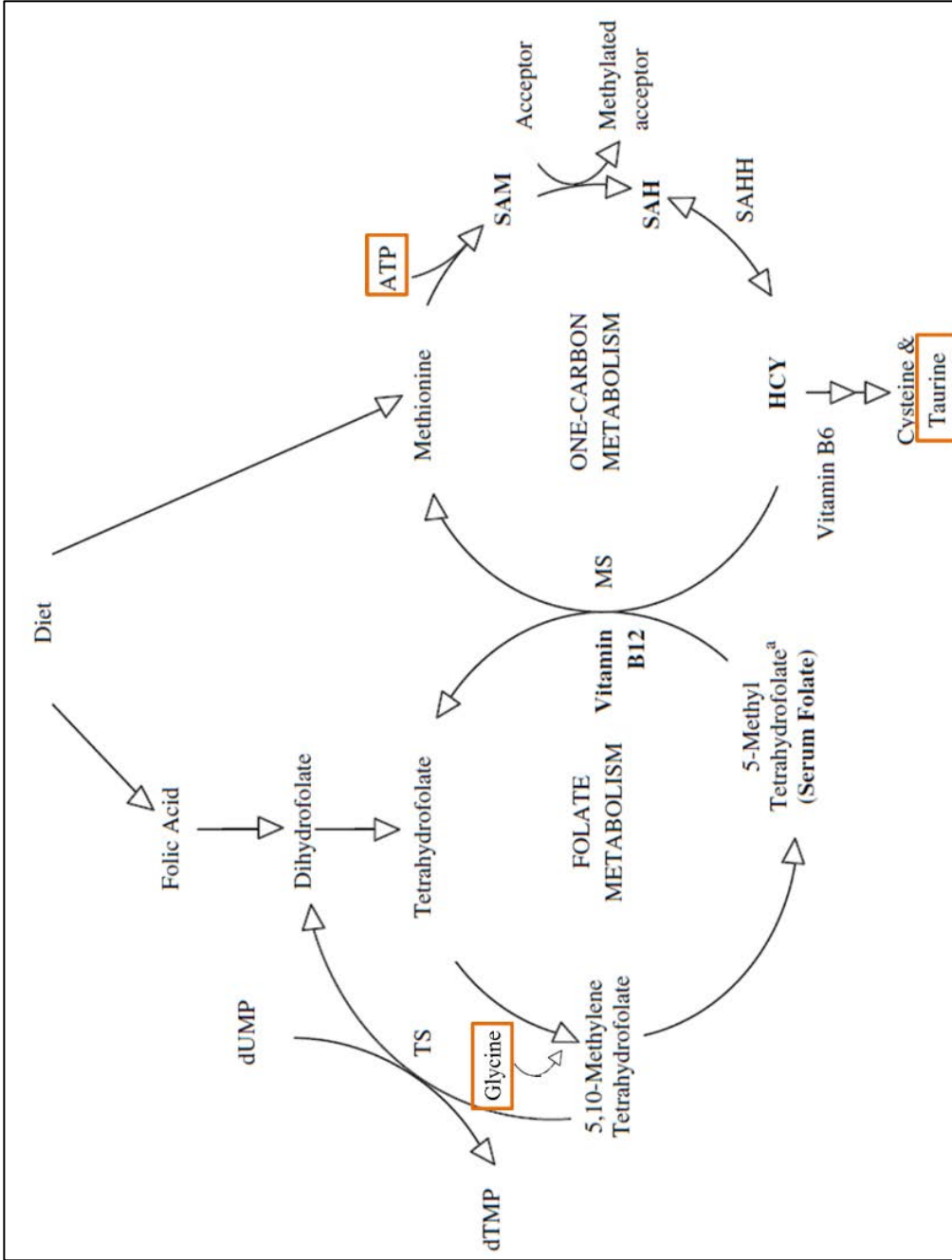


Figure 1.8. The One-Carbon Metabolism pathways, modified from King, et al. (5) to highlight the small molecules changes in response to Hg exposure in bivalves as demonstrated by Liu, et al. (6).

1.12. Overall significance & specific aims

Mercury is a ubiquitous environmental contaminant that is bio-accumulative and toxic, and high mercury concentrations within an organism can lead to a variety of health effects including degeneration of the nervous, cardiac, and muscular systems. Although the most common route of mercury exposure for humans and wildlife is dietary, most of the world's population consumes mercury in low concentrations. However, the consumption and accumulation of a toxic chemical is likely to affect an individual, prior to the onset of degenerative diseases. DNA methylation has been measured as an effect of mercury exposure, with inconsistent results across a variety of species. Metabolomics provides the ability to determine what, if any, cellular-level changes are taking place due to mercury exposure, prior to the onset of any epigenetic or degenerative effect. In plants, bivalves and fish, several small molecules involved in DNA methylation as well as oxidative stress management have been implicated in mercury exposure, but no environmental sentinel has been thoroughly evaluated as a proxy for human health to address these issues.

The body of work that follows examines the overall hypothesis that **increased dietary mercury exposure alters DNA methylation and small molecule profiles in American alligators and diamondback terrapins**. We hypothesized that the concentrations of mercury accumulated by long-lived predators in the Southeastern United States would elicit effects on the epigenome, via increased oxidative stress and GSH utilization. To mimic the natural dietary mercury exposure that coastal human populations are subject to, this hypothesis was examined in two coastal sentinel species living in high mercury environments, the American alligator (*Alligator*

mississippiensis), being newly established as a sentinel with this work, and the Diamondback terrapin (*Malaclemys terrapin*), previously established sentinel for mercury exposure.

Thus, the work presented herein serves the following Specific Aims:

- 1-** Evaluate the American alligator as a sentinel species for mercury exposure by establishing mercury and trace element concentrations along the SE Atlantic Coast of the US, the body distribution, the seasonal variability including changes in body condition, the vertical transmission, and embryonic compartmentalization of mercury.
- 2-** Determine if mercury exposure affects DNA methylation in chronic and acute exposure scenarios in American alligators and diamondback terrapins.
- 3-** Initiate investigations into the biochemical pathways that may be affected by a chronic mercury exposure in diamondback terrapins using an NMR-based metabolomics approach.

This work aims to assess ecologically important species for use as environmental sentinel for health effects of mercury exposure. These effects can be translated to human populations using epigenetic and metabolic endpoints, in effort to better understand the relationship humans have with their environment and how sentinel species can aid in that understanding.

Chapter Two: American alligators as sentinel species for environmental exposure
research

Specific Aim 1, Experiments 1, 2, 3, and 4, have been published in the following three peer-reviewed publications.

- 1- Nilsen FM, Kassim BL, Delaney JP, Lange TR, Brunell AM, Guillette LJ, Long SE, Schock TB. Trace element biodistribution in the American alligator (*Alligator mississippiensis*). *Chemosphere* 2017.
- 2- Nilsen F, Dorsey J, Lowers R, Guillette Jr L, Long S, Bowden J, Schock T. Evaluating mercury concentrations and body condition in American alligators (*Alligator mississippiensis*) at Merritt Island National Wildlife Refuge (MINWR), Florida. *The Science of the total environment* 2017; 607: 1056.
- 3- Nilsen FM, Parrott BB, Bowden JA, Kassim BL, Somerville SE, Bryan TA, Bryan CE, Lange TR, Delaney JP, Brunell AM, Long SE, Guillette Jr LJ. Global DNA methylation loss associated with mercury contamination and aging in the American alligator (*Alligator mississippiensis*). *Science of the Total Environment* 2016; 545–546: 389-397.

2.1. Assessment of the American alligator as a human health sentinel for mercury exposure

The American alligator is a sentinel species for human exposure to numerous environmental contaminants (175, 181, 251, 252). As presented in the previous chapter, the alligator is a good candidate species for evaluating mercury exposure, because they mimic human exposure. Alligators are an upper trophic level predator in their ecosystem, and can accumulate very high mercury concentrations through their position in the food web (43). Alligators can live up to 80 years, and consume similar marine and aquatic food as the human population mimicking human bioaccumulation (e.g. largemouth bass and other freshwater sport fish), making them a natural candidate for sentinels of human dietary mercury exposure (43, 253). Here, the utility of the American alligator as a sentinel species for chronic dietary mercury exposure in the southeastern United States is determined. The experiments that follow will utilize alligators across the southeastern Atlantic coast to determine:

- 1) The mercury and other trace element concentrations in alligators. These experiments will determine if the concentrations are comparable to those observed in the human population. If the concentrations are found to be comparable, then alligators can be used to monitor the effects of mercury exposure in the human population (Figure 2.1, Aim1a).
- 2) The biodistribution of mercury and other trace elements within the body of the American alligator. This information can allow the target organs of mercury accumulation to be identified. Identifying the target organs will enable a comparison between other sentinel species as well as humans. It could also lead to

improved monitoring of alligators in ecosystems contaminated with mercury (Figure 2.1, Aim1b).

3) The seasonality of mercury within the alligator. With this information, research can assess the likelihood of fluctuating seasonal concentrations, complicating the use of the alligator as a sentinel species (Figure 2.1, Aim1c).

4) The relationship between changing body condition and mercury concentrations. Understanding this relationship will enable a better assessment of mercury seasonality, and the health of the alligator population, as well as enable predictions about the changing health status of the human population in terms of mercury exposure (Figure 2.1, Aim1d).

5) If developing alligators are exposed to mercury, and if the mercury concentration they are exposed to is related to the nesting female's mercury concentration. This experiment will assess the utility of using alligator eggs for developmental biology studies related to mercury exposure by elucidating the relationship between mercury concentrations observed in maternal blood samples and those observed in corresponding yolks (Figure 2.1, Aim1e).

6) The efficacy of dosing developing alligator eggs to mimic maternal exposure at highly contaminated sites. This experiment will determine if collections from sites low in mercury contamination can be used for developmental biology studies related to high mercury exposure. Using the relationship describing maternal transfer of mercury elucidated in the previous experiment, *ex situ* dosing will attempt to mimic the natural relationship from highly contaminated areas.

Compartmentalization analyses of mercury within the egg will describe which organs are accumulating mercury during embryonic development (Figure 2.1, Aim1f).

These experiments will enable the evaluation of the American alligator for a sentinel species for mercury exposure at several different biological time points, as well as answer remaining questions for environmental monitoring.

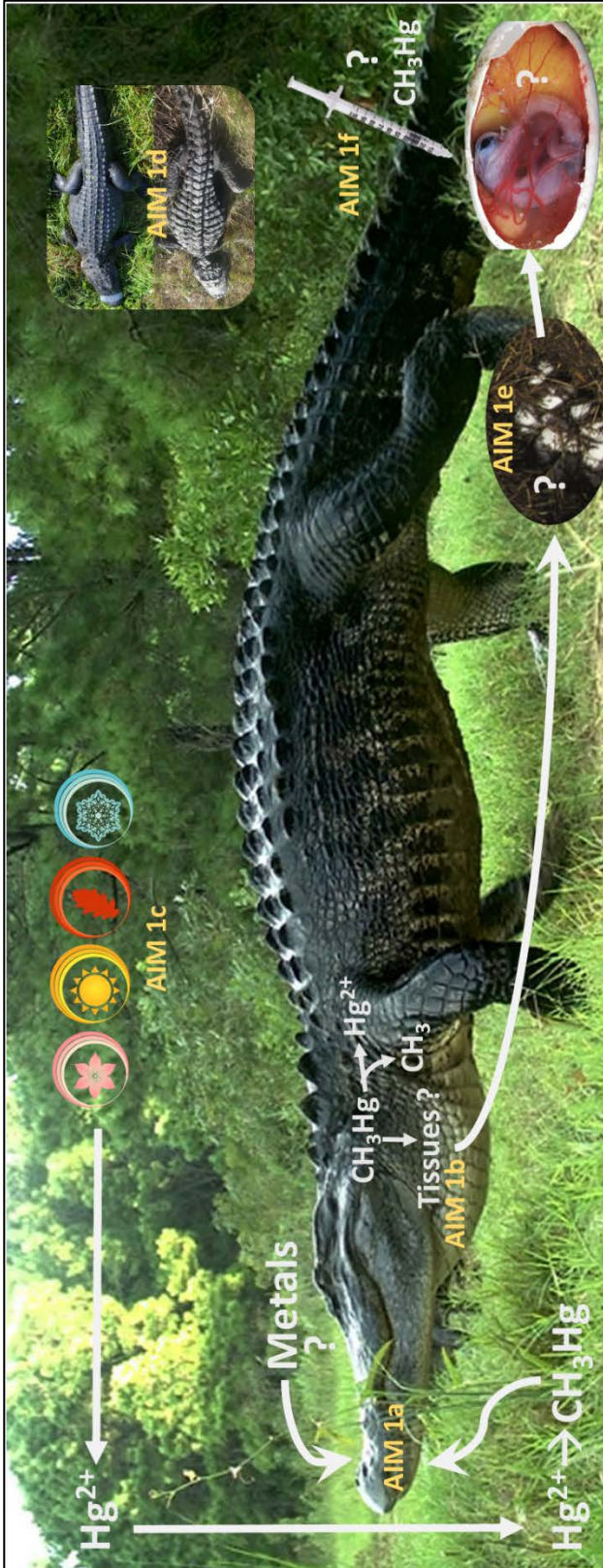


Figure 2.1. The graphical abstract of the experiments of all Specific Aims discussed within this dissertation.

2.2. *General methods*

The methods described below are used throughout this entire chapter to investigate the distribution of mercury and other trace elements in the American alligator throughout various life stages, for the assessment of its utility as a sentinel species of mercury exposure.

The direct mercury analyzer (DMA-80), a combustion atomic absorption spectrometry instrument, was used to conduct the total mercury measurements, as it provides a fast and accurate method of measuring total mercury concentrations in tissues with minimal preparation. The DMA-80 limit of detection (0.05 ng) is amenable to detect changes in complex matrix environmental samples, with a low margin of error. The DMA-80 is preferable to cold vapor inductively coupled plasma mass spectroscopy (CV-ICP-MS) for total mercury measurements, as it is a high throughput method that does not require isotope dilution or complicated sample preparation for instrumental analysis. Previous studies of reptiles and birds have shown that CH₃Hg comprises greater than 70% of the total mercury content in reptilian whole blood, and in the species most closely related to the American alligator, the ratio is nearly 1:1 (176, 254, 255). This measurement is used as a proxy for the most biologically relevant form of mercury, CH₃Hg, until species-specific information regarding the ratio of CH₃Hg to total mercury in crocodilian whole blood becomes available. Also, the speciation of mercury does not change the cellular response by GSH, only the biological ability to remove the mercury from the organism (202).

An inductively coupled plasma quadrupole mass spectrometer (ICP-MS) was also used to determine the total concentration of a suite of trace elements including,

Aluminum (Al), Vanadium (V), Chromium (Cr), Manganese (Mn), Nickel (Ni), Cobalt (Co), Copper (Cu), Zinc (Zn), Arsenic (As), Selenium (Se), Rubidium (Rb), Strontium (Sr), Molybdenum (Mo), Cadmium (Cd), Tin (Sn), and Lead (Pb). These elements were evaluated to determine if any are of interest for the American alligator, as the other toxic heavy metals (As, Cd, Pb) also cause oxidative stress and could elicit a cellular response by GSH, clouding the downstream effects from being directly linked to mercury exposure (199).

2.2.1. Sample collection

The American alligator whole blood samples were collected with 2.54 cm 18.5 gauge needles (Becton Dickinson) and 60 mL Luer lock syringes (Becton Dickinson) or 20 mL Luer lock syringes (Becton Dickinson) for adults and sub-adults, respectively. Samples were transferred from the syringe to lithium-heparin blood collection tubes (Becton Dickinson). Blood samples collected at the time of capture and blanks were stored on wet ice for no more than 5 h before being frozen at -80 °C. Tissue samples were removed using sterile stainless steel scalpel blades and dissection instruments, in the specific manner described for each experiment below. Briefly, tissues were removed and placed into either a Cryovial or Whirlpack and frozen on wet ice for no more than 5 hours before being frozen at -80 °C.

Power & effect statistics

It is important to note that within each of the experiments in this chapter, and all that follow in the text of this dissertation, as many samples as possible were collected, and analyzed. Sampling enough individuals in the environment to ensure statistical power is difficult, since sample sizes are dependent on the presence of, and the ability to interact

with wildlife. Power analyses were not conducted prior to these experiments being conducted, as many of them expand species and contaminant specific issues, so there are no pre-existing long-term data sets, or surveys of perturbations at specific locations (256). Much of the work conducted in this dissertation provides these initial studies that are generally used as the basis of experimental design, and power analysis (256, 257).

The issue of power analysis for wildlife biology is debated in the literature, with many groups suggesting that a power analysis must be conducted to ensure adequate sample sizes, and to remove type II error (the failure to observe a significant effect that is present in the data) (258, 259). The general issue environmental scientists' face in using a power analysis is that there are seldom pilot studies to base the analysis on that are relevant/comparable to the study being conducted. Frequently similar issues are studied in a variety of organisms, and while the questions may be the same, the species or environment may not be biological comparable to the study being conducted.

When there are studies available to use in the analysis, the observed differences and variances from previous studies often yield estimated power that is biased with low precision (260). This could be the result of the underlying data structure of many environmental science studies. As most wildlife data are non-parametric, the heterogeneous variance leads to effect statistics that are biased, confidence intervals that are inaccurate, and incorrect estimations of effect size (257).

Due to these issues, many environmental studies calculate a sensitivity power analysis, after the study has failed to reject the null hypothesis, which is widely considered incorrect in this field (260-263). It is argued that failing to reject, and

accepting, null hypotheses are not the same, and that *post hoc* power analyses on environmental data are subject to the same non-parametric complications that *a priori* power analyses are (262). The consensus is, that *a priori* power analysis should be conducted to aid in experimental design, if applicable. While the use of *post hoc* power analyses should be done with discretion, and serve a specific purpose, particularly when being used alongside an insignificant *p* value.

It is suggested that regardless of the statistical significance of one's study, that the biological importance of the experiment be considered and reported (257, 262). Biological importance is not always associated with a low *p* value, and often leads researchers into conducting unnecessary tests in the hunt for significance (261, 264). Power analysis can provide information about the number of animals needed to characterize nature, but cannot use the data to determine the state of nature (263). For this reason, wildlife biologists well-versed in their area of expertise, are encouraged to examine confidence intervals, choice of hypotheses, and the equivalence between "failing to reject" and "accepting" the null hypothesis to detect environmental impacts (256, 263).

Many environmental and wildlife studies are conducted to support or incite policy measures, and environmental policy is not dependent on significant *p* values. Environmental law frequently defers to the precautionary principle, that states: if something is expected to have an effect on the environment, it is preferable to avoid causing the effect, than to conduct bioremediation afterward (265, 266). To this end, the

studies in this dissertation consider all aspects of the data collected, not just those that are statistically significant.

2.2.2. Analytical chemistry methods

Mercury analysis:

Direct combustion AAS measurements

The mass fraction of mercury was determined using the DMA-80 (Milestone Scientific, Shelton, CT) by external calibration. The samples were thermally decomposed by combustion to release mercury, which catalytically reduces to Hg^0 and binds to the gold amalgamation trap. The method parameters for each sample material follows:

Aqueous Solution under 100 mg

60 s ramp to 200 °C

90 s ramp to 650 °C; 90 s hold

Aqueous Solution over 100 mg

60 s ramp to 200 °C; 60 s hold

90 s ramp to 650 °C; 90 s hold

Fresh/Frozen Tissue under 120 mg

90 s ramp to 200°C; 30 s hold

90 s ramp to 650°C, 180 s hold

The Hg^0 is then thermally desorbed by the increased temperature, and the atomic absorption of Hg^0 is measured at a nominal wavelength of 254 nm. If the experimental samples reached a measured value that approached the plateau of the second order fit line calibration curve, the same sample was analyzed again at a reduced mass, to eliminate the likelihood of the sample concentration being miscalculated.

Calibration & sample measurements

The external calibration curve (peak area versus mercury concentration) for samples measuring between 0.5 ng and 800 ng of mercury was constructed using serial dilutions of SRM 3133 (Mercury in Water), which was tested using other SRMs of varying mercury concentrations. A second order fit was applied to the data to account for an asymptotic or slight rollover effect due to non-ideal Beer-Lambert Law behavior. Coefficients resulting from the second order fit and the instrument signal (peak area) were used to solve the quadratic equation to calculate the concentration of mercury in the whole blood samples. The ordinate is defined as [y * g of mercury per g of sample], where y is the mercury atomic absorption signal and the abscissa is defined as the mass of added mercury spike per gram of sample.

$$y = ax^2 + bx + c$$
$$0 = ax^2 + bx + (c - y)$$

Solving for x using the quadratic formula:

Where:

a , b , and c are coefficient constants

y is the mercury peak area

x is the mercury mass fraction

The uncertainties were combined according to ISO guidelines (267). The expanded uncertainty (U_c), expressed as a 95 % confidence interval was calculated by:

$$U_c = k [A_1^2/n_1 + A_2^2/n_1 + B_1^2 + B_2^2]^{1/2}$$

Where:

- A_1 is the uncertainty for $n_1 =$ replicate measurements of samples
- A_2 is the uncertainty due to the blank corrections
- B_1 is the estimated standard uncertainty of the weighing measurements
- B_2 is the estimated standard uncertainty of SRM 3133
- k is the coverage factor

Blanks

The instrumental and procedural blanks for the analysis of mercury were measured concurrently with all samples. The field blanks were made with Milli-Q water using experiment specific collection materials to mimic the processing of the samples, aliquots of approximately 0.10 g, were run alongside the experimental samples.

Control materials

Matrix matched control materials were used for each of the following experiments and analyzed prior to experimental samples being measured as well as concurrently with the experimental samples to ensure reproducibility and proper instrument function. Ideally, when utilizing standard bracketing for quantitative determinations, the control materials are matrix matched and have a range of analyte mass fractions within which, the experimental samples fall. Specific control materials are described with each experiment that follows.

Sample preparation

As this analytical method requires little sample preparation, samples were either thawed or left frozen for analysis. Liquid samples were thawed to room temperature and gently mixed for homogenization before a sub sample was taken for analysis. Frozen tissue powders were kept frozen and a frozen aliquot was used for analysis. Whole embryonic organ samples were thawed completely and used in their entirety for analysis.

Trace element analysis:

Inductively coupled plasma mass spectrometry

All samples were measured on a Thermo X2 quadrupole ICP-MS system (software build, 2.6.0.334), equipped with a standard introduction system and an Elemental Scientific ESI SC4 auto sampler. The ICP-MS was tuned and optimized using a standard 1 ng/g multi-element tuning solution, and operated in collision cell mode. Collision cell mode utilized 8 % H₂ in 92 % He as the collision gas for *m/z* Al, V, Cr, Mn, Ni, Co, Cu, Zn, As, Se, Rb, Sr, Mo, Cd, Sn, and Pb, and 1 % ammonia in 99 % He as the collision gas for *m/z* 51, 52, 53, 102, and 120. The collision cell ICP-MS optimization was performed with a 10 ng/g, 68 element tuning solution with quadrupole MS routine methods utilize five replicate runs consisting of 50 sweeps, and a dwell time of 25 ms. The data obtained from monitoring the selected isotopes were exported as a csv file to Microsoft Excel spreadsheet for off-line calculations.

Calibration & sample measurements

Working calibration stock solutions were prepared by gravimetric dilution of high-purity primary standards (Table 2.1). Stock solutions were prepared by serial dilution of these standards and external calibration curves were constructed. A first order fit was applied to the data; the equation used to produce the sample concentration estimates (x) was based on a linear fit:

$$y = mx + b$$

Where

- m is the slope
- b is the intercept
- y is counts of analytes / (counts of internal standard)
- x is ng/g of analytes / (g of internal standard)

Analytical signals were corrected for blank contributions. The slope and intercept from the calibration curves were based on the measured isotopic responses from SRM calibration solutions, and utilized to calculate the mass fraction of trace metals in the tissue samples.

Blanks

In addition to the samples, controls, field blanks using experimental specific collection materials, and procedural blanks containing an aliquot of internal standard only, were carried through the entire sample processing and measurement scheme. If the overall mean of these blank measurements was above the limits of detection, the sample measurement data was blank corrected.

Control materials & calibration materials

Seronorm Trace Elements in Whole Blood L-3 (Lot# 1112691) was purchased from SERO (ALS Scandinavia AB, Lulea, Sweden). Ampoules of all NIST SRMs were obtained from the Office of Reference Materials (ORM) (Table 2.1). The trace metal SRMs were used to construct calibration curves. Seronorm was used as a control material that matched the matrix of the experimental samples. The uncertainty values for each solution are provided in Table 2.1.

Table 2.1. A list of the SRM Solutions, mass fractions, uncertainties and lot numbers used in the creation of the Calibration Curves.

SRM Number	SRM Name	Lot #	Symbol	Mass fraction (µg/g)	<i>U</i> (µg/g)
3101a	Aluminum (Al) Standard Solution	060502	Al	10,001	17
3165	Vanadium (V) Standard Solution	992706	V	4,860	20
3112a	Chromium (Cr) Standard Solution	030730	Cr	9,922	25
3132	Manganese (Mn) Standard Solution	050429	Mn	10,000	20
3113	Cobalt (Co) Standard Solution	000630	Co	9,996	23
3136	Nickel (Ni) Standard Solution	000612	Ni	9,738	22
3114	Copper (Cu) Standard Solution	121207	Cu	10,005	24
3168a	Zinc (Zn) Standard Solution	120629	Zn	10,007	20
3103a	Arsenic (As) Standard Solution	100818	As	9,999	15
3149	Selenium (Se) Standard Solution	100901	Se	10,042	51
3145a	Rubidium (Rb) Standard Solution	891203	Rb	10,040	60
3153a	Strontium (Sr) Standard Solution	990906	Sr	9,070	30
3134	Molybdenum (Mo) Standard Solution	891307	Mo	9,990	30
3108	Cadmium (Cd) Standard Solution	060531	Cd	10,005	19
3161a	Tin (Sn) Standard Solution	070330	Sn	10,010	21
3133	Mercury (Hg) Standard Solution	061204	Hg	9,954	53
3128	Lead (Pb) Standard Solution	101026	Pb	9,995	14

Sample preparation

Samples were removed from the freezer, either thawed or left frozen, depending on the sample matrix, and sub-sampled. The sub-sample weighing approximately 0.5 g was gravimetrically weighed into a pre-cleaned Teflon CEM microwave digestion vessel, using a four-place analytical balance. Scandium (Sc), yttrium (Y), rubidium (Ru), rhodium (Rh), and bismuth (Bi) (1000 mg/mL) were added as internal standards by gravimetric addition of 0.25 g into the digestion vessel, followed by the addition of 3.5 mL of nitric acid. The Teflon CEM microwave digestion vessels were then closed and run in the CEM MARS (Microwave Accelerate Reaction System) Xpress microwave, under the method “Tissue Express” which was designed for use with inorganic samples using the following temperature program:

Ramp for 10 minutes to 125 °C, hold for 5 minutes
Ramp for 5 minutes to 210 °C, hold for 15 minutes
Cool for 15 minutes

The samples were then cooled to room temperature and transferred to pre-cleaned auto-sampler vials. Approximately 1.5 mL hydrochloric acid was added to each sample for stabilization and was then diluted to approximately 50 g with Milli-Q water prior to analysis. The control materials, were treated in a similar manner to the samples. Procedural blanks and control materials were run every 20 samples for a total of at least 10 replicates. Field blanks were run alongside experimental samples, for a total of at least 5 replicates.

2.3. Determining the trace elements of concern and their biodistribution in the American alligator in the southeastern United States

2.3.1. Introduction

Historically, mercury is known to be a deleterious contaminant in the southeastern United States, due to a combination of favorable environmental parameters and local point sources of mercury emissions in southern Florida, specifically in the Florida Everglades (4, 43, 268). Since the discovery of mercury concentrations above the 1.0 mg/kg FDA limit within largemouth bass (*Micropterus salmoides*) in the 1990's, as well as identification of the local contributing point sources, extensive bioremediation efforts have taken place (43). Following these bioremediation efforts, mercury concentrations in largemouth bass have declined, however, no updated mercury measurements have been made on the highest trophic level predator consumed by humans, i.e. the American alligator (43). Since alligators are consumed in this region, approximately 8,000 recreationally caught each year, routine monitoring of mercury as well as other trace elements is desirable.

Routine monitoring of mercury in wild populations that have a broad geographical range consumes extensive time and resources. Animals generally must be captured and anesthetized, and then minor surgery is conducted to remove muscle samples for human consumption monitoring efforts. However, since the mercury measurements in Florida have not been updated since prior to the bioremediation efforts in the 1990s, a fast and accurate method of routine monitoring is needed. Such a method

of monitoring would provide important information for both the ecosystem as well as human consumption advisories in areas contaminated with high mercury concentrations.

The American alligator might be helpful in this regard. Although the muscle tissue of this species, which humans consume, is an invasive sample to collect, determining the relationship for mercury and other trace metals between the tissues of the American alligator could greatly alleviate the effort required to routinely monitor muscle concentrations. Investigating the mercury burden of different tissues could also aid in determining if this species accumulates mercury in the same target organs as humans, to further evaluate their use as a sentinel species

Here, we evaluate four tissues from American alligators to determine which organs accumulate the most mercury and fifteen other trace elements (Al, Ni, V, Cr, Mn, Co, Cu, Zn, As, Se, Rb, Mo, Cd, Sn, Pb) as well as to determine if a correlation exists between the tissues for the suite of trace elements examined. We utilized routinely collected monitoring samples (blood and scute), a commonly consumed tissue (muscle), and a classically analyzed tissue for environmental contaminants (liver) to demonstrate how the trace elements were distributed within the American alligator.

The American alligator is used as the sentinel species for humans in these experiments as they reside in mercury contaminated environments, some of which have not been evaluated for other trace elements. The information gained from this experiment will provide valuable information to the public, environmental managers and scientists regarding trace element concentration and exposure for this ecologically important species.

2.3.2. Experiment specific methods

Blood sample collection

Blood samples were collected from healthy American alligators at six sites in Florida, which are known for high and low historic mercury concentrations, and two sites in South Carolina, including one that is currently uncharacterized and expected to be a clean reference site (Figure 2.2, all sites except MINWR, FL). In Florida, the northern sites, Lake Lochloosa and St. John's River are historically low mercury contamination sites (Figure 2.2). Lake Kissimmee and Lake Trafford are both in central Florida, and are moderate mercury contamination sites (Figure 2.2). The Everglades Water Conservation Areas in southern Florida, sites WCA2A and WCA3A, are historically high mercury contamination sites (Figure 2.2). In South Carolina, Tom Yawkey Wildlife Center was chosen as it is downstream from a pulp mill, and currently uncharacterized for mercury contamination. Ace Basin, SC is also currently undescribed for mercury contamination, but is further removed from any potential point sources of contamination, making it a potential reference site for mercury studies (Figure 2.2). All animals that were sampled for the comparison of trace elements in blood samples are detailed in Table 2.2.

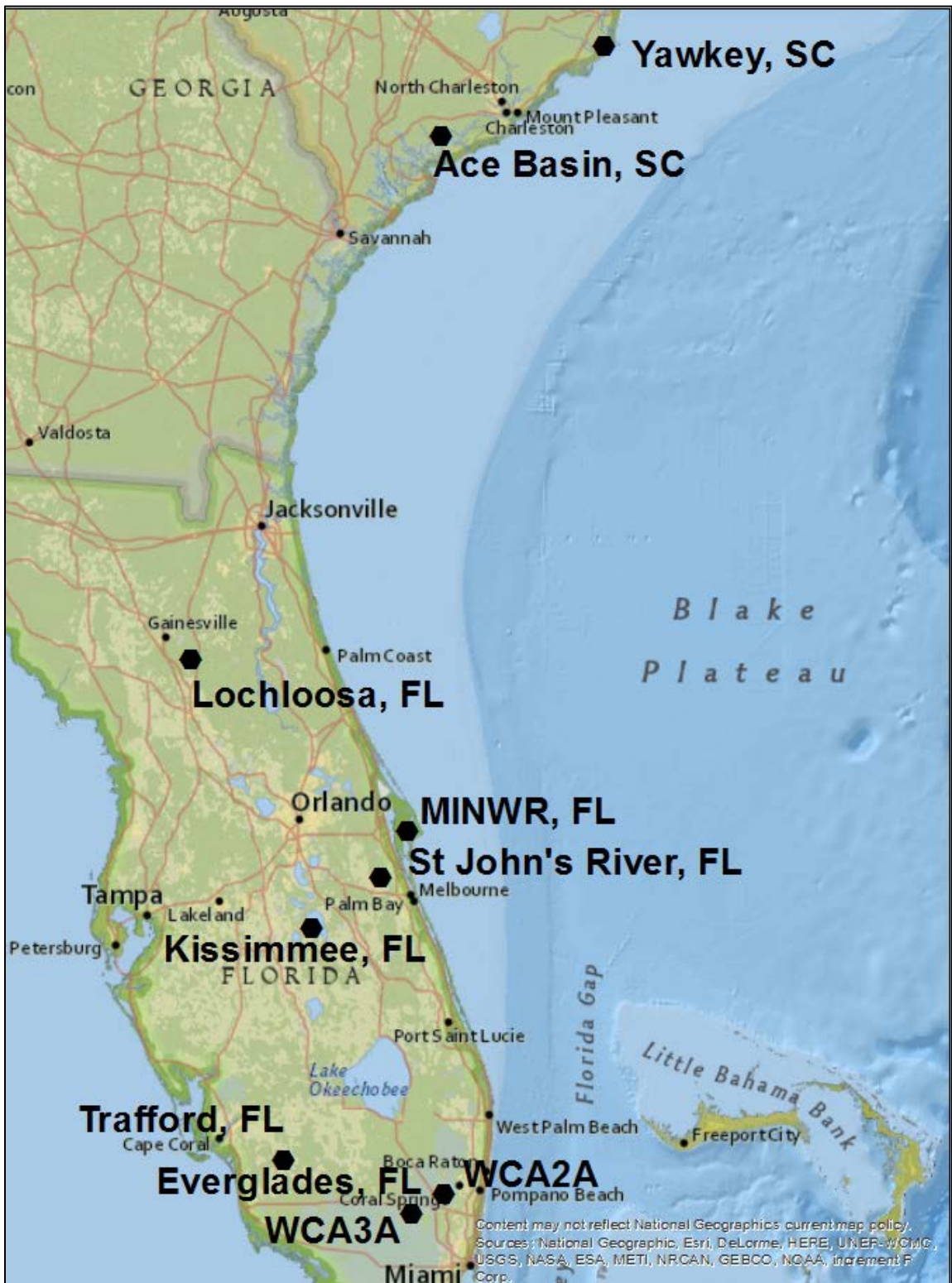


Figure 2.2. Map of all sites used for sample collection in Chapter 2.

Table 2.2. The capture metadata for all alligator with blood samples used in experiment 2.3.

Animal #	Age Class	Location	Latitude-DD (N)	Longitude-DD (W)	SV Length (cm)	Tail Girth (cm)	Sex (M/F)	Condition
2	Adult	L. Kiss	27.98449	81.27867	167	73.1	M	Normal
3	Adult	St. Johns River	28.30001	80.80676	138	70	M	Normal
4	Adult	L. Kiss	27.85359	81.2034	177.5	80.3	M	Normal
5	Adult	L. Kiss	27.98842	81.28396	106.2	44.7	F	Normal
6	Adult	L. Kiss	27.90443	81.223	109.2	49.5	M	Normal
7	Adult	St. Johns River	28.28719	80.8202	146	62.5	M	Normal
8	Adult	WCA3A	26.06168	80.46085	123.5	45	F	
9	Adult	L. Kiss	27.96396	81.29359	115.1	39.2	F	Normal
10	Adult	L. Kiss	27.9219	81.22293	124	54	F	
11	Adult	L. Kiss	27.92968	81.24022	160	49.5	M	Normal
12	Adult	L. Kiss	27.96272	81.32471	142.5	66	M	Normal
13	Adult	L. Kiss	27.87839	81.21207	90.4	42.5	F	Normal
14	Adult	St. Johns River	28.2722	80.83008	126	55	M	Normal
15	Adult	L. Kiss	27.9096	81.22835	173	74	M	Normal
16	Adult	St. Johns River	28.11732	80.74286	96	37	F	
17	Adult	L. Kiss	27.96762	81.31743	96	39.5	M	Normal
18	Adult	L. Kiss	27.97672	81.29482	90	38.5	F	
19	Adult	St. Johns River	28.658	80.82053	152.1	67.4	M	Normal
20	Adult	St. Johns River	28.29604	80.80991	135.6	66	F	Normal
22	Adult	St. Johns River	28.09919	80.74914	155.4	66.7	M	Normal
23	Adult	St. Johns River	28.19143	80.81365	126	53.5	F	
26	Adult	Lochloosa	29.52437	82.14857	144	73.4	F	Fat
29	Adult	St. Johns River	28.17154	80.74515	137	62.5	M	
30	Adult	WCA2A	26.21919	80.39268	94	41.2	F	Normal
31	Adult	Trafford	26.43621	81.49513	99	41	M	
32	Adult	St. Johns River	28.11174	80.75206	117.5	50.4	M	Normal
33	Adult	St. Johns River	28.29033	80.81822	168.2	67.9	M	Normal
34	Adult	WCA3A	26.21176	80.68641	94.3	39.3	F	Normal
36	Adult	Trafford	26.43286	81.49624	134	56	M	
37	Adult	WCA3A	26.06147	80.45958	111	46.5	M	Normal
38	Adult	Lochloosa	29.53641	82.1377	94	45.5	F	Normal
39	Adult	Trafford			153.5	45.8	M	Skinny
41	Adult	Trafford			90	38.5	M	
42	Adult	Trafford			139.9	60.5	M	
43	Adult	WCA2A	26.23712	80.46071	130.2	52	M	
44	Adult	Trafford	26.41976	81.49065	140.2	56.2	M	Normal
45	Adult	Trafford	26.42077	81.50428	109	45	M	
46	Adult	Lochloosa	29.51888	82.133	159	80.7	M	Fat
47	Adult	Trafford	26.42976	81.50338	153	62.3	M	
49	Adult	Trafford			105	43.8	F	
50	Adult	Trafford	26.42557	81.50392	92	41	M	
52	Adult	WCA3A	26.04934	80.47865	99.5	39.5	F	
53	Adult	Trafford	26.41605	81.50302	93	39.5	F	
54	Adult	WCA2A	26.2183	80.40025	140.5	4:48	M	Normal
55	Adult	WCA3A	26.14748	80.63103	154	56	M	Skinny/Normal
56	Adult	Trafford	26.42334	81.459	142	62.7	M	
57	Adult	Lochloosa	29.5418	82.13	179.5	90.1	M	Fat
58	Adult	WCA2A	26.27958	80.49313	91.4	40.5	F	
60	Adult	Lochloosa	29.53319	82.13628	105.5	53.2	F	Normal
61	Adult	Lochloosa	29.5351	82.14065	186	87.5	M	Fat
62	Adult	Lochloosa	29.53374	82.13919	108.8	54.8	M	
63	Adult	Lochloosa	29.53379	82.1393	95.8	47.5	M	Normal
64	Adult	WCA3A	25.76255	80.72896	115.7	49	M	Normal
65	Adult	WCA3A	26.06169	80.46485	94	34.8	M	Skinny/Normal
66	Adult	WCA3A	26.08917	80.5906	157	63.1	M	Fat
67	Adult	Lochloosa	29.52972	82.13016	128.4	69.1	M	Fat
69	Adult	WCA2A	26.23041	80.45899	105	46	F	Normal
70	Adult	WCA3A	26.10992	80.60614	142	56	M	
71	Adult	WCA2A	26.25417	80.3677	91.8	38.9	F	
73	Adult	Lochloosa	29.5272	82.14932	93.5	47.3	M	
75	Adult	Lochloosa	29.50336	82.15189	151.5	66.3	M	Fat
77	Adult	WCA3A	25.7622	80.74733	102.1	38.9	M	Normal
78	Adult	WCA2A	26.3188	80.52347	132	53.5	M	Normal
100	Sub adult	L. Kiss	27.9288	81.23381	89	40	F	
101	Sub adult	L. Kiss	27.95386	81.25823	57.5	23	F	Normal
102	Sub adult	L. Kiss	27.91099	81.22773	82.5	37	M	Normal
103	Sub adult	St. Johns River	28.19582	80.81999	62	25.5	M	
104	Sub adult	L. Kiss	27.90505	81.2225	69.8	30.2	M	Normal
105	Sub adult	L. Kiss	27.91231	81.22723	53.3	23.4	M	Normal
106	Sub adult	L. Kiss	27.98892	81.30901	46.5	17.5	M	
107	Sub adult	L. Kiss	27.93714	81.23738	71.8	31.5	F	Normal

Animal #	Age Class	Location	Latitude-DD (N)	Longitude- DD (W)	SV Length (cm)	Tail Girth (cm)	Sex (M/F)	Condition
109	Sub adult	L. Kiss	27.97738	81.2998	61	25.8	F	
110	Sub adult	L. Kiss	27.93714	81.23738	81	34	M	Normal
111	Sub adult	St. Johns River	28.28141	80.82613	79	33.5	M	Normal
112	Sub adult	L. Kiss	27.8972	81.2184	86.5	38.5	F	Normal
113	Sub adult	WCA3A	26.10006	80.59865	82	33.9	F	Normal
114	Sub adult	Trafford			57	24	F	
115	Sub adult	L. Kiss	27.94872	81.25906	62	24.4	F	Normal
116	Sub adult	St. Johns River	28.29408	80.81126	100.5	46.6	M	Normal
117	Sub adult	St. Johns River	28.18072	80.80492	73	33	M	
118	Sub adult	L. Kiss	27.92754	81.23203	76	33	M	Normal
119	Sub adult	WCA3A	26.16365	80.64969	74.3	29.3	F	Normal
120	Sub adult	Trafford			53	21.1	F	
121	Sub adult	Lochloosa	29.49606	82.15151	60.8	24.8	F	Normal
122	Sub adult	Trafford	26.44522	81.50496	73.5	31	F	
123	Sub adult	Lochloosa	29.49698	82.15193	63.3	26.8	M	Normal
124	Sub adult	Trafford			70.5	29.8	F	
126	Sub adult	WCA2A	26.25162	80.35273	57.7	21.4	M	Fat
127	Sub adult	WCA2A	26.31329	80.51933	89	35.5	F	Normal
128	Sub adult	WCA2A	26.31872	80.52338	84	32	F	Normal
129	Sub adult	Lochloosa	29.5037	82.13558	76.1	33.3	F	Normal
131	Sub adult	WCA3A	26.08386	80.58608	53.9	21.2	M	
132	Sub adult	WCA2A	26.28417	80.49675	47.5	21	M	
133	Sub adult	Trafford	26.43592	81.49872	66.2	27.5	F	
137	Sub adult	Trafford			84	36	M	
138	Sub adult	Trafford			62	25.1	F	
140	Sub adult	WCA2A	26.25	80.35	88	34.4	F	
141	Sub adult	WCA2A	26.2424	80.46444	81.3	31	M	Normal
142	Sub adult	WCA3A	26.08318	80.5856	82.9	30.1	M	Skinny
143	Sub adult	Trafford			52.6	21.7	M	
145	Sub adult	WCA2A	26.29182	80.50263	54	23	M	Normal
146	Sub adult	Trafford	26.41333	81.49485	86.9	36.7	F	
147	Sub adult	WCA2A	26.27773	80.49171	66	26.5	F	
150	Sub adult	WCA3TC	25.76799	80.67432	63.6	24.1	F	Normal
151	Sub adult	WCA3TC	25.76229	80.73094	89.4	34.1	M	Normal
152	Sub adult	WCA2A	26.21894	80.39484	87	37.4	F	Fat
153	Sub adult	WCA2A	26.26769	80.48404	62	26.5	F	
154	Sub adult	Trafford	26.43591	81.49876	50.6	20	F	
155	Sub adult	WCA2A	26.22204	80.36691	78.6	33.5	F	Normal
156	Sub adult	WCA2A	26.22153	80.37025	88	36.1	M	Normal
157	Sub adult	Trafford	26.42814	81.50672	55.8	22.2	F	
158	Sub adult	WCA3A	26.2153	80.6891	68.2	29.4	F	Normal
159	Sub adult	WCA3TC	25.76232	80.77415	43.9	16.5	M	Normal
160	Sub adult	Lochloosa	29.50696	82.15018	47.4	17.1	F	
162	Sub adult	St. Johns River	28.18673	80.81025	79	35.5	M	
163	Sub adult	WCA3A	26.07001	80.57545	81.1	35.9	F	Normal
164	Sub adult	WCA3A	26.2153	80.6891	58.5	28.1	F	Normal
165	Sub adult	St. Johns River	28.17016	80.77918	88	38.5	F	
166	Sub adult	St. Johns River	28.27924	80.83032	59.3	27.3	M	Normal
167	Sub adult	Trafford			71.6	29.6	F	
168	Sub adult	St. Johns River	28.17359	80.78397	74	31.5	F	
169	Sub adult	St. Johns River	28.32151	80.82274	47.7	21.6	F	Normal
172	Sub adult	St. Johns River	28.34319	80.8605	86	38.3	F	Normal
173	Sub adult	WCA3A	26.18148	80.66319	78.2	32.8	F	Normal
174	Sub adult	St. Johns River	28.31413	80.81099	74	32.4	M	Normal
175	Sub adult	St. Johns River	28.12829	80.7293	58.5	24	M	
176	Sub adult	WCA3A	26.2067	80.68246	88.6	37.8	M	Normal
177	Sub adult	St. Johns River	28.11732	80.74285	59	27.5	F	
200	Sub adult	Lochloosa	29.54097	82.11636	56.5	24	M	
201	Sub adult	Lochloosa	29.53981	82.11717	55.9	23	M	
202	Sub adult	Lochloosa	29.54358	82.14153	63	24.9	F	
203	Sub adult	Lochloosa	29.53883	82.11568	72.1	32	M	Normal
205	Sub adult	Lochloosa	29.54031	82.14304	76	34.5	F	
206	Sub adult	Lochloosa	29.53772	82.14436	54.8	21.5	M	
207	Sub adult	Lochloosa	29.53514	82.14535	62.1	26.8	M	
208	Sub adult	Lochloosa	29.49885		62	25.3	F	
MUSC 401	Adult	Ace Basin			135.6	55.5	F	
MUSC 403	Adult	Ace Basin			117.9	52.6	M	
MUSC 404	Adult	Ace Basin	32.59325	80.46284	126	51	F	
MUSC 405	Adult	Ace Basin	32.61375	80.44407	136	66.8	F	
MUSC 406	Adult	Ace Basin	32.61266	80.43929	102	46.5	M	
MUSC 408	Adult	Ace Basin	32.61692	80.44339	131	58.2	F	

Animal #	Age Class	Location	Latitude-DD (N)	Longitude- DD (W)	SV Length (cm)	Tail Girth (cm)	Sex (M/F)	Condition
MUSC 409	Adult	Ace Basin	32.61673	80.44018	164.6	81	M	
MUSC 410	Adult	Ace Basin	32.6251	80.43762	162.2	70.8	F	
MUSC 411	Adult	Ace Basin	32.62506	80.43763	87.2	36.8	M	
MUSC 412	Adult	Ace Basin	32.62961	80.42308	154.2	72.6	M	
MUSC 413	Adult	Ace Basin	32.62959	80.42308	133.5	59.8	M	
MUSC 414	Adult	Ace Basin	32.62962	80.42306	128	54.2	M	
MUSC 417	Adult	Ace Basin	32.63024	80.41964	103.5	43	M	
MUSC 416	Adult	Ace Basin	32.63024	80.41966	155	69.5	M	
MUSC 420	Adult	Ace Basin	32.64208	80.41525	120	51	M	
MUSC 421	Adult	Ace Basin	32.642	80.41565	109	45.5	F	
MUSC 423	Adult	Ace Basin	32.64175	80.42363	134	62.5	F	
MUSC 424	Adult	Ace Basin	32.64273	80.42924	112	46.4	M	
MUSC 426	Adult	Ace Basin	32.64367	80.42915	80.2	35.6	M	
MUSC 427	Adult	Ace Basin	32.64888	80.4258	84.5	36.5	F	
MUSC 428	Adult	Ace Basin	32.64887	80.42579	121.6	52	M	
MUSC 429	Adult	Ace Basin	32.64901	80.42562	117.2	51.5	F	
MUSC 442	Adult	Ace Basin			168	85	M	

DD denotes the decimal degrees format for GPS points

Tissue sample collection

At Lochloosa, St. John's River, Trafford, WCA2A and WCA3A 37 alligators were opportunistically necropsied after having a blood samples taken. The three most anterior caudal scutes (designated A, B and C) were removed at their base/dorsal surface of the tail with a stainless-steel knife. Each scute was placed in an individual Whirlpack (Nasco Lot; #30281). The muscle sample was collected between the 3rd and 6th caudal whorls using a stainless-steel scalpel or knife. A 'deep filet' was taken by removing the hide from beneath the skin to reach the center of the tail muscle. Approximately 300 g of muscle tissue was removed and separated into three individual Whirlpacks. Liver was collected from the right lobe with a stainless-steel scalpel or knife. Approximately 300 g was removed and separated into individual Whirlpacks. Lung was collected from the lower right lobe with a stainless-steel scalpel or knife. Approximately 300 g was removed and separated into individual Whirlpacks. The brain and spinal cord were collected with stainless steel forceps and placed into a 2 mL Cryovial. The entire heart was collected and placed into a Teflon bag. All samples were placed on wet ice upon removal from the animal and kept in that condition for no more than 5 h, until they were placed into a liquid nitrogen vapor freezer for transport and a -80 °C freezer for long term storage.

Preliminary tissue experiments

Prior to experimentally analyzing the alligator tissue samples for the suite of trace elements, preliminary experiments were conducted to determine the most appropriate method of preparation and set of tissues to use to answer the questions we were interested in. Mercury was used as the model trace element in these analyses, as it requires less sample preparation and is a faster measurement than the other trace elements. Scute

tissues were analyzed to determine if mercury is homogeneously deposited across the scute surface and if only a single scute could be used to consistently and accurately determine the mercury concentration of the alligator. After the scute experiment was conducted, a suite of tissues known to be target organs for mercury accumulation were analyzed to determine which tissues had mercury concentrations that were statistically related to each other, as well as the blood samples, for the determination of which tissues to use for the biodistribution of trace elements study.

2.3.2.1. Preliminary scute analysis

Scute processing & homogenization

The three most anterior caudal scutes were removed at their base/dorsal surface of the tail with a stainless-steel knife. Each scute was placed into an individual Whirl-Pak (Nasco Lot; #30281), placed on wet ice upon removal from the animal for no more than 5 h and stored at -80 °C. A homogeneity experiment was conducted to determine how mercury is deposited into the keratin of the scutes. The three scutes from each alligator were cut into small pieces (approximately 100 mg each) and analyzed for total mercury (Figure 2.3).

Instrumental method

The mass fraction of mercury was determined with a DMA-80. The sample size utilized for each measurement was approximately 0.10 g, if the mercury content of the scutes exceeded the calibration range; the weight was reduced by 50 %, then 75 %, if necessary. Each scute was cut into ten to fourteen pieces, weighing approximately 0.1 g, for a total of 115 experimental samples. The procedural blanks for the analysis of mercury and field blanks for the analysis of mercury were measured concurrently with

the samples. The field blanks were made by rinsing the Whirl-Pak (Nasco; Lot#30281) sampling bags and #10 surgical steel scalpel blades (Miltex; Lot#S12J01) with Milli-Q water to emulate the processing and storage conditions of the samples. All samples collected were corrected for the average amount of mercury detected in the field blanks. The standard reference material QC03LH03 (Pygmy Sperm Whale Liver Homogenate, Quality Control Material) was run as a control and was not blank corrected, as the procedural blanks had no detectable mercury.

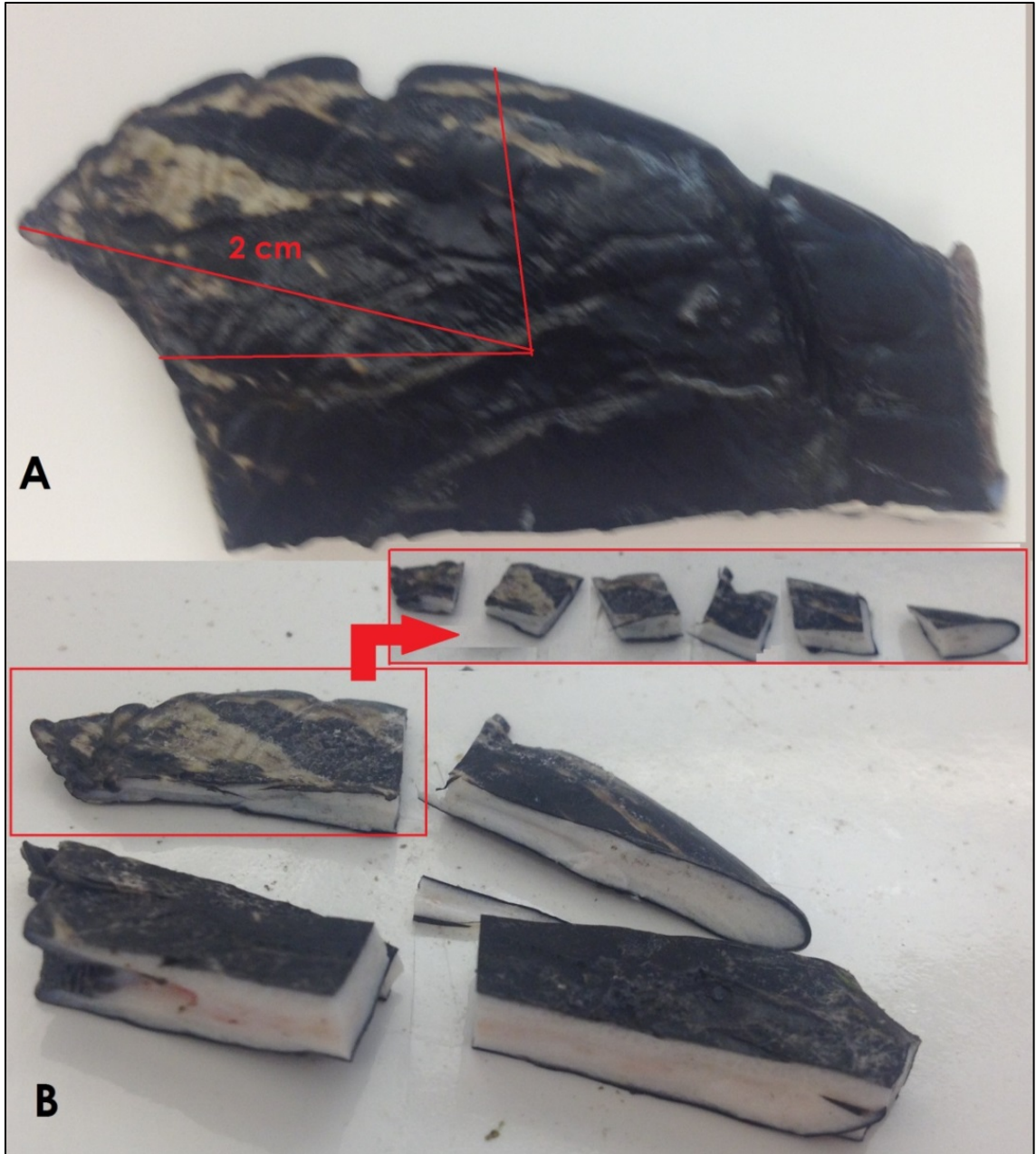


Figure 2.3. The posterior section of caudal scute that was used to standardize the total Hg comparisons is highlighted in red (A). The 2 cm section was then cut into smaller pieces of equal size, to determine variation and concentration across that portion of the scute (B). The anterior portion that was not used in the final analysis is to the right of the red box.

Results

The variability of the mercury deposition in keratin is evident in the total concentration for each scute, as well as in the anterior and posterior 2 cm sections of each scute (Table 2.3, Figure 2.4). The anterior (front) section of the scute is suspected to increase the variability of the entire scute due to the amount of connective tissue that is inside the scute in that portion, as demonstrated by the relative standard deviation, which was 25 % across three scutes from one alligator (Figure 2.4). When the posterior (back) 2 cm sections were analyzed, without the front portion, the total mercury concentrations were much less variable among the three scutes for each alligator (Figure 2.4). The relative standard deviation of mercury determined in the posterior/back 2 cm sections from three scutes of the same alligator was 16 %, which is still highly variable. Hence, the decision was made to cryohomogenize the back 2 cm portions from each of the three scutes collected from the animals and analyze the homogenate as opposed to analyzing the scutes individually to reduce variability, which could be caused by differences in deposition in this tissue as well as abrasive action of the animal.

The caveat to this experiment is that tail scutes in subadult alligators can be smaller than those from adult alligators. This experiment was only conducted using adult scutes, and analyzing those from smaller subadult animals may incorporate more of the connective tissue that the 2 cm delineation attempted to avoid. This caveat could increase the variability in the mercury measurements for sub-adult scutes used. However, for the main experiment, all scutes were large enough to remove the posterior 2 cm section for homogenization and analysis. If the scutes are not large enough to remove a 2 cm section without removing the thicker pieces of connective tissue, we suggest that removing the

top 60% and left 45% of the scute in the upper left corner. These are the proportions of the 2 cm adult scute section, and we propose that this will remove additional variation in the measurement of smaller scutes.

Table 2.3. The total Hg concentration results from the preliminary scute experiment.

Sample ID	[Hg] µg/g	Sample ID	[Hg] µg/g	Sample ID	[Hg] µg/g
Gator66 Sc-B piece 1	2.62	Gator 064 scute C piece 10	2.93	Gator 065 scute B piece 11	1.00
Gator66 Sc-B piece 2	3.04	Gator 064 scute C piece 11	1.82	Gator 065 scute B piece 12	1.25
Gator66 Sc-B piece 3	3.52	Gator 064 scute C piece 12	2.41	Gator 065 scute B piece 13	1.16
Gator66 Sc-B piece 6	4.34	Gator 064 scute C piece 13	2.44	Gator 065 scute B piece 14	1.30
Gator66 Sc-B piece 4	4.58	Gator 064 scute C piece 14	2.09	Gator 065 Scute C piece 1	27.46
Gator66 Sc-B piece 4b	4.46	Gator 064 scute B piece 1	3.36	Gator 065 Scute C piece 2	1.44
Gator66 Sc-B piece 5	3.83	Gator 064 scute B piece 2	1.29	Gator 065 Scute C piece 3	1.36
spongy tissue	2.05	Gator 064 scute B piece 3	2.20	Gator 065 Scute C piece 4	1.46
skin-keratin	2.17	Gator 064 scute B piece 4	2.42	Gator 065 Scute C piece 5	1.24
gator66scuteC piece 01	3.37	Gator 064 scute B piece 5	2.83	Gator 065 Scute C piece 6	1.45
gator66scuteC piece 02	3.08	Gator 064 scute B piece 6	4.03	Gator 065 Scute C piece 7	1.06
gator66scuteC piece 03a	3.01	Gator 064 scute B piece 7	3.94	Gator 065 Scute C piece 8	1.16
gator66scuteC piece 03b	2.93	Gator 064 scute B piece 8	2.73	Gator 065 Scute C piece 9	1.21
gator66scuteC piece 04	3.10	Gator 064 scute B piece 9	2.75	Gator 065 Scute C piece 10	1.14
gator66scuteC piece 05	3.08	Gator 064 scute B piece 10	2.57	Gator 065 Scute C piece 11	1.17
gator66scuteC piece 06	3.15	Gator 064 scute B piece 11	2.34	Gator 065 Scute C piece 12	1.25
gator66scuteC piece 07	2.58	Gator 064 scute B piece 12	2.31	Gator 065 Scute C piece 13	1.36
gator66scuteC piece 08	2.28	Gator 064 scute B piece 13	1.60	Gator 065 Scute C piece 14	1.48
gator66scuteC piece 09	2.03	Gator 064 scute B piece 14	1.59	Gator 065 Scute D piece 1	1.66
gator66scuteC piece 10	2.22	Gator 064 scute B piece 15	1.90	Gator 065 Scute D piece 2	1.45
gator66scuteC piece 11	2.27	Gator 064 scute B piece 16	2.41	Gator 065 Scute D piece 3	1.42
gator66scuteC piece 12	2.84	Gator 064 scute D piece 1	3.11	Gator 065 Scute D piece 4	1.26
gator66scuteD piece 1	3.91	Gator 064 scute D piece 2	3.37	Gator 065 Scute D piece 5	1.22
gator66scuteD piece 2	2.46	Gator 064 scute D piece 3	2.99	Gator 065 Scute D piece 6	1.12
gator66scuteD piece 3	3.01	Gator 064 scute D piece 4	2.91	Gator 065 Scute D piece 7	1.06
gator66scuteD piece 4	2.13	Gator 064 scute D piece 5	3.18	Gator 065 Scute D piece 8	1.07
gator66scuteD piece 5	2.60	Gator 064 scute D piece 6	3.22	Gator 065 Scute D piece 9	1.07
gator66scuteD piece 6	2.65	Gator 064 scute D piece 7	2.59	Gator 065 Scute D piece 10	1.22
gator66scuteD piece 7	2.13	Gator 064 scute D piece 8	2.97	Gator 037 scute B piece 1	2.18
gator66scuteD piece 8	2.31	Gator 064 scute D piece 9	2.55	Gator 037 scute B piece 2	2.08
gator66scuteD piece 9	2.04	Gator 064 scute D piece 10	2.47	Gator 037 scute B piece 3	2.29
gator66scuteD piece 10	2.50	Gator 064 scute D piece 11	2.53	Gator 037 scute B piece 4	2.54
gator66scuteD piece 11	2.47	Gator 064 scute D piece 12	1.97	Gator 037 scute B piece 5	2.25
gator66scuteD piece 12	2.85	Gator 064 scute D piece 13	2.04	Gator 037 scute B piece 6	2.15
gator66scuteD piece 13	3.14	Gator 064 scute D piece 14	2.11	Gator 037 scute B piece 7	2.39
gator66scuteD piece 14	3.68	Gator 065 scute B piece 1	0.91	Gator 037 scute B piece 8	3.01
Gator 064 scute C piece 1	5.19	Gator 065 scute B piece 2	0.93	Gator 037 scute C piece 1	3.11
Gator 064 scute C piece 2	4.02	Gator 065 scute B piece 3	0.95	Gator 037 scute C piece 2	2.58
Gator 064 scute C piece 3	4.23	Gator 065 scute B piece 4	0.96	Gator 037 scute C piece 3	2.60
Gator 064 scute C piece 4	3.30	Gator 065 scute B piece 5	1.01	Gator 037 scute C piece 4	2.21
Gator 064 scute C piece 5	3.28	Gator 065 scute B piece 6	1.02	Gator 037 scute C piece 5	2.50
Gator 064 scute C piece 6	3.17	Gator 065 scute B piece 7	1.05	Gator 037 scute C piece 6	2.72
Gator 064 scute C piece 7	2.68	Gator 065 scute B piece 8	1.08	Gator 037 scute D piece 1	3.22
Gator 064 scute C piece 8	2.01	Gator 065 scute B piece 9	1.01	Gator 037 scute D piece 2	2.64
Gator 064 scute C piece 9	2.50	Gator 065 scute B piece 10	0.95	Gator 037 scute D piece 3	2.83
Gator 37 scute D piece 4	3.00	Gator 037 scute D piece 7	2.49	Gator 037 scute D piece 6	2.77
Gator 37 scute D piece 5	3.06	Gator 037 scute D piece 8	2.28		

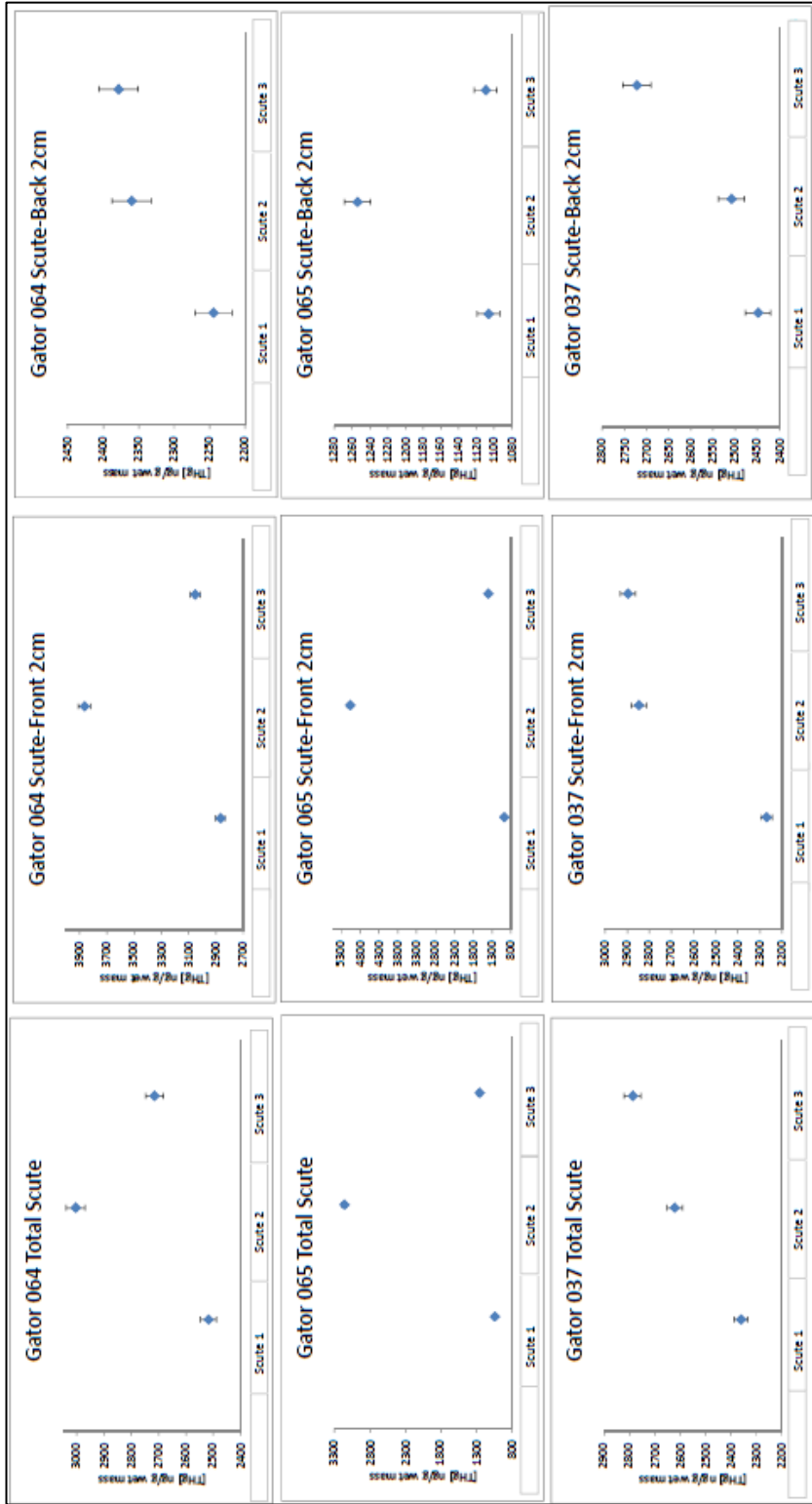


Figure 2.4. The results for the Hg analysis of three different scutes from three adult American alligators collected in Florida, demonstrating the variation in total Hg between individual scutes, as well as variation within scutes. The error bars represent the standard deviation of all pieces measured of each scute or scute section. Samples were consumed upon analysis, so replicate samples were not possible.

2.3.2.2. Preliminary organ tissue analysis

Organ processing & homogenization

The three most anterior caudal scutes were processed as described above and pooled for one scute sample. The muscle sample was collected between the 3rd and 6th caudal whorls using a stainless-steel scalpel or knife. A 'deep filet' of muscle tissue of approximately 300 g was collected by removing the hide from beneath the skin to reach the center of the tail muscle and placed into a Teflon jar. Approximately 300 g of liver tissue was collected from the right lobe with a stainless-steel scalpel or knife. The entire heart was collected using a stainless-steel scalpel blade and placed in a Teflon bag. Approximately 300 g of lung tissue was collected from the bottom left section of the left lung and placed in a Teflon jar. The central nervous system, consisting of the brain and spinal cord was collected with stainless steel forceps and a scalpel blade and placed into a Teflon jar. All samples were stored in a liquid nitrogen vapor shipper upon removal from the animal for no more than 24 h and were placed into a -80 °C freezer for long term storage.

Prior to analysis, the tissue samples were removed from the Teflon jars and placed into Teflon bags. The Teflon bag containing the sample was placed into a cryocart (Chart Industries) and brought down to cryogenic temperatures (below -150 °C) by use of liquid nitrogen vapor. The samples were then removed from the cryocart and broken into smaller pieces for homogenization using a Teflon wrapped hammer. The smaller pieces were then homogenized using a cryomill benchtop homogenizer (Retsch), maintained at -150 °C the entire time. The homogenized tissue was then aliquoted into 2 mL cryovials (Corning; Lot #00612002) and placed in a -80 °C freezer until analysis.

Instrumental method

The determination of mercury was identical to the preliminary scute analysis with a DMA-80. The sample size utilized for each measurement was approximately 0.10 g, for a total of 38 experimental samples. The instrumental ($n = 11$) and procedural blanks ($n = 2$) for the analysis of mercury were measured concurrently with the samples. The procedural blanks made with 8 mL Milli-Q water to mimic the processing of the samples, aliquots of approximately 0.10 g were run alongside the unknown samples. The reference and standard materials were blank corrected since the concentrations of the procedural blanks were detectable (average total mercury concentration = 0.0016 ng/g).

Results

The total mercury fraction measurements for all tissues included in this experiment are presented in Table 2.4. To determine which tissues should be utilized for the main experiment, the total mercury fractions from each tissue were compared using the Pearson product moment correlation. There was positive and statistically significant correlation between all organs measured for total mercury concentration (Table 2.5). This analysis demonstrated that the total mercury concentration in different organ samples from the same animal was correlated. This relationship has been previously observed, and hence was expected. However, this is the first data set of this type to be measured, and the first to demonstrate a statistically significant parametric correlation between tissues from the same animal. The relationships determined in this analysis demonstrate that the total mercury concentration, in many of the tissues of the same animals, is correlated (Table 2.5). Based on these results and the number of correlations observed, the subset of tissues that were chosen in the final experiment were scute and blood, since they are both

non-invasive samples that can be routinely collected; muscle, since this tissue is a target of human consumption; and liver, since it has been historically measured for mercury concentration and other contaminants. The other internal organs that were tested here; heart, lung, and CNS, were not included in the main experiment since they are seldom sampled but were tested initially since they are known target organs for mercury accumulation.

Table 2.4. Total Hg fractions from American alligator tissues collected in Florida in 2014.

Name	[Hg] mg/kg
FL Hg 2014 Blank 01	0
FL Hg 2014 Blank 02	0
Kissimmee Blood	0.3
Kissimmee CNS	0.2
Kissimmee Heart	0.3
Kissimmee Liver	7.6
Kissimmee Lung	0.2
Kissimmee Muscle	0.3
Kissimmee Scute	0.7
St Johns River Blood	0.2
St Johns River CNS	0.1
St Johns River Heart	0.1
St Johns River Liver	3.4
St Johns River Lung	0.1
St Johns River Muscle	0.2
St Johns River Scute	0.3
Trafford Blood	0.5
Trafford CNS	0.3
Trafford Heart	0.3
Trafford Liver	4.4
Trafford Lung	0.2
Trafford Scute	0.8
Trafford Muscle	0.5
WCA2A Blood	2.3
WCA2A CNS	2.1
WCA2A Heart	1.3
WCA2A Liver	15.2
WCA2A Lung	0.8
WCA2A Muscle	1.7
WCA2A Scute	3.1
WCA3A Blood	1.6
WCA3A CNS	2.1
WCA3A Heart	1.6
WCA3A Liver run3	39.7
WCA3A Lung run2	0.8
WCA3A Muscle	2.1
WCA3A Scute	3.2

Table 2.5. American alligator tissue mercury concentration preliminary study ($n = 5$). The relationships between organs are demonstrated using the Pearson product moment correlation and the associated correlation coefficient and calculated p-value ($\alpha = 0.05$) (JMP 11, Cary, NC). The bold text indicates relationships that are statistically significant.

Comparison		Pearson Correlation Coefficient	<i>p</i> -value
(Lung)log10	(CNS)log10	1.000	< 0.01
(Lung)log10	(Heart)log10	0.995	< 0.01
(CNS)log10	(Blood)log10	0.994	< 0.01
(Heart)log10	(CNS)log10	0.993	< 0.01
(Lung)log10	(Blood)log10	0.993	< 0.01
(Heart)log10	(Blood)log10	0.976	< 0.01
(Scute)log10	(CNS)log10	0.974	0.01
(Scute)log10	(Lung)log10	0.972	0.01
(Muscle)log10	(Heart)log10	0.969	0.01
(Scute)log10	(Heart)log10	0.967	0.01
(Muscle)log10	(Lung)log10	0.964	0.01
(Scute)log10	(Blood)log10	0.960	0.01
(Muscle)log10	(CNS)log10	0.959	0.01
(Muscle)log10	(Blood)log10	0.949	0.01
(Scute)log10	(Liver)log10	0.940	0.02
(Liver)log10	(Heart)log10	0.919	0.03
(Lung)log10	(Liver)log10	0.898	0.04
(Liver)log10	(CNS)log10	0.896	0.04
(Scute)log10	(Muscle)log10	0.879	0.05
(Liver)log10	(Blood)log10	0.848	0.07
(Muscle)log10	(Liver)log10	0.824	0.09

2.3.2.3. Experimental tissue processing

After the preliminary experiments were completed, 37 alligators were used in the main tissue experiment, with their metadata presented in Table 2.6. This experiment evaluates a suite of 16 detectable trace elements in alligator blood samples, namely, Al, V, Cr, Mn, Ni, Co, Cu, Zn, As, Se, Rb, Sr, Mo, Cd, Sn, Pb, and Hg, to determine the potential elements of environmental concern. Samples were prepared following the method described in section 2.3.2.2 for soft tissues, and section 2.3.2.1 for blood samples. The homogenized soft tissues were aliquoted into 2 mL cryovials (Corning; Lot #00612002), 20 mL glass scintillation vials (Wheaton; Lot#W8070E) and 30 mL polypropylene jars (Nalgene) for long term storage in a -80 °C freezer until analysis.

Control materials- mercury analysis

SRM 955c Levels 2 and 3 (Toxic Metals in Caprine Blood) were obtained from the NIST Office of Reference Materials (ORM) for use as a control material. SRM 955c was chosen for the similarity of the matrix to that of the whole blood samples. The results of the mercury analysis of the control materials are presented in Table 2.7.

QC03LH03 (Pygmy Sperm Whale Liver Homogenate Quality Control Material) and SRM 1946 (Lake Superior Fish Tissue) were run as control materials for the tissue samples. Ideally, when utilizing standard bracketing for quantitative determinations, the control materials are matrix matched and have a range of analyte mass fractions within which, the experimental samples fall. The high concentration of mercury in QC03LH03 as well as the matching matrix for the liver samples determined its use in this project. Both the mercury concentration and the matrix matched muscle homogenate of the SRM

1946 lead to its use in this experiment. The mercury analysis results of these SRM materials are listed in Table 2.8.

Blanks

The procedural blanks and field blanks for the analysis of mercury were measured concurrently with the samples. The field blanks for the blood samples were made by ‘collecting’ a sample of Milli-Q water with the 2.54 cm 18.5 gauge needles (Becton Dickinson) and 60 mL Luer lock syringes (Becton Dickinson) or 20 mL Luer lock syringes (Becton Dickinson) for adults and sub-adults, respectively. Samples were transferred from the syringe to lithium-heparin blood collection tubes (Becton Dickinson) and then aliquoted into Cryovials (Corning) for freezing and analysis. The field blanks for the tissue samples were made by rinsing the Whirlpack (2-oz., 3"W x 5"L x 2-1/4mil thick, polyethylene; Nasco; Lot#30281) sampling bags and #10 surgical steel scalpel blades (Miltex; Lot#S12J01) with Milli-Q water to mimic the processing and storage conditions of the samples. All samples that were collected using the respective packages were corrected for that average amount of mercury detected. The reference and standard materials were not blank corrected since the concentrations of the procedural blanks were not detectable.

Statistical analysis

The data from the total mercury analysis had a normal distribution and was homoscedastic under a \log_{10} transformation. Since the assumptions of parametric statistics were met, the Pearson Product Moment Correlation was used to determine the relationship between the tissues analyzed using JMP 11 software (SAS Institute Inc., Cary, NC).

Sample preparation- trace element analysis

Single sub-samples were analyzed following the description in section 2.2.2. Briefly, Sc, Y, Ru, Rh, and Bi (1000 mg/mL) were added as internal standards by accurately weighing by difference 0.25 g into the digestion vessel, followed by the addition of 3.5 mL of nitric acid. The Teflon CEM microwave digestion vessels were then closed and run in the manner described in section 2.2.1.

Blanks

In addition to the samples and controls, field blanks using Cryovials ($n = 2$), and procedural blanks ($n = 7$) containing an aliquot of internal standard, were carried through the entire sample processing and measurement scheme. The overall mean of the field blank measurements was found to be below the limits of detection for all elements except cobalt (120 ng/g), zinc (133 ng/g) and lead (0.2 ng/g) and therefore the sample measurement data were field blank corrected for those elements. The overall mean of the procedural blank measurements was found to be below the limits of detection for all elements except aluminum (0.6 ng/g), cobalt (1.0 ng/g), zinc (1.3 ng/g), rubidium (0.3 ng/g), molybdenum (0.1 ng/g) and lead (0.01 ng/g) and therefore the sample measurement data were procedural blank corrected for those elements.

Table 2.6. The metadata associated with the America alligators used for the tissue comparisons in this study.

The locations correspond to locations on the map in Figure 2.1.

Gator #	Location	Age Class	SVL (cm)	Sex
Gator 016	St. Johns River	Adult	96	Female
Gator 020	St. Johns River	Adult	135.6	Female
Gator 023	St. Johns River	Adult	126	Female
Gator 026	Lochloosa	Adult	144	Female
Gator 031	Trafford	Adult	99	Male
Gator 039	Trafford	Adult	153.5	Male
Gator 041	Trafford	Adult	90	Male
Gator 042	Trafford	Adult	139.9	Male
Gator 044	Trafford	Adult	140.2	Male
Gator 045	Trafford	Adult	109	Male
Gator 047	Trafford	Adult	153	Male
Gator 049	Trafford	Adult	105	Female
Gator 050	Trafford	Adult	92	Male
Gator 053	Trafford	Adult	93	Female
Gator 056	Trafford	Adult	142	Male
Gator 060	Lochloosa	Adult	105.5	Female
Gator 113	WCA3A	Sub Adult	82	Female
Gator 119	WCA3A	Sub Adult	74.3	Female
Gator 120	Trafford	Sub Adult	53	Female
Gator 122	Trafford	Sub Adult	73.5	Female
Gator 126	WCA2A	Sub Adult	57.7	Male
Gator 127	WCA2A	Sub Adult	89	Female
Gator 132	WCA2A	Sub Adult	47.5	Male
Gator 133	Trafford	Sub Adult	66.2	Female
Gator 137	Trafford	Sub Adult	84	Male
Gator 142	WCA3A	Sub Adult	82.9	Male
Gator 143	Trafford	Sub Adult	52.6	Male
Gator 145	WCA2A	Sub Adult	86.9	Female
Gator 150	WCA3A	Sub Adult	63.6	Female
Gator 151	WCA3A	Sub Adult	89.4	Male
Gator 156	WCA2A	Sub Adult	88	Male
Gator 158	WCA3A	Sub Adult	68.2	Female
Gator 159	WCA3A	Sub Adult	43.9	Male
Gator 164	WCA3A	Sub Adult	58.5	Female
Gator 167	Trafford	Sub Adult	71.6	Female
Gator 176	WCA3A	Sub Adult	88.6	Male

Control materials – trace element analysis

The trace metal SRMs listed in section 2.2.2 were used to construct calibration curves, NIST SRM 1577c Bovine Liver was used as a control material that matched the matrix of the experimental tissues samples. Seronorm was used as a control material for the blood samples. The mass fractions measured for the control materials Seronorm and, SRM 1577c, are listed in Table 2.9 and 2.10, together with the calculated RSDs. The mean values agreed with the certified value within the stated uncertainties.

Statistical analysis

The elements that were found to be above the limit of detection for this method did not demonstrate a normal distribution or equal variances across the population of alligators sampled. A \log_{10} transformation did not improve either assumption for all elements. Since the assumptions of parametric statistics were not met, the non-parametric Spearman Correlation was used.

Table 2.7. The summaries of the total mercury results for the SRM 955c (Toxic Metals in Caprine Blood) used with the alligator blood samples in Experiment 2.2.

SRM 955c Level 3 was used with two different calibration curves for the samples from Florida, SRM 955c Level 2 was used with the samples from South Carolina. The certified values of the SRMs 955c Level 2 and 3 are $4.95 \pm 0.76 \mu\text{g/kg}$ and $16.9 \pm 1.5 \mu\text{g/kg}$, respectively.

SRM955c level 3		[Hg] mg/kg	SRM955c level 3		[Hg] mg/kg	SRM 955C Level 2 Replicates		[Hg] mg/kg
1 SRM 1641d Low Cal Curve		20.7	1 SRM 3133 Cal Curve		17.5	SRM 955C Level 2 run 01		5.3
2 SRM 1641d Low Cal Curve		19.9	2 SRM 3133 Cal Curve		17.5	SRM 955C Level 2 run 02		5.4
3 SRM 1641d Low Cal Curve		21.3	3 SRM 3133 Cal Curve		18.6	SRM 955C Level 2 run 03		5.2
4 SRM 1641d Low Cal Curve		21.2	4 SRM 3133 Cal Curve		18.5	SRM 955C Level 2 run 04		5.2
5 SRM 1641d Low Cal Curve		19.5	5 SRM 3133 Cal Curve		16.7	SRM 955C Level 2 run 05		5.3
6 SRM 1641d Low Cal Curve		18.9	6 SRM 3133 Cal Curve		16.7	SRM 955C Level 2 run 06		5.4
7 SRM 1641d Low Cal Curve		19.3	7 SRM 3133 Cal Curve		16.7	SRM 955C Level 2 run 07		5.3
8 SRM 1641d Low Cal Curve		20.6	8 SRM 3133 Cal Curve		17.1	SRM 955C Level 2 run 08		5.3
9 SRM 1641d Low Cal Curve		20.2	9 SRM 3133 Cal Curve		17.0	SRM 955C Level 2 run 09		5.2
10 SRM 1641d Low Cal Curve		19.7	10 SRM 3133 Cal Curve		16.9	SRM 955C Level 2 run 10		5.4
11 SRM 1641d Low Cal Curve		19.2	11 SRM 3133 Cal Curve		17.1	SRM 955C Level 2 run 11		5.1
12 SRM 1641d Low Cal Curve		19.6	12 SRM 3133 Cal Curve		17.1	SRM 955C Level 2 run 12		5.3
13 SRM 1641d Low Cal Curve		19.3	13 SRM 3133 Cal Curve		17.2	SRM 955C Level 2 run 13		5.4
14 SRM 1641d Low Cal Curve		19.7	14 SRM 3133 Cal Curve		17.1	SRM 955C Level 2 run 14		5.3
15 SRM 1641d Low Cal Curve		19.9	15 SRM 3133 Cal Curve		17.1	SRM 955C Level 2 run 15		5.3
16 SRM 1641d Low Cal Curve		19.8	16 SRM 3133 Cal Curve		16.8	SRM 955C Level 2 run 16		5.4
17 SRM 1641d Low Cal Curve		19.0	17 SRM 3133 Cal Curve		17.2			
18 SRM 1641d Low Cal Curve		19.9	18 SRM 3133 Cal Curve		17.0			
19 SRM 1641d Low Cal Curve		20.1	19 SRM 3133 Cal Curve		17.4			
20 SRM 1641d Low Cal Curve		19.5	20 SRM 3133 Cal Curve		17.4			
21 SRM 1641d Low Cal Curve		19.9						
22 SRM 1641d Low Cal Curve		19.7						
23 SRM 1641d Low Cal Curve		19.8						
24 SRM 1641d Low Cal Curve		19.6						
25 SRM 1641d Low Cal Curve		20.8						
Average		19.9	Average		17.2	Average		5.3
Standard Deviation		0.6	Standard Deviation		0.5	Standard Deviation		0.1
%RSD		3.2	%RSD		3.0	%RSD		1.8
U		0.3	U		0.8	U		0.1
Overall SRM955c level 3					[Hg] mg/kg			
Average					18.7			
Standard Deviation					1.5			
%RSD					7.8			
U					0.5			

Table 2.8. The summaries of the total mercury results for the SRM QC03LH3 (Pygmy Sperm Whale Liver) and SRM 1946 (Lake Superior Fish Tissue) used with the alligator tissue samples in Experiment 2.3. SRM QC03LH3 was used with two different sample batches. The certified value of the SRM QC03LH3 is $3,642 \pm 143 \mu\text{g/kg}$ and the certified value of the SRM 1946 is $433 \pm 9 \mu\text{g/kg}$ for total Hg.

QC03LH03 Replicates	[Hg] mg/kg	SRM 1946 Replicates	[Hg] mg/kg	QC03LH03 Replicates	[Hg] mg/kg
SRM QC03 run1	3562.01	SRM 1946 run1	409.87	SRM QC03 run1	3495.47
SRM QC03 run2	3472.14	SRM 1946 run2	408.55	SRM QC03 run2	3491.65
SRM QC03 run3	3452.16	SRM 1946 run3	459.14	SRM QC03 run3	3501.18
SRM QC03 run4	3529.51	SRM 1946 run4	395.06	SRM QC03 run4	3525.99
SRM QC03 run5	3445.07	SRM 1946 run5	418.90	SRM QC03 run5	3512.03
SRM QC03 run6	3554.48	SRM 1946 run6	414.20	SRM QC03 run6	3506.23
SRM QC03 run7	3471.99	SRM 1946 run7	422.00	SRM QC03 run7	3512.45
SRM QC03 run8	3436.28	SRM 1946 run8	397.39	SRM QC03 run8	3479.07
SRM QC03 run9	3496.54	SRM 1946 run9	424.50	SRM QC03 run9	3464.41
SRM QC03 run10	3379.55	SRM 1946 run10	414.26	SRM QC03 run10	3472.04
SRM QC03 run11	3514.91	SRM 1946 run11	454.59	SRM QC03 run11	3442.40
SRM QC03 run12	3468.42	SRM 1946 run12	420.85	SRM QC03 run12	3439.10
SRM QC03 run13	3413.01	SRM 1946 run13	420.01		
SRM QC03 run14	3574.43	SRM 1946 run14	400.97		
SRM QC03 run15	3430.58	SRM 1946 run15	410.19		
SRM QC03 run16	3497.50	SRM 1946 run16	412.72		
SRM QC03 run17	3488.52	SRM 1946 run17	411.58		
SRM QC03 run18	3411.08	SRM 1946 run18	413.74		
SRM QC03 run19	3517.91	SRM 1946 run19	405.54		
SRM QC03 run20	3447.59	SRM 1946 run20	415.95		
SRM QC03 run21	3494.92	SRM 1946 run21	399.03		
SRM QC03 run22	3470.52	SRM 1946 run22	404.90		
SRM QC03 run23	3454.24	SRM 1946 run23	418.93		
SRM QC03 run24	3524.33	SRM 1946 run24	400.24		
SRM QC03 run25	3485.34	SRM 1946 run25	442.61		
SRM QC03 run26	3468.05	SRM 1946 run26	424.42		
SRM QC03 run27	3526.00	SRM 1946 run27	393.37		
		SRM 1946 run28	406.82		
Average	3481.59	Average	415.01	Average	3486.84
Standard Deviation	54.00	Standard Deviation	15.9	Standard Deviation	27.86
%RSD	1.55	%RSD	3.8	%RSD	0.80
U	28.87	U	6.8	U	25.55
Total U for SRM QC03LH03	0.01	Total U for SRM 1946	0.02	Total U for SRM QC03LH03	0.01

Table 2.9. The measured values of Seronorm as a control material throughout the analysis of the Alligator blood samples from Florida and South Carolina.

Seronorm	Al	V	Cr	Mn	Co	Ni	Cu	Zn
Average measured value	96.99	6.69	18.97	42.58	10.45	11.07	2274.44	8215.01
Standard deviation	15.34	2.17	1.06	1.89	0.69	1.71	81.85	477.37
RSD	15.81	32.45	5.59	4.45	6.58	15.46	3.6	5.81
SERO- values certified by manufacturer	99.06	5.38	21.89	44.62	10.75	11.89	2330.19	8462.26
<i>U</i>	19.81	1.04	4.43	8.96	1.13	2.36	235.85	622.64
% Difference	-2.1	21.7	-14.3	-4.7	-2.8	-7.1	-2.4	-3

Seronorm	Se	Rb	Sr	Mo	Cd	Sn	Pb
Average measured value	211.85	1260.33	8.53	6.69	11.05	10.33	410.71
Standard deviation	11.8	47.27	1.04	0.84	0.37	1.7	21.89
RSD	5.57	3.75	12.14	12.52	3.32	16.44	5.33
SERO- values certified by manufacturer	256.6	1273.58	14.15	7.08	11.42	9.25	421.7
<i>U</i>	51.89	14.15	0.19	1.42	1.23	1.13	43.4
% Difference	-19.1	-1	-49.6	-5.7	-3.3	11	-2.6

Table 2.10. The measured values of SRM 1577c as a control material throughout the analysis of the Alligator tissue samples using the ICP-MS. Values are presented in ng/g.

Run	Al	V	Cr	Mn	Co	Cu	Zn	Se	Rb	Mo	Cd	Sn	Pb
SRM1577c-1	250.6	9.3	48.8	9493.2	259.0	260038.8	188064.6	2263.5	27326.5	3482.0	102.2	28.9	55.1
SRM1577c-2	263.3	8.9	47.7	11274.9	268.9	306650.2	228362.9	2574.2	33133.2	3942.3	116.6	30.3	63.6
SRM1577c-3	223.2	10.7	51.8	9362.0	275.5	307167.8	190669.9	2408.5	39355.1	3535.9	105.4	28.0	55.4
SRM1577c-4	226.8	9.2	49.8	9367.0	300.0	291096.8	162210.5	2126.2	37116.2	3474.1	100.3	26.0	55.0
SRM1577c-5	234.3	10.0	51.0	9555.2	300.4	293347.0	164689.8	2112.0	37406.0	3480.2	102.1	26.5	57.1
SRM1577c-6	224.9	11.2	51.2	9220.1	305.3	302326.9	176380.0	2129.2	37678.3	3507.5	104.3	27.3	53.7
SRM1577c-7	242.6	6.6	41.8	9821.0	338.2	296855.2	166960.9	2048.8	38526.2	3481.8	104.5	26.3	60.4
SRM1577c-8	273.6	8.2	46.7	9766.7	313.4	288062.7	164389.7	2008.6	37437.2	3472.3	106.1	28.0	65.3
Average	242.4	9.3	48.6	9732.5	295.1	293193.2	180216.0	2208.9	35997.3	3547.0	105.2	27.7	58.2
Standard Deviation	17.5	1.4	3.1	613.4	24.3	14156.1	20902.0	181.9	3694.4	150.7	4.7	1.4	4.1
%RSD	7.2	14.6	6.3	6.3	8.2	4.8	11.6	8.2	10.3	4.2	4.4	4.9	7.0
Certified		8.2	53.0	10460.0	300.0	275200.0	181100.0	2031.0	35300.0	3300.0	97.0		62.8
U		0.7	14.0	470.0	18.0	4600.0	1000.0	45.0	1100.0	130.0	1.4		1.0
% Difference	N/A	13.4	-8.3	-7.0	-1.6	6.5	-0.5	8.8	2.0	7.5	8.5	N/A	-7.4

2.3.3. Results & Discussion

Blood samples

The average blood mercury concentrations of alligators in the Florida Everglades were 1.3 mg/kg and 1.5 mg/kg, which are above the FDA safe consumption limit, despite statewide bioremediation efforts, and statistically greater than any other location measured (with standard deviations of 0.7 and 0.6 mg/kg for WCA3A and WCA2A, respectively; Figure 2.5, Table 2.11, 2.12). The central Florida sites are in the range of moderate mercury concentrations, with concentrations averaging between 0.4 mg/kg and 0.2 mg/kg, depending on location (with standard deviations of 0.02 and 0.08 mg/kg for Kissimmee and Trafford, respectively; Table 2.11, 2.12). The northern sites in both Florida and South Carolina are low for mercury contamination with concentration averages around 0.1 mg/kg at all four locations (with standard deviations of 0.07, 0.08, .004 and 0.05mg/kg for Lochloosa, St. Johns River, Yawkey and Ace Basin, respectively, Table 2.12, Figure 2.5). The reference site, Ace Basin, SC had mercury concentrations significantly lower than all other sites, except for Lochloosa, which was also low for mercury (Figure 2.5, Table 2.11, 2.12). The northern sites being significantly lower in mercury contamination suggests that the environmental parameters of the Everglades ecosystem play a large role in the continual accumulation of mercury, despite the reduction of point source emitters (Table 2.12, 2.13). Across all sites, the mercury values that were observed in the alligators were comparable to the human population. The northern and central sites were comparable to the “average” human population with a varied diet (moderate to low mercury sites), and the southern sites were comparable to “native” human populations with a subsistence diet (Everglades high mercury sites) (132,

269). The remaining trace element concentrations (Al, Cu, Zn, As, Se, Rb, Sr, and Pb) were observed to be more consistent, with very little site specific variation (Table 2.11). When all alligators measured were plotted together, it is easy to see that the trace element of concern in this region is mercury (Figure 2.6, 2.7).

Since these blood concentrations were measured in healthy animals, the higher concentrations of mercury measured in the Everglades is not causing observable health effects. To determine if there is a protective element keeping the adverse effects of mercury at bay, the molar ratio of selenium to mercury was calculated for each group. Selenium (Se) has been shown to alleviate some of the deleterious effects of mercury exposure when Se: Hg molar ratios greater than 1 (201, 270, 271). The molar ratio is an estimation based in the antagonistic effects of Se resulting in less bioaccumulation when Se is in excess (272). However, Se has been shown to aid in the redistribution of mercury from the kidney to the muscle, which is problematic for human consumers (271). Selenium is a component of GPX, which is inhibited by mercury when the ratio is less than 1, leading to the depletion of GSH and oxidative damage (271, 272).

All groups of alligators sampled for this study had Se: Hg ratios greater than 1, except adult alligators from the Florida Everglades (Table 2.12). This suggests that while there are no outward effects of chronic mercury exposure in these animals, there is likely a sub-lethal biochemical effect occurring that Se cannot remediate since it is in such low concentrations relative to mercury.

Table 2.11. The trace element data for the American alligator blood samples analyzed in experiment 2.3. All concentrations are provided in ng/g.

Location	Age Class	ID	Al	V	Cr	Mn	Co	Ni	Cu	Zn	As
Ace Basin	Adult	MUSC320	49.9	0.4	<LOD	<LOD	<LOD	<LOD	199.3	1246.8	33.5
Ace Basin	Adult	MUSC401	72.4	0.4	4.0	<LOD	<LOD	<LOD	339.3	684.2	22.0
Ace Basin	Adult	MUSC402	93.2	0.6	<LOD	<LOD	<LOD	<LOD	284.6	973.9	38.4
Ace Basin	Adult	MUSC403	37.0	1.6	<LOD	<LOD	<LOD	<LOD	272.3	651.8	16.9
Ace Basin	Adult	MUSC404	35.7	1.0	<LOD	<LOD	<LOD	<LOD	376.3	554.6	14.2
Ace Basin	Adult	MUSC405	57.3	0.8	<LOD	<LOD	<LOD	<LOD	319.4	1343.6	44.3
Ace Basin	Adult	MUSC406	28.8	3.1	<LOD	<LOD	<LOD	<LOD	360.1	737.0	25.6
Ace Basin	Adult	MUSC408	24.1	<LOD	<LOD	<LOD	<LOD	<LOD	260.0	852.6	22.9
Ace Basin	Adult	MUSC409	44.1	1.9	<LOD	<LOD	<LOD	<LOD	394.1	741.6	32.3
Ace Basin	Adult	MUSC410	25.6	0.6	<LOD	<LOD	<LOD	<LOD	241.9	418.0	19.6
Ace Basin	Adult	MUSC411	36.5	4.8	<LOD	<LOD	<LOD	<LOD	362.7	755.4	59.4
Ace Basin	Adult	MUSC412	53.3	1.5	<LOD	<LOD	<LOD	<LOD	402.0	678.5	15.4
Ace Basin	Adult	MUSC413	37.2	3.3	<LOD	<LOD	<LOD	<LOD	382.8	689.0	27.6
Ace Basin	Adult	MUSC414	21.4	3.0	<LOD	<LOD	<LOD	<LOD	295.7	718.8	25.6
Ace Basin	Adult	MUSC415	55.3	0.6	<LOD	<LOD	<LOD	<LOD	273.5	1224.6	39.0
Ace Basin	Adult	MUSC416	19.6	1.4	<LOD	<LOD	<LOD	<LOD	304.6	622.4	21.3
Ace Basin	Adult	MUSC417	16.1	1.4	<LOD	<LOD	<LOD	<LOD	159.2	286.4	24.6
Ace Basin	Adult	MUSC418	28.7	0.9	<LOD	<LOD	<LOD	<LOD	250.0	786.2	13.7
Ace Basin	Adult	MUSC419	14.6	<LOD	<LOD	<LOD	<LOD	<LOD	167.7	427.7	7.9
Ace Basin	Adult	MUSC420	14.4	2.1	<LOD	<LOD	<LOD	<LOD	254.1	578.5	23.9
Ace Basin	Adult	MUSC421	23.2	1.1	<LOD	<LOD	<LOD	<LOD	275.6	838.9	30.8
Ace Basin	Adult	MUSC422	28.7	2.7	<LOD	<LOD	<LOD	<LOD	375.9	958.9	27.2
Ace Basin	Adult	MUSC423	27.1	0.4	<LOD	<LOD	<LOD	<LOD	202.2	1276.0	35.1
Ace Basin	Adult	MUSC426	22.6	4.9	<LOD	<LOD	<LOD	<LOD	302.0	891.5	35.7
Ace Basin	Adult	MUSC427	55.3	1.8	<LOD	<LOD	<LOD	<LOD	242.0	874.8	18.8
Ace Basin	Adult	MUSC428	49.9	2.5	<LOD	<LOD	<LOD	<LOD	158.8	749.1	16.6
Ace Basin	Adult	MUSC429	32.9	<LOD	<LOD	<LOD	<LOD	<LOD	306.6	785.4	23.3
Ace Basin	Adult	MUSC430	44.1	3.9	<LOD	<LOD	<LOD	<LOD	325.4	873.1	29.8
Ace Basin	Adult	MUSC440	23.5	2.3	<LOD	<LOD	<LOD	<LOD	182.6	773.4	15.6
Ace Basin	Adult	MUSC441	35.9	1.4	<LOD	<LOD	<LOD	<LOD	253.1	862.3	25.3
Ace Basin	Adult	MUSC442	29.9	4.0	<LOD	<LOD	<LOD	<LOD	311.9	947.7	63.5
Ace Basin	Adult	MUSC443	23.6	0.4	<LOD	<LOD	<LOD	<LOD	350.5	873.2	22.6
Ace Basin	Adult	MUSC444	12.9	1.0	<LOD	<LOD	<LOD	<LOD	213.1	771.2	17.9
Ace Basin	Adult	MUSC445	86.5	1.2	<LOD	<LOD	<LOD	<LOD	245.2	922.8	23.2
Ace Basin	Adult	MUSC446	67.5	5.2	<LOD	<LOD	6.5	<LOD	248.6	973.5	23.3
Ace Basin	Adult	MUSC447	46.7	2.8	<LOD	<LOD	<LOD	<LOD	274.9	1060.6	81.2
Ace Basin	Adult	MUSC448	27.8	6.4	<LOD	<LOD	<LOD	<LOD	364.9	1137.4	51.5
Kissimmee	Adult	Gator002	170.5	<LOD	<LOD	<LOD	<LOD	<LOD	321.0	1046.7	14.9
Kissimmee	Adult	Gator004	50.3	<LOD	<LOD	<LOD	<LOD	<LOD	753.2	1365.1	27.2
Kissimmee	Adult	Gator005	21.5	<LOD	<LOD	<LOD	<LOD	<LOD	389.1	1290.5	26.3
Kissimmee	Adult	Gator006	55.3	<LOD	<LOD	<LOD	<LOD	<LOD	221.0	1025.1	24.4
Kissimmee	Adult	Gator009	12.9	<LOD	<LOD	<LOD	<LOD	<LOD	468.8	1501.0	24.4
Kissimmee	Adult	Gator010	57.6	<LOD	<LOD	<LOD	<LOD	<LOD	353.1	1356.8	16.2
Kissimmee	Adult	Gator012	20.7	1.4	<LOD	<LOD	<LOD	<LOD	233.5	862.6	29.6
Kissimmee	Adult	Gator013	14.7	<LOD	<LOD	<LOD	<LOD	<LOD	363.0	1230.0	23.6
Kissimmee	Adult	Gator015	49.0	<LOD	<LOD	<LOD	<LOD	<LOD	331.7	886.9	22.4
Kissimmee	Adult	Gator017	43.7	<LOD	<LOD	<LOD	<LOD	<LOD	440.8	1347.2	27.2
Kissimmee	Adult	Gator018	18.7	<LOD	<LOD	<LOD	<LOD	<LOD	320.4	1399.7	17.7
Kissimmee	Sub-adult	Gator100	18.5	0.4	<LOD	<LOD	<LOD	<LOD	230.5	983.5	10.6
Kissimmee	Sub-adult	Gator101	<LOD	<LOD	<LOD	<LOD	<LOD	<LOD	344.4	1167.9	11.3
Kissimmee	Sub-adult	Gator102	21.7	5.7	<LOD	<LOD	<LOD	<LOD	303.4	1132.5	21.1
Kissimmee	Sub-adult	Gator104	9.4	7.5	<LOD	<LOD	<LOD	<LOD	400.4	1305.6	28.0
Kissimmee	Sub-adult	Gator105	9.6	2.7	<LOD	<LOD	<LOD	<LOD	280.5	1174.8	21.0
Kissimmee	Sub-adult	Gator106	13.7	<LOD	<LOD	<LOD	<LOD	<LOD	504.4	1283.5	14.1
Kissimmee	Sub-adult	Gator107	23.5	7.0	<LOD	<LOD	<LOD	<LOD	230.4	1032.7	20.8
Kissimmee	Sub-adult	Gator109	11.9	6.1	<LOD	<LOD	<LOD	<LOD	219.9	986.2	19.3
Kissimmee	Sub-adult	Gator11	28.2	<LOD	<LOD	<LOD	<LOD	<LOD	131.0	1127.0	23.5
Kissimmee	Sub-adult	Gator110	39.4	6.0	<LOD	<LOD	<LOD	<LOD	255.1	1055.6	18.3
Kissimmee	Sub-adult	Gator112	18.2	5.4	<LOD	<LOD	<LOD	<LOD	355.6	996.0	24.0
Kissimmee	Sub-adult	Gator115	20.4	2.2	<LOD	<LOD	<LOD	<LOD	275.0	1068.5	18.2
Kissimmee	Sub-adult	Gator118	20.7	2.8	<LOD	<LOD	<LOD	<LOD	252.7	1312.9	17.3
Lochloosa	Adult	Gator026	25.0	<LOD	<LOD	<LOD	<LOD	10.9	334.0	1323.2	37.0
Lochloosa	Adult	Gator038	49.0	<LOD	<LOD	<LOD	<LOD	<LOD	350.4	1149.9	21.8
Lochloosa	Adult	Gator046	<LOD	<LOD	<LOD	<LOD	<LOD	<LOD	334.8	1157.2	11.1
Lochloosa	Adult	Gator057	66.3	<LOD	<LOD	<LOD	<LOD	<LOD	404.6	1031.5	20.1
Lochloosa	Adult	Gator060	101.4	<LOD	3.9	<LOD	<LOD	5.2	430.3	1412.9	27.9
Lochloosa	Adult	Gator062	<LOD	3.8	<LOD	<LOD	<LOD	5.3	357.8	1217.0	26.8

Location	Age Class	ID	Al	V	Cr	Mn	Co	Ni	Cu	Zn	As
Lochloosa	Adult	Gator063	<LOD	3.8	<LOD	<LOD	<LOD	<LOD	320.1	1192.5	22.8
Lochloosa	Adult	Gator067	<LOD	<LOD	<LOD	<LOD	<LOD	<LOD	450.0	1112.8	24.8
Lochloosa	Adult	Gator075	35.7	0.1	<LOD	<LOD	<LOD	<LOD	515.6	1165.0	15.7
Lochloosa	Sub-adult	Gator121	30.4	<LOD	<LOD	<LOD	<LOD	<LOD	358.9	731.4	2.1
Lochloosa	Sub-adult	Gator123	42.0	<LOD	<LOD	<LOD	<LOD	<LOD	315.1	938.7	10.6
Lochloosa	Sub-adult	Gator129	60.1	0.8	4.8	<LOD	<LOD	<LOD	239.2	1215.5	13.4
Lochloosa	Sub-adult	Gator160	72.3	6.8	<LOD	<LOD	<LOD	<LOD	347.4	714.2	17.6
Lochloosa	Sub-adult	Gator200	79.4	1.5	<LOD	<LOD	<LOD	<LOD	320.7	1265.6	12.5
Lochloosa	Sub-adult	Gator201	41.3	4.1	<LOD	<LOD	<LOD	<LOD	318.7	931.7	16.5
Lochloosa	Sub-adult	Gator202	49.9	1.2	<LOD	<LOD	<LOD	<LOD	375.6	848.3	10.0
Lochloosa	Sub-adult	Gator203	26.5	1.5	<LOD	<LOD	<LOD	<LOD	345.9	1227.4	13.3
Lochloosa	Sub-adult	Gator205	29.4	1.4	<LOD	<LOD	<LOD	<LOD	249.2	928.7	10.7
Lochloosa	Sub-adult	Gator206	63.2	1.3	<LOD	<LOD	<LOD	<LOD	381.2	965.1	11.5
Lochloosa	Sub-adult	Gator207	43.9	1.4	<LOD	<LOD	<LOD	<LOD	306.0	1180.0	13.6
Lochloosa	Sub-adult	Gator208	43.3	0.6	<LOD	<LOD	<LOD	<LOD	387.7	748.3	10.6
St. Johns River	Adult	Gator003	44.9	<LOD	3.8	<LOD	<LOD	<LOD	376.8	1237.0	116.7
St. Johns River	Adult	Gator007	76.2	<LOD	16.6	<LOD	9.3	27.7	77.6	782.6	39.1
St. Johns River	Adult	Gator014	19.8	4.8	<LOD	<LOD	<LOD	6.0	177.8	646.2	27.9
St. Johns River	Adult	Gator016	55.8	<LOD	4.2	<LOD	<LOD	<LOD	214.6	758.1	19.6
St. Johns River	Adult	Gator019	25.2	<LOD	<LOD	<LOD	<LOD	<LOD	350.9	1143.9	109.1
St. Johns River	Adult	Gator020	16.9	<LOD	<LOD	<LOD	<LOD	<LOD	269.6	1774.1	81.0
St. Johns River	Adult	Gator022	14.7	<LOD	<LOD	<LOD	<LOD	<LOD	381.5	998.5	21.6
St. Johns River	Adult	Gator023	<LOD	<LOD	<LOD	<LOD	<LOD	<LOD	255.6	1020.8	16.3
St. Johns River	Adult	Gator029	36.2	<LOD	<LOD	<LOD	<LOD	<LOD	334.4	872.1	9.5
St. Johns River	Adult	Gator032	82.9	0.6	<LOD	<LOD	<LOD	<LOD	760.3	891.8	26.2
St. Johns River	Adult	Gator033	34.2	5.0	<LOD	<LOD	<LOD	5.6	270.1	813.3	155.9
St. Johns River	Sub-adult	Gator111	20.4	6.6	<LOD	<LOD	<LOD	<LOD	422.2	913.8	21.5
St. Johns River	Sub-adult	Gator116	20.0	2.0	<LOD	<LOD	<LOD	<LOD	294.1	1311.5	18.2
St. Johns River	Sub-adult	Gator117	15.0	6.6	<LOD	<LOD	<LOD	<LOD	308.2	1236.8	21.4
St. Johns River	Sub-adult	Gator162	19.7	6.1	<LOD	<LOD	<LOD	<LOD	260.2	969.5	20.6
St. Johns River	Sub-adult	Gator165	57.5	5.1	<LOD	<LOD	<LOD	<LOD	289.4	1043.6	20.4
St. Johns River	Sub-adult	Gator166	42.6	6.3	<LOD	<LOD	<LOD	6.0	468.4	1069.2	22.3
St. Johns River	Sub-adult	Gator168	24.3	5.9	<LOD	<LOD	<LOD	<LOD	227.9	774.3	19.5
St. Johns River	Sub-adult	Gator172	58.3	6.3	<LOD	<LOD	<LOD	<LOD	293.3	1101.3	19.2
St. Johns River	Sub-adult	Gator174	14.9	5.8	<LOD	<LOD	<LOD	<LOD	307.7	1069.2	20.1
St. Johns River	Sub-adult	Gator175	24.5	5.3	<LOD	<LOD	<LOD	<LOD	296.4	1050.3	20.2
St. Johns River	Sub-adult	Gator177	30.6	6.0	<LOD	<LOD	<LOD	4.7	388.9	1010.4	21.5
Trafford	Adult	Gator031	<LOD	9.0	<LOD	<LOD	<LOD	7.5	340.6	1098.1	35.3
Trafford	Adult	Gator036	105.5	<LOD	<LOD	<LOD	<LOD	<LOD	291.6	937.7	26.2
Trafford	Adult	Gator039	<LOD	1.8	<LOD	<LOD	<LOD	4.8	240.3	734.7	22.5
Trafford	Adult	Gator041	<LOD	<LOD	<LOD	<LOD	<LOD	<LOD	357.0	1248.2	11.2
Trafford	Adult	Gator042	24.8	0.6	<LOD	<LOD	<LOD	4.8	270.2	728.5	23.9
Trafford	Adult	Gator044	<LOD	<LOD	<LOD	<LOD	<LOD	<LOD	260.9	797.5	16.8
Trafford	Adult	Gator045	37.3	<LOD	<LOD	<LOD	<LOD	4.8	251.4	842.3	19.2
Trafford	Adult	Gator047	<LOD	1.9	<LOD	<LOD	<LOD	5.1	301.5	726.6	25.5
Trafford	Adult	Gator049	<LOD	<LOD	<LOD	<LOD	<LOD	<LOD	513.6	1080.0	20.4
Trafford	Adult	Gator050	<LOD	<LOD	<LOD	<LOD	<LOD	<LOD	264.4	884.7	23.1
Trafford	Adult	Gator053	25.2	0.3	<LOD	<LOD	<LOD	<LOD	279.6	890.0	19.0
Trafford	Adult	Gator056	47.3	<LOD	<LOD	<LOD	<LOD	<LOD	377.4	849.3	20.9
Trafford	Sub-adult	Gator114	35.7	13.4	<LOD	<LOD	<LOD	<LOD	347.8	1071.8	28.2
Trafford	Sub-adult	Gator120	57.9	2.2	<LOD	<LOD	<LOD	<LOD	473.1	1104.5	15.8
Trafford	Sub-adult	Gator122	13.7	4.4	<LOD	<LOD	<LOD	<LOD	310.5	879.8	18.2
Trafford	Sub-adult	Gator124	21.9	2.2	<LOD	<LOD	<LOD	<LOD	424.7	1003.9	15.0
Trafford	Sub-adult	Gator133	64.5	6.2	<LOD	<LOD	<LOD	<LOD	312.0	746.4	19.2
Trafford	Sub-adult	Gator137	22.5	6.5	3.7	<LOD	<LOD	<LOD	325.0	826.8	21.1
Trafford	Sub-adult	Gator138	146.0	7.4	<LOD	<LOD	<LOD	<LOD	314.3	800.8	22.2
Trafford	Sub-adult	Gator143	52.0	7.3	<LOD	<LOD	<LOD	12.9	369.7	1264.1	22.8
Trafford	Sub-adult	Gator146	43.5	2.4	<LOD	<LOD	<LOD	<LOD	306.5	967.0	17.6
Trafford	Sub-adult	Gator154	41.5	6.5	<LOD	<LOD	<LOD	<LOD	384.6	963.3	22.4
Trafford	Sub-adult	Gator157	41.6	10.0	<LOD	<LOD	<LOD	<LOD	423.2	906.3	26.7
Trafford	Sub-adult	Gator167	90.8	7.4	<LOD	<LOD	<LOD	<LOD	351.7	863.0	19.4
WCA2A	Adult	Gator030	<LOD	<LOD	<LOD	<LOD	<LOD	<LOD	282.2	1362.7	33.4
WCA2A	Adult	Gator043	51.8	<LOD	<LOD	<LOD	<LOD	<LOD	249.2	796.9	23.0
WCA2A	Adult	Gator054	20.0	5.7	<LOD	<LOD	<LOD	6.0	376.1	824.1	27.7
WCA2A	Adult	Gator069	215.4	0.2	4.9	<LOD	<LOD	<LOD	295.0	1220.3	28.6
WCA2A	Adult	Gator071	18.2	4.0	<LOD	<LOD	<LOD	4.7	182.4	1153.1	34.0
WCA2A	Adult	Gator078	<LOD	<LOD	<LOD	<LOD	<LOD	<LOD	333.6	1018.3	13.9
WCA2A	Sub-adult	Gator126	25.4	1.5	<LOD	<LOD	<LOD	<LOD	313.2	426.6	13.5
WCA2A	Sub-adult	Gator127	36.5	<LOD	<LOD	<LOD	<LOD	<LOD	296.4	1218.4	7.0
WCA2A	Sub-adult	Gator128	27.4	7.5	<LOD	<LOD	<LOD	<LOD	268.0	1206.2	24.7

Location	Age Class	ID	Al	V	Cr	Mn	Co	Ni	Cu	Zn	As
WCA2A	Sub-adult	Gator132	14.6	3.8	<LOD	<LOD	<LOD	<LOD	311.7	1578.1	23.6
WCA2A	Sub-adult	Gator140	20.3	4.5	<LOD	<LOD	<LOD	<LOD	253.1	815.0	20.9
WCA2A	Sub-adult	Gator145	55.4	5.0	<LOD	<LOD	<LOD	<LOD	330.9	1264.0	24.8
WCA2A	Sub-adult	Gator147	28.4	5.3	<LOD	<LOD	<LOD	<LOD	349.3	1210.0	20.9
WCA2A	Sub-adult	Gator152	39.6	4.9	<LOD	<LOD	<LOD	<LOD	357.1	1006.6	21.5
WCA2A	Sub-adult	Gator152	15.1	<LOD	<LOD	<LOD	<LOD	<LOD	420.5	967.5	14.7
WCA2A	Sub-adult	Gator155	17.1	4.7	<LOD	<LOD	<LOD	<LOD	297.8	1057.5	19.5
WCA2A	Sub-adult	Gator156	45.8	4.8	<LOD	<LOD	<LOD	<LOD	213.0	861.7	22.7
WCA3A	Adult	Gator034	<LOD	0.3	14.6	<LOD	<LOD	<LOD	332.3	1002.9	22.7
WCA3A	Adult	Gator037	60.9	2.8	<LOD	<LOD	<LOD	<LOD	353.2	905.4	25.4
WCA3A	Adult	Gator055	82.6	0.4	<LOD	<LOD	<LOD	<LOD	27.0	867.0	17.9
WCA3A	Adult	Gator064	<LOD	<LOD	<LOD	<LOD	<LOD	<LOD	384.2	972.3	17.1
WCA3A	Adult	Gator065	53.2	0.8	<LOD	<LOD	<LOD	<LOD	240.9	814.1	20.9
WCA3A	Adult	Gator066	67.1	<LOD	<LOD	<LOD	<LOD	<LOD	419.0	1095.3	23.2
WCA3A	Adult	Gator070	<LOD	<LOD	<LOD	<LOD	<LOD	<LOD	395.0	973.7	12.4
WCA3A	Adult	Gator077	25.5	3.3	<LOD	<LOD	<LOD	4.6	364.5	981.0	31.8
WCA3A	Sub-adult	Gator113	13.2	3.1	<LOD	<LOD	<LOD	<LOD	212.1	968.3	19.2
WCA3A	Sub-adult	Gator119	40.1	3.7	<LOD	<LOD	<LOD	<LOD	267.0	1067.1	18.1
WCA3A	Sub-adult	Gator142	62.7	6.6	<LOD	<LOD	<LOD	<LOD	288.1	1006.5	20.7
WCA3A	Sub-adult	Gator150	15.6	4.9	<LOD	<LOD	<LOD	<LOD	316.1	981.3	25.1
WCA3A	Sub-adult	Gator151	34.6	6.2	<LOD	<LOD	<LOD	<LOD	350.9	1000.8	23.7
WCA3A	Sub-adult	Gator158	26.3	8.6	<LOD	<LOD	<LOD	7.4	315.0	790.1	20.4
WCA3A	Sub-adult	Gator159	39.8	6.0	<LOD	<LOD	<LOD	<LOD	328.1	992.9	57.4
WCA3A	Sub-adult	Gator163	47.9	5.0	<LOD	<LOD	<LOD	<LOD	278.1	852.8	22.2
WCA3A	Sub-adult	Gator164	51.5	10.2	<LOD	<LOD	<LOD	<LOD	331.4	1076.6	21.3
WCA3A	Sub-adult	Gator173	19.9	4.8	<LOD	<LOD	<LOD	5.4	275.4	946.8	19.8
WCA3A	Sub-adult	Gator176	35.3	0.7	<LOD	<LOD	<LOD	<LOD	231.7	1063.5	17.5
Yawkey	Adult	MUSC041R	<LOD	<LOD	<LOD	<LOD	<LOD	<LOD	438.9	770.2	5.6
Yawkey	Adult	MUSC047	51.7	10.8	<LOD	<LOD	<LOD	<LOD	390.4	1078.7	29.8
Yawkey	Adult	MUSC048	34.6	8.3	<LOD	<LOD	<LOD	<LOD	332.7	1280.6	23.0
Yawkey	Adult	MUSC050	28.2	7.5	<LOD	<LOD	<LOD	<LOD	382.0	1477.0	33.9
Yawkey	Adult	MUSC051	24.6	5.3	<LOD	<LOD	<LOD	<LOD	270.5	1226.0	20.4
Yawkey	Adult	MUSC052	31.1	7.0	<LOD	<LOD	<LOD	<LOD	278.1	1394.7	26.7
Yawkey	Adult	MUSC054	109.8	6.2	<LOD	<LOD	<LOD	<LOD	353.5	1515.7	21.7
Yawkey	Adult	MUSC055	44.3	2.0	4.4	<LOD	<LOD	<LOD	229.9	1171.1	56.7
Yawkey	Adult	MUSC056	56.9	2.6	<LOD	<LOD	<LOD	<LOD	317.3	1330.9	22.1
Yawkey	Adult	MUSC057	36.3	4.6	<LOD	<LOD	<LOD	<LOD	288.9	1360.3	21.7
Yawkey	Adult	MUSC058	147.9	7.8	<LOD	<LOD	<LOD	<LOD	293.0	1461.4	39.0
Yawkey	Adult	MUSC059	67.5	8.2	<LOD	<LOD	<LOD	<LOD	253.9	1577.5	44.4
Yawkey	Adult	MUSC061	40.1	4.7	<LOD	<LOD	<LOD	<LOD	331.6	1169.6	84.7
Yawkey	Adult	MUSC062	15.3	<LOD	<LOD	<LOD	<LOD	<LOD	280.3	900.0	25.9
Yawkey	Adult	MUSC063	54.2	2.7	<LOD	<LOD	<LOD	<LOD	336.9	1112.3	42.2
Location	Age Class	ID	Se	Rb	Sr	Mo	Cd	Sn	Pb	Hg	
Ace Basin	Adult	MUSC320	119.6	689.3	484.3	2.9	0.8	<LOD	63.9	62.5	
Ace Basin	Adult	MUSC401	184.3	372.2	350.7	2.2	0.6	7.2	26138.5	93.3	
Ace Basin	Adult	MUSC402	190.2	385.3	784.6	3.8	0.8	<LOD	114.8	243.3	
Ace Basin	Adult	MUSC403	150.1	590.6	243.9	2.8	0.9	<LOD	16.1	58.2	
Ace Basin	Adult	MUSC404	170.2	411.8	319.7	3.1	<LOD	<LOD	35271.4	38.3	
Ace Basin	Adult	MUSC405	167.6	491.8	588.7	4.8	0.7	<LOD	72.2	71.4	
Ace Basin	Adult	MUSC406	218.5	432.6	438.0	5.3	0.5	<LOD	36.5	79.1	
Ace Basin	Adult	MUSC408	146.8	532.9	397.3	2.8	0.6	<LOD	12.3	77.3	
Ace Basin	Adult	MUSC409	192.6	654.3	350.1	3.0	0.8	<LOD	17.8	64.5	
Ace Basin	Adult	MUSC410	122.4	331.6	198.7	4.4	<LOD	<LOD	436.9	60.9	
Ace Basin	Adult	MUSC411	204.0	627.6	592.8	6.1	0.8	<LOD	86.1	112.5	
Ace Basin	Adult	MUSC412	186.0	484.0	232.0	4.1	0.6	<LOD	167.8	87.5	
Ace Basin	Adult	MUSC413	216.7	548.1	324.6	3.9	<LOD	<LOD	2841.1	51.1	
Ace Basin	Adult	MUSC414	232.8	605.1	452.5	2.8	0.7	<LOD	23.2	139.5	
Ace Basin	Adult	MUSC415	208.3	659.7	1076.1	2.3	0.8	<LOD	43.9	217.9	
Ace Basin	Adult	MUSC416	158.2	560.7	259.5	2.2	0.6	<LOD	28.5	60.4	
Ace Basin	Adult	MUSC417	114.1	247.5	136.0	2.0	0.3	<LOD	153.8	108.5	
Ace Basin	Adult	MUSC418	147.7	1075.0	218.3	1.5	0.6	<LOD	94.1	212.5	
Ace Basin	Adult	MUSC419	135.6	416.4	186.6	1.7	0.5	<LOD	32.0	166.9	
Ace Basin	Adult	MUSC420	175.9	435.6	230.0	2.8	0.6	<LOD	18.2	90.5	
Ace Basin	Adult	MUSC421	197.0	573.9	241.3	3.8	0.6	<LOD	12.4	116.5	
Ace Basin	Adult	MUSC422	220.2	739.3	244.2	3.6	0.8	<LOD	85.6	178.5	
Ace Basin	Adult	MUSC423	121.7	701.4	483.5	3.2	0.7	<LOD	65.8	132.4	
Ace Basin	Adult	MUSC426	221.7	642.0	256.0	4.1	0.9	<LOD	20.0	168.4	
Ace Basin	Adult	MUSC427	142.4	568.1	236.5	4.0	0.8	<LOD	25.7	112.3	
Ace Basin	Adult	MUSC428	119.9	554.7	183.2	2.3	0.6	<LOD	12.2	151.0	
Ace Basin	Adult	MUSC429	180.8	556.0	225.8	4.4	0.8	<LOD	21.1	97.3	

Location	Age Class	ID	Se	Rb	Sr	Mo	Cd	Sn	Pb	Hg
Ace Basin	Adult	MUSC430	197.5	701.3	275.7	4.7	0.9	<LOD	220.4	102.7
Ace Basin	Adult	MUSC440	165.8	548.1	272.3	3.1	0.6	<LOD	32.2	105.6
Ace Basin	Adult	MUSC441	173.9	662.0	281.4	2.6	<LOD	<LOD	7.7	158.0
Ace Basin	Adult	MUSC442	220.6	1038	266.8	2.3	0.9	<LOD	33.0	215.0
Ace Basin	Adult	MUSC443	194.5	616.8	260.8	2.1	0.7	<LOD	93.7	146.4
Ace Basin	Adult	MUSC444	161.3	442.8	278.7	2.8	0.6	<LOD	265.6	43.9
Ace Basin	Adult	MUSC445	158.3	726.4	299.4	2.4	0.6	<LOD	15.8	52.3
Ace Basin	Adult	MUSC446	204.1	599.2	327.9	4.0	0.9	<LOD	17.3	65.9
Ace Basin	Adult	MUSC447	192.5	594.4	311.5	3.7	0.9	<LOD	77.5	81.2
Ace Basin	Adult	MUSC448	275.9	666.5	370.2	5.6	0.8	<LOD	27.4	92.4
Kissimmee	Adult	Gator002	177.8	1178	105.1	3.2	0.7	<LOD	62.2	N/A
Kissimmee	Adult	Gator004	194.1	1248	124.4	4.8	1.0	<LOD	39.1	792.2
Kissimmee	Adult	Gator005	232.9	1600	111.7	3.6	1.0	<LOD	9.2	331.0
Kissimmee	Adult	Gator006	157.4	857.5	111.6	3.1	1.0	<LOD	5.4	262.7
Kissimmee	Adult	Gator009	150.6	1375	110.3	3.3	1.0	<LOD	11.5	333.7
Kissimmee	Adult	Gator010	178.3	1135	127.3	2.8	<LOD	<LOD	12.0	496.1
Kissimmee	Adult	Gator012	185.1	991.6	88.3	3.0	1.0	<LOD	587.2	305.2
Kissimmee	Adult	Gator013	147.5	1199	109.3	4.2	1.1	<LOD	18.2	284.2
Kissimmee	Adult	Gator015	165.9	749.5	85.6	2.5	1.1	<LOD	197.7	300.9
Kissimmee	Adult	Gator017	178.1	1998	99.4	10.5	1.1	<LOD	26.4	215.7
Kissimmee	Adult	Gator018	165.0	1231	95.4	2.7	0.9	<LOD	8.1	185.3
Kissimmee	Sub-adult	Gator100	134.0	767.8	53.5	1.8	0.7	<LOD	13.1	166.4
Kissimmee	Sub-adult	Gator101	162.3	1099	106.8	2.9	0.9	<LOD	14.5	136.1
Kissimmee	Sub-adult	Gator102	151.1	1093	102.5	4.4	0.9	<LOD	9.1	159.9
Kissimmee	Sub-adult	Gator104	154.1	1339	101.8	9.1	1.2	<LOD	17.7	134.1
Kissimmee	Sub-adult	Gator105	115.5	984.0	93.1	13.4	1.1	<LOD	17.3	113.2
Kissimmee	Sub-adult	Gator106	201.1	958.9	121.0	2.9	1.0	<LOD	49.2	102.9
Kissimmee	Sub-adult	Gator107	93.1	932.4	88.1	6.9	0.9	<LOD	17.3	145.0
Kissimmee	Sub-adult	Gator109	147.6	1101	89.2	2.9	0.9	<LOD	55.0	N/A
Kissimmee	Sub-adult	Gator11	150.8	1147	110.4	2.4	1.0	<LOD	12.5	195.5
Kissimmee	Sub-adult	Gator110	147.6	1102	80.6	2.9	1.0	<LOD	28.5	203.3
Kissimmee	Sub-adult	Gator112	139.0	1031	105.9	3.7	1.1	<LOD	7.5	190.6
Kissimmee	Sub-adult	Gator115	168.7	1285	139.6	3.0	1.0	<LOD	9.7	121.5
Kissimmee	Sub-adult	Gator118	147.1	1154	79.2	3.7	1.1	<LOD	11.3	194.0
Lochloosa	Adult	Gator026	247.6	1731	143.5	3.0	1.1	<LOD	62.9	250.7
Lochloosa	Adult	Gator038	344.6	1530.4	72.7	4.1	1.1	<LOD	467.4	N/A
Lochloosa	Adult	Gator046	265.1	2079	60.7	1.8	0.6	<LOD	3891.2	182.1
Lochloosa	Adult	Gator057	267.1	1849	81.7	3.3	1.0	<LOD	187.6	201.5
Lochloosa	Adult	Gator060	300.3	1587	92.0	5.2	1.2	<LOD	17.2	141.1
Lochloosa	Adult	Gator062	336.4	1639	91.7	3.8	1.3	<LOD	15.8	101.9
Lochloosa	Adult	Gator063	335.9	1476	79.1	3.9	1.1	<LOD	22.0	115.2
Lochloosa	Adult	Gator067	357.3	1646	94.0	4.6	1.0	<LOD	14.4	116.0
Lochloosa	Adult	Gator075	221.4	2715	48.8	2.7	1.0	<LOD	186.0	227.9
Lochloosa	Sub-adult	Gator121	199.6	1674	69.2	2.2	0.7	<LOD	123.6	88.3
Lochloosa	Sub-adult	Gator123	220.9	1988	92.5	2.6	0.8	<LOD	21.7	85.2
Lochloosa	Sub-adult	Gator129	223.0	1566	79.2	2.9	1.3	8.0	29.7	59.4
Lochloosa	Sub-adult	Gator160	201.1	1774	72.5	3.1	0.9	<LOD	22.1	63.8
Lochloosa	Sub-adult	Gator200	231.6	2039	78.9	3.2	2.1	<LOD	24.3	N/A
Lochloosa	Sub-adult	Gator201	231.9	1684	86.2	2.8	1.0	<LOD	27.9	41.3
Lochloosa	Sub-adult	Gator202	218.9	1793	64.9	2.6	0.9	<LOD	5120.6	104.3
Lochloosa	Sub-adult	Gator203	309.1	1931	82.0	3.1	0.9	<LOD	16.8	141.4
Lochloosa	Sub-adult	Gator205	243.0	1648	64.3	2.4	0.7	<LOD	15.5	137.4
Lochloosa	Sub-adult	Gator206	244.1	1707	80.5	2.9	0.8	<LOD	32.1	77.5
Lochloosa	Sub-adult	Gator207	248.8	1561	67.8	2.4	0.9	<LOD	19.0	91.5
Lochloosa	Sub-adult	Gator208	245.4	1820	93.3	3.0	0.8	<LOD	19.0	111.4
St. Johns River	Adult	Gator003	410.3	940.9	383.7	4.4	1.1	<LOD	18.6	161.2
St. Johns River	Adult	Gator007	161.4	651.8	63.9	3.5	1.4	<LOD	19.6	174.0
St. Johns River	Adult	Gator014	128.5	525.2	418.1	2.8	1.0	<LOD	4.6	78.8
St. Johns River	Adult	Gator016	106.1	518.4	325.1	2.7	1.9	<LOD	167.2	100.9
St. Johns River	Adult	Gator019	341.5	1046	283.3	2.7	1.0	<LOD	28.4	149.3
St. Johns River	Adult	Gator020	362.0	1134	993.9	2.3	1.3	<LOD	55.2	194.5
St. Johns River	Adult	Gator022	130.9	746.0	304.8	1.9	1.0	<LOD	5.9	161.8
St. Johns River	Adult	Gator023	180.1	790.1	367.2	2.1	0.9	<LOD	3.3	93.9
St. Johns River	Adult	Gator029	142.6	772.5	413.9	1.5	1.2	<LOD	8.2	236.9
St. Johns River	Adult	Gator032	152.3	793.0	402.2	2.2	1.1	<LOD	5.5	155.2
St. Johns River	Adult	Gator033	222.9	610.4	311.9	3.3	1.3	<LOD	49.4	N/A
St. Johns River	Sub-adult	Gator111	326.4	1136	504.3	2.2	1.0	<LOD	27.2	74.9
St. Johns River	Sub-adult	Gator116	305.2	1526	338.4	2.0	1.0	<LOD	450.6	370.2
St. Johns River	Sub-adult	Gator117	184.7	856.1	535.0	2.9	1.0	<LOD	7.5	202.7
St. Johns River	Sub-adult	Gator162	195.4	1062.0	349.0	3.2	1.0	<LOD	11.2	139.1

Location	Age Class	ID	Se	Rb	Sr	Mo	Cd	Sn	Pb	Hg
St. Johns River	Sub-adult	Gator165	191.4	839.4	336.7	2.4	0.9	<LOD	6.1	152.5
St. Johns River	Sub-adult	Gator166	212.9	843.0	488.5	5.1	1.0	<LOD	15.3	199.8
St. Johns River	Sub-adult	Gator168	218.9	727.1	435.5	3.1	1.0	<LOD	15.7	144.2
St. Johns River	Sub-adult	Gator172	180.8	827.0	411.4	2.9	1.0	<LOD	6.9	233.2
St. Johns River	Sub-adult	Gator174	236.3	1025	444.7	3.1	0.9	<LOD	47.8	164.9
St. Johns River	Sub-adult	Gator175	268.7	1161	434.4	3.9	1.0	<LOD	112.1	54.8
St. Johns River	Sub-adult	Gator177	263.3	927.7	436.8	3.6	1.1	<LOD	16.3	108.7
Trafford	Adult	Gator031	237.4	670.4	83.2	9.0	1.5	<LOD	12.1	241.5
Trafford	Adult	Gator036	209.1	498.5	90.9	9.6	1.1	<LOD	14.0	158.4
Trafford	Adult	Gator039	192.5	463.0	68.5	5.7	1.0	<LOD	139.0	183.6
Trafford	Adult	Gator041	169.4	1192.5	97.7	8.3	<LOD	<LOD	11.6	67.4
Trafford	Adult	Gator042	217.6	602.4	97.2	5.6	1.1	<LOD	4633.5	172.3
Trafford	Adult	Gator044	189.1	460.1	66.0	7.7	0.9	<LOD	20.4	247.0
Trafford	Adult	Gator045	185.4	516.0	74.2	4.9	1.0	<LOD	9.9	222.4
Trafford	Adult	Gator047	202.8	506.3	92.8	6.8	1.1	<LOD	315.0	203.4
Trafford	Adult	Gator049	196.2	498.1	56.5	10.8	1.2	<LOD	10.9	135.6
Trafford	Adult	Gator050	187.7	691.6	72.2	4.7	1.0	<LOD	9.7	358.6
Trafford	Adult	Gator053	162.9	738.2	67.3	5.7	1.1	<LOD	9.6	136.6
Trafford	Adult	Gator056	236.2	557.7	94.2	7.0	1.1	<LOD	5685.5	196.7
Trafford	Sub-adult	Gator114	226.6	699.7	80.7	6.9	1.2	<LOD	11.2	204.8
Trafford	Sub-adult	Gator120	293.6	590.5	97.3	5.5	0.7	<LOD	13.5	193.7
Trafford	Sub-adult	Gator122	161.1	661.0	70.8	4.7	1.1	<LOD	64.8	140.7
Trafford	Sub-adult	Gator124	227.7	730.5	72.7	4.1	1.0	<LOD	38.7	212.3
Trafford	Sub-adult	Gator133	194.5	665.2	79.7	4.6	1.1	<LOD	8.4	175.0
Trafford	Sub-adult	Gator137	191.0	668.2	70.1	4.8	1.0	<LOD	2016.6	142.9
Trafford	Sub-adult	Gator138	271.4	600.9	99.4	6.7	3.8	<LOD	13.7	148.2
Trafford	Sub-adult	Gator143	223.9	605.1	85.4	7.0	1.2	<LOD	14.8	147.0
Trafford	Sub-adult	Gator146	141.1	597.2	74.7	5.0	0.8	<LOD	7.6	275.3
Trafford	Sub-adult	Gator154	217.7	637.7	93.4	5.2	1.0	<LOD	13.3	777.3
Trafford	Sub-adult	Gator157	281.6	697.2	78.7	6.3	1.2	<LOD	16.1	95.6
Trafford	Sub-adult	Gator167	235.2	596.5	75.8	5.8	1.2	<LOD	13.6	100.6
WCA2A	Adult	Gator030	127.0	859.7	925.2	2.1	0.9	<LOD	6.7	1052.7
WCA2A	Adult	Gator043	165.7	800.4	361.0	2.5	1.0	<LOD	10.3	N/A
WCA2A	Adult	Gator054	208.6	918.8	371.4	3.2	1.2	<LOD	165.0	1880.3
WCA2A	Adult	Gator069	142.5	737.4	772.4	3.7	1.0	<LOD	1207.2	1137.5
WCA2A	Adult	Gator071	114.6	726.9	656.4	2.1	1.1	<LOD	13.2	1428.7
WCA2A	Adult	Gator078	204.6	775.1	429.9	2.9	0.8	<LOD	6.2	846.7
WCA2A	Sub-adult	Gator126	131.0	441.4	443.5	3.2	0.6	<LOD	5.3	189.5
WCA2A	Sub-adult	Gator127	199.8	789.9	467.8	3.5	0.7	<LOD	5.0	474.2
WCA2A	Sub-adult	Gator128	141.4	813.3	413.9	2.1	0.9	<LOD	7.4	575.8
WCA2A	Sub-adult	Gator132	182.1	859.3	504.8	4.3	0.8	<LOD	7.2	313.7
WCA2A	Sub-adult	Gator140	139.2	721.5	349.0	2.0	0.8	<LOD	9.5	963.2
WCA2A	Sub-adult	Gator145	175.0	732.0	496.3	3.2	0.9	<LOD	12.3	253.2
WCA2A	Sub-adult	Gator147	177.8	857.6	399.2	3.1	1.1	<LOD	12.8	362.8
WCA2A	Sub-adult	Gator152	190.4	750.4	377.0	2.5	1.1	<LOD	11.1	1447.1
WCA2A	Sub-adult	Gator152	201.1	724.6	417.7	1.7	0.8	<LOD	10.6	104.8
WCA2A	Sub-adult	Gator155	149.9	866.7	475.3	3.1	0.7	<LOD	7.5	N/A
WCA2A	Sub-adult	Gator156	141.4	566.7	378.9	2.6	1.1	<LOD	7.8	736.6
WCA3A	Adult	Gator034	193.5	698.2	191.1	4.2	1.0	<LOD	6.7	700.4
WCA3A	Adult	Gator037	145.6	760.2	232.4	2.3	1.1	<LOD	167.8	1207.6
WCA3A	Adult	Gator055	175.0	582.6	150.0	1.9	2.6	<LOD	4871.6	883.9
WCA3A	Adult	Gator064	148.1	1109	105.0	2.0	1.0	<LOD	6.8	1066.1
WCA3A	Adult	Gator065	141.8	551.0	294.2	3.4	0.9	<LOD	5.1	400.6
WCA3A	Adult	Gator066	165.4	792.9	204.9	3.3	1.1	<LOD	7.0	1554.2
WCA3A	Adult	Gator070	159.2	745.2	152.0	1.8	0.8	<LOD	9.1	3026.9
WCA3A	Adult	Gator077	141.8	1443	90.0	3.6	1.2	<LOD	6.8	1442.2
WCA3A	Sub-adult	Gator113	120.7	537.7	158.3	1.9	0.9	<LOD	5.1	900.4
WCA3A	Sub-adult	Gator119	131.9	603.5	153.4	1.9	1.0	<LOD	4.4	676.2
WCA3A	Sub-adult	Gator142	148.5	611.8	156.4	2.5	1.0	<LOD	8.6	558.5
WCA3A	Sub-adult	Gator150	127.6	674.9	197.3	3.0	0.9	<LOD	6.2	424.7
WCA3A	Sub-adult	Gator151	156.2	1267	94.7	2.9	1.0	<LOD	8.8	1380.6
WCA3A	Sub-adult	Gator158	129.8	548.0	223.1	3.6	0.9	<LOD	15.5	56.4
WCA3A	Sub-adult	Gator159	194.7	1018	124.5	3.3	1.2	<LOD	59.6	80.8
WCA3A	Sub-adult	Gator163	128.0	604.4	210.4	2.4	1.0	<LOD	5.7	792.4
WCA3A	Sub-adult	Gator164	141.8	522.7	218.5	4.0	1.2	<LOD	11.5	68.0
WCA3A	Sub-adult	Gator173	149.0	714.3	217.4	2.6	0.8	<LOD	3.5	707.9
WCA3A	Sub-adult	Gator176	135.9	643.7	162.3	2.4	1.0	<LOD	8.0	580.8
Yawkey	Adult	MUSC041R	181.0	343.2	253.2	2.9	<LOD	<LOD	95.5	154.9
Yawkey	Adult	MUSC047	243.3	285.7	527.3	5.5	0.7	<LOD	27.4	146.7
Yawkey	Adult	MUSC048	194.5	374.2	479.0	3.3	0.6	<LOD	56.7	126.3

Location	Age Class	ID	Se	Rb	Sr	Mo	Cd	Sn	Pb	Hg
Yawkey	Adult	MUSC050	263.9	411.3	436.4	4.5	0.7	<LOD	256.3	141.2
Yawkey	Adult	MUSC051	209.1	328.9	518.0	3.0	<LOD	<LOD	201.7	192.9
Yawkey	Adult	MUSC052	203.1	407.3	381.8	3.4	0.7	<LOD	61.0	151.2
Yawkey	Adult	MUSC054	252.2	457.0	464.6	4.5	0.7	<LOD	199.3	174.1
Yawkey	Adult	MUSC055	250.4	273.1	221.2	7.4	<LOD	<LOD	10.0	59.3
Yawkey	Adult	MUSC056	154.8	455.7	217.1	3.9	0.7	<LOD	23.6	160.5
Yawkey	Adult	MUSC057	293.2	234.5	467.8	4.8	0.7	<LOD	147.9	48.2
Yawkey	Adult	MUSC058	253.7	603.1	332.1	5.4	0.8	<LOD	780.0	238.2
Yawkey	Adult	MUSC059	201.6	253.9	260.9	5.6	0.7	<LOD	43.5	207.7
Yawkey	Adult	MUSC061	275.6	415.2	322.2	3.3	0.6	<LOD	449.2	129.8
Yawkey	Adult	MUSC062	189.5	450.4	307.2	2.8	<LOD	<LOD	87.0	164.8
Yawkey	Adult	MUSC063	252.1	415.2	296.5	2.2	0.6	<LOD	8.5	154.5

Table 2.12. The mean and standard deviation of variation across samples of all trace metals measured for each location and age class.

The selenium: mercury (Se: Hg) molar ratios were calculated using the means presented in this table. The standard deviation is denoted for each element by SD. Uncertainty measures for trace elements are provided in Table 2.1.

Location	Age Class	n	Al		Cu		Zn		As		Se	
			ng/g	SD	ng/g	SD	ng/g	SD	ng/g	SD	ng/g	SD
Lochloosa, FL	Adults	9	39.9	28.6	336.3	71.9	852.2	94.2	47	9.4	260.8	45.8
	Sub Adults	12	57.3	18.6	334.7	44.7	794.2	155.6	38.3	4.8	225.5	25
St. Johns River, FL	Adults	11	42.7	26.2	224.1	142.2	713.6	189.3	62.9	40.9	185.2	83.9
	Sub Adults	11	57	42.1	338.7	51.8	867	99.5	46.7	4.2	214.2	46.7
Trafford, FL	Adults	12	25.6	30.5	274.4	86.2	672.5	129.2	44.9	13.3	186.1	21
	Sub Adults	12	65	39.4	366.1	41.8	792.8	111.3	47.1	7.4	214.5	40.2
Kissimmee, FL	Adults	11	50.5	48.4	241.1	109	813.5	126.7	28.6	4.2	150.7	19.6
	Sub Adults	13	29	9.6	301.7	62.5	863.5	85.9	50	5	150.4	21.7
Everglades WCA2A, FL	Adults	4	61	78.9	259.8	82.3	812.1	166	49.3	13.6	153.5	36.8
	Sub Adults	11	41.6	14.7	327.7	44.6	875.1	219.6	46.6	6	168.4	22
Everglades WCA3A, FL	Adults	9	42.1	33.9	293.7	97.1	719.7	58.4	47.8	7.3	156.3	18.4
	Sub Adults	11	50.3	17.6	318.4	38.3	824.7	66.9	50.4	9.9	147.2	20.3
Yawkey, SC	Adults	15	37.6	35.8	287	56.4	813.7	228.1	28.8	18.9	179.7	39.8
Ace Basin, SC	Adults	37	53	19.5	318.5	68.3	1255	234.9	33.2	15	227.9	37.1
Location	Age Class	n	Rb		Sr		Pb		Hg		Se: Hg Molar Ratio	
			ng/g	SD	ng/g	SD	ng/g	SD	ng/g	SD		
Lochloosa, FL	Adults	9	1279	301	142	24.8	500.3	1032	149	71.2	11.14	
	Sub Adults	12	1328	112	154.9	9.6	384.8	850.4	88	31.5	16.23	
St. Johns River, FL	Adults	11	598	135	363	190.3	71.6	43.6	178	84.9	6.58	
	Sub Adults	11	772	152	454.6	57.9	158.2	85.6	153	53.2	8.92	
Trafford, FL	Adults	12	507	161	134	35.4	796.6	1569	198	79	6.01	
	Sub Adults	12	544	37.3	156.5	13.3	266.5	477.6	165	57.6	8.28	
Kissimmee, FL	Adults	11	904	227	117.6	14.1	102.5	143.8	417	222	2.29	
	Sub Adults	13	829	106	163	18.4	114.5	13.2	161	41.5	5.95	
Everglades WCA2A, FL	Adults	4	632	50.4	555	192.9	253.3	377.5	1569	643	0.62	
	Sub Adults	11	609	93.3	451.8	41.8	120.4	13.7	559	282	1.91	
Everglades WCA3A, FL	Adults	9	662	208	223.9	53.2	519.5	1146	1329	713	0.75	
	Sub Adults	11	580	170	242.6	38.2	128.9	18.1	684	450	1.37	
Yawkey, SC	Adults	15	578	97.1	338.8	108.7	1851	208	150	49	3.04	
Ace Basin, SC	Adults	37	381	164	365.7	180.9	163.2	7102	111	53.3	5.2	

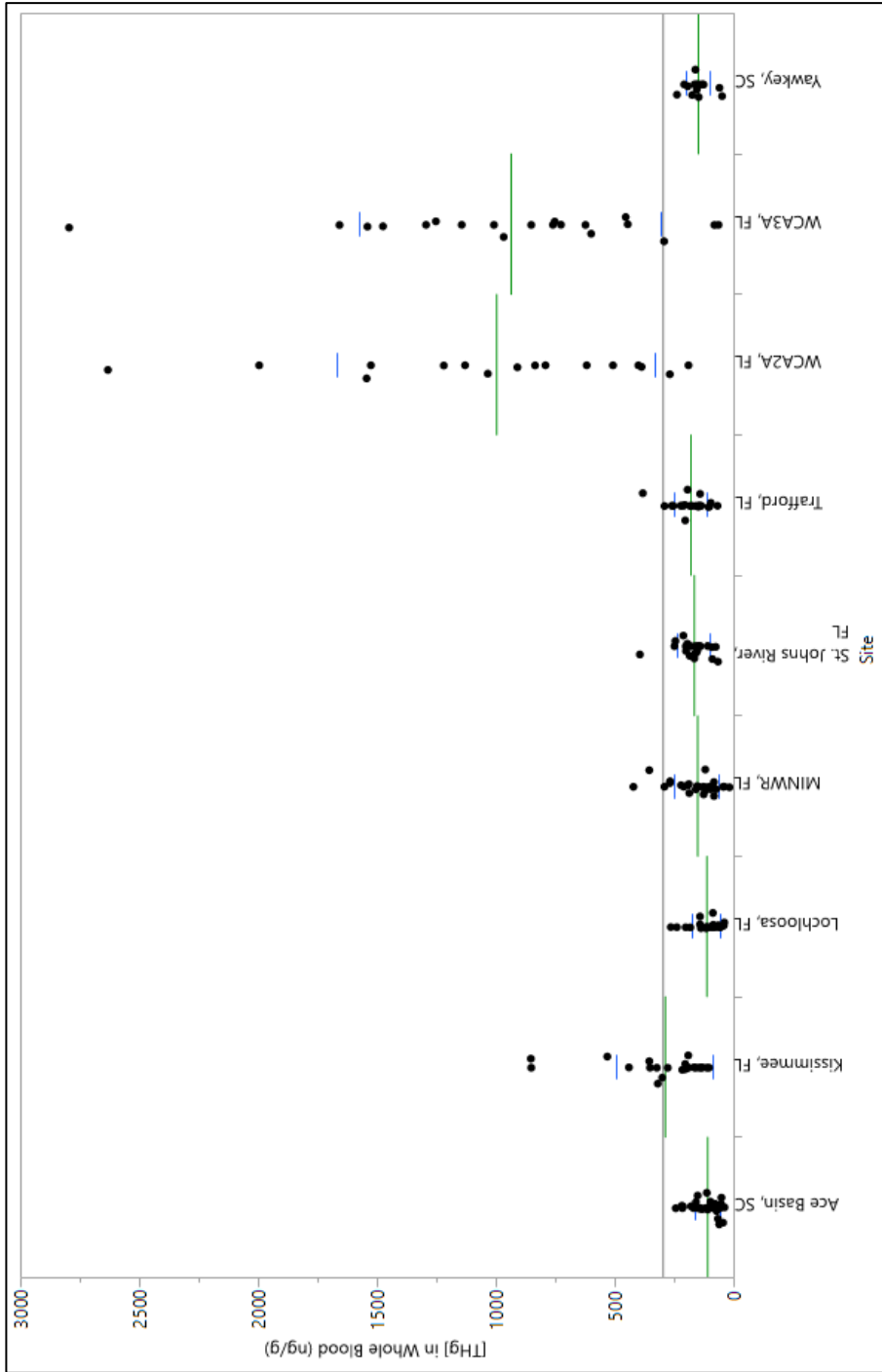


Figure 2.5. The Wilcoxon Each Pair Comparison of the total Hg fraction of whole blood from nine sites in the southeastern United States.

The bars represent the mean and standard deviation for each location, the line at ~300 ng/g is the grand mean of all samples. The significantly different relationships are listed in Table 2.13.

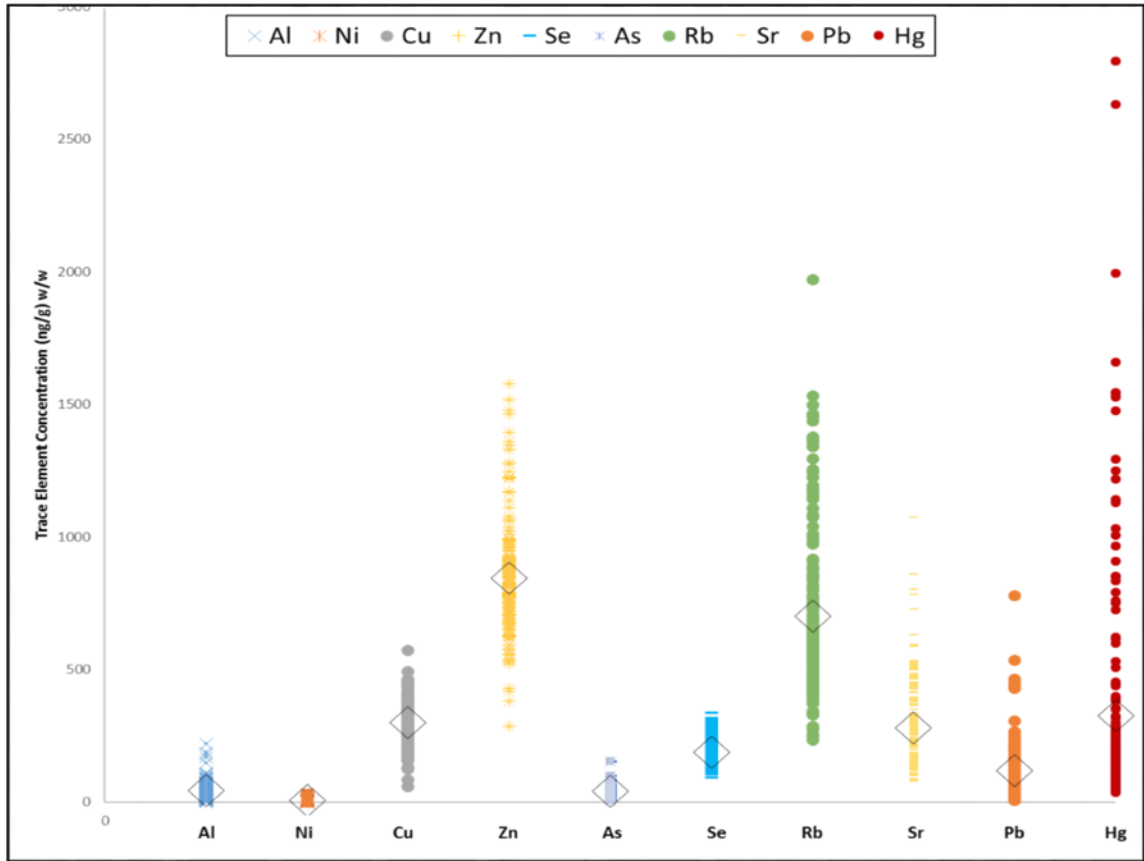


Figure 2.6. The trace element totals measured in all alligators from all nine sites examined in the survey conducted across the southeastern Atlantic coast of the United States. The mean of each trace element is denoted with a hollow diamond overlaid on the individual measurements.

Table 2.13. The Wilcoxon Each Pair Non-Parametric Multiple Comparison and the p-values associated with the data presented in Figure 2.5 (JMP 11, Cary, NC). An asterisk indicates a significant relationship.

Site Comparison		p-Value	Significant
WCA2A, FL	Ace Basin, SC	<.0001	*
WCA3A, FL	Ace Basin, SC	<.0001	*
Kissimmee, FL	Ace Basin, SC	<.0001	*
WCA2A, FL	MINWR, FL	<.0001	*
WCA3A, FL	MINWR, FL	<.0001	*
WCA2A, FL	Trafford, FL	<.0001	*
WCA2A, FL	Lochloosa, FL	<.0001	*
Trafford, FL	Ace Basin, SC	<.0001	*
WCA2A, FL	St. Johns River, FL	<.0001	*
WCA3A, FL	Lochloosa, FL	<.0001	*
WCA3A, FL	Trafford, FL	<.0001	*
WCA3A, FL	St. Johns River, FL	<.0001	*
WCA2A, FL	Kissimmee, FL	<.0001	*
WCA3A, FL	Kissimmee, FL	<.0001	*
Yawkey, SC	WCA3A, FL	<.0001	*
Yawkey, SC	WCA2A, FL	<.0001	*
Lochloosa, FL	Kissimmee, FL	<.0001	*
MINWR, FL	Kissimmee, FL	0.0006	*
Trafford, FL	Lochloosa, FL	0.0009	*
St. Johns River, FL	Ace Basin, SC	0.0011	*
St. Johns River, FL	Lochloosa, FL	0.0047	*
Yawkey, SC	Kissimmee, FL	0.0058	*
St. Johns River, FL	Kissimmee, FL	0.0103	*
Yawkey, SC	Ace Basin, SC	0.0173	*
Yawkey, SC	Lochloosa, FL	0.027	*
Trafford, FL	Kissimmee, FL	0.0466	*
MINWR, FL	Ace Basin, SC	0.0488	*
Trafford, FL	MINWR, FL	0.0833	
MINWR, FL	Lochloosa, FL	0.1176	
St. Johns River, FL	MINWR, FL	0.2258	
Yawkey, SC	Trafford, FL	0.2309	
Yawkey, SC	St. Johns River, FL	0.4375	
Yawkey, SC	MINWR, FL	0.4482	
Trafford, FL	St. Johns River, FL	0.5163	
WCA3A, FL	WCA2A, FL	0.8861	
Lochloosa, FL	Ace Basin, SC	0.9206	



Figure 2.7. The graphical abstract of the results of Specific Aim1, experiment 1 detailed in this section.

Tissue samples

Zn was found to be in the greatest concentration of the trace elements measured in all four tissue types for all animals sampled, followed by Al in the scute, Rb in the muscle and blood, and Cu in the liver (Table 2.14 – 2.17). Mercury concentrations were highest in the liver, followed by the scute, muscle and blood samples (Table 2.14 – 2.17). The observed concentrations of mercury demonstrate that mercury is persistent across all tissues sampled, with great bioaccumulation potential in this species.

While mercury was not the trace element in the highest concentration in all samples, it is important to note that it is the highest in concentration for the toxic heavy metals (including Pb, As, Cd). Elements Sn, Cd and Mo were found in concentrations less than 200 ng/g in liver samples. Very few scute samples and no blood samples had detectable concentrations for these three elements, suggesting that the liver is the sequestration site for these elements (213).

Chromium and Co were found in consistently low concentrations across liver and muscle samples, and not detectable in blood samples; however, the greatest concentration was found in scute samples (Table 2.14 – 2.17). Blood had the lowest Al concentration, but concentrations increased from the muscle to liver to scute samples (Table 2.14 – 2.17). These data suggest that Cr, Co and Al are potentially stored and removed via keratin, which has been demonstrated in Antarctic leopard (*Hydrurga leptonyx*), Baikal (*Pusa sibirica*) and Caspian (*Pusa capica*) seals during molting (273, 274).

Vanadium was not detectable in blood and only found in the muscle of animals from the Everglades, which suggests that it is not at high enough concentrations at the

other locations to be of concern. Vanadium was also detected in scutes and consistently had the greatest concentration in liver samples, demonstrating exposure and subsequent detoxification and excretion via liver and keratin (213, 273, 274).

Lead and Se were lowest in concentration in the muscle and increased from the scute to blood with highest concentrations in liver. The elements that were not detectable in the liver, muscle or scute samples were Ni, As, and Sr, and were only detected in the blood samples (Table 2.15).

It is important to note that many elements are necessary for proper biological function, including some of the trace metals reported here. Some of the trace elements measured in these samples are known to be essential in low concentrations to a variety of physiological processes for humans, namely V, Cr, Mn, Co, Cu, Zn, Mo, and Se (275). Therefore, these elements will always be present in organisms, regardless of environment; and it is the elevated concentration, not the presence of these elements, that can lead to toxicity (275). The necessary concentration for proper biological function of these elements in humans is 100 mg/day or less, which is far less than the daily requirement for other elements, such as potassium (K), which is 4,700 mg/day (275). The concentrations measured here for the essential trace elements (Cu, Mn, Mo, Zn) in adult animals are similar to those measured by Almli, *et al.* (276) in hepatic tissue of another crocodilian apex predator, the Nile crocodile (*Crocodylus niloticus*) in Zambia. The pattern of elemental concentrations is consistent with two other studies in American alligators; however, apparent differences in the studies (i.e. laboratory based, age class, sex, tissue, and dry weight measurements) make direct comparisons difficult (182, 183).

Other trace elements, such as the toxic heavy metals Pb and Hg, are derived from the environment and are biologically detrimental in that they have no physiological purpose (277, 278). In this study, mercury was found in higher concentrations than Pb in all tissues, except blood samples, which appear to be skewed by a few abnormally high concentrations ($n = 3$) across all animals sampled ($n = 37$) (Table 2.15). Additionally, an individual alligator liver had a Pb concentration that was an order of magnitude greater than the other samples. This value was removed from the medians discussed here, but reported in Table 2.17. The overall median for both Pb and mercury was 29.7 ng/g and 243 ng/g in scute, 127 ng/g and 194 ng/g in blood, 9.10 ng/g and 328 ng/g in muscle, and 71.3 ng/g and 3590 ng/g in liver, respectively (Table 2.14 – 2.17). The concentrations of Pb observed in this study are less than those reported in the liver of ringed seals (*Phoca hispida*) in the Arctic, and the muscle concentrations are similar to what has been observed in canned tuna (55, 279). The mercury concentrations, however, are of greater concern as the muscle concentrations are similar to the concentrations found in Arctic cod (*Arctogadus glacialis*) and canned tuna, all of which are approaching the 0.5 mg/kg mark of infrequent consumption by the U.S. Food and Drug Administration, and are over the 0.3 mg/kg limit for the Danish food standards (55, 279).

Measuring this suite of trace elements in the American alligator has shown that mercury is of greater concern than any other element. This may make the alligator a worthy sentinel species for mercury exposure in the environment. This evaluation of trace elements with American alligators shows that at certain research sites, these animals are accumulating detrimental amounts of mercury, and therefore can be used to observe the

effects of chronic exposure. The concentrations of mercury observed here are also comparable to those reported in the human population. Thus, these data suggest that American alligators from the Everglades are good sentinels for chronic exposure to mercury.

Table 2.14. The individual measurements for the 37 American alligator scute, liver tissues analyzed in Experiment 2.3.

All measurements are provided in ng/g unless otherwise noted; S and A denote subadults and adults. <L denotes a concentration that was below the limit of detection

ID	Site	Age	Scute												
			Al	V	Cr	Co	Cu	Zn	Se	Rb	Mo	Cd	Sn	Pb	Hg
Gator 113	WCA3A	S	735	<L	731	142	61.0	5410	59.4	930	<L	<L	<L	66.5	1970
Gator 119	WCA3A	S	5320	<L	11000	742	<L	4440	<L	1840	121	<L	<L	0.83	1240
Gator 120	Trafford	S	2870	<L	759	392	<L	4000	125	1230	<L	<L	<L	6.92	181
Gator 122	Trafford	S	4510	19.6	2260	78.9	159	4640	92.8	871	35.4	<L	<L	29.7	166
Gator 126	WCA2A	S	1260	<L	535	367	316	5120	<L	1250	<L	<L	<L	62.0	952
Gator 132	WCA2A	S	1300	<L	424	112	104	4130	65.0	918	<L	<L	<L	45.0	374
Gator 133	Trafford	S	5940	5.73	483	107	95.4	5090	218	882	25.7	<L	<L	28.2	311
Gator 137	Trafford	S	6970	35.6	766	423	235	5900	291	771	<L	<L	<L	375	240
Gator 142	WCA3A	S	1510	17.7	273	448	205	5170	154	661	<L	<L	<L	82.4	917
Gator 143	Trafford	S	2470	16.7	784	553	85.5	4530	197	704	<L	<L	<L	13.3	109
Gator 145	WCA2A	S	1240	16.9	786	855	27.8	5850	185	935	<L	<L	<L	9.6	319
Gator 150	WCA3A	S	481	11.1	1120	465	149	4850	132	645	<L	<L	<L	36.2	525
Gator 158	WCA3A	S	1100	36.1	653	193	181	4220	152	618	4.73	<L	<L	24.6	119
Gator 159	WCA3A	S	1190	15.6	1390	1020	8.61	4440	148	919	<L	<L	<L	72.3	83.0
Gator 164	WCA3A	S	1830	50.2	336	592	45.0	6060	138	719	<L	<L	<L	12.4	111
Gator 167	Trafford	S	3520	12.2	951	189	177	3250	225	464	10.9	0.61	17.6	17.3	85.4
Gator 176	WCA3A	S	1890	17.8	1100	220	125	4620	130	573	3.56	<L	90.0	27.9	1060
Gator 031	Trafford	A	1390	<L	1110	115	265	5470	191	877	<L	<L	<L	17.2	563
Gator 036	Trafford	A	1770	4.94	344	21.2	292	4840	207	620	<L	<L	<L	98.5	370
Gator 039	Trafford	A	7080	18.0	590	47.7	159	4460	138	590	<L	<L	7.86	58.5	283
Gator 041	Trafford	A	3300	0.814	805	75.6	526	4370	149	1020	4.55	<L	19.8	21.5	62.2
Gator 042	Trafford	A	3880	11.2	248	25.2	146	4770	236	595	<L	27.5	17.7	381	384
Gator 044	Trafford	A	6850	84.1	1020	95.4	472	6430	212	751	72.9	7.06	<L	181	772
Gator 045	Trafford	A	594	<L	189	46.2	103	3840	146	664	<L	<L	11.0	17.4	264
Gator 047	Trafford	A	5350	10.1	315	17.6	195	5180	181	623	6.44	<L	<L	109	546
Gator 049	Trafford	A	21500	60.4	434	53.5	319	5080	154	619	16.0	<L	11.2	45.8	241
Gator 050	Trafford	A	1820	12.7	551	170	93.6	5120	161	917	<L	<L	<L	16.5	582
Gator 053	Trafford	A	2650	12.1	389	103	53.3	4470	118	888	<L	<L	<L	12.7	224
Gator 056	Trafford	A	2020	50.5	84.9	96.0	105	4950	214	712	<L	<L	<L	416	498
Sub Adult Range			481-6970	5.70-50.2	273-11000	78.9-1020	8.61-316	3250-6060	59.4-291	464-1840	3.56-121	-	17.6-90.0	0.827-375	83.0-1970
Sub Adult Median			1830	17.3	766	392	125	4640	148	871	18.3	0.617	53.8	28.2	311
Adult Range			594-21500	0.814-84.1	84.9-1110	17.6-170	53.3-526	3840-6430	118-236	590-1020	4.55-72.9	7.06-27.5	7.86-19.8	12.7-416	62.2-772
Adult Median			2980	12.4	412	64.6	177	4890	171	688	11.2	17.3	11.2	52.2	377
Overall Median			2020	17	653	142	149	4840	154	751	13.5	7.06	17.6	29.7	319

Table 2.15. The individual measurements for the 37 American alligator blood, samples analyzed in Experiment 2.3.

All measurement are provided in ng/g unless otherwise noted; S and A denote subadults and adults. <L denotes a concentration that was below the limit of detection

Blood												
Gator	Location	Age Class	Al	Ni	Cu	Zn	As	Se	Rb	Sr	Pb	Hg
Gator 113	WCA3A	S	27.2	10.7	239	781	52.9	130	462	216	105	900
Gator 119	WCA3A	S	49.6	10.2	274	828	48.4	137	502	208	98.9	676
Gator 120	Trafford	S	67.7	8.67	425	830	45.1	268	491	158	102	194
Gator 122	Trafford	S	26.0	10.4	310	698	50.4	162	546	142	147	141
Gator 126	WCA2A	S	37.0	9.98	318	379	45.4	136	389	451	98.9	189
Gator 127	WCA2A	S	45.4	6.20	290	894	39.0	193	635	475	104	474
Gator 132	WCA2A	S	28.0	10.9	320	1230	56.4	179	684	506	105	376
Gator 133	Trafford	S	78.7	8.23	339	667	43.5	193	561	157	127	175
Gator 137	Trafford	S	33.0	7.89	336	709	42.9	188	558	144	1780	143
Gator 142	WCA3A	S	76.7	8.07	318	863	44.8	155	526	225	129	559
Gator 143	Trafford	S	65.1	17.7	387	1080	47.4	218	523	166	136	147
Gator 145	WCA2A	S	70.1	7.98	348	1070	48.4	177	609	514	130	253
Gator 150	WCA3A	S	26.2	8.26	343	848	49.0	137	570	259	127	425
Gator 151	WCA3A	S	51.2	9.3	368	844	49.4	165	993	178	138	1380
Gator 156	WCA2A	S	57.7	8.14	262	748	46.6	149	495	415	129	737
Gator 158	WCA3A	S	38.0	11.7	330	677	43.1	138	477	278	130	56.4
Gator 159	WCA3A	S	53.8	8.37	353	858	79.1	194	812	198	170	80.8
Gator 164	WCA3A	S	67.4	8.28	354	918	46.6	151	467	281	136	68
Gator 167	Trafford	S	108	7.73	366	742	43.8	228	516	157	134	101
Gator 176	WCA3A	S	44.1	4.43	267	877	39.9	144	546	228	126	581
Gator 016	St. Johns	A	59.9	4.33	131	520	25.0	95.7	415	300	178	101
Gator 020	St. Johns	A	21.7	3.45	179	1220	78.5	303	839	861	76.9	195
Gator 023	St. Johns r	A	8.89	1.70	165	704	23.2	156	603	336	33.3	93.9
Gator 026	Lochloosa	A	29.9	11.9	225	910	40.8	210	1250	148	85.2	251
Gator 031	Trafford	A	13.0	13.6	340	869	64.6	222	551	152	109	280
Gator 036	Trafford	A	103	8.85	282	706	51.0	197	427	155	105	158
Gator 039	Trafford	A	1.54	10.3	246	573	49.5	185	404	137	200	184
Gator 041	Trafford	A	7.03	13.9	365	932	67.9	196	975	216	171	67.4
Gator 042	Trafford	A	30.8	6.19	181	528	30.8	186	473	109	3810	172
Gator 044	Trafford	A	<L	7.08	259	592	44.4	183	404	137	114	247
Gator 045	Trafford	A	43.4	6.15	166	593	26.0	160	412	89.6	38.1	222
Gator 047	Trafford	A	14.9	6.70	212	541	33.3	174	406	106	305	203
Gator 049	Trafford	A	0.835	7.60	440	785	46.2	188	427	125	101	136
Gator 050	Trafford	A	13.1	3.52	174	622	29.2	162	533	87.8	37.8	359
Gator 053	Trafford	A	31.6	8.89	275	678	46.7	161	594	134	102	134
Gator 056	Trafford	A	53.7	9.12	353	650	49.6	221	471	159	4470	197
Gator 060	Lochloosa	A	98.7	9.52	385	1020	52.8	271	1180	158	110	141
Sub Adult Range			26.0-108	4.43-17.7	239-425	379-1230	39.0-79.1	130-268	389-993	142-514	98.9-1780	56.4-1380
Sub Adult Median			50.4	8.33	333	837	46.6	164	536	221	129	224
Adult Range			0.835-103	1.70-13.9	131-440	520-1220	23.2-78.5	95.7-303	404-1250	87.8-861	33.3-4470	67.4-359
Adult Median			25.8	7.60	246	678	46.2	186	473	148	109	184
Overall Median			40.7	8.28	318	781	46.6	179	526	166	127	194

Table 2.16. The individual measurements for the 37 American alligator muscle tissues analyzed in Experiment 2.3.

All measurement are provided in ng/g unless otherwise noted; S and A denote subadults and adults. <L denotes a concentration that was below the limit of detection

ID	Location	Age	Muscle										
			Al	V	Cr	Co	Cu	Zn	Se	Rb	Sn	Pb	Hg
Gator 113	WCA3A	S	171	<L	11.3	<L	91.0	12300	18.5	2260	<L	7.29	1070
Gator 119	WCA3A	S	122	<L	6.42	<L	314	11000	40.5	3830	1.0	11.2	631
Gator 120	Trafford	S	98.8	7.8	35.8	9.02	158	8680	133	3220	<L	1.71	275
Gator 122	Trafford	S	145	<L	4.69	132	46.6	7640	86.2	3480	<L	3.55	129
Gator 126	WCA2A	S	436	<L	20.4	30.4	1390	9410	61.6	3090	2.8	124	683
Gator 127	WCA2A	S	302	<L	27.1	59.9	198	10900	59.0	3290	<L	17.7	543
Gator 132	WCA2A	S	140	<L	6.57	61.2	361	6160	80.9	3160	<L	6.16	263
Gator 133	Trafford	S	231	<L	8.82	59.3	52.1	6600	77.7	3810	0.1	10.8	219
Gator 137	Trafford	S	53.3	<L	17.6	9.63	56.6	9200	115	3100	<L	9.31	170
Gator 142	WCA3A	S	380	<L	64.8	58.9	200	10400	71.1	2750	<L	2.59	542
Gator 143	Trafford	S	74.2	<L	74.2	63.8	73.9	6100	69.3	2890	<L	3.89	162
Gator 145	WCA2A	S	17.0	<L	55.6	6.89	113	5180	76.5	3030	<L	3.95	189
Gator 150	WCA3A	S	188	1.3	234	41.0	141	7560	40.0	2890	31.3	25.3	501
Gator 151	WCA3A	S	70.5	<L	11.6	75.6	266	11000	71.1	4040	<L	8.89	1180
Gator 156	WCA2A	S	65.3	<L	15.3	41.2	45.9	10200	49.3	2480	<L	1.40	766
Gator 158	WCA3A	S	183	<L	19.7	135	2560	10500	41.4	2290	<L	19.1	66.5
Gator 159	WCA3A	S	8.45	<L	23.9	6.82	97.0	6370	105	7740	<L	2.79	127
Gator 164	WCA3A	S	1740	3.3	53.3	61.5	1970	7190	43.6	2170	<L	112	61.5
Gator 167	Trafford	S	77.9	0.1	52.1	22.7	74.0	6670	177	2590	0.9	2.73	110
Gator 176	WCA3A	S	1040	1.7	280	76.6	1350	8320	58.2	2410	<L	29.7	534
Gator 016	St. Johns	A	163	<L	10.8	7.93	29.3	14500	37.9	2900	<L	3.28	188
Gator 020	St. Johns	A	984	<L	<L	0.767	39.4	9940	121	4120	<L	21.7	201
Gator 023	St. Johns	A	600	<L	25.2	<L	924	14100	60.8	4280	<L	54.6	117
Gator 026	Lochloosa	A	109	<L	<L	<L	190	27300	122	8810	7.8	112	243
Gator 031	Trafford	A	185	<L	10.0	<L	122	15400	120	2220	<L	4.82	318
Gator 036	Trafford	A	61.1	<L	0.109	<L	35.5	16100	105	1720	<L	2.13	191
Gator 039	Trafford	A	368	<L	31.9	<L	48.3	30600	68.7	1490	<L	5.80	255
Gator 041	Trafford	A	236	<L	10.8	<L	86.8	11800	98.2	4020	<L	<L	45.3
Gator 042	Trafford	A	325	<L	106	<L	37.6	13000	110	1940	<L	66.9	201
Gator 044	Trafford	A	156	<L	19.0	<L	56.0	18800	96.3	2220	<L	<L	432
Gator 045	Trafford	A	206	<L	20.3	<L	45.9	12300	119	2100	<L	0.195	293
Gator 047	Trafford	A	128	<L	6.11	<L	54.6	17300	110	2110	<L	23.4	343
Gator 049	Trafford	A	314	<L	16.7	<L	61.2	7710	97.8	1670	<L	<L	153
Gator 050	Trafford	A	32.3	<L	6.16	<L	30.0	8660	122	2520	<L	<L	347
Gator 053	Trafford	A	50.3	<L	57.4	37.3	<L	7620	44.0	1200	<L	<L	129
Gator 056	Trafford	A	428	<L	37.0	<L	46.7	15100	111	2120	<L	33.3	329
Gator 060	Lochloosa	A	107	<L	<L	20.2	21.1	12400	97.3	4580	<L	96.0	117
Sub Adult Range			8.45-1740	0.090-7.81	4.69-280	6.82-135	45.9-2560	5180-12300	18.5-177	2170-7740	0.110-31.3	1.40-124	61.5-1180
Sub Adult Median			143	1.66	22.2	59.1	150	8500	70.2	3060	1.02	8.09	269
Adult Range			32.3-984	-	0.109-106	0.767-37.3	21.1-924	7620-30600	37.9-122	1200-8810	-	0.195-112	45.3-201
Adult Median			185	-	17.9	14.1	47.5	14100	105	2220	7.78	22.6	201
Overall Median			163	1.66	20.0	41.1	80.4	10400	80.9	2890	1.89	9.10	243

Table 2.17. The individual measurements for the 37 American alligator liver tissues analyzed in Experiment 2.3.

All measurement are provided in ng/g unless otherwise noted; Age class is noted in preceding tables. <L denotes a concentration that was below the limit of detection. * denotes the Pb value reported herein, but removed from the range and calculations.

Liver															
ID	Site	Al µg/g	V	Cr	Mn	Co	Cu µg/g	Zn µg/g	Se µg/g	Rb µg/g	Mo	Cd	Sn	Pb	Hg µg/g
Gator 113	WCA3A	0.5	85.5	16.1	<L	72.5	14.1	19.0	1.9	3.0	157	10.6	11.7	28.5	7.3
Gator 119	WCA3A	1.4	450	17.0	<L	259	10.5	21.6	1.3	3.5	67.2	15.8	0.7	38.2	5.3
Gator 120	Trafford	2.1	191	23.1	125	37.5	13.8	19.9	1.7	3.9	55.5	6.69	<L	6.63	1.8
Gator 122	Trafford	3.0	241	20.3	96	2.74	26.8	20.1	1.5	5.6	193	33.1	6.4	349	1.9
Gator 126	WCA2A	0.3	26.7	26.4	336	35.0	32.0	19.6	1.3	3.8	86.3	26.2	5.3	63.2	2.9
Gator 127	WCA2A	1.2	395	23.5	305	<L	40.6	19.1	2.9	5.5	172	18.6	9.0	49.6	7.3
Gator 132	WCA2A	2.6	31.2	105	761	12.7	25.6	19.0	1.1	4.1	88.8	12.7	11.5	4.84	1.3
Gator 133	Trafford	1.7	225	16.3	<L	77.6	18.6	29.3	1.3	3.8	80.2	22.5	3.1	9.82	1.6
Gator 137	Trafford	1.6	212	18.4	102	39.8	73.6	18.2	1.4	3.1	112	16.1	19.8	1940	1.7
Gator 142	WCA3A	0.3	115	18.3	283	33.3	10.4	16.6	1.7	3.1	84.1	25.9	15.0	81.5	5.5
Gator 143	Trafford	2.3	297	42.8	348	<L	23.7	20.5	1.4	4.4	116	11.0	1.2	13.3	1.4
Gator 145	WCA2A	4.6	40.2	14.8	497	37.0	11.8	16.3	0.9	5.6	66.7	8.72	<L	15.4	0.8
Gator 150	WCA3A	2.8	79.6	9.45	428	22.8	31.0	23.2	1.3	3.7	125	8.44	1.3	35.8	3.7
Gator 151	WCA3A	6.8	205	33.4	107	12.4	47.4	16.9	3.3	6.9	177	32.2	13.2	186	14
Gator 156	WCA2A	1.3	57.2	26.3	92	46.1	52.9	15.5	1.2	3.8	69.7	10.2	0.2	12.4	3.6
Gator 158	WCA3A	5.9	279	55.9	90	224	68.8	22.3	1.0	3.1	65.9	39.6	31.9	75.2	1.0
Gator 159	WCA3A	1.6	212	101	24	105	36.5	20.0	1.3	11	105	68.4	15.1	222	1.2
Gator 164	WCA3A	1.3	406	25.0	665	12.2	75.3	18.5	0.9	2.3	66.8	13.2	2.4	18.7	0.9
Gator 167	Trafford	2.3	768	30.4	241	3.21	42.1	22.0	1.9	3.4	169	56.6	15.2	67.4	2.5
Gator 176	WCA3A	0.7	143	20.8	147	50.0	89.3	17.8	2.2	3.0	83.2	17.6	2.4	15.7	6.9
Gator 016	St. Johns	3.1	297	15.1	63	<L	10.3	18.8	1.6	4.4	198	12.6	8.9	1940	3.0
Gator 020	St. Johns	6.4	699	9.12	<L	<L	21.1	21.4	2.4	5.6	84.5	19.3	8.2	866	3.6
Gator 023	St. Johns	9.7	278	15.7	28	<L	12.0	21.9	1.4	5.1	105	8.51	23.5	158	1.8
Gator 026	Lochloos	1.2	545	19.3	760	<L	4.0	17.1	2.6	8.4	97.4	14.2	12.0	551	4.9
Gator 031	Trafford	1.6	329	6.62	145	7.69	9.1	22.8	2.6	2.6	148	26.4	6.6	192	4.7
Gator 036	Trafford	2.8	401	109	308	<L	13.5	22.1	3.3	8.1	209	51.5	17.6	673	6.4
Gator 039	Trafford	4.7	736	22.9	<L	<L	6.3	26.2	3.9	2.2	318	20.9	13.7	2900	9.5
Gator 041	Trafford	1.0	210	9.29	219	11.0	6.81	18.9	0.9	4.4	79.7	6.51	<L	28.1	0.7
Gator 042	Trafford	2.1	542	23.0	<L	69.2	4.03	27.0	2.7	2.5	211	15.9	4.5	3440	4.7
Gator 044	Trafford	1.2	262	48.9	41	<L	8.11	33.8	2.9	2.1	130	17.6	7.9	200	6.7
Gator 045	Trafford	3.1	448	27.4	<L	<L	6.46	21.8	2.5	2.5	214	16.1	4.7	84.3	4.6
Gator 047	Trafford	2.2	598	14.0	308	<L	4.72	23.0	4.6	2.1	189	14.2	5.8	1190	11
Gator 049	Trafford	9.1	819	39.6	474	<L	18.5	23.9	1.8	2.1	174	28.9	7.8	41.0	3.9
Gator 050	Trafford	1.5	322	8.22	252	<L	6.95	19.5	2.2	4.3	194	30.2	8.1	18.5	3.7
Gator 053	Trafford	3.9	739	35.7	83	76.8	34.8	25.1	2.2	4.1	269	27.9	15.6	128	3.1
Gator 056	Trafford	2.5	323	22.6	154	32.8	6.08	20.4	3.5	2.5	175	18.1	9.60	12100*	6.4
Gator 060	Lochloos	0.6	57.2	16.4	153	47.4	4.37	12.4	1.0	9.7	43.7	5.38	<L	56.3	0.6
Sub Adult Range		0.1 -	26.7- 768	9.45- 105	24.0 -761	2.74- 259	4.74- 4.21	1.5- 29.3	0.9- 3.3	2.3 5	55.5- 193	6.69- 68.4	0.23 9-	4.84- 1940	0.8- 1.4
Sub Adult Median		0.9	209	23.3	241	37.3	14.0	19.4	1.3	3.8	87.6	16.9	7.71	37.0	2.2
Adult Range		0.6 -	57.2- 819	6.62- 109	27.6- 760	7.69- 76.8	4.0- 34.8	12.4- 33.8	0.9- 4.6	2.1- 9.7	43.7- 318	5.38- 51.5	4.48- 23.5	18.5- 3400	0.6- 11.
Adult Median		2.8	401	19.3	154	40.1	6.95	21.9	2.5	4.1	175	17.6	8.21	196	4.6
Overall Median		1.6	279	22.6	187	37.3	10.4	20.1	1.7	3.8	116	17.6	8.21	71.3	3.6

Tissue correlations

Correlations of elemental concentrations among the tissues were assessed to better inform monitoring efforts and human consumption advisories, using 37 alligators collected across Florida. The concentrations of trace elements between tissues were tested using a Spearman correlation with statistical significance defined as a $p < 0.05$. This analysis found six elements to have statistically significant correlations in the alligator samples, Al, Rb, Zn, Se, Hg, and Pb (Table 2.18). While concentrations are dependent on the element and the tissue, concentration rankings were established. Selenium and Pb had the lowest concentrations in the muscle tissue, whereas the blood contained the lowest concentration of Hg, Se, and Al. These data suggest that Se and Pb are not bioaccumulated in the muscle tissue, even with the higher concentrations that were found in the blood. Previous studies of Pb in alligator tissue found similar results with the lowest concentrations noted in muscle (91).

Predictively, the lowest concentrations of most elements were determined in the blood, as observed with other contaminants, since blood is a dynamic bio-fluid reflective of circulating contaminants and thus has a low accumulation potential comparatively (145, 280). The highest concentrations of Hg, Rb, Zn, Pb and Se were all obtained from the liver tissues, further supporting previously reported Se and mercury high concentrations in the liver (91). Zinc was also found to be the element of highest concentration across all four tissues, followed by Rb in blood, muscle and liver, but by Al in scute (Table 2.18).

Differences were observed in the elemental rankings for the adult compared to the sub-adult alligators; however, these unexpected results are likely due to the different

sampling locations for the subadult and adult animals and are not indicative of an inherent age class difference in trace element biodistribution (Table 2.6). Sampling different age classes at different sites was not intentional, and was the result of opportunistic necropsy when time, staff and resources permitted. Alligators were also only chosen for this experiment if all four tissues (blood, all three scutes, liver and muscle) samples were intact and not compromised between the collection, transport and storage stages of sample collection. The rankings for Hg, Rb, Zn, and Al were consistent for adults and subadults, suggesting that the biodistribution of these elements does not change with age, despite the site-specific differences in this data set (Table 2.6).

The data for all elemental concentrations were log transformed to determine tissue patterns (Figure 2.8). Liver tissues generally had the highest concentration for most elements (9 of 16 elements), which was expected since the liver is a detoxification organ and is known to bioaccumulate high concentrations of many elements (213).

For the six trace elements with significant correlations, Se and Hg appear to co-vary across all four tissues analyzed, a relationship that has been previously described for many animals (Figure 2.9) (82, 183, 188, 281-283). Selenium (Se) is thought to have a protective effect against the toxicity of mercury, which may explain the covariance observed for these elements (Figure 2.9) (201, 270). Rubidium (Rb) and Zn also appear to have the same order in biodistribution, highest in liver and muscle and lowest in blood (Figure 2.8 & 2.9). This potentially is an effect of both elements being present in the alligator's main prey items at all locations and bioaccumulation within the tissues. Lead (Pb) and Al do not appear to co-vary with any of the other four elements that had significant tissue relationships (Se, Hg, Rb and Zn) (Figure 2.9). Aluminum was

significant between the liver and scute tissue (Table 2.19). The effect of Al on reptiles is not well documented in the literature. High concentrations of Al in humans has been associated with certain disease outcomes such as Alzheimer’s disease, but the concentrations we detected here are less than those in the human study and are found in different tissues (284). Lead concentrations, however, have been consistently lower than other trace elements measured in other reptiles, such as snakes and small lizards, so our results are not irregular and demonstrate that there is likely no source of Pb contamination in the sampled sites (285, 286).

These results suggest that American alligators are a good sentinel species for mercury exposure since they are exposed to high concentrations in their natural environment and there are statistically significant relationships between the concentrations in all four tissues examined.

Table 2.18. The median tissue concentration, minimum and maximum (ng/g, w/w), and average ranking for the six trace elements with statistically significant correlations in American alligator samples.

Element	Blood	Muscle	Liver	Scute	Tissue Rank
Se	179.4 (95.7-193.7)	80.9 (18.5-177.5)	1738.8 (899.7-4616)	153.9 (59.4-291.4)	M<S<B<L
Hg	193.7 (56.4-1380)	243.1 (45.3-1183)	3594.1 (566.8-14293.0)	318.5 (62.2-1965.9)	B<M<S<L
Rb	525.8 (389.4-1251.9)	2893.8 (1203.1-8812.3)	3760.6 (2063.0-10507.3)	750.8 (463.9-1841.2)	B<S<M<L
Zn	781.1 (379.3-1227.5)	10443.1 (5180.5-30640.7)	20145.1 (12396.8-33759.5)	4839.8 (3247.5-6428.9)	B<S<M<L
Pb	126.5 (33.3-4470.4)	9.1 (0.2-123.6)	75.2 (4.8-12050.2)	29.6 (0.8-415.6)	M<S<B<L
Al	40.7 (0.8-108.0)	163.1 (8.5-1744.2)	1604.5 (129.3-12064.1)	2015.5 (480.7-21525.8)	B<M<L<S
Elemental Rank	Al<Se<Hg<Pb<Rb<Zn	Pb<Se<Al<Hg<Rb<Zn	Pb<Se<Al<Hg<Rb<Zn	Pb<Se<Hg<Rb<Al<Zn	

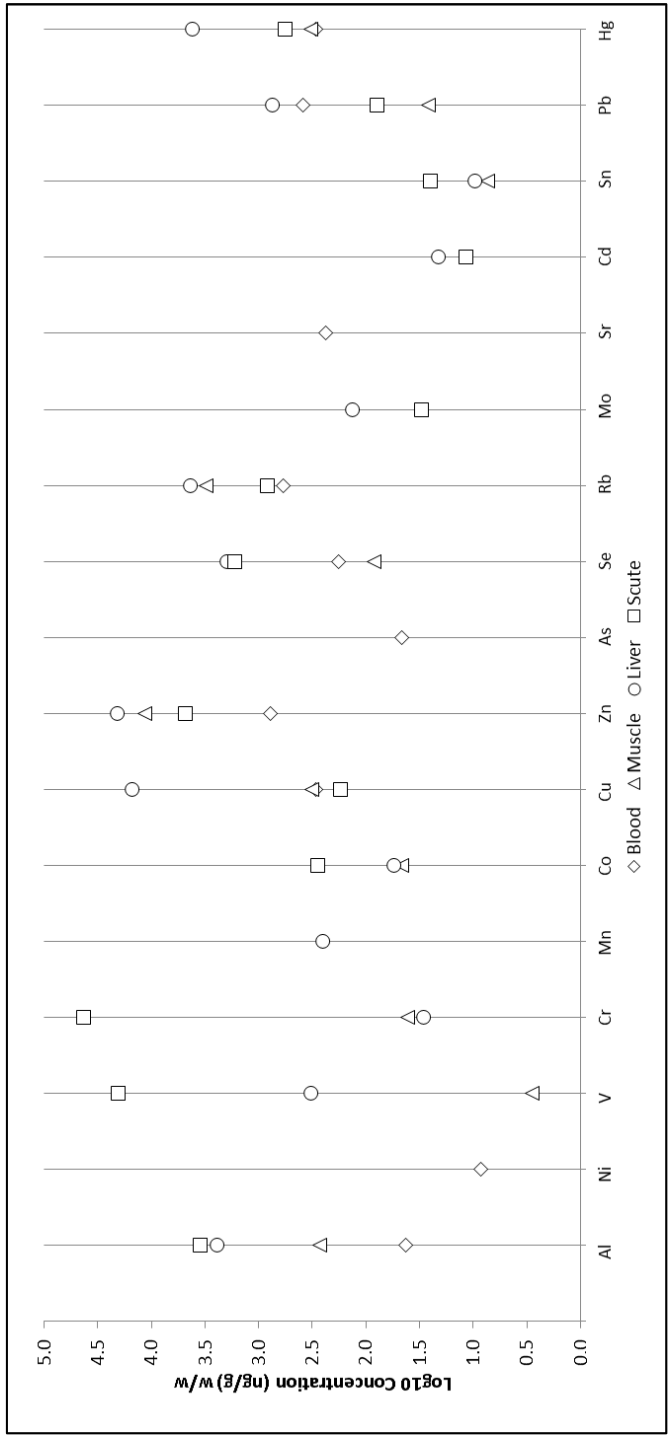


Figure 2.8. Scatter plot of the log transformed tissue averages of each trace element measured in American alligator tissue samples.

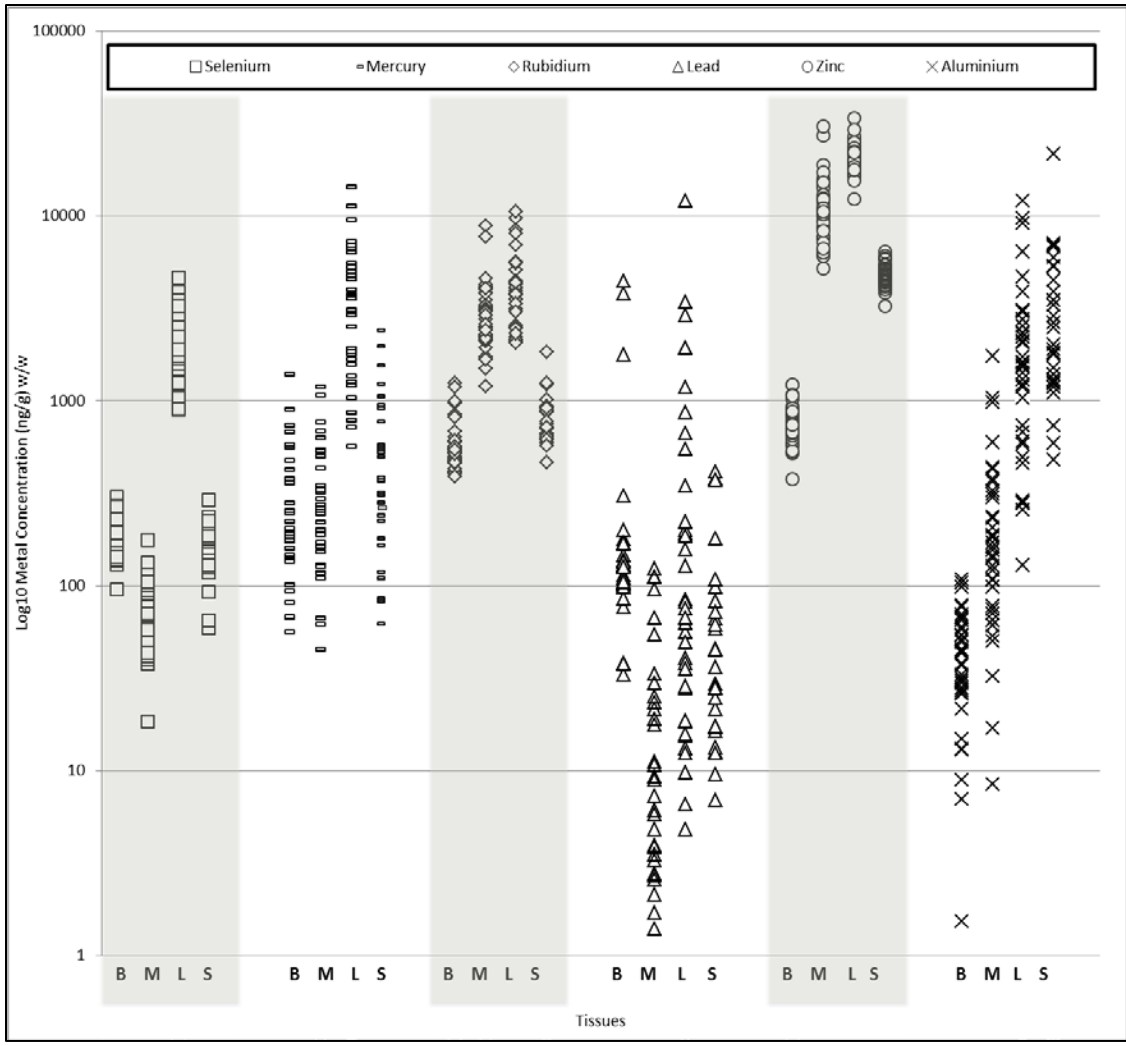


Figure 2.9. Scatter plot of the statistically significant tissue correlations for trace elements in American alligator samples. B, M, L and S represent blood, muscle, liver and scute, respectively.

Table 2.19. The spearman correlation results for significant relationships found for the trace elements measured in whole blood and tissues from the American alligator.

Statistically significant relationships are denoted with bold text ($\alpha = 0.05$)

Element	Tissue Comparison		Spearman's rho	p-value
Aluminum (Al)	Muscle	Liver	0.110	0.52
	Scute	Liver	0.547	<0.01
	Scute	Muscle	0.039	0.84
	Blood	Liver	-0.263	0.12
	Blood	Muscle	-0.274	0.10
	Blood	Scute	-0.241	0.21
Copper (Cu)	Muscle	Liver	0.276	0.11
	Scute	Liver	-0.208	0.31
	Scute	Muscle	-0.025	0.90
	Blood	Liver	0.209	0.22
	Blood	Muscle	0.258	0.13
	Blood	Scute	0.031	0.88
Lead (Pb)	Muscle	Liver	0.176	0.34
	Scute	Liver	0.616	0.00
	Scute	Muscle	0.225	0.29
	Blood	Liver	0.357	0.03
	Blood	Muscle	-0.067	0.72
	Blood	Scute	0.424	0.02
Rubidium (Rb)	Muscle	Liver	0.838	<0.01
	Scute	Liver	0.569	0.00
	Scute	Muscle	0.604	0.00
	Blood	Liver	0.782	<0.01
	Blood	Muscle	0.718	<0.01
	Blood	Scute	0.334	0.08
Selenium (Se)	Muscle	Liver	0.324	0.05
	Scute	Liver	0.246	0.22
	Scute	Muscle	0.420	0.03
	Blood	Liver	0.215	0.21
	Blood	Muscle	0.754	<0.01
	Blood	Scute	0.479	0.01
Zinc (Zn)	Muscle	Liver	0.113	0.51
	Scute	Liver	-0.120	0.54
	Scute	Muscle	0.158	0.41
	Blood	Liver	-0.491	<0.01
	Blood	Muscle	-0.390	0.02
	Blood	Scute	-0.082	0.67
Vanadium (V)	Muscle	Liver	-0.100	0.87
	Scute	Liver	0.039	0.86
	Scute	Muscle	0.800	0.20
Chromium (Cr)	Muscle	Liver	0.227	0.20
	Scute	Liver	-0.093	0.63
	Scute	Muscle	-0.087	0.65
Cobalt (Co)	Muscle	Liver	-0.181	0.47
	Scute	Liver	0.205	0.36
	Scute	Muscle	-0.331	0.19
Molybdenum (Mo)	Scute	Liver	0.152	0.68
Cadmium (Cd)	Scute	Liver	-1.000	<0.01
Tin (Sn)	Muscle	Liver	-0.143	0.79
	Scute	Liver	-0.600	0.21
Mercury (Hg)	Liver	Blood	0.617	<0.01
	Muscle	Blood	0.916	<0.01
	Muscle	Liver	0.711	<0.01
	Scute	Blood	0.892	<0.01
	Scute	Liver	0.698	<0.01
	Scute	Muscle	0.942	<0.01

Using the correlative relationships for biomonitoring

Blood and scute can be routinely sampled for monitoring wild populations without sacrificing animals (287, 288). These routine samples can elucidate the concentrations of Hg, Se, Rb and Zn within muscle tissue (Table 2.19). Blood sample concentrations can be used to infer the muscle concentration of Hg, Se, Rb and Zn, while scute sample concentrations can be used to infer the muscle concentration of Hg, Se and Rb (Figure 2.10). The association of the concentration between scute and muscle that we provide in Figure 2.10 are based on statistical significance ($p \leq 0.05$, using the Pearson correlation). Thus, the concentration in scute could be used for estimating the muscle burden of each trace element in alligator populations but it should be done with caution, as the correlation for mercury is much more direct than it is for Rb, Se or Zn.

The equations are provided to aid in the routine monitoring of alligators but not replace the periodic analysis of the internal tissues to verify the relationship provided here (Figure 2.10, insets). The linear relationship we see in this study would likely change based on habitat characteristics and prey consumption in different locations.

The biodistribution trends demonstrated with the tissue samples for six trace elements, Hg, Se, Rb, Zn, Pb and Al, are the first reported, specifically using routinely collected non-invasive monitoring samples for American alligators. Lead and Al are included because while they did not have a significant relationship between the muscle and blood or scute tissues, there was a significant relationship observed for the liver. The correlative relationships observed in this study for mercury are mirrored in other reptilian studies in blood and scute samples from sea turtles (*Caretta caretta*) and with blood, keratin, liver and muscle of the black caiman (*Melanosuchus niger*) from the Amazon

(289, 290). A relationship for Hg, Se, and Rb, as well as several other elements, has been observed in blood and skin samples from bottlenose dolphins (*Tursiops truncatus*) (171). Previous studies have measured trace metals (Ca, Zn, Mg, Se, Cu and Fe; As, Se, Cd, Se and V) within alligators; however, they utilized other tissues that are not included in this study (plasma only), or calculate the measurements based on dry weight, so a direct comparison cannot be made (182, 183).

On the other hand, the trends and values observed previously for Zn and Se, in both liver and blood samples, are reflected in the data reported here. These findings suggest that these essential trace elements have a consistent pattern for crocodylians, including the American alligator as well as the Nile crocodile (183, 276). Other reptilian studies generally focus on smaller, softer bodied reptiles with shorter lifespans than alligators, which make comparisons difficult (285, 286). Squamate reptiles have shown a similar correlative relationship (between liver, kidney and gonad) to the relationship between liver and kidney in American alligators shown previously and to those that we highlight here (182, 285). However, the concentrations in the present study are orders of magnitude higher those reported for the squamate reptiles. The alligator is an upper level predator, bioaccumulating a lifetime of exposure in a vastly different ecosystem.

The correlative relationships between the blood, scute, muscle and liver samples observed in this study will enable previously published data using one of the tissues a mechanism of comparison to other relevant studies. Liver sample concentrations were significantly correlated to the concentration of Al, Pb, Rb, Se, Zn and Hg in at least scute or blood samples, if not all other measured tissues (Table 2.19). This relationship will

provide an important link between historic studies using liver samples and recent studies using only non-invasive samples.

The correlative relationships between the blood, scute and muscle samples will allow a more comprehensive monitoring effort to take place by using the linear equations identified with this experiment (Figure 2.10, insets). Use of these equations will allow muscle element concentrations, particularly mercury, to be inferred from a routinely collected blood sample. The enhanced monitoring effort will not only provide information for human consumption advisories; it will also provide enhanced mercury data for this species and support the use of alligators as a sentinel for mercury exposure.

The two experiments in this section describe the current trace element burden in American alligators along the Southeastern Atlantic coast of the United States. The first experiment detailed the trace element concentrations in blood samples. These samples allowed a comprehensive analysis of the trace element burden in this upper trophic level predator, and resulted in mercury being identified as the most concentrated trace element, with detrimental concentrations being observed in the Everglades. The second experiment, which detailed the biodistribution of mercury within the tissues of the American alligator, provides useful information that can be used for expanded biomonitoring efforts and human health advisory updates. This experiment also shows that the biodistribution of trace elements in alligators is similar to what has been found in other wildlife species and humans (Figure 2.11). The data from both of these experiments would have been strengthened by having both age classes represented, and if there had been even samples sizes, at all sites.

If the blood sample study is redone, an effort can be made to recapture the same animals that blood samples were taken from, to monitor how quickly the mercury burden within animals and across sites fluctuates. A follow up study like this would determine how frequently updated measurements need to be conducted to improve monitoring. If the biodistribution study were conducted again, additional age classes (i.e. neonate, and juvenile) could be included, to determine if the biodistribution changes throughout the alligator lifespan. Multiple age classes would have to be collected from several sites to make this study robust, and remove site specific effects from the overall analysis.

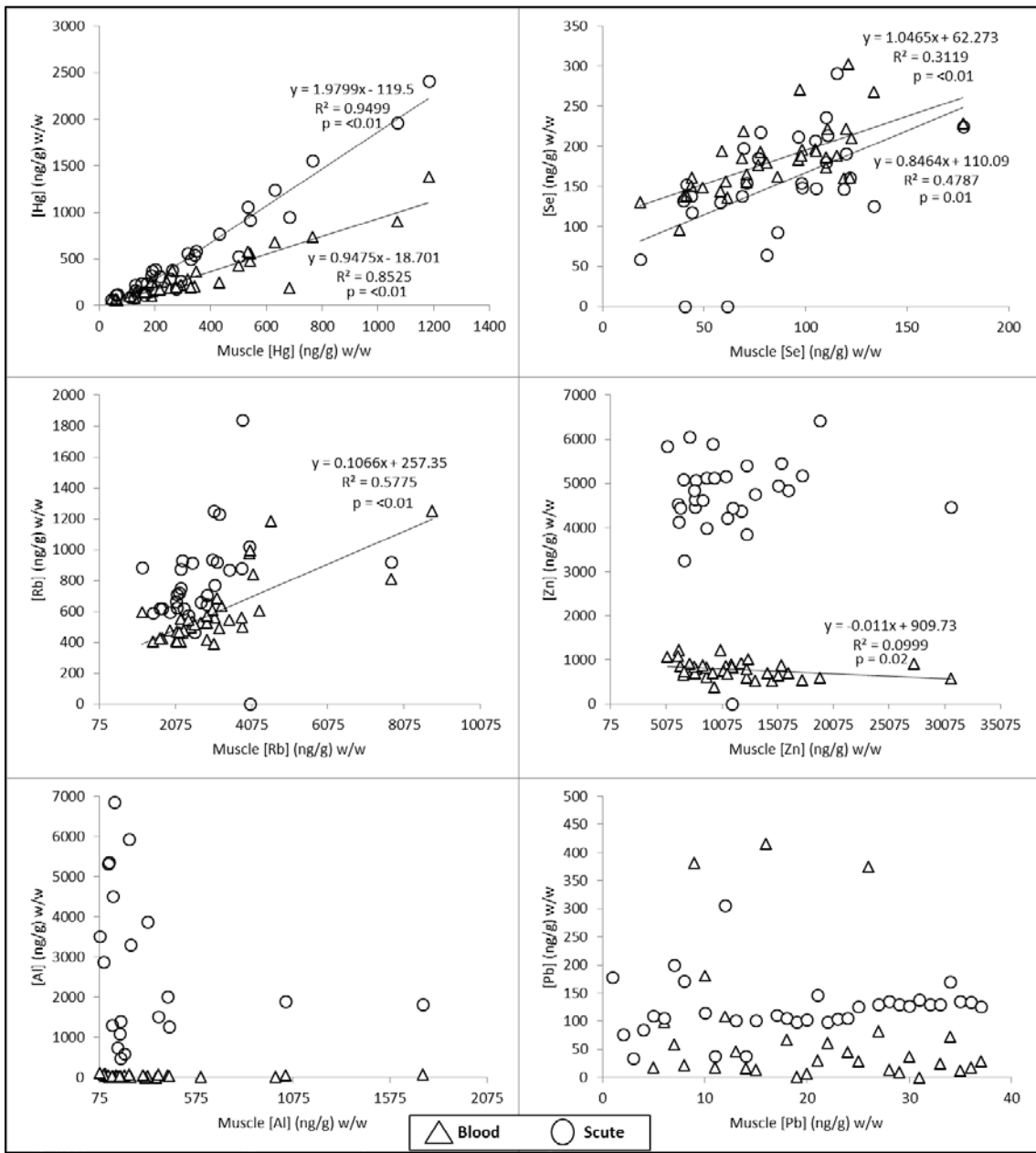


Figure 2.10. American alligator tissue correlations (whole blood and scute tissue vs. muscle tissue) for trace elements (Hg, Se, Rb, Zn, Al, Pb), where statistically significant relationships were observed (Table 2.16). Trend lines, equations and R values are given for those tissues that had a statistically significant correlation.



Figure 2.11. The graphical abstract of the results of Specific Aim 1, experiment 2 detailed in this section.

2.4. Assessing if seasonal changes in mercury concentration exist in alligators

2.4.1. Introduction

In the previous experiment, it was shown that mercury is the trace element of most concern for alligators along the southeastern Atlantic coast of the United States. While mercury was not the highest concentrated of all measured trace elements, it is the highest concentrated of the toxic heavy metals measured (As, Cd, Pb and Hg; Table 2.13). The other toxic heavy metals, despite also being naturally derived and atmospherically transported, are in lower concentrations in alligators in this part of the world (291).

Mercury is a well-established global pollutant with the ability to elicit a myriad of deleterious effects on highly exposed organisms (101, 113, 114, 116, 292, 293). Some studies have shown that mercury can affect seasonal behaviors, such as reproduction, however, these studies have only been conducted in the laboratory over short time periods (105, 113, 116). Here we have the opportunity to examine the potential seasonal changes in mercury concentration in a free ranging population throughout a multi-year sampling regime. Most wildlife species that are used to monitor mercury in the environment are captured seasonally based in their proximity to collection locations or their accessibility in the environment (294, 295). For these reasons, continually sampling one population of animals throughout all four seasons is difficult. At Merritt Island National Wildlife Refuge (MINWR) in Florida, there is a constantly monitored population of alligators that provides this opportunity.

The total mercury concentration found in the blood samples of American alligators is reflective of the mercury burden of their internal tissues, and routine

monitoring can be conducted more easily with this newfound information. As a result, it is important to determine if there are seasonal fluctuations that will confound routine monitoring efforts and reduce the utility of the American alligator as a sentinel for the human health effects of chronic dietary mercury exposure. If seasonal fluctuations in mercury concentrations are found, specific seasons may have to be utilized for human health comparisons, to make the most correct comparison.

2.4.2. Experiment specific methods

Sample selection & preparation

Blood samples were collected during the period 2007 - 2014 at MINWR, using the method described in section 2.2.1. The samples were kept on wet ice until being stored at -20 °C until analysis.

Each year (2007 – 2014) was divided into four seasons: winter (December - March), spring (March - May), summer (June - August) and fall (September – November). At least two adult male and two adult female blood samples were chosen from each season/year. Some seasons did not have representative samples as the quality of the samples while in storage was not optimal, and some vials were cracked and broken. There were also some seasons that were not able to be located in storage and were omitted from this analysis. This resulted in the omission of five total seasons; summer and fall of 2011 and spring, summer and fall of 2013. All individuals that were used in this experiment are listed in Table 2.20, $n = 174$ individual alligators. Over the 7 years that animals were sampled for this experiment, 18 alligators were recaptured (indicated by an R in Table 2.20), for a total of 192 unique blood samples. The recaptured

samples were included as they provide the opportunity to observe change in mercury concentration over time within the same alligator.

Blood samples were thawed to room temperature and gently rocked for 30 s for homogenization of the whole blood and sub-sampled following the method described in section 2.2.2.

Table 2.20. The metadata for all alligators from MINWR used in Experiments 2.4 and 2.5, collected from 2007-2014.

NASA ID*	SEX	Date	Latitude	Longitude	Hg (ng/g)	SVL (cm)	TG (cm)	Status	BMI
NASA5609R	MALE	1/9/2012	28.50915	-80.64557	209.2	154	41.9	Low	0.136
NASA5688R	FEMALE	8/4/2014	28.53594	-80.61543	230.2	124	37.5	Low	0.151
NASA5910	FEMALE	2/28/2014	28.60286	-80.65042	493.7	127	39	Low	0.154
NASA5265	MALE	9/12/2008	28.50765	-80.67764	509.7	156	48	Low	0.154
NASA5539	MALE	2/25/2010	28.594	-80.65428	691.3	156	50	Low	0.160
NASA5087	MALE	1/29/2008	28.5628	-80.6497	151.0	170	55	Low	0.162
NASA5517R	MALE	5/22/2014	28.50828	-80.643777	194.1	174	56.5	Low	0.162
NASA5941	MALE	12/10/2014	28.59447	-80.65428	178.7	153	50	Low	0.163
NASA5818	FEMALE	2/8/2013	28.6024	-80.6604	331.0	112	37	Low	0.165
NASA5164R	MALE	1/26/2009	28.58928	-80.61882	237.6	160	53	Low	0.166
NASA5214	FEMALE	6/25/2008	28.35006	-80.36334	180.5	107	36	Low	0.168
NASA5918	FEMALE	4/17/2014	28.56174	-80.71007	384.0	121	41	Low	0.169
NASA5517R	MALE	4/4/2014	28.50824	-80.64376	251.9	172	59.5	Low	0.173
NASA5105R	MALE	1/23/2013	28.58224	-80.61003	111.6	164	57	Low	0.174
NASA5548	MALE	3/11/2010	28.58902	-80.62968	238.9	146	51	Low	0.175
NASA5152R	MALE	5/16/2008	28.62263	-80.61945	152.6	158	56	Low	0.177
NASA5528R	MALE	2/6/2014	28.56167	-80.71011	227.1	156	56	Low	0.179
NASA5945	MALE	11/21/2014	28.599	-80.65837	334.0	139	50	Low	0.180
NASA5152	MALE	4/25/2008	28.62673	-80.62594	157.7	158	57	Normal	0.180
NASA5083R	MALE	4/14/2011	28.53596	-80.61539	219.8	155	56	Normal	0.181
NASA5053R	FEMALE	1/31/2008	28.5629	-80.64145	158.5	124	45.5	Normal	0.183
NASA5793R	MALE	6/6/2014	28.58788	-80.65741	231.5	144	53	Normal	0.184
NASA5068R	MALE	1/23/2013	28.5897	-80.61909	372.5	153.5	58	Normal	0.189
NASA5911	FEMALE	2/28/2014	28.60305	-80.64971	408.1	127	48	Normal	0.189
NASA5627	FEMALE	12/21/2010	28.58433	-80.65638	168.5	118	45	Normal	0.191
NASA5068	MALE	12/4/2007	28.56288	-80.6496	386.8	149	57	Normal	0.191
NASA3213	FEMALE	5/7/2009	28.52579	-80.60677	174.6	130	50	Normal	0.192
NASA5053	FEMALE	10/17/2007	28.562807	-80.643088	240.2	127	49	Normal	0.193
NASA5799	FEMALE	12/21/2012	28.52163	-80.62594	153.9	131	51	Normal	0.195
NASA5919	MALE	4/4/2014	28.50824	-80.64387	61.9	104	40.5	Normal	0.195
NASA5475	FEMALE	11/4/2009	28.56283	-80.61373	85.9	109	42.5	Normal	0.195
NASA5815	FEMALE	1/31/2013	28.63652	-80.766628	191.5	110	43	Normal	0.195
NASA5070	MALE	12/4/2007	28.60326	-80.6595	286.2	138	54	Normal	0.196
NASA5783	MALE	9/21/2012	28.61615	-80.61415	73.8	161	63	Normal	0.196
NASA5047	MALE	8/20/2007	28.60988	-80.64626	84.3	148	58	Normal	0.196
NASA5132R	FEMALE	3/26/2009	28.59464	-80.66791	124.8	113.5	44.5	Normal	0.196
NASA5906	MALE	2/6/2014	28.56289	-80.67825	133.2	127	50	Normal	0.197
NASA5769	FEMALE	6/11/2012	28.54177	-80.70789	87.1	104	41	Normal	0.197
NASA5751	FEMALE	5/4/2012	28.56283	-80.67688	119.7	109	43	Normal	0.197
NASA5615	FEMALE	11/10/2010	28.61438	-80.66576	200.6	121	48	Normal	0.198
NASA5773	MALE	7/23/2012	28.33774	-80.3823	96.3	93	37	Normal	0.199
NASA5768	FEMALE	6/11/2012	28.55399	-80.70665	100.8	108	43	Normal	0.199
NASA5607	FEMALE	10/29/2010	28.59899	-80.65717	200.6	128	51	Normal	0.199
NASA5132	FEMALE	3/28/2008	28.59463	-80.66801	109.7	115	46	Normal	0.200
NASA5274	FEMALE	9/26/2008	28.55699	-80.60884	120.7	97.5	39	Normal	0.200
NASA5188	FEMALE	6/3/2008	28.56142	-80.71019	445.1	121	48.5	Normal	0.200
NASA5750	MALE	4/30/2012	28.59325	-80.64414	114.8	157	63	Normal	0.201
NASA5328R	FEMALE	2/25/2010	28.6042	-80.65167	342.2	127	51	Normal	0.201
NASA5609	MALE	10/29/2010	28.55979	-80.65593	145.2	153	61.5	Normal	0.201
NASA5164	MALE	5/6/2008	28.5887	-80.61744	149.4	161.5	65	Normal	0.201
NASA5796	FEMALE	12/7/2012	28.61768	-80.66363	127.1	124	50	Normal	0.202
NASA5533	MALE	2/10/2010	28.60504	-80.65812	401.4	152	61.5	Normal	0.202
NASA5903	MALE	1/31/2014	28.54134	-80.70624	114.8	118.5	48	Normal	0.203
NASA5661	FEMALE	4/14/2011	28.56138	-80.71015	128.9	111	45	Normal	0.203
NASA5166	MALE	5/6/2008	28.59253	-80.59573	84.0	162.5	66	Normal	0.203
NASA5253R	FEMALE	8/24/2010	28.53554	-80.61546	226.0	129	52.5	Normal	0.203
NASA5545	FEMALE	3/1/2010	28.60496	-80.65814	121.9	113	46	Normal	0.204
NASA5494	MALE	11/20/2009	28.59237	-80.67857	254.1	140	57	Normal	0.204
NASA5669	FEMALE	5/13/2011	28.53538	-80.61551	88.2	92	37.5	Normal	0.204
NASA5909	MALE	2/28/2014	28.57498	-80.6826	231.3	149	61	Normal	0.205
NASA5411R	FEMALE	3/15/2010	28.5253	-80.63896	101.0	105	43	Normal	0.205
NASA5349	FEMALE	1/16/2009	28.62669	-80.62589	35.8	122	50	Normal	0.205
NASA5606	MALE	11/10/2010	28.6126	-80.6652	108.1	141.5	58	Normal	0.205

NASA ID*	SEX	Date	Latitude	Longitude	Hg (ng/g)	SVL (cm)	TG (cm)	Status	BMI
NASA5790	MALE	11/13/2012	28.60381	-80.64693	82.3	158.5	65	Normal	0.205
NASA5450	FEMALE	9/21/2009	28.45095	-80.5972	159.0	129	53	Normal	0.205
NASA5793	MALE	11/30/2012	28.58754	-80.65739	186.0	146	60	Normal	0.205
NASA5348	MALE	1/16/2009	28.60548	-80.64296	175.2	163	67	Normal	0.206
NASA5788	FEMALE	11/7/2012	28.606	-80.6536	144.0	104.5	43	Normal	0.206
NASA5934	MALE	10/3/2014	28.58096	-80.64085	156.0	97	40	Normal	0.206
NASA5348R	MALE	12/15/2011	28.60361	-80.64148	318.1	160	66	Normal	0.206
NASA3402	MALE	4/15/2009	28.56178	-80.71001	94.8	126	52	Normal	0.206
NASA5537R	MALE	11/22/2011	28.60207	-80.62697	173.6	130	54	Normal	0.208
NASA5050	MALE	8/20/2007	28.57757	-80.59428	83.1	151	63	Normal	0.209
NASA3218	MALE	8/13/2010	28.56292	-80.67043	92.6	88.5	37	Normal	0.209
NASA5204	MALE	6/17/2008	28.5688	-80.599	137.4	110	46	Normal	0.209
NASA5061	MALE	11/6/2007	28.460671	-80.650692	137.1	165	69.1	Normal	0.209
NASA5167R	FEMALE	5/8/2009	28.56161	-80.59058	218.6	130	54.5	Normal	0.210
NASA5658	MALE	3/23/2011	28.52451	-80.63053	48.1	93	39	Normal	0.210
NASA5933	FEMALE	8/11/2014	28.48203	-80.6431	243.6	93	39	Normal	0.210
NASA5082	FEMALE	12/31/2007	28.50917	-80.64442	175.3	129	54.2	Normal	0.210
NASA5051	FEMALE	10/5/2007	28.562704	-80.701552	133.5	114.2	48	Normal	0.210
NASA5791	FEMALE	11/13/2012	28.59334	-80.66473	87.4	107	45	Normal	0.210
NASA3021R	FEMALE	4/26/2012	28.50826	-80.64327	188.2	116.5	49	Normal	0.210
NASA5900	MALE	1/31/2014	28.5891	-80.62948	140.7	145	61	Normal	0.210
NASA5716	FEMALE	1/9/2012	28.60271	-80.66033	421.3	114	48	Normal	0.211
NASA5772	MALE	7/23/2012	28.30493	-80.386	82.5	95	40	Normal	0.211
NASA5935	FEMALE	10/3/2014	28.60267	-80.75211	163.5	121	51	Normal	0.211
NASA3021	FEMALE	8/1/2007	28.503232	-80.633473	55.2	92.5	39	Normal	0.211
NASA5907	FEMALE	2/17/2014	28.6235	-80.72834	122.7	92.5	39	Normal	0.211
NASA3210	MALE	5/12/2009	28.56283	-80.62685	75.2	118.5	50	Normal	0.211
NASA5371	MALE	2/13/2009	28.59518	-80.6546	235	141	59.5	Normal	0.211
NASA5904	FEMALE	1/31/2014	28.57623	-80.64544	77.1	109	46	Normal	0.211
NASA5207R	MALE	10/16/2014	28.57324	-80.58794	310.9	142	60	Normal	0.211
NASA5779	MALE	8/16/2012	28.58892	-80.63004	354.4	130	55	Normal	0.212
NASA5537	MALE	2/15/2010	28.60324	-80.64991	188.6	125	53	Normal	0.212
NASA5688	FEMALE	8/15/2011	28.53968	-80.61118	286.1	125	53	Normal	0.212
NASA5542	FEMALE	2/25/2010	28.60493	-80.65228	159.1	113	48	Normal	0.212
NASA5379R	FEMALE	4/30/2012	28.59371	-80.6657	86.8	120	51	Normal	0.213
NASA5905	MALE	2/6/2014	28.58911	-80.62959	233.5	143.5	61	Normal	0.213
NASA5780	MALE	8/17/2012	28.58892	-80.64384	39.4	174	74	Normal	0.213
NASA5430	MALE	7/28/2009	28.4378	-80.65858	155.5	135	57.5	Normal	0.213
NASA5289	MALE	10/14/2008	28.59177	-80.67936	205.6	117	50	Normal	0.214
NASA5036	FEMALE	7/9/2007	28.594669	-80.652126	91.5	105	45	Normal	0.214
NASA5253	FEMALE	8/14/2008	28.54533	-80.60665	173.0	126	54	Normal	0.214
NASA5376	FEMALE	2/25/2009	28.59486	-80.65452	293.2	112	48	Normal	0.214
NASA5183R	MALE	4/10/2014	28.52301	-80.62735	217.9	163	70	Normal	0.215
NASA5299R	MALE	6/22/2009	28.56283	-80.61089	123.9	163	70	Normal	0.215
NASA5753	MALE	5/4/2012	28.59416	-80.66646	290.9	142	61	Normal	0.215
NASA5749	FEMALE	4/30/2012	28.50736	-80.64321	125.8	87	37.5	Normal	0.216
NASA3112	FEMALE	7/9/2010	28.53383	-80.6161	129.7	109	47	Normal	0.216
NASA3223	MALE	8/17/2010	28.56631	-80.59049	199.9	155	67	Normal	0.216
NASA5413	FEMALE	6/22/2009	28.47694	-80.63929	187.8	135	58.5	Normal	0.217
NASA5125	MALE	3/20/2008	28.58952	-80.61576	150.7	159	69	Normal	0.217
NASA5095R	MALE	4/27/2011	28.5354	-80.6155	98.0	161	70	Normal	0.217
NASA5411	FEMALE	6/17/2009	28.52574	-80.63791	67.0	103.5	45	Normal	0.217
NASA5784	MALE	10/5/2012	28.4755	-80.64668	266.9	96.5	42	Normal	0.218
NASA5212R	MALE	10/22/2010	28.52678	-80.6108	124.6	163	71	Normal	0.218
NASA5814	FEMALE	1/31/2013	28.60985	-80.7663	147.7	89.5	39	Normal	0.218
NASA5527	FEMALE	1/29/2010	28.45276	-80.6185	275.0	117	51	Normal	0.218
NASA3118	FEMALE	7/26/2010	28.50083	-80.5884	92.6	94	41	Normal	0.218
NASA5592R	MALE	4/30/2012	28.59438	-80.66723	16.9	142	62	Normal	0.218
NASA3121	FEMALE	4/9/2009	28.57794	-80.64851	134.6	119	52	Normal	0.218
NASA5365	MALE	2/6/2009	28.59047	-80.62626	198.8	160	70	Normal	0.219
NASA5487	MALE	11/13/2009	28.59369	-80.66562	185.1	160	70	Normal	0.219
NASA5695	FEMALE	9/16/2011	28.46845	-80.64854	243.6	130	57	Normal	0.219
NASA5085	FEMALE	1/29/2008	28.6183	-80.6753	114.6	107	47	Normal	0.220
NASA5671R	MALE	9/12/2014	28.50823	-80.64382	134.9	170.5	75	Normal	0.220
NASA5042	MALE	8/1/2007	28.496396	-80.63727	168.0	118	52	Normal	0.220

NASA ID*	SEX	Date	Latitude	Longitude	Hg (ng/g)	SVL (cm)	TG (cm)	Status	BMI
NASA5781	FEMALE	8/20/2012	28.58296	-80.61288	119.1	93	41	Normal	0.220
NASA3113	MALE	7/19/2010	28.58953	-80.65801	237.6	127	56	Normal	0.220
NASA5422	FEMALE	7/17/2009	28.45718	-80.59748	176.6	133.5	59	Normal	0.221
NASA5156R	MALE	5/20/2009	28.56281	-80.67676	275.1	165	73	Normal	0.221
NASA5387	MALE	3/13/2009	28.61825	-80.67506	191.9	139	61.5	Normal	0.221
NASA5697	FEMALE	10/7/2011	28.6037	-80.60345	188.6	101.5	45	Normal	0.222
NASA5808	MALE	1/23/2013	28.64121	-80.7559	221.3	106	47	Normal	0.222
NASA5428	FEMALE	7/22/2009	28.5158	-80.62489	91.6	124	55	Normal	0.222
NASA5286	FEMALE	10/9/2008	28.54072	-80.61302	220.9	127	56.5	Normal	0.222
NASA5168R	MALE	11/17/2009	28.54682	-80.59146	112.8	155	69	Normal	0.223
NASA5534	MALE	2/15/2010	28.59455	-80.65446	278.7	137	61	Normal	0.223
NASA5510	FEMALE	12/31/2009	28.5924	-80.6787	146.0	110	49	Normal	0.223
NASA5549	FEMALE	3/15/2010	28.52474	-80.63851	121.0	110	49	Normal	0.223
NASA5081	MALE	12/31/2007	28.50917	-80.64442	125	143.3	64	Normal	0.223
NASA5517	MALE	1/27/2010	28.50914	-80.64416	157.8	178	79.5	Normal	0.223
NASA5691	FEMALE	8/25/2011	28.5564	-80.7057	149.8	98.5	44	Normal	0.223
NASA5414	MALE	6/22/2009	28.56287	-80.64146	191.4	125	56	Normal	0.224
NASA5603	MALE	9/17/2010	28.56164	-80.71012	100.9	120.5	54	Normal	0.224
NASA3224	MALE	8/17/2010	28.54606	-80.59282	208.4	136	61	Normal	0.224
NASA5797	MALE	12/21/2012	28.50915	-80.64629	159.0	169	76	Normal	0.225
NASA5203R	MALE	9/29/2011	28.30479	-80.38611	188.1	146.5	66	Normal	0.225
NASA5297	MALE	10/15/2008	28.47816	-80.59027	109.8	187.2	84.5	Normal	0.226
NASA5712R	MALE	2/13/2013	28.60438	-80.60286	170.8	155	70	Normal	0.226
NASA5747	MALE	3/23/2012	28.56164	-80.71013	268.1	124	56	Normal	0.226
NASA5095	MALE	2/5/2008	28.561	-80.6045	287.4	166	75	Normal	0.226
NASA5505	MALE	12/17/2009	28.59358	-80.66466	166.0	126	57	Normal	0.226
NASA5715	MALE	1/9/2012	28.60271	-80.66033	192.6	145	66	Normal	0.228
NASA5913	FEMALE	4/10/2014	28.54105	-80.67845	186.9	123	56	Normal	0.228
NASA5491	FEMALE	11/20/2009	28.50828	-80.6437	97.1	125	57	Normal	0.228
NASA5785	MALE	11/2/2012	28.567	-80.6	220.9	171	78	Normal	0.228
NASA5696	MALE	10/7/2011	28.50734	-80.64473	113.0	105	48	Normal	0.229
NASA5604	FEMALE	9/17/2010	28.56314	-80.70869	212.9	118	54	Normal	0.229
NASA5049	MALE	8/20/2007	28.60006	-80.5982	183.2	142	65	Normal	0.229
NASA5074	FEMALE	12/13/2007	28.556	-80.7015	91.3	107	49	Normal	0.229
NASA3222	FEMALE	8/17/2010	28.55942	-80.60285	97.1	113.5	52	Normal	0.229
NASA5212R	MALE	12/9/2010	28.53574	-80.61541	105.7	157	72	Normal	0.229
NASA5195R	MALE	7/16/2010	28.56121	-80.71	177.4	146	67	Normal	0.229
NASA5092	MALE	1/31/2008	28.5626	-80.70691	127.7	148	68	Normal	0.230
NASA5519	MALE	1/27/2010	28.59515	-80.6706	450.1	150	69	Normal	0.230
NASA5257	MALE	8/15/2008	28.52165	-80.61919	244.8	139	64	Normal	0.230
NASA5008R	FEMALE	1/20/2009	28.54664	-80.61522	242.8	117	54	Normal	0.231
NASA5042R	MALE	8/4/2011	28.50738	-80.64708	253.8	145	67	Normal	0.231
NASA5576R	MALE	4/7/2010	28.64338	-80.70582	135.6	147	68	Normal	0.231
NASA5472R	MALE	9/1/2011	28.50787	-80.64821	60.3	176	82	Normal	0.233
NASA5213	MALE	6/25/2008	28.563	-80.69516	97.6	144	67.1	Normal	0.233
NASA5807	MALE	1/23/2013	28.63578	-80.76557	206.3	148	69	Normal	0.233
NASA5712	MALE	1/5/2012	28.60356	-80.60342	147.1	154	72	Normal	0.234
NASA5066	MALE	11/21/2007	28.49295	-80.58965	94.6	172	80.5	Normal	0.234
NASA5483	MALE	11/4/2009	28.5933	-80.66454	234.4	136	64	Normal	0.235
NASA5369R	MALE	7/22/2009	28.5418	-80.61284	138.6	156	73.5	Normal	0.236
NASA5062	FEMALE	11/6/2007	28.475249	-80.645959	236.3	125	59	Normal	0.236
NASA5657	FEMALE	4/14/2011	28.53566	-80.61549	139.5	125	59	Normal	0.236
NASA5602	MALE	9/17/2010	28.56164	-80.71012	191.2	163	77	Normal	0.236
NASA5519R	MALE	3/1/2010	28.59501	-80.66994	567.9	150	71	Normal	0.237
NASA5147	FEMALE	4/23/2008	28.6035	-80.6036	113.3	103	49	Normal	0.238
NASA5177	FEMALE	5/23/2008	28.49621	-80.63748	188.4	126	60	Normal	0.238
NASA5229	FEMALE	7/10/2008	28.48951	-80.60416	151.9	131	63	Normal	0.240
NASA5256	MALE	8/15/2008	28.4882	-80.59129	197.9	159.5	77	Normal	0.241
NASA5592R	MALE	12/7/2012	28.5957	-80.6721	44.1	142	69	Normal	0.243
NASA5064	MALE	11/21/2007	28.47205	-80.5944	205.3	162	79	Normal	0.244
NASA5267	MALE	9/26/2008	28.58988	-80.72374	169.1	158	78.5	Normal	0.248
NASA5037	FEMALE	7/9/2007	28.6223	-80.61419	123.8	110	55	Normal	0.250
NASA5067	MALE	11/29/2007	28.5629	-80.64966	91.7	109	55	Normal	0.252
NASA5932	MALE	8/11/2014	28.50822	-80.64376	177.0	159	81	Normal	0.255

*R after ID number indicates that the animal was re-captured. GPS points in decimal degrees.

Control materials

An ampoule of SRM 3133 (Mercury Standard Solution) and SRM 955c Level 2 & 4 (Toxic Metals in Caprine Blood) were obtained from the NIST Office of Reference Materials (ORM). SRM 3133 was used to construct a new calibration curve for this experiment, following the method detailed in section 2.2.2. SRM 955c Level 2 & 4 (Toxic Metals in Caprine Blood) were run as control materials for the blood samples since they are matrix matched and the ranges of analyte mass fractions bracket the concentrations that we expect the experimental samples to fall within. The results of the total mercury analysis for these SRMs are listed in Table 2.21.

Table 2.21. Summary of total mercury results for SRM 955C Levels 2 and 4 (Toxic Metals in Caprine Blood; total mercury $4.95 \pm 0.76 \mu\text{g}/\text{kg}$, and $33.9 \pm 2.1 \mu\text{g}/\text{kg}$, respectively) used during the analysis of American alligator blood samples in Experiment 2.4.

SRM 955C Level 2 Replicates	[Hg] ng/g	SRM 955C Level 4 Replicates	[Hg] mg/kg
SRM 955C Level 2 run 01	4.38	SRM 955C Level 2 run 01	29.6
SRM 955C Level 2 run 03	4.39	SRM 955C Level 2 run 02	28.3
SRM 955C Level 2 run 04	4.47	SRM 955C Level 2 run 03	28.6
SRM 955C Level 2 run 05	4.84	SRM 955C Level 2 run 04	28.7
SRM 955C Level 2 run 06	4.97	SRM 955C Level 2 run 05	28.9
SRM 955C Level 2 run 07	6.09	SRM 955C Level 2 run 06	29.4
SRM 955C Level 2 run 09	4.99	SRM 955C Level 2 run 07	27.7
SRM 955C Level 2 run 10	4.90	SRM 955C Level 2 run 08	34.8
SRM 955C Level 2 run 11	4.83	SRM 955C Level 2 run 09	33.9
SRM 955C Level 2 run 12	4.75	SRM 955C Level 2 run 10	34.1
SRM 955C Level 2 run 13	4.85	SRM 955C Level 2 run 11	34.5
SRM 955C Level 2 run 14	4.70	SRM 955C Level 2 run 12	33.8
SRM 955C Level 2 run 15	5.30	SRM 955C Level 2 run 13	34.1
SRM 955C Level 2 run 16	4.90	SRM 955C Level 2 run 14	34.8
SRM 955C Level 2 run 17	4.78	SRM 955C Level 2 run 15	31.7
SRM 955C Level 2 run 18	5.56	SRM 955C Level 2 run 16	31.9
SRM 955C Level 2 run 19	5.61	SRM 955C Level 2 run 17	32.3
SRM 955C Level 2 run 20	5.15	SRM 955C Level 2 run 18	32.8
SRM 955C Level 2 run 21	5.29	SRM 955C Level 2 run 19	32.8
SRM 955C Level 2 run 22	6.34	SRM 955C Level 2 run 21	33.2
Average	5.1	Average	31.8
Standard Deviation	0.5	Standard Deviation	2.5
%RSD	10.3	%RSD	7.8
Total U for SRM 955c Level 2	0.06	Total U for SRM 955c Level 2	0.04

Blanks

The MINWR blood samples were collected over an extended time-period, and field blanks were not made in concert with the collected samples, so exact representation for each lot number, type of syringe, and blood collection tube used, in the form of a blank is not possible. In lieu of exact match field blanks, field blanks using 2.54 cm 18.5 gauge needles (lot # 305196 BD) and 60 mL Luer lock syringes (lot # 09F058B BD) or 20 mL Luer lock syringes (lot # W11883 BD) were made using Milli-Q water. The Milli-Q water was transferred from the syringe to lithium-heparin blood collection tubes (lot # 1178410; 0246555) and then analyzed with the experimental samples. Procedural blanks using an empty weigh boat filled with Milli-Q water were also made and measured

concurrently with the samples. The experimental samples were blank corrected as the laboratory-produced field blanks measured an average mercury concentration = 0.2 ng/g.

Field and procedure blanks can be above the detection limit of the instrument for several reasons, and each blank provides different information about the sample processing workflow. If the field blank, created with sample collection materials, is above the limit of detection, (LOD) the equipment used in sample collection was contaminated with mercury. This can occur by the equipment being stored improperly, for long periods of time, or close to sources of contamination. If the procedural blank is above the LOD this is indicative of contamination during the analytical steps in the laboratory and could be from cross contamination of samples into the procedural blank, or from replaceable parts inside the instrument, such as the catalyst tube or mercury amalgamator reaching their maximum number of uses.

Instrumental method & quantification

The mass fraction of mercury was determined with a DMA-80 is described in section 2.2.2. The newly created calibration curve was tested with experiment specific control material prior to analyzing samples. Blood samples from 174 individuals collected at MINWR were analyzed for a total of 193 experimental measurements, 22 measurements of SRM 955c Level 2 and 21 measurements of SRM 955c Level 4 (Toxic Metals in Caprine Blood). Procedural blanks and SRMs used as control materials were analyzed every 8-12 experimental samples, to ensure proper function of the instrument. Laboratory produced field blanks were run in tandem with the experimental samples.

Statistical analysis

The data from the total mercury analysis of the MINWR, FL alligator whole blood samples demonstrated a non-normal distribution that was verified by the Shapiro-Wilk goodness-of-fit test. Transformation by \log_{10} normalized the data for each season. The \log_{10} transformed data were found to be homoscedastic under Levene's Test for Equality of Variances. These tests were conducted for samples grouped by sex, season, health status, and sampling location. With the \log_{10} transformation, the assumptions of parametric statistics could be met, therefore parametric analyses (ANOVA and MANOVA) were used for the comparisons within Kennedy Space Center, FL. The recaptured animal health status comparison samples were also \log_{10} transformed to meet the assumptions of parametric statistics under Levene's and Shapiro-Wilk tests, where $p = 0.05$ for both tests.

Spatial analysis

The total mercury concentration data were visually described using ArcMap 10.3 (ESRI, Redlands, CA). Shape files were downloaded from <http://geodata.myfwc.com/> and trimmed to display only the results from the study site. GPS points for alligator capture locations were plotted using the WGS 1984 plotting system. All points were entered as positive or negative decimal degrees. The total mercury concentration data were interpolated on the map using the spline with barriers spatial analysis tool. Data were re-sampled for display using the nearest neighbor method for discrete data and manually classified into four groups based on increments of 50 ng/g of total mercury concentration. Seasonal average rainfall (SAR) data were taken from the two closest monitoring stations and averaged (Daytona Beach, FL (north of MINWR) and Melbourne, FL (south of MINWR)).

2.4.3. Results & Discussion

The alligators sampled at MINWR between 2007 and 2014 did not have statistically different blood mercury concentrations between the sexes, so both sexes were combined for the seasonal analysis. The individual seasons varied in their average mercury concentrations, ranging from 112 ng/g to 252 ng/g (Table 2.22; does not include an anomalously high value of 1023 ng/g observed in spring 2010). The total average mercury concentration across all samples was $177 \text{ ng/g} \pm 110 \text{ ng/g}$, placing MINWR as a low mercury site, compared to the other sites in this chapter.

Samples were analyzed seasonally and annually to determine the presence of recurring trends in alligator blood sample mercury concentrations (Figure 2.12). Some seasons had greater variation in mercury concentrations than others, determined by the standard deviation of the measurements that season (Table 2.22). The variation could be reflective of the seasonal changes in environmental variables or alligator behavior, such as breeding in late spring, nesting in early summer, and brumating in winter (Figure 2.12) (176, 296). The mercury concentration differences between winter and spring in the alligators in this study coincide with vastly different seasonal behaviors that could affect the mercury concentration.

In the winter, alligators enter a brumation period, where body temperature drops and foraging decreases from the warmer months (176). The brumation period leads to higher mercury concentrations in the blood as the animals become dehydrated and both muscle and fat are metabolized for energy (280). Though winter temperatures at MINWR are warm ($14.8 \text{ }^{\circ}\text{C}$ - $15.9 \text{ }^{\circ}\text{C}$), suggesting the brumation period is short (taking place below $16 \text{ }^{\circ}\text{C}$), the decrease in foraging activity resulting in metabolism of tissues and

mobilization of mercury are likely responsible for the statistically significant mercury concentration observed in this season (Figure 2.12) (176). In the spring, the alligators are emerging from brumation and begin the breeding season, when foraging and resource utilization go from very limited to nearly maximal in a short period to ensure there is enough fuel for this energetically expensive behavior.

During the summer, increased activity —such as foraging, mating, nesting and rearing hatchlings—may result in variable mercury concentrations among individuals, as not all alligators participate in breeding every year (176). Much of the population is foraging in earnest while less than 50 % of the sexually mature female population is nesting. Mercury is vertically transferred to the eggs from the nesting female (Nilsen, *unpublished data*; (297, 298)). However, the effect of maternal transfer of mercury on the adult female blood mercury concentration is unknown for alligators and other reptiles. In mammals, the mother: fetus mercury concentration ratios reflect weak offloading, and mother mercury concentration is lower than male mercury concentration, suggesting that even the weak offloading via maternal transfer can elicit changes in adult female circulation blood concentrations (79). A decrease in maternal mercury concentration as a result of nesting, combined with the reduced foraging associated with nesting could contribute to the variation observed in this season (Figure 2.12, bottom) (176). During the fall, the population comes back to synchronous behavior as temperatures begin to decrease and preparations for brumation begin, which could explain the decrease in mercury concentration variation in the fall from the wider range observed in the summer (Figure 2.12, bottom).

Table 2.22. The mean mercury concentration for each season/year, followed by the standard deviation and number of alligators in each group.

Season	Year	Mean [Hg] (ng/g)	Standard Deviation	<i>n</i>
Fall	2007	162.7	63.8	7
Summer	2007	112.7	47.6	7
Winter	2007	212.9	122.0	5
Fall	2008	165.2	49.5	5
Spring	2008	138.2	33.3	8
Summer	2008	203.5	106.8	8
Winter	2008	167.8	69.1	5
Fall	2009	161.2	66.7	7
Spring	2009	161.2	66.8	8
Summer	2009	141.6	45.4	8
Winter	2009	186.6	77.4	8
Fall	2010	168.0	43.9	8
Spring	2010	402.7	417.9	5
Summer	2010	171.1	57.4	8
Winter	2010	252.7	115.9	10
Fall	2011	158.7	72.0	5
Spring	2011	120.4	58.5	5
Summer	2011	229.9	71.2	3
Fall	2012	164.6	73.8	6
Spring	2012	151.4	92.3	8
Summer	2012	132.9	111.8	6
Winter	2012	181.9	88.2	12
Winter	2013	187.5	29.1	5
Fall	2014	191.3	80.6	4
Spring	2014	141.9	72.8	4
Summer	2014	210.3	47.1	2
Winter	2014	175.7	113.0	7
Total		176.9	109.6	170

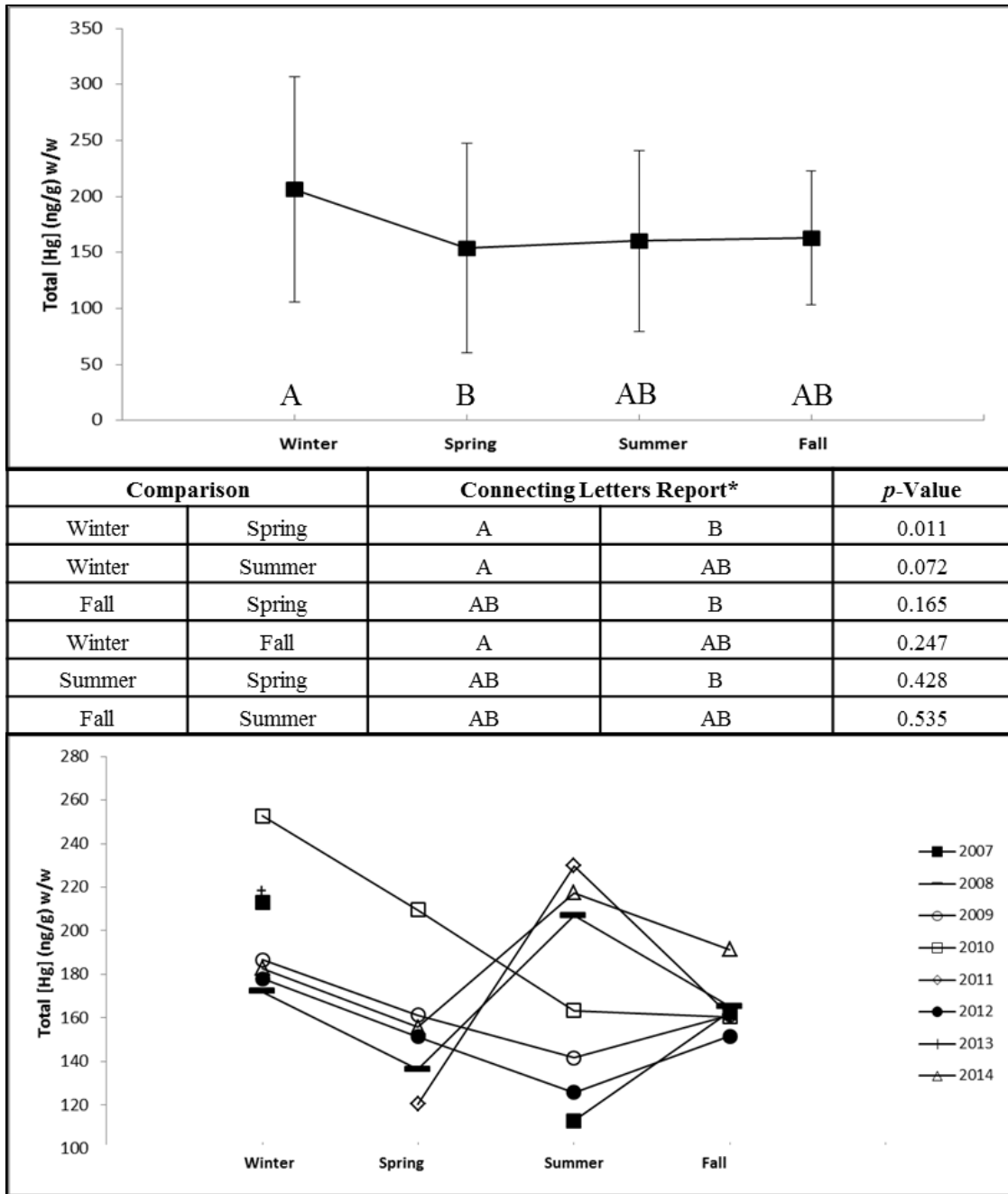


Figure 2.12. The average total Hg concentration for all alligators collected in each season from 2007-2014 at Merritt Island National Wildlife Refuge (MINWR) (top). The seasonal comparisons of total Hg concentration in alligators, using Student's t-Test and Connecting Letters Report (center). The total Hg concentration for all alligators collected in each season from 2007-2014 at Merritt Island National Wildlife Refuge (MINWR), separated by year (bottom). The error bars represent the standard deviation of all samples from that season (top). *Different letters in the Connecting Letters Report indicate statistical significance.

While seasonal behaviors appear to correspond to changes in the concentration of mercury in alligator blood, we also considered the possibility of seasonal effects related to changes in mercury transformation by bacteria, which is dependent on deposition and fluctuating environmental parameters (4, 17). During the winter in Florida, dry mercury deposition is dominant since there is less seasonal rainfall and can lead to a greater accumulation of mercury in the environment than in seasons dominated by wet deposition (Figure 2.12) (299, 300). The increased amounts of rainfall in the spring and summer in Florida lead to a greater amount of wet mercury deposition, bringing less mercury from the atmosphere into the wetland ecosystem (Figure 2.13) (299, 300). The change in the amount of rainfall and switch in wet and dry depositions between these seasons could be related to the variability in alligator mercury concentration, since less mercury is present in the environment in the spring and summer while much of the population is foraging in earnest.

However, for the amount and type of atmospheric mercury deposition to affect the mercury concentration found in apex predators, mercury must have a very fast residence time through the food web in this environment, which has not been assessed. The toxicokinetics of mercury in reptiles is also not well defined, making a definitive connection impossible. In mammals, there is fast assimilation from digestion to being detectable in whole blood, and the subsequent elimination half-life in whole blood is on average seven weeks (range 4.3 weeks to 7.5 weeks) (202, 203). There could be similarly fast assimilation in reptiles, which would make the seasonally changing environmental parameters of this ecosystem incredibly relevant to the mercury

accumulation discussion, but further research is needed. The seasonal data observed here more likely are attributed to the seasonal behavior, individual variation, and physiology.

The fluctuations in seasonal mercury concentration observed here will not likely hinder the use of American alligators as a sentinel for human mercury exposure, despite the statistical difference (Figure 2.12, 2.14). This data provides an excellent example of statistically significant environmental data, which does not correspond to an actual environmental effect that was discussed in Chapter 2 (259, 261, 262). The statistical differences between the seasons are related to the synchronous seasonal behaviors of the entire population, particularly in the winter when alligators undergo brumation. During brumation, the alligators are often hidden and more difficult to sample routinely, so the fluctuation in mercury concentration due to this behavior is not likely to influence samples collected for human health monitoring related to dietary exposure of mercury.

These data presented in this section describe the seasonal mercury concentrations that coincide with seasonal behaviors of the American alligator over 7 years. The length of time that these samples cover as well as the number of samples examined makes this data set informative and valuable. However, since only a few alligators were recaptured over that 7-year period, the conclusions were limited to population-level behaviors and mercury concentrations. If this study were conducted again, an effort could be made to recapture the same animals every season for several years, so the changes within animals based on their specific behaviors could be determined. This experimental design would also provide additional life history information for the species at MINWR, such as specific date/temperature at which brumation begins and ends, frequency of participation in breeding activities, and site fidelity following continued disturbance in their

environment. All of this information would allow Kennedy Space Center to make the best management decisions possible for this resident population of American alligators.

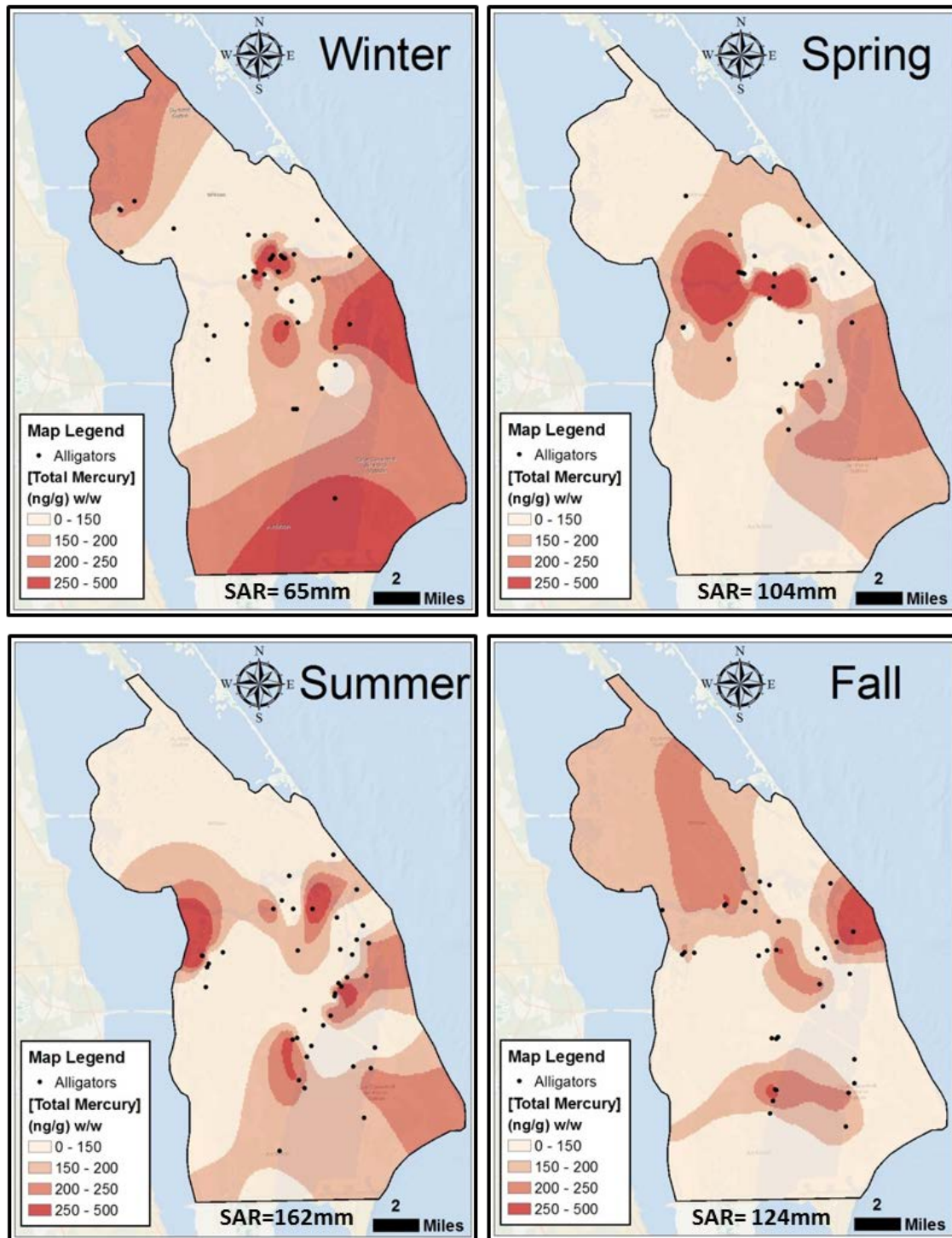


Figure 2.13. The GIS interpolation of the total Hg measurements taken at MINWR from 2007- 2014 by season. Winter = December – February, $n = 49$; spring = March – May, $n = 37$; summer = June – August, $n = 44$; fall = September – November, $n = 43$. The seasonal average rainfall (SAR) provided within each map.

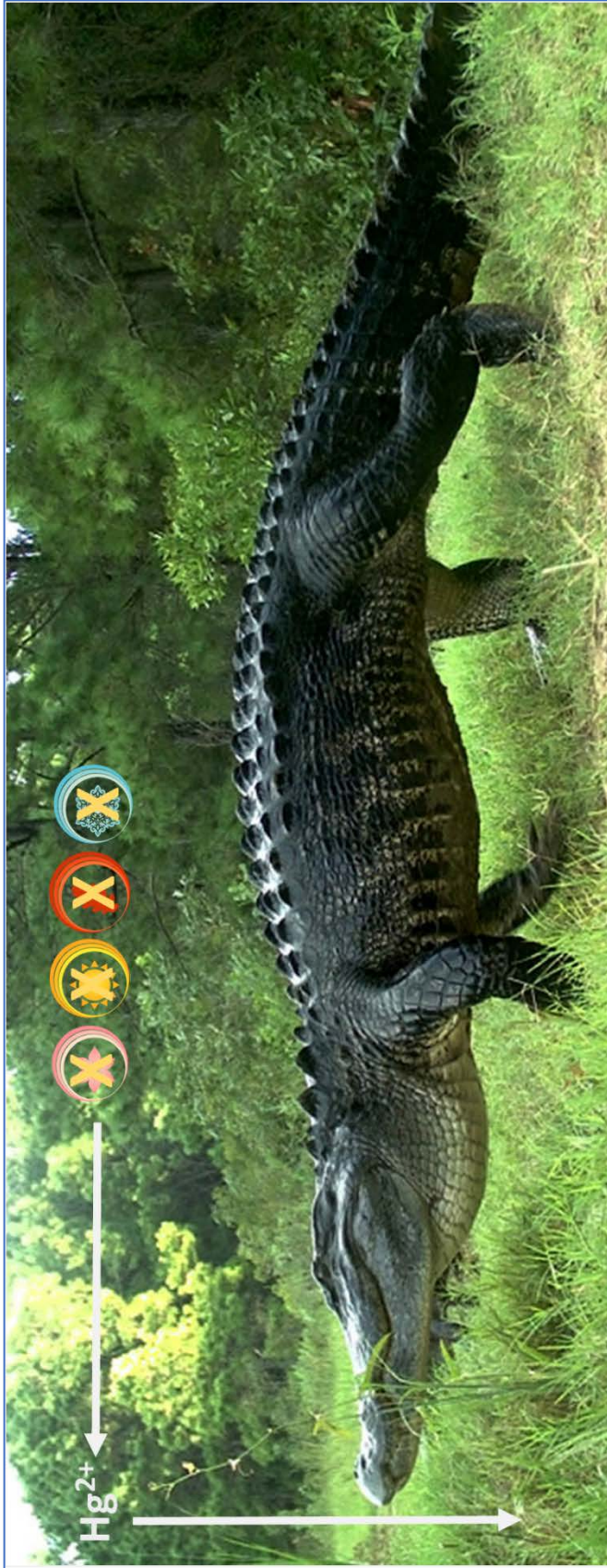


Figure 2.14. The graphical abstract of the results of Specific Aim 1, experiment 3 detailed in this section.

2.5. Elucidating the relationship between mercury concentration & body condition

2.5.1. Introduction

Over the course of the 7-year seasonal mercury concentration study period conducted using alligators at MINWR, some animals were captured appearing drastically emaciated, the cause of which is unknown and may not be related to illness (Figure 2.15). This provided an opportunity to assess the relationship between reduced body condition and mercury concentration, and to discern if the change in body condition could be used analogously to the same change in humans.

To understand how mercury burden is affected by the changing body condition of human behaviors (i.e. diet, exercise, pregnancy), alligators with both low and normal body mass indexes (BMI, defined in Methods section) were compared. This comparison served to determine if significant weight loss/gain in humans is correlated to changing mercury concentrations, potentially increasing the toxicity during certain BMI changes, as the stored mercury is remobilized into circulation making it once again biologically available. Previous studies have demonstrated that a correlation can exist between the health status of a wildlife population and their respective contaminant burdens, generally with reduced body condition resulting in the metabolism of stored contaminants, elevating the circulating concentration in the blood (280, 301).



Figure 2.15. The observable difference in alligators with normal BMI (top) and low BMI (bottom) at MINWR.

2.5.2. *Experimental specific methods*

Sample collection, identification & preparation

Animals captured and sampled for the previous study at MINWR that were classified as having a low body mass index (BMI) by their observed emaciation upon capture were noted (Table 2.20). To better describe the emaciation observed in the field, we developed a mathematical description of BMI to coincide with the noted field observations: tail girth (TG, in cm) divided by double the snout to vent length (SVL, in cm) ($BMI = TG / (SVL \times 2)$). SVL x 2 was used as used instead of total length, since alligators can damage their tails throughout their lives which would make a calculation that included the tail prone to errors. An alligators tail is half of its total length, so doubling the SVL serves to include total body length and protecting for the possible error that could occur from using the length of the alligator's tail. BMI of less than 0.18 equated to a 'low' BMI (18 individuals fit this description; Table 2.20). The TG and SVL are the circumference of the tail at the urogenital slit and the length from the snout to the urogenital slit, respectively. Over this time period, 19 animals were recaptured. All 19 were initially captured as healthy/normal; 12 alligators were recaptured captured with normal BMI and 7 alligators recaptured as low BMI. These animals are compared to determine how an individual's mercury concentration changes with changed body condition.

Statistical analysis

Total mercury concentration data were tested for a normal distribution using a \log_{10} transformation across the general population, seasons, sex, and health status by Kolmogorov's D goodness of fit test. Homoscedasticity was assessed using Levene's

Test of equal variances, and subsequently parametric analyses were used to determine statistical significance. The comparison of total mercury concentration with health status (normal or low BMI) was conducted using ANOVA. Mean values are presented as ± 1 standard deviation (SD).

The 18 alligators that were captured with a low BMI were matched to 18 healthy counterparts, so a comparison of mercury burden across BMI status could be conducted. The counterpart alligators were of normal BMI (value > 0.18), of the same sex, capture season, and snout to vent length (SVL) as the low BMI alligators. The group of healthy counterparts was used instead of the entire population of healthy alligators at MINWR so the different sample sizes or possible mercury differences across the seasons would not mask a statistical difference between the BMI groups. The recaptured alligators were compared using the Matched-Pair Wilcoxon Signed Rank comparison for non-parametric data, due to the small sample sizes.

2.5.3. Results & Discussion

The normal and low BMI alligators sampled at MINWR had average mercury concentrations of $160 \text{ ng/g} \pm 74 \text{ ng/g}$ and $279 \text{ ng/g} \pm 145 \text{ ng/g}$, respectively (Table 2.23). The alligators with low BMI exhibited significantly higher ($p < 0.0087$) total mercury concentration in blood than alligators with normal BMI (Figure 2.17). While the low BMI alligators had a higher average mercury concentration than the normal BMI alligators, both of these values fall in the “low mercury” category compared to other sites in Florida determined in this chapter. The average SVL of the low BMI alligators was 8 cm greater than the average SVL of the normal BMI alligators, however, this difference

is not likely the reason for the higher mercury concentrations in the low BMI alligators, as the highest mercury concentrations were not from the largest alligators (Figure 2.16).

The elevated total mercury concentration observed in the low BMI animals may be due to increased metabolism of muscle and fat tissues. Muscle and fat become metabolized due to starvation, illness, foraging difficulties, or due to normal behavioral changes such as brumation. The remobilization of mercury from the storage tissues can elevate the circulating contaminant burden. We find this explanation more likely than the alligators with a reduced BMI having greater mercury exposure and accumulation, since they are all foraging at the same location (280, 301). To remove the possibility that the animals in this study were of different biological status (different sex, age, behavior differently due to the season), the low BMI animals were matched to healthy BMI counterparts to control for these variables (see section 2.5.2.).

The recaptured alligators had a similar result, we observed that there was a significant difference ($p = 0.04$) in the change in total mercury concentration between recaptured normal and recaptured low BMI status alligators (Figure 2.18). These results further support the assumption that increased mercury concentrations might be linked to further health deficits in these alligators (secondary effect). Though we do not know the etiology of low BMI in the alligators sampled, it appears that mercury burden may be a contributing factor. Despite the unknown etiology of the BMI change, these results show that with a reduced BMI, mercury is consistently found at elevated levels compared to normal BMI counterparts (Figure 2.19).

The relationship between BMI and mercury concentration is translational to humans as a significant amount of BMI change takes place throughout the various life

stages of both males and females. This is of particular importance to females as body condition changes drastically throughout gestation and lactation. As BMI increases during pregnancy, an increase in mercury may be a result of increased food consumption. For this reason, guidance is given for pregnant females to avoid high mercury foods, such as sushi. However, the subsequent decrease in BMI after birth and during lactation may be detrimental to both the individual and the offspring, as the mercury accumulated during pregnancy is released into circulation as BMI decreases. In humans, there is also a significant decrease in BMI with age. This could correspond to the onset of neurodegenerative diseases, like Alzheimer's disease, that are normally associated with old age. With the mobilization of stored contaminants, additional neurodegenerative effects may be a result of their bioavailability. The alligators at MINWR that are experiencing drastic changes in their BMI could be used to model these changes, and further elucidate the effects of mercury exposure.

The data presented in this section define the mathematical equation to discern body condition, and describe the inverse relationship between lowered BMI and mercury concentration in American alligators. The relationship between BMI and mercury is new information for this species, but is supported by studies of other organisms. This relationship could be strengthened by recapturing the same alligators throughout their BMI changes, to determine not only the rate of increasing mercury within a single alligator, but also the rate of emaciation. Observations could also be made to determine how much time each alligator spends foraging through the BMI change, to determine when foraging decreases, and when the peak mercury concentration reach the blood stream. Maximal mercury concentrations are likely when the alligator is still foraging but

BMI loss is occurring, once the alligator stops foraging, the mercury concentration may decrease after all the fat stores have been mobilized. Understanding the relationship between foraging and BMI changes would also aid in identifying the etiology of this health issue, and would allow remediation efforts to begin.

Table 2.23. The mean mercury concentration of the two BMI statuses identified in this experiment, followed by the standard deviation, mean SVL, and number of alligators in each group.

BMI Status	Mean [Hg] (ng/g)	Standard Deviation	Mean SVL (cm)	<i>n</i>
Normal	160.2	74.2	140.9	22
Low	278.7	145.2	147.9	22

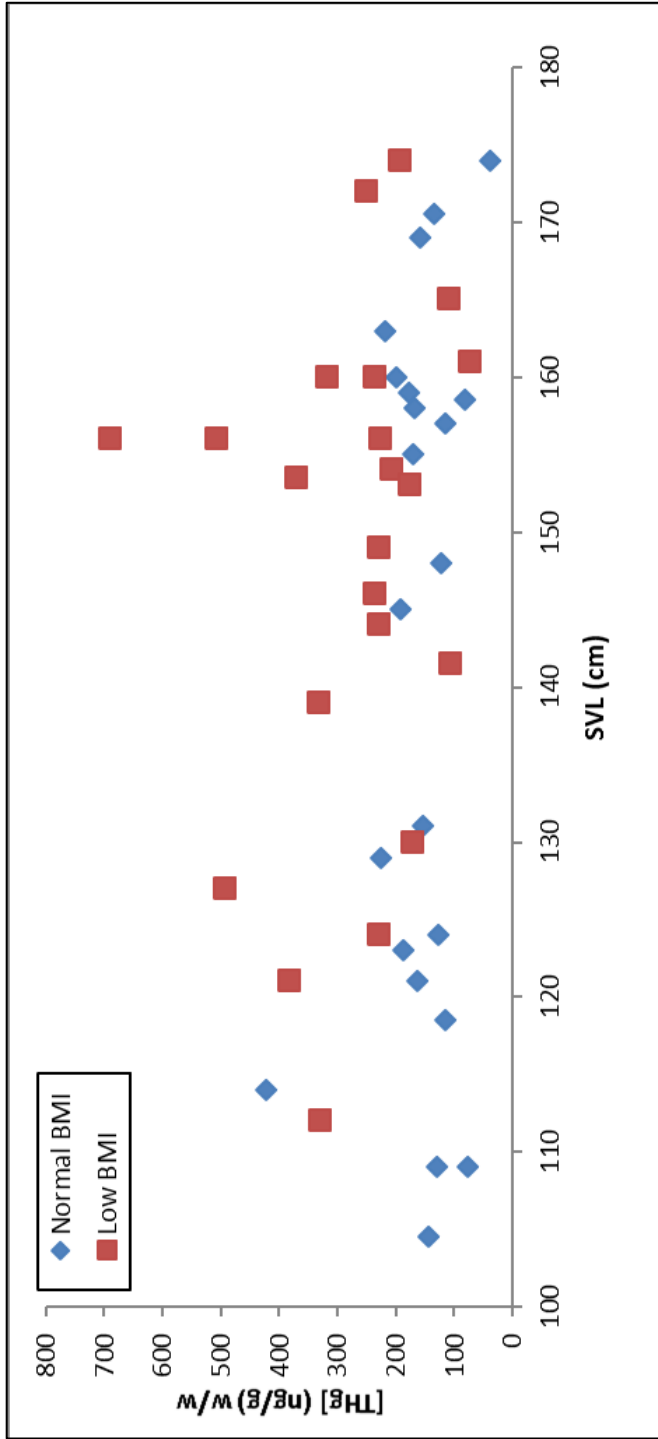


Figure 2.16. The individual mercury concentrations for each of the alligators in the BMI assessment, separated by group and plotted against their SVL (cm).

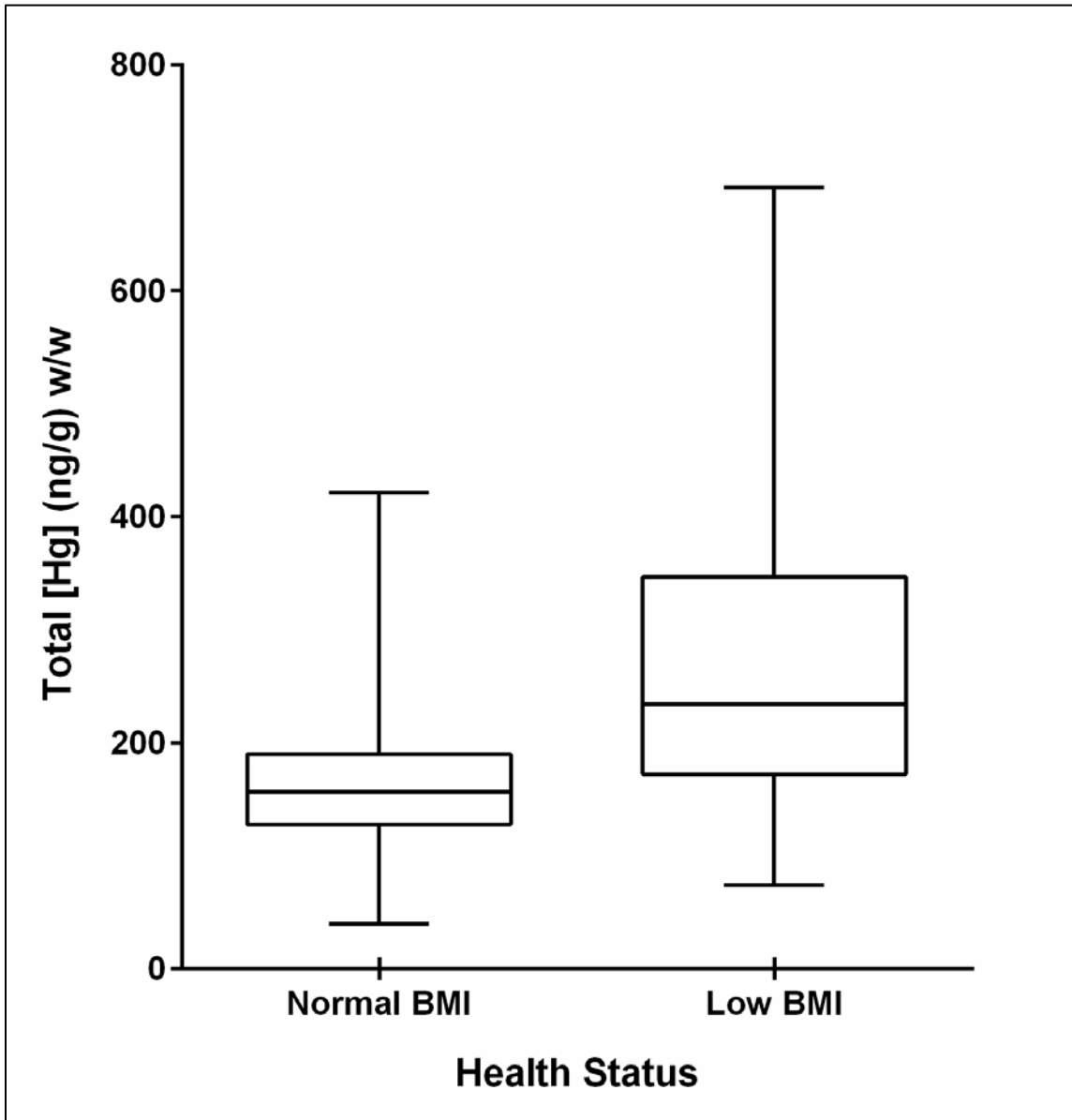


Figure 2.17. A boxplot demonstrating the statistically significant difference in total Hg concentration between American alligators with a low ($n = 22$) and normal ($n = 22$) body mass index (BMI) (by season/year of collection, sex and length) at MINWR, FL from 2007-2014 ($p < 0.0087$).

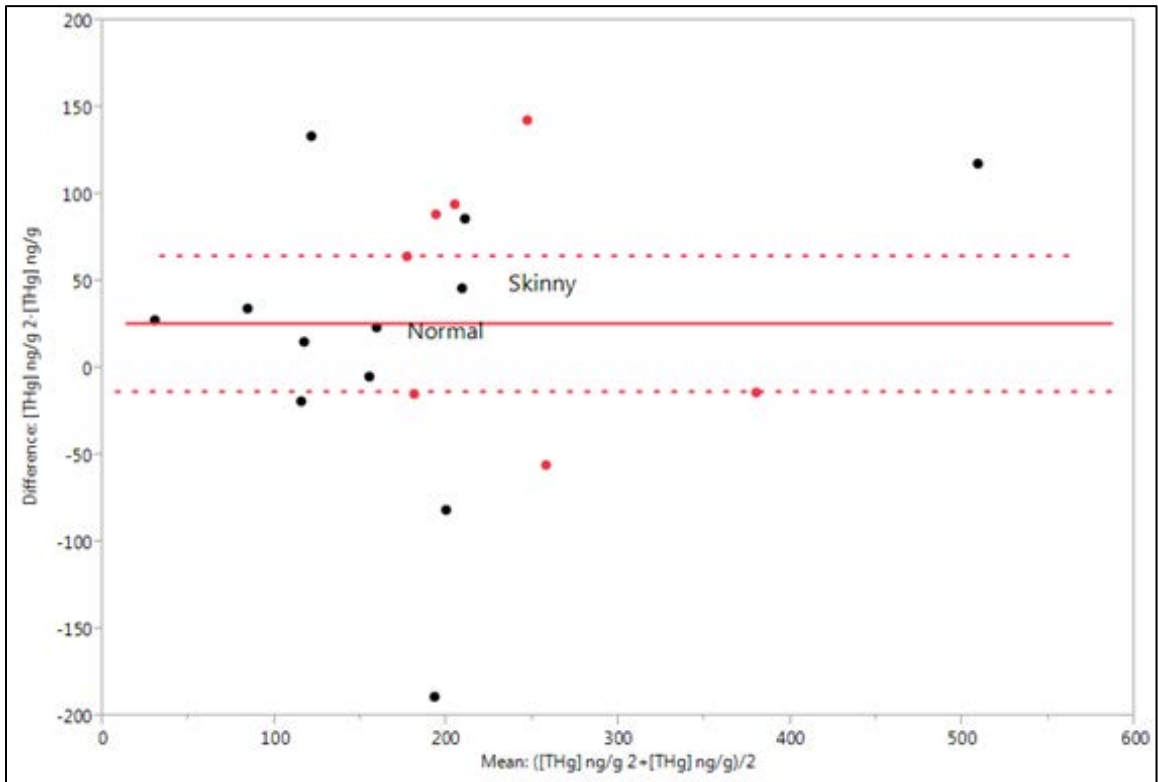


Figure 2.18. The amount of change in mercury concentration each BMI group experience between initial and recapture sampling, as indicated by the Wilcoxon Matched Pair analysis. The low BMI group is denoted by the black dots, and the amount of change is indicated by how far away the word “Skinny” is from the red line that represents the grand mean. The red dots and the word “Normal” represents the normal BMI group.



Figure 2.19. The graphical abstract of the results of Specific Aim 1, experiment 4 which was detailed in this section.

2.6. Determining if developing alligators are exposed to mercury

2.6.1. Introduction

The previous experiment elucidated the changing mercury concentrations in relation to body condition in American alligators. As human body condition changes drastically with pregnancy, and many contaminants are transferred vertically. Here, we investigate the amount of mercury detectable in alligator egg yolk, to determine if developing embryos are exposed to mercury, and if the alligator could be a developmental model for human exposure. Yolk was chosen as the representative egg tissue to determine mercury concentration, because egg is produced in the liver of the nesting female, and is what “feeds” the developing embryo until it hatches.

This experiment examines egg yolk from three sites, one that has been previously deemed to have low mercury concentrations in adult alligators (Yawkey Wildlife Preserve, SC; Chapter 2), and two sites that are frequently used by the Guillette lab as contaminated and control sites, Lakes Apopka and Woodruff, respectively, but have never been assessed for mercury. Using Yawkey will enable the determination of how little mercury may be in eggs at low mercury sites, as well as determine if those concentrations are below the detection limit of the Mercury Analyzer (DMA-80, Milestone), which is approximately 0.05 ng/g. This experiment will also characterize two commonly sampled sites that are undescribed for mercury.

2.6.2. *Experiment specific methods*

Sample collection

The eggs used in this experiment were collected from Lakes Woodruff and Apopka in Florida, and Yawkey Wildlife Preserve in South Carolina in June of 2011. The eggs were brought back to the Hollings Marine Laboratory and incubated at 32 °C until reaching developmental stage 19, which is the sexual determination stage. The eggs were opened with clean dissection scissors, and yolk was collected using a 10 mL syringe (BD). The yolk was then placed in a 50 mL centrifuge tube (Falcon) and homogenized by rocking the tube gently several times. The yolk was then aliquoted into 2 mL cryovials (Corning) frozen at -20 °C until being analyzed. The metadata for the egg samples is presented in Table 2.24.

Table 2.24. The metadata associated with the egg yolk samples analyzed in this experiment.

Site	Nest	Sample ID	Site	Nest	Sample ID	Site	Nest	Sample ID
Apopka, FL	1	AP-01-01	Woodruff, FL	1	WO-01-20	Yawkey, SC	2	YK-02-22
		AP-01-04			WO-01-28		3	YK-03A-16
		AP-01-06			WO-01-34		4	YK-03B-3
		AP-01-38		WO-02-19	5		YK-04-02	
	AP-01-48	WO-02-20		YK-05-35				
	2	AP-02-10		WO-02-21	6		YK-05-03	
		AP-02-21		WO-03-10	7		YK-05-36	
		AP-02-23		WO-03-22			YK-06-04	
		AP-02-26		WO-03-23			YK-07-01	
		AP-02-32		WO-04-14	YK-07-02			
	AP-02-34	WO-04-28		YK-07-03				
	3	AP-03-15		WO-05-17	8		YK-07-4	
		AP-03-18		WO-05-24			YK-08-##	
		AP-03-22		WO-06-02			YK-08-01	
		AP-03-23		WO-06-11	YK-08-02			
	AP-03-33	WO-06-18		YK-08-4				
	4	AP-04-01		WO-06-43	9		YK-09-41	
		AP-04-03		WO-07-25			YK-09-43	
		AP-04-39		WO-07-32			YK-09-44	
	5	AP-05-11		WO-07-39	10		YK-09-46	
		AP-05-17		WO-08-10			YK-10-22	
		AP-05-19		WO-08-12	11		YK-11-01	
		AP-05-20		WO-08-14			YK-11-02	
		AP-05-27		WO-09-05			YK-11-03	
	AP-05-37	WO-09-10		YK-11-4				
	6	AP-06-02		WO-09-17	12		YK-12-01	
		AP-06-10		WO-10-01			YK-12-02	
		AP-06-21		WO-10-08	YK-12-4			
		AP-06-26		WO-10-14	13		YK-13-17	
		AP-06-44		WO-13-01	14		YK-14-4	
	13	WO-13-20		16	YK-16-17			
		WO-13-21			YK-16-09			
	14	WO-14-11			YK-16-15			
	15	WO-15-04		YK-16-22				
		WO-15-32		17	YK-17-35			
		WO-15-37		18	YK-18-01			
	WO-16-12	YK-18-03						
	16	WO-16-19		YK-18-4				
		WO-16-25		19	YK-19-3			
		WO-17-11			YK-19-4			
	18	WO-17-19		20	YK-20-4			
		WO-18-02		21	YK-21-4			
		WO-18-04						
	19	WO-18-18						
		WO-19-34						
	20	WO-19-37						
		WO-20-05						
		WO-20-07						
	WO-20-27							

Instrumental method, quantification & control materials

The mass fraction of mercury was determined with a DMA-80, as described above in section 2.2.2. The quality control material used for this study was egg contents homogenate from NIST's inter-laboratory comparison study, QC04-ERM 1, which is certified at $101.0 \text{ ng/g} \pm 3.0 \text{ ng/g}$ mercury with our measurements falling within that range. Some of the replicates of the reference material are outside the certified range, and we suspect this is because the end of one container of reference material was used in the beginning of these measurements, and a new container was used throughout the rest of the yolk measurements. We provide the measurements that are outside the range of the certified reference material to demonstrate that there is slightly more uncertainty in the unknown yolk samples than is preferred, but the measurements are still reliable, as the average QC measurement is in the desired range. For this experiment, 135 egg yolk sample measurements, were analyzed alongside 50 replicates of the matrix matched control material. The sample size utilized for each measurement was approximately 0.10 g. The results of the mercury analysis of the reference material are listed in Table 2.25.

Blanks

The instrumental and procedural blanks for the analysis of mercury were measured concurrently with the samples. The procedural blanks made with Milli-Q water to mimic the processing of the samples. Aliquots of approximately 0.10 g were run alongside the experimental samples. The concentrations of the procedural blanks were below the limit of detection (LOD) and therefore not subtracted from any experimental samples.

Table 2.25. The measurements of the QC04-ERM 1 reference material used in the egg yolk analysis. QC04 ERM 1 is certified for mercury at 101 ng/g \pm 3 ng/g, which is the range in which these measurements fall.

QC04-ERM 1 Replicates	[Hg] mg/kg	QC04-ERM 1 Replicates	[Hg] mg/kg
QC04 ERM 1 run 01	96.6	QC04 ERM 1 run 26	99.0
QC04 ERM 1 run 02	99.1	QC04 ERM 1 run 27	97.4
QC04 ERM 1 run 03	98.7	QC04 ERM 1 run 28	97.6
QC04 ERM 1 run 04	97.2	QC04 ERM 1 run 29	93.3
QC04 ERM 1 run 05	96.4	QC04 ERM 1 run 30	96.2
QC04 ERM 1 run 06	94.3	QC04 ERM 1 run 31	98.3
QC04 ERM 1 run 07	92.3	QC04 ERM 1 run 32	96.9
QC04 ERM 1 run 08	107.6	QC04 ERM 1 run 33	96.7
QC04 ERM 1 run 09	105.0	QC04 ERM 1 run 34	98.7
QC04 ERM 1 run 10	102.9	QC04 ERM 1 run 35	98.2
QC04 ERM 1 run 11	103.4	QC04 ERM 1 run 36	94.9
QC04 ERM 1 run 12	104.7	QC04 ERM 1 run 37	100.4
QC04 ERM 1 run 13	104.5	QC04 ERM 1 run 38	97.1
QC04 ERM 1 run 14	104.3	QC04 ERM 1 run 39	99.4
QC04 ERM 1 run 15	108.5	QC04 ERM 1 run 40	97.8
QC04 ERM 1 run 16	104.6	QC04 ERM 1 run 41	100.0
QC04 ERM 1 run 17	106.6	QC04 ERM 1 run 42	99.8
QC04 ERM 1 run 18	102.4	QC04 ERM 1 run 43	98.2
QC04 ERM 1 run 19	99.1	QC04 ERM 1 run 44	99.8
QC04 ERM 1 run 20	97.3	QC04 ERM 1 run 45	98.5
QC04 ERM 1 run 21	99.3	QC04 ERM 1 run 46	100.7
QC04 ERM 1 run 22	99.5	QC04 ERM 1 run 47	98.4
QC04 ERM 1 run 23	97.2	QC04 ERM 1 run 48	96.4
QC04 ERM 1 run 24	97.9	QC04 ERM 1 run 49	99.9
QC04 ERM 1 run 25	99.6	QC04 ERM 1 run 50	99.4
Average		97.5	
Standard Deviation		3.5	
% RSD		3.6	

Statistical analysis

The egg yolk data from the total mercury analysis demonstrated a normal distribution, but were not homoscedastic, even under a log₁₀ transformation. Since the assumptions of parametric statistics were not met, the Wilcoxon Each Pair test was used to determine the statistical differences between locations. The statistical analysis was carried out using JMP 11 software (SAS Institute Inc., Cary, NC).

2.6.3. Results & Discussion

The egg yolk samples from the three sites ranged in mercury concentration from approximately 2 to 50 ng/g (Table 2.26). The average egg yolk mercury concentration from Apopka, Woodruff and Yawkey were 8.8 ± 5.1 ng/g, 22.6 ± 6.3 ng/g, 26.3 ± 11.0 ng/g, respectively (Table 2.27, Figure 2.20). The results from Apopka are surprising, as this is a historically contaminated site for organic contaminants (302). While there is no relationship between concentration of organic contaminants and the presence/concentration of mercury, we expected this location to have higher mercury than was observed. The Guillette laboratory has been using Apopka as a “contaminated site” for over a decade, and the observation that there is very low mercury at this site changes how it is characterized by the laboratory.

The Wilcoxon Each Pair Comparison was used to determine the statistical difference between the total mercury fractions in the egg yolk at the three locations. Lake Apopka, FL (average mercury = 8.75 µg/kg) was shown to be highly significantly different from both Lake Woodruff, FL (average mercury = 26.26 µg/kg) and Yawkey Wildlife Center, SC (average mercury = 22.64 µg/kg), both comparisons having *p* values <0.0001.

Yawkey Wildlife Center, SC and Lake Woodruff, FL were not significantly different from each other (p value = 0.26, Figure 2.20).

These data from Yawkey, SC show that mercury is detectable in egg yolk at low mercury sites, and above the limit of our detection. These data from Lakes Apopka and Woodruff suggest that there are additional low mercury sites in northern Florida, and that Apopka may be the lowest site for mercury that has been measured by the Guillette laboratory. However, since adults were not sampled at Apopka and Woodruff, definitively characterizing these two sites as low mercury is based on the assumption that the egg yolk mercury concentration is related to the blood concentration of the nesting females. Vertical transfer of contaminants, particularly mercury, is known to widely occur in mammals, and has been shown in certain amphibians, and reptiles (189, 190, 303-305). The assumption that it occurs in alligators is supported by the known maternal transfer of selenium, but more in depth investigations need to be conducted to determine if mercury is also vertically transferred in this species (306).

Table 2.26. The individual mercury concentrations of the yolk samples collected at Yawkey, Apopka and Woodruff in 2011.

Sample ID	[Hg] ng/g	Sample ID	[Hg] ng/g	Sample ID	[Hg] ng/g
AP13 01-03	4.1	AP-02-23 (261)	5.3	YK-09-44 (364)	18.5
AP13 01-19	8.0	AP-02-26 (262)	10.7	YK-09-46 (365)	21.0
AP13 01-22	7.5	AP-02-32 (260)	6.4	YK-16-09 (354)	14.1
AP13 01-23	2.5	AP-02-34 (272)	24.7	YK-16-15 (355)	20.8
AP13 01-41	2.3	AP-06-02 (357)	5.2	YK-16-22 (356)	20.6
AP13 01-42	2.3	AP-06-10 (358)	1.9	YK-18-01 (273)	14.3
AP13 01-44	8.8	AP-06-21 (359)	5.2	YK-18-03 (274)	16.9
YK-02-22	28.7	AP-06-26 (360)	4.8	AP-01-38	10.2
YK-03A-16	45.8	AP-06-44 (361)	5.9	AP-01-48	6.8
YK-03B-37	42.4	WO-01-20 (254)	23.5	AP-03-15	14.4
YK-04-02	39.5	WO-01-28 (253)	21.8	AP-03-18	5.1
YK-05-35	16.2	WO-01-34 (252)	15.3	AP-03-22	9.2
YK-07-4	18.1	WO-06-02 (268)	22.5	AP-03-23	8.6
YK-08-4	31.6	WO-06-18 (266)	21.7	AP-03-33	10.2
YK-09-41	25.7	WO-06-43 (269)	24.0	WO-04-14-278	20.7
YK-10-22	24.1	WO-08-10 (251)	17.8	WO-04-28-279	20.1
YK-11-01	42.6	WO-08-12 (256)	15.7	WO-05-17-282	18.6
YK-11-02	38.4	WO-08-14 (255)	15.3	WO-05-24-283	20.3
YK-11-03	47.0	WO-10-01 (222)	25.8	WO-06-11-281	17.8
YK-11-4	31.5	WO-10-08 (223)	31.2	WO-20-05	20.5
YK-12-01	45.4	WO-10-14 (224)	30.6	WO-20-07	20.8
YK-12-02	31.6	WO-13-01 (257)	10.0	YK-05-03-287	18.7
YK-12-4	35.3	WO-13-20 (258)	13.6	YK-05-36-288	17.3
YK-13-17	19.3	WO-13-21 (259)	13.7	YK-19-3	12.9
YK-14-4	45.0	WO-16-12 (216)	26.4	AP-01-01 (no #)	8.5
YK-16-17	27.4	WO-16-19 (217)	23.8	AP-01-04 (no #)	4.1
YK-17-35	33.0	WO-16-25 (218)	22.2	AP-01-06	3.5
YK-18-4	11.8	WO-17-11 (219)	16.4	AP-04-01 (no#)	5.0
YK-19-4	15.9	WO-17-19 (220)	18.9	AP-04-03 (no#)	3.8
YK-20-4	13.2	WO-19-34 (270)	22.4	AP-04-39 (no#)	4.8
YK-21-4	45.1	WO-19-37 (271)	25.6	AP-05-11 (160)	13.0
AP-02-10 (263)	6.4	WO-20-27 (no #)	21.3	AP-05-17 (111)	12.4
AP-02-21 (264)	4.6	YK-07-01 (351)	13.7	AP-05-19 (112)	17.1
WO-02-20 (no #)	39.2	YK-07-02 (352)	18.4	AP-05-20 (113)	15.0
WO-02-21 (no #)	38.7	YK-07-03 (353)	19.2	AP-05-27 (114)	16.6
WO-03-10 (no#)	23.0	YK-08-## (369)	25.7	AP-05-37 (105)	12.0
WO-03-22 (no#)	26.0	YK-08-01 (367)	28.4	WO-02-19 (no #)	29.5
WO-03-23 (no#)	28.3	YK-08-02 rep 01	26.2	WO-15-32 (no #)	21.4
WO-07-25 (159)	10.0	YK-08-02 rep 04	27.5	WO-15-37 (no #)	23.5
WO-07-32 (168)	13.5	YK-09-43 (363)	24.8	WO-18-02 (no#)	34.3
WO-07-39 (161)	21.8	WO-18-04 (no#)	27.3	WO-15-04 (no#)	27.8
WO-09-05 (no #)	23.2	WO-09-17 (no#)	24.2	WO-18-18 (no#)	24.9
WO-09-10 (no#)	27.7	WO-14-11 (157)	28.9	YK-06-04(no#)	15.7

Table 2.27. The descriptive statistics for the average mercury concentrations found in the yolk samples at Yawkey, Apopka and Woodruff in 2011.

2011 Egg Yolk Comparison Descriptive Statistics						
Site	n eggs	n nests	Mean [THg] ng/g	Standard Deviation ng/g	Range [THg] ng/g	
Yawkey	42	18	26.26	10.94	11.82	46.97
Woodruff	50	18	22.64	6.27	9.97	39.20
Apopka	30	6	8.75	5.09	1.92	24.68

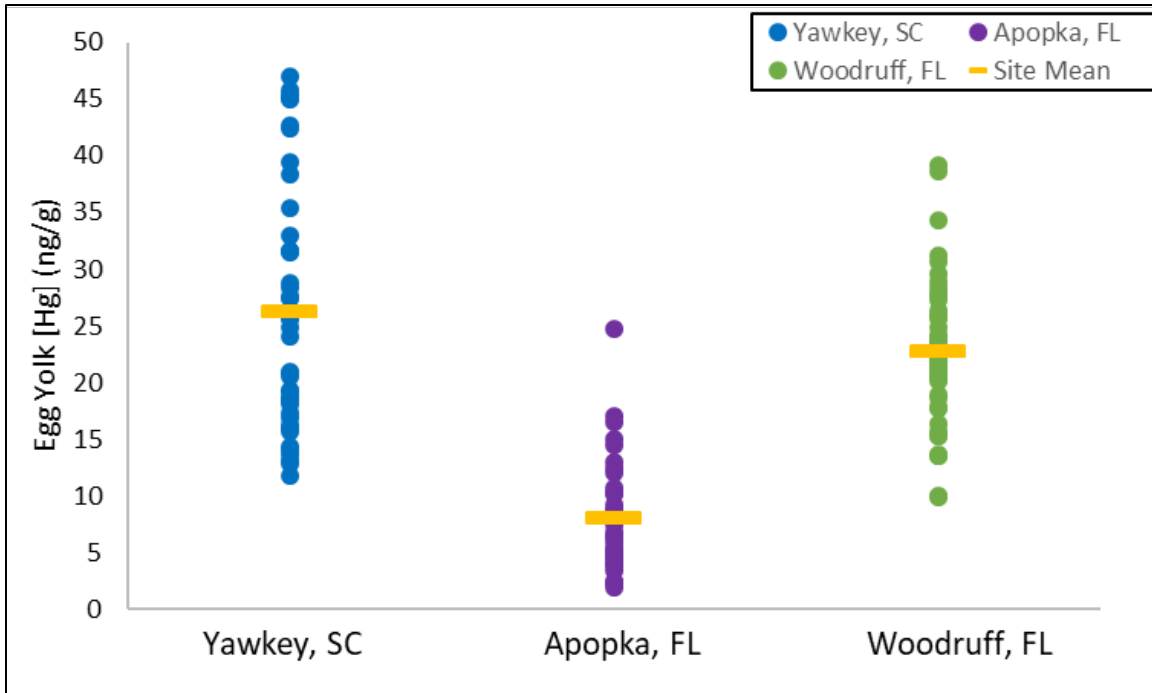


Figure 2.20. The individual mercury measurements from the yolk samples collected at Yawkey, Apopka and Woodruff in 2011. The mean mercury concentration for each site is denoted with a yellow bar overlaid on the individual samples for that site.

2.7. Investigating maternal transfer of mercury to developing embryos in American alligators

2.7.1. Introduction

This experiment will examine maternal blood samples and corresponding eggs and embryos to determine if maternal transfer of mercury is occurring in the American alligator. We have shown that adult American alligators are worthy environmental sentinels for chronic dietary mercury exposure throughout the seasons, and for modeling mercury changes associated with decreasing BMI. The previous experiment determined that mercury is detectable in alligator egg yolk, and present in different amounts at different sites. The vertical transfer of mercury in this species is currently undescribed, and understanding the relationship between mercury in nesting females and their embryos will aid in the determination if this species can be used as a developmental model.

Many species of animals; including fish, amphibians, mammals and humans maternally transfer mercury during gestation and embryonic development. (131, 189, 305, 307-311). A few studies using mammals have shown that there is greater mercury transfer during gestation compared to the lactation period, making reptiles, which do not lactate, worthy candidates for sentinel species of maternal exposure (312, 313).

2.7.2. Experiment specific methods

Sample collection

Using a routinely monitored population of alligators at Tom Yawkey Wildlife Center, South Carolina, egg samples were collected from nests where putative mother alligators were found (Figure 2.21). The putative mother was also captured and a blood

sample was taken, following the method described in section 2.2.2. The metadata for the female alligators and their nests is provided in Table 2.19. Samples were collected over three nesting seasons (2011, 2013 and 2014), totaling 23 nesting pairs comprised of a nesting female blood sample and at least three egg samples from the corresponding nest. Embryos from some eggs were opportunistically collected for a single year (2014) by the following method for egg processing. The egg samples were collected from each nest less than 48 hours after the eggs were laid, during the early stages of embryonic development.

Collected alligator eggs were packed into their own nesting material for transport to the Hollings Marine Laboratory from Yawkey, South Carolina, under the direction of Dr. Louis Guillette. Upon arrival, eggs were “candled” to determine if they were viable using a microscope staging light in a dark room (Figure 2.22, top). If a white band was observed around the equator of the egg, the egg was fertilized and developing. The eggs were cut open on the outside of the band using stainless-steel dissection instruments (Figure 2.22, bottom). Yolk samples were collected using a 10 mL Luer-lock syringe (BD, lot # 9K783), placed into a 5 % nitric acid leached 50 mL Falcon tube (Corning, lot # 35013005), gently rocked for homogenization and then aliquoted into 2 mL Cryovials (Corning, lot # 00612002). Samples were placed on wet ice for no longer than 2 h before being stored at -80 °C until analysis. Between three and eleven eggs were sampled per nest, depending on availability and compliance with the permitted guidelines. The embryos were collected from the eggshell with stainless-steel dissection instruments, compared to an embryonic staging guide to determine developmental stage, and placed into a Cryovial for storage at -80 °C until the time of analysis.

All experiments performed in this study conform to the guidelines set forth by the Institutional Animal Care and use Committee (IACUC) at the Medical University of South Carolina. All fieldwork and collections were performed under permits issued from the Florida Fish and Wildlife commission, South Carolina Department of Natural Resources, and United States Fish and Wildlife Service.

Sample preparation

Blood and egg yolk samples were thawed, gently rocked to mix the contents and pipetted into nickel weigh boats for mercury analysis in the DMA-80. The embryonic samples were thawed completely, removed from the Cryovials and analyzed in their entirety.

Instrumental method, & quantification

The mass fraction of mercury was determined with a DMA-80, as described above in section 2.2.2. For this experiment, 23 blood sample measurements, 68 yolk sample measurements, and 20 embryo samples were analyzed alongside replicates of the matrix matched control materials described below. The sample size utilized for each measurement was approximately 0.10 g.

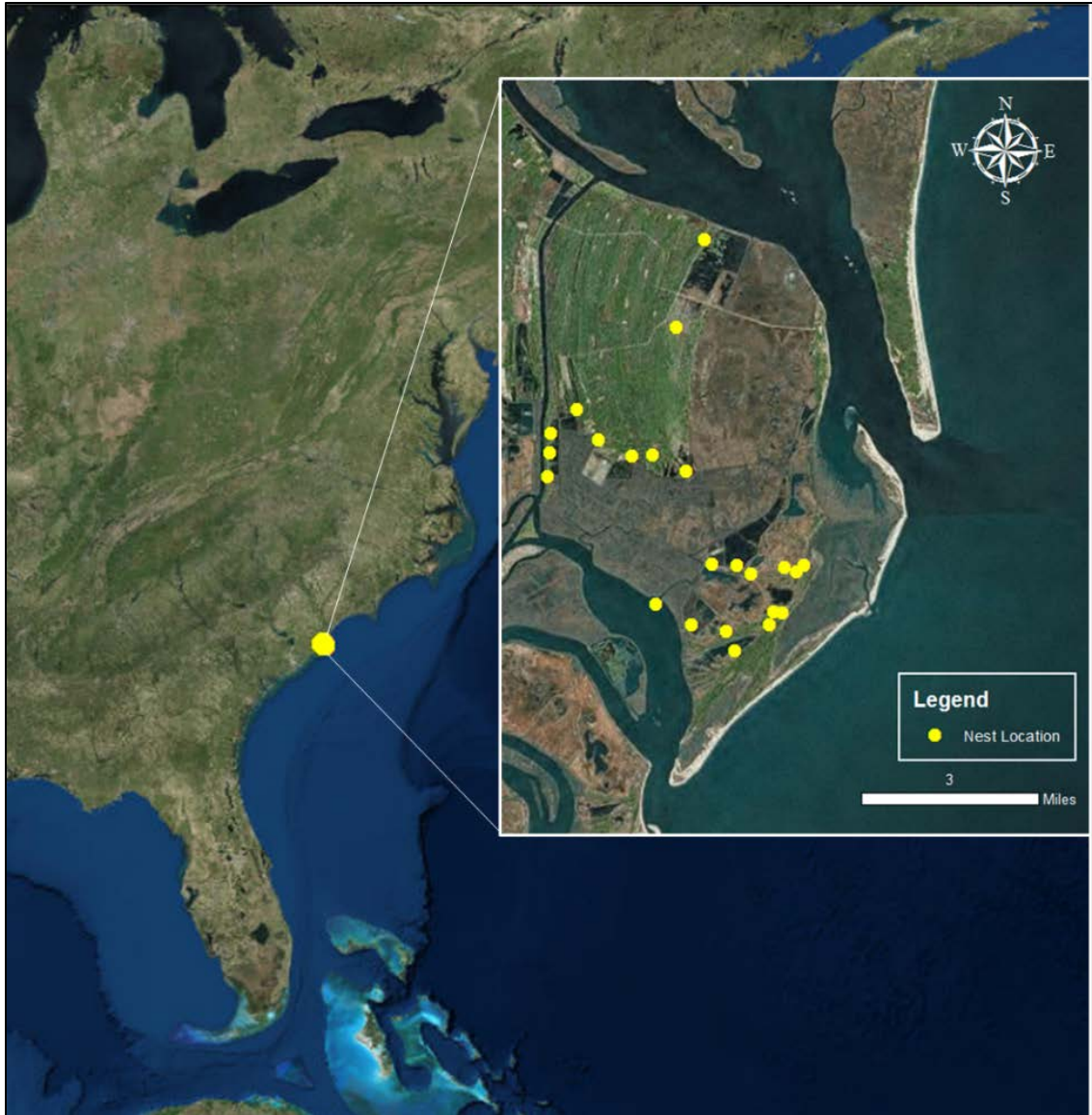


Figure 2.21. The GPS locations of the nests sampled at Yawkey, SC during the summers of 2011, 2013 and 2014. The coordinates are provided in Table 2.28.

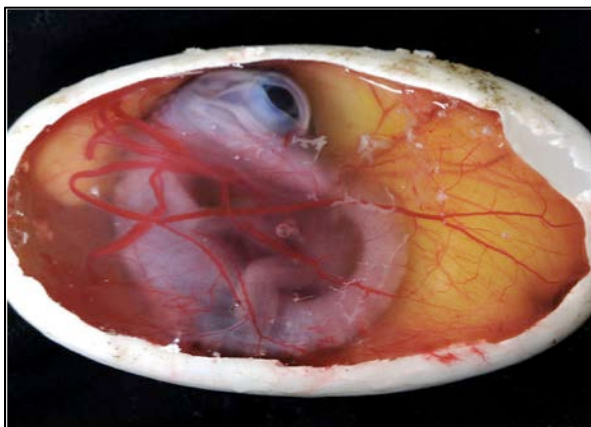
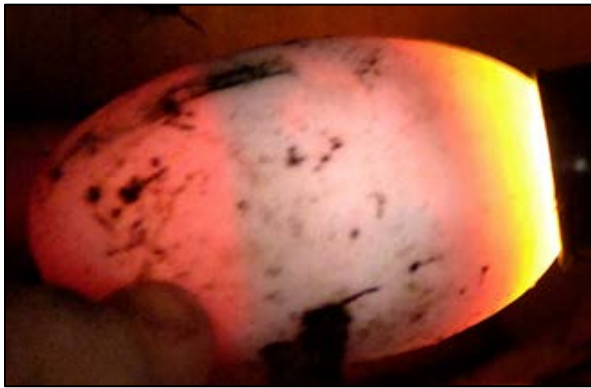


Figure 2.22. Embryonic alligator photos. The candling process (top) and the procedural opening of a viable alligator egg in the laboratory to ensure that the embryo can be sampled intact (center). The embryo shown was staged at Stage 8 of embryonic development according to Ferguson (314). A developing alligator embryo at Stage 18 according to the guide by Ferguson (1987) (bottom -photo courtesy of Theresa Cantu).

Table 2.28. The metadata associated with the nesting females and their nests from Yawkey, SC during 2011, 2013 and 2014.

Nest #	GPS coordinate (N)	GPS coordinate (W)	Oviposition date	Clutch size	% viability	Female captured	Date captured	Female scute ID	Female toe tag #
1	33°14.124	79°14.347	Gravid	ND	ND	Yes	6/10/2011	CF-65	MUSC-038
2	33°12.604	79°15.753	6/15/2011	44	100	Yes	6/16/2011	CF-67	MUSC-040
3(A,B)	33°13.720	79°14.324	6/18/2011	A-31, B-52	.	Yes	6/20/2011	CF-73	MUSC-046
4	33°14.808	79°13.912	6/13/11- 6/18/11	56	.	Yes	6/21/2011	CF-34	MUSC-047
5	33°10.234	79°12.892	Before 6/20/11	45	.	Yes	6/23/2011	BF-57	MUSC-041
6	33°12.576	79°16.163	Before 6/20/11	45	98	Yes	6/23/2011	CF-74	MUSC-048
7	33°11.890	79°16.203	Before 6/20/11	49	100	Yes	6/24/2011	CF-75	MUSC-050
8	33°12.429	79°16.165	6/22/2011	48	97.9	Yes	6/24/2011	CI-5	MUSC-051
9	33°12.346	79°15.456	6/21/2011	56	.	Yes	6/24/2011	DEFUJ	MUSC-054
10	33°10.811	79°13.797	After 6/20/11	30	.	Yes	6/28/2011	CI-43	MUSC-057
11	33°10.071	79°12.951	6/27/2011	34	97	Yes	6/29/2011	CF-77	MUSC-058
12	33°10.222	79°12.760	6/28/2011	34	85	Yes	6/30/2011	CF-78	MUSC-059
YK-13-03	33°10.327'	79°12.959'	.	41	.	YES	6/22/2013	CG-14	MUSC-132
YK-13-04	33°10.773'	79°12.723'	.	41	.	YES	6/25/2013	CF-40	MUSC-141
YK-13-06	33°13.730	79°14.316'	6/23/2013	46	.	YES	6/24/2013	CG-15	MUSC-137
YK-13-10	33°10.700'	79°13.222'	.	58	.	YES	6/27/2013	CF-35	MUSC-203
YK-13-12	33°09.983'	79°13.580	6/26/2013	36	.	YES	6/26/2013	CF-13B	MUSC-135
YK-13-15	33° 09.754'	79°13.456'	6/28/2013	25	84	YES	6/28/2013		MUSC 107
YK-13-22	33°10.73'	79°12.55'	.	14	93	YES	6/30/2013	CF-32	MUSC 164
YK14-01	33°12.143'	79°14.973'	6/21/2014	48	.	YES	6/21/2014	CDI-8	MUSC 214
YK14-02	33° 10.81'	79° 12.44'	6/23/2014	48	.	YES	6/23/2014	CF-52	21
YK14-03	33° 10.798'	79° 13.433'	6/20/2014	43	.	YES	6/25/2014	CF-32	MUSC 206
YK14-04	33° 12.152'	79° 14.664'	6/26/2014	50	.	YES	6/26/2014	BF-94	MUSC 211
YK14-05	33° 12.26'	79°14.35'	6/28/2014	55	.	YES	6/28/2014	CF-37	NONE
YK14-06	33° 12.188'	79° 16.176'	6/27/2014	43	.	YES	6/24/2014	CG-31	MUSC 120
YK14-07	33° 12.069'	79° 14.089'	6/29/2014	36	100	YES	6/29/2014	CG-25	MUSC-174
YK14-09	33° 11.965'	79° 14.173'	7/3/2014	46	83	YES	7/3/2014	CG-28	MUSC 220
YK14-12	33° 10.795'	79° 03.592'	6/30/2014	54	91	YES	6/30/2014	CF-30	NONE
YK14-14	33° 09.997'	79° 13.582'	6/29/2014	51	94	YES	6/29/2014	BF-24	MUSC 172
YK14-15	33° 10.711'	79° 13.240'	6/30/2014	43	.	YES	6/30/2014	CG-26	MUSC 173
YK14-17	33° 12.390'	79° 15.476'	7/13/2014	55	87	YES	7/13/2014	DEF15-10	NONE
YK14-18	33° 12.721'	79° 15.777'	7/4/2014	45	64	YES	7/4/2014	CFG-29	MUSC 218

Blanks

The instrumental and procedural blanks for the analysis of mercury were measured concurrently with the samples. The procedural blanks made with Milli-Q water to mimic the processing of the samples. The procedural blanks made with 8 mL Milli-Q water in either a Vacutainer or Corning tube, to mimic the processing of the samples, aliquots of approximately 0.10 g were run alongside the experimental samples. The reference and standard materials as well as the whole blood samples were blank corrected since the concentrations of the whole blood procedural blanks were detectable (average mercury concentration = 0.2 ng/g). The concentrations of the yolk procedural blanks were below the limit of detection (LOD) and therefore not subtracted from any experimental yolk samples. The procedural blanks for the embryo samples were below the LOD, and the embryo samples were not blank corrected. Some sample blanks may be above the LOD while others are not due to contamination of those specific sample collection materials. When this occurs, only the samples that were collected with those materials are corrected for the contamination.

Control materials

QC04-ERM-1 (Egg Reference Material) was used as a control material for the alligator egg yolk samples. SRM 955c Level 2 (Toxic Metals in Caprine Blood) (10 replicates) was run as control materials for the nesting female blood samples. SRM 955c Level 2 and 3 were both used as control materials for the embryo samples, as the expected mercury concentration of the embryos was unknown. The results of the mercury analysis of the SRMs are listed in Table 2.29.

Table 2.29. Summary of total mercury (Hg) results for QC04-ERM-1, and SRM 955C Levels 2 and 3, used during the analysis of American alligator blood, yolk and embryo samples in Experiment 2.6. QC04-ERM-1 Egg Reference Material is certified at $101 \pm 3 \mu\text{g/kg}$; SRM955C Toxic Metals in Caprine Blood Levels 2 and 3 are certified at $4.95 \pm 0.76 \mu\text{g/kg}$, and $33.9 \pm 2.1 \mu\text{g/kg}$, respectively. SRM 955c level 2 was run alongside the embryo samples (center) and SRM 955c levels 2 and 3 were run alongside the blood samples, to span the possible range of Hg concentrations (right).

QC04 ERM1 Replicates	[Hg] ng/g	SRM 955c Replicates	[Hg] ng/g	SRM 955c Replicates	[Hg] ng/g
QC04 ERM1 run 01	93.0	SRM 955c level 2 rep 01	5.1	955c Level 3 run 01	17.49
QC04 ERM1 run 02	91.4	SRM 955c level 2 rep 02	5.1	955c Level 3 run 02	17.68
QC04 ERM1 run 03	98.0	SRM 955c level 2 rep 03	5.2	955c Level 3 run 03	17.56
QC04 ERM1 run 04	91.4	SRM 955c level 2 rep 04	5.2	955c Level 3 run 04	17.33
QC04 ERM1 run 05	97.6	SRM 955c level 2 rep 05	5.1	955c Level 3 run 05	17.66
QC04 ERM1 run 06	96.8	SRM 955c level 2 rep 06	5.5	955c Level 3 run 06	17.63
QC04 ERM1 run 07	101.2	SRM 955c level 2 rep 07	5.0		
QC04 ERM1 run 08	100.0	SRM 955c level 2 rep 08	5.4	Average	17.6
QC04 ERM1 run 09	100.7	SRM 955c level 2 rep 09	5.0	Standard Deviation	0.1
QC04 ERM1 run 10	102.8	SRM 955c level 2 rep 10	5.1	%RSD	0.8
QC04 ERM1 run 11	100.4			U	0.2
QC04 ERM1 run 12	96.0				
QC04 ERM1 run 13	97.1			Total U for SRM 955c 3	0.009
QC04 ERM1 run 14	97.9				
QC04 ERM1 run 15	103.0			955c Level 2 run 01	4.67
QC04 ERM1 run 16	104.4			955c Level 2 run 02	4.88
				955c Level 2 run 03	4.84
				955c Level 2 run 04	5.60
				955c Level 2 run 05	4.72
				955c Level 2 run 06	4.86
Average	98.23	Average	5.2	Average	4.9
Standard Deviation	3.96	Standard Deviation	0.1	Standard Deviation	0.3
%RSD	4.03	%RSD	2.7	%RSD	0.1
U	3.10	U	0.1	U	0.2
Total U for QC04 ERM1	0.03	Total U for SRM 955c 2	0.02	Total U for SRM 955c 2	0.005

Statistical analysis

The data from the mercury analysis of the blood samples demonstrated a normal distribution while the data from the total mercury analysis of the yolk samples demonstrated a non-normal distribution, verified by the Shapiro-Wilk goodness-of-fit test. The data were not homoscedastic. Transforming the data by \log_{10} did demonstrate a normal distribution for both sample types, but did not reduce the variance between samples. Since the assumptions of parametric statistics could not be met, the non-parametric Spearman Correlation was used to determine the statistical relationship between the mercury concentrations in the whole blood, egg yolk, and embryo samples using JMP 11 software (SAS Institute Inc., Cary, NC).

2.7.3. Results & Discussion

The nesting females at Yawkey, SC that were sampled in 2011, 2013 and 2014 displayed an average mercury concentration of $169.3 \text{ ng/g} \pm 62.9 \text{ ng/g}$. This value places these females alongside the general population of adult alligators at Yawkey that were sampled and measured in experiment 2.3 (Table 2.12). The yolk samples displayed an average mercury concentration of $17.8 \text{ ng/g} \pm 5.2 \text{ ng/g}$ (Table 2.30). These measurements show that developing eggs have low mercury concentrations at sites where the adult mercury concentrations are low (Figure 2.23).

In 2014, the nesting females could be paired to yolk and embryo samples. The embryos from these females displayed more variable mercury concentrations than those that were observed in the yolk samples (Table 2.31). The varying concentrations observed in the embryos may suggest that there are individual differences in the way that

the yolk is assimilated into the embryo, but could also be due to the small mass of the embryos yielding inconsistent results via the DMA-80.

Over the three years when eggs and adult females were sampled, a positive correlation ($\rho = 0.77$) was observed in total mercury concentration between the nesting female and the yolk of her eggs. Each year's pairs had different correlation coefficients, with the greatest coefficient corresponding to the year with the greater number of pairs, 2011 ($\rho = 0.91$; Figure 2.24). The varying correlation coefficients are not surprising, since different female–nest pairs were sampled each year, as female alligators do not reproduce annually (253). In 2014, embryos were added to the correlation and the resulting relationship was not as strong as when only yolk and blood were examined ($\rho = 0.11$ and $\rho = 0.51$, respectively; Figure 2.24). The weaker correlation could be due to the timing of exposure, since the embryos used in this study were early stage embryos, from the first stages of development (stages 3 - 9). These stages were chosen as they would most closely match the yolk mercury concentrations from the 2011 and 2013 eggs sampled 48 hours after being laid, when no embryos were collected. A stronger correlation may have been observed if the embryos were collected at a later developmental stage, when more of the yolk had been incorporated.

Throughout embryonic development for the alligator, the embryo “consumes” the yolk. Initially, the alligator embryo is very small, barely visible to the unassisted eye. At this stage, the rest of the eggshell is full of yolk and albumin (stage 1-3). Throughout development, the embryo grows and consumes the yolk to fuel this energetic process (stages 4-26). By the end of embryonic development, the yolk is almost completely consumed and has begun to be internalized into the abdomen of the stage 27 embryo.

When the neo-natal hatchling emerges, sometimes it is still tethered to the inside of the eggshell, where the chorioallantoic membrane (CAM) once was.

The relationship observed here shows that the amount of total mercury observed in a nesting female can be used to predict how much mercury is in the yolk. There is not a large amount “off-loading” of mercury from the nesting females to offspring in reptiles, like what occurs with organic contaminants in other species, as reptiles do not transfer energy through lactation (190, 308). This study does not answer the question of how much mercury is transferred to the developing embryo, since early embryonic stages before the yolk was incorporated into the embryo, were used in this analysis. The data from this experiment do show that there is a relationship between the nesting females’ blood mercury concentration, and their egg yolk concentrations, which is suggestive of vertical transfer, and has not previously been shown for large reptiles (Figure 2.25). These data add to the growing body of life history information for this species as well as provide some insight to the seasonal variability observed in the spring and summer for adult alligators in experiment 2.4 (Figure 2.12). Previously, we believed that some of the annual variation observed in the spring and summer could be related to the nesting females depositing mercury into their eggs. While there appears to be a consistent proportion of mercury deposited, this is not likely the cause of the springtime variation observed over the 7 year sampling period. The mobilization of the synthesized egg material from the liver to the ovary via the blood prior to egg laying may be the cause of some of the variation observed, as well as the altered foraging pattern of the nesting females during this season (253, 315). However, an experiment that specifically addresses this question would have to be conducted to make this statement, such as

sampling the same females multiple times throughout the breeding and nesting season to determine how a single females blood mercury concentration changes based on seasonal behaviors, as well as if she lays eggs that year.

Using the correlation and equation that was derived from the 3 years of paired data, predictions can be made estimating how much mercury embryos at other locations are exposed to, based on the nesting female blood concentrations. The relationship described in this chapter could improve monitoring efforts for high exposure populations that are experiencing lowered breeding success, by estimating the amount of mercury the embryos are exposed. Mercury is known to cause reproductive impairment, and using the developed equation could identify or rule out mercury as a source of embryonic lethality (113).

The data presented in this section is the first nesting female – embryo pair samples collected from a wild reptilian species, to the best of our knowledge. Reptiles do not care for their young throughout neonatal development the way that most mammals do, so identifying maternity is difficult. The few embryos that were collected for this study are a limiting factor in understanding how much mercury developing alligators are exposed to. If this study were conducted again, sampling additional locations would be advantageous to determine if varying mercury concentrations in nesting females affects the amount of mercury that is transferred to the embryo, or if the proportion is always the same. Also, collecting eggs from many different nests and allowing them to incubate until the late stages of development would provide additional information regarding the amount of mercury that is incorporated into the embryo from the yolk. Since the females in this study were only sampled after they laid their eggs, future studies could sample

females throughout the breeding and nesting period, to determine how much their blood mercury concentration changes based on their behaviors, and determine if there is a more accurate time point to compare egg yolk mercury concentrations to than post-laying. . However, blood samples collected from the nesting female post-egg laying may be a more accurate representation of the normal circulating concentration of mercury in the female blood, rather than prior to egg laying. The egg material is synthesized in the liver, where the highest concentrations of mercury are observed in alligators, and then transported to the ovary via the blood (315). The transportation of the egg material could elevate the nesting female's blood concentration of mercury, complicating sampling females prior to egg laying. Using blood sample collected after egg laying removes the possibility of observing an artificially high concentration, and likely provides a realistic ambient concentration.

Table 2.30. The total Hg data for the nesting female blood samples and yolk sampled collected at Yawkey, SC in 2011, 2013 and 2014.

<i>Nesting Female Blood Samples</i>		<i>Egg yolk Samples</i>							
Sample	[Hg] ng/g	Sample	[Hg] ng/g	Sample	[Hg] ng/g	Sample	[Hg] ng/g	Sample	[Hg] ng/g
MUSC 041	154.9	YK11-04-02	39.5	YK11-12-02	31.6	YK14-02-48	12.0	YK14-06-03	17.8
MUSC 047	146.7	YK11-05-35	16.2	YK13-03-01	11.9	YK14-03-05	28.8	YK14-06-04	1.5
MUSC 050	141.2	YK11-05-03	18.7	YK13-03-01	28.3	YK14-03-12	22.7	YK14-06-04	17.6
MUSC 051	192.9	YK11-05-36	17.3	YK13-03-02	13.6	YK14-03-13	34.9	YK14-06-17	15.9
MUSC 054	174.1	YK11-06-04	15.7	YK13-03-02	25.6	YK14-03-16	28.1	YK14-06-18	14.8
MUSC 057	48.2	YK11-07-01	13.7	YK13-03-13	16.7	YK14-03-17	28.5	YK14-06-26	16.0
MUSC 058	238.2	YK11-07-02	18.4	YK13-03-27	29.2	YK14-03-27	29.3	YK14-06-27	17.0
MUSC 059	207.7	YK11-07-03	19.2	YK13-04-12	19.8	YK14-03-37	25.2	YK14-06-31	15.1
MUSC 107	103.8	YK11-07-4	17.3	YK13-04-01	12.0	YK14-04-03	14.9	YK14-06-35	16.2
MUSC 120	125.5	YK11-08-4	31.6	YK13-04-01	17.2	YK14-04-06	10.6	YK14-06-37	16.0
MUSC 132	111.9	YK11-08-##	25.7	YK13-04-02	17.6	YK14-04-07	19.3	YK14-06-39	18.5
MUSC 137	208.0	YK11-08-01	28.4	YK13-04-04	17.7	YK14-04-10	15.3	YK14-06-41	13.0
MUSC 141	161.7	YK11-08-02	27.8	YK13-04-30	18.7	YK14-04-11	16.1	YK14-07-02	17.0
MUSC 174	143.2	YK11-09-43	24.8	YK13-06-01	19.1	YK14-04-18	14.9	YK14-07-03	17.3
MUSC 203	72.3	YK11-09-44	18.5	YK13-06-31	20.2	YK14-04-21	14.7	YK14-07-04	18.7
MUSC 21	134.4	YK11-09-46	21.0	YK13-06-46	18.7	YK14-04-26	14.4	YK14-09-01	14.5
MUSC 211	152.3	YK11-09-41	25.7	YK13-15-03	7.6	YK14-04-28	14.1	YK14-09-02	20.6
MUSC 214	155.6	YK11-10-22	24.1	YK13-15-05	12.7	YK14-04-34	14.8	YK14-09-03	15.0
MUSC 218	176.3	YK11-11-01	42.6	YK14-01-47	14.5	YK14-04-35	14.5	YK14-09-04	11.6
MUSC 220	196.7	YK11-11-02	38.4	YK14-01-48	20.7	YK14-04-37	14.9	YK14-14-03	29.6
MUSC 164	316.2	YK11-11-03	47.0	YK14-01-49	18.6	YK14-04-38	12.9	YK14-18-02	16.1
MUSC 206	253.5	YK11-11-4	31.5	YK14-01-50	21.8	YK14-04-43	14.4	YK14-18-03	26.4
MUSC 172	278.0	YK11-12-01	45.4	YK14-02-45	15.0	YK14-02-46	18.6	YK14-04-49	12.6
Average Hg	169.3	YK11-12-4	35.3	Average Hg			20.4		
Standard Deviation	62.9				Standard Deviation			8.2	

Table 2.31. The paired nesting female, yolk and embryo total Hg results from Yawkey, SC 2014.

Mother	Hg ng/g		Hg ng/g	Embryo	Hg ng/g
MUSC 214	155.6	YK14-01-48	20.7	YK14-01-48 embryo	9.03
MUSC 21 (CF-52)	134.4	YK14-02-48	12.0	YK14-02-48 embryo	25.37
MUSC 206	253.5	YK14-03-05	28.8	YK14-03-05 embryo	46.32
MUSC 206	253.5	YK14-03-16	28.1	YK14-03-16 embryo	32.35
MUSC 211	152.3	YK14-04-06	10.6	YK14-04-06 embryo	44.86
MUSC 211	152.3	YK14-04-18	14.9	YK14-04-18 embryo	23.18
MUSC 211	152.3	YK14-04-26	14.4	YK14-04-26 embryo	24.18
MUSC 211	152.3	YK14-04-28	14.1	YK14-04-28 embryo	7.85
MUSC 211	152.3	YK14-04-43	14.4	YK14-04-43 embryo	14.90
MUSC 120	125.5	YK14-06-03	17.8	YK14-06-03 embryo	20.99
MUSC 120	125.5	YK14-06-37	16.0	YK14-06-37 embryo	20.18
MUSC 120	125.5	YK14-06-41	13.0	YK14-06-41 embryo	39.92
MUSC 174	143.2	YK14-07-04	18.7	YK14-07-04 embryo	11.85
MUSC 220	196.7	YK14-09-03	15.0	YK14-09-03 embryo	16.59

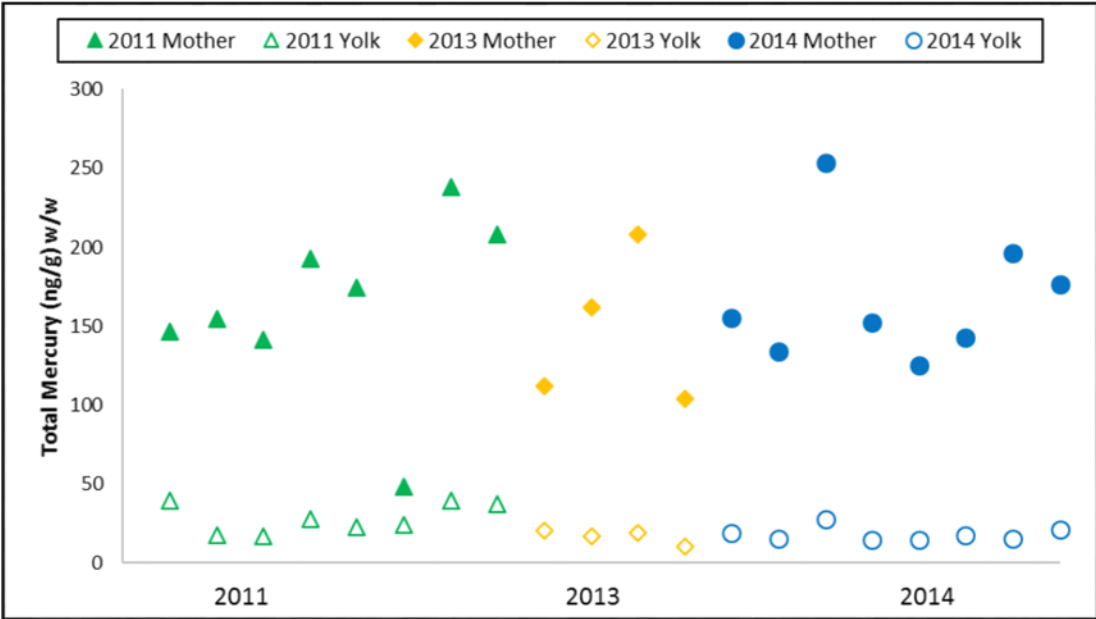


Figure 2.23. The mercury concentrations from the individual nesting female blood samples (filled markers), and the corresponding yolk samples (hollow markers) from Yawkey, SC in 2011, 2013, and 2014.

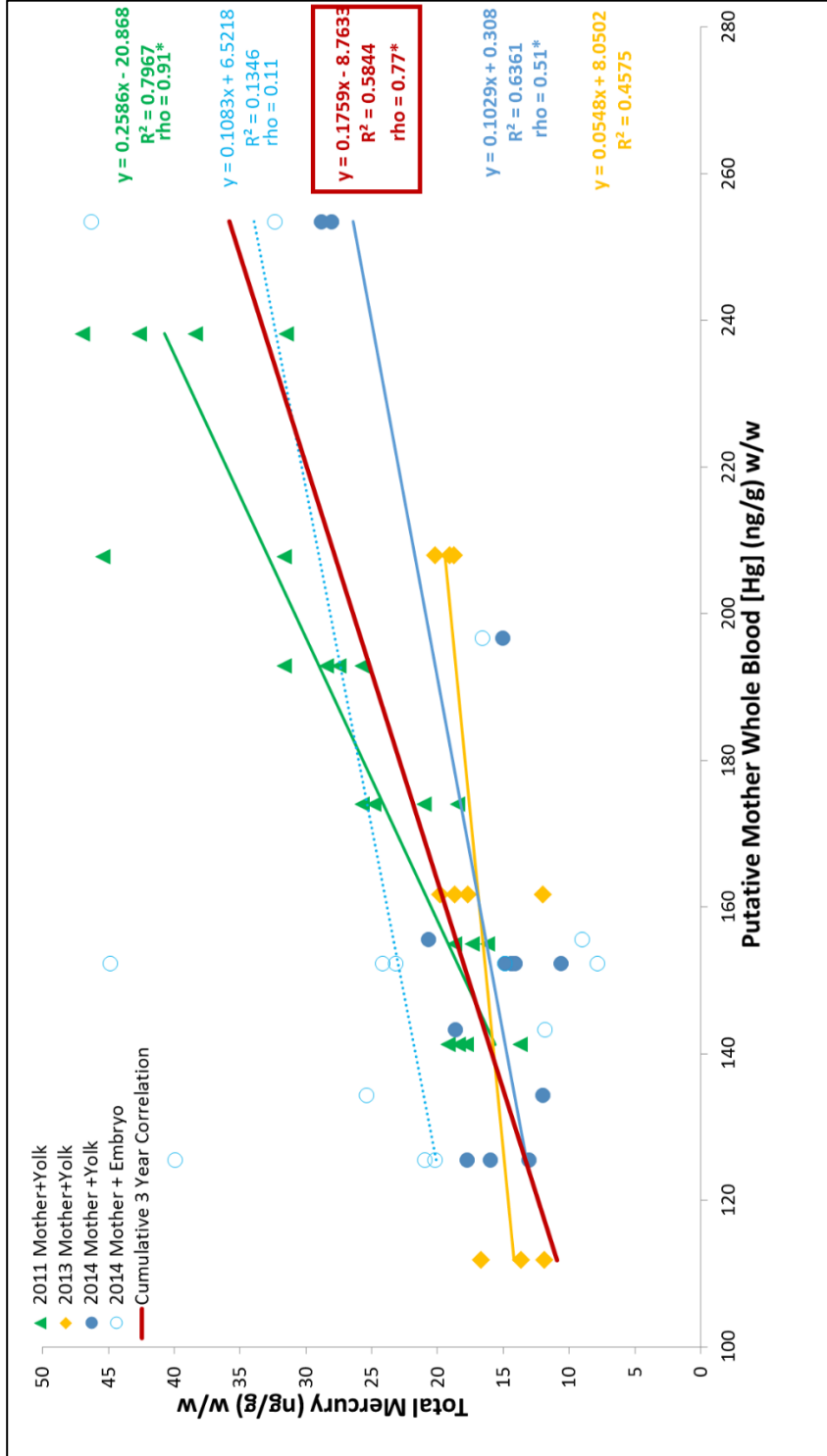


Figure 2.24. The relationship between putative mother blood samples, egg yolk and embryonic total Hg concentrations. The * denotes statistical significance in the Spearman Correlation.



Figure 2.25. The graphical abstract of the results of Specific Aim 1, experiment 5, which was detailed in this section.

2.8. Determining the feasibility of mercury dosing for American alligator eggs

2.8.1. Introduction

The previous experiment provided information regarding the correlative relationship between the mercury concentrations that developing alligator embryos are exposed to, and the mercury concentration measured in the blood of the nesting females (Figure 2.24). Since multiple years of samples were collected, a cumulative 3-year correlation was derived to assist with the prediction of yolk mercury concentrations based on adult female blood concentrations (Figure 2.24).

The Florida Everglades are an area of high mercury contamination where egg collection is prohibited. Developing alligators in high mercury contamination areas, such as the Everglades, are likely subject to a greater dose of maternally transferred mercury, as the females in those locations have greater mercury concentrations compared to those at Yawkey, SC (Table 2.12). To this end, we use the cumulative 3-year correlation linear equation from experiment 2.6 ($y = 0.1759x - 8.7633$; Figure 2.24), to predict egg yolk concentrations in the Everglades based on total mercury concentrations in nesting females from that location. This prediction was then used to carry out a dosing study, to “create” eggs from the Everglades as well as from a lower mercury site, for comparison to elucidate the effect mercury exposure has on developing alligator embryos.

There are only two methods available to dose calcified eggs, such as chicken and crocodilian eggs, either by topical application or injection (316, 317). Neither method appears to be a reproducible way to dose crocodilian eggs. The topical method has come under scrutiny in the field of environmental toxicology, as few studies provide any quality control measurements to determine if the dose transferred through the eggshell

(316). The injection method is very effective with chicken eggs, but crocodilian eggs do not have an air cell for the solution to be injected into, instead the injection goes directly into the yolk (317). Exposing the yolk and other egg contents to the air, and humid incubation environment has not resulted in any successful dosing study attempted by the Guillette laboratory. This experiment investigates the efficacy of each method for American alligator eggs.

2.8.2. Experiment specific methods

Sample collection & egg incubation

American alligator eggs were collected from Lake Woodruff National Wildlife Refuge, Florida under the direction of Dr. Louis Guillette with the assistance of the Florida Fish and Wildlife Conservation Commission (Figure 2.26). Once a nest was located, the adult female was driven away, and the nest was excavated by two field collectors wearing nitrile gloves. Nest excavation consisted of removing the top layer of plant material from the nest to reveal the eggs. The eggs were removed from the nest and carefully placed in a bin lined with nesting material from the top nest layer, and were marked to note the location of the developing embryo, as well as to note the original location within the nest. The location of the embryo within the egg is important, as alligator eggs cannot be turned during incubation. The alligator embryo is fused to the inside of the eggshell, which creates the banding pattern that can be observed through candling. If the egg is rotated, the embryo will detach from the eggshell and the developing CAM will rip and stop facilitating gas exchange to the embryo. The eggs were transported back to the dock via airboat, and secured within the back of the lab van using straps, cushioning and tarps, then transported back to HML in air conditioning.

At HML, the eggs were candled as described in section 2.6.2. One egg from each clutch was opened to determine the embryonic stage of each nest at the day of collection/sorting, according to the guide by Ferguson (314). The eggs were then placed on a bed of farmed sphagnum moss in plastic bins in incubators set to the female producing temperature of 30 °C. Each nest inside the incubator had a temperature monitoring device, a thermistor (Hobo, Onset, Bourne, MA), which was read once daily to ensure a constant temperature was maintained throughout the experiment.

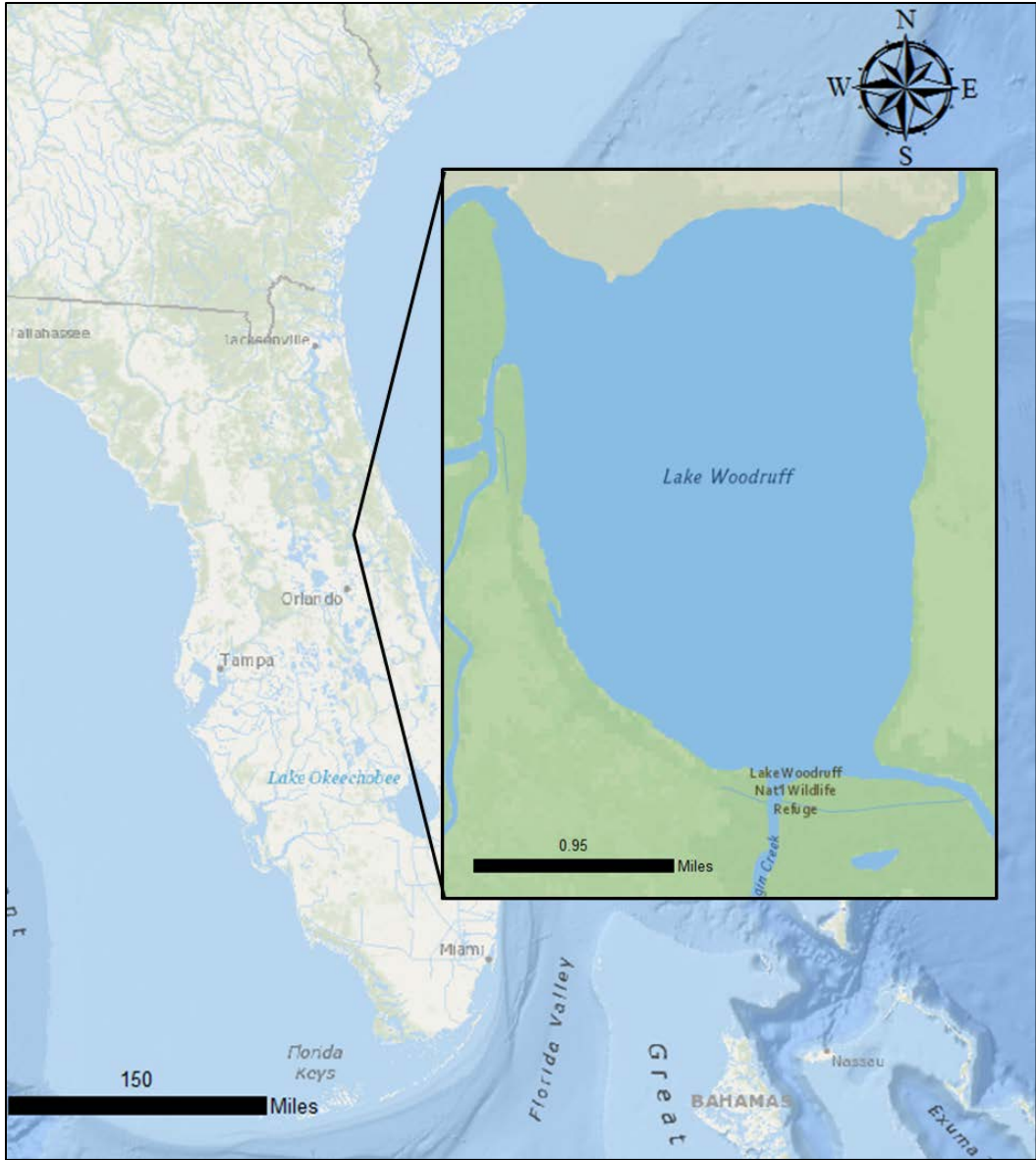


Figure 2.26. A map of Lake Woodruff National Wildlife Refuge, FL where alligator eggs for experiment 2.7 were collected.

Methylmercury cysteine solutions

Methylmercury chloride and cysteine chloride salts were acquired from Sigma Aldrich for the creation of a methylmercury–cysteine solution following the method used by Roos, *et al.* (318). The desired doses were determined based on the amount of mercury that is predicted to be in the eggs in the Everglades, (a high mercury site) based on the 3-year correlation equation ($y = 0.1759x - 8.7633$), and the relative amount of dosed chemicals that have previously been observed to penetrate reptile eggs (~30% through the eggshell and 8% to the embryo) (319). Podreka, *et al.* (319) observed that only one third of the dosed amount of Dichlorodiphenyldichloroethylene (DDE) penetrates sea turtle eggs. Due to the similar physical characteristics between DDE and methylmercury-cysteine, such as molecular weight, and boiling point, we based our dose requirements on their findings (Figure 2.27). We calculated the average mercury concentration we observed in the Everglades, as well as the lowest observed mercury concentration in adult female alligators in section 2.3 (Table 2.32). Using the information provided by Podreka, *et al.* (319), we used the “normal” Everglades dose as calculated by the equation, and then a triple dose, in the event that the alligator eggs have similar penetrability as sea turtle eggs. The created doses were designed to fall between the average and lowest adult female blood mercury concentrations in the Everglades, as to not over dose the eggs with a toxic concentration of mercury. We also considered the low concentration of mercury that has been previously observed at Woodruff, and subtracted that from the dose amount. The results of the calculations are provided in Table 2.32.

The neat salt compounds were weighed gravimetrically into a 50 mL Falcon tube (BD) and suspended in Milli-Q water. A high dose solutions was created using the

approximate mass of 28,800 ng of methylmercury-cysteine dissolved in 30.2 g of Milli-Q water, and a low dose solution was created using an approximate mass of 8,000 ng methylmercury-cysteine dissolved in 22.5 g of Milli-Q water. These doses would require 750 μ L for a 70 g alligator egg, to achieve the desired doses of \sim 100 ng/g for the low dose and 360 ng/g for the high dose eggs. These doses would provide eggs with approximately 120 and 30 ng/g above the baseline average mercury concentration of 20 ng/g measured in the egg yolk upon collection (Table 2.32).

Prior to use, the mercury concentration of the dosing solutions were measured using the DMA-80, following methods described in section 2.2.2, using NIST SRM 1641e (Mercury in Water), which is certified for $101.6 \text{ ng/g} \pm 1.7 \text{ ng/g}$, as the control material. The SRM measurements 1-4 are within the range expected for this SRM, the measurements 5-7 are higher than the certified value (Table 2.32). The higher values are likely the result of mercury carry over from the high dose solution, and not a contaminated vial of the SRM. The high dose solution also have the greatest amount of variation between them - a standard deviation of $\sim 900 \text{ ng/g}$, which may also be a result of the mercury carry over between samples, since this liquid has such a high concentration of mercury. The vehicle control, low dose solution, and high dose solution had average mercury concentrations of $4 \text{ ng/g} \pm 0.5 \text{ ng/g}$, $5730 \text{ ng/g} \pm 82 \text{ ng/g}$ and $32,040 \text{ ng/g} \pm 897 \text{ ng/g}$, respectively (Table 2.32).

When 750 μ L is applied to an alligator egg weighing \sim 70 g, the expected dose was \sim 340 ng/g and 60 ng/g for the high and low doses, respectively (Table 2.33). The mean mercury concentration for each of the dosing solutions (low and high) were similar to what was desired (100 ng/g for the low dose, 360 ng/g for the high dose). The low dose

solution was ~ 40 ng/g lower than anticipated, and the high dose solution was 20 ng/g lower than anticipated. This could be due to slightly more water being added to the Falcon tube than was initially calculated, or the salts not reacting completely and releasing Hg^{2+} . These doses are still within the range of concentrations that the initial estimations were based on (Table 2.32). The detectable mercury concentration observed in the control solution was unexpected (Table 2.33). This small but consistent value is indicative of contamination from the laboratory supplies used in the solution preparation. Despite the contamination, the concentration is very low, at approximately 4 ng/g, which would not have an effect on the control group eggs that were dosed with this solution, since only one third of the applied dose is expected to transfer into the yolk, and only 8% into the embryo (319).

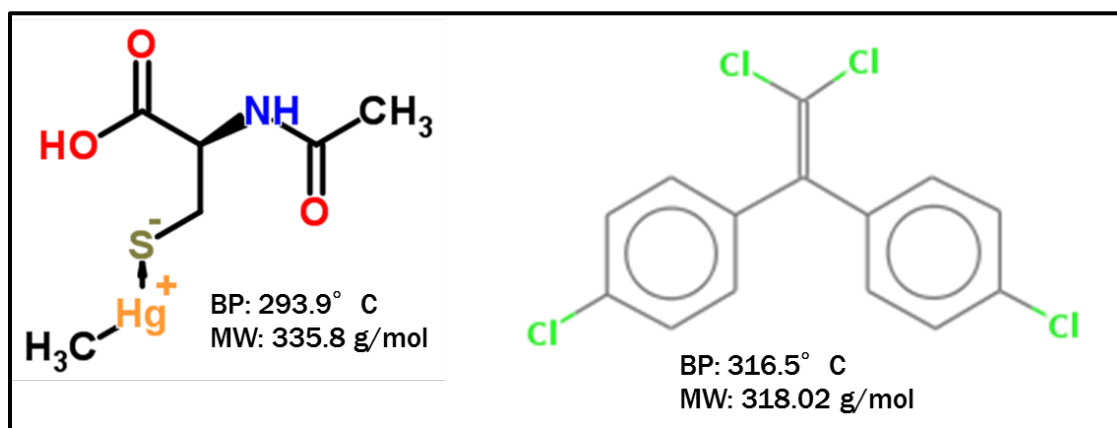


Figure 2.27. The chemical structures, boiling point and molecular weight of Methylmercury-cysteine and Dichlorodiphenyldichloroethylene.

Table 2.32. The Hg concentrations used to determine the doses needed to create high Hg eggs in the laboratory.

All concentrations are provided in ng/g. Data is extrapolated from the results presented in section 2.3, the mean Hg concentration for Woodruff, FL is provided since that is where the eggs for this study were collected from.

Location	Adult Female Mean [Hg]	Adult Female Lowest [Hg]	Projected Egg [Hg] based on mean female	Projected Egg [Hg] based on Lowest female	Woodruff, FL egg yolk mean [Hg]	Hg needed to create desired dose (mean)	Hg needed to create desired dose (Low)	Dose Of Hg Given	Hg Projection based on Dose
Everglades 3x	1079	882	181	146	20	161	126	344	115
Everglades	326	213	49	29	20	29	9	60	20

Table 2.33. The total Hg results for the methylmercury-cysteine solutions used in the laboratory dosing of American alligator eggs in experiment 2.7, and the SRM 1641e replicates used as a control material (certified values 101.6 ± 1.7 ng/g Hg).

SRM Replicates	[Hg] ng/g	Dosing Solution	[Hg] ng/g	Dosing Solution	[Hg] ng/g	Dosing Solution	[Hg] ng/g
SRM 1641e run 01	99.5	Vehicle Control run 01	3.4	Low Dose run 01	5825.8	High Dose run 01	33311.8
SRM 1641e run 02	98.9	Vehicle Control run 02	3.3	Low Dose run 02	5695.9	High Dose run 02	31734.4
SRM 1641e run 03	98.3	Vehicle Control run 03	4.1	Low Dose run 03	5643.4	High Dose run 03	32150.3
SRM 1641e run 04	101.7	Vehicle Control run 04	4.4	Low Dose run 04	5803.2	High Dose run 04	32179.7
SRM 1641e run 05	139.1	Vehicle Control run 05	4.5	Low Dose run 05	5671.4	High Dose run 05	30825.4
SRM 1641e run 06	122.8	Average	3.9	Average	5727.9	Average	32040.3
SRM 1641e run 07	123.7	Standard Deviation	0.5	Standard Deviation	81.6	Standard Deviation	896.9
Average	112.0	%RSD	13.1	%RSD	1.4	%RSD	2.8
Standard Deviation	16.4						
%RSD	14.6						

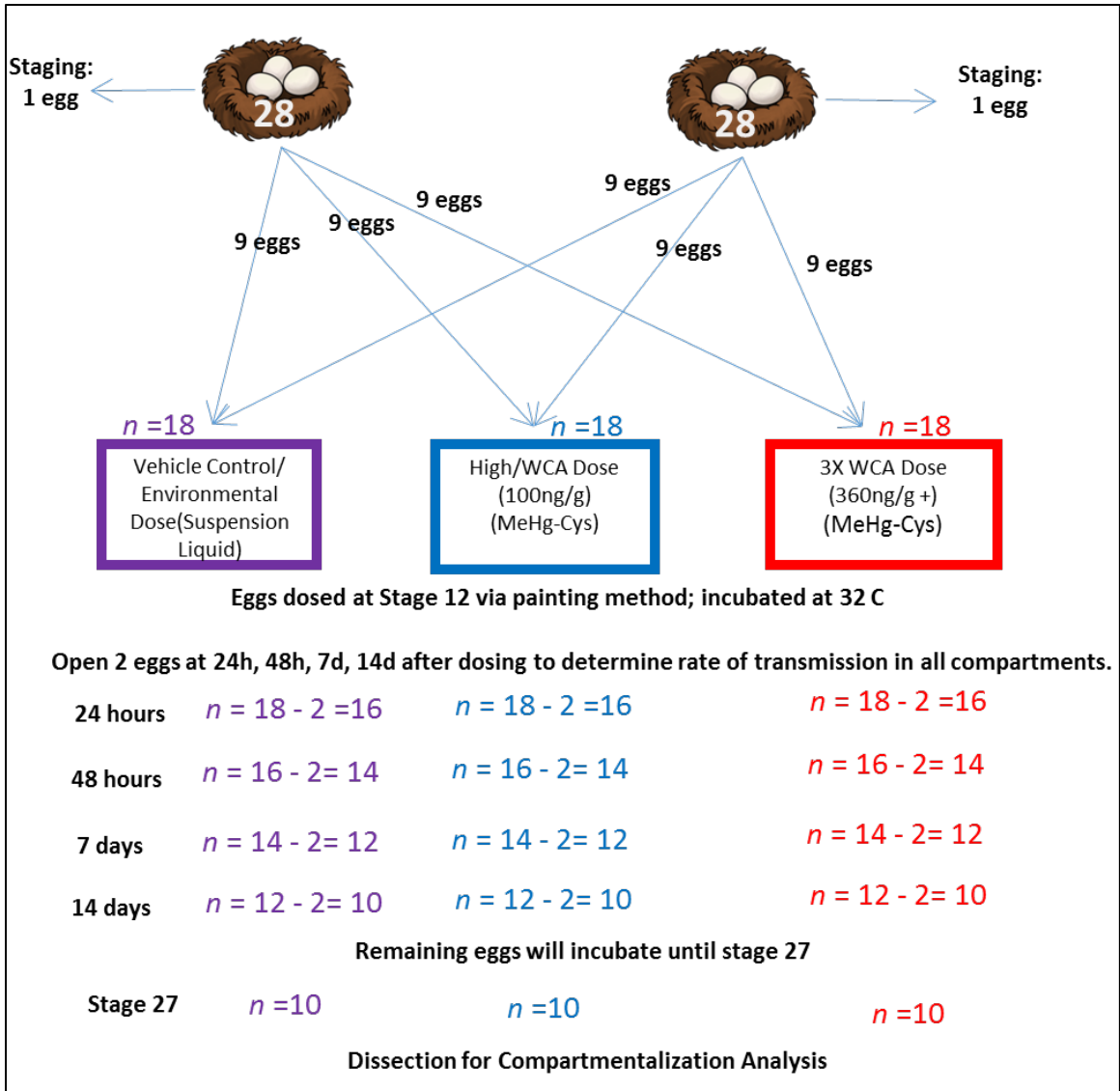


Figure 2.28. The pictorial description of the experimental design for the topical dosing experiment described in section 2.7.2.

Dose group design

Eggs from two different nests (clutches) were used in this experiment; 28 eggs were collected from each nest for a total of 56 eggs. One egg from each nest was opened and staged according to the guide by Ferguson (314). The remaining 54 eggs were divided into three groups of 18 eggs each (with 9 each from each nest). These three groups of 18 eggs became the control, low and high dose groups for this experiment (Figure 2.28).

Topical egg dosing & sampling

The eggs were topically dosed with a mercury solution at Stage 12 of embryonic development. Stage 12 was selected as it is the latest stage that either of the two collected nests were at when they were brought back to the laboratory. Using this stage enabled all eggs from the less developed nest to develop to Stage 12 and then be dosed. Two eggs (one from each of the two original nests, based on limited number of eggs collected in 2014) were then harvested from each treatment at 24 h, 48 h, 7 d and 14 d after dosing. These four time points were selected to enable the determination of the rate of transfer for methylmercury-cysteine through the eggshell, into the various egg compartments (Figure 2.28).

Eggshell, chorioallantoic membrane (CAM), albumin, yolk and embryo samples were collected from these eggs to determine rate that the mercury dose penetrated into these egg compartments. Yolk and albumin samples were collected following the methods used for yolk described above. Embryos were removed following the same method as described above. CAM samples were scraped from the inside of the eggshell after the other contents had been removed using stainless-steel dissection instruments and

placed into a Cryovial. The eggshells were then wiped clean of all remaining contents using a Tex-wipe, and then cut into strips for storage inside a 50 mL nitric acid pre-rinsed Falcon tube. The remaining eggs ($n = 10$ per dose) were developed to Stage 27 and then a blood sample was collected, to determine how much mercury transferred into the embryo by the end of development. The blood samples were vortexed for 30 s and split into erythrocyte and plasma fractions that were frozen at $-20\text{ }^{\circ}\text{C}$ until time of total mercury analysis.

Injection dosing design

Twenty-four eggs were allocated for this experiment (12 from each of two nests), collected at the same time/location/nests as those used in the main experiment in this section. These 24 eggs were then split into two 12 egg groups, with 6 eggs from each nest in each of the two groups, the control group and the dose group (Figure 2.29). The dose group received the low dose mercury solution from the main experiment ($\sim 100\text{ ng/g}$) since the entire concentration was being injection into the yolk. Stage 19 was used as it is the sexual differentiation stage that was under investigation in the previous Guillette Lab experiments, and as we aimed to change as few variables as possible, used this same developmental stage (320).

At stage 19, eggs were dosed using an insulin needle inserted directly into the yolk, through the eggshell, after a small hole was made using a larger gauge needle. Both groups received $75\text{ }\mu\text{L}$ injections of either the control dosing liquid or the 100 ng low dose dosing liquid. The hole was sealed using a hot glue gun. When the glue was dry, the eggs were then placed back in the bed of sphagnum moss inside the incubator. Eggs were sampled from both groups 14 days after injection ($n = 4$), following the method described

above, for all egg compartments. The remaining eight eggs in each group were developed to stage 27, when they were sampled for all egg compartments as previously described (Figure 2.29).

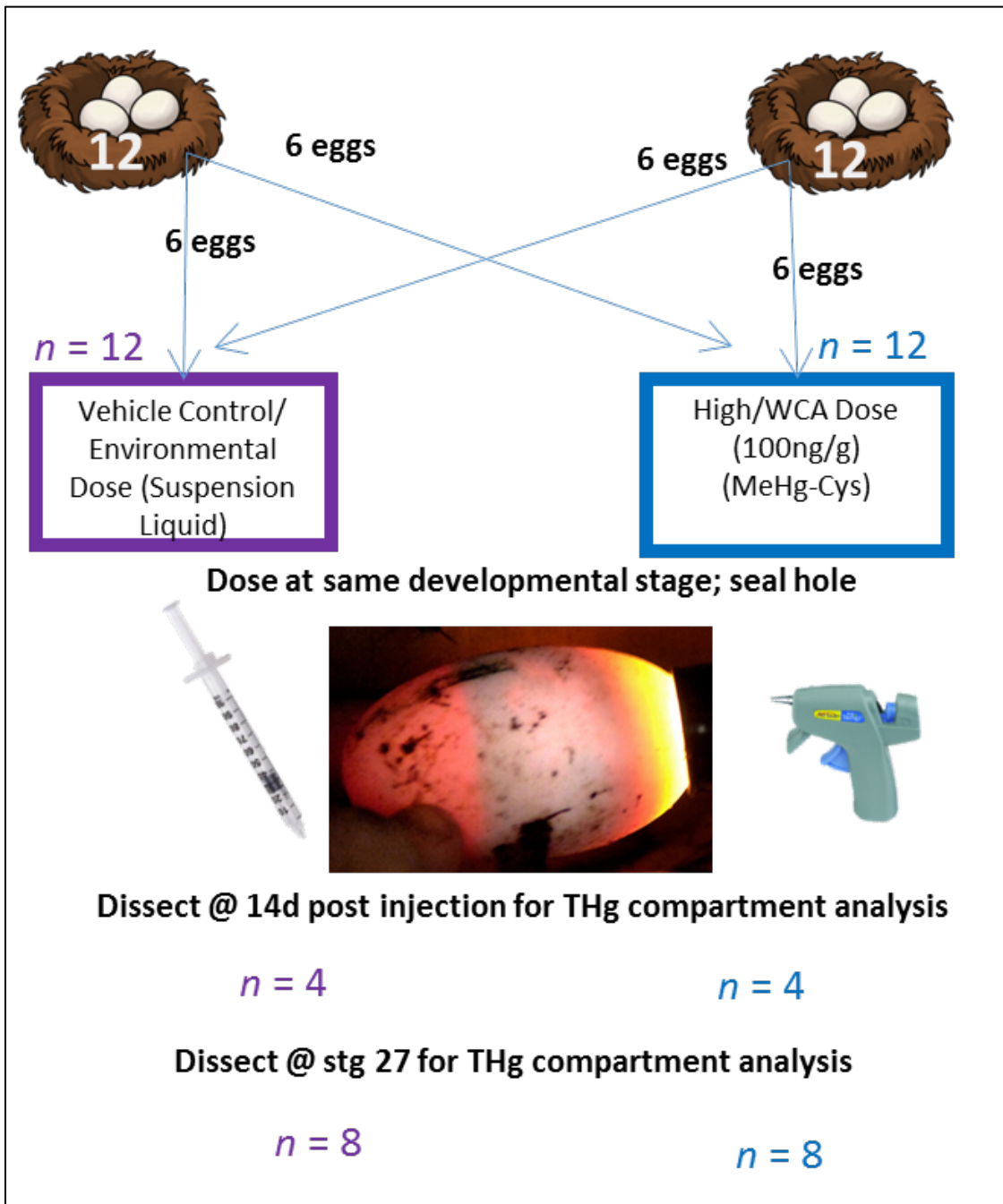


Figure 2.29. The pictorial description of the experimental design for the injection dosing experiment described in section 2.7.2.

Sample preparation

The egg yolk, albumin, and CAM samples were removed from the freezer, thawed to room temperature and gently rocked for homogenization prior to being pipetted into the nickel weigh boats on the DMA-80. The eggshell samples were cryohomogenized into a fine powder following the method described in section 2.2.2. Approximately 0.1 g of sample was weighed into a pre-cleaned nickel weight boat and analyzed. Samples that weighed more than 0.10 g (CAM) were measured successively, and the sum of the total mercury measured was divided by the total mass of the sample aliquot to determine the correct concentration of total mercury in ng/g units.

Instrumental method, quantification & control materials

The mass fraction of mercury was determined with a DMA-80, as described in section 2.2.1. A total of 185 experimental sample measurements, nine measurements of SRM 1641e (Mercury in Water) and 37 measurements of QC04 ERM-1 (Egg Contents Reference Material) and ten measurements of SRM 955c Level 2 (Trace Elements in Caprine Blood). The results of the mercury analysis of the SRMs are listed in Table 2.34.

Blanks

The instrumental blanks using an empty weigh boat for the analysis of mercury were measured concurrently with the samples. The reference and standard materials were blank corrected since the concentrations of the procedural blanks were detectable (average mercury concentration = 0.1 ng/g).

Table 2.34. Summary of total Hg results for SRM 1641e, QC04 ERM-1, and SRM 955c Level 2, used for the analysis of American alligator dosing solutions, egg compartments, and embryonic erythrocyte samples, respectively.

The certified values for the SRM 1641e (Mercury in Water) is $101.6 \pm 1.7 \mu\text{g/kg}$, for QC04 ERM-1 (Egg Contents Reference Material) is $101 \pm 3 \mu\text{g/kg}$ and for SRM 955c Level 2 (Toxic Metals in Caprine Blood) is $4.95 \pm 0.76 \mu\text{g/kg}$.

SRM 1641e Replicates	[Hg] ng/g	ERM-1 Replicates	[Hg] ng/g	955c Level 2 Replicates	[Hg] ng/g
SRM 1641e run 01	97.20	ERM-1 run 01	96.26	955c Level 2 run 01	5.07
SRM 1641e run 02	101.51	ERM-1 run 02	98.63	955c Level 2 run 02	5.11
SRM 1641e run 03	97.08	ERM-1 run 03	99.07	955c Level 2 run 03	5.22
SRM 1641e run 04	99.23	ERM-1 run 04	97.11	955c Level 2 run 04	5.18
SRM 1641e run 05	96.86	ERM-1 run 05	95.55	955c Level 2 run 05	5.11
SRM 1641e run 06	99.04	ERM-1 run 06	98.00	955c Level 2 run 06	5.46
SRM 1641e run 07	101.49	ERM-1 run 07	99.26	955c Level 2 run 07	5.04
SRM 1641e run 08	100.07	ERM-1 run 08	97.00	955c Level 2 run 08	5.35
SRM 1641e run 09	101.69	ERM-1 run 09	101.49	955c Level 2 run 09	5.04
		ERM-1 run 10	99.04	955c Level 2 run 10	5.15
		ERM-1 run 11	100.06		
		ERM-1 run 12	97.77		
		ERM-1 run 13	97.46		
		ERM-1 run 14	96.26		
		ERM-1 run 15	97.56		
		ERM-1 run 16	117.14		
		ERM-1 run 17	110.76		
		ERM-1 run 18	95.83		
		ERM-1 run 19	96.32		
		ERM-1 run 20	101.2		
		ERM-1 run 21	97.9		
		ERM-1 run 22	100.1		
		ERM-1 run 23	96.9		
		ERM-1 run 24	99.1		
		ERM-1 run 25	97.6		
		ERM-1 run 26	97.8		
		ERM-1 run 27	96.1		
		ERM-1 run 28	99.3		
		ERM-1 run 29	97.4		
		ERM-1 run 30	96.1		
		ERM-1 run 31	98.9		
		ERM-1 run 32	99.6		
		ERM-1 run 33	100.7		
		ERM-1 run 34	95.0		
		ERM-1 run 35	101.3		
		ERM-1 run 36	97.1		
		ERM-1 run 37	96.7		
Average	99.4	Average	98.9	Average	5.2
Standard Deviation	2.0	Standard Deviation	4.1	Standard Deviation	0.1
%RSD	2.0	%RSD	4.1	%RSD	2.7
U	1.6	U	1.4	U	0.1
Expanded U	0.016	Expanded U	0.015	Expanded U	0.020

2.8.3. *Results & Discussion*

Topical dosing

The eggs that were analyzed to determine how quickly the mercury solution transferred into the egg compartments (time points between 24 h and 14 days) do not show a dose specific pattern (Table 2.35, Figure 2.30). There are several missing time points in the data because the eggs corresponding to those time point were not viable, and did not develop an embryo so they were omitted from the data analysis. Since there are so few individual samples for each time point in this experiment, the mean and standard deviation cannot be calculated for the egg compartments mercury concentrations. The egg compartments from each of the eggs analyzed from those time points have inconsistent results; the albumin, CAM, and embryo mercury concentrations are varied; the yolk samples are more consistent, but no dose effects are seen in any group (Table 2.35, Figure 2.30). The eggshell samples appear to have an increasing trend with dose group, specifically the high dose groups (Table 2.35, Figure 2.30). Since the eggshell samples are the only egg compartment to have observable mercury changes with the dose groups, these results suggest that the topically applied mercury did not penetrate the eggshell within 14 days of dosing (Table 2.35, Figure 2.30).

Despite the initial results, the remaining eggs were developed to stage 27 and erythrocyte samples were collected from the embryos to determine if the dosed solution could to penetrate the eggshell, and be incorporated into the embryo by the end of development. The erythrocyte mercury concentration of the low and high dose group stage 27 embryos did not increase compared to the control group embryos ($n = 10$ each dose group; Table 2.35, Figure 2.30). The erythrocytes from the stage 27 embryos do not

show a dose specific pattern, but we observed clutch-effects related to mercury concentration, as all dose groups from each of the two clutches have very similar mercury concentrations (Table 2.35, Figure 2.30). The clutches average mercury concentration in the stage 27 erythrocytes across all three doses were $14.3 \text{ ng/g} \pm 2.2 \text{ ng/g}$, and $26.8 \text{ ng/g} \pm 3.8 \text{ ng/g}$, with very narrow standard deviations across the three large dosing concentrations. The clutch based difference are likely the result of different mercury concentration being transferred from the two different female alligators that each laid one of the clutches that was used in this study. The clutch based differences are still observed at the end of the study since the eggshells become calcified approximately 24 h after being laid, and may become impenetrable to exogenous materials, as the pores on the surface of the eggshell only facilitate gas exchange, which would have led to the dosing solution not penetrating the calcified eggshell at stage 12.

This experiment sought to mimic maternal transfer by dosing the eggs at the earliest developmental stage possible based on the time of collection. These results suggest that all mercury that the developing embryo is exposed to comes from maternal transfer, and that exogenous sources cannot easily penetrate the eggshell once it has been calcified. We did not anticipate that the dosed mercury would not penetrate the eggshell, as many previous studies in the Guillette lab have dosed alligator eggs using this method for a variety of chemicals (251, 302, 320). However, the previous studies did not measure how much of the dosed chemicals penetrated the eggshell. While the results of these previous studies suggest that the chemical did affect the dosed embryos differently than the controls, without direct measurement of the chemicals in each egg compartment, there is no certainty that the affects observed are the result of the dosed chemicals (320).

Injection dosing

All eggs dosed by injection did not survive more than a few days. Each egg that was opened to be sampled was rotten and full of undiscernible necrotic tissue. Only one egg had an identifiable embryo by the time stage 27 should have been reached. This embryo was at stage 21, suggesting that the embryo died shortly after injection at stage 19. We speculate that the humidity inside the incubator kept the glue from staying attached to the eggshell, and once removed, the eggs began to degrade. Based on these results, injection-style dosing is not a reliable option for alligator eggs.

Conclusions

Since consistently exposing the developing alligator embryos to exogenous mercury has proven difficult, these data show that American alligator eggs currently are not good models for *ex situ* embryonic mercury exposure (Figure 2.30, 2.31). Alligator eggs cannot be successfully dosed with mercury without making a hole in the eggshell, which causes other issues. However, these data do elucidate the strength of the calcareous eggshell and how effective it is in resisting exogenous substances from permeating through to the developing embryo. This protective effect lends insight into the resiliency of this species; and may be one of the factors that have allowed alligators to thrive in proximity to humans.

Alligators are routinely documented in highly contaminated areas and in close proximity to humans, while other large predators like the Florida panther (*Puma concolor coryi*) and Burmese python (*Python bivittatus*) that share their natural habitat, are seldom observed (43). The evolutionary adaptation of protective calcareous eggshells may be an advantage the alligator has, as it's habitat suffers anthropogenic change. Understanding

the effects of Hg exposure in this species will allow a more comprehensive analysis of their evolutionary adaptations, that make them different from other large predators, and potential sentinels for human dietary mercury exposure.

The data presented here did not serve the specific goal of this experiment, they lend insight into the evolutionary adaptations of reptilian breeding strategies, and life history characteristics. The few clutches of eggs that were collected during the 2014 nesting season and used for this experiment prevent population level conclusions from being made, as these results herein pertain only to the two clutches of eggs examined.

To further investigate the ability of the calcified eggshell to resist chemical dosing, several things can be tested. A comparison between freshly laid eggs that have not yet been calcified (less than 24 h post-lay) and calcified eggs (more than 24 h post-lay) to determine the transmission of dosed solutions through each type of eggshell would be useful for future dosing studies. Also, testing the efficacy of a variety of solvents to dissolve the mercuric salts, and their ability to permeate the eggshells would provide useful information. This comparison would enable the determination if: 1) transmission through the eggshell is possible before, and/or after calcification and, 2) if the solute used in the topical application makes a difference in the permeability of the dosing solution.

If the injection experiment is repeated in the future, a few improvements might increase the chance of success. A sealant that is not affected by the humid environment may prevent the eggs from degrading. The sphagnum moss could also be autoclaved to help remove some of the bacteria or other agents that may have initially caused the infection. In lieu of moss, a synthetic substitute could be used to further reduce the risk of infection.

Table 2.35. The total Hg results for all embryonic samples collected during experiment 2.7. Sample IDs are provided with each sample for reference, each ID denotes one egg. CAM denotes chorioallontic membrane. Timepoints that did not yield a sample that could be analyzed are omitted from this table.

Clutch	Dose	Timepoint	Albumin	Albumin [Hg] ng/g	Yolk	Yolk [Hg] ng/g	CAM	CAM [Hg] ng/g
Clutch 1	Control	48hr	Early Stg Alb WO15-01-46	1.2	Early Stg WO15-01-40	23.7	EarlyCAM WO15-01-40	0.5
		Stage 27						
		Stage 27						
		Stage 27						
	100 ng	24hr	Early Stg Alb WO15-01-34	0.9	Early Stg WO15-01-34	25.8	EarlyCAM WO15-01-34	11.0
		48hr	Early Stg Alb WO15-01-31	0.9	Early Stg WO15-01-31	22.3	EarlyCAM WO15-01-31	9.3
		7d	Early Stg Alb WO15-01-05	1.1	Early Stg WO15-01-05	31.1	EarlyCAM WO15-01-05	8.4
		14d	Early Stg Alb WO15-01-17	0.9	Early Stg WO15-01-17	27.6	EarlyCAM WO15-01-17	3.5
		Stage 27						
		Stage 27						
		Stage 27						
		Stage 27						
	360 ng	24hr	Early Stg Alb WO15-01-32	0.9	Early Stg WO15-01-32	24.0	EarlyCAM WO15-01-32	3.9
		48hr	Early Stg Alb WO15-01-02	3.3	Early Stg WO15-01-02	21.9	EarlyCAM WO15-01-02	14.3
		7d	Early Stg Alb WO15-01-30	0.7	Early Stg WO15-01-30	25.8	EarlyCAM WO15-01-30	7.2
		Stage 27						
		Stage 27						
		Stage 27						
		Stage 27						
Clutch 9	Control	24hr	Early Stg Alb WO15-09-25	0.8	Early Stg WO15-09-25	28.0	EarlyCAM WO15-09-25	0.4
		48hr	Early Stg Alb WO15-09-02	1.0	Early Stg WO15-09-02	25.3	EarlyCAM WO15-09-02	19.0
		7d	Early Stg Alb WO15-09-12	0.7	Early Stg WO15-09-12	13.0	EarlyCAM WO15-09-12	21.8
		4d	Early Stg Alb WO15-09-07	0.6	Early Stg WO15-09-07	25.3	EarlyCAM WO15-09-07	7.0
		Stage 27						
		Stage 27						
	100 ng	24hr	Early Stg Alb WO15-09-26	0.6	Early Stg WO15-09-26	25.4	EarlyCAM WO15-09-26	19.9
		7d	Early Stg Alb WO15-09-21	0.9	Early Stg WO15-09-21	25.4	EarlyCAM WO15-09-21	18.9
		14d	Early Stg Alb WO15-09-24	0.3	Early Stg WO15-09-24	24.3	EarlyCAM WO15-09-24	15.5
		Stage 27						
		Stage 27						
	360 ng	48hr	Early Stg Alb WO15-09-03	7.3	Early Stg WO15-09-03	25.7	EarlyCAM WO15-09-03	24.0
		7d	Early Stg Alb WO15-09-20	6.1	Early Stg WO15-09-20	23.2	EarlyCAM WO15-09-20	28.4
		14d	Early Stg Alb WO15-09-27	0.8	Early Stg WO15-09-27	21.5	EarlyCAM WO15-09-27	6.5
		Stage 27						
		Stage 27						

Eggshell	Eggshell [Hg] ng/g	Embryo	Embryo [Hg] ng/g	Stage 27 RBCs	Stg 27 RBCs [Hg] ng/g	Stg 27 RBCs Average [Hg] ng/g
Eggshell WO15-01-40	5.9	Embryo WO15-01-40	6.8			
Eggshell WO15-01-43	5.5			WO15-01-43 RBC	16.01	14.9
Eggshell WO15-01-19	5.8			WO15-01-19 RBC	15.74	
Eggshell WO15-01-36	5.8			WO15-01-36 RBC	12.82	
Eggshell WO15-01-34	28.3	Embryo WO15-01-34	6.7			
Eggshell WO15-01-31	9.9	Embryo WO15-01-31	7.1			
Eggshell WO15-01-05	13.6	Embryo WO15-01-05	6.9			
Eggshell WO15-01-17	7.6	Embryo WO15-01-17	10.0			
Eggshell WO15-01-21	7.6			WO15-01-21 RBC	17.10	14.0
Eggshell WO15-01-41	7.1			WO15-01-41 RBC	13.10	
Eggshell WO15-01-38	8.9			WO15-01-38 RBC	12.46	
Eggshell WO15-01-06	7.3			WO15-01-06 RBC	14.79	
Eggshell WO15-01-01	14.2			WO15-01-01 RBC	12.38	
Eggshell WO15-01-32	38.8	Embryo WO15-01-32	7.1			
Eggshell WO15-01-02	41.4	Embryo WO15-01-02	6.4			
Eggshell WO15-01-30	20.9	Embryo WO15-01-30	9.6			
Eggshell WO15-01-20	12.6			WO15-01-20 RBC	11.20	14.2
Eggshell WO15-01-11	16.2			WO15-01-11 RBC	13.73	
Eggshell WO15-01-39	18.2			WO15-01-39 RBC	12.38	
Eggshell WO15-01-23	15.4			WO15-01-23 RBC	15.01	
Eggshell WO15-01-14	25.2			WO15-01-14 RBC	18.52	
Eggshell WO15-09-25	8.0	Embryo WO15-09-25	4.4			
Eggshell WO15-09-02	6.9	Embryo WO15-09-02	6.3			
Eggshell WO15-09-12	6.5	Embryo WO15-09-12	7.3			
Eggshell WO15-09-07	7.5	Embryo WO15-09-07	14.5			
Eggshell WO15-09-31	5.0			WO15-09-31 RBC	22.81	25.2
Eggshell WO15-09-13	5.0			WO15-09-13 RBC	22.83	
Eggshell WO15-09-18	4.9			WO15-09-18 RBC	26.38	
Eggshell WO15-09-24	14.9			WO15-09-24 RBC	28.91	
Eggshell WO15-09-26	13.7	Embryo WO15-09-26	4.6			
Eggshell WO15-09-21	9.3	Embryo WO15-09-21	6.9			
Eggshell WO15-09-24	14.9	Embryo WO15-09-24	11.4			
Eggshell WO15-09-14	6.9			WO15-09-14 RBC	22.54	27.51
Eggshell WO15-09-09	8.3			WO15-09-09 RBC	32.48	
Eggshell WO15-09-03	75.1	Embryo WO15-09-03	4.5			
Eggshell WO15-09-20	40.0	Embryo WO15-09-20	10.4			
Eggshell WO15-09-27	24.5	Embryo WO15-09-27	11.9			
Eggshell WO15-09-08	22.9			WO15-09-08 RBC	30.85	29.25
Eggshell WO15-09-22	23.2			WO15-09-22 RBC	27.66	

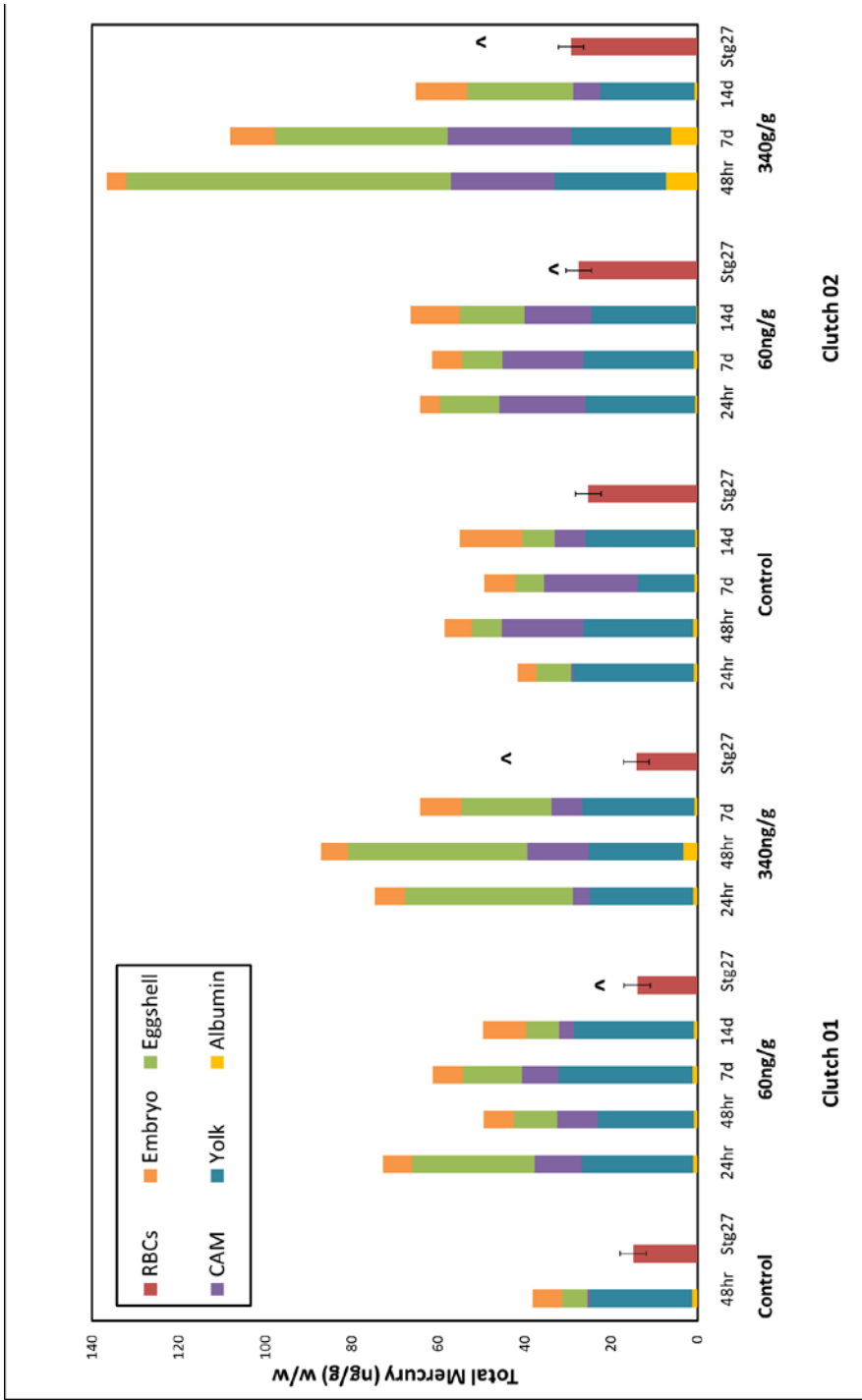


Figure 2.30. The compartmental analysis of total Hg in American alligator eggs after dosing via the painting method. Carets denote the expected Hg concentration in stage 27 embryos.



Figure 2.31. The graphical abstract of the experiments and results of Specific Aim 1, experiment 6 detailed in this section.

2.9. Chapter Discussion

The results of the experiments within this chapter suggest that the adult American alligator makes an excellent sentinel species for dietary mercury exposure for the human population (Figure 2.32). Alligators are subject to the same mercury concentrations as the human population, have the same biodistribution of mercury in their tissues as humans, are able to be sampled throughout the year, demonstrate maternal transfer of mercury similar to humans, and can provide a developmental model for endogenous, but not exogenous, mercury exposures.

This was established through the assessment that examined the American alligator for its utility as a sentinel for dietary mercury exposure, by determining if alligators experience the same exposure as the human population. This assessment examined numerous locations in Florida and South Carolina for trace elements, and demonstrated that mercury is the trace element in highest concentration in this region, and that many types of human diets can be mimicked using alligators from these different sites. The bio-distribution of the trace elements within the alligator was also determined; the tissue distribution of mercury, and several other trace elements, in the alligator is similar to humans and other species. This experiment also determined that a routine blood sample can be used to estimate the concentration of four trace elements, including mercury, found in the muscle tissue consumed by humans. This information makes alligator blood samples useful for human consumption biomonitoring efforts, since it is predictive of body mercury burden. Understanding the bio-distribution of mercury in a proposed sentinel species is important, as the adverse outcomes associated with the exposure will

likely be related to the bio-distribution pattern. The bio-distribution will elucidate the target organ that accumulate the highest mercury concentrations, which is where adverse outcomes may originate.

To further assess the alligator as a sentinel, blood samples over seven consecutive years and in each of the four seasons were assessed for mercury concentration. This analysis demonstrated that the mercury concentration measured in alligator blood may change according to their behaviors, but not enough to inhibit their utility as a sentinel species. The slightly higher mercury concentrations observed in the winter suggest that while an alligator is brumating, they may have higher mercury concentrations because they are fasting, and metabolizing stored mercury back into their blood stream. Fortunately, while alligators are brumating they are very difficult to locate for capture and sampling, so this variable does not detract from their utility as a sentinel species. The seasonal analysis did reveal that there are highly variable concentrations of mercury in adult alligators in the spring, when mating and nesting are occurring. This could be due to the proportion of the population that are nesting females, that continue to fast later into the season than males and non-nesting females (253). Body condition was also assessed to determine how mercury concentrations change with increasing or decreasing BMI, which is relevant to human health. We observed that mercury concentration increases with decreasing BMI, but the change in body condition in alligators is of an unknown etiology. However, since body condition changes drastically in humans during gestation, and the alligator comparisons can be used to provide information regarding the changing mercury concentrations when humans undergo drastic body changes. While body

condition is not drastically altered during alligator breeding activities, it relates to maternal transfer of contaminants during gestation. We find that mercury is present in alligator eggs from low mercury sites, and significant relationship between the nesting female blood mercury concentration and the mercury concentration measured in the egg yolk was observed. While this does not explain the springtime variation seen in blood samples, it suggests that females transfer mercury to their developing eggs.

These data highlight the Everglades as a region of concern for mercury contamination, particularly since the eggs in that region are likely receiving a high dose of mercury early in development. The alligators in the Everglades would make exceptional sentinels for mercury exposure, as they have been observed to accumulate high concentrations in all measured tissues. Using eggs from the Everglades to study the developmental effects of such high concentrations of mercury would prove translational to human populations thriving on subsistence style diets. However, egg collection in the Everglades is prohibited. In effort to circumvent this, and determine if high mercury alligator eggs are useful developmental models, eggs were dosed with mercury, topically and via injection. None of the dosed mercury was observed to penetrate the eggshell, and when dosed by injection, the eggs did not survive. These data suggest that while the alligator is a worthy sentinel species for dietary mercury exposure, using it for developmental studies related to mercury currently is not ideal.

While the lack of differing mercury concentrations in each nest, despite dosing efforts, removes the developmental time point from use as a sentinel (unless eggs can be collected directly from high mercury sites), we are confident in the data presented here

due to the rigorous analytical quality of the analysis, and the large sample sizes, both of which are uncommon in many environmental studies. Conducting these analyses according to the National Institute of Standards and Technology guidelines ensures that the results presented in this chapter are consistent and reliable. The large sample sizes for each of these experiments which most studies using free-ranging animals do not have is a testament to the large effort put forth by the Guillette laboratory and its partners at the Florida Fish and Wildlife Conservation Commission (FFWCC) and Integrated Mission Support Systems (IMSS) at MINWR and NASA's Kennedy Space Center. Since season-specific sampling occurs in a short window of a few days, large teams were deployed at multiple locations to conduct sampling efforts in an IACUC and ASIH approved manner, simultaneously. The large number of samples that came from these collection efforts allowed statistical analyses to be conducted, and definitive statements to be made regarding many of the experiments in this chapter.

The experimental design of these studies sought to answer a single question related to the assessment of the American alligator as a sentinel species for mercury exposure. While the large number of samples, diverse locations and variety of variable included in the data sets make them attractive to conduct additional analyses, but samples selected were only intended for the specific experiments conducted, and other analyses can include additional confounding factors that were not controlled for in the initial planning of these experiments. The experiments in this chapter could be improved if the same alligators could be resampled for repeated analysis, which have remove some of the uncertainty of the seasonal mercury assessment and the recaptured BMI study, both

conducted at MINWR, FL. There was also an issue with the storage conditions of some of the samples, which lead to the integrity of many samples being too questionable for use, which is easily improved. Another limitation is the unanticipated results of the egg dosing experiment. The topical and injection style dosed eggs were only able to show that these methods of dosing with mercury are not appropriate for alligator eggs. We can confidently state that all the mercury within an alligator egg comes from maternal transfer, but we must concede that this biological time point is not appropriate for mercury exposure studies based on our data. There is also a significant limitation in the information we can gain from the maternal transfer study in terms of how nesting affects seasonal mercury concentration in an alligator population as a whole. Our study sampled nesting females while they were at their nest, and not before or after nesting. Additional samples throughout the season from the same females would provide the necessary information regarding maternal transfer and off-loading of mercury to the eggs that this data suggests occurs. Without the additional time points the conclusions we can draw in relation to seasonal mercury variation in the population are limited.

To the best of our knowledge, this assessment of a species prior to its use as a sentinel is the first of its kind. Conducting a critical assessment of a species of interest for a particular issue can provide insight as well as guide researchers in the right direction with their experiments. While the alligator has been used extensively as a developmental model for organic contaminant exposure, we have shown that the same methods are not feasible for mercury exposure. Existing sentinel species should be evaluated for new types of exposure, as the same sentinel can provide very different information to the

researcher depending on the type of exposure under investigation.

We propose that the experiments in this chapter be used to devise a “sentinel species assessment framework” to guide researchers through determining the most salient exposure for each species under investigation. A framework such as this would provide detailed information to researchers, and the outcome would allow improvements to ecological monitoring based on the specific exposure. This framework would also allow researchers to understand the greater picture of environmental health in the context of the “one health” paradigm, as a solid assessment would explicitly make the links between the sentinel and humans, as well as allow the ecosystem health to be evaluated using the improved monitoring efforts.

**Chapter Three: Investigating the relationship between mercury exposure
& an epigenetic modification**

Specific Aim 2, Experiment 1 has been published in the following peer-reviewed publication.

Nilsen, F. M.; Parrott, B. B.; Bowden, J. A.; Kassim, B. L.; Somerville, S. E.; Bryan, T. A.; Bryan, C. E.; Lange, T. R.; Delaney, J. P.; Brunell, A. M.; Long, S. E.; Guillette Jr, L. J., Global DNA methylation loss associated with mercury contamination and aging in the American alligator (*Alligator mississippiensis*). *Science of the Total Environment* **2016**, 545–546, 389-397.

3.1. Determination of DNA methylation changes in response to chronic & acute mercury exposure scenarios in American alligators & diamondback terrapins

Mercury is a persistent problem among mid and upper level predators due to its bioaccumulation potential. High mercury concentrations are known to cause adverse effects, including impaired reproductive function and neurodegenerative disorders (113, 126). However, in many wild populations, high mercury concentrations are not always linked to an observable effect of exposure.

Once mercury is ingested, it binds to intracellular thiol groups and creates oxidative stress (152). Approximately 90% of the available thiol groups in cells are derived from the antioxidant glutathione (GSH) (199). However, binding exogenous mercury is not the only function of GSH. The endogenous function of GSH is to remove reactive oxygen species (ROS) that accumulate due to normal cellular function and mitochondrial respiration. GSH also removes any toxic xenobiotic that enters the cell, in this case mercury (208, 209). Under normal circumstances, GSH binds to a ROS or mercury, is translocated out of the cell, enters the blood plasma, and is removed by the excretion organs (210). GSH is used and recycled by glutathione S-transferase (GST) once the cell is detoxified, so there is a continual supply of the protective antioxidant within the cell (210).

GSH metabolism is critical for the detoxification/toxic response of cells to metals, as one mercury molecule can irreversibly bind two GSH molecules. Irreversible bindings does not allow GSH to be recycled, which effectively stops the detoxification process at the first step, when the Hg-GSH complex is translocated out of the cell (199). In dosed

animals, mercury has been shown to inhibit the detoxification enzyme, GST, which is critical to the recycling of GSH, supporting the idea that mercury exposure lowers GSH availability (199, 211, 244).

The reduced abundance of GSH in the cells leads to an increase in oxidative stress, and removing ROS is the endogenous function of GSH (321, 322). Without GSH the ROS build up, and cause many forms of oxidative damage. The oxidative damage to the DNA strand occurs particularly through the hydroxyl ions that attach to guanine bases (Figure 3.1). The hydroxyl ions change the shape of the DNA strand and affect methylation on cytosine residues, forming hydroxyl “lesions” (216-218). The addition of these hydroxyl lesions can cause deletions, strand breakages, chromosomal rearrangements, and interfere with the potential of DNA to function as a substrate for the DNA methyl transferases (DNMTs), resulting in altered DNA methylation (216).

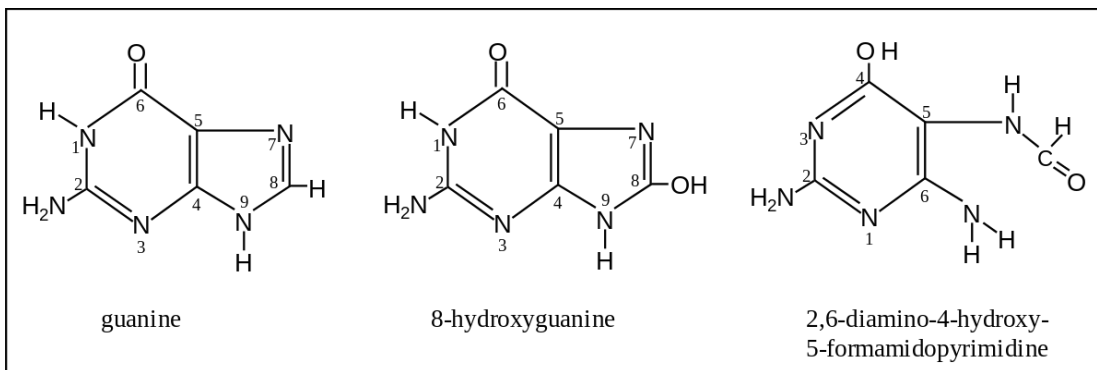


Figure 3.1. The oxidation of DNA with hydroxyl adducts to the guanine base residue.

DNA methylation—consisting of the covalent addition of a methyl-group to the 5' carbon end of cytosine—regulates gene expression, promotes chromosome stability, and silences the transcription of transposons (3, 323, 324). Alterations in DNA methylation can occur at specific loci or more broadly across the genome.

Studies in humans and other lab models have demonstrated the highly dynamic nature of DNA methylation throughout an organism's lifetime. Shortly after fertilization, the maternal and paternal pronuclei undergo genome-wide demethylation and begin to acquire tissue- and cell-type specific methylomes during development and differentiation (325, 326). Later in life, variation in the DNA methylome becomes tightly associated with age, with global measures of genomic DNA methylation consistently found to decline as a function of increasing age (327-330). However, the drivers of these age-associated changes in DNA methylation remain unclear. In humans, altered levels of global DNA methylation have been associated with lifestyle and environmental factors such as diet, smoking, alcohol consumption, pollution, and exposure to environmental contaminants (331-335). These studies, however, have not consistently analyzed the same section of DNA, or DNA from the same source tissue, which makes comparisons difficult (331-333). Many differences can arise between tissues due to the tissue-specific methylomes that affect gene regulation, such as those associated with reproductive senescence (331). Study specific differences also arise from different methods of analysis. Some studies use promoter specific methods, while some use enzyme immunoassay methods to directly measure methylation based on fluorescence of a probe

on a small section of DNA, and others use direct measurement with analytical techniques to assess the entire genome (99, 333, 336).

Very few studies to date have examined how mercury exposure might affect the epigenome, especially in free-living animals (99, 101, 337). Previous targeted genomic studies have provided detailed information about a specific region of the genome's response to mercury exposure, but frequently leave large areas of the genome uninvestigated (106, 107, 338). To determine the total effects of an exposure on an organism, a non-targeted method is preferred, and since genome wide sequencing studies are prohibitively expensive compared to the wide variety of global epigenetic analyses available, the epigenome is often analyzed for changes related to contaminant exposures. In one study, indirect measures of global DNA methylation trended negative with increasing mercury concentrations in brain tissues from polar bears, but a clear correlation was not observed (99). Studies using captive animals have shown a relationship between DNA hypomethylation in brain tissue and environmentally relevant mercury concentrations for mink, but not for fish or chickens (101). There is not a clear consensus regarding the relationship between DNA methylation and mercury exposure. Although, it appears clearer in longer-lived mammals, separating the age related effects on the epigenome from those resulting solely from mercury exposure remains difficult (99, 101).

The American alligator (*Alligator mississippiensis*) and diamondback terrapin (*Malaclemys terrapin*) have characteristics that make them ideal models to study the long-term effects of chronic mercury exposure on the epigenome. These predators are

long-lived (≈ 80 and 40 years, respectively), consume animals known to accumulate mercury, and display high site fidelity in mercury contaminated areas, such as the Florida Everglades (83, 84, 176, 178).

Here, we use three experiments to investigate this relationship. In the first experiment, the relationship between global DNA methylation and mercury concentration is examined using blood samples of adult and sub-adult alligators from six sites in Florida. This investigation will enable the determination of a relationship between chronic mercury exposure and DNA methylation changes. In the second experiment, the effect of a high quality diet on DNA methylation is examined, as this epigenetic modification is reversible, and could be used to develop preventative and therapeutic strategies to alleviate the effects of mercury exposure (339). The third experiment examines the relationship between short-term dietary mercury exposure and DNA methylation from a laboratory dietary dosing study mimicking Everglades' exposure levels, using diamondback terrapins. This laboratory study will allow the determination of individual epigenomes changes over time with increased mercury exposure and a standardized diet. All experiments will provide new information regarding the relationship between mercury exposure and DNA methylation (Figure 3.2).

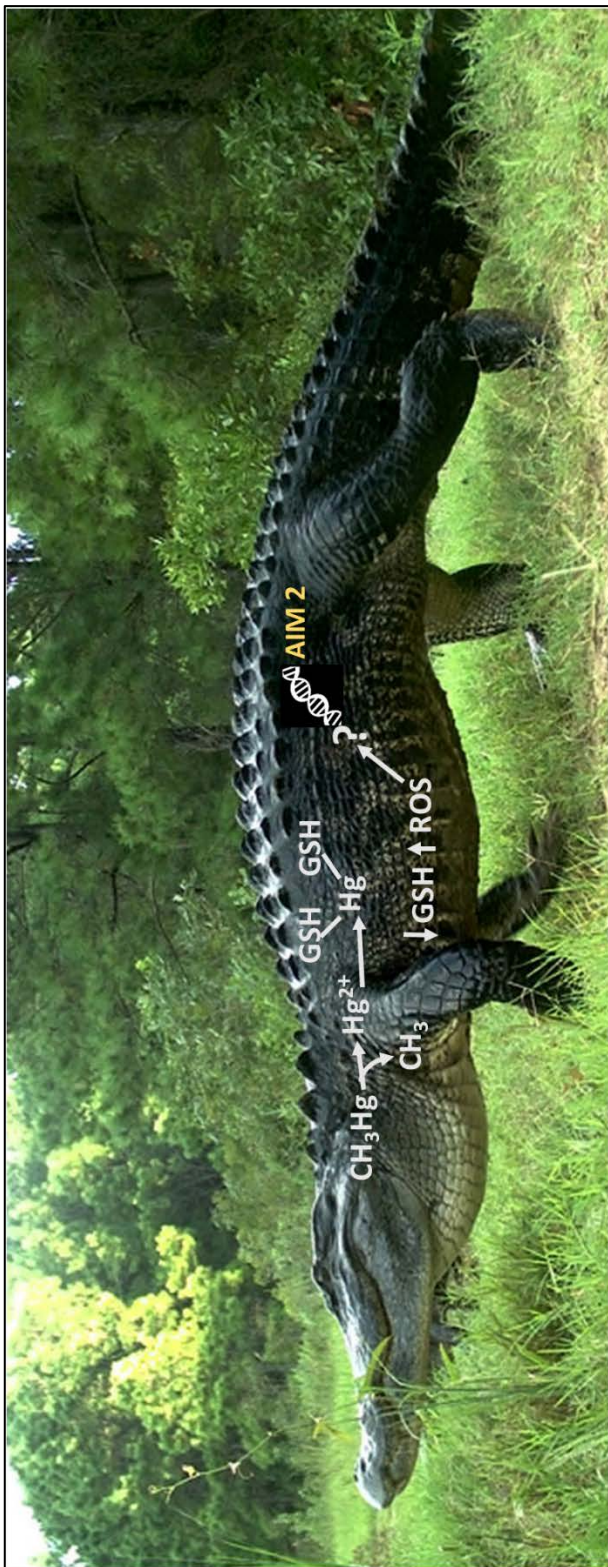


Figure 3.2. The graphical abstract of the experiments of Specific Aims 2 detailed in this chapter.

3.2. General methods

3.2.1. DNA isolation

DNA was extracted using the Promega total DNA Isolation protocol for erythrocytes (Madison, WI). DNA concentration and purity were assessed by measuring optical density using a Nano Drop UV-Vis Spectrophotometer at wavelengths of 260 nm and 280 nm (Thermo, Wilmington, DE). The wavelength at 260 nm measures the optical density of nucleic acids in the sample, and the wavelength at 280 nm measures the optical density for the protein content of the sample. The ratio of these two measurements, 260:280, is used to determine DNA quality, with a ratio of ~1.8 being considered “pure” DNA. A ratio lower than 1.8 can be indicative of low nucleic acid concentration or extraction solvent carry over. A ratio higher than 1.8 can indicate that there is residual RNA from the extraction in the sample (340).

3.2.2. Preparation of deoxyribonucleoside solutions for calibration

To create the deoxyribonucleoside standards, 2'-deoxyguanosine monohydrate (dG, Sigma Aldrich, St. Louis, MO) and 5-methyl-2'-deoxycytidine (5mdC, Santa Cruz Biotechnology Inc., Dallas, TX) were used (Table 3.1). Initial stock solutions of each deoxyribonucleoside standard were made by gravimetric addition of ≈ 10 mg neat standard into 10 mL of Milli-Q water to produce ≈ 1000 ng standard/mg water solutions (Table 3.2). To enhance solubility, sodium hydroxide pellets (402.24 mg, Sigma Aldrich, 97 % ACS reagent) were gravimetrically added to the dG stock solution. Using the initial stock solutions, 20 ng standard/mg water solutions were prepared by gravimetric addition (Table 3.3). The final calibration solutions included the gravimetric addition of 200 mg of

the 20 ng/mg dG solution and incrementally increasing amounts of the 20 ng/mg 5mdC solution to produce twelve serial dilutions from 0.1 % to 10 % solutions of 5mdC to dG (Tables 3.4 and 3.5).

Table 3.1. The details for the deoxyribonucleoside standards used in the LC-MS/MS DNA methylation analysis.

Nucleoside	Abbreviation	Purity (%)	MW	Manuf.	Product #	Lot #
2'-deoxycytidine	dC	≥ 99	227.22	Sigma	D3897	060M5158V
2'-deoxyguanosine monohydrate	dG	99 - 100	285.26	Sigma	D7145	051M1268V
Thymidine	T	≥ 99	242.23	Sigma	T9250	041M0151V
2'-deoxyadenosine monohydrate	dA	≥ 99	269.26	Sigma	D7400	099K1642V
5-methyl-2'-deoxycytidine	5mdC	≥ 99	241.24	Santa Cruz	SC-278256	I2111
5-hydroxymethyl-2'-deoxycytidine	5hmdC	≥ 99	257.24	Berry	PY7588	DT205-5

MW denotes molecular weight. Manuf. denotes manufacturer. Sigma = Sigma Aldrich; Santa Cruz = Santa Cruz Biotechnology, Inc.; Berry = Berry and Associates. The masses in bold indicate that the mass listed in the monohydrate mass.

Table 3.2. Initial stock solutions for each deoxyribonucleoside standard for the LC-MS/MS DNA methylation analysis.

Nucleoside	Empty Tube (g)	Tared Solid (mg)	Tube + 10 mL Water (g)	Add for Solubility	Total Wt. (g)	Final Concentration mg/g	ng/mg
dC	6.72613	10.18000	16.56151	No	16.56151	1.03504	1035.03881
dG	14.04482	9.36000	24.01391	NaOH (1M)*	24.01391	0.93890	938.90200
T	6.78418	10.90000	16.73188	No	16.73188	1.09573	1095.73067
dA	6.78622	11.10000	16.74986	No	16.74986	1.11405	1114.05100
5mdC	6.78634	9.51000	16.77853	No	16.77853	0.95174	951.74331
5hmdC	6.77020	7.36000	16.69289	No	16.69289	0.74173	741.73435

* Indicates that 402.24 mg of NaOH pellets were added to the vial (included in total weight measurement). The stock solutions were prepared between 7/23/13 and 7/24/13. Nucleosides are defined in Table 1.

Table 3.3. Preparation of 20 ng standard/mg stock solutions from initial stock solutions for each deoxyribonucleoside standard for the LC-MS/MS DNA methylation analysis.

Nucleoside	Stock Solution ng/mg	Empty vial (g)	Tared Stock Added (mg)	Total Weight (g)	Weight of Water (g)	Weight of Water (mg)	ng Added To Each Vial	20 ng/mg Stock
dC	1035.03881	6.76890	192.96000	16.72207	9.95317	9953.17000	199721.08856	20.06608
dG	938.90215	6.77562	220.82000	16.71161	9.93599	9935.99000	207328.37200	20.86640
T	1095.73067	6.78385	182.78000	16.69159	9.90774	9907.74000	200277.65212	20.21426
dA	1114.05069	6.78717	178.30000	16.68531	9.89814	9898.14000	198635.23772	20.06794
5mdC	951.74331	6.73810	209.68000	16.67178	9.93368	9933.68000	199561.53756	20.08939
5hmdC	741.73435	6.72594	270.45000	16.65316	9.92722	9927.22000	200602.05448	20.20727
dC**	1035.03881	63.36626	2885.87000	213.09139	149.72513	149725.13000	2986987.44736	19.94981

** Indicates the use of the “larger volume” 150 mL dC stock solution. ng/μL = ng/mg. The 20 ng/mg solutions were prepared between 9/23/13 and 9/24/13. Nucleosides are defined in Table 1.

Table 3.4. Preparation of final calibration solutions (Cal) (1 – 13) for LC-MS/MS DNA methylation analysis.

	Cal 1	Cal 2	Cal 3	Cal 4	Cal 5	Cal 6	Cal 7	Cal 8	Cal 9	Cal 10	Cal 11	Cal 12	Cal 13
percent (5hmdC/total dC)	0	0.005	0.01	0.025	0.05	0.075	0.1	0.2	0.3	0.4	0.5	1	3
percent (5mdC/total dC)	0	0.1	0.5	1	1.5	2	2.5	3	4	5	6	7	10
Empty vial, g	1.087	1.082	1.086	1.079	1.086	1.081	1.086	1.081	1.078	1.80	1.080	1.083	1.089
dA, 300 µL added (g)	0.296	0.294	0.297	0.289	0.293	0.294	0.294	0.298	0.294	0.289	0.295	0.295	0.294
T, 300 µL added (g)	0.295	0.296	0.296	0.295	0.296	0.295	0.295	0.296	0.295	0.296	0.295	0.293	0.296
dG, 200 µL added (g)	0.200	0.198	0.197	0.198	0.197	0.198	0.198	0.199	0.197	0.197	0.198	0.199	0.197
dC Mix, 200 µL added (g)	0.200	0.199	0.198	0.199	0.198	0.199	0.199	0.199	0.199	0.199	0.199	0.199	0.198
total weight of solvent (g)	2.078	2.071	2.078	2.061	2.073	2.069	2.073	2.073	2.063	2.062	2.066	2.071	2.078
dA (mg added to vial)	296.1	294.6	297.7	289.23	293.95	294.09	294.39	298.46	294.02	289.43	294.62	295.33	294.9
T (mg added to vial)	295.8	296.6	296.9	295.49	296.28	295.87	295.48	295.52	295.08	296.14	294.83	293.31	296.6
dG (mg added to vial)	199.6	198.4	197.7	198.34	197.84	198.32	197.94	198.73	196.69	197.04	197.77	199.96	197.5
dC Mix (mg added to vial)	199.9	199.0	198.7	199.10	198.87	198.85	198.55	199.31	198.71	199.50	198.83	198.93	198.99

Each calibration solution (levels 1 -13) had a total of 20 µg of total deoxyribonucleoside. dC mix constituted dC + 5mdC + 5hmdC. The composition of each dC mix used for each calibration level is shown in Table 7 (solutions A – M). Nucleosides are defined in Table 1.

Table 3.5. The final concentrations of each deoxyribonucleoside standard in the final calibration solutions (1 – 13) for the LC-MS/MS DNA methylation analysis.

	Cal 1	Cal 2	Cal 3	Cal 4	Cal 5	Cal 6	Cal 7	Cal 8	Cal 9	Cal 10	Cal 11	Cal 12	Cal 13
percent (5hmdC/total dC)	0	0.005	0.01	0.025	0.05	0.075	0.1	0.2	0.3	0.4	0.5	1	3
percent (5mdC/total dC)	0	0.1	0.5	1	1.5	2	2.5	3	4	5	6	7	10
dA (µg in final mix)	5.943	5.913	5.974	5.804	5.898	5.901	5.907	5.989	5.900	5.808	5.912	5.926	5.918
T (µg in final mix)	5.978	5.996	6.002	5.973	5.989	5.980	5.972	5.973	5.964	5.986	5.959	5.929	5.994
dG (µg in final mix)	4.164	4.141	4.126	4.138	4.128	4.138	4.130	4.147	4.104	4.112	4.127	4.172	4.121
dC Mix													
dC (µg in final mix)	3.989	3.967	3.945	3.932	3.906	3.885	3.860	3.850	3.794	3.768	3.710	3.652	3.455
5mdC (ng in final mix)	0	3.733	19.42	39.50	59.82	79.92	97.75	119.38	159.66	197.94	238.45	279.11	400.19
5hmdC (ng in final mix)	0	0.177	0.314	0.946	1.941	2.925	3.965	7.829	11.793	15.794	19.782	39.970	118.99
Total weight, mg	991.4	988.8	991.1	982.1	986.9	987.1	986.3	992.02	984.50	982.11	986.05	987.53	987.96
dA (ng/mg)	5.994	5.979	6.028	5.910	5.977	5.979	5.989	6.0376	5.9932	5.9140	5.9960	6.0015	5.9909
T (ng/mg)	6.031	6.064	6.056	6.082	6.068	6.059	6.056	6.0217	6.0587	6.0953	6.0440	6.0039	6.0675
dG (ng/mg)	4.200	4.188	4.163	4.214	4.183	4.192	4.187	4.1801	4.1688	4.1864	4.1851	4.2251	4.1709
dC Mix													
dC (ng/mg)	4.023	4.011	3.981	4.003	3.958	3.935	3.913	3.8808	3.8538	3.8364	3.7627	3.6981	3.4970
5mdC (ng/mg)	0	0.003	0.020	0.040	0.061	0.081	0.099	0.1203	0.1621	0.2015	0.2418	0.2826	0.4050
5hmdC (ng/mg)	0	0.001	0.001	0.001	0.002	0.003	0.004	0.0078	0.0119	0.0160	0.0200	0.0404	0.1204

3.2.3. Hydrolysis of final calibration solutions & experimental DNA extracts

The calibration solutions were hydrolyzed along with experimental DNA extracts for accurate determination of methylation. The calibration solutions contained specific amounts of nucleosides that were used to make a calibration line (Table 3.5). By hydrolyzing the calibration solutions, the samples will be measured against a calibration line with known amounts of nucleosides for comparison that also went through identical processing to the samples. This ensures that if any nucleosides are lost or modified because of the hydrolysis, the calibration line will reflect this, and the samples will not be measured against a calibration line containing a set of nucleosides that has not been subject to the same potential degradation.

To hydrolyze genomic DNA into individual nucleosides, the method described by Quinlivan and Gregory (2008) was used and modified as follows (341). The genomic DNA extracted from whole blood (18 μL at [20 $\mu\text{g}/\mu\text{L}$]) was added to hydrolysis buffer in a 1:1 ratio (final volume = 36 μL). The hydrolysis buffer was made as previously reported by Quinlivan and Gregory (2008), with the Tris-HCl Buffer at a pH = 7.75 (341). Both the genomic DNA samples and the final calibration curve solutions (18 μL of each final calibration solution and 18 μL of hydrolysis buffer) were incubated at 37 °C for 11 h in an Innova 4200 Incubator (New Brunswick Scientific, Edison, NJ). To confirm hydrolysis, aliquots of five samples were assessed with their non-hydrolyzed counterparts via 1% agarose gel electrophoresis (Figure 3.3). Post-hydrolysis, 30 μL of each hydrolyzed sample/calibration solution, and 40 μL of Milli-Q water were added to auto sampler vials, for a final volume of 70 μL . The calculated amounts (ng) in each

calibration vial were used for the gravimetrically derived weight ratios were calculated for 5mdC to dG. The weight ratios (x-axis) were used to construct calibration lines for the % 5mdC to dG (Table 3.6).

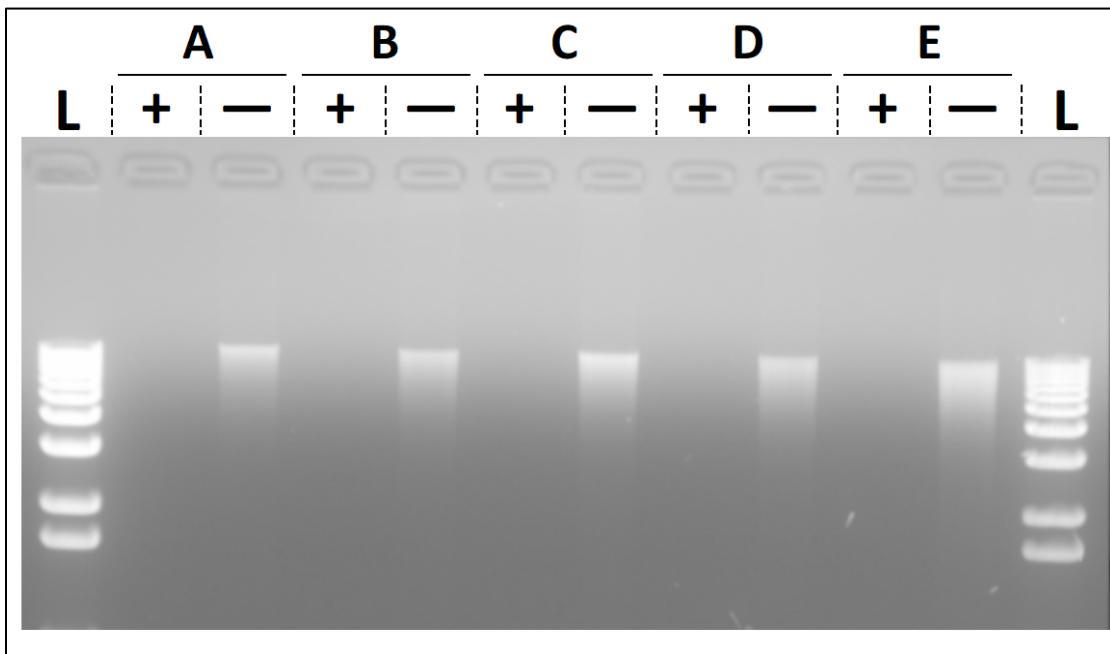


Figure 3.3. Confirmation of Hydrolysis Reaction. 15 μ L of five representative genomic DNA samples (labeled A-E) were tested for hydrolysis by agarose gel electrophoresis. Mock reactions including incubations in Tris only (indicated by [-]) show high molecular weight genomic DNA is still present after 11 h of incubation at 37°C, whereas reactions containing the full hydrolysis buffer (indicated by [+]) lack any detectable high molecular weight DNA. Size standards (L; 1Kb plus DNA Ladder, Life Technologies) include DNA bands ranging from 12,000 base pairs (top band) to 1,650 base pairs (bottom band). DNA smears are likely a result of the 11hr incubation.

Table 3.6. Preparation of hydrolyzed calibration solutions for the LC-MS/MS DNA methylation analysis.

	Cal 1	Cal 2	Cal 3	Cal 4	Cal 5	Cal 6	Cal 7
percent (5hmdC/total dC)	0	0.005	0.01	0.025	0.05	0.075	0.1
percent (5mdC/total dC)	0	0.1	0.5	1	1.5	2	2.5
Empty Hydrolysis Tube (g)	0.51628	0.52237	0.51790	0.52019	0.51687	0.51806	0.52035
18 µL Std Added Wt (g)	0.53445	0.54049	0.53607	0.53824	0.53490	0.53630	0.53831
18 µL Hyd Buff - Total Vol (g)	0.55247	0.55864	0.55401	0.55647	0.55332	0.55419	0.55636
Total Weight Std Added (g)	0.01817	0.01812	0.01817	0.01805	0.01803	0.01824	0.01796
Total Weight Std Added (mg)	18.17000	18.12000	18.17000	18.05000	18.03000	18.24000	17.96000
Total Solvent Volume (g)	0.03619	0.03627	0.03611	0.03628	0.03645	0.03613	0.03601
Total Solvent Volume (mg)	36.19000	36.27000	36.11000	36.28000	36.45000	36.13000	36.01000
dA, ng in Hyd Samples	108.91624	108.35529	109.52534	106.66968	107.76585	109.05195	107.57135
T, ng in Hyd Samples	109.57704	109.88621	110.03489	109.77303	109.41206	110.51197	108.75691
dG, ng in Hyd Samples	76.31571	75.89362	75.64412	76.05939	75.41655	76.46533	75.20592
dC, ng in Hyd Samples	73.10599	72.69343	72.33139	72.25896	71.35889	71.78198	70.28515
5mdC, ng in Hyd Samples	0	0.06841	0.35611	0.72590	1.09282	1.47675	1.77988
5hmdC, ng in Hyd Samples	0	0.00325	0.00576	0.01739	0.03547	0.05404	0.07220
dA, ng/mg in Hyd Samples	3.00957	2.98746	3.03310	2.94018	2.95654	3.01832	2.98726
T, ng/mg in Hyd Samples	3.02783	3.02967	3.04721	3.02572	3.00170	3.05873	3.02019
dG, ng/mg in Hyd Samples	2.10875	2.09246	2.09482	2.09646	2.06904	2.11639	2.08847
dC, ng/mg in Hyd Samples	2.02006	2.00423	2.00308	1.99170	1.95772	1.98677	1.95182
5mdC, ng/mg in Hyd Samples	0	0.00189	0.00986	0.02001	0.02998	0.04087	0.04943
5hmdC, ng/mg in Hyd Samples	0	0.00009	0.00016	0.00048	0.00097	0.00150	0.00201

	Cal 8	Cal 9	Cal 10	Cal 11	Cal 12	Cal 13
percent (5hmdC/total dC)	0.2	0.3	0.4	0.5	1	3
percent (5mdC/total dC)	3	4	5	6	7	10
Empty Hydrolysis Tube (g)	0.52075	0.52090	0.52053	0.51688	0.52149	0.51799
18 µL Std Added Wt (g)	0.53863	0.53907	0.53829	0.53489	0.53968	0.53620
18 µL Hyd Buff - Total Vol (g)	0.55645	0.55711	0.55614	0.55319	0.55815	0.55436
Total Weight Std Added (g)	0.01788	0.01817	0.01776	0.01801	0.01819	0.01821
Total Weight Std Added (mg)	17.88000	18.17000	17.76000	18.01000	18.19000	18.21000
Total Solvent Volume (g)	0.03570	0.03621	0.03561	0.03631	0.03666	0.03637
Total Solvent Volume (mg)	35.70000	36.21000	35.61000	36.31000	36.66000	36.37000
dA, ng in Hyd Samples	107.95330	108.89772	105.03380	107.98905	109.16733	109.09553
T, ng in Hyd Samples	107.66929	110.08721	108.25246	108.85399	109.21120	110.49087
dG, ng in Hyd Samples	74.74086	75.74764	74.35066	75.37421	76.85518	75.95236
dC, ng in Hyd Samples	69.39021	70.02367	68.13565	67.76774	67.26835	63.68082
5mdC, ng in Hyd Samples	2.15172	2.94669	3.57939	4.35530	5.14119	7.37633
5hmdC, ng in Hyd Samples	0.14110	0.21766	0.28562	0.36132	0.73624	2.19330
dA, ng/mg in Hyd Samples	3.02390	3.00739	2.94956	2.97409	2.97783	2.99960
T, ng/mg in Hyd Samples	3.01595	3.04024	3.03995	2.99791	2.97903	3.03797
dG, ng/mg in Hyd Samples	2.09358	2.09190	2.08792	2.07585	2.09643	2.08832
dC, ng/mg in Hyd Samples	1.94370	1.93382	1.91339	1.86637	1.83492	1.75092
5mdC, ng/mg in Hyd Samples	0.06027	0.08138	0.10052	0.11995	0.14024	0.20281
5hmdC, ng/mg in Hyd Samples	0.00395	0.00601	0.00802	0.00995	0.02008	0.06031

3.2.4. *LC-MS/MS method*

LC-MS/MS was used to directly calculate the proportion of methylated deoxy cytosine (5mdC) to deoxy guanosine (dG) within genomic DNA extracted from erythrocytes. Deoxyribonucleosides (5mdC and dG) present in the DNA extracts, calibration solutions, and blanks were chromatographically separated using an Agilent 1100 LC and Auto sampler. The deoxyribonucleosides were separated on a temperature-controlled (20 °C) Kinetex C18 column (100 x 3.0 mm, 2.6 µm, Phenomenex, Torrance, CA). After each injection (7.5 µL) separation of the nucleosides was achieved using the solvent mixtures of (A) Optima LC-MS grade acetonitrile (ACN, Fisher Scientific, Fair Lawn, NJ) with 0.1 % formic acid ((98 %, EMD, Germany) and (B) water with 0.1 % formic acid in a gradient as follows: 0 to 1 min (100 % B), 1 to 14 min (92 % B), 14 to 15 min (100 % B), and continued from 15 to 20 min for re-equilibration, with a flow rate of 250 µL/min.

Chromatographically separated deoxyribonucleosides were detected by multiple reaction monitoring (MRM) using an AB Sciex API 4000 triple quadrupole (Q1, Q2, Q3) mass spectrometer (equipped with a TurboV electrospray ionization source). Operation of the LC and MS was controlled using Analyst software (v.1.52, SCIEX, Framingham, MA). The method employed scheduled MRM, which was set to scan using a 180 s scan window from the retention times noted in Table 3.7. The target scan time for each MRM scan was 2 s. The MRM transition for each deoxyribonucleoside (Q1 mass (Daltons (Da)) → Q3 mass (Da)), and the tune-optimized compound-specific MS/MS parameters are also shown in Table 3.1. The tune-optimized source parameters were: collisionally

activated dissociation (8.0), curtain gas (15 psi), gas 1 (50 psi), gas 2 (30 psi), source temperature (500 °C), interface heater (on), and ion spray voltage (5000 V).

Table 3.7. The multiple reaction monitoring (MRM) transitions and optimized compound-specific MS/MS parameters for each deoxyribonucleoside measured in the LC-MS/MS DNA methylation analysis.

Nucleoside	Q1 Mass (Da)	Q3 Mass (Da)	RT (min)*
5hmdC	258.2	142.0	3.76
dC	228.2	112.0	3.79
5mdC	242.2	126.1	7.02
dA	252.1	136.1	10.84
dG	268.4	152.1	12.36
T	243.3	127.0	13.65

RT indicates retention time; Q indicates quadrupole, Da represents Daltons

3.2.5. Global DNA methylation quantification

The peaks for each nucleoside were integrated using the Analyst software. The percent global methylation (% 5mdC, or 5mdC/dG) was calculated using a calibration curve constructed by relating the calibration solution peak area ratios to the weight ratios of 5mdC and dG, as previously described, with some modification (contribution of deoxyribonucleoside adducts was negligible and was not factored into this analysis) (Table 3.8) (3, 336). Equimolar solutions were used to normalize differences in ionization efficiency between 5mdC and dG, the dG peak area was multiplied by a response factor (RSF) (0.8971) before the peak area ratio was calculated (3) (Table 3.9). The QC and calibration solutions were run throughout the sample queue. Peak areas for each deoxyribonucleoside in each sample ($n = 3$) were corrected (dG, as previously described), and averages as well as the percent (%) of 5mdC were calculated using the calibration line.

Table 3.8. Targeted and experimentally calculated average weight ratio for calibration solutions used in the LC-MS/MS DNA methylation analysis.

Cal #	% 5mdC	% 5hmdC	5mdC/dC	5hmdC/dC	5mdC/dG	5hmdC/dG
1	0	0	0	0	0	0
2	0.1	0.005	0.00094	4.47E-05	0.000901	4.29E-05
3	0.5	0.01	0.004899	7.92E-05	0.004708	7.61E-05
4	1	0.025	0.009944	0.000238	0.009544	0.000229
5	1.5	0.05	0.015076	0.000489	0.01449	0.00047
6	2	0.075	0.020143	0.000737	0.019313	0.000707
7	2.5	0.1	0.024673	0.001001	0.023667	0.00096
8	3	0.2	0.030017	0.001968	0.028789	0.001888
9	4	0.3	0.040262	0.002974	0.038901	0.002874
10	5	0.4	0.049713	0.003967	0.048142	0.003841
11	6	0.5	0.060086	0.004985	0.057782	0.004794
12	7	1	0.070287	0.010065	0.066894	0.00958
13	10	3	0.1007	0.029943	0.097118	0.028877

The weight ratios (for both 5mdC and 5hmdC) were expressed in two ways, calculated to total dC or dG. The values in grey indicate the values used to calculate percent global methylation (% 5mdC to dG) and were used in the calibration line.

Table 3.9. Corrected peak area ratios (5mdC/dG) for each calibration solution replicate used in the LC-MS/MS DNA methylation analysis.

Cal #	Rep 1	Rep 2	Rep 3	Rep 4	Average	Standard	RSD
	5mdC/dG	5mdC/dG	5mdC/dG	5mdC/dG		Deviation	
1	0.000625	0.000375	0.000382	0.000343	0.000431	0.000130	30.30%
2	0.006395	0.006115	0.006436	0.007673	0.006655	0.000693	10.42%
3	0.028602	0.030443	0.028073	0.029982	0.029275	0.001119	3.82%
4	0.054853	0.064285	0.060591	0.057904	0.059408	0.004008	6.75%
5	0.095678	0.08316	0.101193	0.085242	0.091318	0.008563	9.38%
6	0.117207	0.120949	0.100381	0.110008	0.112136	0.009057	8.08%
7	0.137745	0.144697	0.140312	0.133856	0.139153	0.004550	3.27%
8	0.180009	0.175347	0.174128	0.167754	0.174309	0.005052	2.90%
9	0.227752	0.231849	0.260047	0.18717	0.226705	0.030012	13.24%
10	0.285740	0.283978	0.302439	0.273537	0.286424	0.011958	4.18%
11	0.312947	0.337789	0.365138	0.320079	0.333988	0.023244	6.96%
12	0.398108	0.401936	0.391762	0.359376	0.387796	0.019405	5.00%
13	0.563995	0.539304	0.557351	0.538977	0.549907	0.012725	2.31%

3.3. Examining the relationship between mercury & DNA methylation in wild American alligators

3.3.1. Introduction

To elucidate the relationship between mercury exposure and epigenetic changes in DNA methylation, we utilize the “natural dosing” gradient of mercury concentrations observed in American alligators from Florida. These alligators are subject to mercury exposure throughout their lives and depending on where they reside, the mercury concentrations can be high. Thus, this exposure scenario provides the opportunity to examine changes to DNA methylation induced by chronic lifetime exposure to mercury. The comparison will allow the examination of a correlational link between mercury exposure and DNA methylation in a long-lived reptilian sentinel species. The natural variation will allow observation of the relationship over a wide range of mercury concentrations in adult and sub-adult animals that cannot be replicated in the laboratory.

3.3.2. Experiment specific methods

Sample collection

Alligators were collected by researchers with the Florida Fish and Wildlife Conservation Commission and the Medical University of South Carolina using guidelines provided by the American Society of Ichthyologists and Herpetologists (342). Alligators were captured from six sites known to have either a low, moderate, or high concentrations of mercury in the upper trophic levels (Figure 3.4) (90, 186). Twenty-four alligators (12 sub-adults and 12 adults, grouped based on size with a 50: 50 sex ratio), were sampled from each location during the spring of 2012 (Figure 3.4, Tables 3.10 & 3.11). Whole blood was collected from the post-occipital venous sinus with a sterile

needle and syringe immediately following capture as described by Myburgh, *et al.* (288). Whole blood samples were then transferred to 8 mL lithium-heparin Vacutainer blood collection tubes (BD, Franklin Lakes, NJ), and kept on wet ice for no longer than 5 h. For mercury measurement, whole blood was frozen at $-80\text{ }^{\circ}\text{C}$ until analysis. Red blood cell samples were collected from a separate 8 mL lithium-heparin Vacutainer blood collection tube by centrifugation, fixed in RNA Later (Sigma-Aldrich, St. Louis, MO), and frozen at $-20\text{ }^{\circ}\text{C}$ until DNA extraction.

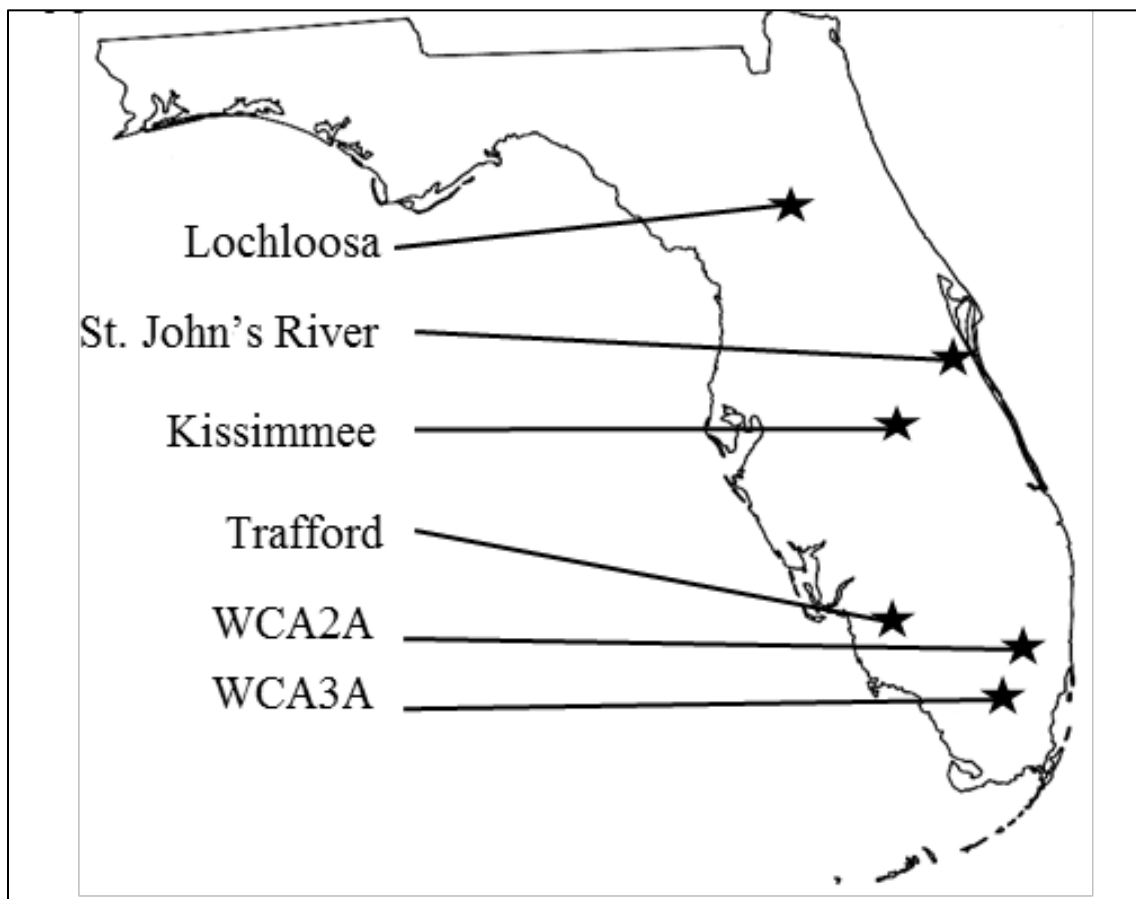


Figure 3.4. A map of the six sites used for collection of American alligator blood samples in experiment 3.3.

Table 3.10. Capture and morphometric information for adult alligators examined in experiment 3.3.

Age Class	Location	Tag #	Latitude (N)	Longitude (W)	Head Length (cm)	SV Length (cm)	Total Length (cm)	Tail Girth (cm)	Weight (kg)	Sex (M/F)
Adult	Kissimmee	FLM1259970	27.98449	81.27867	45	167	279	73	118	M
Adult	St Johns River	FLM1260030	28.30001	80.80676	37	138	277	70	75	M
Adult	Kissimmee	FLM1259952	27.85359	81.2034	48	178	340	80	154	M
Adult	Kissimmee	FLM1259963	27.98842	81.28396	28	106	212	45	27	F
Adult	Kissimmee	FLM1259953	27.90443	81.223	29	109	191	50	-	M
Adult	St Johns River	FLM1259965	28.28719	80.8202	40	146	279	63	76	M
Adult	Kissimmee	FLM1259972	27.96396	81.29359	32	115	191	39	-	F
Adult	Kissimmee	FLM1259968	27.9219	81.22293	32	124	242	54	-	F
Adult	Kissimmee	FLM1259964	27.92968	81.24022	43	160	301	50	-	M
Adult	Kissimmee	FLM1260043	27.96272	81.32471	39	143	287	66	-	M
Adult	Kissimmee	FLM1260046	27.87839	81.21207	25	90	180	43	21	F
Adult	Kissimmee	FLM1259951	27.9096	81.22835	49	173	330	74	143	M
Adult	St Johns River	FLM1259983	28.11732	80.74286	26	96	193	37	19	F
Adult	Kissimmee	FLM1260044	27.96762	81.31743	25	96	142	40	19	M
Adult	Kissimmee	FLM1259969	27.97672	81.29482	25	90	181	39	18	F
Adult	St Johns River	FLM1259991	28.658	80.82053	41	152	295	67	-	M
Adult	St Johns River	FLM1260022	28.29604	80.80991	35	136	256	66	-	F
Adult	St Johns River	FLM1260002	28.09919	80.74914	40	155	296	67	-	M
Adult	St Johns River	FLM1259985	28.19143	80.81365	32	126	245	54	-	F
Adult	Lochloosa	FLM1259997	29.52437	82.14857	38	144	268	73	100	F
Adult	WCA2A	FWC52769	26.21919	80.39268	26	94	186	41	-	F
Adult	Trafford	FLM1260063	26.43621	81.49513	27	99	195	41	22	M
Adult	St Johns River	FLM1260001	28.11174	80.75206	31	118	231	50	-	M
Adult	St Johns River	FLM1260023	28.29033	80.81822	45	168	317	68	-	M
Adult	WCA3A	FWC52740	26.21176	80.68641	26	94	184	39	-	F
Adult	Trafford	FLM1260066	26.43286	81.49624	38	134	247	56	62	M
Adult	WCA3A	FWC52255	26.06147	80.45958	31	111	218	47	-	M
Adult	Lochloosa	FLM1231575	29.53641	82.1377	25	94	187	46	-	F
Adult	Trafford	FLM1260039	-	-	41	154	291	46	61	M
Adult	Trafford	FLM1259980	-	-	24	90	180	39	18	M
Adult	Trafford	FLM1259977	-	-	39	140	272	61	65	M
Adult	WCA2A	FWC52745	26.23712	80.46071	37	130	249	52	-	M
Adult	Trafford	FLM1260047	26.41976	81.49065	38	140	270	56	61	M
Adult	Trafford	FLM1260050	26.42077	81.50428	29	109	212	45	30	M
Adult	Lochloosa	FLM1260057	29.51888	82.133	44	159	306	81	-	M
Adult	Trafford	FLM1260062	26.42976	81.50338	43	153	291	62	79	M
Adult	Trafford	FLM1260000	-	-	28	105	204	44	30	F
Adult	Trafford	FLM1260035	26.42557	81.50392	27	92	184	41	20	M
Adult	Trafford	FLM1260049	26.41605	81.50302	26	93	191	40	21	F
Adult	WCA2A	FWC52772	26.2183	80.40025	38	141	267	55	-	M
Adult	WCA3A	FWC52739	26.14748	80.63103	42	154	289	56	-	M
Adult	Trafford	FLM1260061	26.42334	81.459	38	142	270	63	68	M
Adult	Lochloosa	FLM1260032	29.5418	82.13	50	180	339	90	-	M
Adult	Lochloosa	FLM120016	29.53319	82.13628	28	106	211	53	-	F
Adult	Lochloosa	FLM1259999	29.53374	82.13919	27	109	215	55	40	M
Adult	Lochloosa	FLM1259998	29.53379	82.1393	26	96	187	48	26	M
Adult	WCA3A	FWC52742	25.76255	80.72896	32	116	224	49	-	M
Adult	WCA3A	FWC52253	26.06169	80.46485	26	94	181	35	-	M
Adult	WCA3A	FWC51820	26.08917	80.5906	45	157	291	63	-	M
Adult	Lochloosa	FLM1231574	29.52972	82.13016	36	128	259	69	-	M
Adult	WCA2A	FWC52759	26.23041	80.45899	28	105	205	46	-	F
Adult	WCA3A	FWC52256	26.10992	80.60614	37	142	267	56	-	M
Adult	WCA2A	FWC52768	26.25417	80.3677	25	92	183	39	-	F
Adult	Lochloosa	FLM1260055	29.5272	82.14932	25	94	186	47	26	M
Adult	Lochloosa	FLM1260053	29.50336	82.15189	41	152	283	66	Est 84	M
Adult	WCA3A	FWC52741	25.7622	80.74733	27	102	193	39	-	M
Adult	WCA2A	FWC52747	26.3188	80.52347	34	132	253	54	-	M

Dashes indicate that we do not have this information.

Table 3.11. Capture and morphometric information for sub-adult alligators examined in experiment 3.3

Age Class	Location	Tag #	Latitude (N)	Longitude (W)	Head Length (cm)	SV Length (cm)	Total Length (cm)	Tail Girth (cm)	Weight (kg)	Sex (M/F)
Sub adult	Kissimmee	FLM1259967	27.9288	81.23381	24	89	175	40	18	F
Sub adult	Kissimmee	FLM1259954	27.90505	81.22225	19	70	144	30	8	M
Sub adult	Kissimmee	FLM1259959	27.91231	81.22723	15	53	107	23	4	M
Sub adult	Kissimmee	FLM1259962	27.98892	81.30901	13	47	97	18	2	M
Sub adult	Kissimmee	FLM1259955	27.93714	81.23738	19	72	145	32	9	F
Sub adult	Kissimmee	FLM1259961	27.97738	81.2998	16	61	124	26	5	F
Sub adult	Kissimmee	FLM1259956	27.93714	81.23738	22	81	160	34	12	M
Sub adult	St Johns River	FLM1259966	28.28141	80.82613	21	79	160	34	12	M
Sub adult	WCA3A	FLM1260068	26.10006	80.59865	23	82	161	34	13	F
Sub adult	Trafford	FLM1259990	-	-	16	57	119	24	4	F
Sub adult	St. Johns River	FLM1260024	28.29408	80.81126	27	101	195	47	-	M
Sub adult	St Johns River	FLM1259974	28.18072	80.80492	20	73	149	33	-	M
Sub adult	WCA3A	FLM1259992	26.16365	80.64969	21	74	147	29	9	F
Sub adult	Trafford	FLM1259989	-	-	15	53	104	21	3	F
Sub adult	Lochloosa	FLM1260052	29.49606	82.15151	17	61	128	25	5	F
Sub adult	Trafford	FLM1259993	26.44522	81.50496	20	74	150	31	11	F
Sub adult	Lochloosa	FLM1260051	29.49698	82.15193	18	63	125	27	5	M
Sub adult	Trafford	FLM1260040	-	-	19	71	142	30	7	F
Sub adult	WCA2A	FLM1260037	26.25162	80.35273	16	58	116	21	4	M
Sub adult	WCA2A	FLM1260004	26.31329	80.51933	23	89	175	36	15	F
Sub adult	WCA2A	FLM1260003	26.31872	80.52338	23	84	164	32	12	F
Sub adult	Lochloosa	FLM1260065	29.5037	82.13558	19	76	149	33	10	F
Sub adult	WCA2A	FLM1260008	26.28417	80.49675	14	48	100	21	3	M
Sub adult	Trafford	FLM1259995	26.43592	81.49872	18	66	134	28	6	F
Sub adult	Trafford	FLM1259988	-	-	24	84	166	36	15	M
Sub adult	Trafford	FLM1259978	-	-	17	62	107	25	5	F
Sub adult	WCA2A	FLM1260038	26.25	80.35	23	88	174	34	14	F
Sub adult	WCA3A	FLM1260070	26.08318	80.5856	23	83	158	30	10	M
Sub adult	Trafford	FLM1260026	-	-	14	53	199	22	3	M
Sub adult	WCA2A	FLM12960007	26.29182	80.50263	15	54	111	23	4	M
Sub adult	Trafford	FLM1260048	26.41333	81.49485	23	87	172	37	14	F
Sub adult	WCA2A	FLM1260009	26.27773	80.49171	17	66	134	27	7	F
Sub adult	WCA3A	FLM1260018	25.76799	80.67432	18	64	119	24	5	F
Sub adult	WCA3A	FLM1260020	25.76229	80.73094	27	89	178	34	15	M
Sub adult	Trafford	FLM1259996	26.43591	81.49876	14	51	103	20	3	F
Sub adult	WCA2A	FLM1260042	26.92204	80.36691	21	79	157	34	11	F
Sub adult	WCA2A	FLM1260041	26.22153	80.37025	24	88	177	36	16	M
Sub adult	Trafford	FLM1259994	26.42814	81.50672	15	56	110	22	4	F
Sub adult	WCA3A	FLM1260017	26.2153	80.6891	18	68	131	29	7	F
Sub adult	WCA3A	FLM1260019	25.76232	80.77415	13	44	87	17	2	M
Sub adult	Lochloosa	FLM1260060	29.50696	82.15018	13	47	93	17	2	F
Sub adult	St. Johns River	FLM1259984	28.18673	80.81025	22	79	163	36	-	M
Sub adult	WCA3A	FLM1260067	26.07001	80.57545	23	81	160	36	13	F
Sub adult	WCA3A	FLM1260015	26.2153	80.6891	16	59	123	28	6	F
Sub adult	St Johns River	FLM1259982	28.17016	80.77918	25	88	178	39	17	F
Sub adult	St. Johns River	FLM60011	28.27924	80.83032	16	59	124	27	6	M
Sub adult	Trafford	FLM1260027	-	-	19	72	127	30	8	F
Sub adult	St Johns River	FLM1259981	28.17359	80.78397	20	74	149	32	11	F
Sub adult	St. Johns River	FLM1260013	28.32151	80.82274	13	48	99	22	3	F
Sub adult	St Johns River	FLM1260014	28.34319	80.8605	22	86	171	38	17	F
Sub adult	WCA3A	FLM1260034	26.18148	80.66319	21	78	155	33	10	F
Sub adult	St. Johns River	FLM1260012	28.31413	80.81099	20	74	148	32	10	M
Sub adult	St Johns River	FLM1259986	28.12829	80.7293	16	59	120	24	5	M
Sub adult	WCA3A	-	26.2067	80.68246	25	89	175	38	15	M
Sub adult	St. Johns River	FLM1259975	28.11732	80.74285	17	59	125	28	-	F
Sub adult	Lochloosa	FLM1260006	29.54097	82.11636	15	57	110	24	4	M
Sub adult	Lochloosa	FLM1259957	29.53981	82.11717	15	56	107	23	385	M
Sub adult	Lochloosa	FLM1260005	29.54358	82.14153	17	63	121	25	5	F
Sub adult	Lochloosa	FLM1259979	29.53883	82.11568	19	72	145	32	9	M
Sub adult	Lochloosa	FLM1260058	29.54031	82.14304	20	76	149	35	11	F
Sub adult	Lochloosa	FLM1260054	29.53772	82.14436	15	55	107	22	3	M
Sub adult	Lochloosa	FLM1260059	29.53514	82.14535	16	62	121	27	6	M
Sub adult	Lochloosa	FLM1260064	29.49885	-	16	62	124	25	5	F

Dashes indicate that we do not have this information

Mercury analysis

The mercury analysis of these samples was conducted and detailed in Chapter 2. Briefly, blood samples were thawed and gently rocked for homogenization. The mass fraction of total mercury was determined in one aliquot (100 μ L) of alligator whole blood with a direct mercury analyzer (DMA-80, Milestone, Shelton, CT). NIST Standard Reference Material (SRM) 3133, Mercury Standard Solution was used for external calibration (Figure 3.5). NIST SRM 955c Level 3, Toxic Metals in Caprine Blood was used as a control material certified for total mercury at 17.8 ± 1.6 ng/g. Procedural blanks were analyzed by use of an empty sample vessel, and concurrently, field blanks were analyzed by use of Milli-Q water. If blanks were found to be above the detection limit, the samples were blank corrected.

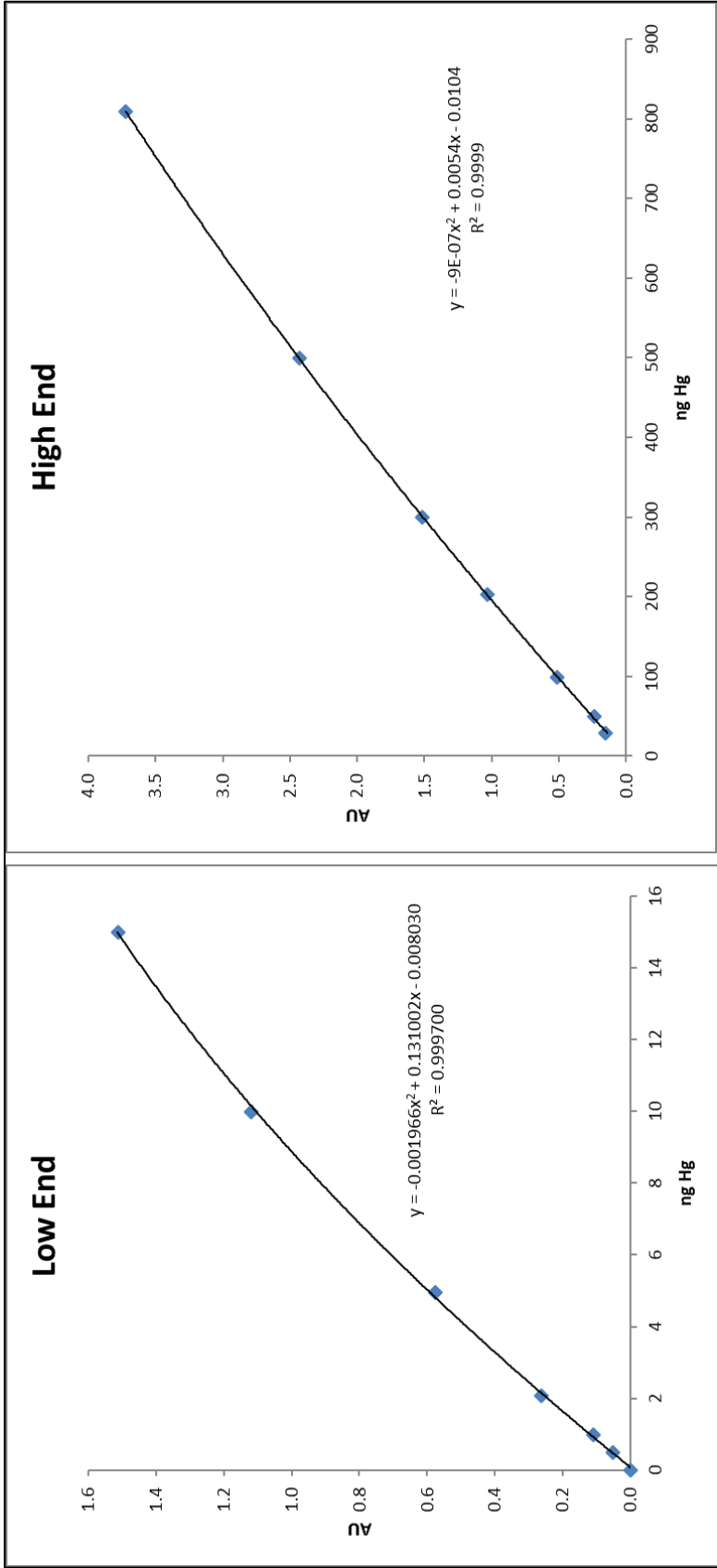


Figure 3.5. The calibration lines created using NIST SRM 3133 (Mercury in Water) for use with the alligator blood samples collected from six sites in Florida in 2012. Ng denotes Nano grams; AU denotes absorbance in the Direct Mercury Analyzer (DMA-80).

DNA methylation analysis

To assess the reproducibility of the LC-MS/MS assay and serve as a Quality Control (QC) measure, three separate aliquots of a pooled alligator blood DNA sample were prepared, and each was analyzed in triplicate (RSD < 10 %). Previously made alligator tissue DNA QC material was also used (RSD < 10 %). The alligator whole blood DNA extracts ($n = 122$), calibration solutions ($n = 13$), alligator tissue DNA QC samples ($n = 9$), alligator blood DNA QC samples ($n = 3$), and blanks ($n = 3$) were queued in randomized sets and analyzed by LC-MS/MS as described above, in triplicate.

The resulting calibration line is pictured in Figure 3.6.

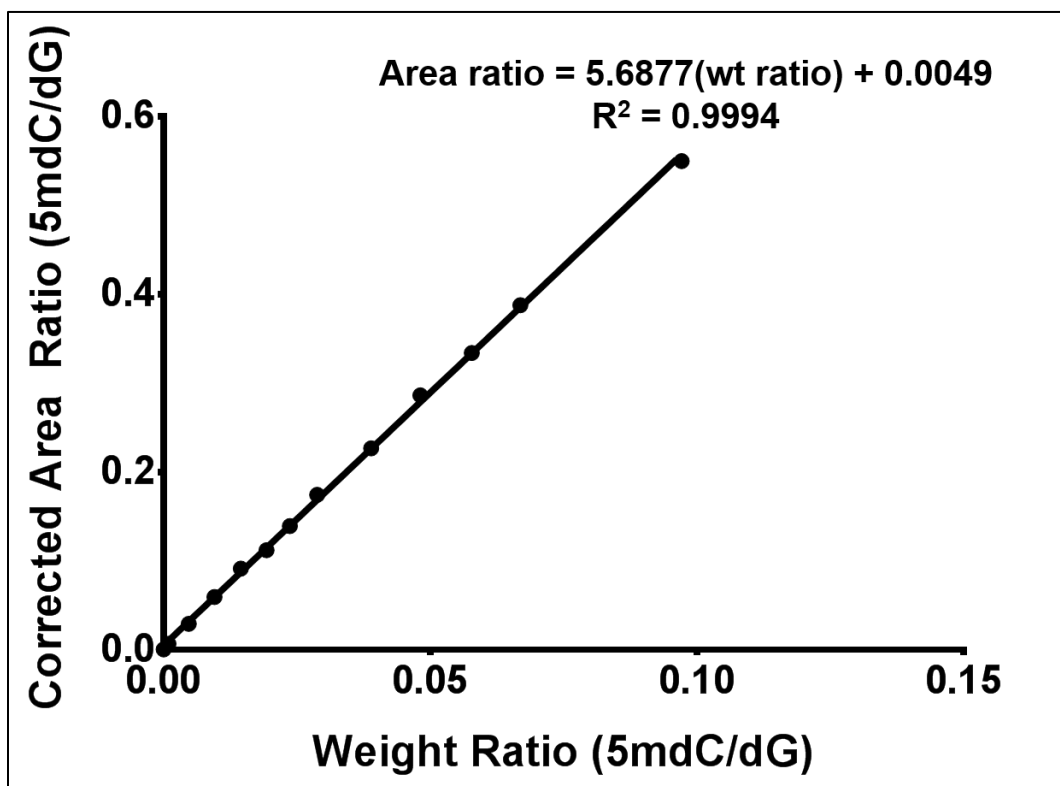


Figure 3.6. A standard calibration line for calculating global DNA methylation (% 5mdC, 5mdc/dG). The calibration solutions used were 0.0, 0.1, 0.5, 1.0, 1.5, 2.0, 2.5, 3.0, 4.0, 5.0, 6.0, 7.0 and 10.0% of 5mdc to dG.

Statistical analysis

All total mercury concentration of the alligator blood samples data failed to meet the assumptions of normality and homoscedasticity based on the Shapiro-Wilk Goodness of Fit Test and Levene's Test for Unequal Variances. After the data were \log_{10} transformed, the mercury measurements met the parametric assumptions. Linear Regression and Pearson Product Moment Correlations were used to compare the mercury data to the DNA methylation data. The Student's T-test was used to assess differences in mercury concentration and DNA methylation pattern due to sex. No significant differences were found and both sexes were grouped for the remaining analyses: the Two-Way Factorial ANOVA was used to compare mercury concentrations found at each of the six sites, with the Tukeys' HSD Multiple Comparison post-hoc test for comparisons among sites and age classes. An ANCOVA analysis was not used as all the parameters did not meet the assumptions, particularly the homogeneity of regression. All statistical analyses were conducted using Graph Pad (Prism 6, La Jolla, CA) and JMP 11 (SAS, Cary, NC). Statistical significance was determined by $p < 0.05$ for all tests.

3.3.3. Results

Variation in mercury concentrations

The replicated measurements of the control material, NIST SRM 955c Level 3, had an average value of $17.2 \text{ ng/g} \pm 0.5 \text{ ng/g}$, falling within the certified confidence interval ($16.2 - 19.4 \text{ ng/g}$) (Table 3.12).

The mercury concentrations in the whole blood of American alligators from six sites in Florida varied from $88 \text{ ng/g} \pm 32 \text{ ng/g}$ to $1,569 \text{ ng/g} \pm 643 \text{ ng/g}$ (Figure 3.7, Table 3.13). At each site, adults had greater concentrations of mercury than sub-adults did;

however, statistically significant differences between age classes were only observed at the three locations with the greatest mercury concentrations (WCA2A, WCA3A, and Kissimmee), as these adult alligators had nearly double the mercury concentration of the subadults from the same location (Figure 3.7, Table 3.14). Suggesting, that above a certain threshold of mercury, age class has an effect on mercury concentration.

Comparisons of mercury concentrations across the sites revealed significant differences among many of the groups (Table 3.14). With exception of one site, Lake Trafford, higher concentrations of mercury were observed towards the southern part of the state. Animals sampled at the two sites within the Everglades, WCA2A and WCA3A, were observed to have the greatest concentrations of mercury. These findings are consistent with previous studies identifying the Everglades region but particularly WCA3A, as a “hotspot” for mercury accumulation. Alligators from this region show elevated mercury concentrations in comparison to alligators from other regions of the state (4, 90).

Table 3.12. The summaries of the total Hg results for the SRM 955c used with the alligator blood samples in Experiment 3.3.

The certified values of the SRMs 955c (Toxic Metals in Caprine Blood) Level 3 is $16.9 \pm 1.5 \mu\text{g}/\text{kg}$.

SRM955c level 3	[Hg] mg/kg
1 SRM 3133 Cal Curve	17.5
2 SRM 3133 Cal Curve	17.5
3 SRM 3133 Cal Curve	18.6
4 SRM 3133 Cal Curve	18.5
5 SRM 3133 Cal Curve	16.7
6 SRM 3133 Cal Curve	16.7
7 SRM 3133 Cal Curve	16.7
8 SRM 3133 Cal Curve	17.1
9 SRM 3133 Cal Curve	17.0
10 SRM 3133 Cal Curve	16.9
11 SRM 3133 Cal Curve	17.1
12 SRM 3133 Cal Curve	17.1
13 SRM 3133 Cal Curve	17.2
14 SRM 3133 Cal Curve	17.1
15 SRM 3133 Cal Curve	17.1
16 SRM 3133 Cal Curve	16.8
17 SRM 3133 Cal Curve	17.2
18 SRM 3133 Cal Curve	17.0
19 SRM 3133 Cal Curve	17.4
20 SRM 3133 Cal Curve	17.4
Average	17.2
Standard Deviation	0.5
%RSD	3.0
U	0.8

Table 3.13. The mean and standard deviation of Hg for each location and age class from experiment 3.3. The correlation coefficients and *p*-values for each location's Hg values compared to the DNA methylation pattern found in the same blood samples are also shown. The coefficient is reflective of the Pearson Product Moment Correlation.

<i>Location</i>	<i>Age Class</i>	<i>n</i>	<i>Average Hg (ng/g)</i>	<i>Standard Deviation</i>
Kissimmee	Adult	12	417.2	222.1
	Sub-adult	7	160.5	41.5
Lochloosa	Adult	10	148.5	71.2
	Sub-adult	12	88.0	31.5
St. John's River	Adult	10	177.7	84.9
	Sub-adult	12	152.9	53.2
Trafford	Adult	12	198.1	79.0
	Sub-adult	12	164.5	57.6
WCA2A	Adult	6	1568.5	642.5
	Sub-adult	9	558.8	282.3
WCA3A	Adult	8	1329.4	712.6
	Sub-adult	11	683.6	450.2

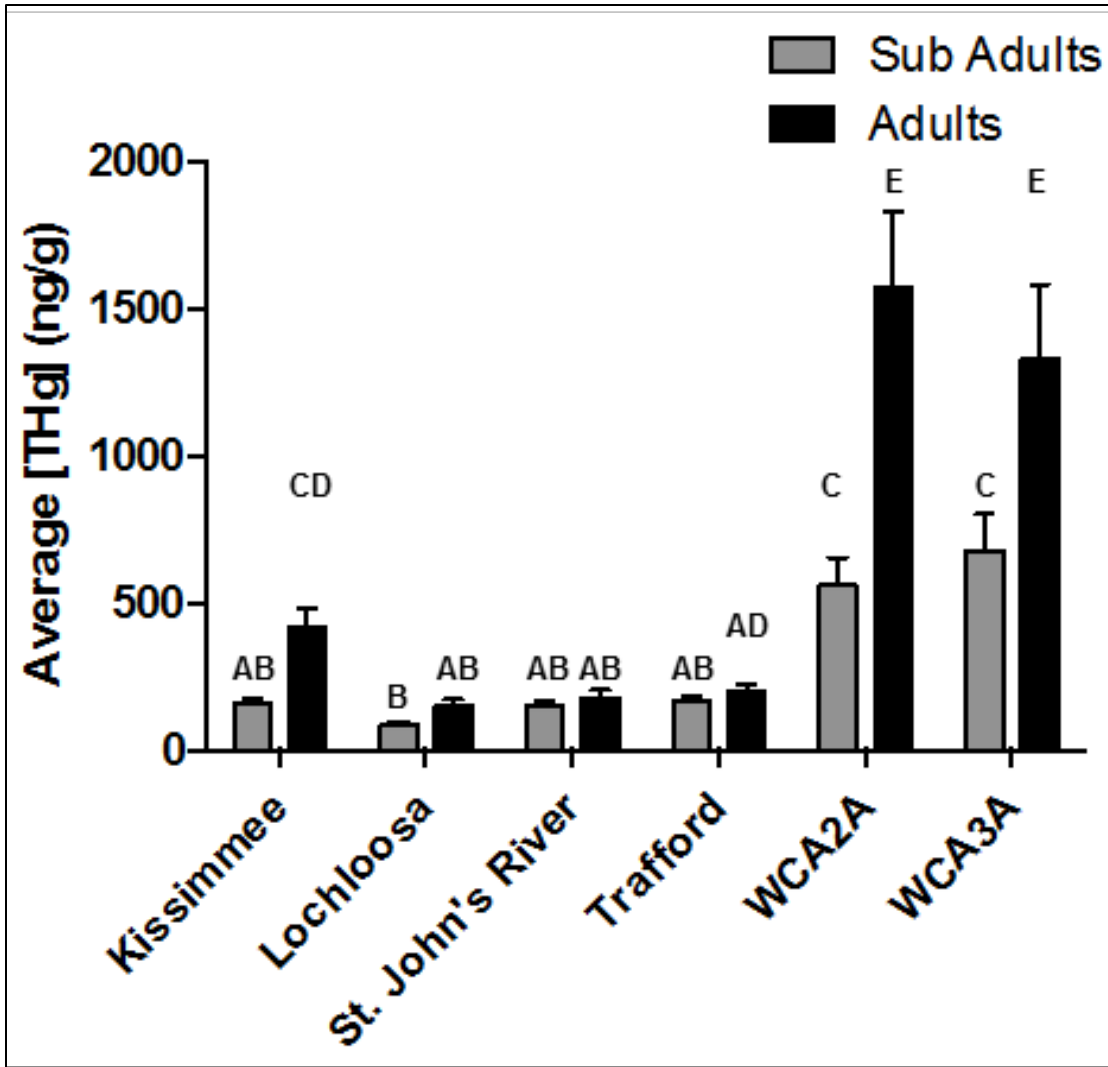


Figure 3.7. The mean (\pm SD) total Hg concentrations (ng/g, wet mass) in alligator whole blood partitioned as a function of age class and sampling location in Florida. Significantly different letters (significance noted by $p < 0.05$) denote different average Hg concentrations.

Table 3.14. The Tukey's HSD Multiple Comparison results for total Hg concentration compared to location and age class.

Comparisons from the same location are denoted in bold. Only statistically significant ($p < 0.05$) comparisons are presented here.

Comparison		p-Value
Adults, WCA2A	Sub-Adults, Lochloosa	<.0001
Adults, WCA3A	Sub-Adults, Lochloosa	<.0001
Adults, WCA2A	Adults, Lochloosa	<.0001
Adults, WCA2A	Sub-Adults, St. John's River	<.0001
Adults, WCA2A	Sub-Adults, Kissimmee	<.0001
Adults, WCA2A	Sub-Adults, Trafford	<.0001
Adults, WCA2A	Adults, St. John's River	<.0001
Adults, WCA3A	Adults, Lochloosa	<.0001
Adults, WCA3A	Sub-Adults, St. John's River	<.0001
Adults, WCA2A	Adults, Trafford	<.0001
Adults, WCA3A	Sub-Adults, Kissimmee	<.0001
Adults, WCA3A	Sub-Adults, Trafford	<.0001
Adults, WCA3A	Adults, St. John's River	<.0001
Adults, WCA3A	Adults, Trafford	<.0001
Sub-Adults, WCA2A	Sub-Adults, Lochloosa	<.0001
Sub-Adults, WCA3A	Sub-Adults, Lochloosa	<.0001
Adults, Kissimmee	Sub-Adults, Lochloosa	<.0001
Adults, WCA2A	Adults, Kissimmee	<.0001
Sub-Adults, WCA2A	Adults, Lochloosa	<.0001
Sub-Adults, WCA3A	Adults, Lochloosa	<.0001
Sub-Adults, WCA2A	Sub-Adults, St. John's River	<.0001
Sub-Adults, WCA3A	Sub-Adults, St. John's River	<.0001
Sub-Adults, WCA2A	Sub-Adults, Kissimmee	0.0019
Sub-Adults, WCA2A	Sub-Adults, Trafford	0.0002
Adults, WCA3A	Adults, Kissimmee	0.0004
Sub-Adults, WCA3A	Sub-Adults, Kissimmee	0.0012
Sub-Adults, WCA3A	Sub-Adults, Trafford	<.0001
Adults, WCA2A	Sub-Adults, WCA3A	0.0037
Sub-Adults, WCA2A	Adults, St. John's River	0.0008
Adults, WCA2A	Sub-Adults, WCA2A	0.0077
Sub-Adults, WCA3A	Adults, St. John's River	0.0004
Adults, Kissimmee	Adults, Lochloosa	0.0006
Sub-Adults, WCA2A	Adults, Trafford	0.0026
Sub-Adults, WCA3A	Adults, Trafford	0.0014
Adults, Kissimmee	Sub-Adults, St. John's River	0.0012
Adults, WCA3A	Sub-Adults, WCA3A	0.0224
Adults, Kissimmee	Sub-Adults, Kissimmee	0.0317
Adults, Kissimmee	Sub-Adults, Trafford	0.0050
Adults, WCA3A	Sub-Adults, WCA2A	0.0435
Adults, Kissimmee	Adults, St. John's River	0.0188
Adults, Trafford	Sub-Adults, Lochloosa	0.0173

As reported in Chapter 2, there was an increasing gradient of mercury along the north-to-south axis, through the central Florida drainage system, from Lake Kissimmee to the Everglades (Figure 3.7 and 3.8). There was also a significant increase in mercury concentrations within the Everglades compared to Lake Trafford, Lake Kissimmee and St. John's River, with the mean mercury concentrations more than tripling (Table 2.12). The gradient in average mercury concentration was seen in adults ($417 \text{ ng/g} \pm 222 \text{ ng/g}$, $1570 \text{ ng/g} \pm 643 \text{ ng/g}$, $1330 \text{ ng/g} \pm 713 \text{ ng/g}$) and sub-adults ($160 \text{ ng/g} \pm 41 \text{ ng/g}$, $560 \text{ ng/g} \pm 282 \text{ ng/g}$, and $680 \text{ ng/g} \pm 450 \text{ ng/g}$) for Kissimmee, WCA2A, and WCA3A, respectively.

The increasing concentrations of mercury observed in animals from Lake Kissimmee to the Everglades locations suggests that anthropogenic influence could be an additional source of mercury in this drainage system. This series of connected watersheds begins north of Lake Kissimmee, drains through part of urban Orlando and nearby tourist attractions, which both add to the water effluent filtering through the more southern watersheds. This drainage system continues through central Florida down through the Everglades to Florida Bay (343). The combined effects of the anthropogenic influence on the central Florida drainage system and the unique biogeochemical characteristics of the Everglades that control production of CH_3Hg —as well as transport, binding, and bioaccumulation— provides a unique opportunity to study the effects of mercury exposure. Mercury concentrations in animals from the three sites that are not part of this drainage system—Lochloosa Lake, St. John's River and Lake Trafford—were below those concentrations observed in the Everglades, despite being near Lake Trafford.

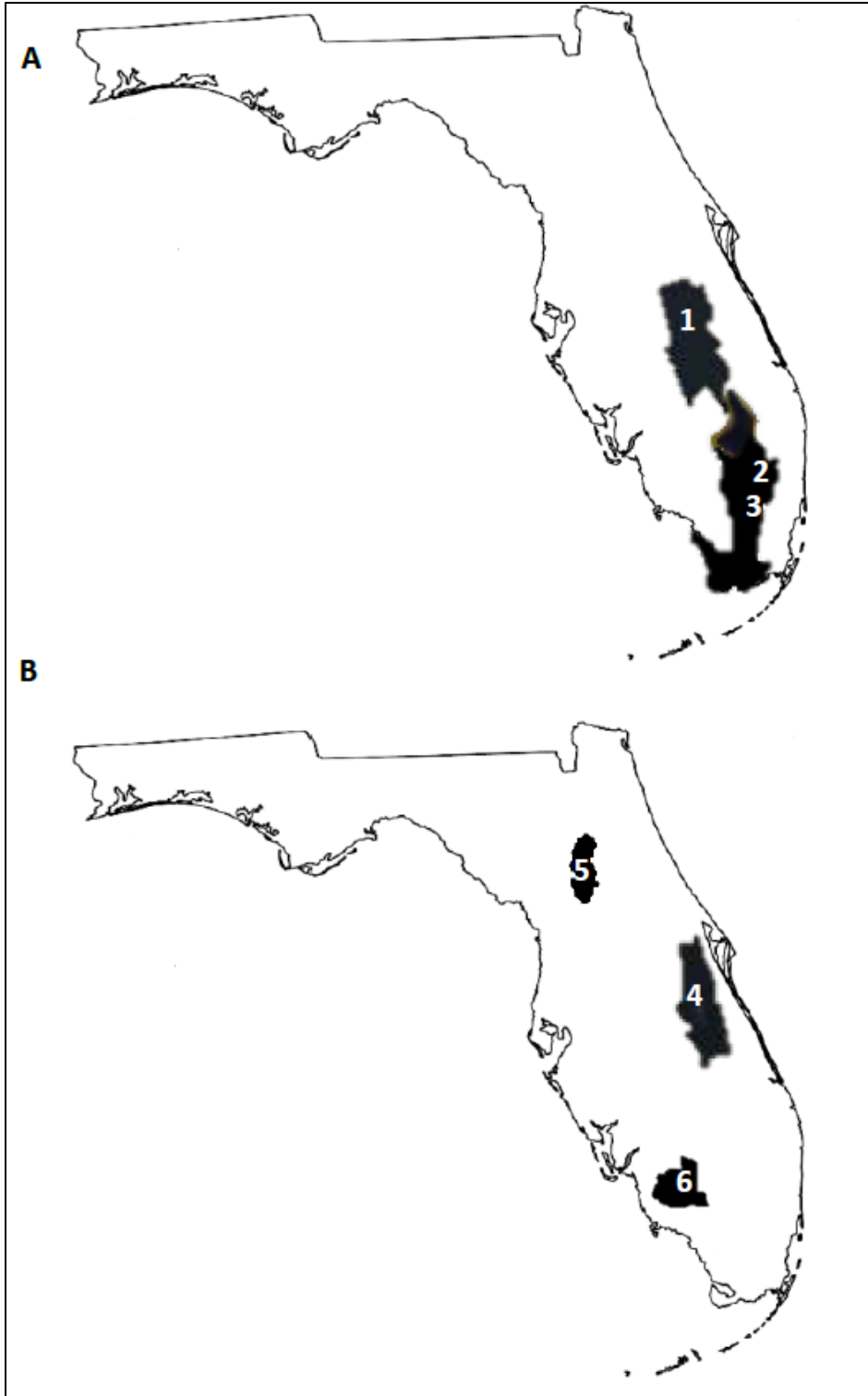


Figure 3.8. A map of the sampling sites within the connected drainage system flowing south to Florida Bay (A) and sites located in other watersheds. Sites 4 and 5 are part of a connected system that flows north to the Atlantic Ocean, site 6 has isolated drainage to the Gulf of Mexico (B). Sites are as follows: 1- Kissimmee, 2- WCA2A, 3- WCA3A, 4- St. John's River, 5- Lochloosa, and 6- Trafford. Images modified from the Florida Department of Environmental Protection.

Variation in DNA methylation

The alligators sampled across Florida provide the opportunity to examine the effects of mercury exposure over a wide range of mercury concentrations. Previous studies have shown that DNA methylation changes are related to high mercury exposure, and could provide a biomarker of effect prior to the onset of the classical adverse outcome such as neurodegeneration, muscle tremors, and impaired reproductive success (99, 101, 108, 338, 344-347). In this study, we examined DNA methylation changes over a wider range of mercury concentrations than ever examined before.

The quality control materials used in this experiment, the replicated whole blood DNA extracts ($n = 2$) and QC samples ($n = 3$), had an average RSD 0.18, or less, throughout the sample queue (Table 3.15). The final % DNA methylation for the alligator samples was calculated from the average of three replicates from the same sample, corrected using the RSF described in section 3.2.5. The measured % DNA methylation for the alligators with mercury concentration data is presented in Table 3.16 and summarized in Table 3.17.

The alligators from six sites in Florida had % global DNA methylation that ranged from 3.3% to 3.5%, which is a narrow margin (Table 3.17). However, since this experiment measured global methylation, a small change in % can equate to large changes in methylation across the genome. DNA methylation is known to change with age, and since alligators undergo prolonged growth, animal length (or SVL) is the closest available proxy to age (253). When all animals are separated by age class alone, a slight difference is observed (Figure 3.9), but when they are plotted using a linear regression analysis a significant inverse relationship was found between % global DNA methylation

(5mdC/dG) and SVL ($p = 0.03$; Figure 3.10, top). However, when the age classes are separated, the consistent trend disappears, suggesting that age/size is not the only variable influencing DNA methylation in this group of alligators (Figure 3.10, bottom). The difference in global DNA methylation for sub-adults compared to adults observed here is consistent with a previous study in which captive juvenile alligators were found to have increased global DNA methylation when compared to wild adults (3).

To probe this relationship further, we separated the age classes based on location, as differences in diet, lifestyle, and environmental contaminant exposure can affect DNA methylation (217, 219, 332, 348). We found that both variables are significantly associated with global DNA methylation (location ($p = 0.02$) and age class ($p < 0.001$)) using a two-way ANOVA. When separated this way, the adults display decreased global DNA methylation when compared to sub-adults (Figure 3.10).

In Figure 3.10, the differences between sub-adult and adult global DNA methylation are more pronounced in alligators captured at sites observed to have the greatest concentrations of mercury (Kissimmee, WCA2A, and WCA3A, Figure 3.13, 3.14, and 3.15). Given that increased mercury concentrations are associated with decreased global DNA methylation, we hypothesize that alligators living in sites with the greatest concentrations of mercury could undergo a more pronounced reduction in global DNA methylation. However, the relationship with SVL described above suggests that there is an age class component to DNA methylation loss in alligators. To observe how much influence SVL has on DNA methylation compared to mercury concentration, all three variables were plotted together in Figure 3.12. The locations are plotted from left to right with increasing mercury concentrations, and as mercury increases DNA methylation

decreases, while SVL remains consistent between the age classes (Figure 3.12). At the high mercury sites (Kissimmee, WCA2A, and WCA3A) the DNA methylation pattern inversely oscillates with mercury concentration, showing an apparent decrease in methylation in the adults from each site. These data suggest that mercury is influencing DNA methylation more than age does at the high mercury sites.

Table 3.15. The quality control materials used in the LC-MS/MS analysis of the alligator blood sample extracts for DNA methylation.

Nucleoside	Sample Name	Rep 1	Rep 2	Rep 3	Rep 4	Rep 1 w/ RSF	Rep 2 w/ RSF	Rep 3 w/ RSF	Rep 4 w/ RSF	Mean	SD	RSD
5mdC	GDNA1	7.04	6.96	10.22	8.24	0.077	0.055	0.071	0.052	0.064	0.012	0.195
dG		91.4	127.23	143.19	159.3							
5mdC	GDNA2	6.99	6.88	8.85	8.58	0.064	0.054	0.072	0.051	0.060	0.009	0.158
dG		109.58	126.46	123.22	168.9							
5mdC	GDNA3	6.44	9.04	8.9	8.31	0.064	0.081	0.067	0.049	0.065	0.013	0.200
dG		100.59	111.22	132.45	168.6							
5mdC	100	5.21	6.34	5.91		0.051	0.062	0.054		0.055	0.006	0.103
dG		102.92	102.95	110.37								
5mdC	100(2)	7.03	5.91	6.22		0.075	0.051	0.048		0.058	0.015	0.257
dG		94.22	116.94	130.43								
5mdC	104	6.6	6.69	6.52		0.062	0.050	0.053		0.055	0.006	0.115
dG		105.89	133.18	122.96								
5mdC	104(2)	7.77	7.31	7.22		0.069	0.059	0.049		0.059	0.010	0.171
dG		112.2	124.67	147.21								

Table 3.16. The alligator DNA methylation data for experiment 3.3.

The replicates from the instrument software (Rep 1- Rep 3) are given in relative abundance units. The standard deviation (SD) and coefficient of variance (CV = SD/mean of replicates) are provided as quality assessment measures.

Nucleoside	Sample ID	Rep 1 mdC/dG (w RSF)	Rep 2 mdC/dG (w RSF)	Rep 3 mdC/dG (w RSF)	Average	Standard Deviation	Coefficient of Variance	% DNA Methylation
dC	2	0.169	0.167	0.169	0.168	0.001	0.005	0.029
dC	3	0.193	0.164	0.175	0.178	0.012	0.067	0.030
dC	4	0.188	0.187	0.180	0.185	0.004	0.019	0.032
dC	5	0.182	0.201	0.188	0.190	0.008	0.040	0.033
dC	6	0.177	0.193	0.200	0.190	0.010	0.052	0.033
dC	7	0.234	0.206	0.226	0.222	0.012	0.052	0.038
dC	9	0.184	0.181	0.187	0.184	0.002	0.013	0.032
dC	10	0.213	0.195	0.209	0.206	0.008	0.039	0.035
dC	11	0.198	0.174	0.169	0.180	0.013	0.071	0.031
dC	12	0.179	0.177	0.196	0.184	0.009	0.047	0.031
dC	13	0.201	0.198	0.193	0.198	0.003	0.016	0.034
dC	14	0.193	0.167	0.183	0.181	0.011	0.060	0.031
dC	15	0.187	0.182	0.180	0.183	0.003	0.017	0.031
dC	16	0.188	0.193	0.187	0.189	0.003	0.013	0.032
dC	17	0.192	0.194	0.210	0.199	0.008	0.039	0.034
dC	18	0.185	0.183	0.182	0.183	0.001	0.007	0.031
dC	19	0.216	0.206	0.205	0.209	0.005	0.025	0.036
dC	20	0.200	0.197	0.193	0.197	0.003	0.016	0.034
dC	22	0.193	0.180	0.211	0.195	0.013	0.066	0.033
dC	23	0.216	0.189	0.183	0.196	0.015	0.075	0.034
dC	26	0.213	0.189	0.212	0.205	0.011	0.054	0.035
dC	30	0.227	0.206	0.203	0.212	0.011	0.050	0.036
dC	31	0.206	0.160	0.188	0.184	0.019	0.103	0.032
dC	32	0.230	0.200	0.212	0.214	0.012	0.058	0.037
dC	33	0.191	0.202	0.180	0.191	0.009	0.047	0.033
dC	34	0.215	0.181	0.177	0.191	0.017	0.090	0.033
dC	36	0.196	0.172	0.169	0.179	0.012	0.068	0.031
dC	37	0.194	0.192	0.206	0.197	0.006	0.031	0.034
dC	38	0.184	0.170	0.187	0.180	0.008	0.042	0.031
dC	39	0.235	0.174	0.182	0.197	0.027	0.138	0.034
dC	41	0.206	0.211	0.213	0.210	0.003	0.012	0.036
dC	42	0.190	0.217	0.181	0.196	0.015	0.078	0.034
dC	43	0.249	0.194	0.215	0.219	0.023	0.104	0.038
dC	44	0.198	0.160	0.182	0.180	0.015	0.085	0.031
dC	45	0.208	0.173	0.207	0.196	0.016	0.082	0.034
dC	46	0.201	0.187	0.186	0.191	0.006	0.034	0.033
dC	47	0.235	0.210	0.215	0.220	0.010	0.047	0.038
dC	49	0.188	0.172	0.174	0.178	0.007	0.038	0.030
dC	50	0.231	0.199	0.176	0.202	0.023	0.113	0.035
dC	53	0.172	0.193	0.170	0.178	0.010	0.058	0.031
dC	54	0.180	0.176	0.187	0.181	0.004	0.023	0.031
dC	55	0.176	0.189	0.172	0.179	0.008	0.042	0.031
dC	56	0.192	0.184	0.204	0.193	0.008	0.042	0.033
dC	57	0.183	0.175	0.185	0.181	0.004	0.024	0.031
dC	60	0.198	0.190	0.204	0.197	0.006	0.028	0.034
dC	62	0.220	0.192	0.199	0.204	0.012	0.058	0.035
dC	63	0.203	0.197	0.213	0.204	0.007	0.033	0.035
dC	64	0.212	0.194	0.166	0.191	0.019	0.099	0.033
dC	65	0.186	0.206	0.175	0.189	0.013	0.070	0.032
dC	66	0.241	0.192	0.214	0.215	0.020	0.094	0.037
dC	67	0.204	0.183	0.182	0.190	0.010	0.054	0.032
dC	69	0.201	0.210	0.185	0.199	0.010	0.051	0.034
dC	70	0.189	0.179	0.166	0.178	0.009	0.053	0.030
dC	71	0.200	0.189	0.180	0.190	0.008	0.042	0.032
dC	73	0.211	0.194	0.192	0.199	0.008	0.042	0.034
dC	75	0.171	0.175	0.167	0.171	0.003	0.019	0.029
dC	77	0.210	0.212	0.226	0.216	0.007	0.033	0.037
dC	78	0.202	0.191	0.189	0.194	0.006	0.029	0.033
dC	100	0.176	0.202	0.209	0.196	0.014	0.074	0.034
dC	104	0.210	0.177	0.218	0.202	0.018	0.087	0.035
dC	105	0.189	0.182	0.196	0.189	0.006	0.030	0.032

Nucleoside	Sample ID	Rep 1 mdC/dG (w RSF)	Rep 2 mdC/dG (w RSF)	Rep 3 mdC/dG (w RSF)	Average	Standard Deviation	Coefficient of Variance	% DNA Methylation
dC	106	0.189	0.189	0.194	0.191	0.002	0.013	0.033
dC	107	0.209	0.189	0.230	0.209	0.017	0.082	0.036
dC	108	0.178	0.220	0.187	0.195	0.018	0.094	0.033
dC	109	0.172	0.215	0.225	0.204	0.023	0.112	0.035
dC	110	0.187	0.193	0.220	0.200	0.014	0.072	0.034
dC	111	0.206	0.224	0.226	0.219	0.009	0.042	0.038
dC	113	0.198	0.197	0.233	0.209	0.017	0.080	0.036
dC	114	0.198	0.203	0.222	0.207	0.010	0.050	0.036
dC	116	0.184	0.189	0.202	0.192	0.007	0.039	0.033
dC	117	0.219	0.207	0.214	0.213	0.005	0.023	0.037
dC	119	0.181	0.181	0.212	0.191	0.015	0.076	0.033
dC	120	0.205	0.210	0.238	0.218	0.015	0.068	0.037
dC	121	0.192	0.198	0.219	0.203	0.011	0.057	0.035
dC	122	0.192	0.220	0.233	0.215	0.017	0.081	0.037
dC	123	0.175	0.182	0.196	0.185	0.009	0.048	0.032
dC	124	0.191	0.207	0.226	0.208	0.014	0.069	0.036
dC	126	0.172	0.175	0.189	0.178	0.007	0.042	0.030
dC	127	0.188	0.212	0.213	0.205	0.011	0.056	0.035
dC	128	0.194	0.192	0.202	0.196	0.004	0.022	0.034
dC	129	0.188	0.213	0.206	0.202	0.011	0.053	0.035
dC	132	0.227	0.228	0.201	0.219	0.013	0.057	0.038
dC	133	0.198	0.198	0.223	0.206	0.012	0.058	0.035
dC	137	0.213	0.205	0.211	0.210	0.003	0.015	0.036
dC	138	0.189	0.190	0.192	0.190	0.001	0.007	0.033
dC	140	0.235	0.187	0.190	0.204	0.022	0.109	0.035
dC	142	0.220	0.201	0.195	0.205	0.011	0.052	0.035
dC	143	0.215	0.225	0.176	0.205	0.021	0.104	0.035
dC	145	0.206	0.206	0.166	0.192	0.019	0.097	0.033
dC	146	0.189	0.190	0.212	0.197	0.011	0.053	0.034
dC	147	0.184	0.185	0.185	0.185	0.001	0.004	0.032
dC	150	0.186	0.170	0.192	0.183	0.010	0.052	0.031
dC	151	0.212	0.208	0.184	0.202	0.012	0.061	0.035
dC	154	0.212	0.221	0.199	0.211	0.009	0.044	0.036
dC	155	0.197	0.189	0.221	0.202	0.014	0.067	0.035
dC	156	0.219	0.201	0.233	0.218	0.013	0.060	0.037
dC	157	0.199	0.187	0.201	0.196	0.006	0.033	0.034
dC	158	0.185	0.169	0.185	0.180	0.007	0.042	0.031
dC	159	0.211	0.212	0.199	0.207	0.006	0.029	0.036
dC	160	0.195	0.191	0.181	0.189	0.006	0.031	0.032
dC	162	0.207	0.193	0.213	0.204	0.008	0.042	0.035
dC	163	0.165	0.187	0.184	0.179	0.010	0.055	0.031
dC	164	0.192	0.207	0.198	0.199	0.006	0.032	0.034
dC	165	0.197	0.184	0.212	0.198	0.011	0.057	0.034
dC	166	0.226	0.199	0.212	0.212	0.011	0.051	0.036
dC	167	0.172	0.192	0.201	0.188	0.012	0.062	0.032
dC	168	0.186	0.156	0.200	0.181	0.018	0.102	0.031
dC	169	0.193	0.201	0.191	0.195	0.004	0.021	0.033
dC	171	0.202	0.209	0.194	0.202	0.006	0.030	0.035
dC	172	0.207	0.220	0.229	0.219	0.009	0.042	0.038
dC	173	0.213	0.184	0.190	0.196	0.013	0.065	0.034
dC	174	0.195	0.209	0.201	0.202	0.005	0.027	0.035
dC	175	0.232	0.236	0.217	0.228	0.008	0.034	0.039
dC	176	0.226	0.189	0.183	0.199	0.019	0.097	0.034
dC	177	0.284	0.266	0.200	0.250	0.036	0.144	0.043
dC	200	0.184	0.201	0.193	0.192	0.007	0.036	0.033
dC	201	0.156	0.199	0.214	0.190	0.025	0.130	0.033
dC	202	0.195	0.263	0.227	0.228	0.028	0.122	0.039
dC	203	0.201	0.212	0.213	0.209	0.006	0.027	0.036
dC	205	0.187	0.182	0.201	0.190	0.008	0.042	0.033
dC	206	0.216	0.210	0.237	0.221	0.012	0.053	0.038
dC	207	0.187	0.195	0.181	0.188	0.005	0.029	0.032
dC	208	0.203	0.227	0.222	0.217	0.011	0.049	0.037

Table 3.17. The average snout vent length (SVL), % DNA methylation and Hg concentrations for each site and age class of alligators in Florida used in experiment 3.3.

<i>Location</i>	<i>Age Class</i>	<i>n</i>	<i>% DNA Methylation</i>		<i>Hg Concentration (ng/g)</i>		<i>SVL (cm)</i>	
			<i>Average</i>	<i>Standard Deviation</i>	<i>Average Hg (ng/g)</i>	<i>Standard Deviation</i>	<i>Average</i>	<i>Standard Deviation</i>
Kissimmee	Adult	12	3.211%	0.173%	417.2	222.1	129.2	33.2
	Sub-adult	7	3.441%	0.185%	160.5	41.5	67.5	15.0
Lochloosa	Adult	10	3.438%	0.237%	148.5	71.2	126.0	31.0
	Sub-adult	12	3.582%	0.233%	88.0	31.5	62.5	8.7
St. John's River	Adult	10	3.395%	0.229%	177.7	84.9	133.5	23.6
	Sub-adult	12	3.424%	0.227%	152.9	53.2	70.7	12.8
Trafford	Adult	12	3.349%	0.248%	198.1	79.0	120.9	25.0
	Sub-adult	12	3.286%	0.187%	164.5	57.6	65.3	12.2
WCA2A	Adult	6	3.184%	0.160%	1568.5	642.5	115.6	21.2
	Sub-adult	9	3.444%	0.169%	558.8	282.3	72.5	16.4
WCA3A	Adult	8	3.275%	0.197%	1329.4	712.6	121.3	26.1
	Sub-adult	11	3.521%	0.152%	683.6	450.2	73.7	14.0

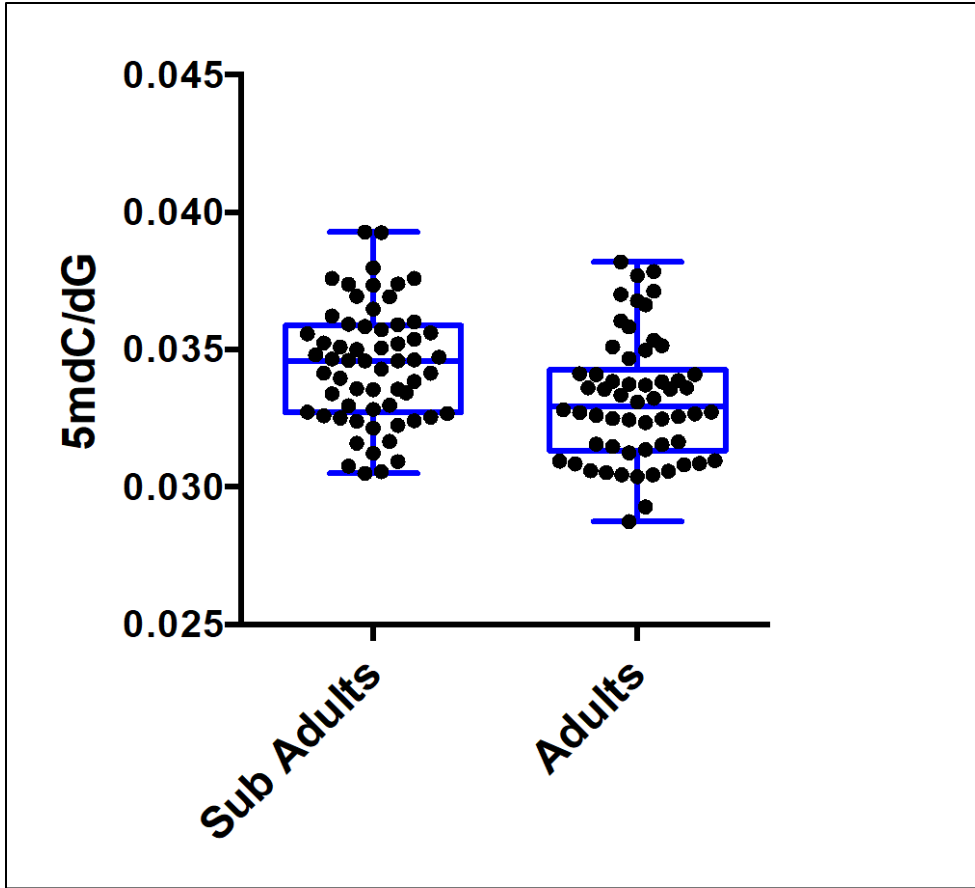


Figure 3.9. Box and whisker plots showing the difference in % DNA methylation (5mdC/dG) between the two age classes of alligators in experiment 3.3.

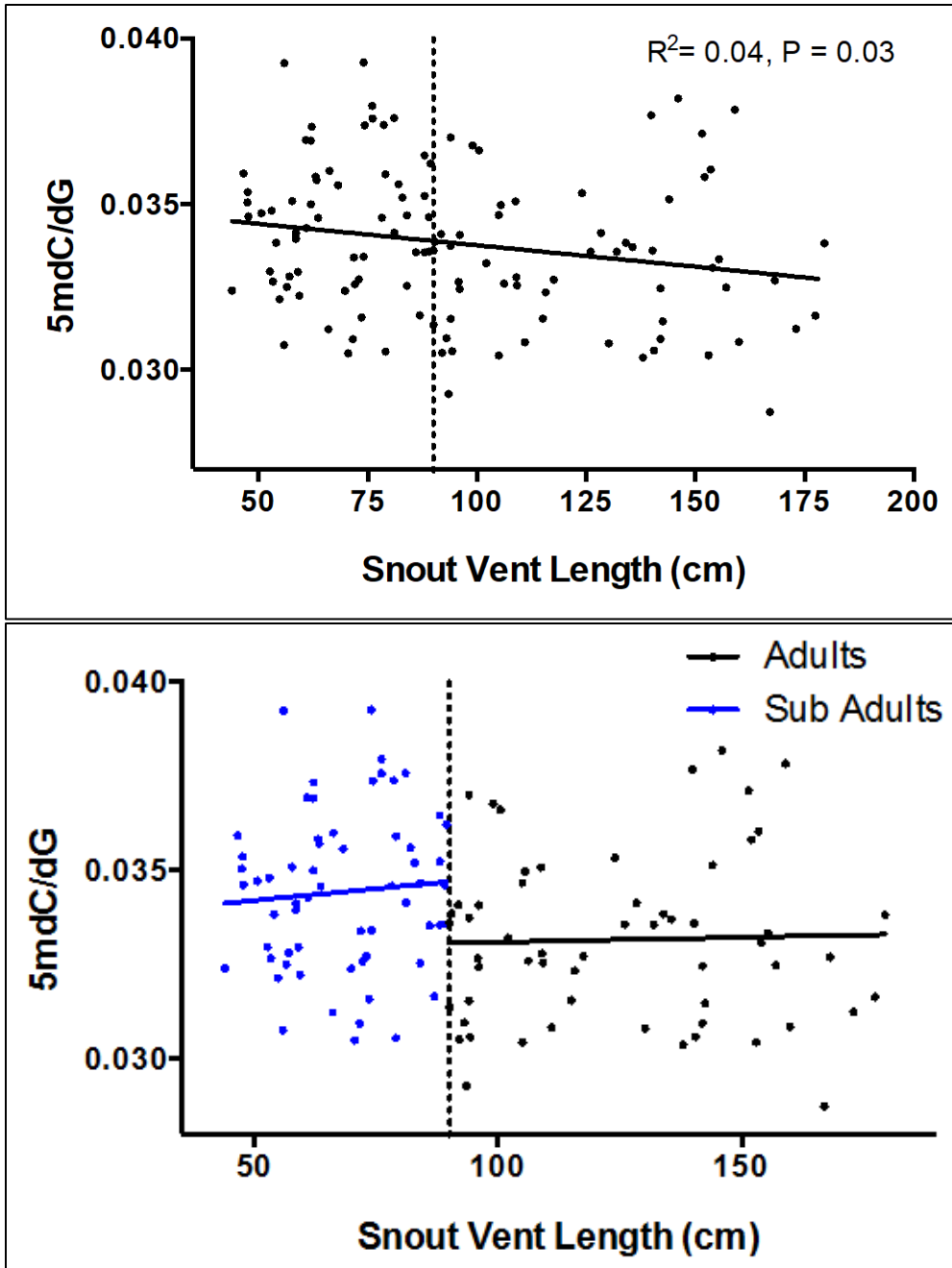


Figure 3.10. Snout-vent length is plotted against 5mdC/dG for each alligator from experiment 3.3. *Top:* Results of a linear regression analysis is reported; dotted line demarcates the sub-adults and adults. *Bottom:* Measures of global DNA methylation and snout-vent length are not correlated within each size class. Dotted line (90 cm) demarcates sub-adults from adults

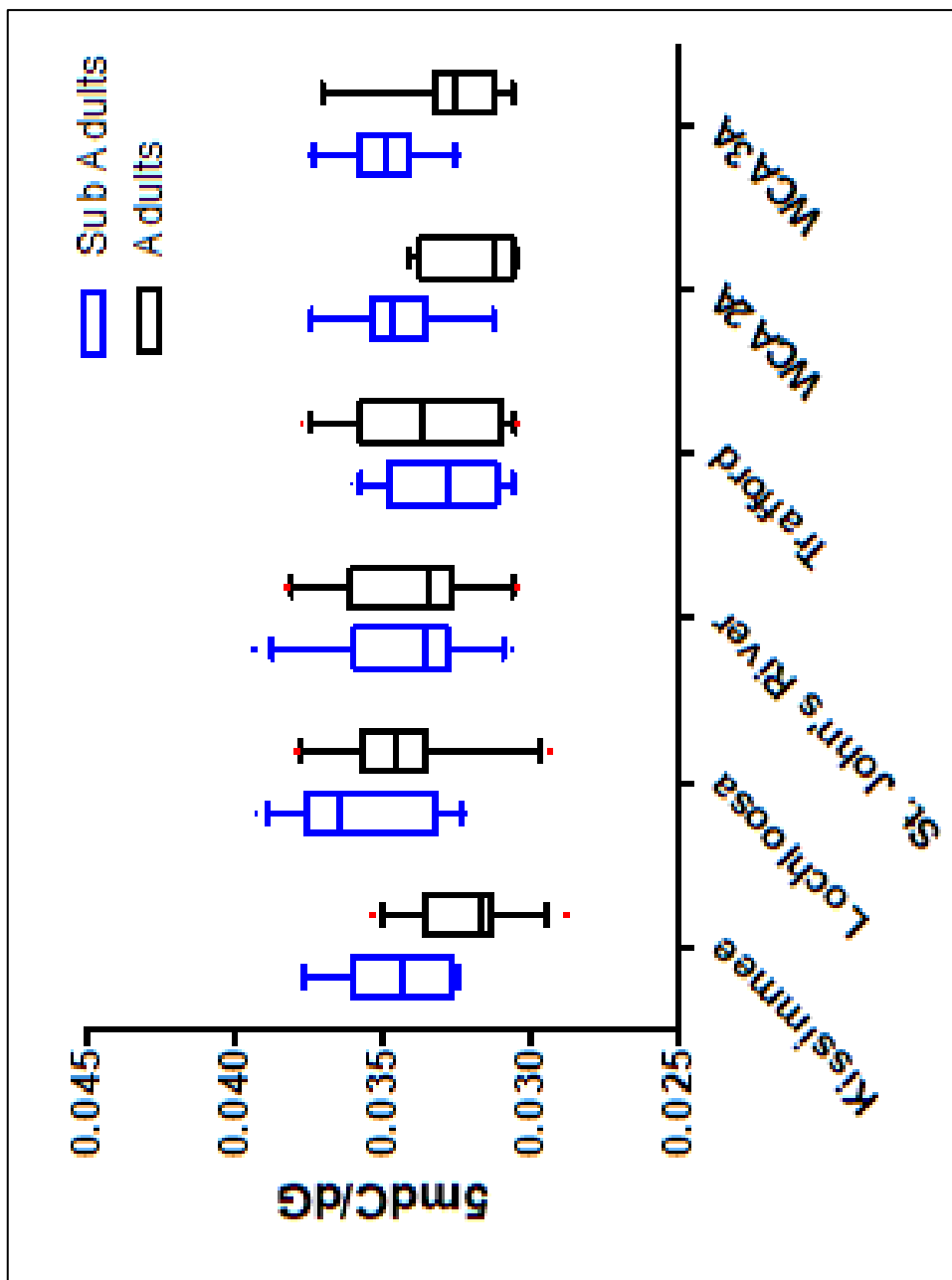


Figure 3.11. Box-and-whisker plots of global DNA methylation measurements across site and age class from the alligator blood samples used in experiment 3.3. Two-way factorial ANOVA indicates the interaction between age class ($p < 0.001$) and location ($p = 0.02$) has a significant impact on DNA methylation.

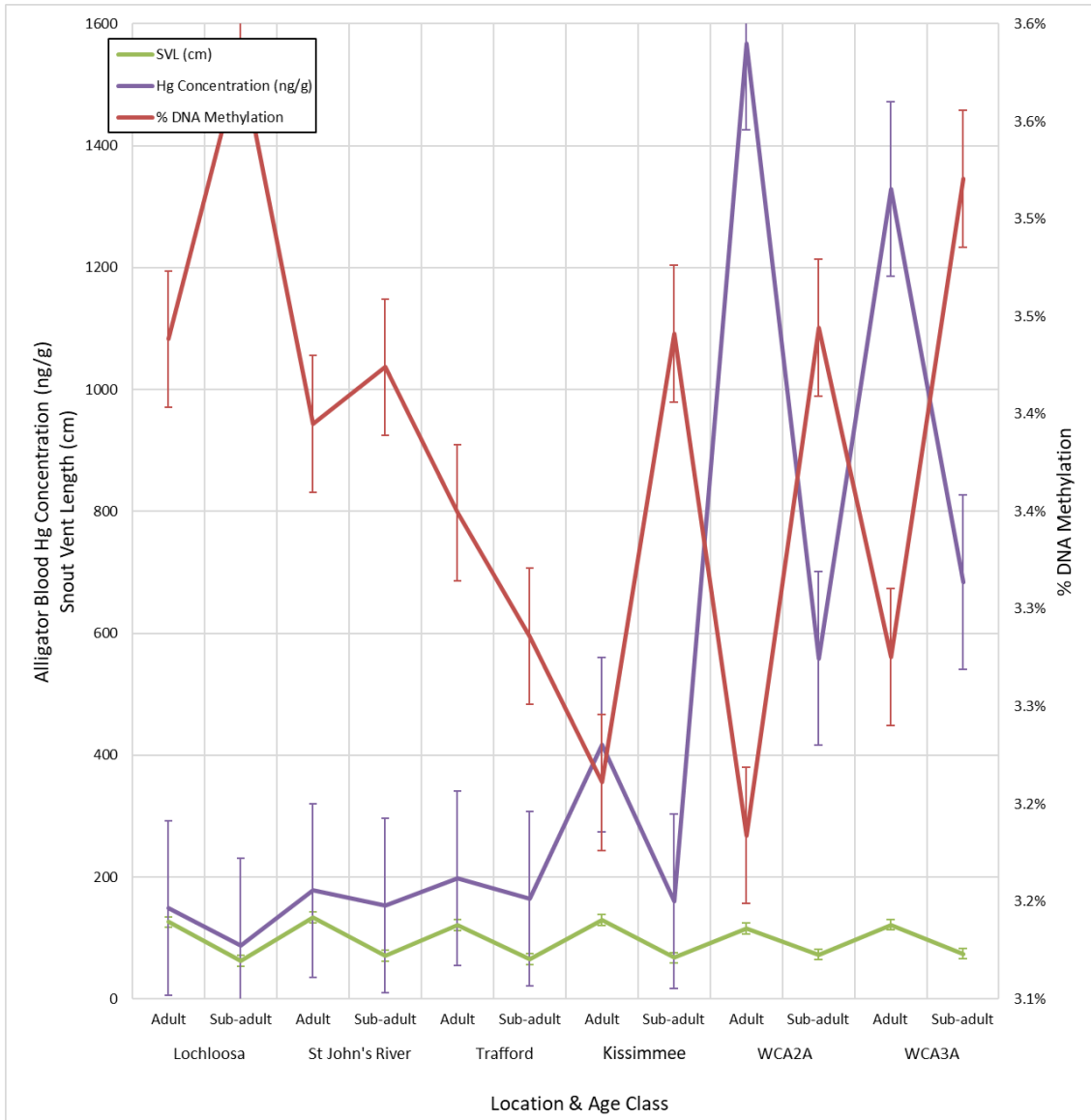


Figure 3.12. The graphical representation of SVL (cm), average mercury concentration, and DNA methylation across all six sites, separated by age class.

DNA methylation loss & mercury concentration

In effort to determine if the loss of DNA methylation is more directly related to mercury exposure or age class, adults and subadults from each site were compared using SVL and DNA methylation (Figure 3.13, 3.14 and 3.15). The sites with low and moderate mercury concentrations have a weak inverse relationship between SVL and % DNA methylation (Figure 3.13 and 3.14). The two Everglades sites (WCA2A and WCA3A), that have the greatest mercury concentrations, both show the lack of a relationship between SVL and % DNA methylation (Figure 3.15).

Since the locations with the highest concentrations of mercury, WCA2A and WCA3A, had weaker R^2 values of the linear comparison between DNA methylation and SVL than the other locations, this suggests that in areas of high mercury contamination SVL is not as important in determining DNA methylation compared to the low mercury sites. To investigate how mercury alone relates to DNA methylation, all alligators were combined and analyzed based on their mercury concentration. We found that decreased global DNA methylation (5mdC/dG) was significantly correlated to increasing mercury concentrations across all alligators by linear regression ($p = 0.04$), and Pearson Product Moment Correlation ($p = 0.03$; correlation coefficient = -0.19; Figure 3.16, top). The relationship between global DNA methylation and mercury levels in different size classes was also examined. This relationship was different across the two size classes ($p < 0.01$), with a significant inverse relationship observed between the larger and sexually mature adult animals ($p = 0.02$, correlation coefficient = -0.30), but not for sub-adults ($p = 0.21$; Figure 3.16, bottom) or between the sexes. Because adults were found to have greater

mercury concentrations than sub-adults, these findings suggest that only at the higher ranges of mercury exposure may affect the global DNA methylation.

To further understand the relationship between high mercury concentrations and global DNA methylation, each site was analyzed independently. The relationship between global DNA methylation and mercury were found to be statistically significant in alligators from Kissimmee ($R^2 = 0.27$; Linear Regression; $p = 0.02$) and WCA2A ($R^2 = 0.28$; Linear Regression; $p = 0.04$), two of the three sites with the greatest mercury concentrations (Figure 3.17). A significant relationship was not observed at WCA3A, which could indicate an environmental dietary difference between the two sites that is resulting in different amounts of DNA methylation over the same range of mercury concentrations, or an effect of different sample sizes at the two Everglades sites (WCA2A = 6 adults & 9 subadults; WCA3A = 8 adults & 10 subadults) (Table 3.17). However, the similarity between the regression lines of the two Everglades sites suggests that the same relationship is present at both locations. The lack of statistical significance at WCA3A may have been due to three anomalously low mercury concentrations in three subadult alligators (gators 158, 159, & 164; mercury concentrations 56 ng/g, 81 ng/g, & 68 ng/g, respectively). These three alligators were smaller subadults (SVL = 68 cm, 44 cm, and 59 cm, respectively), but were not outside the range of SVL measurements that resulted in high mercury concentrations, except gator 159 (SVL = 44 cm), which was 10 cm smaller than the next smallest subadult from WCA3A (gator 131, SVL = 54 cm). The low mercury concentrations in these three alligators could indicate that they are not as old as the other subadults, or have not fully transitioned to the subadult food source from the juvenile food source at this location. Since the lowest mercury concentration in the

subadults from WCA2A was approximately 100 ng/g (gator 152), but had a similar range of SVLs compared to WCA3A, this may be another example of statistical significance not being an adequate metric of environmental effect. As there was no discernible relationship between global DNA methylation and mercury at the three sites with the lowest measured mercury concentrations (Lochloosa, St John's River and Trafford; Figure 3.17), these data further suggest that there is a relationship at WCA3A that cannot be detected statistically using the samples collected in 2012.

Since the adults at the high mercury locations (Kissimmee, WCA2A and WCA3A) have more than double the mercury concentrations of the subadults, we corrected for the DNA methylation differences observed between the age classes. This was done by plotting the average mercury concentration of each site against the ratio of adult to sub-adult global DNA methylation (Figure 3.18). The ratio describes the amount of DNA methylation that was retained between the two age classes, with 100% being no DNA methylation loss. The three sites with the greatest mercury concentrations showed the most dramatic loss of DNA methylation. The adults from WCA3A, WCA2A, and Kissimmee respectively retained only 91%, 92%, and 93% of the global DNA methylation levels measured in their sub-adult counterparts. In contrast, adult alligators living in the three sites with the lowest mercury concentrations retained greater than 95% of the DNA methylation observed in their sub-adult counterparts. The differences in the % of DNA methylation that the adults retained shows that at high mercury sites, a greater DNA methylation loss is experienced than at the lower mercury sites (Figure 3.18). It is important to note that small % changes in global DNA methylation represents a substantially larger change in the proportion of methylated genomic locations where most

DNA methylation takes place (commonly referred to as CpG dinucleotides or “islands”; where cytosine is followed by a guanine in the linear 5' → 3' sequence on one side of the DNA strand, not as a base pair) relative to all cytosine bases across the genome. The small % changes may have been responsible for the lack of statistical significance, but both linear ($R^2 = 0.55$, $p = 0.09$) and 2nd order polynomial regressions ($R^2 = 0.80$, $p = 0.27$) support the hypothesis that adult alligators living in sites with the greatest mercury concentrations undergo the greatest decrease in global DNA methylation (Figure 3.17. 3.18).

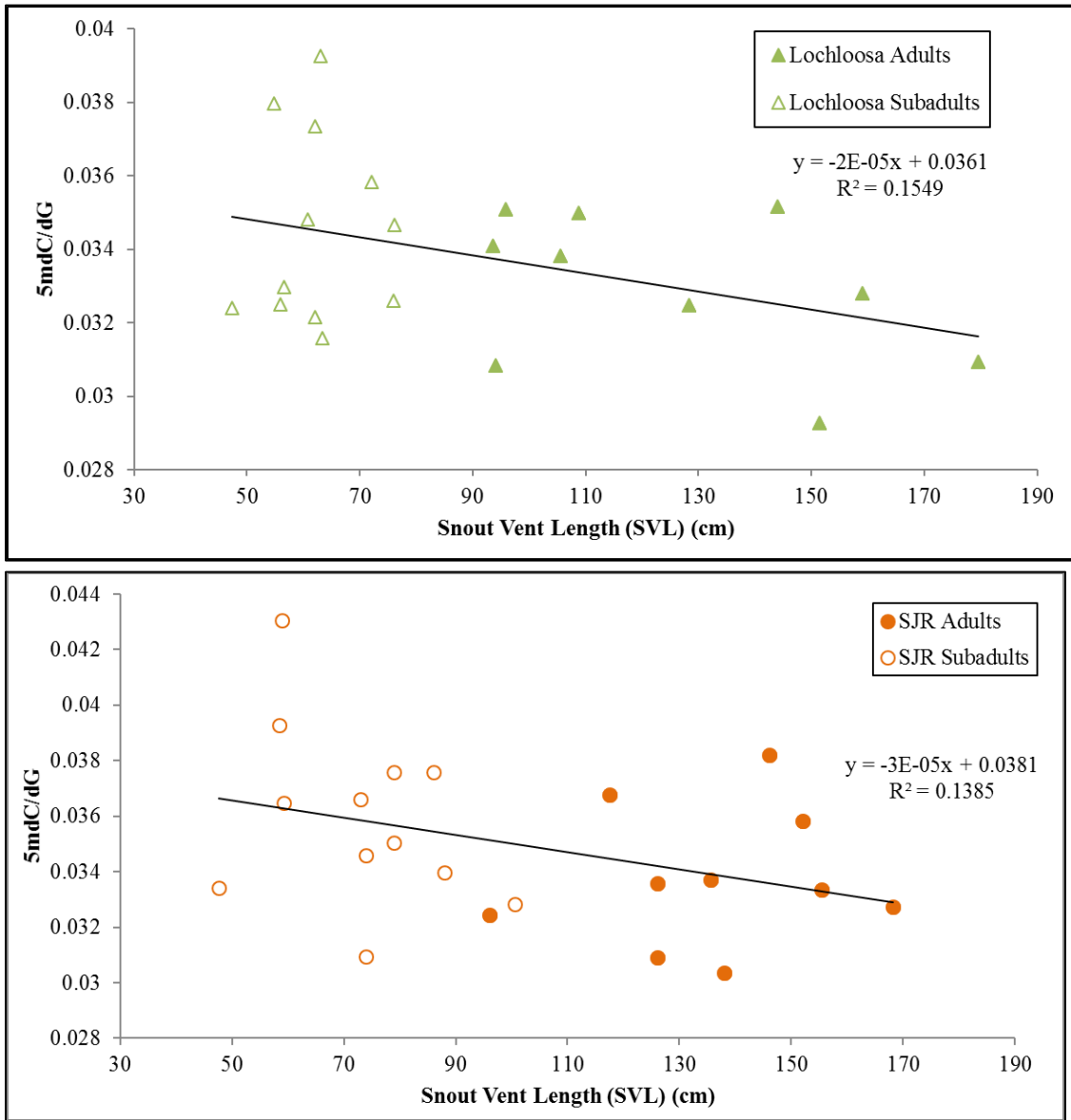


Figure 3.13. The % DNA methylation data plotted against snout vent length (SVL) for alligators from Lake Lochloosa and St. Johns River (SJR), two low Hg sites.

Age class separates the alligators, but the linear equation fits all alligators from that site.

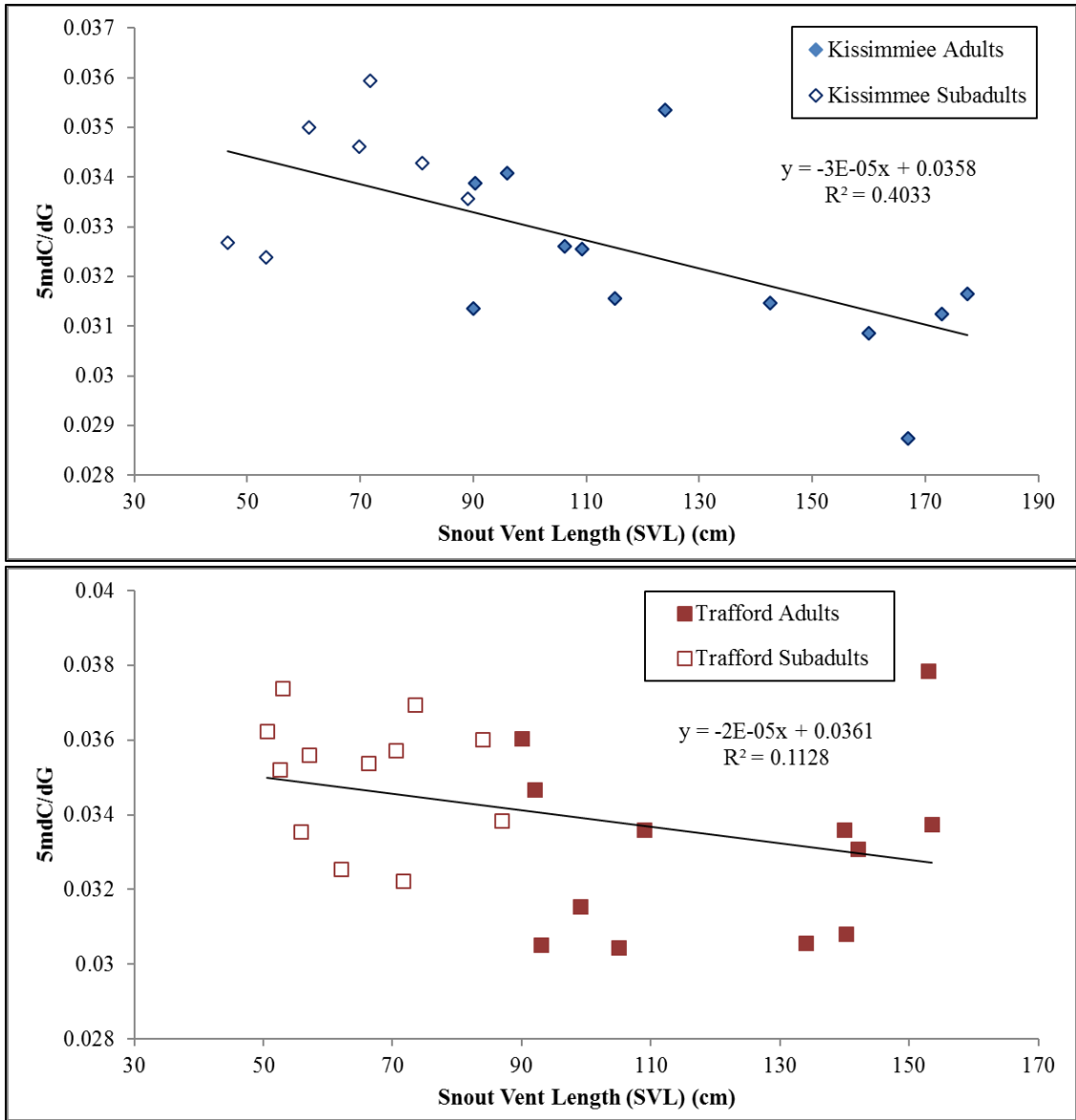


Figure 3.14. The % DNA methylation data plotted against snout vent length (SVL) for alligators from the Lake Kissimmee and Lake Trafford, two moderate Hg sites. The alligators are separated by age class, but the linear equation fits all alligators from that site.

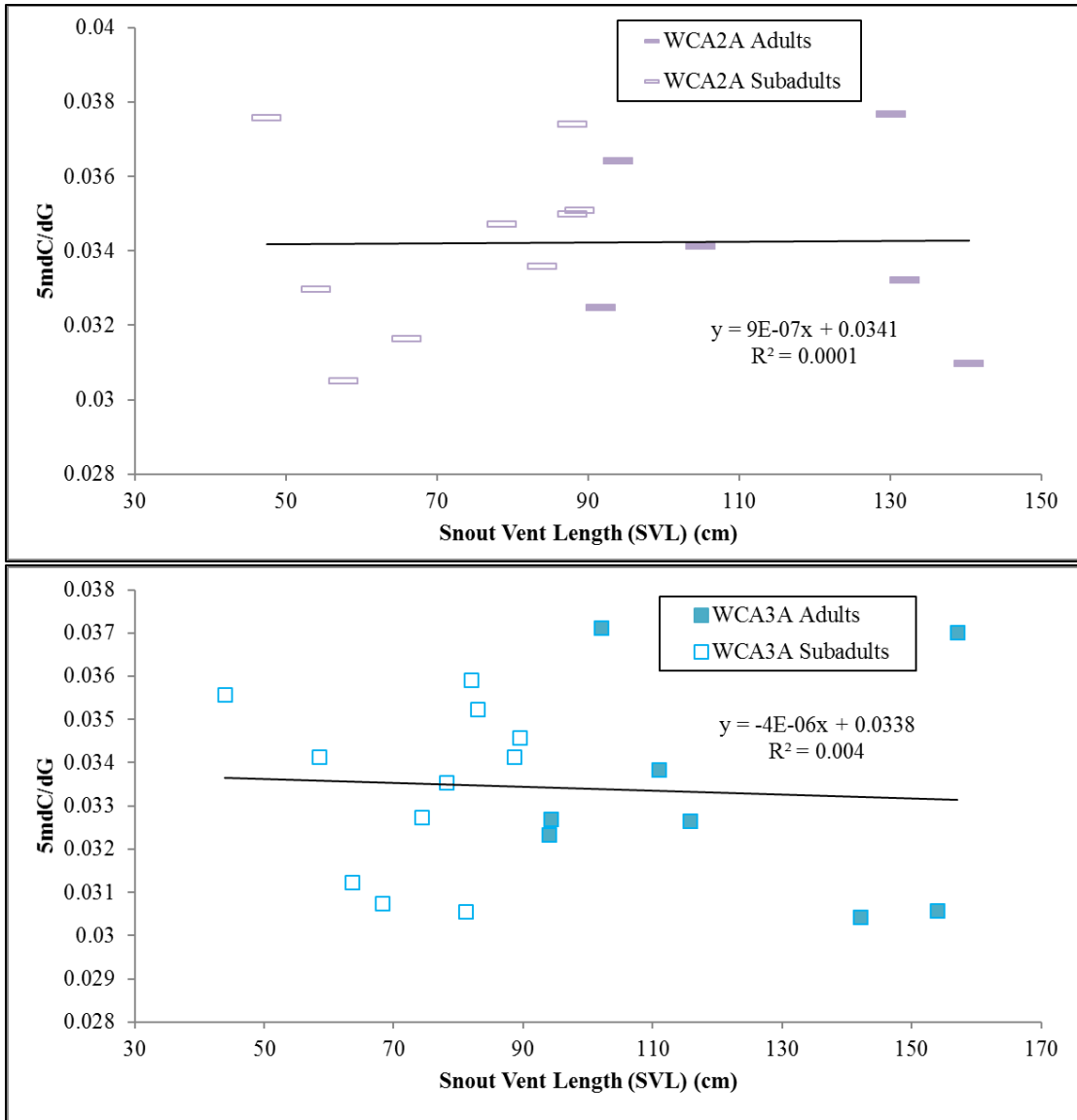


Figure 3.15. The % DNA methylation data plotted against snout vent length (SVL) for alligators from the two Everglades sites, WCA2A and WCA3A, two high Hg sites.

The alligators are separated by age class, but the linear equation fits all alligators from that site.

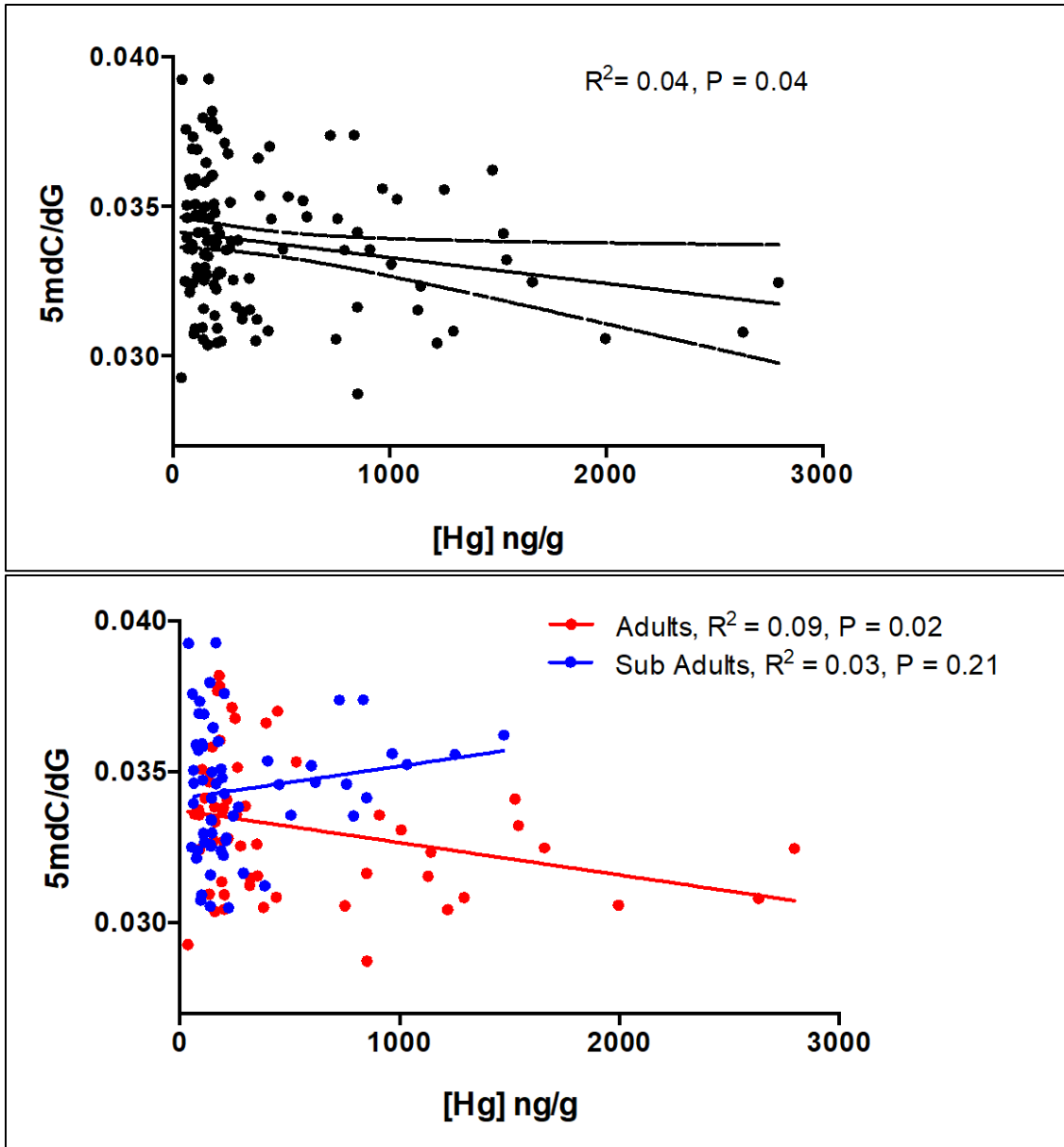


Figure 3.16. Global measures of DNA methylation are correlated to concentrations of Hg. All individuals ($n = 119$) are plotted together (top), and according to age class (bottom). Results of linear regression analyses are reported. Top and bottom lines in the top graph represent 95% confidence intervals.

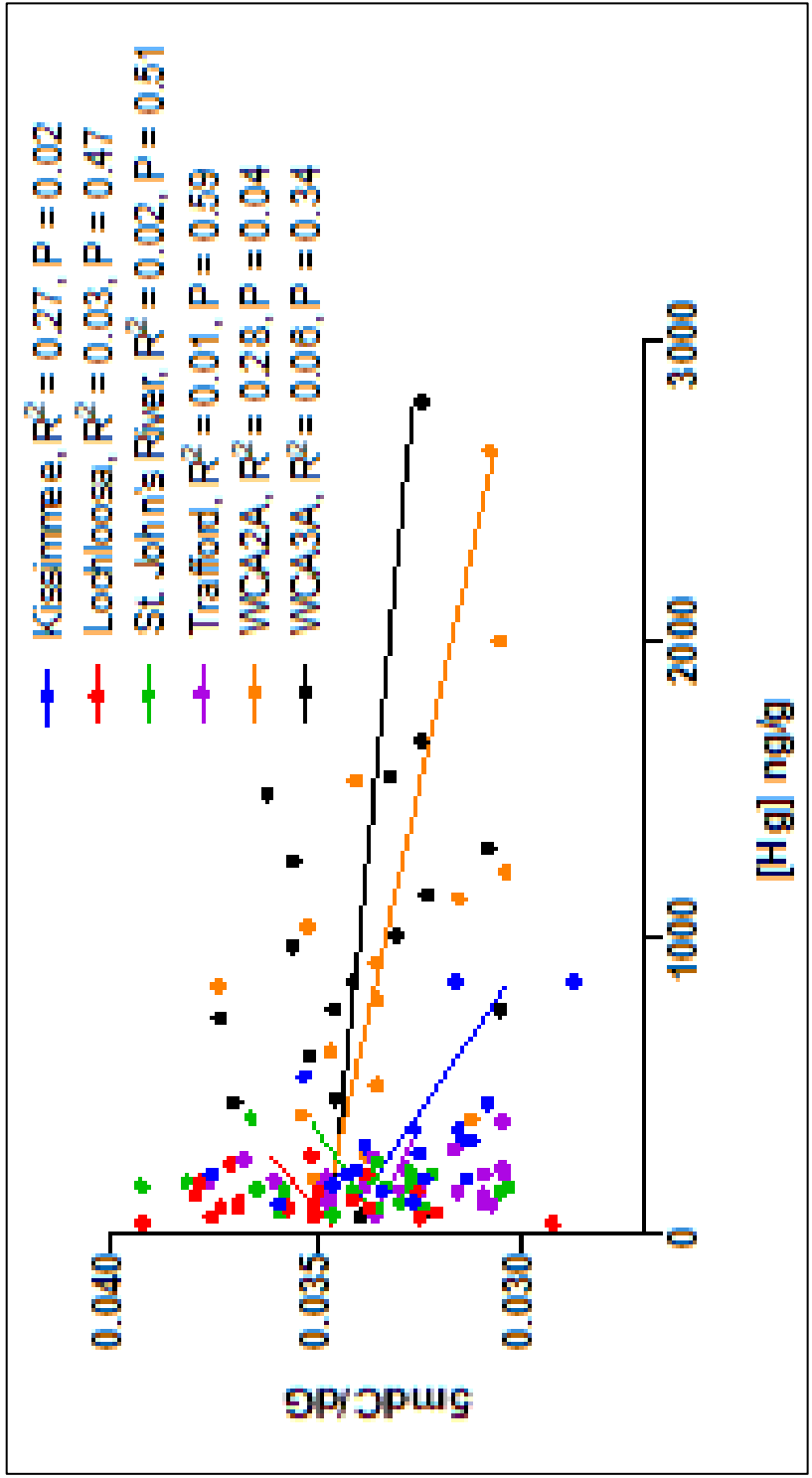


Figure 3.17. Global measures of DNA methylation are correlated to concentrations of Hg. All individuals ($n = 119$) are plotted according to site. Results of linear regression analyses are reported.

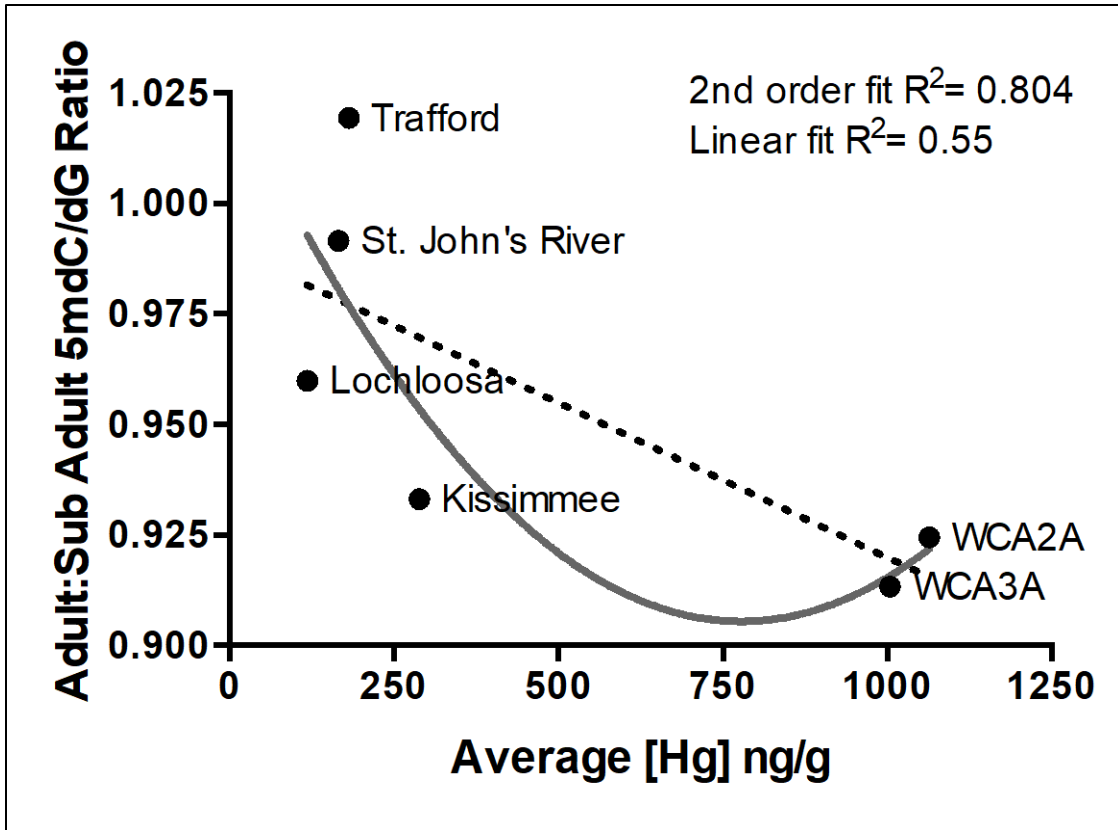


Figure 3.18. The proportion of global DNA methylation in adults relative to sub-adults from the same site is plotted against the mean concentrations of THg measured for each site. R^2 values are reported for regression analyses.

3.3.4. Discussion

Taken together, these data suggest that mercury exposure is one of several variables that are related to changes in global DNA methylation. When age was corrected for, the effect of mercury exposure on DNA methylation became apparent at the high mercury locations (Kissimmee, WCA2A and WCA3A; Figure 3.18). By examining the relationship between small changes in DNA methylation over the wide range of mercury concentrations observed in alligators at the high mercury sites, the small changes were able to be observed. If a range of mercury concentrations that span an order of magnitude (WCA2A and WCA3A; Kissimmee had concentrations that span a 700 ng/g range, but did not reach an order of magnitude) are required to observe DNA methylation changes, this may explain the lack of significant relationship between mercury concentration and DNA methylation in other wildlife studies (99, 101). Pilsner et al. (2010) examined DNA methylation changes related to mercury exposure in a population of polar bears, which are a species known to accumulate high mercury concentrations. Their sample population was heavily skewed towards sub-adults, with an average mercury concentration of 370 ng/g \pm 160 ng/g in brain tissue. Despite their use of brain tissue, which has been shown to have a greater mercury concentrations than blood for many species, the range examined is much smaller than those observed at the Everglades locations, which spanned an order of magnitude (270 ng/g – 2,200 ng/g at WCA2A, 230 ng/g – 2,000ng/g at WCA3A) (67, 94, 349). If small % changes in global DNA methylation are dependent on mercury concentration in polar bears and in brain tissues, our results of small % changes over a wide range of mercury concentrations might explain why a correlation was not observed in their study.

The greater % change in DNA methylation between the adults and subadults in the Everglades (WCA2A and WCA3A) than at the low mercury sites may lend insight into the mercury concentrations that can be managed by the biochemical pathways controlling xenobiotic and oxidative stress response. Mercury is known to cause oxidative stress which leads to hydroxyl adducts binding to DNA and altering DNA methylation maintenance (217, 218, 321, 322, 350). The increased DNA hypomethylation at the Everglades sites may be indicative of this process taking place; where the increased oxidative stress from mercury exposure can be managed at the low mercury locations that experienced less hypomethylation, but at high mercury concentrations the oxidative stress results in hypomethylation (Figure 3.17). However, these data do not investigate the biochemical link between mercury and DNA methylation, so the proposed mechanism of action is speculated based on the literature.

The differences in % DNA methylation across all sites can be further elucidated by considering the drainage systems and ecosystems of each site (Figure 3.8). Lake Trafford, which is the only site to undergo DNA hypermethylation when corrected for age, is vastly different from the other sites in that it is far removed from the other sampling location, has a completely separate drainage system, and the environment at Trafford is different than the other sites (Figure 3.17). Trafford is a very deep circular lake with little incline from the shore, whereas the other sites have sloping inclines from the bank and have a variety of depths and bathymetric features. The diet that the animals at Trafford are exposed to is likely different from the diets at all the other similar sites; these dietary differences could be providing the resident alligators with the necessary biochemical components to alleviate oxidative stress much more efficiently than the other sites. The

other five sites are similar in their features, three of which have a connected drainage system. Lochloosa and St. John's River have separate drainage systems and the alligators experience different amounts of DNA hypomethylation while their mercury concentrations are similar (Figure 3.8, 3.17). These differences could be the effects of different diets, or slightly different environmental conditions between Lochloosa and St. John's River, but both groups of alligators experienced low %s of DNA hypomethylation. The remaining three sites, Kissimmee, WCA2A and WCA3A, area all part of one large drainage system (Figure 3.8). Lake Kissimmee has higher mercury concentrations than the three aforementioned locations, and a greater amount of DNA hypomethylation (Figure 3.17, 3.18). Whether there is a resource that is depleted, or if the mercury concentrations are becoming great enough for the biochemical pathways to be inefficient at detoxification, or a combination of the two, there is a change at Kissimmee that is not observed in the low mercury locations. Kissimmee is at the beginning of the drainage system that include the Everglades sites (WCA2A and WCA3A), so any resource that is depleted at Kissimmee will only continue to be depleted throughout the drainage system to the Everglades. The alligators in the Everglades are subject to higher mercury concentrations than any other sites measured here due to the favorable environmental parameters for methylation of mercury, the increased mercury combined with a potential depleted food source, or nutrient, that aids in the biochemical detoxification process could be what lead to the greater amount of DNA hypomethylation at both of these sites (Figure 3.17).

These data support the hypothesis that increased mercury can lead to DNA hypomethylation, with the relationship observed in adult alligators. While the

mechanism of mercury induced oxidative stress leading to DNA hypomethylation is tangible based on the literature and the relationship observed here, this may not be the only factor responsible for the relationship. There is also the potential for transgenerational epigenetic inheritance and/or genomic mutations that result from generations of alligators living in high mercury environments leading to DNA hypomethylation at the Everglades sites. Directly testing transgenerational inheritance in wild populations is incredibly difficult, so examining this potential confounding factor without the ability to dose animals in the laboratory, is unlikely. However, captive juvenile alligators have been shown to have hypermethylated DNA compared to wild adults (3). While this relationship is tenuous based on many different factors between the two examined populations, the hypermethylated DNA of the juveniles suggests that epigenetic inheritance is not the source of DNA hypomethylation. To further investigate the potential confounding factor of epigenetic inheritance, the population of captive juvenile alligators reared by Parrott, *et al.* (3) will be used in the following experiment.

3.4. Using captive American alligators to elucidate the relationship between diet & DNA methylation

3.4.1. Introduction

The previous experiment elucidated the inverse relationship between mercury concentration and DNA methylation in wild American alligators. However, since the relationship was observed at locations with historically high mercury concentrations throughout the ecosystem, determining if the epigenetic differences occurred during the lifespan and exposure of the alligators measured, or if the DNA methylation changes are the result of heritable genomic mutations from adults persisting in a highly contaminated environment was not possible (351, 352). Parrott, *et al.* (3) observed that wild adult alligators had hypomethylated DNA compared to juveniles that were collected as eggs and captively reared, from the same location. While the high quality captive diet may have had an effect on this result, the captive juvenile alligator samples provide the opportunity to examine DNA methylation across a standardized diet in relation to mercury concentrations, which was a confounding factor of the site specific relationship observed in the previous experiment.

3.4.2. Experiment specific methods

Sample collection

In June of 2010 Parrott, *et al.* (3) collected alligator eggs shortly after oviposition from ten nests at Lake Woodruff, FL; six nests at Lake Apopka, FL, and ten nests at Yawkey Wildlife Center, SC. An egg from each nest was opened upon returning to Hollings Marine Laboratory to determine developmental stage, yolk from this egg was pipetted into a Falcon tube and stored at -20 °C for future analysis, then all eggs were

incubated on damp sphagnum moss at 30 °C until hatching, when an ID tag was applied to the rear foot webbing. Hatchlings were then housed in flow through tanks and fed a commercial crocodilian diet (Mazrui) until reaching 1 kg in body weight. When the hatchlings weighed 1 kg, a blood sample was collected, and pelleted to separate the erythrocyte fraction, which was preserved with RNAlater and stored at -20 °C until analysis.

DNA methylation analysis

The DNA methylation analysis was conducted by Parrott, *et al.* (3) following the method described in section 3.2, which he helped design. Ben Parrott provided the DNA methylation data collected from the juvenile erythrocyte and ovary samples, so they could be paired to the mercury analysis conducted in this experiment (Figure 3.19).

Mercury analysis

The mercury analysis of these samples was conducted following the method detailed in section 2.2. Briefly, the erythrocyte ($n = 136$) samples were thawed and aliquoted for analysis. The mass fraction of total mercury was determined in one aliquot (100 μ L) of alligator whole blood with a direct mercury analyzer (DMA-80, Milestone, Shelton, CT). NIST Standard Reference Material (SRM) 3133, Mercury Standard Solution was used for external calibration. NIST SRM 955c Level 2, Toxic Metals in Caprine Blood was used as a control material for the erythrocyte samples, which is certified for total mercury at 4.95 ± 0.75 ng/g. Procedural blanks were analyzed by use of an empty sample vessel, and concurrently, field blanks were analyzed by use of Milli-Q water. If blanks were found to be above the detection limit, the samples were blank corrected.

Statistical analysis

All total mercury concentration of the alligator erythrocyte samples data failed to meet the assumptions of normality and homoscedasticity based on the Shapiro-Wilk Goodness of Fit Test and Levene's Test for Unequal Variances. Spearman's Correlations was used to compare the mercury data to the DNA methylation data provided by Ben Parrott. All statistical analyses were conducted using JMP 11 (SAS, Cary, NC). Statistical significance was determined by $p < 0.05$ for all tests.

3.4.3. Results & Discussion

The replicated measurements of the control material, NIST SRM 955c Level 2, had an average value of $5.42 \text{ ng/g} \pm 0.19 \text{ ng/g}$, falling within the certified confidence interval (4.2 - 5.6 ng/g) (Table 3.18).

The average mercury concentrations in the 2011 "Grow Out" hatchlings erythrocytes from Apopka, Woodruff and Yawkey were $13.0 \pm 1.9 \text{ ng/g}$, $13.6 \pm 3.6 \text{ ng/g}$, and $14.7 \pm 4.2 \text{ ng/g}$, respectively (Table 3.19, 3.20; Figure 3.20). The yolk mercury measurements from the same eggs (from Chapter 2) are plotted alongside the erythrocyte data for comparison (Figure 3.20). The variation that was observed in the yolk samples, demonstrated by the standard deviation, is reduced in the erythrocytes from 18 months post-hatch (Table 3.20, Figure 3.20). The reduction in mercury between these two tissues could be due to less mercury being incorporated into the embryo from the yolk than was present in the yolk, and/or if the captive diet standardized the mercury concentrations in the erythrocytes after 18 months.

When the individual erythrocyte mercury measurements were compared to the erythrocyte DNA methylation data from Parrott, *et al.* (3) using the Spearman correlation,

there was no statistical relationship ($p = 0.32$; $\rho = -0.10$) (Figure 3.21, left). However, when the erythrocyte mercury measurements were compared to the DNA methylation data from the ovary samples, there was a significant relationship ($p = 0.003$; $\rho = 0.27$) (Figure 3.21, right). When each site and tissue were separated and compared using the Spearman correlation, only the ovary samples from Yawkey, SC were significantly related to the erythrocyte mercury concentration ($p = 0.001$; $\rho = 0.45$).

These results were unexpected, but may lend insight to the effects of epigenetic inheritance and standardized diet on DNA methylation. The standardized diet that the hatchlings were fed removed the variation in mercury concentration that was observed from the same nests using egg yolk in Chapter 2 (Table 3.20). The standardized diet, that likely included some mercury based on the very similar concentrations found in the erythrocytes of hatchlings from the three sites, also standardized the DNA methylation in their erythrocyte samples. Measuring the mercury in the captive diet would have elucidated this effect, but no remaining food pellets remained after the study was completed, and the batches of captive diet produced vary depending on which fish are used in their production (Mazrui). However, it appears that this was not the case for the ovary samples, which still display different DNA methylation. The significant relationship observed between the ovary samples and the mercury concentration in the erythrocytes from Yawkey may suggest two things; 1-the wider range of mercury concentrations in both the erythrocyte and yolk samples from this site allow the observation of the changing methylation in neonates, similar to what was observed in the wild adults; and 2- DNA methylation in the internal tissues does not change as quickly as in the erythrocytes when diet is standardized. The ovary samples may be indicative of the

DNA methylation that was inherited from the nesting female, or could be indicative the mercury concentrations in the yolk that fed the embryo during development (the data from Chapter 2 suggest that mercury is transferred from the nesting female).

To test this theory, the average nesting females blood mercury concentration was compared to the average DNA methylation observed in the juvenile tissue samples from corresponding nests ($n = 4$ pairs). Surprisingly, the juvenile erythrocyte DNA methylation did not appear to be dependent on the nesting females' blood concentration when plotted, but the ovary methylation did (Figure 3.21). Despite the small sample sizes, an exploratory correlation analysis revealed that 98% of the variation in the average ovary methylation values can be explained by the mercury concentration measured in their nesting female's blood (correlation = 0.98, $p = 0.01$). While this comparison is based on a few pairs of nesting females and juvenile tissue measurements, the relationship is interesting and follows what we observed in Chapter 2, that all eggs from the same nest have very similar mercury concentrations that are related to the nesting female's concentration, which could also lead to similar DNA methylation values.

These data demonstrate that diet plays a large role in the DNA methylation observed in alligator blood samples, but may exert less of an influence on the DNA methylation of their internal organs. The mercury measurements in yolk samples from the juveniles' nests show that Yawkey had a wider range of mercury concentrations *in ovo*, and that wider range is still reflected in the erythrocyte samples, but is becoming very narrow after consuming a standardized diet with a consistent mercury concentration for 18 months. The relationship between the DNA methylation of the ovary samples and the mercury concentration of the erythrocytes may be elucidating the change in methylation

that is reflective of the dietary switch from yolk to the standardized hatchling diet. The effect of diet is supported by the tight relationship between the juvenile ovary methylation with the nesting females' mercury concentration, and the lack of relationship between the juvenile erythrocyte methylation and the nesting females' mercury concentrations (Figure 3.21). However, without mercury measurements from the ovary samples, as well as larger sample sizes for the comparison with the nesting females, the information gleaned from these results is purely speculative. The relationship between DNA methylation, mercury, and diet is investigated further in the following experiment, using a standardized diet with varying concentrations of mercury.

These data provided by this experiment raise more questions than they answer, since not all tissue DNA methylation data can be matched to mercury measurements of the same tissue, and small sample sizes plague the nesting female comparison. The relationships speculated in this section could be clarified by determining the mercury concentration of the ovary samples, as well as analyzing an earlier hatchling time point erythrocyte sample, between developmental stage 19 and 18 months post-hatch, for both DNA methylation and mercury concentration. These samples would provide the ability to observe a step-wise change in both parameters, if it is occurring. Comparison of the earlier time point to the nesting females' blood concentration may also elucidate the role diet plays in changing DNA methylation.

Table 3.18. The individual measurements of the NIST SRM 955c Level 2 used in this experiment. The average value was 5.42 ng/g \pm 0.19 ng/g, falling within the certified confidence interval (4.2 - 5.6 ng/g).

SRM 955c Level 2 Replicates	[Hg] mg/kg
SRM 955c Level 2 run 01	5.15
SRM 955c Level 2 run 02	4.94
SRM 955c Level 2 run 03	5.26
SRM 955c Level 2 run 04	5.44
SRM 955c Level 2 run 05	5.07
SRM 955c Level 2 run 06	5.74
SRM 955c Level 2 run 07	5.49
SRM 955c Level 2 run 08	5.45
SRM 955c Level 2 run 09	5.38
SRM 955c Level 2 run 10	5.36
SRM 955c Level 2 run 11	5.55
SRM 955c Level 2 run 12	5.39
SRM 955c Level 2 run 13	5.35
SRM 955c Level 2 run 14	5.52
SRM 955c Level 2 run 15	5.4
SRM 955c Level 2 run 16	5.55
SRM 955c Level 2 run 17	5.52
SRM 955c Level 2 run 18	5.57
SRM 955c Level 2 run 19	5.51
SRM 955c Level 2 run 20	5.51
SRM 955c Level 2 run 21	5.36
SRM 955c Level 2 run 22	5.77
Average	5.42
Standard Deviation	0.19
%RSD	3.56

Table 3.19. The mercury measurements for all erythrocyte (RBC) and ovary tissue, listed with the corresponding DNA methylation value provided by Parrott, *et al.* (3).

Egg ID	Site	TISSUE	5mdC/dG	RBC [Hg] ng/g
AP-01-05	APOPKA	RBCs	0.01806	10.9
AP-05-05	APOPKA	RBCs	0.01926	10.6
AP-05-24	APOPKA	RBCs	0.02627	11.8
AP-05-39	APOPKA	RBCs	0.0171	12.9
AP-02-45	APOPKA	RBCs	0.02231	11.4
AP-02-12	APOPKA	RBCs	0.01777	12.0
AP-03-27	APOPKA	RBCs	0.01402	14.0
AP-01-11	APOPKA	RBCs	0.02139	13.5
AP-05-46	APOPKA	RBCs	0.02177	14.1
AP-02-46	APOPKA	RBCs	0.01897	12.7
AP-03-41	APOPKA	RBCs	0.02165	15.1
AP-06-49	APOPKA	RBCs	0.01728	16.8
AP-06-34	APOPKA	RBCs	0.01441	15.8
AP-06-27	APOPKA	RBCs	0.02091	15.5
AP-02-39	APOPKA	RBCs	0.01352	14.2
AP-03-47	APOPKA	RBCs	0.01805	13.9
AP-04-12	APOPKA	RBCs	0.01975	14.8
AP-04-08	APOPKA	RBCs	0.02345	15.6
AP-06-43	APOPKA	RBCs	0.0218	14.0
AP-06-40	APOPKA	RBCs	0.0124	12.6
AP-04-18	APOPKA	RBCs	0.02014	12.0
AP-06-06	APOPKA	RBCs	0.02377	11.8
AP-02-01	APOPKA	RBCs	0.02819	12.1
AP-05-21	APOPKA	RBCs	0.01901	11.4
AP-04-14	APOPKA	RBCs	0.01632	11.6
AP-04-10	APOPKA	RBCs	0.01888	11.9
AP-03-13	APOPKA	RBCs	0.02087	8.6
WO-18-05	WOODRUFF	RBCs	0.0143	10.6
WO-09-11	WOODRUFF	RBCs	0.01805	10.3
WO-15-05	WOODRUFF	RBCs	0.02067	10.5
WO-07-06	WOODRUFF	RBCs	0.0217	10.0
WO-15-13	WOODRUFF	RBCs	0.02152	11.1
WO-15-08	WOODRUFF	RBCs	0.01957	11.0
WO-19-07	WOODRUFF	RBCs	0.02515	11.1
WO-07-38	WOODRUFF	RBCs	0.01993	10.5

Egg ID	Site	TISSUE	5mdC/dG	RBC [Hg] ng/g
WO-03-05	WOODRUFF	RBCs	0.02329	11.7
WO-15-20	WOODRUFF	RBCs	0.01887	12.1
WO-03-30	WOODRUFF	RBCs	0.02112	12.0
WO-09-18	WOODRUFF	RBCs	0.02438	12.2
WO-01-08	WOODRUFF	RBCs	0.02741	11.6
WO-07-21	WOODRUFF	RBCs	0.02405	13.1
WO-06-31	WOODRUFF	RBCs	0.01566	28.0
WO-18-01	WOODRUFF	RBCs	0.0239	19.7
WO-06-16	WOODRUFF	RBCs	0.0189	22.3
WO-03-35	WOODRUFF	RBCs	0.01662	13.8
WO-19-26	WOODRUFF	RBCs	0.0171	14.4
WO-19-11	WOODRUFF	RBCs	0.01381	14.6
WO-07-45	WOODRUFF	RBCs	0.01286	13.3
WO-01-24	WOODRUFF	RBCs	0.02356	15.3
WO-10-34	WOODRUFF	RBCs	0.02459	15.0
WO-20-10	WOODRUFF	RBCs	0.02059	15.9
WO-10-22	WOODRUFF	RBCs	0.02254	15.3
WO-10-09	WOODRUFF	RBCs	0.02219	14.5
WO-07-31	WOODRUFF	RBCs	0.02271	15.3
WO-06-35	WOODRUFF	RBCs	0.01953	17.1
WO-18-03	WOODRUFF	RBCs	0.01991	8.7
WO-01-31	WOODRUFF	RBCs	0.01482	13.2
WO-06-28	WOODRUFF	RBCs	0.013	11.4
WO-20-19	WOODRUFF	RBCs	0.01682	13.8
WO-20-22	WOODRUFF	RBCs	0.02256	15.9
WO-06-03	WOODRUFF	RBCs	0.02317	13.2
WO-01-23	WOODRUFF	RBCs	0.01567	16.0
WO-09-16	WOODRUFF	RBCs	0.02725	12.6
WO-10-37	WOODRUFF	RBCs	0.02222	18.2
WO-08-03	WOODRUFF	RBCs	0.01795	12.2
WO-20-01	WOODRUFF	RBCs	0.02059	14.8
WO-01-12	WOODRUFF	RBCs	0.02144	14.3
WO-09-08	WOODRUFF	RBCs	0.02357	13.7
YK-17-24	YAWKEY	RBCs	0.02709	12.7
YK-16-04	YAWKEY	RBCs	0.02151	12.6
YK-17-14	YAWKEY	RBCs	0.01369	24.0
YK-17-46	YAWKEY	RBCs	0.02097	24.8
YK-09-49	YAWKEY	RBCs	0.01798	24.7
YK-3B-11	YAWKEY	RBCs	0.02332	24.3
YK-04-39	YAWKEY	RBCs	0.01877	26.4
YK-16-31	YAWKEY	RBCs	0.01924	14.4
YK-10-29	YAWKEY	RBCs	0.02144	13.6
YK-16-29	YAWKEY	RBCs	0.02176	14.2
YK-10-28	YAWKEY	RBCs	0.01958	14.7
YK-09-56	YAWKEY	RBCs	0.02394	13.7
YK-10-05	YAWKEY	RBCs	0.0211	14.0
YK-04-34	YAWKEY	RBCs	0.01851	14.3
YK-09-12	YAWKEY	RBCs	0.01869	15.1
YK-16-35	YAWKEY	RBCs	0.01807	14.4
YK-17-23	YAWKEY	RBCs	0.01421	12.4
YK-10-02	YAWKEY	RBCs	0.01817	14.4
YK-09-06	YAWKEY	RBCs	0.01773	14.8
YK-04-45	YAWKEY	RBCs	0.01867	16.0
YK-3B-03	YAWKEY	RBCs	0.01197	15.6
YK-13-15	YAWKEY	RBCs	0.02447	15.3
YK-05-07	YAWKEY	RBCs	0.0202	15.5
YK-3b-47	YAWKEY	RBCs	0.01379	17.6
YK-3B-34	YAWKEY	RBCs	0.01853	16.2
YK-13-34	YAWKEY	RBCs	0.02409	16.1
YK-3a-22	YAWKEY	RBCs	0.02051	16.2
YK-04-22	YAWKEY	RBCs	0.0216	11.7
YK-3B-17	YAWKEY	RBCs	0.01579	16.6
AP-01-05	APOPKA	ovary	0.02994	10.9
AP-05-05	APOPKA	ovary	0.01754	10.6
AP-05-24	APOPKA	ovary	0.02356	11.8
AP-05-39	APOPKA	ovary	0.03043	12.9
AP-02-45	APOPKA	ovary	0.02646	11.4
AP-02-12	APOPKA	ovary	0.02788	12.0
AP-03-27	APOPKA	ovary	0.03215	14.0
AP-01-11	APOPKA	ovary	0.02891	13.5
AP-05-46	APOPKA	ovary	0.02856	14.1
AP-02-46	APOPKA	ovary	0.02614	12.7
AP-03-41	APOPKA	ovary	0.02737	15.1
AP-06-49	APOPKA	ovary	0.0297	16.8

Egg ID	Site	TISSUE	5mdC/dG	RBC [Hg] ng/g
AP-06-34	APOPKA	ovary	0.02079	15.8
AP-06-27	APOPKA	ovary	0.02719	15.5
AP-03-47	APOPKA	ovary	0.0195	13.9
AP-04-12	APOPKA	ovary	0.02325	14.8
AP-04-08	APOPKA	ovary	0.02791	15.6
AP-06-43	APOPKA	ovary	0.02467	14.0
AP-06-40	APOPKA	ovary	0.02386	12.6
AP-04-18	APOPKA	ovary	0.02431	12.0
AP-06-06	APOPKA	ovary	0.02783	11.8
AP-02-01	APOPKA	ovary	0.02824	12.1
AP-05-21	APOPKA	ovary	0.02783	11.4
AP-04-14	APOPKA	ovary	0.02175	11.6
AP-04-10	APOPKA	ovary	0.02603	11.9
AP-03-13	APOPKA	ovary	0.03161	8.6
WO-18-05	WOODRUFF	ovary	0.01901	10.6
WO-09-11	WOODRUFF	ovary	0.02233	10.3
WO-15-05	WOODRUFF	ovary	0.0216	10.5
WO-07-06	WOODRUFF	ovary	0.02092	10.0
WO-15-13	WOODRUFF	ovary	0.02109	11.1
WO-15-08	WOODRUFF	ovary	0.02159	11.0
WO-19-07	WOODRUFF	ovary	0.0262	11.1
WO-07-38	WOODRUFF	ovary	0.02033	10.5
WO-03-05	WOODRUFF	ovary	0.02572	11.7
WO-15-20	WOODRUFF	ovary	0.02903	12.1
WO-03-30	WOODRUFF	ovary	0.02209	12.0
WO-09-18	WOODRUFF	ovary	0.02611	12.2
WO-01-08	WOODRUFF	ovary	0.01971	11.6
WO-07-21	WOODRUFF	ovary	0.03253	13.1
WO-06-31	WOODRUFF	ovary	0.02106	28.0
WO-18-01	WOODRUFF	ovary	0.02926	19.7
WO-06-16	WOODRUFF	ovary	0.02253	22.3
WO-03-35	WOODRUFF	ovary	0.02198	13.8
WO-19-26	WOODRUFF	ovary	0.0302	14.4
WO-19-11	WOODRUFF	ovary	0.03	14.6
WO-07-45	WOODRUFF	ovary	0.02774	13.3
WO-01-24	WOODRUFF	ovary	0.02922	15.3
WO-10-34	WOODRUFF	ovary	0.03194	15.0
WO-20-10	WOODRUFF	ovary	0.03012	15.9
WO-10-22	WOODRUFF	ovary	0.02712	15.3
WO-10-09	WOODRUFF	ovary	0.02182	14.5
WO-07-31	WOODRUFF	ovary	0.02068	15.3
WO-06-35	WOODRUFF	ovary	0.02232	17.1
WO-18-03	WOODRUFF	ovary	0.02414	8.7
WO-01-31	WOODRUFF	ovary	0.02097	13.2
WO-06-28	WOODRUFF	ovary	0.02284	11.4
WO-20-19	WOODRUFF	ovary	0.02349	13.8
WO-20-22	WOODRUFF	ovary	0.0238	15.9
WO-06-03	WOODRUFF	ovary	0.02677	13.2
WO-01-23	WOODRUFF	ovary	0.02332	16.0
WO-09-16	WOODRUFF	ovary	0.02278	12.6
WO-10-37	WOODRUFF	ovary	0.02247	18.2
WO-08-03	WOODRUFF	ovary	0.03084	12.2
WO-20-01	WOODRUFF	ovary	0.02504	14.8
WO-01-12	WOODRUFF	ovary	0.02695	14.3
WO-09-08	WOODRUFF	ovary	0.02894	13.7
YK-17-24	YAWKEY	ovary	0.0257	12.7
YK-16-04	YAWKEY	ovary	0.02584	12.6
YK-17-14	YAWKEY	ovary	0.02711	24.0
YK-17-46	YAWKEY	ovary	0.02861	24.8
YK-09-49	YAWKEY	ovary	0.02811	24.7
YK-3B-11	YAWKEY	ovary	0.02685	24.3
YK-04-39	YAWKEY	ovary	0.02855	26.4
YK-16-31	YAWKEY	ovary	0.03525	14.4
YK-10-29	YAWKEY	ovary	0.02225	13.6
YK-16-29	YAWKEY	ovary	0.02216	14.2
YK-10-28	YAWKEY	ovary	0.02374	14.7
YK-09-56	YAWKEY	ovary	0.01788	13.7
YK-10-05	YAWKEY	ovary	0.01965	14.0
YK-09-12	YAWKEY	ovary	0.02667	15.1
YK-16-35	YAWKEY	ovary	0.03297	14.4
YK-17-23	YAWKEY	ovary	0.03011	12.4
YK-10-02	YAWKEY	ovary	0.02261	14.4
YK-09-06	YAWKEY	ovary	0.02759	14.8
YK-04-45	YAWKEY	ovary	0.02342	16.0

Egg ID	Site	TISSUE	5mdC/dG	RBC [Hg] ng/g
YK-3B-03	YAWKEY	ovary	0.0233	15.6
YK-13-15	YAWKEY	ovary	0.03249	15.3
YK-05-07	YAWKEY	ovary	0.03115	15.5
YK-3b-47	YAWKEY	ovary	0.0284	17.6
YK-3B-34	YAWKEY	ovary	0.02843	16.2
YK-13-34	YAWKEY	ovary	0.02987	16.1
YK-3a-22	YAWKEY	ovary	0.02877	16.2
YK-04-22	YAWKEY	ovary	0.02997	11.7
YK-3B-17	YAWKEY	ovary	0.02776	16.6
YK-05-18	YAWKEY	ovary	0.02559	14.8
YK-16-01	YAWKEY	ovary	0.02064	15.4
YK-13-03	YAWKEY	ovary	0.02611	13.1
YK-05-16	YAWKEY	ovary	0.02401	14.1
YK-02-26	YAWKEY	ovary	0.02549	14.3
YK-02-30	YAWKEY	ovary	0.02043	12.3
YK-13-22	YAWKEY	ovary	0.02274	12.3
YK-04-14	YAWKEY	ovary	0.02278	11.8
YK-13-42	YAWKEY	ovary	0.02216	11.3
YK-10-07	YAWKEY	ovary	0.02605	11.4
YK-09-17	YAWKEY	ovary	0.03444	12.4
YK-3B-24	YAWKEY	ovary	0.02041	11.3
YK-3a-06	YAWKEY	ovary	0.0231	13.5
YK-3a-28	YAWKEY	ovary	0.02242	11.8
YK-05-14	YAWKEY	ovary	0.02195	11.3
YK-16-40	YAWKEY	ovary	0.02915	15.7
YK-16-10	YAWKEY	ovary	0.02012	14.5
YK-02-07	YAWKEY	ovary	0.0258	13.4
YK-13-37	YAWKEY	ovary	0.01902	8.1

Table 3.20. The descriptive statistics for the yolk and erythrocyte (RBC) mercury concentrations from the 2011 “grow out” captive juvenile alligator study conducted by Parrott, *et al.* (3).

2011 Grow Out Yolk Hg Descriptive Statistics						
Site	n eggs	n nests	Mean [THg] ng/g	Standard Deviation ng/g	Range [THg] ng/g	
Yawkey	42	18	26.3	10.9	11.8	47.0
Woodruff	50	6	22.6	6.3	10.0	39.2
Apopka	30	18	8.8	5.1	1.9	24.7
2011 Grow Out RBC Hg Descriptive Statistics						
Site	n hatchlings	Mean [THg] ng/g	Standard Deviation ng/g	Range [THg] ng/g		
Yawkey	66	14.7	4.2	7.4	26.4	
Woodruff	44	13.6	3.6	5.8	28.0	
Apopka	26	13.0	1.9	8.6	16.8	

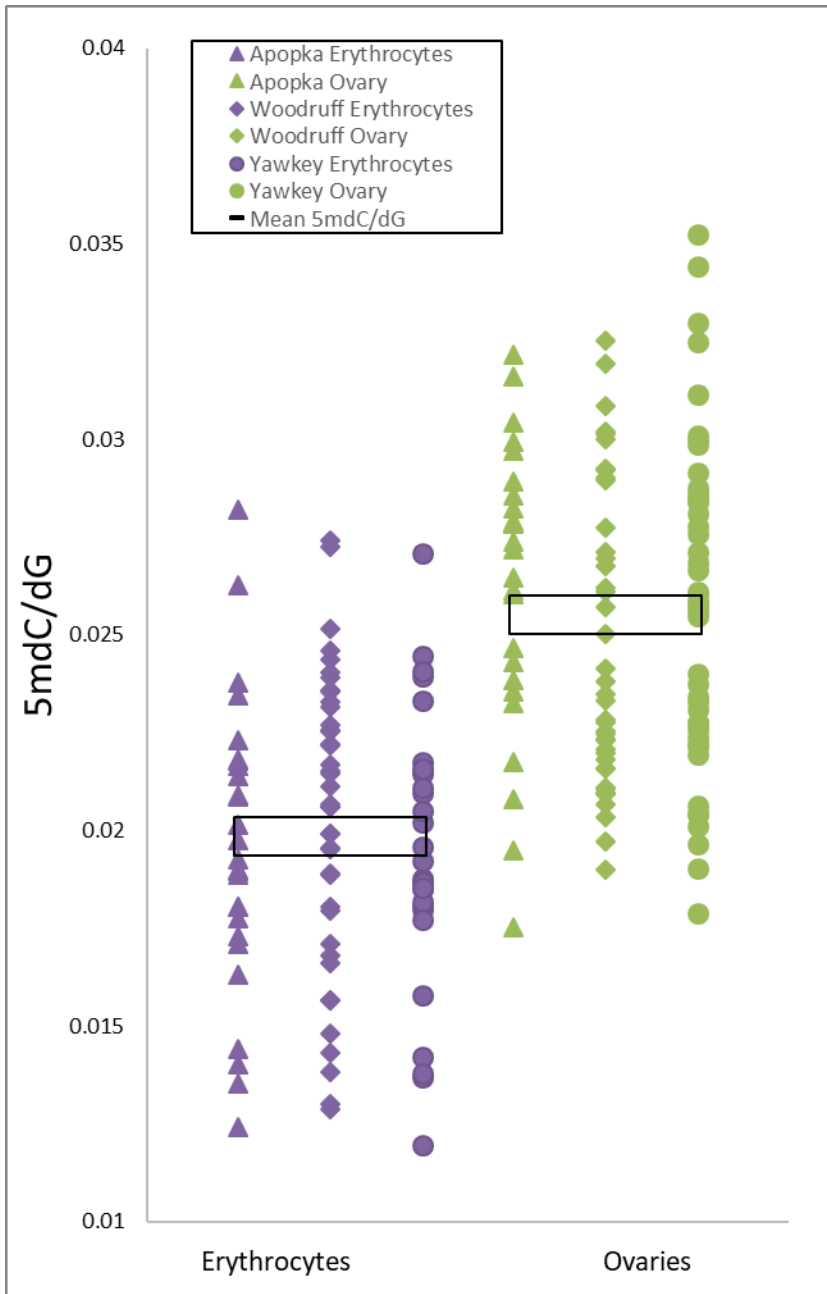


Figure 3.19. The DNA methylation for the erythrocytes and ovary samples from Parrott et al. (3).

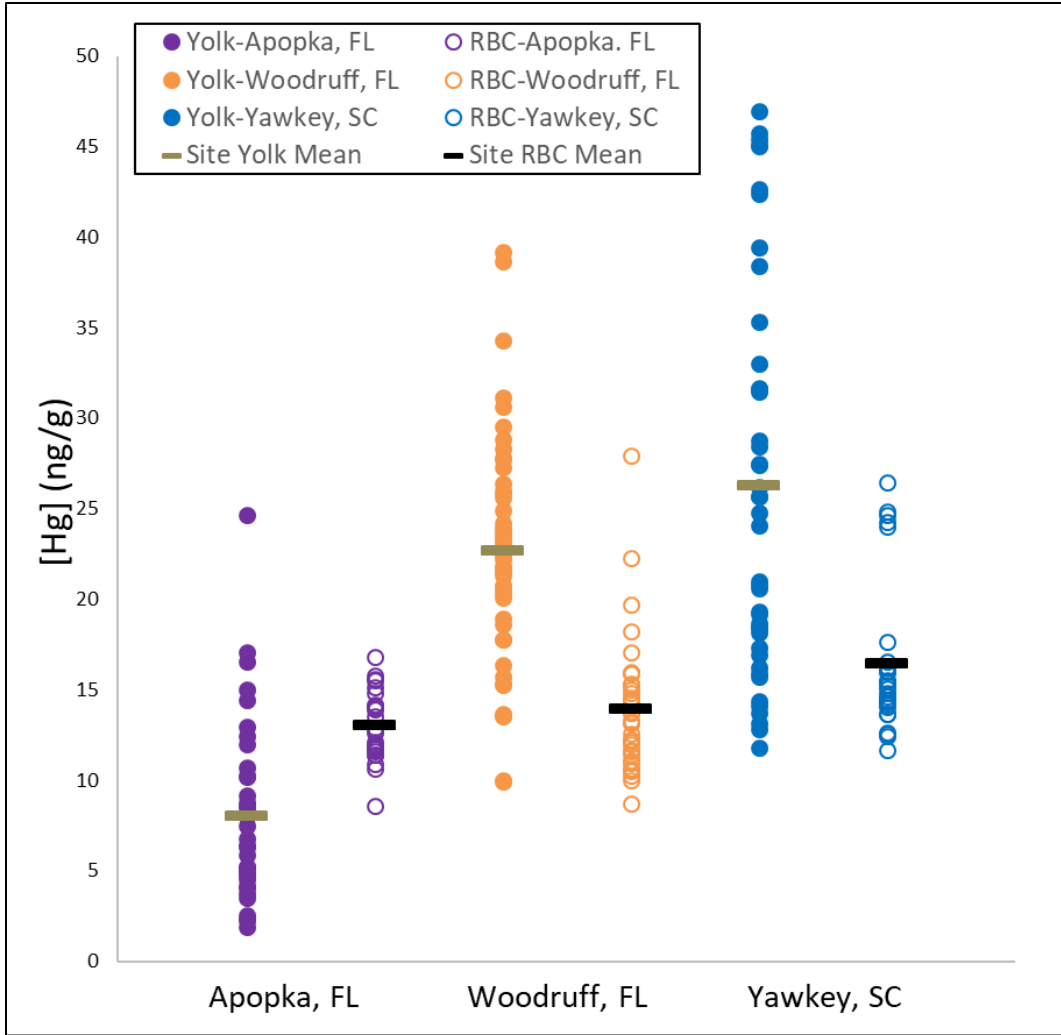


Figure 3.20. The mercury concentration for the egg yolk and erythrocytes (RBCs) from the 2011 Grow Out study conducted by Parrott et al. (3).

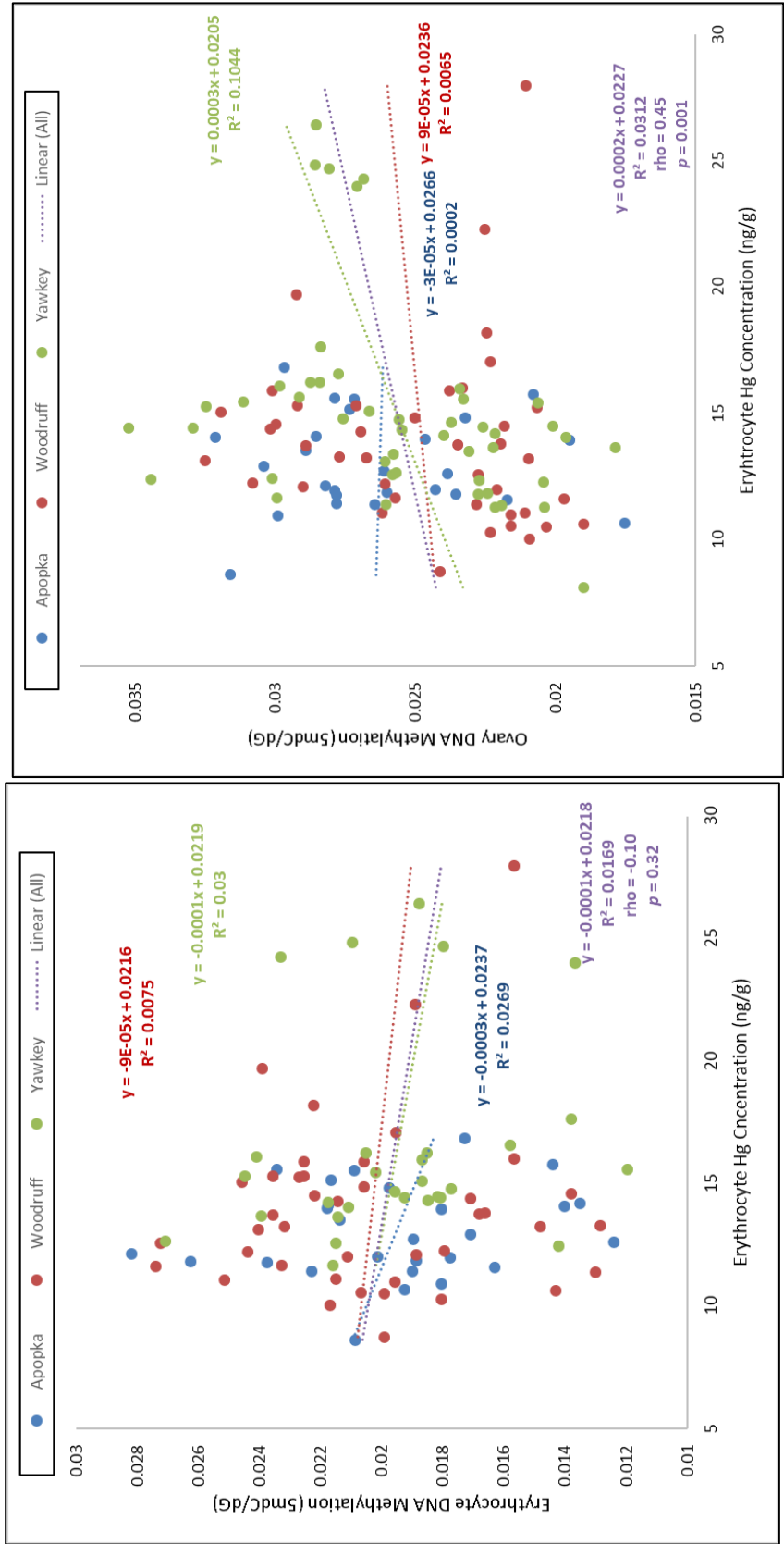


Figure 3.21. The comparison between captive juvenile erythrocyte mercury concentration and the erythrocyte (left) and ovary (right) DNA methylation provided by Parrott, *et al.* (3).

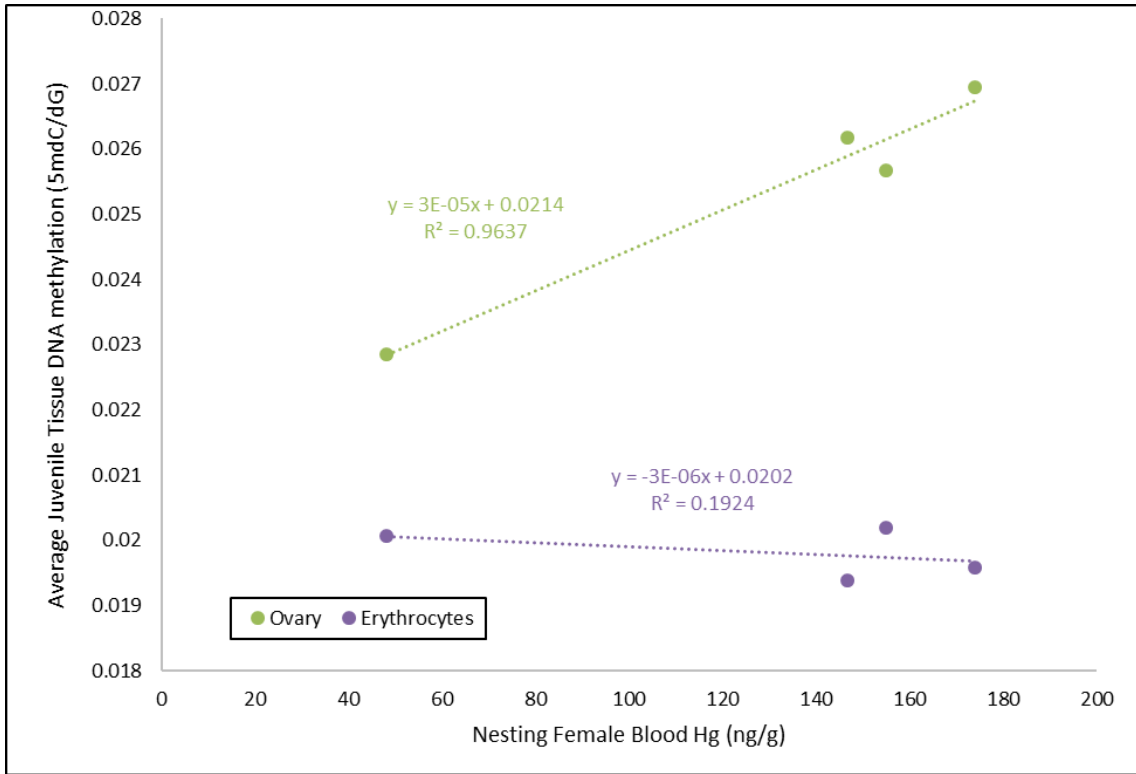


Figure 3.22. The relationship between the DNA methylation of captive juvenile alligator tissues, provided by Parrott, *et al.* (3), and the corresponding nesting females blood mercury concentration. The ovary average DNA methylation and nesting female relationship had a correlation coefficient = 0.98, $p = 0.01$.

3.5. Examining the relationship between DNA methylation & mercury exposure in captive diamondback terrapins

3.5.1. Introduction

The first experiment using wild alligators elucidated a relationship between mercury exposure and DNA methylation loss. However, that relationship was observed only at high mercury sites that were far removed from the other sites examined, and while we believe the observed relationship was dependent on the mercury concentration measured within the alligator at high mercury concentrations, these difference could have been the result of different environmental parameters at the high mercury locations. We attempted to determine if the observed relationship was a site- specific effect, an effect of mercury exposure, or simply an effect of aging. While we were able identify hypomethylation in the adults in the high mercury locations, the question as to the source of the relationship being the local environment or the mercury exposure remained.

The second experiment investigated the relationship between diet and DNA methylation, in effort to resolve one confounding factor of the first experiment. We observed that when a diet is standardized, without varying concentrations of mercury, DNA methylation in blood samples was not correlated to mercury concentration. However, we did observe that the DNA methylation of the ovary of captive juveniles that are fed a standardized diet was correlated to the nesting females blood mercury concentration, which suggests that DNA methylation may be inherited, and that DNA methylation in the blood has a greater plasticity than that of the organs.

In an effort to examine the source of the DNA hypomethylation observed in the experiment, we utilize diamondback terrapin samples from a laboratory mercury dosing

study previously conducted by Schwenter (353). This group of diamondback terrapins are from the same age class and location, and were measured as having low blood mercury concentrations at the beginning of the dosing experiment. The captive dosing experiment samples will allow us to remove the previous confounding factor of site specific and dietary differences, and solely examine the relationship between mercury exposure and DNA methylation changes.

3.5.2. Experiment specific methods

Sample collection

As per Schwenter (353), thirty-six terrapins (18 female, 18 male) were collected during July and August 2004 from the Ashley River—near Charleston, South Carolina—and returned to the Grice Marine Laboratory (Figure 3.20). The experiment was conducted and described in detail by Schwenter (353). Briefly, terrapins were measured, tagged and subjected to ultrasound analysis to determine if each terrapin was participating in breeding that season (Table 3.21). Only adult male terrapins and adult female terrapins that had completed nesting for the season, as determined via ultrasound, were kept for the experiment. The selected terrapins were divided into three groups (control, low dose and high dose), placed into separate tanks, and allowed to acclimatize to their new living conditions for one year (July 2004 – April 2005), including one hibernation period (November 2004 – April 2005). Beginning in May 2005, weekly dietary dosing began via CH₃Hg soaked shrimp supplemented to their captive food (Freshwater Turtle Diet gelatin, Mazrui). The dosing scheme was not designed to achieve a specific mercury concentration within each terrapin and dose group, but to dose the terrapins with dose group specific mercury concentrations to allow for individual

variation in accumulation and excretion. The shrimp were delivered based on an estimated 3% body mass/week diet. Male low-dose terrapins received one dosed shrimp piece while female low-dose terrapins received three dosed shrimp pieces per week. Male high-dose terrapins received five dosed shrimp pieces while female high-dose terrapins received 15 dosed shrimp pieces per week. Additionally, control and low-dose terrapins received shrimp pieces soaked in control solution (high-purity water and ethanol) to maintain all individuals in each dose group on the same diet (total shrimp diet of 5 g for males or 15 grams for females). Nominal doses were based on an estimated average mass of 0.25 kg for male terrapins and 1 kg for female terrapins (Schwenter 2007). The concentration of CH₃Hg in the shrimp pieces were measured throughout the experiment and are provided in Table 3.22. Consumption of dosed shrimp pieces was monitored to ensure the desired dose was administered (Table 3.23, 3.24). Monthly blood and scute samples were collected and analyzed for mercury concentration, to monitor the doses of mercury that the terrapins received, and to understand the uptake into the terrapin tissues (Table 3.25). Blood samples were collected from the femoral artery directly into a sodium heparin 3ml Vacutainer tube (BD), the pelleted to separate the erythrocytes, and stored a -80 ° C. Dosing and sampling continued through October 2006 when the animals were necropsied by Schwenter (353) (Figure 3.24).

Erythrocyte samples were obtained from Jeffrey Schwenter from -20°C storage for DNA methylation analysis. Samples from three time points were chosen: 1- prior to the first hibernation period- before dosing began (October 2004); 2- one year later, after dosing began but prior to the second hibernation (October 2005); 3- and the following year, prior to necropsy at the end of the experiment (September 2006) (Figure 3.24).

These three time points were chosen to allow us to observe the maximum change in DNA methylation that could be attained because of the mercury exposure.



Figure 3.23. The sampling area where diamondback terrapins were collected along the Ashley River near Charleston, SC in 2004 denoted with yellow bars. Terrapins were collected on both sides of the Ashley River, taken from Schwenter (2007).

Table 3.21. Terrapin morphometric data taken from Schwenter (2007).
 Straight carapace length (SCL), straight carapace width (SCW) and straight plastron length (SPL) are provided in centimeters. Dose group and tank locations are indicated for each individual.

Turtle ID	Sex	Mass (g)	SCL	SCW	SPL	Tail Measurements		Head Width	Dose Group	Tank #
						Base- Cloaca	Cloaca- Tip			
M2	M	290	12.95	9.6	11.1	3.1	2.6	2.2	C	1
M4	M	330	13.7	10.1	11.3	4.2	2.7	2.3	C	
M5	M	250	12.3	9.15	9.95	3.4	2.6	2.3	L	2
M15	M	265	12.6	9.6	10.5	3.3	2.8	2.3	L	
M9	M	260	11.8	8.9	10	3.6	2.7	2.3	H	3
M14	M	280	12.7	9.4	10.6	3.7	2	2.4	H	
M3	M	395	13.9	10.3	11.9	4.2	3.3	2.5	L	4
M8	M	225	11.7	9	9.95	3	2.4	2.2	L	
M11	M	215	11.3	8.7	9.8	3.1	2.8	2.2	H	5
M20	M	235	11.9	8.7	10.05	3.2	2.9	2.3	H	
M6	M	290	12.8	9.6	10.3	3.4	2.5	2.4	C	6
M17	M	255	12.4	9.2	10.4	3.7	2.7	2.2	C	
M18	M	238	12	9.05	10	3.3	3.1	2.3	H	7
M19	M	310	13.15	9.9	10.9	3.7	2.9	2.4	H	
M7	M	275	12.45	9.4	10.15	3.5	3.15	2.2	C	8
M16	M	240	11.7	8.9	10.4	3	2.4	2.3	C	
M1	M	250	11.95	8.85	10	3.1	2.6	2.2	L	9
M12	M	280	12.3	9	10.2	4.1	3	2.3	L	
Average		271.28	12.42	9.30	10.42	3.48	2.73	2.29		
SD		42.82	0.70	0.47	0.56	0.39	0.31	0.09		
K1	F	725	16.9	12.7	14.9	3.2	3.7	3.3	C	1
K3	F	1175	18.7	14.4	16.7	2.8	3.9	4.5	C	
F9	F	760	16.3	12.8	14.7	2.6	3.1	3.2	L	2
F11	F	1150	19.4	14	17.1	2.55	3.6	3.95	L	
F8	F	1025	17.95	13.1	16.4	2.7	3.5	4.1	H	3
K9	F	900	18.2	14.1	16	2.1	3.8	3.6	H	
F4	F	850	17.05	12.6	15.45	2.6	3.7	3.55	L	4
K8	F	800	16.4	12.9	14.7	2.5	3.5	3.5	L	
K4	F	800	18	13.4	15.7	2.4	3.4	3.5	H	5
F6	F	1060	17.8	13.5	15.8	2.5	3.8	4.1	H	
F3	F	975	17.9	13.7	15.7	2	3.15	3.9	C	6
K7	F	720	16.5	12.1	14.7	2.9	3.4	3.4	C	
F10	F	790	17.4	12.5	15.8	2.3	3.5	3.6	H	7
K10	F	950	17.9	13.4	16.1	3	2.4	3.8	H	
F2	F	1150	19	14.1	17.2	3	3	4.25	C	8
F5	F	750	17.2	12.8	14.9	3	3.7	3.2	C	
K2	F	710	16.7	12.4	14.5	2	3.6	3.3	L	9
K11	F	1290	19.9	15.6	18.3	2.8	3.8	4.6	L	
Average		921.11	17.73	13.34	15.81	2.61	3.48	3.74		
SD		183.09	1.04	0.87	1.04	0.35	0.37	0.43		

Table 3.22. The concentrations of control and Hg soaked shrimp pieces taken from Schwenter (2007).

Values represent the average \pm the standard deviation of three randomly chosen shrimp pieces from the monthly allotment of shrimp pieces for all control or dosed terrapins. The average concentration \pm one standard deviation for all months in the study is also indicated. Control group concentrations are ppb (ng/g), Hg-soaked concentrations are ppm ($\mu\text{g/g}$). Mercury treatment group terrapins were provided control soaked shrimp pieces during June and August 2005.

		May	June	July	August	September	Average (ng/g)	SD
2005	Control	5.0 \pm 1.8	2.3 \pm 0.2	1.5 \pm 1.0	10.3 \pm 3.1	11.6 \pm 8.5	6.2	4.6
2006	Control	7.8 \pm 2.1	6.4 \pm 4.9	34.0 \pm 7.3	5.2 \pm 1.00	6.9 \pm 2.1	12	12.3
		May	June	July	August	September	Average ($\mu\text{g/g}$)	SD
2005	Mercury	91.8 \pm 10.3	-----	81.8 \pm 30.3	-----	85.1 \pm 2.1	86.2	5.1
2006	Mercury	93.3 \pm 4.2	94.2 \pm 5.2	87.5 \pm 12.5	77.6 \pm 12.5	70.0 \pm 7.4	84.5	10.5

Table 3.23. Shrimp consumption chart for 2005 taken from Schwenter (2007). Numbers indicate the actual number of shrimp pieces consumed by an individual turtle each dosing day. Males received five shrimp pieces each dosing day. Females received 15 shrimp pieces each dosing day. High-dose terrapins received 5 or 15 shrimp pieces soaked in 37-ppm MeHg solution. In Low-dose treatment, males received 1 Hg-soaked and 4 control shrimp pieces, females received 3 Hg-soaked and 12 control shrimp pieces. Control terrapins received shrimp pieces soaked in ethanol and water. Black boxes indicate the death of a turtle. Red shaded “Code” squares denote terrapins that exhibited overt health decline towards the conclusion of the experiment (during 2006). Gray shaded squares represent dosing days where low-dose turtles received shrimp pieces soaked in a solution of enriched $M^{200}Hg$. Only one terrapin (M3) that received the $Me^{200}Hg$ dosed shrimp pieces survived and was included in analyses.

Tank	Dose	Code	Sex	# To Eat	ACTUAL NUMBER CONSUMED																															
					2-May	9-May	16-May	23-May	30-May	6-Jun	13-Jun	20-Jun	27-Jun	4-Jul	11-Jul	18-Jul	25-Jul	1-Aug	8-Aug	15-Aug	22-Aug	29-Aug	5-Sep	12-Sep	19-Sep	26-Sep	3-Oct	10-Oct	17-Oct							
1		K1	F	15	15	15	10	15	15	15	15	15	15	15	15	15	15	15	15	15	15	15	15	15	15	15	15	15	15	15	15	15	15	15		
1		K3	F	15	14	15	15	15	15	15	15	15	15	15	15	15	15	15	15	15	15	15	15	15	15	15	15	15	15	15	15	15	15	15		
1		C	M2	M	5	3.5	4.5	3.5	3	4.5	5	5	5	5	5	5	5	5	5	5	5	5	5	5	5	5	5	5	5	5	5	5	5	5		
1		M4	M	5	5	5	5	5	5	5	5	5	5	5	5	5	5	5	5	5	5	5	5	5	5	5	5	5	5	5	5	5	5	5		
2		F9	F	3 dose/12 extra	3/12	3/12	0	1/0	0	0	0	0	0	0	0	0	0	0	0	0	0	0	0	0	0	0	0	0	0	0	0	0	0	0	0	
2		F11	F	3 dose/12 extra	3/8	3/12	3/4	0	1/0	0	0	0	0	0	0	0	0	0	0	0	0	0	0	0	0	0	0	0	0	0	0	0	0	0	0	
2		L	M5	M	1 dose/4 extra	1/4	1/4	1/2	1/3	0	0	0	0	0	0	0	0	0	0	0	0	0	0	0	0	0	0	0	0	0	0	0	0	0	0	0
2		M15	M	1 dose/4 extra	5	5	5	1/4	4/1	0	0	0	0	0	0	0	0	0	0	0	0	0	0	0	0	0	0	0	0	0	0	0	0	0	0	0
3		K5	F	15	15	15	15	15	15	14	15	14	15	15	15	15	15	15	15	15	15	15	15	15	15	15	15	15	15	15	15	15	15	15	15	
3		F8	F	15	15	15	15	15	15	15	15	15	15	15	15	15	15	15	15	15	15	15	15	15	15	15	15	15	15	15	15	15	15	15	15	
3		H	M14	M	5	5	5	5	5	5	5	5	5	5	5	5	5	5	5	5	5	5	5	5	5	5	5	5	5	5	5	5	5	5	5	
3		M9	M	5	5	5	5	5	5	5	5	5	5	5	5	5	5	5	5	5	5	5	5	5	5	5	5	5	5	5	5	5	5	5	5	
4		F4	F	3 dose/12 extra	3/12	15***	3/10	3/12	3/12	14	7	15	15	15	3/12	3/12	3/12	3/12	3/12	3/12	3/12	3/12	3/12	3/12	3/12	3/12	3/12	3/12	3/12	3/12	3/12	3/12	3/12	3/12	3/12	
4		K8	F	3 dose/12 extra	3/12	3/12	3/12	3/12	3/12	15	15	15	15	15	3/12	3/12	3/12	3/12	3/12	3/12	3/12	3/12	3/12	3/12	3/12	3/12	3/12	3/12	3/12	3/12	3/12	3/12	3/12	3/12	3/12	
4		L	M8	M	1 dose/4 extra	1/4	1/4	1/4	1/4	1/4	5	5	5	5	5	5	5	5	5	5	5	5	5	5	5	5	5	5	5	5	5	5	5	5	5	5
4		M3	M	1 dose/4 extra	1/4	1/4	1/4	1/4	1/4	1/4	5	5	5	5	5	5	5	5	5	5	5	5	5	5	5	5	5	5	5	5	5	5	5	5	5	5
5		K4	F	15	15	15	15	15	15	15	15	15	15	15	15	15	15	15	15	15	15	15	15	15	15	15	15	15	15	15	15	15	15	15	15	15
5		F8	F	15	15	15	15	15	15	15	15	15	15	15	15	15	15	15	15	15	15	15	15	15	15	15	15	15	15	15	15	15	15	15	15	15
5		H	M11	M	5	5	5	5	5	5	5	5	5	5	5	5	5	5	5	5	5	5	5	5	5	5	5	5	5	5	5	5	5	5	5	5
5		M20	M	5	1	1.5	2	4	5	3	4	5	5	5	5	5	5	5	5	5	5	5	5	5	5	5	5	5	5	5	5	5	5	5	5	5
6		K7	F	15	15	15	15	15	15	15	15	15	15	15	15	15	15	15	15	15	15	15	15	15	15	15	15	15	15	15	15	15	15	15	15	15
6		F3	F	15	15	15	15	15	15	15	15	15	15	15	15	15	15	15	15	15	15	15	15	15	15	15	15	15	15	15	15	15	15	15	15	15
6		C	M17	M	5	5	5	5	5	5	5	5	5	5	5	5	5	5	5	5	5	5	5	5	5	5	5	5	5	5	5	5	5	5	5	5
6		M8	M	5	0	0	0	0	0	0	0	0	0	0	0	0	0	0	0	0	0	0	0	0	0	0	0	0	0	0	0	0	0	0	0	0
7		F6	F	15	15	15	15	15	15	15	15	15	15	15	15	15	15	15	15	15	15	15	15	15	15	15	15	15	15	15	15	15	15	15	15	15
7		K10	F	15	15	15	15	15	15	15	15	15	15	15	15	15	15	15	15	15	15	15	15	15	15	15	15	15	15	15	15	15	15	15	15	15
7		H	M19	M	5	5	5	5	5	5	5	5	5	5	5	5	5	5	5	5	5	5	5	5	5	5	5	5	5	5	5	5	5	5	5	5
7		M18	M	5	5	5	5	5	5	5	5	5	5	5	5	5	5	5	5	5	5	5	5	5	5	5	5	5	5	5	5	5	5	5	5	5
8		F2	F	15	15	15	15	15	15	15	15	15	15	15	15	15	15	15	15	15	15	15	15	15	15	15	15	15	15	15	15	15	15	15	15	15
8		F5	F	15	15	15	15	15	15	15	15	15	15	15	15	15	15	15	15	15	15	15	15	15	15	15	15	15	15	15	15	15	15	15	15	15
8		C	M7	M	5	5	5	5	5	5	5	5	5	5	5	5	5	5	5	5	5	5	5	5	5	5	5	5	5	5	5	5	5	5	5	5
8		M16	M	5	5	5	5	5	5	5	5	5	5	5	5	5	5	5	5	5	5	5	5	5	5	5	5	5	5	5	5	5	5	5	5	5
9		K11	F	3 dose/12 extra	3/10	3/12	3/12	3/12	3/12	15	15	15	15	15	3/12	3/12	3/12	3/12	3/12	3/12	3/12	3/12	3/12	3/12	3/12	3/12	3/12	3/12	3/12	3/12	3/12	3/12	3/12	3/12	3/12	3/12
9		K2	F	3 dose/12 extra	3/10	3/12	3/12	3/11	3/12	15	15	15	15	15	3/12	3/12	3/12	3/12	3/12	3/12	3/12	3/12	3/12	3/12	3/12	3/12	3/12	3/12	3/12	3/12	3/12	3/12	3/12	3/12	3/12	3/12
9		L	M1	M	1 dose/4 extra	1/4	1/4	1/4	1/4	5	5	5	5	5	5	5	5	5	5	5	5	5	5	5	5	5	5	5	5	5	5	5	5	5	5	5
9		M12	M	1 dose/4 extra	1/2	1/4	1/4	1/4	1/4	1/3	4	4	4	4	5	5	5	5	5	5	5	5	5	5	5	5	5	5	5	5	5	5	5	5	5	5

* Asterisks for females F4 and K4 denote an error in dosing of these two females on May 9, 2005. Terrapin F4 was administered 15 mercury-soaked shrimp pieces instead of the normal 3 dose/12 extra allotment. Terrapin K4 was administered 3 mercury soaked and 12 control shrimp pieces instead of the normal allotment of 15 mercury soaked pieces.

Table 3.24. Shrimp consumption chart for 2006 taken from Schwenter (2007). Shaded empty squares indicate terrapins that were absent from the study during 2006. Black squares indicate the death of a turtle. Red shaded "Code" squares denote terrapins that exhibited overt health decline towards the conclusion of the experiment. Failure to consume shrimp pieces was evident after the onset of these symptoms.

Tank	Dose	Code	Sex	# To Eat	ACTUAL NUMBER CONSUMED																													
					1-May	8-May	15-May	22-May	29-May	5-Jun	12-Jun	19-Jun	26-Jun	3-Jul	10-Jul	17-Jul	24-Jul	31-Jul	7-Aug	14-Aug	21-Aug	28-Aug												
1		K1	F	15	12	15	15	15	15	15	15	15	15	15	15	15	15	15	15	15	15	15	15	15	15	15	15	15	15	15	15			
1		K3	F	15	15	15	15	15	15	15	15	15	15	15	15	15	15	15	15	15	15	15	15	15	15	15	15	15	15	15	15	15		
1	C	M2	M	5	5	5	5	5	5	5	5	5	5	5	5	5	5	5	5	5	5	5	5	5	5	5	5	5	5	5	5			
1		M4	M	5	5	5	5	5	5	5	5	5	5	5	5	5	5	5	5	5	5	5	5	5	5	5	5	5	5	5	5			
2		F9	F	3 dose/12 extra																														
2		F11	F	3 dose/12 extra																														
2	L	M5	M	1dose/4 extra																														
2		M15	M	1dose/4 extra																														
3		K9	F	15	15	15	15	9	12	11	0	0	0	13	15	15	15	15	15	15	15	15	15	15	15	15	15	15	15	15	15	15		
3		F8	F	15	15	15	15	15	15	15	15	15	15	15	15	15	15	15	15	15	15	15	15	15	15	15	15	15	15	15	15	15		
3	H	M14	M	5	5	5	5	5	5	5	5	5	5	5	5	5	5	5	5	5	5	5	5	5	5	5	5	5	5	5	5	5		
3		M9	M	5																														
4		F4	F	3 dose/12 extra																														
4		K8	F	3 dose/12 extra																														
4	L	M8	M	1dose/4 extra																														
4		M3	M	1dose/4 extra	1/4	1/4	1/4	1/4	1/4	1/4	1/4	1/4	1/4	1/4	1/4	1/4	1/4	1/4	1/4	1/4	1/4	1/4	1/4	1/4	1/4	1/4	1/4	1/4	1/4	1/4	1/4	1/4	1/4	
5		K4	F	15	15	15	15	15	15	15	15	15	15	15	15	15	15	15	15	15	15	15	15	15	15	15	15	15	15	15	15	15	15	
5		F6	F	15	13	15	15	-----	15	15	15	15	15	15	15	15	15	15	15	15	15	15	15	15	15	15	15	15	15	15	15	15	15	
5	H	M11	M	5	1	3	3	4	5	5	5	5	5	5	5	5	5	5	5	5	5	5	5	5	5	5	5	5	5	5	5	5	5	
5		M20	M	5																														
6		K7	F	15	15	15	15	15	15	15	15	15	15	15	15	15	15	15	15	15	15	15	15	15	15	15	15	15	15	15	15	15	15	
6		F3	F	15	15	15	15	15	15	15	15	15	15	15	15	15	15	15	15	15	15	15	15	15	15	15	15	15	15	15	15	15	15	
6	C	M17	M	5	5	5	5	5	5	5	5	5	5	5	5	5	5	5	5	5	5	5	5	5	5	5	5	5	5	5	5	5	5	
6		M6	M	5	0	0	0	0	0	0	0	0	0	0	0	0	0	0	0	0	0	0	0	0	0	0	0	0	0	0	0	0	0	
7		F10	F	15	15	15	15	15	15	15	15	15	15	15	15	15	15	15	15	15	15	15	15	15	15	15	15	15	15	15	15	15	15	
7		K10	F	15	3	14	14	15	15	15	15	15	15	15	15	15	15	15	15	15	15	15	15	15	15	15	15	15	15	15	15	15	15	
7	H	M19	M	5	5	5	5	5	5	5	5	5	5	5	5	5	5	5	5	5	5	5	5	5	5	5	5	5	5	5	5	5	5	
7		M18	M	5	5	5	5	5	5	5	5	5	5	5	5	5	5	5	5	5	5	5	5	5	5	5	5	5	5	5	5	5	5	
8		F2	F	15	15	15	15	15	15	15	15	15	15	15	15	15	15	15	15	15	15	15	15	15	15	15	15	15	15	15	15	15	15	
8		F5	F	15	15	15	15	15	15	15	15	15	15	15	15	15	15	15	15	15	15	15	15	15	15	15	15	15	15	15	15	15	15	
8	C	M7	M	5	5	5	5	5	5	5	5	5	5	5	5	5	5	5	5	5	5	5	5	5	5	5	5	5	5	5	5	5	5	
8		M16	M	5																														
9		K11	F	3 dose/12 extra	3/12	3/12	3/12	3/12	3/12	3/12	3/12	3/12	3/12	3/12	3/12	3/12	3/12	3/12	3/12	3/12	3/12	3/12	3/12	3/12	3/12	3/12	3/12	3/12	3/12	3/12	3/12	3/12	3/12	
9		K2	F	3 dose/12 extra	3/12	3/12	3/12	3/12	3/12	3/12	3/12	3/12	3/12	3/12	3/12	3/12	3/12	3/12	3/12	3/12	3/12	3/12	3/12	3/12	3/12	3/12	3/12	3/12	3/12	3/12	3/12	3/12	3/12	
9	L	M11	M	1dose/4 extra	1/3	1/4	1/4	1/4	1/4	1/4	1/4	1/4	1/4	1/4	1/4	1/4	1/4	1/4	1/4	1/4	1/4	1/4	1/4	1/4	1/4	1/4	1/4	1/4	1/4	1/4	1/4	1/4	1/4	
9		M12	M	1dose/4 extra	1/4	1/4	1/4	1/4	1/4	1/4	1/4	1/4	1/4	1/4	1/4	1/4	1/4	1/4	1/4	1/4	1/4	1/4	1/4	1/4	1/4	1/4	1/4	1/4	1/4	1/4	1/4	1/4	1/4	1/4

Table 3.25. Terrapin Hg concentrations in red blood cells and scutes, reported as ppb (ng/g) taken from Schwenter (2007).

Missing values indicate samples were not obtained for that compartment during that month.

Treatment Group	Tank #	Turtle ID	Sex	Month	Blood THg (ppb)	Scute THg (ppb)
H	7	M19	M	October-04	----	----
				April-05	42.4	----
				May-05	28549	----
				June-05	17520	2630
				July-05	28552	----
				August-05	17997	41557
				October-05	52121	51178
				April-06	61022	----
				At Sacrifice	82533	197981
				H	7	M18
April-05	39.3	----				
May-05	26771	326.3				
June-05	19666	439.1				
July-05	35399	33872				
August-05	17789	----				
October-05	53430	93893				
April-06	70531	----				
At Sacrifice	159711	229378				
H	7	F10	F			
				April-05	37.3	----
				May-05	24777	2728
				June-05	23200	----
				July-05	46862	38606
				August-05	18021	----
				October-05	65185	21079
				April-06	56816	----
				At Sacrifice	134199	151258
				H	7	K10
April-05	57.2	----				
May-05	9493	----				
June-05	16162	3060				
July-05	31851	----				
August-05	18834	71567				
October-05	54620	73172				
April-06	54996	----				
At Sacrifice	98384	219010				
L	4	M3	M			
				April-05	59.7	----
				May-05	3732	836.8
				June-05	2462	----
				July-05	4787	5391
				August-05	3774	----
				October-05	8822	9516
				April-06	8249	----
At Sacrifice	18780	26339				

Treatment Group	Tank #	Turtle ID	Sex	Month	Blood THg (ppb)	Scute THg (ppb)				
C	1	M2	M	October-04	55.1	-----				
				April-05	46.9	-----				
				May-05	44.1	504.8				
				June-05	55.3	276.2				
				July-05	44.4	-----				
				August-05	31.8	286.4				
				October-05	39.0	275.6				
				April-06	26.6	-----				
				At Sacrifice	36.8	245.5				
				C	1	M4	M	October-04	63.6	-----
April-05	52.3	-----								
May-05	59.6	490.7								
June-05	58.0	-----								
July-05	50.4	402.8								
August-05	42.7	-----								
October-05	47.8	409.0								
April-06	35.7	-----								
At Sacrifice	37.6	294.9								
C	1	K1	F					October-04	43.0	-----
				April-05	36.8	-----				
				May-05	32.0	-----				
				June-05	55.1	260.6				
				July-05	48.0	-----				
				August-05	34.3	316.1				
				October-05	44.5	345.4				
				April-06	37.0	-----				
				At Sacrifice	48.6	302.3				
				C	1	K3	F	October-04	44.7	-----
April-05	39.9	-----								
May-05	69.6	397.1								
June-05	79.5	-----								
July-05	88.3	418.4								
August-05	57.0	-----								
October-05	42.1	266.5								
April-06	33.5	-----								
At Sacrifice	32.7	218.2								
H	3	M14	M					October-04	39.9	-----
				April-05	28.2	-----				
				May-05	19831	3815				
				June-05	18589	-----				
				July-05	35005	60754				
				August-05	20386	-----				
				October-05	54308	99163				
				April-06	48814	-----				
				At Sacrifice	127757	192983				
				H	3	M9	M	October-04	66.1	-----
April-05	48.5	-----								
May-05	30963	-----								
June-05	24047	466.8								
July-05	39330	80544								
August-05	25242	93708								
October-05	66677	-----								
H	3	K9	F					October-04	54.4	-----
								April-05	46.7	-----
								May-05	24730	-----
				June-05	24260	6082				
				July-05	34864	-----				
				August-05	23402	110363				
				October-05	57722	104152				
				April-06	64708	-----				
				At Sacrifice	75852	231506				
				H	3	F8	F	October-04	44.53	-----
April-05	46.36	-----								
May-05	25666	3041								
June-05	19245	-----								
July-05	32572	46930								
August-05	24760	-----								
October-05	53327	117210								
April-06	60209	-----								
At Sacrifice	107915	175280								

Treatment Group	Tank #	Turtle ID	Sex	Month	Blood THg (ppb)	Scute THg (ppb)
H	5	M11	M	October-04	36.8	-----
				April-05	30.2	-----
				May-05	37149	712.2
				June-05	27059	-----
				July-05	60380	43162
				August-05	28795	-----
				October-05	72972	70836
				April-06	89915	-----
				October-04	-----	-----
				April-05	44.2	-----
May-05	19979	190.2				
June-05	19111	2450				
July-05	36719	-----				
August-05	88834	16104				
H	5	K4	F	October-04	77.6	-----
				April-05	55.5	-----
				May-05	30072	-----
				June-05	16826	11455
				July-05	37409	-----
				August-05	26623	70004
				October-05	69874	139368
				April-06	72853	-----
				At Sacrifice	122853	188247
				October-04	53.7	-----
April-05	62.1	-----				
May-05	38528	6514				
June-05	17602	-----				
July-05	29386	93544				
August-05	14418	-----				
October-05	49577	117039				
April-06	56695	-----				
At Sacrifice	115061	196325				
C	6	M6	M	October-04	53.7	-----
				April-05	52.4	-----
				May-05	69.6	284.4
				June-05	60.7	-----
				July-05	49.9	350.9
				August-05	44.4	-----
				October-05	52.2	285.8
				April-06	63.4	-----
				At Sacrifice	43.0	270.5
				October-04	75.9	-----
April-05	49.7	-----				
May-05	70.6	454.0				
June-05	45.4	394.2				
July-05	49.7	433.4				
August-05	41.6	291.9				
October-05	37.3	239.0				
April-06	51.2	-----				
At Sacrifice	48.3	236.7				
C	6	K7	F	October-04	33.9	-----
				April-05	25.5	-----
				May-05	35.2	-----
				June-05	37.0	158.4
				July-05	29.3	-----
				August-05	24.1	179.3
				October-05	44.6	163.9
				April-06	57.3	-----
				At Sacrifice	56.8	202.9
				October-04	41.4	-----
April-05	40.6	-----				
May-05	49.3	339.9				
June-05	68.9	268.3				
July-05	78.7	193.8				
August-05	83.3	-----				
October-05	94.4	303.8				
April-06	103.1	-----				

Treatment Group	Tank #	Turtle ID	Sex	Month	Blood THg (ppb)	Scute THg (ppb)
C	8	M7	M	October-04	50.5	-----
				April-05	39.5	-----
				May-05	48.0	-----
				June-05	48.1	195.7
				July-05	35.8	-----
				August-05	38.8	225.5
				October-05	42.9	212.0
				April-06	51.4	-----
				At Sacrifice	39.2	213.0
				October-04	50.6	-----
C	8	M16	M	April-05	39.3	-----
				May-05	49.4	133.9
				June-05	38.9	155.0
				July-05	29.4	340.8
				August-05	28.6	-----
				October-05	27.2	248.3
				October-04	46.2	-----
C	8	F2	F	April-05	41.3	-----
				May-05	49.1	191.0
				June-05	43.2	106.9
				July-05	39.2	206.5
				August-05	38.1	-----
				October-05	42.5	211.7
				April-06	55.8	-----
				At Sacrifice	34.0	207.5
				October-04	77.8	-----
				April-05	65.2	-----
C	8	F5	F	May-05	65.9	410.0
				June-05	60.0	392.8
				July-05	43.4	261.6
				August-05	35.1	252.1
				October-05	52.2	215.3
				April-06	63.4	-----
				At Sacrifice	47.2	265.8
				October-04	-----	-----
				April-05	29.5	-----
				May-05	3759	439.3
L	9	M1	M	June-05	3488	-----
				July-05	7287	12081
				August-05	5796	-----
				October-05	10880	13062
				April-06	8454	-----
				At Sacrifice	28798	32454
				October-04	69.0	-----
				April-05	52.8	-----
				May-05	4175	460.7
				June-05	3736	530.5
L	9	M12	M	July-05	6988	2373
				August-05	5185	8607
				October-05	8550	13158
				April-06	10729	-----
				At Sacrifice	22754	32904
				October-04	39.5	-----
				April-05	39.1	-----
				May-05	5110	-----
				June-05	5522	1079
				July-05	15224	-----
L	9	K2	F	August-05	7011	15262
				October-05	12532	2736
				April-06	16908	-----
				At Sacrifice	23298	55573
				October-04	49.3	-----
				April-05	46.7	-----
				May-05	3486	616.0
				June-05	3182	901.3
				July-05	5623	3788
				August-05	3576	-----
L	9	K11	F	October-05	8149	2522
				April-06	9254	-----
				At Sacrifice	12711	40020

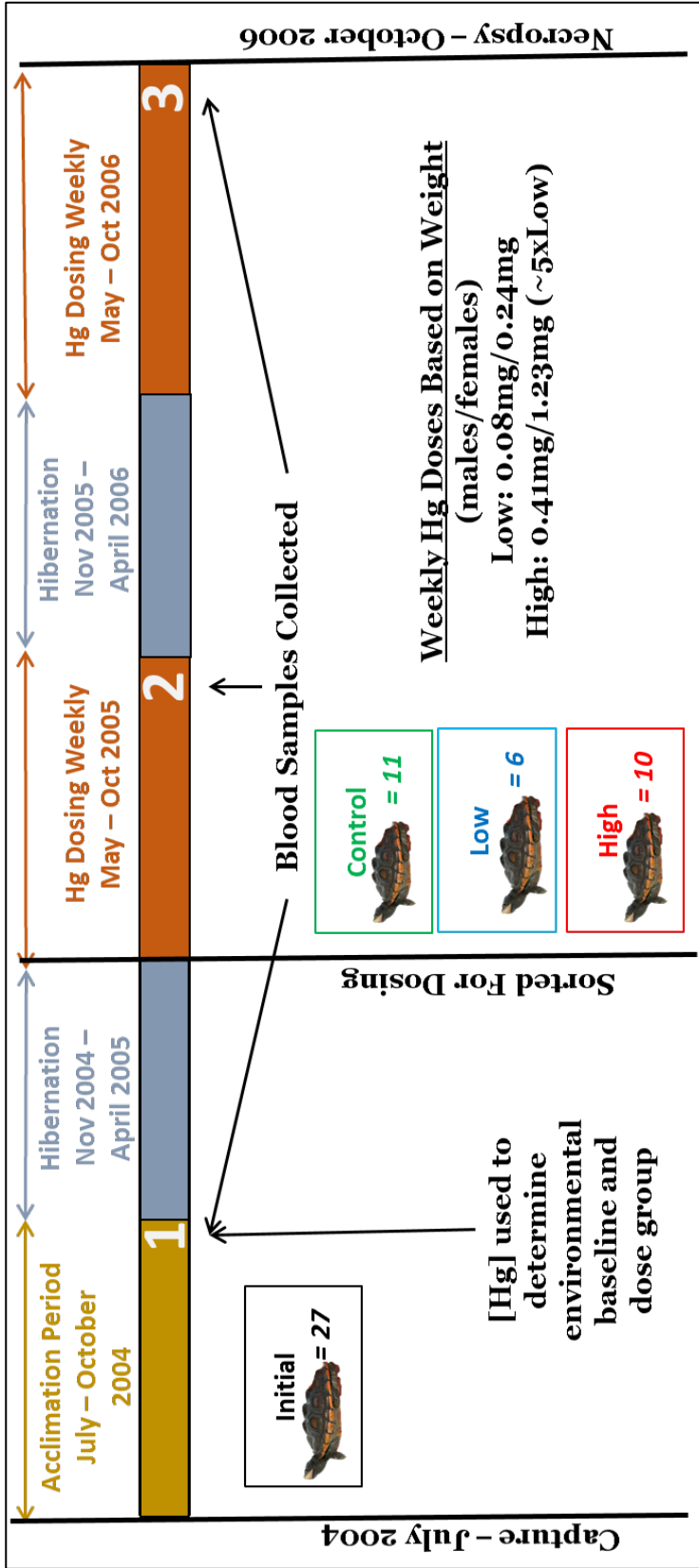


Figure 3.24. A schematic for the diamondback terrapin dosing experiment conducted by Schwenter (2007).

Sample preparation & LC-MS/MS analysis

Samples were prepared and analyzed following the methods described in section 3.2. An experiment-specific QC material was made from pooled terrapin DNA extracts, separated into four aliquots, and run in tandem with the samples throughout the duration of the analysis on the instrument, after each of the three replicated samples, for a total for three measurements of the four aliquots of the same QC material. The QC material was made and used for two reasons: first, to ensure that the instrument was providing consistent results throughout the experiment; and second, to ensure that the method designed and used for alligator DNA extracts (detailed in section 3.2) was also appropriate for terrapin DNA extracts.

3.5.3. Results & Discussion

Instrument calibration

A calibration curve was made following the description in section 3.2.5, using serial dilutions of powdered nucleosides dissolved in water. A test calibration curve was conducted prior to any terrapin DNA extracts being analyzed, to ensure that the powdered nucleotide standards purchased in 2013 were still usable, and that the instrument was performing optimally. The resulting calibration line had an R^2 value of 0.9862 (Figure 3.25). This is less than the calibration line from 2013 ($R^2 = 0.9994$, Figure 3.6), so stored alligator DNA extract samples from 2013 were analyzed against the test curve, to determine if the serial dilutions could be used for this experiment. The alligator DNA samples had both nucleotides of interest, dC and 5mdC, observed in the correct proportions. Based on these results, and since the calibration curve is analyzed multiple

times throughout the sample queue in order to reduce the variation, the terrapin samples were analyzed.

The replicates of the serial dilution measurements did not improve the calibration curve (Figure 3.26). The R^2 value dropped even lower, at 0.9517. Inspection of the individual calibration measurements showed that the abundance of each peak was not consistent (Reps 1-4 without RSF; Table 3.26). The calibration solutions consist of powered nucleotides that have been dissolved in water, so there should not have been any matrix effects of the solutions that would interfere with the analysis in the instrument. Since the alligator sample that was run as a test sample returned the proper ratio of 5mdC : dG, the terrapin QC samples were analyzed to determine if the calibration line was producing consistent results in the terrapin samples, since the equation of the average calibration replicates is used, not the individual measurements.

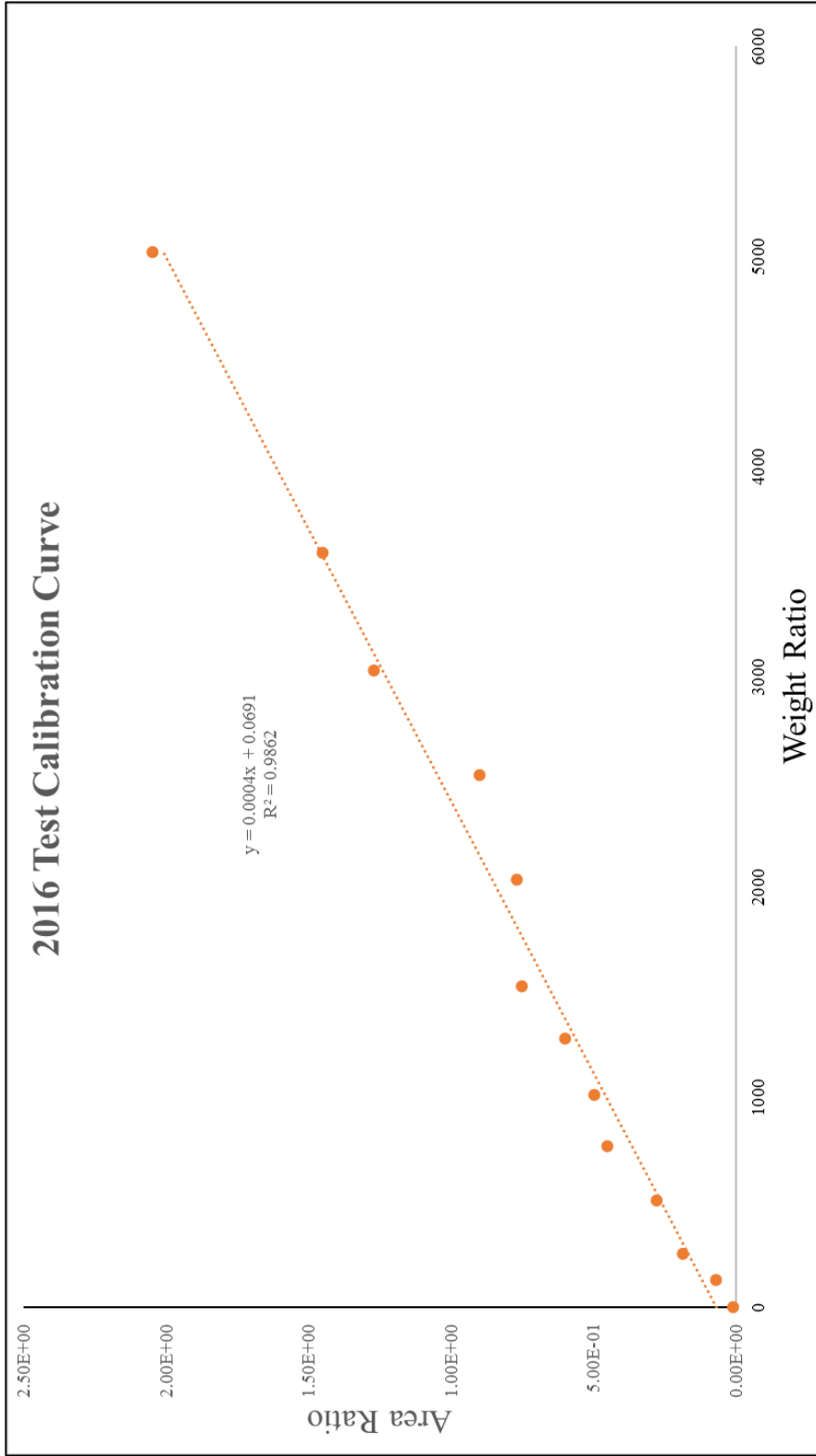


Figure 3.25. The test DNA methylation calibration curve generated in September 2016 using the LC-MS/MS method. The point at 0 was generated by the lack of any calibration solution in water.

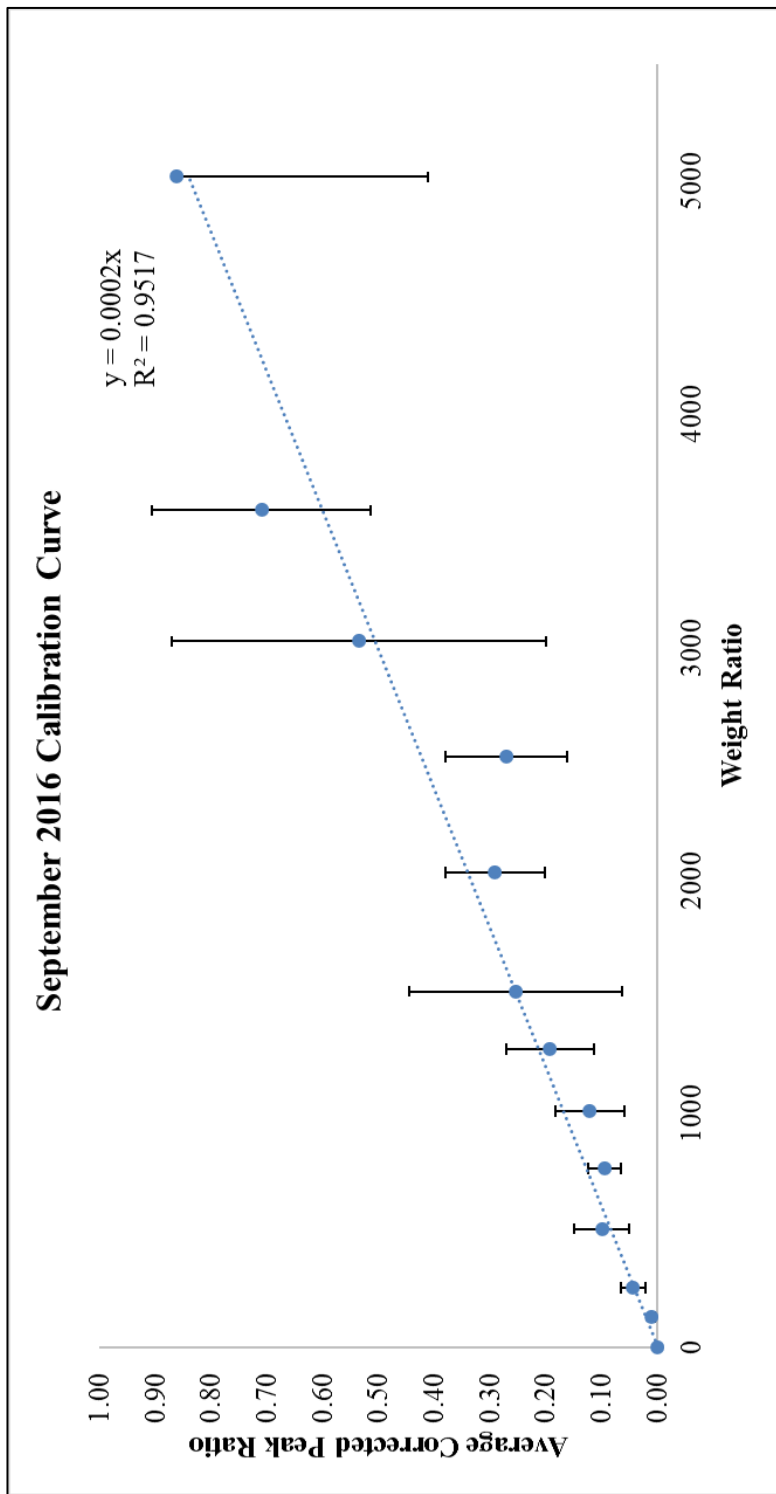


Figure 3.26. The hydrolyzed DNA methylation calibration curve generated in September 2016 using the LC-MS/MS method. The error bars represent the standard deviation of all four replicates of each calibrant. The point at 0 was generated by the lack of any calibration solution in water.

Table 3.26. The relative abundances, ratios and descriptive statistics for the calibration solutions used in the terrapin DNA methylation experiment. The replicates from the instrument software (Rep 1- Rep 4) are given in relative abundance units. The standard deviation (SD) and coefficient of variance (CV = SD/mean of replicates) are provided as quality assessment measures.

Nucleoside	Sample Name	Rep 1	Rep 2	Rep 3	Rep 4	Rep 1 (5mdC/dG) w RSF	Rep 2 (5mdC/dG) w RSF	Rep 3 (5mdC/dG) w RSF	Rep 4 (5mdC/dG) w RSF	MEAN	SD	CV	CURVE INTEGRATE
		14	101	125	363	0.00	0.00	0.00	0.00	0.00	0.00	0.43	-0.001
5mdC	CAL_1	38200	517000	1230000	1670000								
dG	CAL_1												
5mdC	CAL_2	635	7430	6240	3210	0.01	0.02	0.00	0.01	0.01	0.01	0.55	0.001
dG	CAL_2	59100	450000	1510000	658000								
5mdC	CAL_3	2590	21700	29400	37200	0.07	0.05	0.03	0.02	0.04	0.02	0.50	0.007
dG	CAL_3	39000	448000	1030000	2570000								
5mdC	CAL_4	6070	55900	61600	87500	0.13	0.16	0.05	0.06	0.10	0.05	0.49	0.016
dG	CAL_4	51300	384000	1480000	1720000								
5mdC	CAL_5	8140	95400	121000	110000	0.10	0.14	0.07	0.07	0.09	0.03	0.31	0.015
dG	CAL_5	88000	765000	2040000	1740000								
5mdC	CAL_6	36800	183000	123000	153000	0.23	0.10	0.07	0.09	0.12	0.06	0.51	0.020
dG	CAL_6	181000	2120000	2070000	1800000								
5mdC	CAL_7	13900	87500	233000	189000	0.32	0.13	0.20	0.12	0.19	0.08	0.41	0.032
dG	CAL_7	48900	770000	1270000	1720000								
5mdC	CAL_8	18900	11800	341000	48100	0.58	0.11	0.18	0.15	0.25	0.19	0.75	0.043
dG	CAL_8	36100	116000	2170000	366000								
5mdC	CAL_9	24600	234000	289000	332000	0.43	0.30	0.21	0.22	0.29	0.09	0.30	0.049
dG	CAL_9	63400	870000	1530000	1670000								
5mdC	CAL_10	69500	209000	311000	408000	0.45	0.16	0.23	0.24	0.27	0.11	0.40	0.045
dG	CAL_10	171000	1430000	1480000	1930000								
5mdC	CAL_11	28700	421000	467000	440000	0.59	1.06	0.22	0.27	0.54	0.34	0.63	0.090
dG	CAL_11	54400	442000	2380000	1800000								
5mdC	CAL_12	34500	372000	583000	158000	0.94	0.84	0.63	0.43	0.71	0.20	0.28	0.120
dG	CAL_12	41000	492000	1030000	411000								
5mdC	CAL_13	49100	428000	673000	894000	1.55	0.96	0.36	0.58	0.86	0.45	0.52	0.146
dG	CAL_13	35400	495000	2070000	1730000								

Quality control materials

The four aliquots of the pooled terrapin DNA extracts QC material resulted in four different measurements for % DNA methylation (QC1, 5%; QC2, 8%; QC3, 7%; QC4, 5%; Table 3.27). The RSD for these four measurements spanned 0.17 through 0.75. The mean of the three replicates of each of the four QC samples were also different (QC1, 0.33; QC2, 0.5; QC3, 0.39; QC4, 0.32; Table 3.27). The four QC samples are aliquoted from the same pooled DNA extract, which means these values should be identical as they are all the same sample. Upon closer inspection of each replicate from the four QC samples, the inconsistency in the QC replicates stems from the inconsistent relative abundances of the two nucleotides analyzed, 5mdC and dG, detected by the instrument (Rep 1-4, Table 3.27). Each replicate of the QC material should yield identical results, specifically, the ratio of 5mdC and dG should be the same in each replicate, even if the relative abundances are different based on potential instrumental errors in injection volume, because each replicate is an aliquot of the same sample. Since the ratios in each replicate are different, there may be a problem with the detection of the nucleotides in the mass spectrometer section of the instrument.

To determine how different the terrapin QC materials were from what was considered acceptable margins of error for biological samples, their descriptive statistics were compared to those from the 2013 alligator QC materials. The alligator experiment utilized QC materials from visceral organs and erythrocyte samples, for an accurate comparison only the erythrocyte DNA extraction QC materials were compared (Table 3.28). The alligator QC materials had a low standard deviation, between 1% and 2%, and relative standard deviations that are acceptable for this work, between 10% and 25%

(Table 3.28). The terrapin QC materials had SD values between 6% and 38%, and RSD values between 17% and 75%. Using the alligator QC values as a metric for acceptable measurements, only one of the terrapin QC aliquots (QC4) is acceptable for use (Table 3.28). The average SD and RSD for the experimental alligator samples was 1% and 5%, which is lower than the QC material. The experimental terrapin samples had an SD value of 12% and RSD value of 34%. These values are lower than some of the terrapin QC values, but the values are higher than acceptable, and so variable across measurements that there is very little confidence in the data.

Table 3.27. The pooled terrapin quality control (QC) material replicates used in the terrapin DNA methylation analysis conducted in September 2016 using the LC-MS/MS method. The replicates from the instrument software (Rep 1- Rep 3) are given in relative abundance units. The standard deviation (SD) and coefficient of variance (CV = SD/mean of replicates) are provided as quality assessment measures.

Nucleoside	Sample Name				Rep 1	Rep 2	Rep 3				% DNA Methylation
		Rep 1	Rep 2	Rep 3	(5mdC/dG) w RSF	(5mdC/dG) w RSF	(5mdC/dG) w RSF	MEAN	SD	CV	
5mdC dG	QC1	26500	86200	147000	0.61	0.14	0.24	0.33	0.20	0.62	5%
		48100	689000	685000							
5mdC dG	QC2	195000	112000	148000	0.24	1.04	0.23	0.50	0.38	0.75	8%
		888000	120000	733000							
5mdC dG	QC3	71400	89400	140000	0.64	0.29	0.26	0.39	0.17	0.43	7%
		125000	348000	598000							
5mdC dG	QC4	105000	238000	211000	0.38	0.35	0.25	0.32	0.06	0.17	5%
		310000	764000	950000							

Nucleosides are defined in Table 3.1. Standard deviation is denoted by SD, relative standard deviation is denoted by RSD. The mean, SD, and RSD are calculated using the replicates that have been corrected with the RSF.

Table 3.28. The QC materials from the alligator experiment conducted in 2013, and the terrapin experiment conducted in 2016, used in the DNA methylation analyses using the LC-MS/MS method. The standard deviation (SD) and coefficient of variance (CV = SD/mean of replicates) are provided as quality assessment measures.

Alligator Experiment QC Data			Terrapin Experiment QC Data		
Sample Name	SD	CV	Sample Name	SD	CV
100	0.01	0.10	QC1	0.20	0.62
100(2)	0.02	0.26	QC2	0.38	0.75
104	0.01	0.12	QC3	0.17	0.43
104(2)	0.01	0.17	QC4	0.06	0.17
Experimental Samples	0.01	0.05	Experimental Samples	0.12	0.34

Sample data

While the QC materials for the terrapin experiment were not acceptable for continued biological analysis, the experimental sample data was analyzed for consistency and variation, to better understand the suspected issue with the instrument. The terrapin samples were separated by dose group, to aid in the visualization of variation between samples that were presumed to be similar in DNA methylation, as well as to observe the variation of each replicate within each sample. The control, low and high dose samples had an average % DNA methylation of $3.24\% \pm 0.73\%$, $3.54\% \pm 1.25\%$, and $3.49\% \pm 1.39\%$, respectively. While the averages are all similar, there is a wide amount of variation both within and between samples of each group (Table 3.29, 3.30, 3.31). All time points are included in each of the dose group averages, so the control group should have a low standard deviation as no dose was applied. The low and high dose groups should have a greater standard deviation than the control group, and DNA methylation should be changing with mercury dosing, if mercury is the cause of the relationship observed in the wild alligator experiment. By only inspecting the averages and standard deviations, one may assume that the dosing experiment was a success in supporting our observed relationship. However, it is upon inspection of the relative abundances of each samples replicates that one can see how inconsistent the measurements are, making the very tenuous relationship suggested by the averages and standard deviations unreliable (Reps 1-3, Table 3.29, 3.30, 3.31).

The experimental samples do appear less variable than the QC replicates, but this may be due to the QC material being analyzed so many times throughout the sample

queue, and each experimental sample being run only in triplicate. While the samples are run in triplicate to account for instrumental drift or small inconsistencies in the injection process, using data from replicates of each sample that are this variable would be disingenuous, because we cannot be sure that the values are correct, despite the low average SD. Removing individual replicates as outliers is an attractive option, but since the QC replicates are inconsistent, we cannot be sure which of the three sample replicates are the 'true' value, and which could be considered an outlier value, since all three replicates are different for some of the experimental samples.

Table 3.29. DNA methylation measurements made on the LC-MS/MS in September 2016 of the diamondback terrapin control group samples.

Samples highlighted in grey did not have any consistent measurements among all sample replicates. These samples were assessed as inconsistent by comparison of replicate values and fluctuation over the three years of % DNA methylation measurements. The replicates from the instrument software (Rep 1- Rep 3) are given in relative abundance units. The standard deviation (SD) and coefficient of variance (CV = SD/mean of replicates) are provided as quality assessment measures.

Dose Group	Time Point	Sample Name	5mdC/dG w RSF			Mean	SD	CV	Curve Integrate	Mean % DNA Methylation	% DNAME Change (1-3)
			Rep 1	Rep 2	Rep 3						
Control	1	K1-2004	0.28	0.28	0.30	0.29	0.01	0.04	0.028	2.83%	-0.36%
Control	2	K1-2005	0.24	0.28	0.19	0.24	0.04	0.16	0.023	2.29%	
Control	3	K1-2006	0.24	0.26	0.25	0.25	0.01	0.02	0.025	2.47%	
Control	1	F2-2004	0.15	0.49	0.37	0.33	0.14	0.43	0.033	3.34%	-0.71%
Control	2	F2-2005	0.29	0.50	0.26	0.35	0.11	0.31	0.035	3.52%	
Control	3	F2-2006	0.20	0.38	0.22	0.27	0.08	0.29	0.026	2.63%	
Control	1	F5-2004	0.28	0.74	0.16	0.39	0.25	0.63	0.040	3.99%	-0.16%
Control	2	F5-2005	0.28	0.34	0.19	0.27	0.06	0.23	0.027	2.67%	
Control	3	F5-2006	0.59	0.39	0.16	0.38	0.18	0.47	0.038	3.83%	
Control	1	K3-2004	0.23	0.43	0.24	0.30	0.09	0.31	0.030	2.97%	0.04%
Control	2	K3-2005	0.18	0.29	0.24	0.24	0.05	0.20	0.023	2.29%	
Control	3	K3-2006	0.41	0.26	0.23	0.30	0.08	0.26	0.030	3.01%	
Control	1	K7-2004	0.51	0.37	0.27	0.38	0.10	0.26	0.038	3.84%	-1.01%
Control	2	K7-2005	0.19	0.59	0.20	0.33	0.19	0.58	0.033	3.27%	
Control	3	K7-2006	0.33	0.34	0.18	0.29	0.07	0.25	0.028	2.83%	
Control	1	M17-2004	0.50	0.23	0.22	0.32	0.13	0.42	0.032	3.16%	-0.72%
Control	2	M17-2005	0.07	0.63	0.26	0.32	0.23	0.72	0.032	3.21%	
Control	3	M17-2006	0.25	0.22	0.28	0.25	0.03	0.11	0.024	2.44%	
Control	1	M4-2004	0.64	0.50	0.27	0.47	0.15	0.33	0.048	4.82%	-2.41%
Control	2	M4-2005	0.21	0.63	0.19	0.34	0.20	0.59	0.035	3.45%	
Control	3	M4-2006	0.26	0.27	0.21	0.25	0.02	0.10	0.024	2.41%	
Control	1	M6-2004	0.26	0.19	0.24	0.23	0.03	0.14	0.022	2.21%	0.47%
Control	2	M6-2005	0.63	0.25	0.32	0.40	0.16	0.41	0.041	4.05%	
Control	3	M6-2006	0.25	0.32	0.25	0.27	0.03	0.12	0.027	2.68%	
Control	1	M7-2004	0.84	0.23	0.24	0.44	0.28	0.65	0.044	4.45%	-1.06%
Control	2	M7-2005	0.34	0.42	0.25	0.34	0.07	0.20	0.034	3.39%	
Control	3	M7-2006	0.45	0.42	0.26	0.38	0.08	0.22	0.038	3.83%	
Control	1	M2-2004	0.33	0.24	0.23	0.27	0.04	0.16	0.026	2.62%	1.44%
Control	2	M2-2005	0.49	0.66	0.20	0.45	0.19	0.42	0.046	4.61%	
Control	3	M2-2006	0.41	0.51	0.29	0.40	0.09	0.22	0.041	4.06%	
Average										3.24%	-0.45%
Standard Deviation										0.73%	0.010

Nucleosides are defined in Table 1. Standard deviation is denoted by SD, relative standard deviation is denoted by RSD. The mean, SD, and RSD are calculated using the replicates that have been corrected with the response factor (RSF).

Table 3.30. DNA methylation measurements made on the LC-MS/MS in September 2016 of the diamondback terrapin low dose group samples.

Boxes highlighted in grey did not have all three time points for measurement. The replicates from the instrument software (Rep 1- Rep 3) are given in relative abundance units. The standard deviation (SD) and coefficient of variance (CV = SD/mean of replicates) are provided as quality assessment measures.

Dose Group	Time Point	Sample Name	5mdC/dG w RSF			Mean	SD	CV	Curve Integrate	Average % DNA Methylation	% DNAm Change (1-3)
			Rep 1	Rep 2	Rep 3						
Low	1	M3-2004	0.23	0.58	0.20	0.34	0.17	0.51	0.034	3.40%	-0.60%
Low	3	M3-2006	0.38	0.28	0.24	0.30	0.06	0.19	0.030	2.96%	
Low	1	K11-2004	0.50	0.24	0.11	0.28	0.16	0.57	0.028	2.80%	0.13%
Low	2	K11-2005	0.38	0.23	0.22	0.28	0.08	0.28	0.027	2.72%	
Low	3	K11-2006	0.34	0.26	0.29	0.30	0.03	0.11	0.029	2.93%	
Low	1	K2-2004	1.21	0.18	0.23	0.54	0.47	0.88	0.056	5.56%	
Low	2	K2-2005	1.00	0.66	0.23	0.63	0.31	0.50	0.065	6.54%	
Low	2	M1-2005	0.48	0.29	0.24	0.34	0.10	0.31	0.034	3.37%	
Low	3	M1-2006	0.12	0.34	0.23	0.23	0.09	0.39	0.022	2.21%	
Low	1	M12-2004	0.36	0.34	0.32	0.34	0.02	0.05	0.034	3.38%	-0.41%
Low	2	M12-2005	0.23	0.58	0.21	0.34	0.17	0.50	0.034	3.42%	
Low	3	M12-2006	0.22	0.43	0.25	0.30	0.10	0.32	0.030	2.97%	
Average									3.54%	-0.29%	
Standard Deviation									1.25%	0.004	

Nucleosides are defined in Table 1. Standard deviation is denoted by SD, relative standard deviation is denoted by RSD. The mean, SD, and RSD are calculated using the replicates that have been corrected with the response factor (RSF).

Table 3.31. DNA methylation measurements made on the LC-MS/MS in September 2016 of the diamondback terrapin high dose group samples.

The replicates from the instrument software (Rep 1- Rep 3) are given in relative abundance units. The standard deviation (SD) and coefficient of variance (CV = SD/mean of replicates) are provided as quality assessment measures.

Dose	Time Point	Sample Name	5mdC/dG w RSF			Mean	SD	CV	Curve Integ	Average % DNAm	% DNAm Change (1-3)
			Rep 1	Rep 2	Rep 3						
High	1	F10-2004	0.46	1.62	0.21	0.76	0.62	0.81	0.080	7.96%	-5.27%
High	2	F10-2005	0.62	0.67	0.37	0.55	0.13	0.24	0.057	5.68%	
High	3	F10-2006	0.22	0.37	0.23	0.27	0.07	0.26	0.027	2.69%	
High	1	F6-2004	0.45	0.51	0.29	0.42	0.09	0.22	0.042	4.25%	-2.13%
High	2	F6-2005	0.33	0.67	0.25	0.42	0.18	0.43	0.042	4.22%	
High	3	F6-2006	0.16	0.23	0.27	0.22	0.04	0.20	0.021	2.12%	
High	1	F8-2004	0.44	0.31	0.26	0.34	0.07	0.22	0.034	3.36%	0.48%
High	2	F8-2005	0.26	0.24	0.17	0.22	0.04	0.17	0.021	2.14%	
High	3	F8-2006	0.61	0.29	0.24	0.38	0.16	0.43	0.038	3.84%	
High	1	M18-2004	0.15	0.12	0.28	0.18	0.07	0.37	0.017	1.72%	0.78%
High	2	M18-2005	0.25	0.46	0.33	0.35	0.09	0.25	0.035	3.49%	
High	3	M18-2006	0.37	0.14	0.26	0.26	0.09	0.36	0.025	2.50%	
High	1	M19-2004		0.25	0.27	0.26	0.01	0.04	0.025	2.52%	0.78%
High	2	M19-2005	0.47	0.44	0.21	0.38	0.11	0.31	0.038	3.79%	
High	3	M19-2006	0.54	0.10	0.16	0.26	0.20	0.74	0.026	2.58%	
High	1	K10-2004	0.14	0.51	0.20	0.28	0.16	0.57	0.028	2.79%	0.04%
High	2	K10-2005	0.13	0.37	0.22	0.24	0.10	0.41	0.023	2.32%	
High	3	K10-2006	0.35	0.28	0.23	0.29	0.05	0.16	0.028	2.83%	
High	1	K9-2004	0.24	0.35	0.30	0.30	0.04	0.15	0.030	2.96%	0.27%
High	2	K9-2005	0.73	0.12	0.28	0.38	0.26	0.68	0.038	3.82%	
High	3	K9-2006	0.22	0.49	0.26	0.32	0.12	0.37	0.032	3.23%	
High	1	M14-2004	0.39	0.66	0.23	0.42	0.18	0.41	0.043	4.32%	-1.33%
High	2	M14-2005	0.90	0.35	0.39	0.55	0.25	0.46	0.057	5.66%	
High	3	M14-2006	0.37	0.28	0.25	0.30	0.05	0.17	0.030	2.99%	
Average										3.49%	-0.80%
Standard Deviation										1.39%	0.021

Nucleosides are defined in Table 1. Standard deviation is denoted by SD, relative standard deviation is denoted by RSD. The mean, SD, and RSD are calculated using the replicates that have been corrected with the response factor (RSF).

Instrument malfunction – September 2016

When the diamondback terrapin DNA methylation data were analyzed, it became clear that the LC-MS/MS was not performing well throughout the duration of the week-long sample queue. Each of the four replicates of the calibration curve that were run did not result in a straight line (Figure 3.25), and the QC material did not produce consistent results (Table 3.26). This malfunction led to the inconsistent number of ions inside the detector and varied results obtained during analysis. We made this determination based on the variation seen in the calibration curve measurements, which were made immediately prior to the start of the experiment from neat powder nucleosides and water (Figure 3.25). The matrix of these solutions should not vary between injections or over time, as the powders were completely dissolved during the preparation process. The inconsistent measurements of the replicated QC material also indicated that there was a problem with the instrument detection over time. It was determined that the instrument was not functioning properly because it had not been cleaned thoroughly in over 6 months— the sample residue clogged the ionization pore leading into the quadrupole of the mass spectrometer. The clogged residue resulted in poor throughput of the ionized sample spray into the detector, because the residue was physically blocking the entrance, as well as attracting the ions from the sample.

Plans for future analysis

The loss of the data from these terrapin samples is unfortunate, since they were collected over a decade ago by Jeff Schwenter while he was a student at College of Charleston, and very little of the each of the DNA extracts, and original samples remain. There is also very little of the erythrocyte samples remaining; some of the samples have

been used in their entirety. In effort to salvage the data presented here, the remaining 5-7 μL of hydrolyzed DNA extract will be diluted with water to 20 μL and reanalyzed, using only 5 μL injections instead of the 7 μL previously used. The concentration of nucleotides in the diluted samples will be lower than it was initially, and since the samples were stored in $-20\text{ }^{\circ}\text{C}$ conditions, there was low concentrations of DNA to begin with. Conducting this analysis again, may provide assurance that some the terrapin QC material values here are usable, and perhaps the experimental data collected between the reliable QC replicates can be used in addition to the newly collected data. However, until the QC replicates are reanalyzed and provide consistent measurements, these data cannot be analyzed for biological significance.

3.6. Chapter Discussion

In this experiment, an inverse relationship between the mercury concentration and the % DNA methylation in blood samples of American alligators was observed. The inverse relationship was best observed in adult alligators exposed to high mercury concentrations. While we aimed to highlight the relationship between mercury exposure and DNA methylation for long-lived reptiles, in both the wild, and captive setting. The captive alligator experiment illustrated the effect of diet on blood mercury concentrations, and suggests that maternal transfer may influence DNA methylation. High mercury concentrations are problematic in many regions, as upper level predators are often object of human consumption, as well as keystone species in the ecosystem. Conservation biologists are continually developing tools to improve monitoring of many wildlife species, however most tools used are reactionary in nature and have been developed due to a problem occurring the ecosystem previously. With additional research, DNA

methylation analysis could provide a preemptive approach to wildlife monitoring, where the precursors of ecosystem issues could be identified prior to the problem occurring in the environment.

DNA methylation for risk assessment

The experiments detailed herein describe a common epigenetic modification, global DNA methylation, which is altered as an effect of mercury exposure and age (3, 93). Changes in global DNA methylation that are solely from mercury exposure cannot be determined without mercury measurements, but global DNA methylation can be used as a metric for environmental quality. If a population of animals is sampled in their environment, the range of the % methylation can lend insight to the age, reproductive status, and level of contamination in their food source (3, 354). If there were a large discrepancy in DNA methylation between sites of the same population, this would point to a location in need of further characterization, since some aspect of their environment is causing a change in methylation compared to animals at other locations. This characterization could include nutrient profiling, contaminant analysis, comparing food web dynamics and/or assessing ecosystem quality based on land use changes.

The effects of environmental quality could also be assessed by measuring global methylation or by comparing differentially methylated regions (DMR) at specific loci between the high risk and low risk location/groups, using specific polymerase chain reaction experiments, or bisulfate sequencing. Specific genetic regions and genes that are related to the known adverse outcomes of mercury would make a good starting point for these investigations. However, the same tissue and age class would have to be sampled for accurate comparison, as different tissues are differentially methylated at different life

stages, specifically DMR1, which has recently been shown to have tissue dependent methylation in juvenile alligators (3). Instead, DMR2 may be a more advantageous comparison, as many animals from the same site may have inherited their methylation pattern from the same female, based on the maternal transfer observed in Chapter 2 (355).

Adverse outcome pathways

Filling in the blanks between changes in global DNA methylation and known adverse outcomes can be simplified using the adverse outcome pathway (AOP) framework. Following the AOP framework guidelines put forth by Villeneuve, *et al.* (195), the increased oxidative stress as a response to mercury exposure can be considered a chemical initiator (CI) that begins the cascade leading to adverse outcomes. This CI then leads to increased oxidative stress and results in the molecular initiating event (MIE), reduced DNA methylation.

Villeneuve, *et al.* (195) state that while the MIE is necessary to further describe the AOP, there can be more than one CI that initiates it, making reduced global DNA methylation an acceptable candidate, since multiple mechanisms cause it. In this case, the exposure to mercury begins the cascade of events that elicits the MIE because of increased ROS from GSH uptake and limitation by mercury, but many environmental exposures can cause increased oxidative stress. Other KEs that could follow this CI would be lipid peroxidation and protein damage, which also occur due to increased oxidative stress (Figure 1.6). Reduced global DNA methylation due to mercury exposure can be used as a guide for linking the other effects of oxidative stress to environmental exposures and adverse outcomes, as many studies have presented pieces of the AOP puzzle for mercury exposures.

Several of the known adverse outcomes of mercury exposure have been observed in wildlife, including impaired reproduction, behavioral changes, and muscular atrophy (113, 353). If a definitive link could be made between the adverse outcomes and specific genes with altered DNA methylation, then predicting, identifying and preventing population level effects would be simplified. Using the known adverse outcomes, investigators could work backwards toward DNA methylation by sequencing and analyzing genes that are known to be related to the adverse outcomes. Once the genes are sequenced, the methylation patterns, and any other changes, of the genes' promoter regions can be determined, and compared between locations (Figure 3.27). Methylation changes that are not caused by altered DNA, such as hydroxyl lesions or a sequence mutation, would not be the effect of mercury but could be related to other environmental quality issues. While reduced methylation, or hypomethylation, is what we observed in this experiment, increased or hypermethylation has also been shown to be problematic for gene regulation and has been linked to a variety of diseases (99, 324, 334, 351, 356, 357).

If a difference is found, using DNA methylation as a risk assessment tool through the AOP framework will have not only improved species monitoring, but also provided substantial data in support of improving the quality of the environment at the high-risk location through policy. In the case of human populations, prevention efforts can be taken when a high-risk group is identified, using the changes in methylation related to diet observed.

Depending upon the adverse outcome associated with the genes identified, several different management strategies can be put in place at a high-risk location, to prevent population level effects (Figure 3.27). If genes associated with muscular disorders are

identified as altered at a specific location, food supplementation can be done to avoid the effects of starvation throughout the population that would occur from decreased foraging ability. If genes related to behavior disorders are altered in a population, monitoring efforts can be increased until the specific behavioral changes are observed. If necessary, measures can be taken to separate predators from this population, provide an additional food source, otherwise alter the environment to protect the population, such as the way lights are prohibited in areas close to sea turtle nesting ground, to prevent disorientation of hatchlings and subsequent population declines. If genes related to lower reproductive success are altered in a population, captive breeding programs can begin to circumvent the effects of lowered recruitment through wild breeding populations. The AOP framework provides the opportunity to link the results of many studies relating negative effects of chemical exposure, as well as enables management decisions based on the data and relationships elucidated (Figure 3.27, 3.28).

The relationship observed between mercury concentration and DNA hypomethylation at the high mercury sites provides not only a significant statistical analysis of the relationship, but we also provide a rationale as to why previous wildlife studies have not produced consistent results or statistical significance (93, 99, 229, 337, 354, 358).

The DNA methylation data in this chapter was measured using a highly sensitive, and accurate method of analysis. Due to the extensive QC measures taken prior to analysis on the instrument, these data have been thoroughly examined for accuracy and reproducibility, and provided justification for reduced analysis of low quality data.

The unfortunate circumstance surrounding the diamondback terrapin samples leaves a question unanswered, and was not able to provide insight for the mercury and DNA methylation relationship observed with the wild alligator samples. While the original dosing study yielded uneven sample sizes between the dose groups, this is not an uncommon complication in wildlife biology. If the data from these samples had been usable, the statistical power would have been low especially between the individual plasma time points. The low statistical power would have limited the conclusions we could have drawn from these samples, but may have provided enough rationale to conduct a larger follow-up dosing experiment.

Apart from the suggested experiments described above, there are additional analyses that could be conducted to strengthen the data presented here, answer additional questions, and advance the field of environmental epigenetics. To strengthen the data presented here, additional methods of DNA methylation measurement could be employed, as many wildlife studies do not use this LC-MS/MS method (99, 229). Analyzing the alligator DNA extracts with an enzyme linked immunosorbent (ELISA) style assay would make these results more comparable to previously conducted studies, as well as determine if ELISA style method can detect the small changes observed in this study. If the ELISA assay fails to detect the changes that the LC-MS/MS did detect, this could provide an explanation for the lack of statistically significant results observed in some studies (99, 229). An immunoprecipitation (IP) assay specific for DNA methylation could also be used to confirm these results, using an anti-methylated DNA antibody specific for epigenetic analysis.

DNA methylation is the most extensively studied epigenetic modification, but there are others that could be investigated to determine their relationship with mercury exposure, including histone modification and changes in micro-RNAs. Histones are proteins that can undergo post-translational covalent modifications via acetylation, methylation, phosphorylation, ubiquitination, sumoylation, citrullination, and ADP-ribosylation, which can make determining a specific mechanism difficult (359). Measuring the modifications to histones is done via the same methods as DNA Methylation: LC-MS/MS, immunostaining and immunoprecipitation (356). Measuring the histone modifications in the alligator samples used in the study would be relatively easy using the LC-MS/MS, the preparation would require a different method than the DNA methylation analysis, but erythrocytes could be used as reptilian red blood cells are nucleated (93, 360).

Transgenerational epigenetic inheritance experiments aimed at elucidating how much of the effects of a chronic exposure is transferred through the germline could provide additional information for understanding the site/dose relationships observed in wildlife. Most epigenetic marks are lost during the early stages of development, through a process known as epigenetic reprogramming, where all the marks accumulated on the parents genome are erased and new epigenetic marks are established (361). However, epigenetic changes that are the result of chemical exposure are transferred to subsequent generations in rodent studies (311, 352, 359, 362). Deciphering transgenerational epigenetic inheritance for reptiles may be complicated, due to the varying degrees of methylation observed between the different classes of reptiles as these class specific differences in DNA methylation could lead to inconsistent results in DNA methylation

changes and different epigenetic modifications as a result (228, 361). Additional studies would need to be conducted to determine the “baseline” methylation for a specific organism, and then determine if exposure to chemicals changes the exposed animals’ epigenome before attempting to determine if transgenerational epigenetic inheritance occurs in reptiles because of chemical exposure.

This study also bypassed the direct effects of increased oxidative stress on the genome, and examines the epigenome, which may be considered an oversight. However the epigenome was specifically chosen since one type of DNA damage resulting from oxidative stress, hydroxyl adducts on the DNA strands, results in altered methylation (217, 218). The genetic mutations related to DNA methyl transferases have been shown to cause developmental abnormalities, but no research has been done of the effects of the mutations on adult organisms (363). These mutations would provide a good starting point for future research regarding the effects of mercury on the genome. Investigating these mutations in relation to mercury exposure would not only provide information about the persistent effects of mercury exposure, it may serve to link the disparate literature regarding the genetic mutations caused by mercury exposure. One study has shown that mutations and deletions in the glutamic-pyruvic transaminase gene increase with increasing mercury exposure (364). The glutamic-pyruvic transaminase gene is involved in glucose metabolism, and is used as a biomarker of liver injury, so it may be related to the secondary effects of mercury exposure discussed in Chapter 4. Another study identifies a mechanism of mercury mutagenicity related to GSH depletion, which suggests that oxidative stress is involved in this mechanism, making DNA methylation potentially indicative of this mutation (365). There have also been studies that examine

the effects of mercury on a single gene, or genomic region, but focus on specific effects of mercury exposure, such as impaired reproductive ability, intellectual disability, and liver toxicity. The genetic mutations associated with altered DNA methylation may elucidate a commonality between these studies, and serve as a starting point for a genome-wide investigation.

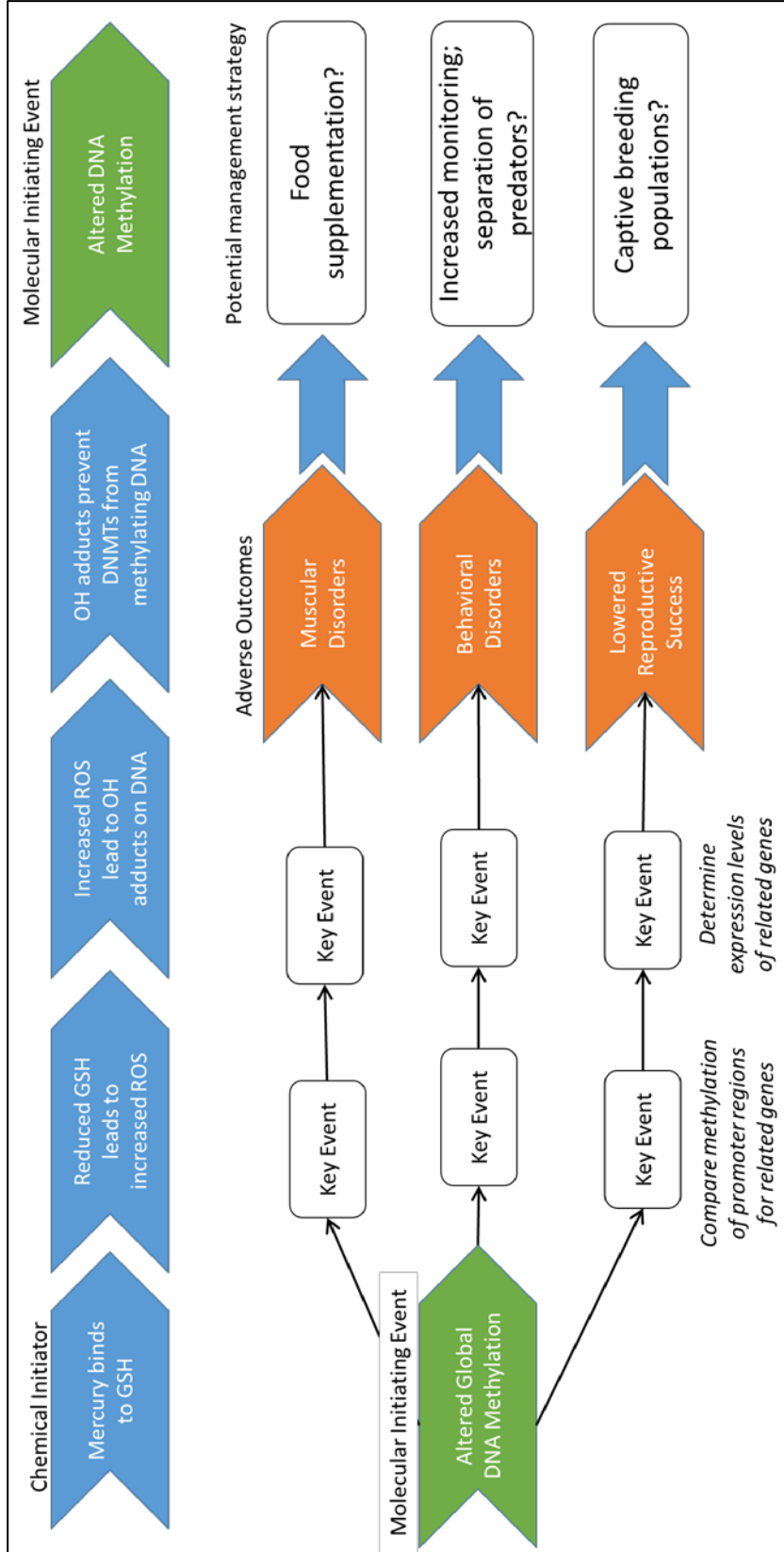


Figure 3.27. The proposed AOP design to utilize DNA methylation as an indicator of decreased environmental quality and population level changes to improve wildlife management strategies.

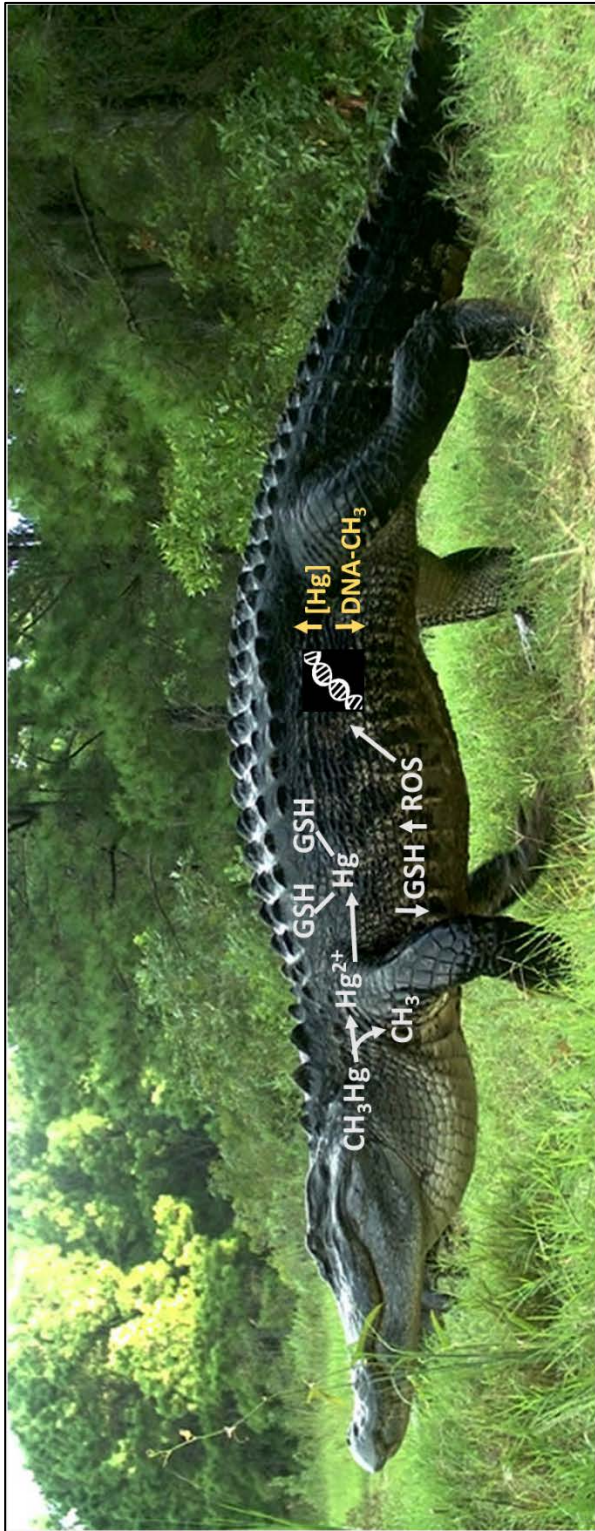


Figure 3.28. The graphical abstract of the results of Specific Aims 2 detailed in this chapter

Chapter Four: Using NMR-based metabolomics to elucidate the biochemical pathways affected by chronic mercury exposure in diamondback terrapins

4.1. Investigating the effect of mercury exposure on the metabolome

Mercury is a global pollutant, and a problem in all ecosystems. Many ecosystems have detrimental mercury concentrations throughout their food webs, but observable effects seen only at the highest concentrations in the laboratory setting (113, 116, 366). The underlying biological mechanisms related to organism-environment interactions, including mercury exposure can be elucidated by using a metabolomics approach (230, 236, 237). The biochemical impacts of these interactions can be assessed by analyzing profiles of small molecules associated with cellular pathways and biological functions (236). Investigating the small molecule profiles of animals that are exposed to mercury in their environment may elucidate the biochemical precursors that lead to the onset of the classical symptoms of mercury poisoning, such as neurodegeneration and muscular disorders (100, 124, 126, 133, 166).

As there are many adverse outcomes associated with mercury exposure, a discovery tool is preferred to identify changing molecules, rather than a tool that is highly sensitive for specific metabolites, so all changes with the exposure can be identified (367). Non-targeted metabolomics methods provide information about a diverse group of low-molecular-weight structures including lipids, amino acids, peptides, nucleic acids, organic acids, vitamins, thiols and carbohydrates, which makes the analysis complex, but highly informative (368). The non-targeted methods often identify classes of metabolites and cellular pathways that are related to an exposure or response that can be investigated in greater detail using a targeted method (369).

Previous discovery studies using non-targeted ^1H NMR based metabolomics have utilized aquatic model organisms to investigate the effects of mercury exposure (242, 244, 246). The studies using bivalves (*Ruditapes philippinarum*) and wild mullet (*Liza aurata*) have identified several biochemical pathways that are altered as a result of mercury exposure, including oxidative stress management, osmoregulation, energy metabolism and neurotransmitter synthesis (242, 244, 246, 370). The biochemical pathways identified in these studies are related to some of the known adverse effects of mercury exposure, including neurodegeneration and increased oxidative stress (7, 244, 292, 305, 321, 322, 371, 372). The similarity of the biochemical pathways affected illustrates that mercury has a common measurable effect across species, and that the cumulative results can be used for risk assessment of mercury exposure (242, 244, 246, 373).

While these, and most other metabolomics studies investigating mercury exposure use model aquatic organisms, there is a great deal of information to be gained from using non-model species that are established as sentinel species for mercury exposure, such as diamondback terrapins (*Malaclemys terrapin*) or American alligators (*Alligator mississippiensis*), sampled from field populations experiencing detrimental exposure (374). Many studies take captive bred model organisms, and subject them to polluted environmental conditions, which allows the observation of the specific effects of a short term exposure (239, 240). However, the captive bred models, such as earthworms (*Lumbricus rubellus*) and zebrafish (*Danio rerio*), do not provide information regarding the chronic effects of lifetime exposure, the way that organisms sampled from environmentally exposed populations can, despite increasing the variation between

individuals (374). To advance the metabolomic investigations of mercury exposure, a species that is exposed to mercury in its natural habitat and uses more than one area of the ecosystem (i.e. aquatic, terrestrial, benthic) is desirable, as the aquatic models only utilize the water and not the rest of their environment, so the species can be used to model more than one type of exposure (242, 244, 245).

The diamondback terrapin is an ecologically important species, which utilizes all aspects of its environment throughout its life cycle, and is exposed to high mercury concentrations throughout its natural range (83, 84, 193, 303, 375). This species has been previously identified as a sentinel species for monitoring mercury pollution in coastal ecosystems, and an indicator of the human health effects of mercury exposure (83, 303, 353). These qualities make the diamondback terrapin a candidate species for expanding the metabolomic analysis of mercury exposure, to gain a deeper understanding of the biochemical response (374).

In this experiment, wild diamondback terrapins are used as a non-model species to determine if any small molecules change in response to mercury exposure using a non-targeted metabolomic analysis. Wild adult terrapins were collected from a single location, to ensure similar lifetime environmental exposures and brought to Grice Marine Laboratory for a controlled dosing experiment mimicking environmental doses. Conducting this experiment in a controlled setting allows the individual metabolomic variation due to different dietary and environmental preferences to be reduced, but allows any potential effects of chronic mercury exposure to be observed. This experiment will provide a comprehensive analysis of the biochemical effects of mercury exposure over

time, as well as the systemic effect of chronic mercury exposure on the diamondback terrapin.



Figure 4.1. The graphical abstract of the goal of the experiments of Specific Aim 3 in this chapter.

4.2. Methods

4.2.1. Experimental design

Considering the results of experiment 2.5, in that dosing American alligator eggs has proven difficult in the laboratory setting and that adult alligators cannot be kept at the Hollings Marine Lab, previously collected samples from another species are used for metabolic analysis of mercury exposure. Samples were chosen from a previous mercury dosing experiment using wild caught captive diamondback terrapins conducted by Schwenter (353), that were also used in Chapter 3. This experiment was conducted in a high-quality manner, with samples preserved for future analyses. The experimental design is detailed in section 3.4.2 (Figure 3.24), with the terrapin metadata provided in Table 3.21. The mercury measurements were conducted using cold vapor-inductively coupled plasma mass spectroscopy (CV-ICP-MS) (Schwenter 2007). The tissue-specific mercury concentration results indicate a successful dosing scheme, with the respective average mercury concentrations for the control, low and high dose groups being 47.9 ± 19.7 ng/g; $21,268.2 \pm 5,967.2$ ng/g; $100,463 \pm 26,535$ ng/g in their erythrocytes (Table 4.1).

The results discussed by Schwenter (353) suggest that the captive animals experienced dose-specific effects of mercury exposure, but their analytical capability at the time limited the questions that could be answered. Revisiting this experiment with the analytical capabilities of a ^1H NMR metabolomics approach would enable a more comprehensive investigation of the effects of mercury exposure on the diamondback terrapin.

Schwenter (353) collected weekly blood samples throughout the duration of the dosing experiment, and liver samples at the end of the study via necropsy.

The plasma samples selected for this experiment were collected after the terrapins were captured and acclimatized to the laboratory setting with a standardized diet; after the first dosing season; and at the end of the second dosing season prior to necropsy (numbers 1, 2, and 3 in Figure 3.24). To observe the changes in organisms over time, blood samples are commonly used as they are non-invasive, can be repeatedly collected, and are correlated to mercury concentrations in the internal organs that have been historically sampled for mercury analysis (75, 78, 89, 94, 376). These time points were chosen as they would enable comparisons between the un-dosed terrapin metabolome (Figure 3.24, 1), and the cumulative effects of one and two years of mercury exposure (Figure 3.24, 2 and 3, respectively). The plasma was separated from the erythrocytes after collection, and stored at -20° C.

Terrapin liver samples were also used because liver is a commonly monitored tissue for mercury exposure, as the body cannot easily detoxify mercury, mercury accumulates in this organ proportionally to other tissues, which could lend insight to the biochemical effects of chronic mercury exposure (Table 4.1) (97, 188, 213, 283, 376-378). The liver samples were collected by necropsy. The right lobe of the liver was used by Schwenter (2007) for histological analyses that did not yield dose specific results, and the left lobe was stored whole in plastic bags at -20° C. At the start of this experiment the samples were transferred to -80° C storage at the Hollings Marine Lab.

Table 4.1. The total Hg concentration data for liver, kidney, brain and erythrocytes (RB) from the terrapin dosing study taken from Schwenter (2007).

Replicates from liver, kidney and brain are presented, along with the average and relative standard deviation. The RBC and scute samples had one aliquot for analysis, so the single value is presented. The control, low and high dose groups are denoted by the letters C, L and H. Values are presented in ng/g, or parts per billion (ppb).

Turtle ID	Treatment Group		Liver THg (ppb)	Kidney THg (ppb)	Brain THg (ppb)	RBC THg (ppb)	Scute THg (ppb)
M2	C	Run 1:	231.11	52.38	10.68		
		Run 2:	218.82	57.53	13.46		
		Run 3:	221.49	59.07	13.38		
		Average:	223.8	56.33	12.5	36.8	245.46
		RSD:	2.89	6.22	12.66		
M4	C	Run 1:	537.42	117.82	49.64		
		Run 2:	529.44	105.97	48.91		
		Run 3:	534.97	106.5	49.75		
		Average:	533.94	110.09	49.43	37.57	294.94
		RSD:	0.77	6.08	0.92		
K1	C	Run 1:	73.08	47.7	8.46		
		Run 2:	75.84	49.24	8.75		
		Run 3:	75.72	48.45	8.64		
		Average:	74.88	48.46	8.62	48.58	302.31
		RSD:	2.08	1.58	1.68		
K3	C	Run 1:	192.39	50.03	14.69		
		Run 2:	193.12	51.25	13.95		
		Run 3:	195.6	49.27	14.06		
		Average:	193.7	50.18	14.23	32.75	218.22
		RSD:	0.87	1.98	2.82		
M6	C	Run 1:	376.57	121.49	14.54		
		Run 2:	364.38	128.55	15.08		
		Run 3:	377.95	123.99	15.03		
		Average:	372.97	124.68	14.88	43.02	270.5
		RSD:	2	2.87	2.02		
M17	C	Run 1:	307.05	107.11	25.66		
		Run 2:	311.59	97.34	24.82		
		Run 3:	307.21	97.88	25.33		
		Average:	308.62	100.78	25.27	48.31	236.7
		RSD:	0.84	5.45	1.66		
K7	C	Run 1:	126.3	57.62	16.73		
		Run 2:	126.58	57.44	18.22		
		Run 3:	124.81	60.73	16.51		
		Average:	125.9	58.59	17.15	56.85	202.91
		RSD:	0.76	3.15	5.42		
F3	C	Run 1:	1659.38	247.62	20.54		
		Run 2:	1682.34	229.84	20.79		
		Run 3:	-	214.93	19.93		
		Average:	1670.86	238.73	20.67	103.12	303.84
		RSD:	0.97	5.27	0.84		
M7	C	Run 1:	307.05	74.14	15.51		
		Run 2:	311.59	78.2	15.61		
		Run 3:	307.21	75.2	16.44		
		Average:	308.62	75.85	15.85	39.19	213
		RSD:	0.84	2.78	3.22		
F2	C	Run 1:	229.06	37.85	11.49		
		Run 2:	229.14	38.31	12.39		
		Run 3:	226.82	40.24	11.14		
		Average:	228.34	38.8	11.67	33.98	207.48
		RSD:	0.58	3.28	5.56		
F5	C	Run 1:	101.04	51.6	13.13		
		Run 2:	102.93	52.46	13.32		
		Run 3:	100.63	51.97	13.2		
		Average:	101.53	52.01	13.18	47.21	265.82
		RSD:	1.21	0.84	0.88		
M3	L	Run 1:	18580.5	30588.82	5465.5		
		Run 2:	18718.28	30281.59	5576.1		
		Run 3:	17496.6	31146.38	5237.08		
		Average:	18265.13	30672.26	5426.23	18780.11	26339.48
		RSD:	3.66	1.43	3.19		

Turtle ID Treatment Group		Liver THg (ppb)	Kidney THg (ppb)	Brain THg (ppb)	RBC THg (ppb)	Scute THg (ppb)	
M1	L	Run 1:	17415.87	18787.78	4723.14	28798.04	32454.13
		Run 2:	17737.77	18656.75	4789.25		
		Run 3:	17550.07	18835.91	4851.2		
		Average:	17567.90	18760.15	4787.86		
		RSD:	0.92	0.49	1.34		
M12	L	Run 1:	14385.33	6678.61	3166.12	22753.56	32903.63
		Run 2:	14192.08	6684.37	3348.13		
		Run 3:	14173.03	6831.88	3147.75		
		Average:	14250.15	6731.62	3220.67		
		RSD:	0.82	1.29	3.44		
K2	L	Run 1:	21382.96	24296.63	1344.48	23297.67	55573.26
		Run 2:	21295.04	23964.24	1293.8		
		Run 3:	22036.05	23750.57	1318.6		
		Average:	21571.35	24003.81	1318.96		
		RSD:	1.88	1.15	1.92		
K11	L	Run 1:	13930.45	9365.74	3477.95	12711.47	39149.34
		Run 2:	13809.20	9178.09	3431.16		
		Run 3:	14592.50	9333.12	3468.74		
		Average:	14110.72	9292.32	3459.28		
		RSD:	2.99	1.08	0.72		
M14	H	Run 1:	81998.68	133967.38	37370.23	127757.39	192982.97
		Run 2:	81317.73	144466.24	35437.6		
		Run 3:	90703.14	150876.51	37719.8		
		Average:	84673.18	143103.37	36842.54		
		RSD:	6.18	5.97	3.34		
K9	H	Run 1:	32159.13	73285.82	16032.21	75852.47	231505.85
		Run 2:	33126.90	71907.13	16905.56		
		Run 3:	32772.41	70747.39	16121.52		
		Average:	32686.15	71980.11	16353.1		
		RSD:	1.50	1.77	2.94		
F8	H	Run 1:	72869.94	145302.29	25625.02	107914.68	175279.55
		Run 2:	74324.63	146300.73	25517.36		
		Run 3:	70944.23	141209.83	24645.87		
		Average:	72712.93	144270.95	25262.75		
		RSD:	2.33	1.87	2.13		
M11	H	Run 1:	55716.09	91481.74	25274.78	89915.3	70835.54
		Run 2:	58807.28	97189.23	26887.53		
		Run 3:	58979.27	100973.87	26884.59		
		Average:	57834.21	96548.28	26348.97		
		RSD:	3.18	4.95	3.53		
M20	H	Run 1:	62180.29	47249.75		88833.69	16103.56
		Run 2:	73788.14	36183.86			
		Run 3:	77696.84	37177.25			
		Average:	71221.76	40203.62			
		RSD:	11.33	15.23			
K4	H	Run 1:	129820.77	89746.38	21195.11	122853.46	188246.56
		Run 2:	105172.10	81248.87	2202.53		
		Run 3:	90088.32	83235.45	21907.25		
		Average:	108360.39	84743.56	21768.3		
		RSD:	18.51	5.25	2.38		
F6	H	Run 1:	41306.26	282821.11	23509.01	115060.68	196325.46
		Run 2:	45430.64	320373.7	23457.26		
		Run 3:	52517.82	258016.25	24379.32		
		Average:	46418.24	287070.35	23781.86		
		RSD:	12.22	10.94	2.18		
M19	H	Run 1:	49439.42	94020.9	13394.99	82533.12	197980.65
		Run 2:	53373.69	91819.38	13439.34		
		Run 3:	51280.25	97258.82	13252.95		
		Average:	51364.45	94366.36	13362.43		
		RSD:	3.83	2.9	0.73		
M18	H	Run 1:	80942.17	185247.08	30362.35	159710.83	229377.59
		Run 2:	83032.33	173453.74	30173.24		
		Run 3:	84661.58	183487.43	29117.44		
		Average:	82878.69	174062.75	29884.35		
		RSD:	2.25	6.26	2.24		
F10	H	Run 1:	65344.13	75256.26	23566.37	134199.18	151258.42
		Run 2:	80432.07	76481.19	22789.56		
		Run 3:	110707.87	78562.6	23110.36		
		Average:	85494.69	76766.68	23152.1		
		RSD:	27.02	2.18	1.69		
K10	H	Run 1:	46263.18	81641.09	10513.29	98384.11	219010.22
		Run 2:	47606.53	82788.19	11122.17		
		Run 3:	46346.18	87991.89	11239.3		
		Average:	46738.63	84140.39	10958.25		
		RSD:	1.61	4.02	3.56		

* THg measurements in selected internal tissues obtained at the conclusion of the long term accumulation experiment. Included for reference are the blood and scute THg concentration at time of sacrificing for each individual.

4.2.2. *Methods development*

Non-targeted metabolomic analysis of tissues is used for a variety of different applications (379, 380). Many studies utilize bio-fluids, such as plasma or urine, which can be easily and repeatedly collected, and require little laboratory preparation (380-382). Tissue samples, such as liver, require extensive laboratory preparation, including homogenization, lyophilization and extraction (382). Optimization of tissue extraction methods is critically important to ensuring that the metabolites in the sample are consistently replicated and that metabolites are not degrading as a function of the extraction method used (380).

The Bligh and Dyer method was used for tissue extraction. This method consists of a methanol/chloroform/water solvent extraction technique that has been shown to yield good fractionation of polar and non-polar molecules, low contamination of larger non-polar molecules, and produce reproducible results with both wet and dry tissue samples (383). Determination of the sample preparation method (wet or dry) that provides the most consistent extraction of polar metabolites, with low variability between extractions, and the greatest sample stability with less feature changing over time, ensures that the highest quality of data is collected from the tissue samples. The dry method adds the additional step of lyophilizing the sample prior to solvent extraction, to remove any water within the sample, which reduces variation between samples (383). However, lyophilizing does not always yield greater data quality due to species specific and tissue differences, so testing each method on a new sample ensures that the most reproducible method is used for each tissue experiment.

Liver sample preparation

The left lobe of the diamondback terrapin frozen liver tissues were acquired from -20°C storage at the Grice Marine Laboratory and transferred to -80 °C storage at the beginning of this experiment. The liver tissues were cryohomogenized using a benchtop Retsch CryoMill (Haan, Germany), following the method described in section 2.2.2. The powdered liver samples were aliquoted into cryovials, and stored at -80 °C until time of extraction. Any excess liver tissue was pooled to create a control material, the terrapin liver control material (TLCM) that would serve as a species and experiment specific quality measure throughout these experiments. Five TLCM replicates were used to test both, the wet and dry, sample preparation methods to determine the best method for this experiment.

Control material sample processing

TLCM samples ($n = 10$) weighing approximately 0.100 g were added to bead homogenization tubes. Five TLCM samples were put under a vacuum pressure drying system for 12 hours, and then weighed again so the % water loss could be calculated for extraction with the appropriate amount of solvent. The average water loss for the TLCM replicates was 61%, the average mass of the dry tissue was 0.039 g, and the average mass of the water loss was 0.062 g. The % water loss calculations were then used to determine the volume of extraction solvent required according to the 2.0:2.0:1.8 ratio of methanol/chloroform/water put forth by Bligh and Dyer (384) to extract non-polar lipids from a biological sample. This method is appropriate for NMR-based metabolomic analysis of polar metabolites, as all non-polar molecules must be separated from the

sample. The extraction solvent volumes, for both wet and dry samples, were 0.404 mL methanol and 0.16 mL water pipetted directly into the bead homogenization tube containing each sample, for homogenization using a Precellys homogenizer (Atkinson, NH) at 6500 rpm for two 15s increments. The wet and dry samples were then pipetted into a glass culture tube containing 0.404 mL chloroform and 0.20 mL water, and vortexed quickly.

Each sample was vortexed and incubated on ice for 10 minutes before centrifuging for 5 min at 2000 rpm, to separate the polar and non-polar layers. The polar layer was pipetted into an Eppendorf tube, without disturbing the protein pellet or non-polar layer. The polar fraction was dried in the Eppendorf tube, using the pressure vacuum dryer for 2 hours, once dried, the weight of the dried metabolites was recorded. The polar metabolite pellet was reconstituted using phosphate buffer, vortexed and transferred to a glass 7-inch 5mm NMR tube. The tubes were centrifuged by hand to collect the sample in the bottom of the tube, wiped to remove any dust or fingerprints, and placed in the auto sampler and put in queue for analysis. The wet and dry extraction replicates were analyzed repeatedly for 52 hours, to determine the stability of each tissue preparation method type over time.

Results

The results of the tissue preparation comparison showed that the dry preparation method had less variation between samples. The dry extraction was observed to be more reproducible for this tissue type, since the metabolite peaks are less variable (Figure 4.2). This was observed by overlaying the chemical shift spectra for all samples, with the

different preparation methods denoted by different colors; the wet preparation samples are colored blue, and the dry preparation samples are colored black (Figure 4.2). There is a greater amount of variation in the peak height of the wet (blue) TLCM samples, which fluctuate around the solid black line (dry preparation TLCM replicates), giving a different peak height for each sample (Figure 4.2). The dry preparation TLCM samples are much more consistent in peak height, which is observed by all 5 sample chemical shifts coming together to form a thick black line, whereas all of the wet preparation samples are separate (Figure 4.2). Less time related changes were observed in the dry TLCM replicates, the wet TLCM replicates had new metabolite peaks emerging after 18 hours, and had more over all variability (Figure 4.3). Both preparation methods had the same metabolite peaks shift over time (Figure 4.3, 2.93 ppm), and a peak that changed peak height with every analysis (Figure 4.3, 2.89 ppm). However, the rest of the metabolite peaks had less variation in peak height over time in the dry preparation samples, and the wet preparation samples had new metabolite peaks appearing after 18 hrs. (Figure 4.3, black arrows). These results lead to the determination that the dry preparation method provides a more stable and reproducible metabolite profile, with less features changing over time than the wet preparation method.

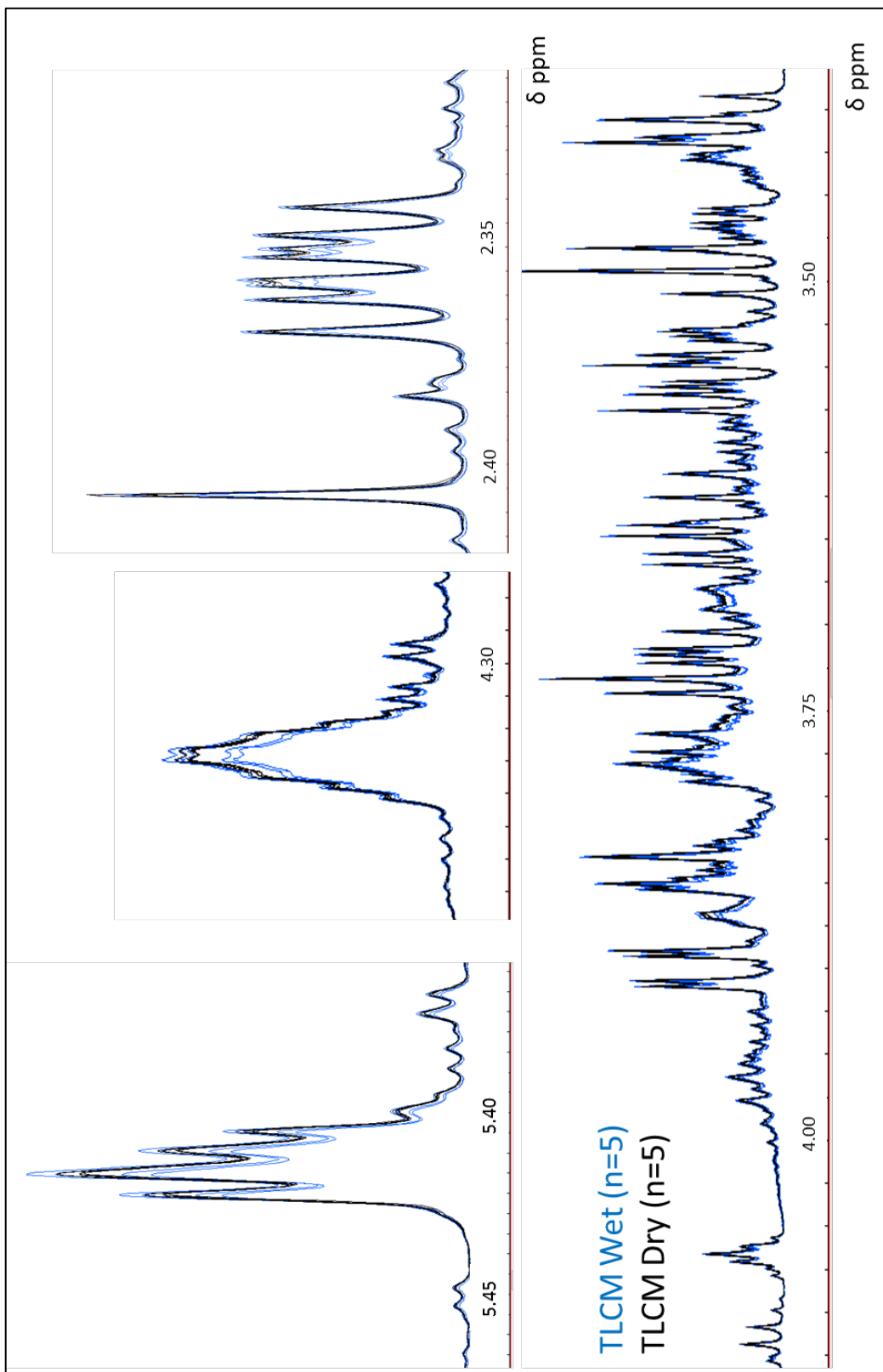


Figure 4.2. The overlaid sections of the TLCM replicate spectra showing peaks that differ in relative abundance when the wet/dry extraction methods are compared.

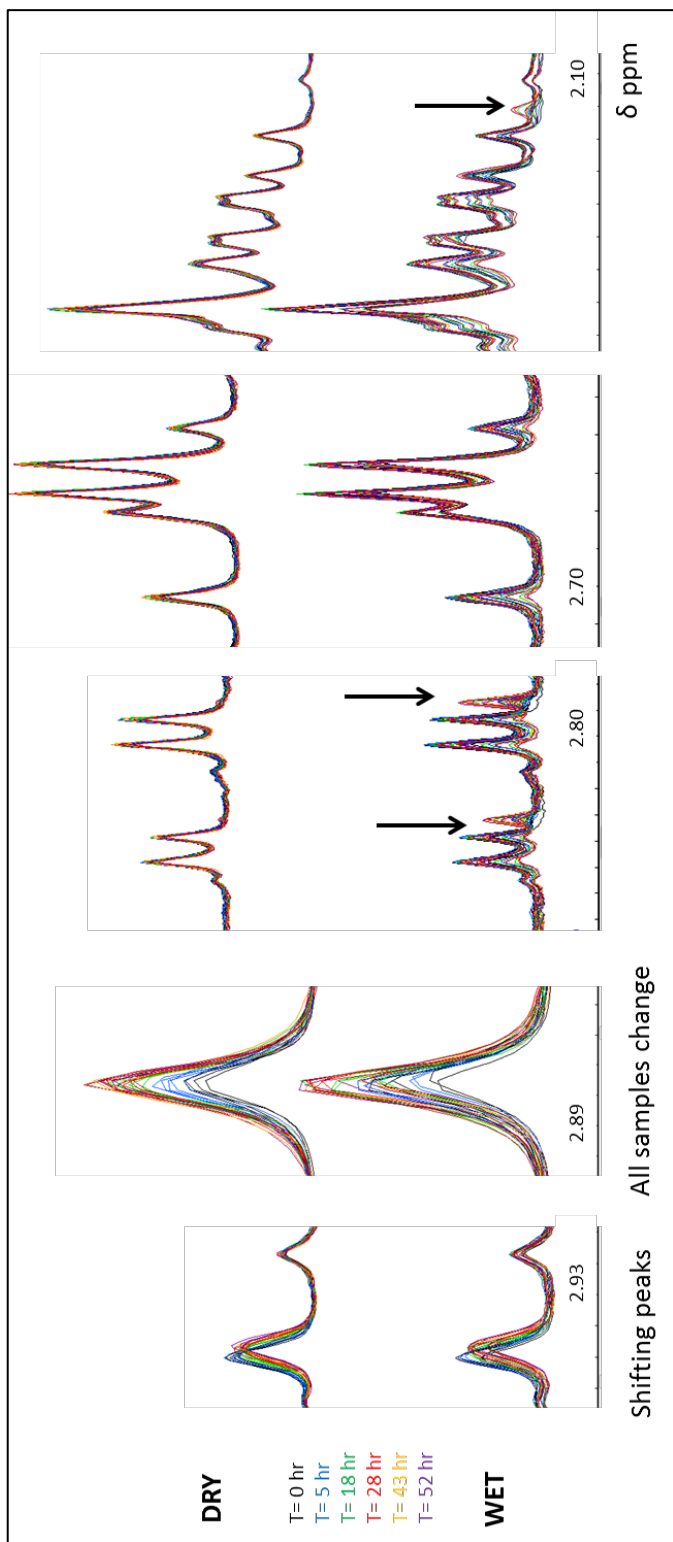


Figure 4.3. The overlaid sections of the spectra with peaks that change in relative abundance between the wet/dry extraction methods stability comparison for the terrapin liver control material replicates. The black vertical arrows indicate new peaks emerging after 18 hours in the auto sampler.

4.2.3. *Experimental sample extraction*

Plasma samples

The diamondback terrapin plasma samples were prepared using a size exclusion filter to remove high molecular weight compounds from the plasma sample, leaving the small molecules of interest. Prior to use, the size exclusion filters were vortexed in a beaker with Milli Q-water overnight, using a solvent cleaned stir bar over a room temperature stir plate with the speed set to spin each filter continuously. This step served to remove any impurities that may interfere with the analysis; Milli-Q water was used as the pH \approx 7.0, which is close to that of the phosphate buffer used in the subsequent sample preparation (pH = 7.29). Excess water was removed from the filters by pipette, and each 500 μ l plasma sample was split between two filters (250 μ l each) for separation by centrifugation. Any samples that had excess plasma after the 550 μ L was removed were pooled to create a species and experiment specific terrapin plasma control material (TPCM), to analyze alongside the samples and replicates of the NIST SRM 1950 (Metabolites in Frozen Human Plasma), to assess data quality throughout the experiment. The plasma was centrifuged at 10,000 rpm at 4°C for 90 minutes. The total volume of the TPCM pool was slightly lower than expected, so to ensure our analysis included four control material replicates, so only 170 μ l of plasma filtrate was removed from each size exclusion filter and added to the Eppendorf tube with 430 μ l phosphate buffer. NIST SRM 1950 replicates had 200 μ l of plasma filtrate removed from each filter and added to an Eppendorf tube. Then 400 μ l of 0.1 M phosphate buffer with deuterated water and 1.0 mM 3-Trimethylsilyl 2,2,3,3,-d₄ propionate (TMSP) which served as the chemical shift reference, was added to each Eppendorf tube, and vortexed for 10 seconds. Finally, 550

μl of the plasma filtrate and phosphate buffer solution was pipetted into a glass 7-inch 5mm NMR tube. The stability of the plasma samples was determined similar to the liver methods development samples, with less changing metabolites being observed in samples analyzed under 18 h post extraction, than those analyzed after 18 h.

Liver samples

The powdered diamondback terrapin liver samples were removed from $-80\text{ }^{\circ}\text{C}$ storage with the TLCM, and NIST SRM 1946 (Fish Tissue) control materials, and were lyophilized, and extracted following the method described in the Methods Development section above. Briefly, the % water was calculated for the lyophilized control and experimental samples. The average % water for the liver samples was 64.9%, and 71.7% for the NIST SRM 1946 replicates. The extraction solvent volumes were calculated for each group of samples, using the 2.0/2.0/1.8 methanol/chloroform/water solvent ratio (384). Once the samples were extracted, the extracts were dried and the dried metabolite weight was recorded before the metabolite pellets were reconstituted with TMSP buffer. When fully dissolved, the sample extracts were pipetted into glass 7-inch 5mm NMR tubes and put in queue for analysis on the instrument.

4.2.4. NMR measurement

NMR operation & experiments

A Bruker 700 MHz NMR set to a temperature of 298 K was used in these analyses. The magnetic field of the NMR was shimmed to achieve greater uniformity in the magnetic field for each sample type. The NMR was tuned and matched using the wobble curve minimum as a guide for adjustment. Optimal conditions were achieved when the wobble curve was centered at the bottom of the screen, which indicates that the NMR probe has been tuned to each sample matrix.

Each sample was analyzed using the 1D Nuclear Overhauser Effect spectroscopy (1D NOESY) experiment, and a representative sample of each tissue type (plasma and liver) was analyzed using the 2D Heteronuclear Single-Quantum Correlation (HSQC) experiment. Each of these methods of data acquisition provides different information about the molecules in the sample by using different sequences of electromagnetic pulses, and both are used for accurate identification of metabolites (385).

The 1D NOESY pulse sequence is a 90° electromagnetic pulse, which puts the sample under a transverse magnetization, and puts all the molecules that normally spin in different directions into the same plane. The time it takes for the molecules to go back to their initial state, or free induction decay (FID), is measured, and then converted to a spectra using the Fourier transformation (386, 387). The molecules in the sample will take different amounts of time to get back to their initial state based on their chemical properties, which results in separate peaks along the spectra generated from the FID data.

The HSQC experiment has a different and longer pulse sequence than the 1D NOESY experiment. This experiment detects the less abundant ^{13}C nuclei by making use of the ^1H nuclei that are more abundant, and using the ^{13}C - ^1H bond's spin-spin coupling interactions between the nuclei to determine the relationship (380, 386). The transverse magnetization affects the ^1H nuclei, which is transferred to the ^{13}C nuclei, and then back to the ^1H nuclei for detection. The pulse gradient ratio for $^{13}\text{C}:^1\text{H}$ is 4:1, since ^{13}C is much less abundant than ^1H , it is more difficult to detect (387).

NMR acquisition parameters

The NMR acquisition parameters for the 1D NOESY experiment were set to conduct 8 steady state scans with 80 transient scans for the liver samples and 160 transient for the plasma samples. The spectra width was set to 20 ppm, with an acquisition time of 2.34 s, and a dwell time of 35.7 μs .

For the HSQC experiment the NMR was set to conduct 256 steady state scans with 128 transient scans for each sample. The spectral width was set to 11 ppm on the second frequency axis (F2), and 180 ppm on the first frequency axis (F1). The increment for delay was 1.5 s, with the acquisition times of 0.13s (F2), and 0.008 s (F1), and a dwell time of 65 μs .

NMR spectrum processing

The FID data collected by the NMR was Fourier transformed into a chemical shift (δ or ppm). The plasma and liver 1D chemical shifts were manually phase corrected according to the internal standard (TMSP) peak, with the baseline automatically corrected. The phase corrected chemical shift data were exported for additional analysis.

The 2D HSQC data required manual phase corrections for both frequency axes (F1 and F2) of both the plasma and liver samples.

4.2.5. Data analysis

Quality control

To determine the quality of the data in this experiment the differences in the replicate control materials were assessed using the % relative standard deviation (%RSD). To calculate the %RSD, a bucket table was generated (described below) using the control material replicates, and the experimental samples. This bucket table was then examined using a principle component analysis (PCA) to determine commonalities between the samples. The PCA allows control materials to be inspected for similarity by relative abundance and presence/absence of metabolites (PCA described in further detail below). Irregularities in the SRM replicates could be indicative of inconsistent extract methods or other steps in the preparation process. The bucket table was then exported from AMIX to Excel for mathematical analysis. The 1960 buckets across the chemical shift spectra were divided into 32 sections, with the standard deviation calculated for each section. The noise level of the spectra was estimated at $3 \times$ the smallest standard deviation of those 32 sections. The noise level was then subtracted from the spectral bins to allow calculation of the % RSD of just the metabolite abundances across the spectrum (388). If the median RSD values of the control materials were within the published ranges of being acceptable for 1D NMR, the additional analyses were conducted (388).

Plasma quality control measures

The PCA conducted using the plasma control materials and NIST reference materials showed that there was little variation within the TPCM and NIST SRM 1950 replicates (Figure 4.4). The median % RSD of the TPCM and of the NIST SRM 1950 replicates that were analyzed alongside the experimental plasma samples was 11.5% and 8.54%, respectively. The median % RSD of the experimental terrapin plasma samples was 39.3% (Table 4.3). The low % RSD of the control materials provides confidence that the results of this analysis are reproducible, as they are less than the technical variation expected from human cell lines, 14%, and are expected to have greater variation than tissue replicates (388).

Liver quality control measures

The PCA conducted using the liver sample control materials showed that there was little variation within the TLCM and NIST SRM 1946 replicates (Figure 4.5). The median % RSD of the TLCM replicates, and of the NIST SRM 1946 that were analyzed alongside the experimental liver samples was 3.3% and 5.7%, respectively (Table 4.3). The low % RSD of the NIST SRM 1946 replicates and the TLCM replicates represent a high degree of control on the measurement process, as the technical variation is below 10%, which is average among fish liver studies using 1D NMR (388).

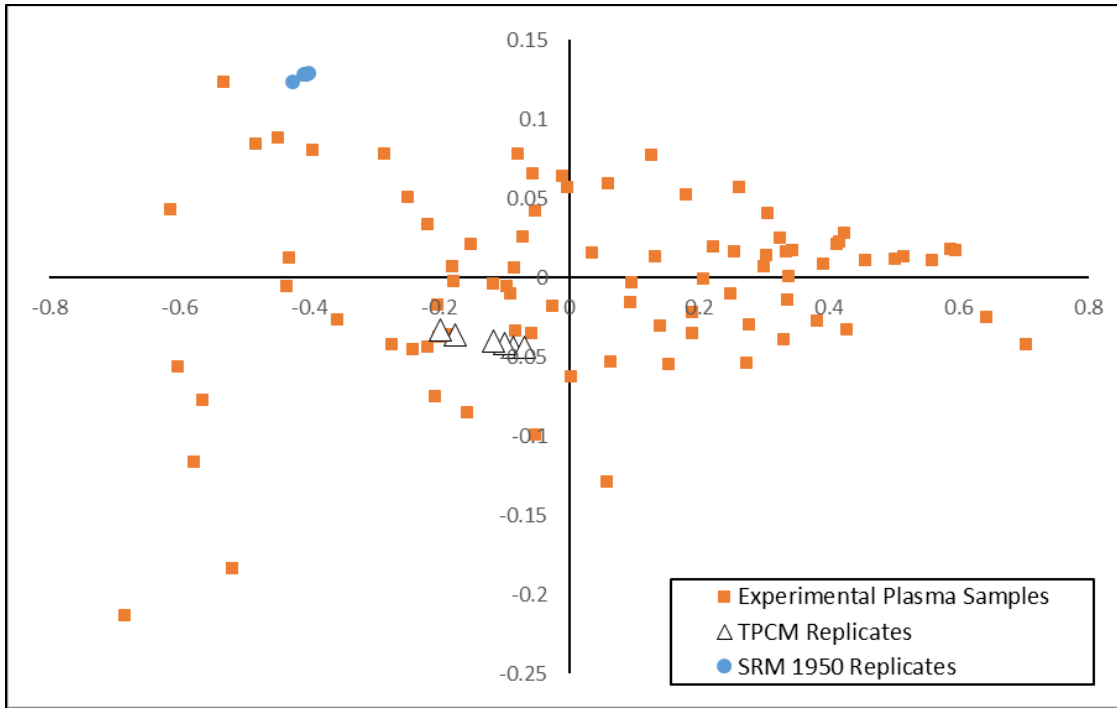


Figure 4.4. The Principle Component Analysis (PCA) showing the technical and individual variance between the control materials and experimental samples in the plasma analysis. The figure shows the five SRM 1950 replicates, the six TPCM replicates and the 85 experimental terrapin plasma samples.

Table 4.2. The summary statistics for the relative standard deviation (RSD) calculations of the terrapin plasma control material (TPCM) replicates.

<i>Terrapin Plasma Quality Measures</i>		
Summary Statistics	TPCM %RSD	SRM 1950 %RSD
Min:	0.57	0.37
Max:	181.63	69.06
Average:	20.14	10.82
Confidence:	1.54	0.57
Median:	11.50	8.54
Interquartile Range:	21.83	11.40
3rd quartile:	27.15	15.36
1st quartile:	5.32	3.96

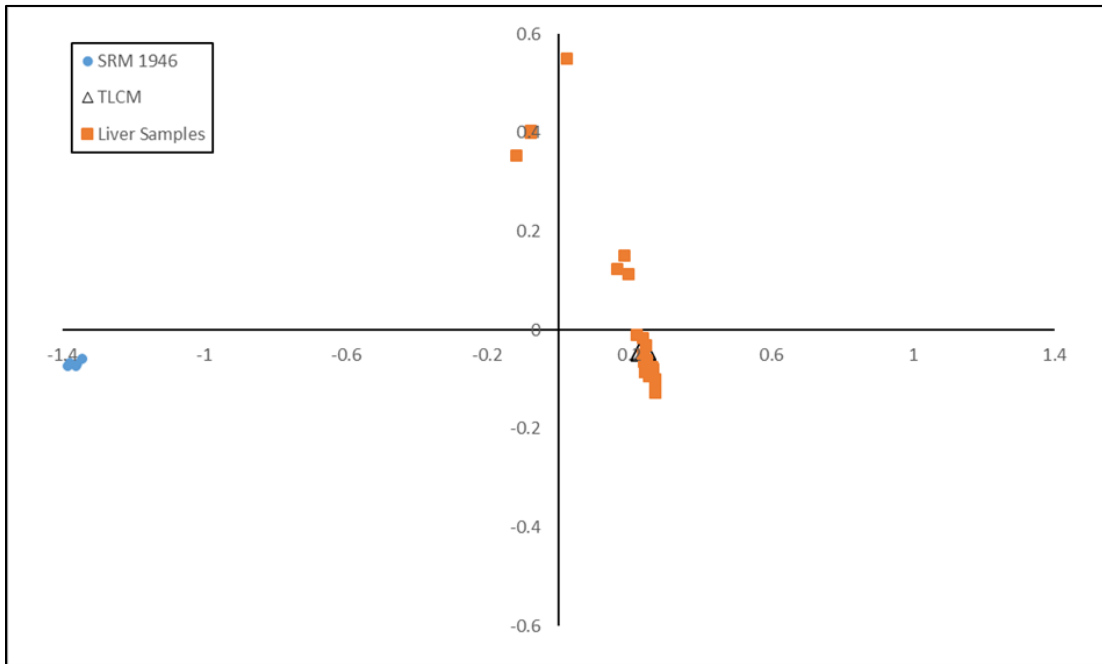


Figure 4.5. The Principle Component Analysis (PCA) showing the technical and individual variance between the control materials and experimental samples in the liver analysis. The figure shows the five SRM 1946 replicates, the four TLCM replicates and the 29 experimental terrapin liver samples.

Table 4.3. The summary statistics for the relative standard deviation (RSD) calculations of the terrapin liver control material (TLCM) replicates, NIST SRM 1946 replicates, and experimental terrapin liver samples.

<i>Terrapin Liver Quality Measures</i>		
Summary Statistics	TLCM %RSD	SRM 1946 %RSD
Min:	0.15	0.47
Max:	92.90	99.60
Average:	6.21	8.94
Confidence:	0.44	0.64
Median:	3.31	5.70
Interquartile Range:	6.26	8.66
3rd quartile:	7.81	11.66
1st quartile:	1.55	3.00

Generating bucket tables

NMR chemical shift spectra include data for the relative abundance of thousands of small molecules. To examine the changes across peaks between samples, the spectra are divided into smaller sections called buckets, which calculate the total area of the peak within each bucket. The buckets can be compared between samples, since they are a numeric representation of the entire NMR spectrum. The only regions that will be excluded from the bucketing process are the regions that are specifically entered into the software, and generally relate to extraction solvent peaks. The method used to generate the buckets across the NMR spectrum affects the data that is incorporated into the bucket table, which can affect the results of the statistical analysis. The two bucketing techniques chosen were uniform rectangular and intelligent bucketing, as each offers distinct benefits in inspecting the data (389).

Uniform rectangular bucketing evenly divides the entire NMR spectrum into 1960 evenly spaced buckets, 0.005 ppm in width. This method includes all regions on the spectra, including large sections of background noise.

Intelligent bucketing allows the user to choose sections of the spectra that include spectral peaks and omit sections that are not of interest, such as regions of background noise or exclusion regions. This method should highlight the most important buckets, since only areas of interest are included.

Sample bucketing

The terrapin plasma and liver sample spectra were uniformly bucketed, after the regions pertaining to chemicals used in the preparation process (water (4.5307-5.2003)

and phosphate buffer (2.2208-2.22526)), as well as the region pertaining to urea (5.9920-5.5454; plasma), were excluded. To build the intelligent bucket table, regions without spectral peaks were not included. Uniform bucketing resulted in 1825 buckets, whereas intelligent bucketing resulted in 460 buckets in the plasma samples, and 1918 and 350 buckets, respectively, in the liver samples.

It is important to now that multiple buckets can correspond to a single molecule, since molecules disassociate along the chemical shift based on their physical properties. The ID NOESY experiment detects hydrogens, which are shielded by electrons and other atoms in a molecule, with the amount shielding increasing with the number of electrons (390). The magnetic resonance is influenced by the amount of shielding each nucleus has, so nuclei that are shielded differently give different resonance signals along the chemical shift spectrum (390). When a molecule has multiple sections that are chemically equivalent, multiple resonance peaks appear very close to each other along the chemical shift. Both situations, nuclei that are and are not chemically equivalent to each other can occur in one molecule, which results in resonance peaks in separate regions of the chemical shift, as well as multiple peaks within one region of the chemical shift all corresponding to the same molecule. So while many buckets may be significant, they may correspond to the same molecule.

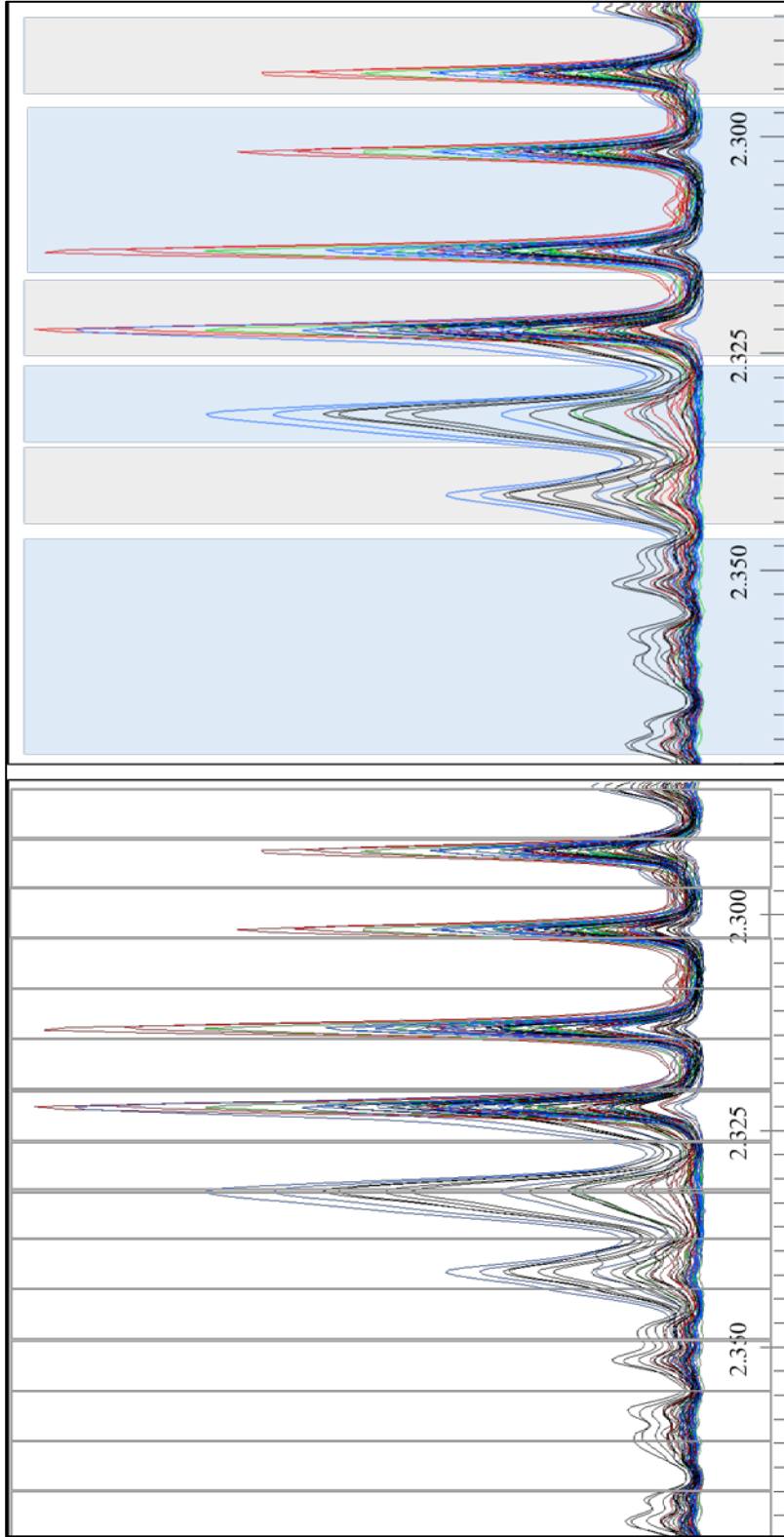


Figure 4.6. A representation of uniform (left) and intelligent (right) bucketing techniques.

Multivariate statistical analysis - principle component analysis

The principle component analysis (PCA) is a multivariate statistical tool that transforms a set of observations/samples with many variables that are expected to be correlated by some biological relationship, into a set of linearly uncorrelated values (391). The transformation is done by reducing the dimensionality of the data through linear algebra into a specified number of “principle components” of the data (391, 392). The principle components simplify the data by emphasizing strong patterns and building a visual model to describe the variation that was simplified (391). This analysis provides several plots to describe the model made from the variance in the data (391-393). The loadings plot shows the buckets from the chemical shift spectra organized by the amount of influence each bucket has on the model. The principle components are derived from the vectors through the loadings plots that explain the greatest amount of variance in the data (392). The principle components (PCs) are provided in descending order, making PC1 the most important component of the data. The PC scores plot is the result of the model generated, and shows how much influence each included PC has on each sample/observation. The influence plot shows how well the observations/samples fit the model, by combining residual and leverage values into a scatter plot, making possible outliers to be easily observed (391-393).

The bucket table contains the data from which the PCA derives the model of variance. The bucket tables can be normalized and scaled in multiple ways to observe differences in the data more clearly (392). Normalization affects the buckets within each sample, and the scaling method affects the peaks across the samples. Both methods can influence the data incorporated into the PCs, and affect the PCA scores plot. The PCA

can be biased toward the largest spectral peaks in the samples, as they have the highest values in the bucket table (392). To understand the inherent bias in the analysis, as well as the differences that exist in the data set, two different bucketing and scaling methods are used. After bucketing is complete the buckets are either not scaled or, Pareto scaled. However, the unscaled buckets are not reflective of raw data, all bucketed data that is incorporated into a PCA is mean centered, which reduces variability across each bucket, making the buckets more comparable to each other. After mean centering, the data is still subject to the bias of large peaks, regardless of the amount of change in the large peaks between the samples. This bias can be observed by using different scaling methods to view the data. To observe these differences, we use unscaled mean centered data to observe what the bias in the PCA may be, and the Pareto scaling technique, which reduces this bias by using the mean centered value, divided by the square root of the standard deviation of each variable. Using both visualization methods across both bucketing techniques will allow an assessment of the variation in the data, as well as demonstrate the effects of bucketing and scaling technique on the results, since each of these influence the loadings that are incorporated in the PCA, and are what the PCs are based on.

Univariate statistical analysis- t-test comparisons

To conduct the univariate t-tests across all buckets, the exported bucket tables were sorted in Microsoft Excel. The average of each bucket was calculated for each dose group. A t-test with a significant difference spectra (SDS) comparison and subsequent false discovery rate correction (FDR) was applied to the individual bucket comparisons (394, 395). The SDS comparison is done by comparing the t-test p value for the buckets

being compared between the two groups to the alpha value of 0.05, if the t-test p value is smaller than the alpha value, this denotes significantly different spectra (SDS) between the two groups. Listing the SDS results allows the inspection of the significant buckets without the spectral features, so the single bins that are significant and the adjacent bins with opposing signs (+ or -), can be removed as false discoveries by using the spectra and loadings plots or confirmation because they are likely areas with high variance in background noise and not a metabolite peak. The significant buckets are then sorted by p value for the FDR calculations. The FDR correction uses the rank of each bucket, determined by p values in ascending order, multiplied by 0.05, and then divided by the total number of buckets as the FDR p-value (394). The FDR p value is then multiplied by the total number of buckets, and then divided by the original t-test p value (394). This provides the FDR q value, which is the new basis for statistical significance, since the FDR correction at the q-level is used to protect against Type I error, false discoveries, that become more likely with a large number of comparisons (394, 395). The statistically significant buckets were visually scrutinized along the chemical shift spectra to ensure that the difference was indicative of metabolite peaks and not background noise (395).

Metabolite identification

The significant buckets that were identified by the loadings plots, univariate statistical analysis and confirmed as spectral peaks in the chemical shift were putatively identified using Chenomx NMR Suite (Chenomx Inc., Alberta Canada) by matching spectral peaks to known metabolites in the Chenomx database. These identifications were verified using the 2D HSQC ^1H - ^{13}C bonding data. Verification can be tenuous if there is a very low abundance of a metabolite in the sample, as well as if wider compound peaks

that obstruct some of the smaller peaks. The quality of the identification, according to the standard set by the Metabolomics Standards Initiative (MSI) is also provided (396).

Biochemical pathway identification

To identify the biochemical pathways and the potential biochemical effects that the identified metabolites are involved in, Cytoscape 3.1 with the Metscape plug – in was used (397, 398). These software applications integrate publically available biomolecular data bases, such as PubMed and KEGG, with literature databases that enables a comprehensive visual analysis of metabolomics data, which is otherwise cumbersome to interpret.

4.3. Results

4.3.1. Plasma experimental samples

Multivariate analysis

For the PCA, all plasma samples were grouped according to dose, combining both 2005 and 2006 samples. When the samples from 2005 and 2006 are combined for each dose group, the control group had 22 samples; with 2 samples from each of the 11 terrapins, that represent 2005 and 2006 individually. The low dose group had 10 samples; with 2 samples from each of the 5 terrapins that represent 2005 and 2006 individually. The high dose group had 18 samples; 2 from each terrapin, except for two terrapins that only have a sample from 2005, which will be discussed below. The initial group that was sampled prior to dosing has 33 samples.

A PCA of all plasma samples, separated by dose group, was conducted on each the uniform, and the intelligent bucketed data, using both mean centered and Pareto scaling techniques (Figure 4.7). The PCA scores plot comparison of the uniform, and intelligent bucketed mean centered data show that PC1 explains most of the variance in all the plasma samples (89%, uniform; 78%, intelligent), but the bucketing technique affects how much variance can be explained by PC2 (3%, uniform; 13%, intelligent) (Figure 4.7). The effects of the Pareto scaling technique can be observed in those loadings plots, compared to the unscaled loadings plots. The few buckets that separate from the dense cluster of buckets are the same each loadings plot, but the pareto method reduces the influence of the large spectral features, so smaller features can be observed and included in the comparison (Figure 4.7). The inclusion of the smaller features in

Pareto scaled data may reveal additional buckets that are causing variation within those loadings plots.

The PCA scores plots of the Pareto scaled uniform and intelligent bucketed data are more similar to each other than the two PCA scores plots of the unscaled data (Figure 4.7). For both bucketing techniques, the Pareto scaling provides approximately the same amount of explained variance by PC1 and PC2 (43% and 17%, uniform; 42% and 17%, intelligent). The loadings plots of the Pareto scaled PCAs show that the buckets which had the greatest effect in the unscaled scores plots are suppressed, and brought closer to the group in the Pareto scaled scores plots (Figure 4.7). But, the differences in the Pareto scaled loadings plots are not drastically different than the unscaled loadings plots. There is very little change in the shape of the scores plots between all four combinations of techniques.

Throughout the subsequent analyses, several outlier terrapins were observed, based on their behavior throughout the experiment (outliers: K11, F3, M20) and at the end of the experiment, which are thought to be the drastic result of mercury dosing (F10, K9, M11). In this experiment, we aim to investigate the sub-lethal effects of mercury exposure, which would be best observed in the group of terrapins that did not experience extreme effects. In effort to observe the sub-lethal effects the terrapin population experienced in this experiment, all plasma samples from those six terrapins; were removed from the dose group analyses. The situations that lead to each of the six terrapins being removed as outlier is described in detail in the analysis of the liver samples below.

With the outliers removed, the PCA scores plot of the unscaled data drastically changes shape and the PCA scores plot of the Pareto scaled data does not (Figure 4.8). The two unscaled scores plots are different, with PC1 and PC2 explaining different amounts of variance (90% and 3%, uniform; 79% and 12%, intelligent). Pareto scaling of both the uniform and intelligent bucketed data provides a similar explanation of variance between the two bucketing techniques (44% and 14%, uniform; 44% and 14%, intelligent) (Figure 4.8). The similarity of the Pareto scaled loadings plots demonstrates that Pareto scaling incorporates a greater number of buckets in the explanation of variance in PC1 and PC2, which may allow the small changes that are the result of mercury exposure to be observed.

The lack of an observable difference in the dose groups may be due to the inclusion of the initial sample group. The initial group includes a sample from every terrapin prior to dosing. The initial samples (grey circles) in the scores plots cover a wide range of the plot, as these samples represent the individual terrapins adjustment to captivity, specifically, altered shelter, food, and location. Since we aim to understand the differences in the terrapins relating to mercury exposure, the initial samples were removed, and the PCA was conducted without the initial samples.

With the initial samples removed, the unscaled PCA scores plots do not change shape or either bucketing technique (Figure 4.9). The pattern of the unscaled scores plots changes drastically, but the explained variance between PC1 and PC2 based on the bucketing technique changes very slightly (89.5 % and 2.8%, uniform; 88.9% and 2.9%, intelligent). The corresponding loadings plots are also very similar to each other, and those generated from the data that included the initial samples (Figure 4.9 and 4.7). The

Pareto scaled scores plots without the initial samples are also similar to those with the initial samples, with no clear difference between any of the dose groups. The corresponding loadings plots are also similar to those that included the initial samples (Figure 4.9). This indicates that the same buckets are influencing the variation of the data in both scenarios, which suggests that a commonality between all groups is heavily influencing the analysis. The terrapins experienced many commonalities across the groups during their time in captivity including standardized microenvironments, and a high quality diet. Compared to the standardization of many conditions for the terrapins, the effect of mercury on their metabolome will likely be small in comparison, and may be difficult to observe in a PCA where all variables are included.

Closer inspection of the uniform and intelligent bucketed Pareto scaled scores plots show that the high and low dose groups (orange and yellow circles, respectively) separate along PC1 (Figure 4.9). The control samples (blue circles) span all four quadrants of the scores plot. The standardized diet, and captive environment are likely responsible for the lack of separation of the three groups, as the same buckets continually appear in the loadings plots, even when the initial samples are removed (Figure 4.9). However, the separation of the high and low dose groups along PC1, suggests that the mercury exposures may be responsible for some of the variation explained by PC1.

While the specific buckets shift depending on the bucketing and scaling techniques applied, the same molecules are consistently identified as being influential in the terrapin samples. However, a bucket or molecule being influential in the PCA does not ensure that it will be statistically significant between all sample groups, it means that

those buckets are prominent spectral features in all groups. The significant buckets are determined in the following univariate analysis.

The 20 most influential buckets in PC1 for all the terrapin plasma samples pertain to just four molecules; lactate, 3-hydroxybutyrate, acetate, and glucose (description of identification below; Table 4.4 and 4.5). These four molecules lend insight to what the dosed terrapins were experiencing as a population, rather than provide details of the dose specific effects of exposure. Glucose, lactate and 3-hydroxybutyrate are all involved in different aspects of energy metabolism. Since these have all been identified as influential molecules in the terrapin population, it can be ascertained that significant differences related to energy metabolism may be revealed in the univariate comparisons of the dose groups. Acetate is involved in a wide variety of biochemical processes and may be related to the change in diet, or many other factors. The specific univariate analysis may elucidate other significant buckets that are not including in these 20.

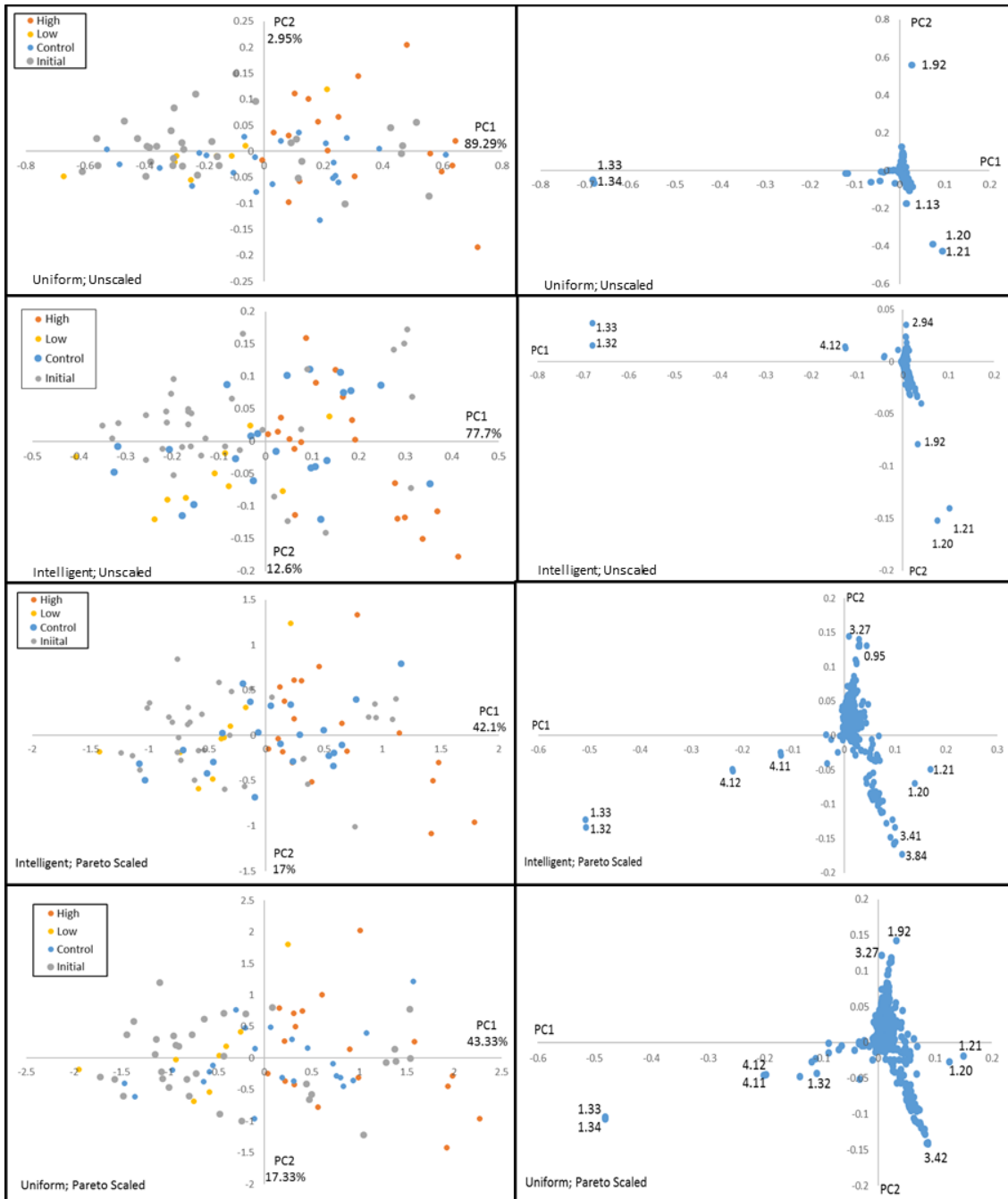


Figure 4.7. All plasma samples from the Hg dosed terrapin experiment conducted by Schwenter (2007). Initial samples $n = 33$; control group $n = 22$; low dose group $n = 10$; high dose group $n = 18$.

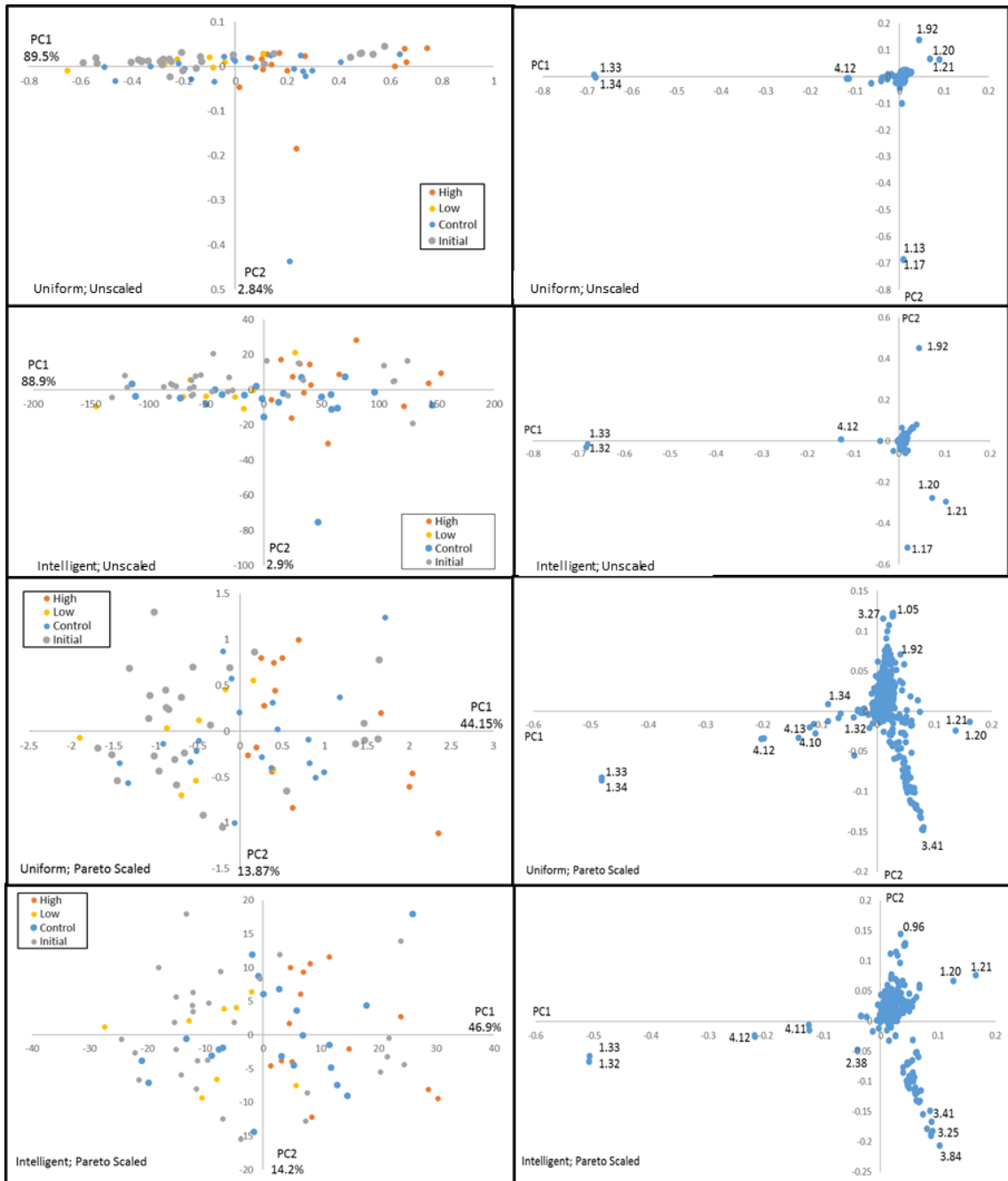


Figure 4.8. All plasma samples from the Hg dosed terrapin experiment conducted by Schwenter (2007), excluding the samples from outlier terrapins K11, M20, F3, F10, K9, M11. Initial samples $n = 33$; control group $n = 21$; low dose group $n = 19$; high dose group $n = 14$.

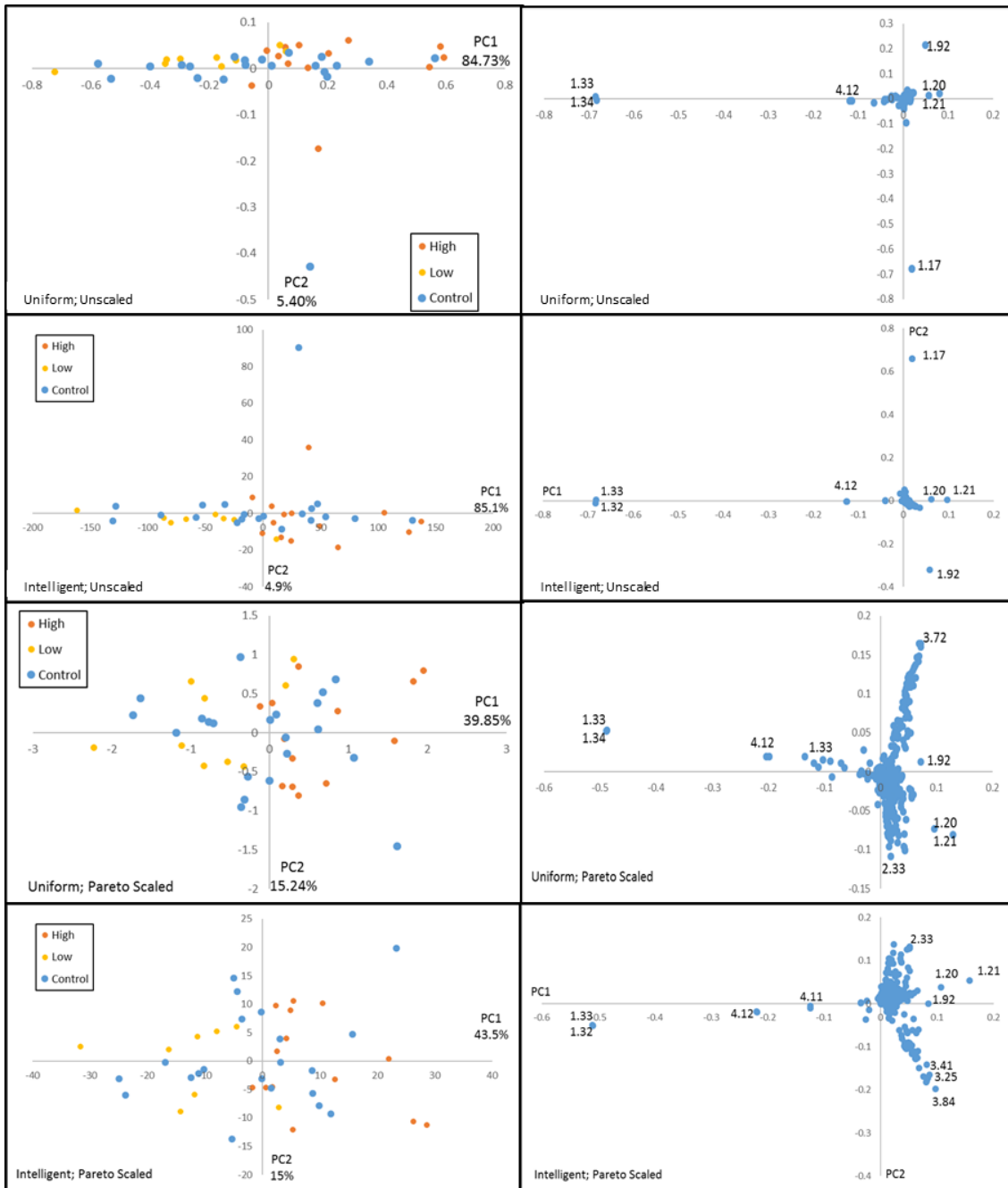


Figure 4.9. All plasma samples from the Hg dosed terrapin experiment conducted by Schwenter (2007), excluding the samples from outlier terrapins K11, M20, F3, F10, K9, M11 and the initial samples collected before dosing began.

Control group $n = 21$; low dose group $n = 19$; high dose group $n = 14$.

Table 4.4. The top 20 uniform buckets for each the unscaled and Pareto scaled data, sorted by loadings intensity. The metabolites listed with each bucket were identified using Chenomx, 1D and 2D NMR data, and the HMDB.

<i>Uniform Buckets PC1 Loadings Intensity Comparison</i>						
Rank	Unscaled	Compound Name	Intensity	Pareto Scaled	Compound Name	Intensity
1	1.33750 ppm	Lactate	0.685	1.33750ppm	Lactate	0.488
2	1.32750 ppm	Lactate	0.683	1.32750ppm	Lactate	0.488
3	4.11250 ppm	Lactate	0.119	4.11250ppm	Lactate	0.203
4	4.12250 ppm	3-hydroxybutyrate	0.114	4.12250ppm	3-hydroxybutyrate	0.198
5	1.20750 ppm	3-hydroxybutyrate	0.082	1.33250ppm	Lactate	0.134
6	1.33250 ppm	Lactate	0.065	1.20750ppm	3-hydroxybutyrate	0.130
7	1.19750 ppm	3-hydroxybutyrate	0.057	4.10250ppm	Lactate	0.119
8	1.92250 ppm	Acetate	0.049	4.13250ppm	3-hydroxybutyrate	0.111
9	1.32250 ppm	Lactate	0.043	1.32250ppm	Lactate	0.102
10	4.10250 ppm	Lactate	0.040	1.19750ppm	3-hydroxybutyrate	0.096
11	4.13250 ppm	3-hydroxybutyrate	0.036	4.11750ppm	Lactate	0.089
12	4.11750 ppm	Lactate	0.026	1.34250ppm	Lactate	0.086
13	1.34250 ppm	Lactate	0.024	1.92250ppm	Acetate	0.072
14	3.40750 ppm	Glucose	0.023	3.71750ppm	Glucose	0.072
15	3.71750 ppm	Glucose	0.022	3.40750ppm	Glucose	0.072
16	3.48250 ppm	Glucose	0.022	4.10750ppm	Lactate	0.070
17	3.83750 ppm	Glucose	0.020	3.48250ppm	Glucose	0.069
18	3.73250 ppm	Glucose	0.019	3.83750ppm	Glucose	0.069
19	1.18250 ppm	3-hydroxybutyrate	0.019	3.73250ppm	Glucose	0.068
20	1.17250 ppm	3-hydroxybutyrate	0.019	3.89250ppm	Glucose	0.065

Table 4.5. The top 20 intelligent buckets for each the unscaled and Pareto scaled data, sorted by loadings intensity.

The metabolites listed with each bucket were identified using Chenomx, 1D and 2D NMR data, and the HMDB.

<i>Intelligent Buckets PC1 Loadings Intensity Comparison</i>						
Rank	Unscaled	Compound Name	Intensity	Pareto Scaled	Compound Name	Intensity
1	1.3381	Lactate	0.683	1.3381	Lactate	0.510
2	1.3181	Lactate	0.682	1.3181	Lactate	0.510
3	4.1215	3-hydroxybutyrate	0.127	4.1215	3-hydroxybutyrate	0.220
4	4.1110	Lactate	0.126	4.1110	Lactate	0.219
5	1.2088	3-hydroxybutyrate	0.097	1.2088	3-hydroxybutyrate	0.157
6	1.1967	3-hydroxybutyrate	0.062	4.1316	3-hydroxybutyrate	0.125
7	1.9217	Acetate	0.058	4.1012	Lactate	0.124
8	4.1316	3-hydroxybutyrate	0.041	1.1967	3-hydroxybutyrate	0.107
9	4.1012	Lactate	0.041	3.8370	Glucose	0.097
10	3.8370	Glucose	0.036	3.2489	Glucose	0.087
11	3.2489	Glucose	0.028	1.9217	Acetate	0.085
12	3.7155	Glucose	0.027	3.7155	Glucose	0.084
13	3.4960	Glucose	0.026	3.4960	Glucose	0.082
14	3.4834	Glucose	0.026	3.7334	Glucose	0.081
15	3.7334	Glucose	0.024	3.4834	Glucose	0.081
16	3.4081	Glucose	0.023	3.4081	Glucose	0.075
17	1.3475	Lactate	0.019	3.4215	Glucose	0.068
18	1.1818	3-hydroxybutyrate	0.019	3.7669	Glucose	0.067
19	1.1697	3-hydroxybutyrate	0.019	3.7428	Glucose	0.066
20	3.4215	Glucose	0.018	1.3475	Lactate	0.065

Univariate analysis of plasma dose groups

Using the univariate t-test with the FDR correction, significant differences were observed between the control and high dose (CvH) groups, and the low and high (LvH) dose groups of the terrapin plasma samples, and not for any other comparison (CvL). The statistical analysis was conducted on both the uniform, and intelligent bucketed data, with both, the unscaled, and Pareto scaling techniques applied. Each t-test gave slightly different results, which are clear in the SDS plot of each group, based on the bucketing and scaling methods used (Table 4.6, Figure 4.10). The uniform bucketing provided a different number of significant buckets for each comparison, while the intelligent bucketing resulted in a consistent number of significant buckets for each dose group comparison. This is likely due to the inherent differences in the two bucketing techniques. The uniform and intelligent bucketing methods also provide different results based on the scaling technique applied. The number of significant intelligent buckets does not change based on the scaling technique, but the number significant of uniform buckets does. This is also likely due to the difference in type and number of buckets included in the analysis. The changes in the number of significant uniform buckets demonstrate the effect that scaling method has on the outcome of a statistical analysis.

The buckets that were identified as being statistically different in each t-test were visually scrutinized along the chemical shift spectra, to determine if the statistical significance corresponded to an area of noise, anomalous sample, or a potential metabolite peak. After the spectra were inspected, the buckets were identified as metabolites as described in section 4.2.5.

Table 4.6. The number of significant buckets for each of the plasma dose group t-test comparisons.

Univariate t-test results comparisons			
Plasma			
<i>Uniform Buckets</i>		<i>Intelligent Buckets</i>	
LvC pareto	LvC unscaled	LvC pareto	LvC unscaled
CvH pareto	CvH unscaled	CvH pareto	CvH unscaled
79	50	69	69
LvH pareto	LvH unscaled	LvH pareto	LvH unscaled
99	48	136	136

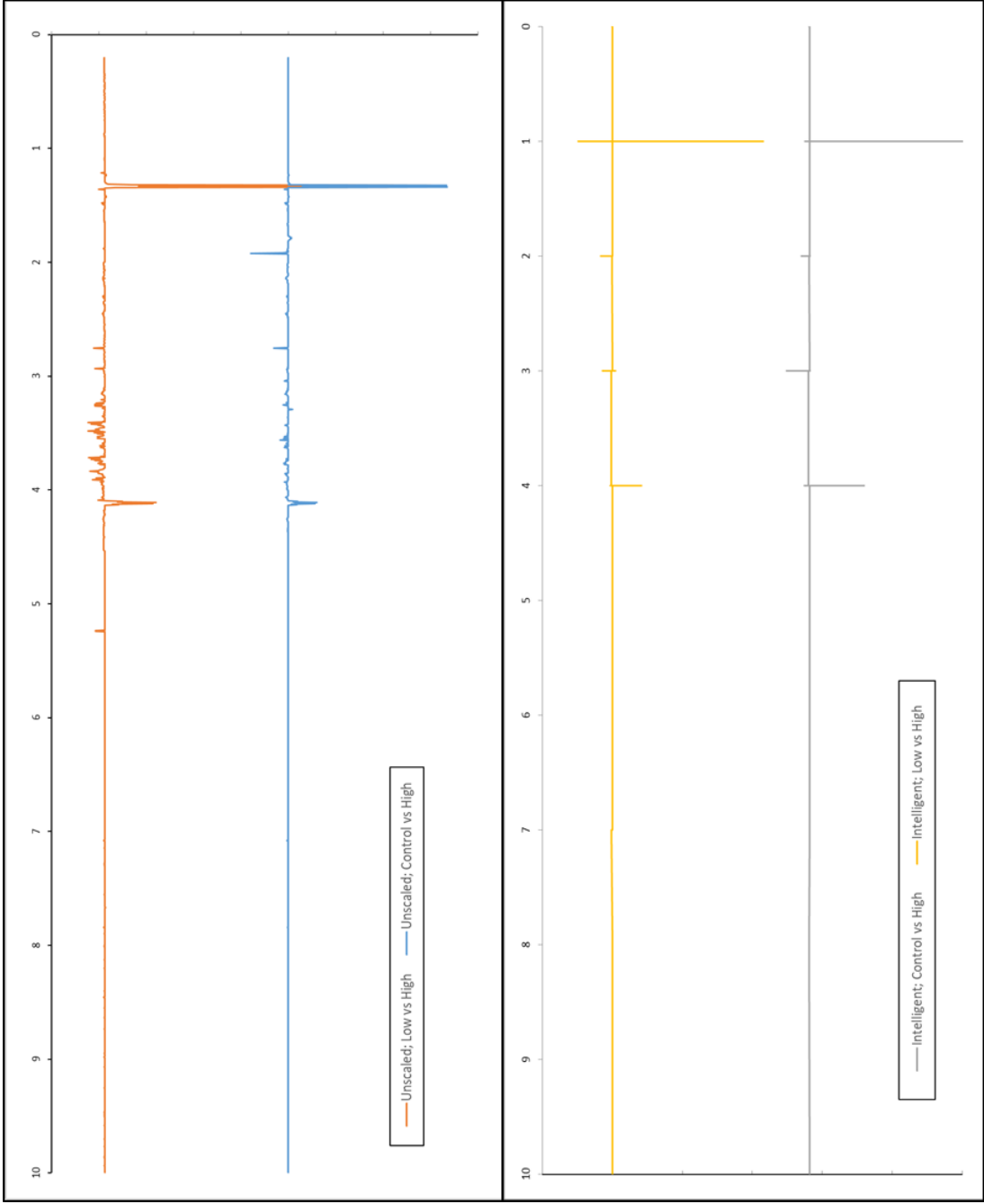


Figure 4.10. The significant difference spectra (SDS) for the different groups of plasma samples.

Metabolites identified in plasma

The different metabolites identified between the CvH and LvH comparisons are likely due to the differences in mercury exposure. The different bucketing techniques did not always detect the same suite of metabolites. Each method failed to recognize some statistically significant buckets that the other detected, so the level of confidence of the metabolite identification according to the Metabolomics Standards Initiative is also provided (Table 4.7)(396).

The high dose group had changes in the following metabolites compared to the control group; leucine, methyl malonate, lactate, acetate, N-methylhydantoin, glucose; 3-hydroxybutyrate, and unknown metabolites at 2.75 ppm, 2.95 ppm, and 3.86 ppm (Table 4.7). The high dose group also had alterations in methyl malonate, acetate, myo-inositol, glycerate, sarcosine, N-methylhydantoin, and unknown metabolites at 1.41 ppm, 1.42 ppm and 2.75 ppm, than the low dose group (Table 4.7). The identified metabolites, that have been verified, along with their ID numbers for several web based databases, are provided in Table 4.7.

Since the univariate analysis revealed differences between the high dose samples and the other groups, and several of the identified metabolites have been previously related to mercury exposure, a dose specific analysis was conducting using PC1 to represent the spectral features of each group.

Table 4.7. The statistically significant buckets identified in AMIX and NMRProcFlow for the comparison of terrapin plasma samples, with the metabolites identified using Chenomx, and verified using the ¹H and ¹³C NMR spectra with the HMDB.

C v H	L v H	Metabolite	Annotation	Pattern	Chenomx Match ppm	CAS #	HMDB ID	Pub Chem ID	KEGG ID	MSI #
✓	✓	Leucine	High Dose less	multiplet	0.9 , 1.0, 1.7 , 1.7, 1.7, 3.7	61-90-5	<i>Too few peaks in spectra</i>	7045798	C00123	2
✓	✓	Methyl Malonate	High Dose less	doublet	1.2 , 3.2	516-05-2	<i>Low abundance peaks in spectra</i>	487	C02170	2
✓		3- hydroxybutyrate	High Dose more	doublet	1.2 , 2.3 , 2.4, 4.1	300-85-6	HMDB00357	441	C01089	1
✓	✓	Lactate	High Dose less	doublet	1.3 , 4.1	79-33-4	HMDB00190	107689	C00186	1
✓	✓	Acetate	High Dose less	singlet	1.9	64-19-7	HMDB00042	176	C00033	1
✓	✓	Methyl- hydantoin	High Dose less	singlet	2.9 , 4.1	616-04-6	<i>Low abundance peaks in spectra</i>	69217	C02565	2
✓		Glucose	High Dose less	multiplet	3.2 , 3.4 , 3.4 , 3.5 , 3.5, 3.5, 3.7 , 3.7, 3.8 , 3.8 , 3.8, 3.8, 3.9, 4.6*, 5.2*	50-99-7	HMDB00122	79025	C00029	1
	✓	Isoleucine	High Dose more	triplet	0.9 , 1.0, 1.2, 1.5, 2.0, 3.7	73-32-5	HMDB003392 3	6306	C00407	1
	✓	Glycerate	High Dose less	multiplet	3.7 , 3.8 , 4.1	473-81-4	HMDB00139	439194	C00258	1
	✓	Sarcosine	High Dose more	singlet	2.7 , 3.6	107-97-1	HMDB00271	1088	C00213	1
	✓	Myo-Inositol	High Dose less	two doublets	3.3 , 3.5 , 3.6 , 4.1	87-89-8	HMDB00211	892	C00137	1
✓		Unknown 2.75	High Dose more	singlet	<i>No matches</i>					4
✓		Unknown 2.95	High Dose more	multiplet	<i>No matches</i>					4
✓		Unknown 3.86	High Dose more	singlet	<i>No matches</i>					4
	✓	Unknown 1.41	High Dose less	doublet	<i>No Matches</i>					4
	✓	Unknown 1.42	High Dose less	doublet	<i>No Matches</i>					4

Dose group mercury concentrations

Since the PCA scores plots do not indicate a difference in the mercury dose groups, but the univariate analysis indicated that there was a difference in several metabolites previously associated with mercury exposure, PC1 was compared to the average mercury concentration for each dose group, to determine if there was a difference related to mercury concentration. PC1 was chosen because this PC includes the most important differences in the NMR spectra, as well as had a greater amount of variation without a clear difference in the groups compared to PC2. To compare these parameters, the PC1 scores were taken from all samples and averaged based on dose group (excluding the outliers and terrapins identified as having overt health declines (OHD), which are discussed in the liver samples), and plotted against the average mercury concentration for each dose group reported by Schwenter (2007) (Table 3.25, Figure 4.11). This comparison shows distinct separation of the high dose terrapins from the other dose groups for PC1 and mercury concentration, which may become more apparent if they are separated annually as mercury dosing continued.

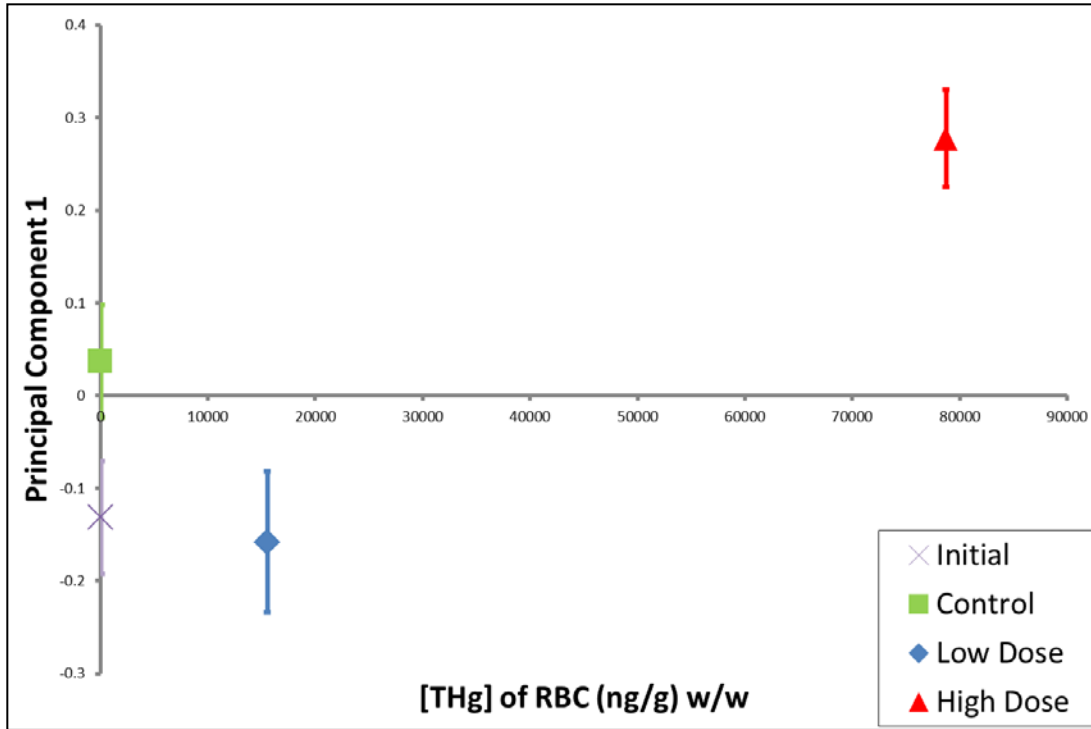


Figure 4.11. The average pareto scales PC1 scores for each dose group plotted against the average Hg concentration for each group of the diamondback terrapin Hg dosing experiment, as reported by Schwenter (2007).

The error bars represent the standard error of the mean of the PC1 values for each dose group.

Metabolic trajectory of mercury exposure

To explore this data, the dose groups were separated by sampling year, then plotted using the average PC1 and PC2 scores of each year/dose group (Figure 4.12). Separating the samples by year made the number of terrapins in each group smaller; initial group still has 33 samples; the control group had 10 samples in each 2005 and 2006; the low dose group had 5 samples in each 2005 and 2006; the high dose group had 10 samples in 2005 and 8 samples in 2006.

The initial samples that were collected before dosing began and both years of the control and low dose groups are not different from each other (Figure 4.12). However, the high dose group is different from the other groups in 2005, and continues to diverge further in 2006 (Figure 4.12). The direction of the trajectory of the high dose samples away from the other groups supports the idea that mercury exposure is playing a role in the dose group separation along PC1 that was observed in the previous section. This comparison shows the change in the average PC scores over time, but with such large error bars, it is difficult to determine if these groups are significantly different. To investigate the pattern observed here, multi- and univariate statistics were conducted on these groups of samples.

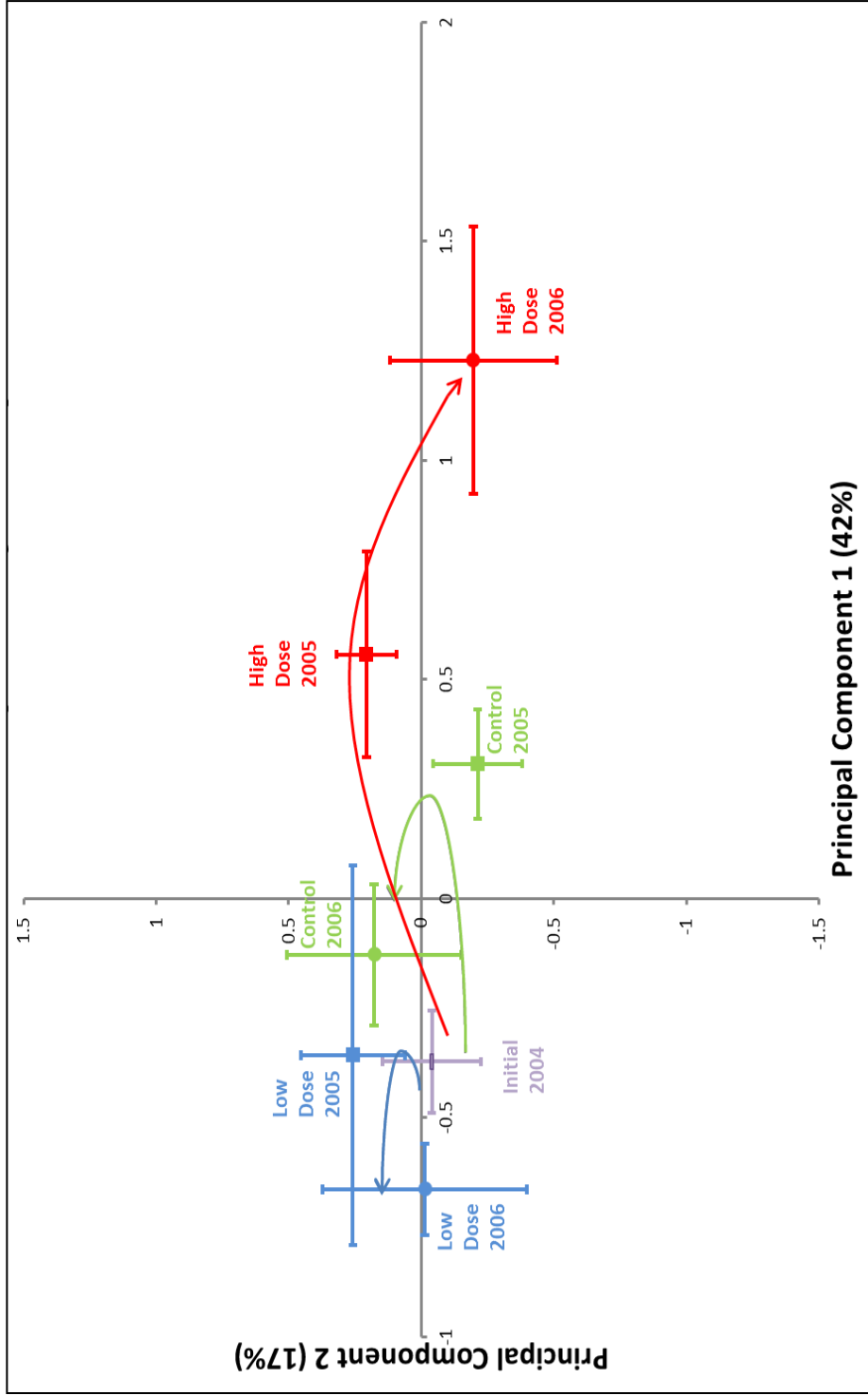


Figure 4.12. The average pareto scaled PC1 and PC2 scores for each dose group, separated by year of the diamondback terrapin Hg dosing experiment. The error bars represent the standard error of the mean of PC1 on the y-axis, and PC2 on the x-axis.

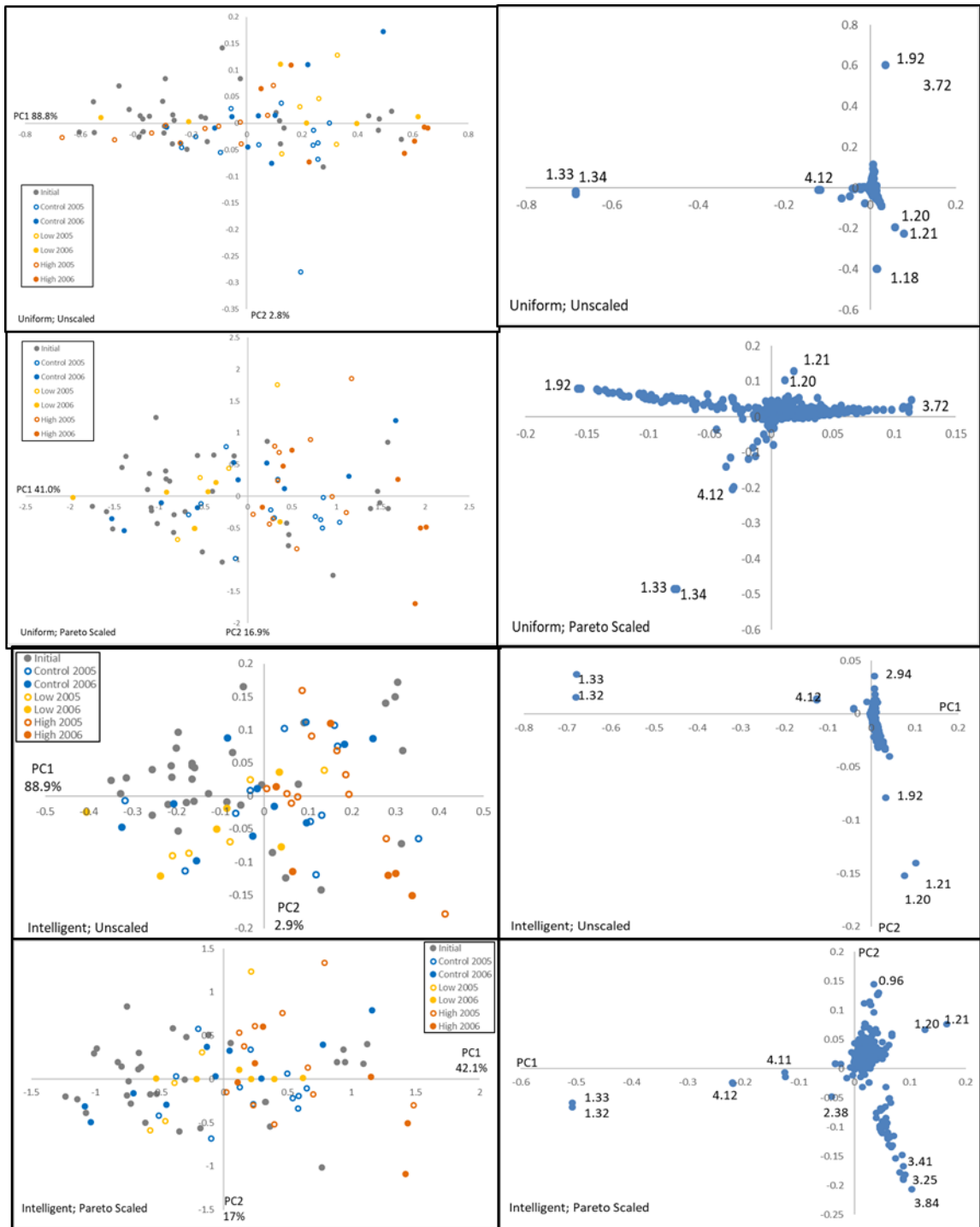


Figure 4.13. The PCA scores and loadings plots for all Hg dose terrapin plasma samples. The initial group having 33 samples; the control group had 10 samples in 2005 and 9 in 2006 (due to 1 outlier being removed); the low dose group had 5 samples in 2005 and 4 in 2006 (due to 1 outlier being removed); the high dose group had 10 samples in 2005 and 7 samples in 2006 (due to 1 outlier being removed). The uniform bucketed, Pareto scaled data (second row) was used in the trajectory analysis.

Univariate analysis of dose groups through time

The differences between the years within each dose group were examined by the univariate t-tests with the FDR correction at the q-level. No significant differences were observed for the following comparisons: control 2005 vs control 2006; low dose 2005 vs low dose 2006; high dose 2005 vs high dose 2006. The lack of any significant buckets between the annual comparisons supports the PCAs above in which all samples appear similar (Figure 4.13). The comparison between the average PC scores for the annual dose groups, also suggests that there is no difference within the groups (Figure 4.12).

To further investigate the initial samples grouping across all dosed samples in the PCAs, the initial group was compared to the 2005 control group samples, and yielded a statistically significant difference. This result suggests a difference between the dosing regimen that began in 2005 and the pre-dosed samples, which could be a result of the water in the enclosures being changed on a different schedule, and/or the honey that was added to the dosed shrimp pieces (353). Even though there was a significant difference between the initial and the 2005 control groups, no additional comparisons were conducted, since the diet changed by the addition of honey between 2004 and 2005 that could influence the metabolome, and these comparisons would not serve to elucidate the effects of mercury exposure with the additional variables as confounding factors.

4.3.2. Liver experimental samples

Multivariate analysis

A PCA including all terrapin liver samples was conducted on the uniform and intelligent bucketed data, using both the mean centered and Pareto scaling techniques. The control group had 10 liver samples, the low dose group had 5 liver samples, and the high dose group had 10 liver samples.

Identification of outlier samples

Throughout the terrapin experiment, several outlier terrapins were identified by Schwenter (2007). Schwenter (2007) noted that F3 did not consume any of the provided gelatin, and that her mercury concentration continued to rise throughout the experiment, despite being in the control group where no mercury was administered (Table 4.1). Terrapin M20, from the high dose group, was described by Schwenter (2007) as displaying signs of sickness early in the experiment and did not consume all the provided dosed shrimp pieces (Table 4.8). For these reasons, the samples from terrapins M20 and F3 can be removed as outliers, as they were also not included in the final analyses conducted by Schwenter (2007). The third outlying sample is from terrapin K11, a low dose terrapin. There was nothing anomalous about this terrapin throughout the duration of the experiment, except for being the largest terrapin in the experiment (Table 3.21). However, the spectral features of this terrapin changed in the same manner that the spectra of M20 and F3 did, so this terrapin can also be removed from the analysis.

Initially, these terrapins were included in the PCA comparisons of all liver samples to understand the spectral features that were associated with them. The PCA

scores plot show that they drastically separate from the rest of the liver samples, but are not tightly grouped (Figure 4.14). The loadings plots that correspond to both, the unscaled and Pareto scaled data show several buckets that are influencing the separation of the outlying samples (Figure 4.14). The influence plot also indicates that K11 and F3 do not fit the PCA model as well as the other samples, which is indicated by these samples separating from the other samples in the PCA scores plot. Due to the observations made during the dosing experiment, and the large variance in the spectral features, these three terrapins were removed from further liver analyses (Figure 4.18).

Identification of mercury affected terrapins

When the three outlying terrapin liver samples were removed, all four PCA scores plots changed shape (Figure 4.15). All four of these PCA scores plots show an additional three samples separating from the main group of samples. These samples are from three high dose terrapins, F10, K9, and M11. These three terrapins were noted as suffering overt health declines (OHD) that are generally associated with mercury poisoning (Schwenter 2007). Schwenter (2007) describes this as the inability to swim, right themselves or consume food. Terrapin M11 was not included in the later stages of the dosing experiment since he had slowed his eating habits early in the experiment (Table 4.8). Terrapins F10 and K9 had drastically slowed their eating habits by the end of the study (Schwenter 2007). Terrapins F10, K9, and M11 were also unable to ‘right’ themselves by the end of the study. Righting response is a common test for turtles that measured their ability to reorient themselves when flipped carapace down in a specific amount of time (Table 4.9).

The three OHD terrapin liver samples appear to be outliers based on their separation from the rest of the high dose samples in the PCA scores plot, but the terrapins suffered the behavioral changes commonly associated with mercury exposure (Schwenter, 2007). Removing these samples from the analysis removes the ability to determine what biochemical effects lead to their altered behavior. So that the observable effects of mercury exposure may be linked to their biochemical precursors, the three OHD terrapin liver samples are included in the univariate analysis of the terrapin liver samples, but as a separate group.

Liver analysis by dose group

After the removal of the three OHD terrapins (F10, K9, and M11) the PCA scores plots changed shape, and little variance could be explained by this model (Figure 4.16). The loadings plots that correspond to these PCA scores plots are not very different from those that included the OHD terrapins, with a similar group of buckets influencing the model.

The most influential buckets from all the PCA comparisons in Figure 4.16 are listed in Tables 4.10 and 4.11. The influential buckets in the uniform comparisons are provided in Table 4.10, and those from the intelligent comparisons are provided in Table 4.11. The buckets shift around in rank depending on the scaling and bucketing techniques applied, but the same metabolites are present in both tables. This suggests that the same buckets are influencing the model, regardless of the bucketing and scaling techniques applied. These buckets likely correspond to prominent spectral features in the spectra.

The influential buckets from the liver samples correspond to more metabolites than those of the plasma samples. Choline was consistently observed to be influential in the loadings plots (3.21, 3.23, 3.24 ppm), which could be due to the standardized diet the terrapins were given, since it is a dietary molecule and it is an ingredient in the turtle gelatin (Mazrui). Choline is also a precursor to acetylcholine, which is an important neurotransmitter for muscular control, and is known to be important to the transmission at neuromuscular junctions (399, 400). The influence of the buckets related to choline could be related to the behavioral changes observed in the OHD terrapins, since these buckets were also influential to the model when the OHD terrapins were included.

Several metabolites that are influential in the PCA model of the liver samples are repeated from what was observed in the plasma samples (glucose, leucine, myo-inositol, and lactate) and additional metabolites were observed in the liver samples: taurine, glycerol, glycerophosphocholine and cholate. Cholate is a bile acid that is produced in the liver, and taurine is a component of many bile acids, so it is not surprising for these to be influential metabolites in liver samples. Taurine and glycerol are also molecules that can be attained from diet, and are components of the gelatin the turtles were fed, as are leucine and inositol (Mazrui). Glycerol is also found in honey, which was added to the dosed shrimp pieces fed to the terrapins. These metabolites had such influence on the PCA model since they were components of the standardized diet of the terrapins, and while some of the terrapins were given mercury with their food, the changes that result from mercury are likely small compared to the effect that a very consistent suite of metabolites that come from their diet would have on the PCA model, even when the data

was pareto scaled. Univariate analysis across all buckets may be able to elucidate the small changes related to mercury exposure, which are conducted below.

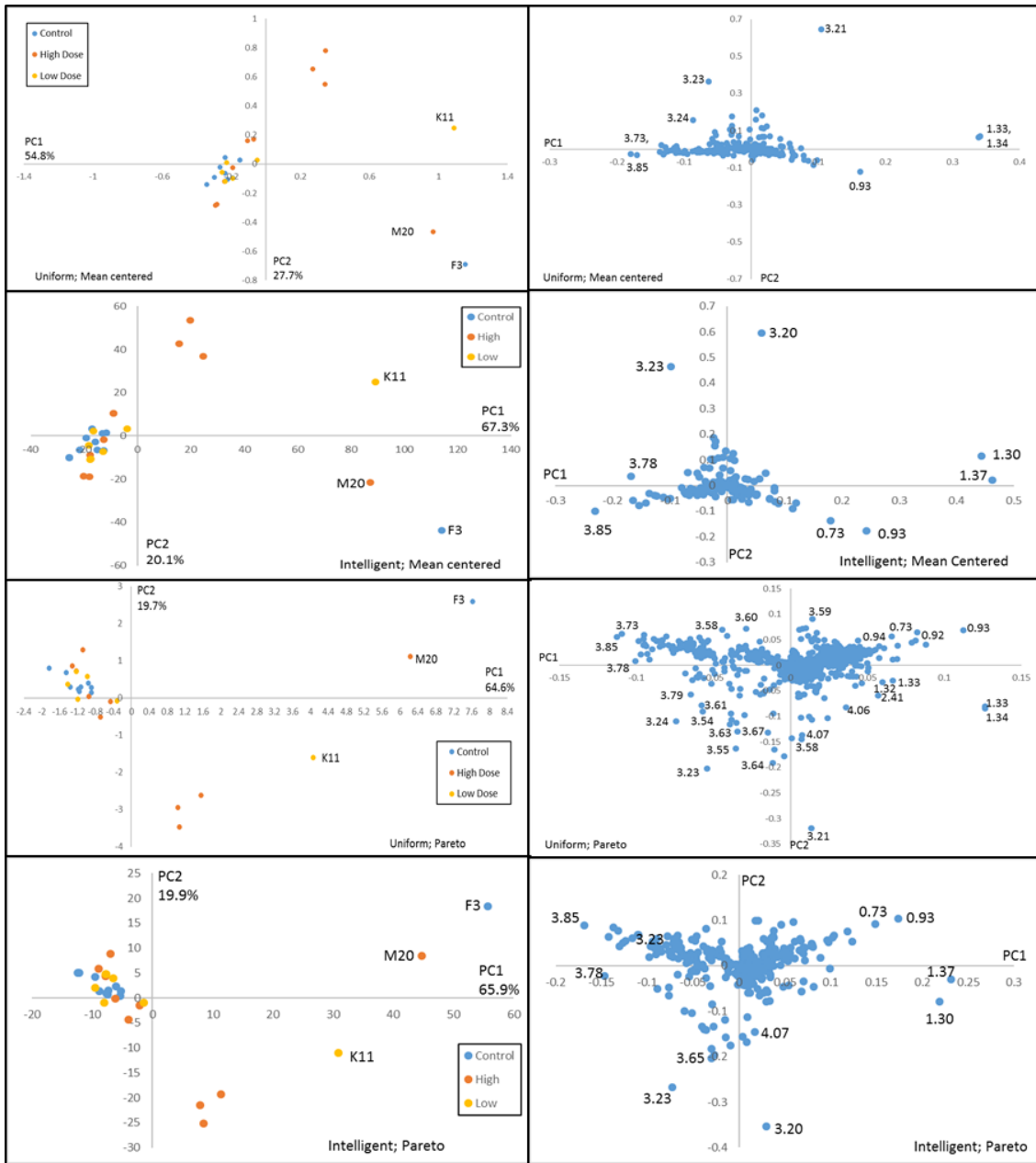


Figure 4.14. The PCA scores and loadings plots for all Hg dosed terrapin liver samples. Control group $n = 10$ samples; low dose $n = 6$ samples, high dose $n = 10$ samples.

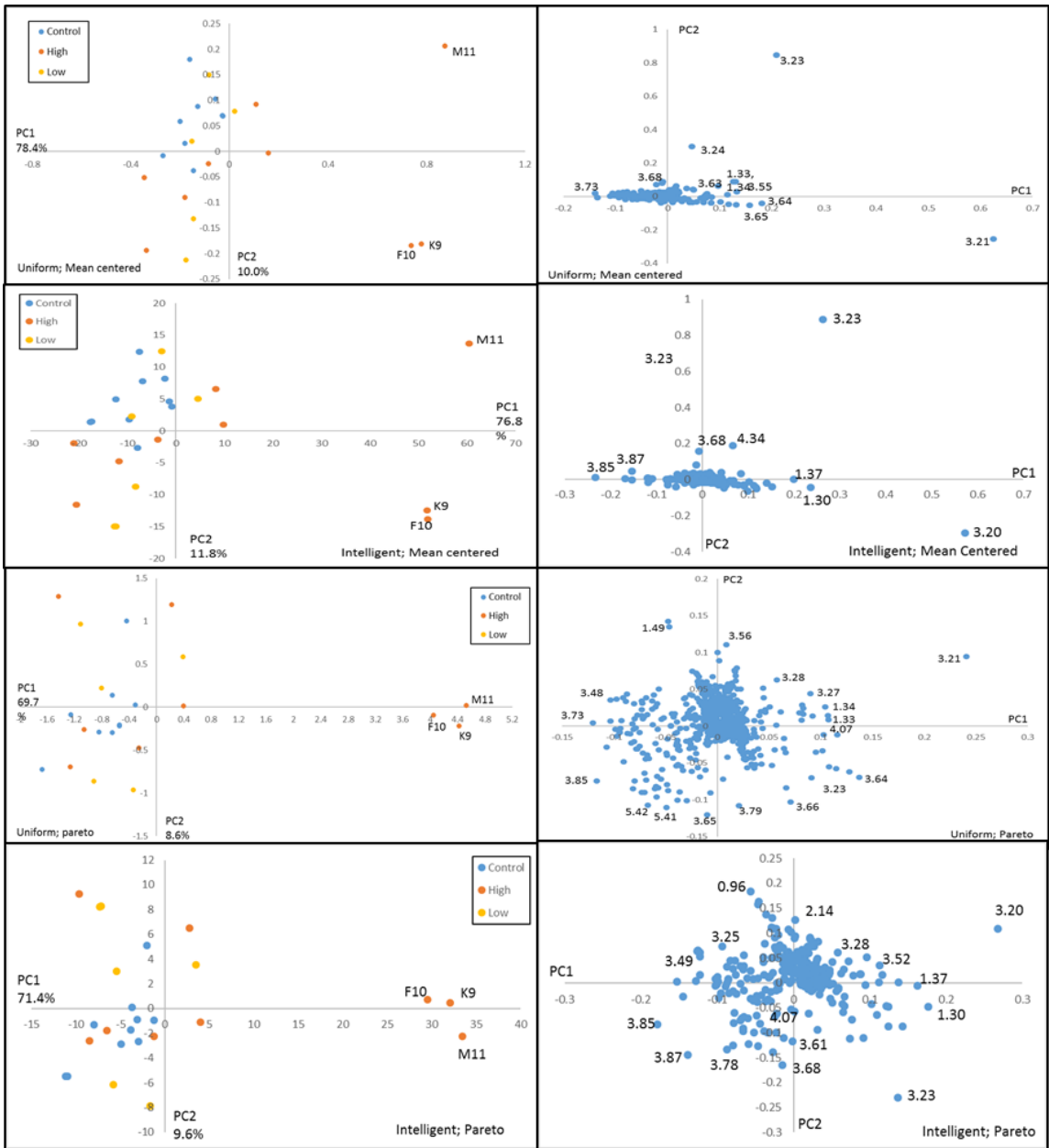


Figure 4.15. The PCA scores and loadings plots for all Hg dosed terrapin liver samples with the three outlying samples removed (M20, F3 and K11).

Control group $n = 9$ samples; low dose $n = 5$ samples, high dose $n = 9$ samples.

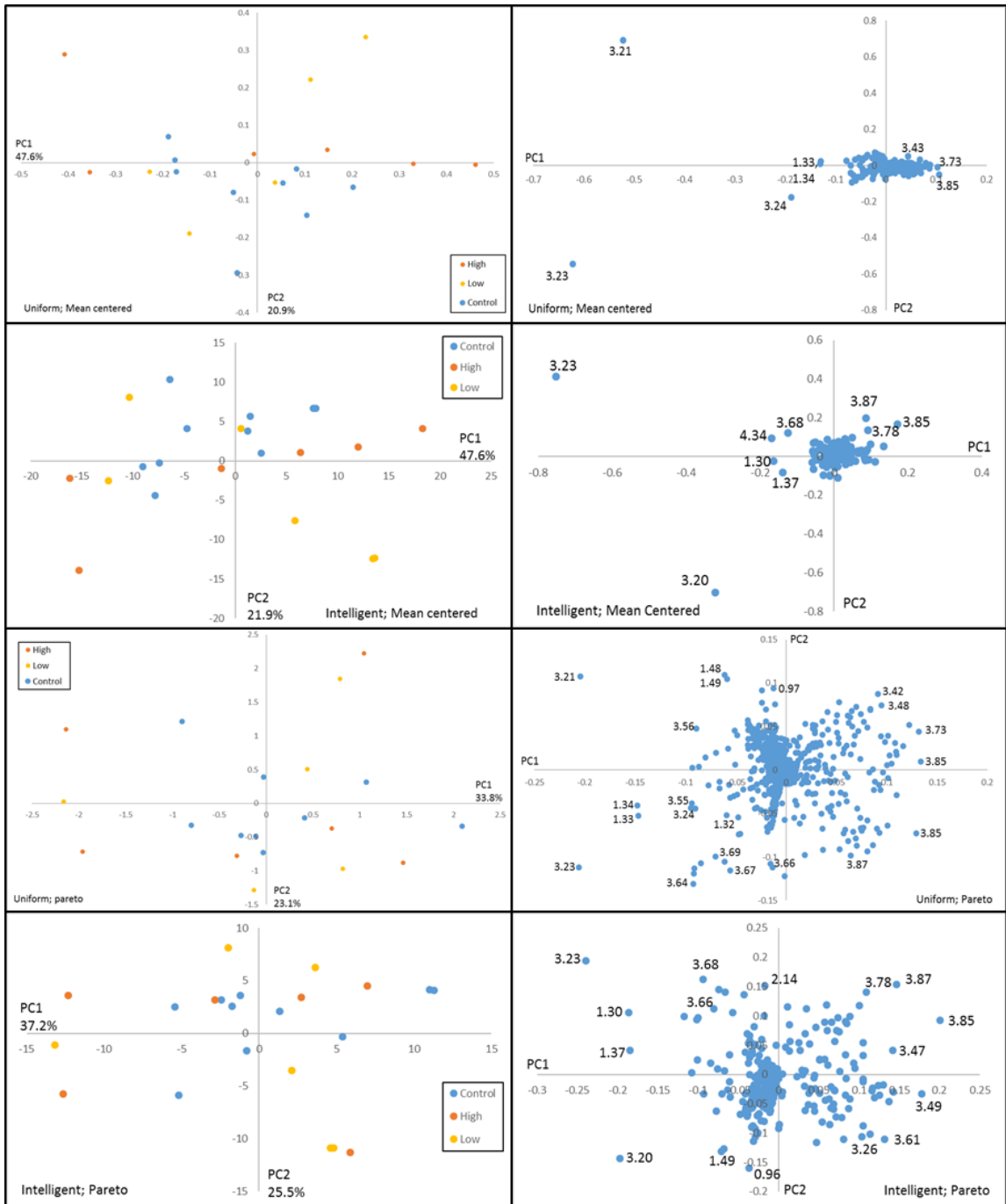


Figure 4.16. The PCA scores and loadings plots for all Hg dosed terrapin liver samples with the three outlying samples removed (M20, F3 and K11), and the three OHD samples removed (M11, F10, K9). Control group $n = 9$ samples; low dose $n = 5$ samples, high dose $n = 6$ samples.

Table 4.8. The average number of pieces of Freshwater Turtle Gelatin (Mazuri) that each terrapin consumed during the 30-minute feeding period for each month. Dashes denote months where the terrapin was no longer included in the experiment. Taken from Schwenter (2007).

Sex	ID	Tank #	June-05	July-05	September-05	October-05	May-06	June-06	July-06	August-06	September-06
F	K1	1	12	15	14	7	8	15	19	12	9
F	K3	1	1	0	27	13	16	19	18	12	7
M	M2	1	8	8	5	3	7	9	6	3	3
M	M4	1	8	10	5	3	6	8	6	4	3
F	K9	3	13	19	17	11	13	5	11	8	2
F	F8	3	11	15	26	12	14	11	11	7	2
M	M14	3	7	9	10	4	2	2	3	1	0
M	M9	3	8	9	11	8	---	---	---	---	---
M	M3	4	7	7	5	3	5	5	4	5	3
F	K4	5	14	10	9	11	8	7	1	1	1
F	F6	5	23	22	16	10	5	4	8	0	0
M	M11	5	5	5	5	2	1	2	1	---	---
M	M20	5	2	3	0	0	---	---	---	---	---
F	K7	6	14	11	11	6	9	11	8	7	6
F	F3	6	0	0	0	0	0	1	1	---	---
M	M17	6	6	8	6	2	3	6	4	4	3
M	M6	6	5	5	5	4	6	6	4	3	2
F	F10	7	11	11	13	8	9	4	3	4	0
F	K10	7	19	17	21	13	12	15	11	7	10
M	M19	7	8	8	4	2	6	5	4	4	1
M	M18	7	7	9	6	4	3	6	4	2	2
F	F2	8	19	19	19	14	15	19	20	16	15
F	F5	8	23	17	10	6	8	9	13	12	8
M	M7	8	9	7	3	2	4	6	5	3	1
M	M16	8	11	10	2	1	---	---	---	---	---
F	K11	9	18	22	19	15	14	22	23	16	15
F	K2	9	13	14	12	7	10	14	13	10	6
M	M1	9	9	8	4	2	3	5	3	3	1
M	M12	9	8	8	4	1	6	7	5	1	1

Table 4.9. The average time (in seconds) each terrapin required to right itself after being paced carapace-down on the ground. Maximum time allotted was 600 seconds. Dashed lines indicate months where the terrapin was no longer included in the experiment.

Sex	ID	Tank #	June-05	July-05	September-05	October-05	May-06	June-06	July-06	August-06
M	M2	1	2.16	1.74	3.89	3.81	6.96	5.36	1.86	1.63
M	M4	1	4.08	2.17	2.57	6.04	4.77	2.32	2.95	2.53
F	K1	1	4.87	3.89	4.03	7.57	7.08	3.70	2.90	3.12
F	K3	1	67.36	328.04	4.64	6.89	7.36	4.19	3.26	2.60
F	K9	3	48.07	9.36	16.52	32.22	37.29	250.45	600.00	600.00
F	F8	3	2.96	2.34	3.78	7.48	7.22	5.67	164.98	378.76
M	M14	3	2.92	1.69	2.75	4.34	7.54	9.84	8.66	22.98
M	M9	3	2.07	2.51	3.19	5.09	---	---	---	---
M	M3	4	1.84	1.79	6.29	10.14	14.90	6.40	12.53	3.83
F	K4	5	3.90	9.34	3.78	20.96	9.28	432.69	600.00	600.00
F	F6	5	6.51	3.30	3.61	8.94	7.97	5.92	11.73	600.00
M	M11	5	5.90	2.95	4.72	5.95	7.85	8.27	315.95	---
M	M20	5	31.74	50.63	503.40	600.00	---	---	---	---
F	K7	6	8.85	2.44	8.54	13.62	14.87	9.85	11.56	16.80
F	F3	6	121.83	392.96	710.00	600.00	600.00	600.00	600.00	---
M	M17	6	1.79	56.34	2.07	4.65	4.17	2.50	144.42	2.79
M	M6	6	6.76	5.51	8.05	13.62	12.96	4.25	9.07	14.20
F	F10	7	10.12	4.18	8.24	21.56	27.18	182.72	526.75	600.00
F	K10	7	3.66	2.96	3.11	4.77	4.28	3.26	3.04	3.35
M	M19	7	2.74	1.89	2.97	4.84	4.04	2.47	2.80	3.42
M	M18	7	2.29	1.92	2.20	3.33	5.05	3.28	4.76	5.78
F	F2	8	5.91	4.12	4.49	7.98	9.89	4.21	5.02	4.26
F	F5	8	3.52	1.83	3.02	4.02	8.57	3.33	14.01	13.47
M	M7	8	3.81	2.34	2.25	18.57	4.03	1.82	1.81	1.79
M	M16	8	2.94	3.00	2.46	3.70	---	---	---	---
F	K11	9	12.00	5.80	6.75	12.80	14.18	9.66	5.32	7.99
F	K2	9	3.16	2.88	6.26	6.81	6.68	4.23	3.88	3.12
M	M1	9	1.78	1.78	2.81	4.73	5.41	2.96	2.97	2.44
M	M12	9	10.32	2.57	3.95	4.92	7.76	4.13	2.53	3.67

Table 4.10. The top 20 uniform buckets for each the mean centered and Pareto scaled liver sample data, sorted by loadings intensity.

The metabolites listed with each bucket were identified using Chenomx, 1D and 2D NMR data, and the HMDB.

<i>Uniform Buckets PCI Loadings Intensity Comparison</i>						
Rank	Mean Centered	Compound Name	Intensity	Pareto Scaled	Compound Name	Intensity
1	3.20750ppm	Choline	0.624	3.20750ppm	Choline	0.241
2	3.23250ppm	Taurine	0.209	3.64250ppm	Glycerol	0.137
3	3.64250ppm	Glycerol	0.181	3.64750ppm	Glycerol	0.128
4	3.64750ppm	Glycerol	0.158	3.73250ppm	Leucine	0.120
5	3.73250ppm	Leucine	0.139	3.85250ppm	Glucose	0.117
6	3.85250ppm	Glucose	0.135	3.54750ppm	Glycerol	0.116
7	3.54750ppm	Glycerol	0.133	3.56750ppm	Glycerol	0.115
8	3.56750ppm	Glycerol	0.132	3.57750ppm	Myo-inositol	0.108
9	1.32750ppm	Lactate	0.130	4.06750ppm	Choline	0.107
10	1.33750ppm	Lactate	0.126	3.84750ppm	Glucose	0.107
11	3.57750ppm	Myo-inositol	0.117	1.32750ppm	Lactate	0.107
12	4.06750ppm	Choline	0.115	1.33750ppm	Lactate	0.104
13	3.84750ppm	Glucose	0.110	3.48250ppm	Glucose	0.103
14	3.48250ppm	Glucose	0.106	3.71750ppm	Myo-inositol	0.103
15	3.71750ppm	Myo-inositol	0.102	3.55750ppm	Glycerol	0.102
16	3.55750ppm	Glycerol	0.101	3.23250ppm	Taurine	0.102
17	3.62750ppm	Glycerol	0.097	3.76250ppm	Glycerol	0.099
18	3.40750ppm	Taurine	0.094	3.40750ppm	Taurine	0.097
19	3.76250ppm	Glycerol	0.094	3.83250ppm	Glucose	0.097
20	3.83250ppm	Glucose	0.090	3.62750ppm	Glycerol	0.095

Table 4.11. The top 20 intelligent buckets for each the mean centered and Pareto scaled data, sorted by loadings intensity.

The metabolites listed with each bucket were identified using Chenomx, 1D and 2D NMR data, and the HMDB. Question marks denote metabolites that could not be verified using the HMDB.

<i>Intelligent Buckets PCI Loadings Intensity Comparison</i>						
Rank	Mean Centered	Compound Name	Intensity	Pareto Scaled	Compound Name	Intensity
1	B3 2326	Taurine	0.75196	B3 2326	Taurine	0.2395
2	B3 2039	Choline	0.32114	B3 8518	Glucose	0.20078
3	B3 8518	Glucose	0.17061	B3 2039	Choline	0.19733
4	B4 3353	Glycerophosphocholine?	0.16931	B1 2973	Cholate?	0.1864
5	B1 2973	Cholate?	0.1635	B1 3695	Cholate?	0.18426
6	B1 3695	Cholate?	0.13863	B3 7317	Leucine	0.17748
7	B3 7317	Leucine	0.13332	B3 8694	Glucose	0.14659
8	B3 6804	Glycerol	0.12433	B3 8343	Glucose	0.14262
9	B3 4174	Taurine	0.11149	B3 7624	Glycerol	0.14206
10	B3 7624	Glycerol	0.098435	B3 7411	Myo-inositol	0.13727
11	B3 4835	Glucose	0.092773	B3 4174	Taurine	0.13188
12	B3 7824	Glucose	0.090628	B5 2454	Glucose	0.13016
13	B3 8343	Glucose	0.08929	B3 7123	Myo-inositol	0.12572
14	B3 8694	Glucose	0.085916	B3 7234	Glucose	0.12376
15	B3 7411	Myo-inositol	0.085409	B3 7183	Myo-inositol	0.11879
16	B3 4045	Taurine	0.084211	B4 3353	Glycerophosphocholine?	0.11758
17	B3 4965	Myo-inositol	0.082962	B3 4287	Glucose	0.11709
18	B3 4287	Glucose	0.08237	B4 6583	Glucose	0.11592
19	B5 2454	Glucose	0.073381	B3 4835	Glucose	0.11328
20	B3 7123	Glucose	0.067924	B3 7824	Glucose	0.10912

Univariate analysis

Using t-tests with the FDR q-level 0.1% correction, all combinations of bucketing and scaling techniques were analyzed for significance between the dose groups, LvH, CvH, HvL, and OHD terrapins compared to the rest of the high dose liver samples (OHDvH). The LvH, CvH, CvL, and HvL comparisons yielded no significant differences in either the uniform or intelligent bucketed data with no scaling or Pareto scaling applied (Table 4.12). The OHDvH comparisons yielded many significant differences; the uniform bucketed data had approximately 1000 significant buckets, and the intelligent bucketed data had over 200 significant buckets (Table 4.12). The intelligent bucketed data has fewer significant buckets since only spectral features were included in that data, and not any background noise.

The significant buckets from all OHDvH comparisons are the results of the very different spectra of the OHD terrapins (Figure 4.17, 4.18). To determine if the significant buckets pertained to a spectral peak or background noise, the two group's spectra were visually inspected at the significant chemical shift values. Large regions of significance pertained to areas where neither group had a spectral peak and the abundance of background noise differed, since the OHD spectra are depressed in many regions due to their reduced feeding behavior (Figure 4.18). The buckets that corresponded to spectral peaks, and metabolites are discussed below.

Univariate analysis of the OHD terrapins in plasma

To complement the liver analysis, the three terrapins that experienced 'overt health declines' (OHD) associated with mercury exposure, were compared to the rest of

the terrapins in the high dose group using their plasma samples. Due to the declines the OHD terrapins experienced, all three terrapins were not all sampled in 2006, so only their samples from 2005 were compared to the high dose 2005 and 2006 samples, separately. Neither of these comparisons yielded any statistically significant buckets, even when the singular OHD 2006 sample was included in the comparisons. It appears that the declines the terrapins observed were not discernable in their plasma samples.

Table 4.12. The number of significant buckets for each of the liver dose group t-test comparisons.

Univariate t-test results comparisons			
Liver			
Uniform Buckets		Intelligent Buckets	
CvL pareto	CvL mean centered	CvL pareto	CvL mean centered
0	0	0	0
CvH pareto	CvH mean centered	CvH pareto	CvH mean centered
0	0	0	0
LvH pareto	LvH mean centered	LvH pareto	LvH mean centered
0	0	0	0
OHDvH pareto	OHDvH mean centered	OHDvH pareto	OHDvH mean centered
997	998	254	254

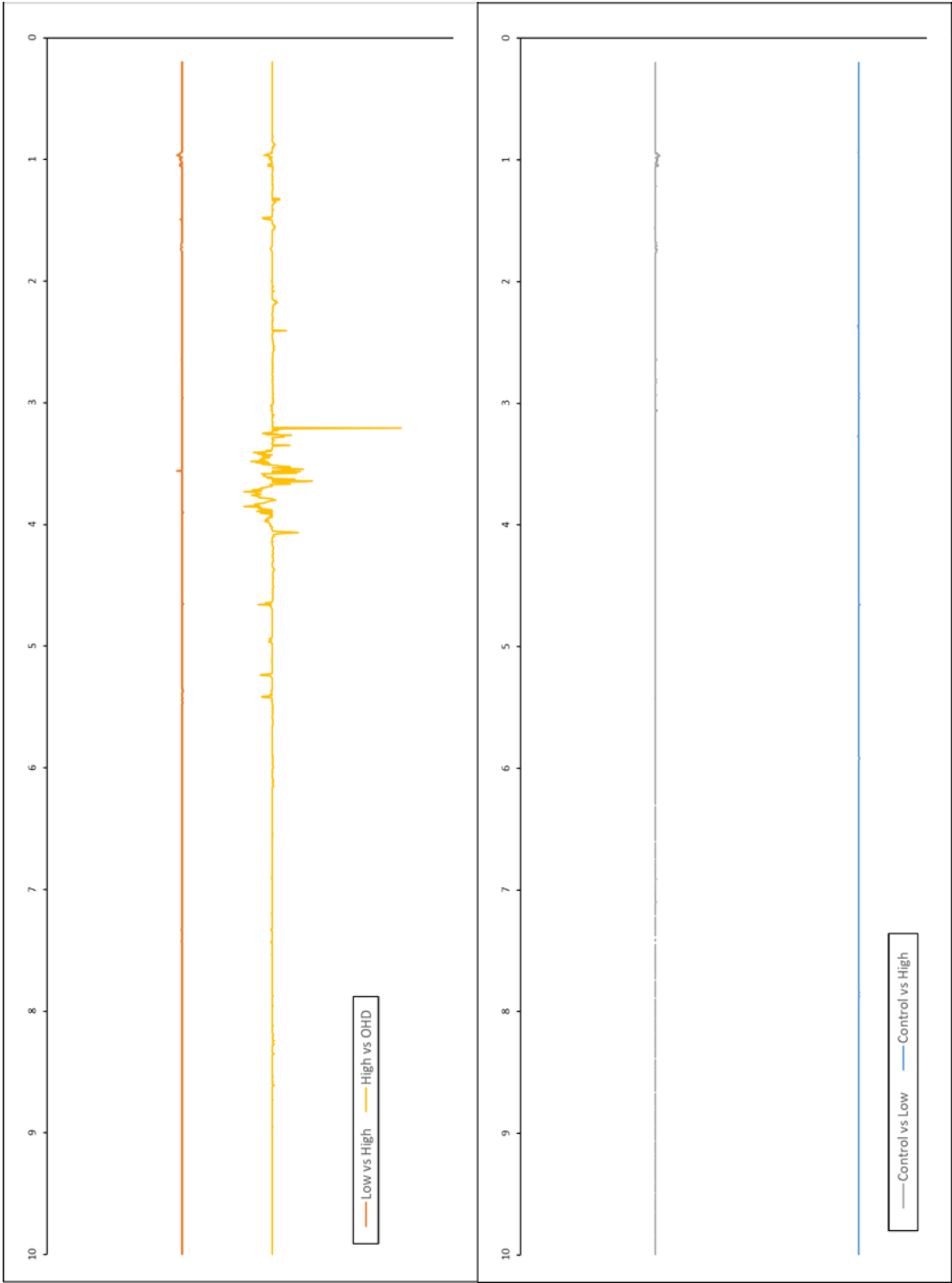


Figure 4.17. The significant difference spectra (SDS) for the different groups of liver tissue.

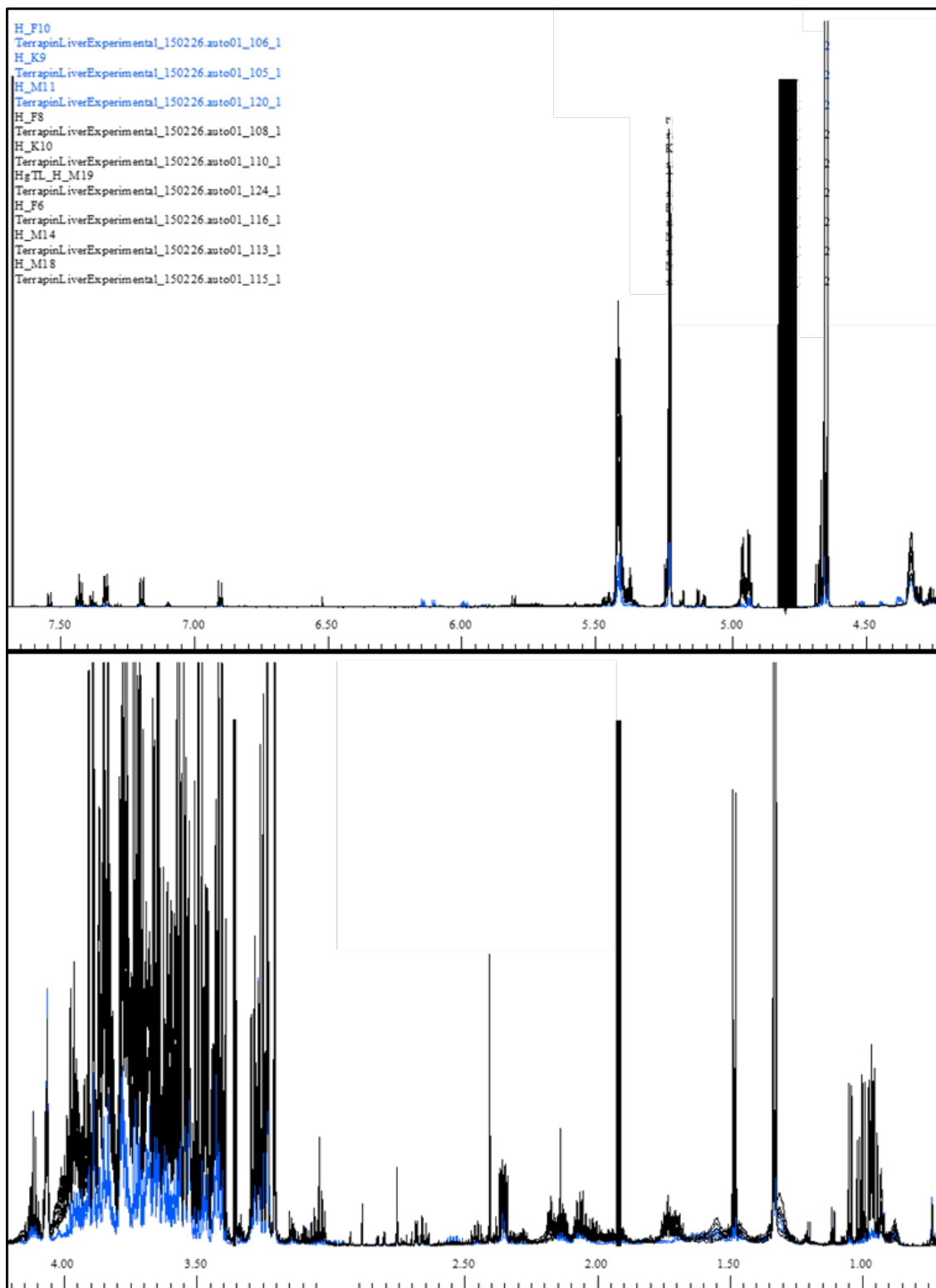


Figure 4.18. The chemical shift spectra comparing the differences between the OHD and high dose terrapin liver samples.

OHD terrapin samples are in blue, high dose samples are in black.

Metabolites identified

Overall, the OHD terrapins had a depressed metabolome, with most of the significant metabolites being in lower relative concentration than the high dose terrapins (Table 4.13). The OHD terrapin liver metabolomes were depressed for leucine, valine, isoleucine, putrescine, succinate, lactate, alanine, glutamate, taurine, glycerol, methionine, aspartate, choline, glucose, uracil and phenylalanine (Table 4.13).

The OHD terrapins had increased relative concentrations of a hypoxanthine containing compound, as well as unknown metabolite peaks at 8.23 ppm, 8.24 ppm, 8.27 ppm, 8.35 ppm.

4.3.3. Cumulative results

To determine the entire effect of mercury exposure on the dose diamondback terrapins, the metabolites that were identified high dose plasma samples, and the OHD liver samples were combined (Tables 4.10 and 4.17). The combined list of metabolites was entered into the Metscape plugin for Cytoscape, to determine which biochemical pathways are affected by the metabolites. The identified molecules affect the synthesis, degradation and abundance of many other compounds in the body, and can effect a wide variety of enzymes and reactions, including amino acid metabolism, glycolysis, methionine, cysteine and folate metabolism, and the citric acid cycle (Table 4.14, 4.15, 4.16). The seemingly small changes in these metabolites may lead to changes in over 100 genes related to these compounds, enzymes and reactions (Table 4.17, Figure 4.19). The potential extended effects demonstrate how detrimental mercury exposure can be.

Table 4.13. The statistically significant buckets identified in AMIX and NMRProcFlow for the comparison of the OHD and high dose terrapins, with the metabolite identified using Chenomx, and verified using the ¹H and ¹³C NMR spectra with the HMDB.

OHD vs High Dose Terrapins									
Metabolite	Annotation	Pattern	Chenomx Match ppm	CAS #	HMDB ID	PubChem ID	KEGG ID	MSI #	
Leucine	OHD less	multiplet	.09, 1.0, 1.7, 1.7, 1.7, 3.7	61-90-5	HMDB00687	6106	C00123	1	
Valine	OHD less	doublet	1.0, 1.0, 2.3, 3.6	72-18-4	HMDB00883	6287	C00183	1	
Isoleucine	OHD less	doublet	0.9, 1.0, 1.3, 1.5, 2.0, 3.7	73-32-5	HMDB00172	6306	C00407	1	
Lactate	OHD less	multiplet	1.3, 4.1	79-33-4	HMDB00190	107689	C00186	1	
Alanine	OHD less	doublet	1.5, 3.8	56-41-7	HMDB00161	5950	C00041	1	
Putrescine	OHD less	singlet	1.7, 3.0	110-60-1	HMDB01414	1045	C00134	1	
Glutamate	OHD less	multiplet	2.0, 2.1, 2.3, 2.4, 3.7	56-86-0	HMDB00148	33032	C00025	1	
Succinate	OHD less	Singlet	2.4	110-15-6	HMDB00254	1110	C00042	1	
Glutamine	OHD less	multiplet	2.1, 2.1, 2.4, 2.5, 3.8, 6.9, 7.6	56-85-9	<i>Low abundance peak in spectra</i>	5961	<i>C00064</i>	2	
Methionine	OHD less	triplet	2.1, 2.1, 2.2, 2.6, 3.9	63-68-3	<i>Not enough peaks to confirm in spectra</i>	6137	<i>C00073</i>	2	
Aspartate	OHD less	singlet	2.7, 2.8, 3.9	56-84-8	HMDB00191	5960	C00049	1	
Phenylalanine	OHD less	small peak	3.1, 3.1, 4.0, 7.3, 7.4, 7.4	63-91-2	HMDB00159	6140	C00079	1	
Choline	OHD less	singlet	3.2, 3.5, 4.1	62-49-7	HMDB00097	305	C00114	1	
Glucose	OHD less	multiplet	3.2, 3.4, 3.4, 3.5, 3.5, 3.5, 3.7, 3.7, 3.8, 3.8, 3.8, 3.8, 3.9, 4.6*, 5.2*	50-99-7	HMDB00122	5793	C00031	1	
Taurine	OHD less	triplet	3.3, 3.4	107-35-7	HMDB00251	1123	C00245	1	
Glycerol	OHD less	multiplet	3.5, 3.6, 3.8	473-81-4	HMDB00139	752	C00258	1	
Uracil	OHD less	doublet	5.8, 7.5	66-22-8	HMDB00300	1174	C00106	1	
Hypoxanthine-N	OHD more	doublet	8.2, 8.2	68-94-0	<i>Component of several close matches</i>	6021	<i>C00262</i>	3	
Unknown	OHD more	singlet	<i>No Matches</i>						4
Unknown	OHD more	singlet	<i>No Matches</i>						4
Unknown	OHD more	singlet	<i>No Matches</i>						4
Unknown	OHD more	singlet	<i>No Matches</i>						4

Table 4.14. The altered metabolites identified in the Hg dosed terrapins (input compounds), and the other compounds that are effected by the changed metabolite abundances.

This list was generated using Cytoscape 3.1 with the Metscape plug-in.

Category	Canonical Compound Name	Compound PubMed ID	Category	Canonical Compound Name	Compound PubMed ID
Input Compound	L-Glutamate	33032	Compound	N-Acetyl-L-glutamate	7345
Input Compound	UDPglucose	439156	Compound	5-Formiminotetrahydrofolate	530
Input Compound	D-Glucose	5793	Compound	gamma-L-Glutamyl-L-cysteine	123938
Input Compound	Acetate	176	Compound	Amylose	0
Input Compound	L-Alanine	5950	Compound	D-Sorbitol	5780
Input Compound	Succinate	1110	Compound	L-Alanyl-tRNA	
Input Compound	L-Aspartate	5960	Compound	2-Oxoglutarate	48
Input Compound	L-Phenylalanine	6140	Compound	N,N-Dimethylglycine	673
Input Compound	Uracil	1174	Compound	N-Acetyl-L-aspartate	65065
Input Compound	Choline	305	Compound	N-Formyl-L-aspartate	
Input Compound	L-Leucine	6106	Compound	alpha,alpha-Trehalose	1143
Input Compound	Putrescine	1045	Compound	S-Adenosylmethioninamine	1078
Input Compound	myo-Inositol	892	Compound	L-Glutamate 5-semialdehyde	193305
Input Compound	L-Valine	1182	Compound	Pseudouridine 5'-phosphate	439424
Input Compound	(S)-Lactate	107689	Compound	1L-myo-Inositol 1-phosphate	107737
Input Compound	Sarcosine	1088	Compound	1-Phosphatidyl-D-myo-inositol	
Input Compound	Taurine	1123	Compound	(R)-3-Amino-2-methylpropanoate	
Input Compound	D-Glycerate	439194	Compound	1-alpha-D-Galactosyl-myo-inositol	439451
Input Compound	L-Isoleucine	791	Compound	N-Acetyl-beta-D-glucosaminylamine	897
Input Compound	(R)-3-Hydroxybutanoate	92135	Compound	Cys-Gly	439498
Compound	ATP	5957	Compound	tRNA(Ala)	
Compound	NH3	222	Compound	tRNA(Asp)	
Compound	UDP	6031	Compound	tRNA(Glu)	
Compound	AMP	6083	Compound	tRNA(Ile)	
Compound	Pyruvate	1060	Compound	tRNA(Leu)	
Compound	Acetyl-CoA	6302	Compound	tRNA(Phe)	
Compound	2-Oxoglutarate	51	Compound	tRNA(Val)	
Compound	Oxaloacetate	970	Compound	Glycogenin	
Compound	Glycine	750	Compound	Acylcholine	
Compound	Glutathione	124886	Compound	Choloyl-CoA	383
Compound	UDP-D-galactose	18068	Compound	5-Oxoproline	7405
Compound	Formate	284	Compound	Acetylcholine	187
Compound	Carboxylate		Compound	L-Leucyl-tRNA	
Compound	L-Glutamine	5961	Compound	R-S-Glutathione	
Compound	L-Serine	5951	Compound	2-Phenylacetamide	7680
Compound	L-Ornithine	6262	Compound	L-Valyl-tRNA(Val)	
Compound	L-Tyrosine	6057	Compound	Taurolithocholate	439763
Compound	Acetaldehyde	177	Compound	Glucosylglycogenin	
Compound	Sucrose	5988	Compound	N-Acetylputrescine	122356
Compound	Succinyl-CoA	439161	Compound	Phosphatidylserine	0
Compound	D-Glucose 6-phosphate	208	Compound	Peptide L-aspartate	
Compound	D-Fructose		Compound	L-Aspartyl-tRNA(Asp)	
Compound	L-Cysteine	5862	Compound	L-Glutamyl-tRNA(Glu)	
Compound	beta-Alanine	239	Compound	L-Isoleucyl-tRNA(Ile)	

Category	Canonical Compound Name	Compound PubMed ID	Category	Canonical Compound Name	Compound PubMed ID
Compound	Tetrahydrofolate	1129	Compound	L-Glutamyl 5-phosphate	193475
Compound	D-Glucose 1-phosphate	65533	Compound	N-(L-Arginino)succinate	439998
Compound	UMP	6030	Compound	3-Methyl-2-oxopentanoate	
Compound	Fumarate	723	Compound	L-Phenylalanyl-tRNA(Phe)	
Compound	D-Galactose	439357	Compound	Tetrahydrofolyl-[Glu](n)	442163
Compound	IMP	8582	Compound	myo-Inositol 4-phosphate	440043
Compound	dATP	15993	Compound	N-Acyl-O-acetylneuraminic acid	
Compound	3-Methyl-2-oxobutanoic acid	49	Compound	N6-(1,2-Dicarboxyethyl)-AMP	440122
Compound	L-Asparagine	6267	Compound	(S)-1-Pyrroline-5-carboxylate	
Compound	Phosphatidylcholine	452110	Compound	Peptide 3-hydroxy-L-aspartate	
Compound	Citrate	311	Compound	3alpha-Hydroxy-5beta-cholanate	9903
Compound	Acetoacetate	96	Compound	1D-myo-Inositol 3-phosphate	440194
Compound	Phenylpyruvate	997	Compound	1-Organyl-2-lyso-sn-glycero-3-phosphocholine	0
Compound	UDPglucuronate	17473	Compound	N4-(Acetyl-beta-D-glucosaminy)asparagine	123826
Compound	Hydroxypyruvate	964	Compound	1-Alkyl-2-acetyl-sn-glycero-3-phosphocholine	2503
Compound	Carbamoyl phosphate	278	Compound	Taurocholate	440567
Compound	5'-Methylthioadenosine	149	Compound	Phenethylamine	1001
Compound	Agmatine	199	Compound	Chenodeoxycholoyl-CoA	11966205
Compound	D-Glucuronate	444791	Compound	Melibiose	440658
Compound	dADP	188966	Compound	Taurodeoxycholate	10594
Compound	Acetyl phosphate	186	Compound	Taurochenodeoxycholate	10591
Compound	Succinate semialdehyde	1112	Compound	R-S-Alanylglycine	
Compound	4-Methyl-2-oxopentanoate		Compound	5-Glutamyl-aurine	0
Compound	Lactose	84571	Compound	Acetyl adenylate	440867
Compound	Dihydrobiopterin		Compound	L-Glutamyl-tRNA(Gln)	
Compound	N-Acetylneuraminic acid	439197	Compound	L-Aspartyl-tRNA(Asn)	
Compound	Tetrahydrobiopterin	1125	Compound	Tetrahydrofolyl-[Glu](2)	442163
Compound	Uridine	6029	Compound	4-Hydroxyphenyl acetate	
Compound	Spermidine	1102	Compound	gamma-L-glutamyl-L-alanine	
Compound	L-Citrulline	9750	Compound	N-acetyl-L-alanine	
Compound	4-Aminobutanoate	119	Compound	deoxycholoyl-CoA	
Compound	2-Methyl-3-oxopropanoate	296	Compound	tetrahydrobiopterin-4a-carbinolamine	
Compound	Phosphatidate	5873088	Compound	acetamidopropanal	
Compound	5,6-Dihydrouracil	649	Compound	3(S)-phytanoyl-CoA	
Compound	N-Carbamoyl-L-aspartate	93072	Compound	3(S)-2-hydroxyphytanoyl-CoA	
Compound	N-Formimino-L-glutamate	13160	Compound	somatostatin	
Compound	alpha-D-Galactose 1-phosphate	439995	Compound	Somatostatin fragment 3-14	
Compound	L-Cysteate	25701	Compound	kinetensin	
Compound	Deoxyuridine	13712	Compound	kinetensin 1-3	
Compound	Hydroquinone	785	Compound	kinetensin 1-7	
Compound	4-Aminobutanal	118	Compound	kinetensin 1-8	
Compound	Betaine aldehyde	249	Compound	kinetensin 4-7	
Compound	D-Glyceraldehyde		Compound	kinetensin 4-8	
Compound	Choline phosphate	1014	Compound	neuromedin N	
Compound	N1-Acetylspermidine	496	Compound	neuromedin N (1-4)	

Table 4.15. The enzymes that are effected by the altered metabolites identified in the Hg dosed terrapins. This list was generated using Cytoscape 3.1 with the Metscape plug-in.

Category	Canonical Enzyme Name	Category	Canonical Enzyme Name
Enzyme	Aldehyde reductase	Enzyme	UTP--glucose-1-phosphate uridylyltransferase
Enzyme	UDP-glucose 6-dehydrogenase	Enzyme	Transferases for other substituted phosphate groups
Enzyme	Glyoxylate reductase	Enzyme	3-oxoacid CoA-transferase
Enzyme	L-lactate dehydrogenase	Enzyme	Arylesterase
Enzyme	Glycerate dehydrogenase	Enzyme	1-alkyl-2-acetylglucero-phosphocholine esterase
Enzyme	3-hydroxybutyrate dehydrogenase	Enzyme	Sialate O-acetyltransferase
Enzyme	Glyoxylate reductase (NADP(+))	Enzyme	Acetylcholinesterase
Enzyme	L-lactate dehydrogenase (cytochrome)	Enzyme	Cholinesterase
Enzyme	Choline dehydrogenase	Enzyme	Acetyl-CoA hydrolase
Enzyme	Peroxidase	Enzyme	Inositol-phosphate phosphatase
Enzyme	Inositol oxygenase	Enzyme	Phosphoethanolamine/phosphocholine phosphatase
Enzyme	Peptide-aspartate beta-dioxygenase	Enzyme	Phospholipase D
Enzyme	Phytanoyl-CoA dioxygenase	Enzyme	Lactase
Enzyme	Phenylalanine 4-monoxygenase	Enzyme	Alpha-glucosidase
Enzyme	Succinate-semialdehyde dehydrogenase	Enzyme	Alpha-galactosidase
Enzyme	Aldehyde dehydrogenase (NAD(+))	Enzyme	Alpha, alpha-trehalase.
Enzyme	Aldehyde dehydrogenase (NAD(P)(+))	Enzyme	Tripeptide aminopeptidase
Enzyme	Dihydropyrimidine dehydrogenase (NADP(+))	Enzyme	Carboxypeptidase A
Enzyme	Succinate dehydrogenase (ubiquinone)	Enzyme	Tissue kallikrein
Enzyme	Glutamate dehydrogenase (NAD(P)(+))	Enzyme	Chymase
Enzyme	L-amino-acid oxidase	Enzyme	Tryptase
Enzyme	Amine oxidase (copper-containing)	Enzyme	Aminoacylase
Enzyme	1-pyrroline-5-carboxylate dehydrogenase	Enzyme	Aspartoacylase
Enzyme	Sarcosine oxidase	Enzyme	Glutaminase
Enzyme	Polyamine oxidase	Enzyme	N(4)-(beta-N-acetylglucosaminyl)-L-asparaginase
Enzyme	Sarcosine dehydrogenase	Enzyme	5-oxoprolinase (ATP-hydrolyzing)
Enzyme	Dimethylglycine dehydrogenase	Enzyme	Agmatinase
Enzyme	Glycine N-methyltransferase	Enzyme	Acylphosphatase
Enzyme	Glutamate formimidoyltransferase	Enzyme	Nucleotide diphosphatase
Enzyme	Aspartate carbamoyltransferase	Enzyme	Glutamate decarboxylase
Enzyme	Amino-acid N-acetyltransferase	Enzyme	Ornithine decarboxylase
Enzyme	Diamine N-acetyltransferase	Enzyme	Arginine decarboxylase
Enzyme	Choline O-acetyltransferase	Enzyme	Aromatic-L-amino-acid decarboxylase
Enzyme	Bile acid-CoA:amino acid N-acyltransferase	Enzyme	Sulfinoalanine decarboxylase
Enzyme	Gamma-glutamyltransferase	Enzyme	Citrate (pro-3S)-lyase
Enzyme	Glycogen(starch) synthase	Enzyme	Pseudouridylyl synthase
Enzyme	Glycogenin glucosyltransferase	Enzyme	UDP-glucose 4-epimerase
Enzyme	Purine-nucleoside phosphorylase	Enzyme	Aspartate--tRNA ligase
Enzyme	Uridine phosphorylase	Enzyme	Glutamate--tRNA ligase
Enzyme	Thymidine phosphorylase	Enzyme	Phenylalanine--tRNA ligase
Enzyme	Spermidine synthase	Enzyme	Leucine--tRNA ligase
Enzyme	Aspartate transaminase	Enzyme	Isoleucine--tRNA ligase
Enzyme	Alanine transaminase	Enzyme	Alanine--tRNA ligase
Enzyme	(R)-3-amino-2-methylpropionate--pyruvate transaminase	Enzyme	Valine--tRNA ligase
Enzyme	Branched-chain-amino-acid transaminase	Enzyme	Acid--thiol ligases
Enzyme	Alanine--glyoxylate transaminase	Enzyme	Acetate--CoA ligase
Enzyme	Tyrosine transaminase	Enzyme	Succinate--CoA ligase (GDP-forming)
Enzyme	Glutamine--phenylpyruvate transaminase	Enzyme	Succinate--CoA ligase (ADP-forming)
Enzyme	Hexokinase	Enzyme	Glutamate--ammonia ligase
Enzyme	ADP-specific glucokinase	Enzyme	Tetrahydrofolate synthase
Enzyme	Choline kinase	Enzyme	Glutamate--cysteine ligase
Enzyme	Glutamate 5-kinase	Enzyme	Adenylosuccinate synthase
Enzyme	UDP-glucose--hexose-1-phosphate uridylyltransferase	Enzyme	Argininosuccinate synthase
Enzyme	Asparagine synthase (glutamine-hydrolyzing)		

Table 4.16. The reactions affected by the sixteen altered metabolites identified in the Hg dosed terrapins. This list was generated using Cytoscape 3.1 with the Metscape plug-in.

<u>Category</u>	<u>Canonical Name</u>	<u>Reaction Location</u>	<u>Reaction Pathway</u>
Reaction	R00010	cytosol	
Reaction	R00196	cytosol	Glycolysis and Gluconeogenesis
Reaction	R00227	cytosol	Glycolysis and Gluconeogenesis
Reaction	R00235	cytosol, mitochondria	Glycolysis and Gluconeogenesis
Reaction	R00239	cytosol, mitochondria	Urea cycle and metabolism of arginine, proline, glutamate, aspartate and asparagine
Reaction	R00243	cytosol, mitochondria	Urea cycle and metabolism of arginine, proline, glutamate, aspartate and asparagine
Reaction	R00245	mitochondria	Urea cycle and metabolism of arginine, proline, glutamate, aspartate and asparagine
Reaction	R00248	cytosol, mitochondria	Urea cycle and metabolism of arginine, proline, glutamate, aspartate and asparagine
Reaction	R00251	cytosol	Urea cycle and metabolism of arginine, proline, glutamate, aspartate and asparagine
Reaction	R00253	cytosol, mitochondria	Urea cycle and metabolism of arginine, proline, glutamate, aspartate and asparagine
Reaction	R00256	mitochondria	Urea cycle and metabolism of arginine, proline, glutamate, aspartate and asparagine
Reaction	R00258	cytosol	Urea cycle and metabolism of arginine, proline, glutamate, aspartate and asparagine
Reaction	R00259	mitochondria	Urea cycle and metabolism of arginine, proline, glutamate, aspartate and asparagine
Reaction	R00261	Golgi apparatus, cytosol, mitochondria	Urea cycle and metabolism of arginine, proline, glutamate, aspartate and asparagine
Reaction	R00286	cytosol	
Reaction	R00287	cytosol, extracellular	Pyrimidine metabolism
Reaction	R00289	cytosol	
Reaction	R00291	cytosol	Galactose metabolism
Reaction	R00292	cytosol	
Reaction	R00316	cytosol, mitochondria	Glycolysis and Gluconeogenesis
Reaction	R00317	cytosol	Glycolysis and Gluconeogenesis
Reaction	R00355	cytosol, mitochondria	Urea cycle and metabolism of arginine, proline, glutamate, aspartate and asparagine
Reaction	R00357	lysosomes	Urea cycle and metabolism of arginine, proline, glutamate, aspartate and asparagine
Reaction	R00362	cytosol, mitochondria	TCA cycle
Reaction	R00367	cytosol	Glycine, serine, alanine and threonine metabolism
Reaction	R00369	peroxisomes	Glycine, serine, alanine and threonine metabolism
Reaction	R00405	mitochondria	TCA cycle
Reaction	R00410	cytosol, mitochondria	Butanoate metabolism
Reaction	R00432	mitochondria	TCA cycle
Reaction	R00488	cytosol	Urea cycle and metabolism of arginine, proline, glutamate, aspartate and asparagine
Reaction	R00489	Golgi apparatus, cytosol	Urea cycle and metabolism of arginine, proline, glutamate, aspartate and asparagine
Reaction	R00494	cytosol	Urea cycle and metabolism of arginine, proline, glutamate, aspartate and asparagine
Reaction	R00526	cytosol	Urea cycle and metabolism of arginine, proline, glutamate, aspartate and asparagine
Reaction	R00578	mitochondria	Urea cycle and metabolism of arginine, proline, glutamate, aspartate and asparagine
Reaction	R00610	peroxisomes	Glycine, serine, alanine and threonine metabolism
Reaction	R00611	cytosol, mitochondria	Glycine, serine, alanine and threonine metabolism
Reaction	R00670	cytosol, mitochondria	Urea cycle and metabolism of arginine, proline, glutamate, aspartate and asparagine

<u>Category</u>	<u>Canonical Name</u>	<u>Reaction Location</u>	<u>Reaction Pathway</u>
Reaction	R00689	lysosomes	Tyrosine metabolism
Reaction	R00694	cytosol	Tyrosine metabolism
Reaction	R00698	lysosomes, cytosol	Tyrosine metabolism
Reaction	R00699	cytosol	Tyrosine metabolism
Reaction	R00703	cytosol	Glycolysis and Gluconeogenesis
Reaction	R00707	mitochondria	Urea cycle and metabolism of arginine, proline, glutamate, aspartate and asparagine
Reaction	R00708	mitochondria	Urea cycle and metabolism of arginine, proline, glutamate, aspartate and asparagine
Reaction	R00710	cytosol, mitochondria	Glycolysis and Gluconeogenesis
Reaction	R00711	cytosol, mitochondria	Glycolysis and Gluconeogenesis
Reaction	R00713	cytosol, mitochondria	Urea cycle and metabolism of arginine, proline, glutamate, aspartate and asparagine
Reaction	R00725	mitochondria, cytosol	
Reaction	R00727	mitochondria	TCA cycle
Reaction	R00801	Golgi apparatus, lysosomes, endoplasmic reticulum, cytosol	
Reaction	R00894	cytosol	Urea cycle and metabolism of arginine, proline, glutamate, aspartate and asparagine
Reaction	R00942	cytosol, mitochondria	Vitamin B9 (folate) metabolism
Reaction	R00955	cytosol	Galactose metabolism
Reaction	R00978	cytosol	Pyrimidine metabolism
Reaction	R01021	endoplasmic reticulum	Glycerophospholipid metabolism
Reaction	R01023	cytosol, nucleus	Glycerophospholipid metabolism
Reaction	R01025	mitochondria	Glycine, serine, alanine and threonine metabolism
Reaction	R01026	Golgi apparatus, cytosol, extracellular	Glycerophospholipid metabolism
Reaction	R01029	endoplasmic reticulum, extracellular, nucleus	
Reaction	R01055	cytosol, nucleus	Pyrimidine metabolism
Reaction	R01090	cytosol, mitochondria	Valine, leucine and isoleucine degradation
Reaction	R01100	Golgi apparatus, lysosomes, cytosol	Galactose metabolism
Reaction	R01101	Golgi apparatus, lysosomes, cytosol, extracellular	Galactose metabolism
Reaction	R01135	cytosol	Purine metabolism
Reaction	R01139	cytosol, mitochondria	
Reaction	R01151	cytosol, mitochondria	Urea cycle and metabolism of arginine, proline, glutamate, aspartate and asparagine
Reaction	R01154	mitochondria	Urea cycle and metabolism of arginine, proline, glutamate, aspartate and asparagine
Reaction	R01157	mitochondria	Urea cycle and metabolism of arginine, proline, glutamate, aspartate and asparagine
Reaction	R01184	cytosol	Phosphatidylinositol phosphate metabolism
Reaction	R01185	cytosol	Phosphatidylinositol phosphate metabolism
Reaction	R01186	cytosol	Phosphatidylinositol phosphate metabolism
Reaction	R01187	cytosol	Phosphatidylinositol phosphate metabolism
Reaction	R01194	Golgi apparatus, cytosol	Phosphatidylinositol phosphate metabolism
Reaction	R01214	cytosol, mitochondria	Valine, leucine and isoleucine degradation
Reaction	R01310	Golgi apparatus, endoplasmic reticulum, cytosol, nucleus	Glycerophospholipid metabolism
Reaction	R01361	cytosol, mitochondria	Butanoate metabolism

<u>Category</u>	<u>Canonical Name</u>	<u>Reaction Location</u>	<u>Reaction Pathway</u>
Reaction	R01375	cytosol	
Reaction	R01388	cytosol	Glycine, serine, alanine and threonine metabolism
Reaction	R01392	cytosol	Glycine, serine, alanine and threonine metabolism
Reaction	R01397	cytosol	Pyrimidine metabolism
Reaction	R01565	cytosol, mitochondria	Glycine, serine, alanine and threonine metabolism
Reaction	R01682	Golgi apparatus, cytosol	Methionine and cysteine metabolism
Reaction	R01687	cytosol	Methionine and cysteine metabolism
Reaction	R01752	endoplasmic reticulum, cytosol, extracellular, mitochondria	Glycerophospholipid metabolism
Reaction	R01795	cytosol	Tyrosine metabolism
Reaction	R01810	lysosomes	
Reaction	R01876	cytosol, extracellular, nucleus	Pyrimidine metabolism
Reaction	R01920	cytosol	Urea cycle and metabolism of arginine, proline, glutamate, aspartate and asparagine
Reaction	R01954	cytosol	Urea cycle and metabolism of arginine, proline, glutamate, aspartate and asparagine
Reaction	R02048	mitochondria	
Reaction	R02050	mitochondria	
Reaction	R02164	cytosol, mitochondria	TCA cycle
Reaction	R02197	cytosol	Valine, leucine and isoleucine degradation
Reaction	R02198	cytosol, mitochondria	Valine, leucine and isoleucine degradation
Reaction	R02287	cytosol	Histidine metabolism
Reaction	R02483	cytosol, extracellular	Pyrimidine metabolism
Reaction	R03038	cytosol, mitochondria	Glycine, serine, alanine and threonine metabolism
Reaction	R03421	lysosomes	Urea cycle and metabolism of arginine, proline, glutamate, aspartate and asparagine
Reaction	R03647	cytosol, mitochondria	Urea cycle and metabolism of arginine, proline, glutamate, aspartate and asparagine
Reaction	R03651	cytosol, mitochondria	Urea cycle and metabolism of arginine, proline, glutamate, aspartate and asparagine
Reaction	R03656	cytosol, mitochondria	Valine, leucine and isoleucine degradation
Reaction	R03657	cytosol, mitochondria	Valine, leucine and isoleucine degradation
Reaction	R03660	cytosol, mitochondria	Tyrosine metabolism
Reaction	R03665	cytosol, mitochondria	Valine, leucine and isoleucine degradation
Reaction	R03681	cytosol	
Reaction	R03720	cytosol, peroxisomes	Bile acid biosynthesis
Reaction	R03916	cytosol	Urea cycle and metabolism of arginine, proline, glutamate, aspartate and asparagine
Reaction	R04073	endoplasmic reticulum, cytosol, nucleus	
Reaction	R04241	cytosol, mitochondria	Vitamin B9 (folate) metabolism
Reaction	R04452	cytosol, extracellular, nucleus	Glycerophospholipid metabolism
Reaction	R05577	cytosol, mitochondria	Urea cycle and metabolism of arginine, proline, glutamate, aspartate and asparagine
Reaction	R05578	cytosol, mitochondria	Urea cycle and metabolism of arginine, proline, glutamate, aspartate and asparagine
Reaction	R05804	cytosol	
Reaction	R06871	endoplasmic reticulum	Glycerophospholipid metabolism
Reaction	R06893	cytosol, extracellular	

<u>Category</u>	<u>Canonical Name</u>	<u>Reaction Location</u>	<u>Reaction Pathway</u>
Reaction	RE1342	cytosol	Fructose and mannose metabolism
Reaction	RE1465	cytosol	Tyrosine metabolism
Reaction	RE1473	cytosol	Glycine, serine, alanine and threonine metabolism
Reaction	RE1537	cytosol, peroxisomes	Urea cycle and metabolism of arginine, proline, glutamate, aspartate and asparagine
Reaction	RE1845	cytosol, peroxisomes	Bile acid biosynthesis
Reaction	RE1846	cytosol, peroxisomes	Bile acid biosynthesis
Reaction	RE2031	mitochondria	Glycine, serine, alanine and threonine metabolism
Reaction	RE2265	cytosol	
Reaction	RE2268	cytosol, extracellular	
Reaction	RE2269	cytosol, extracellular	
Reaction	RE2270	cytosol, extracellular	
Reaction	RE2273	cytosol, extracellular	
Reaction	RE2304	extracellular	
Reaction	RE2637	cytosol, peroxisomes	Bile acid biosynthesis
Reaction	RE2642	cytosol	Glycine, serine, alanine and threonine metabolism
Reaction	RE2650	cytosol	Biopterin metabolism
Reaction	RE3066	peroxisomes	Phytanic acid peroxisomal oxidation
Reaction	RE3273	Golgi apparatus, endoplasmic reticulum, cytosol	Phosphatidylinositol phosphate metabolism
Reaction	RE3299	cytosol	Glycerophospholipid metabolism

Table 4.17. The gene effected by the sixteen altered metabolites identified in the Hg dosed terrapins. This list was generated using Cytoscape 3.1 with the Metscape plug-in.

Category	Canonical Name/ Gene Symbol	Gene Description	Gene Location
Gene	FARSB	phenylalanyl-tRNA synthetase, beta subunit	soluble fraction, cytoplasm, cytosol
Gene	FARS2	phenylalanyl-tRNA synthetase 2, mitochondrial	soluble fraction, cytoplasm, mitochondrion, mitochondrial matrix
Gene	FTCD	formiminotransferase cyclodeaminase	cytoplasm, Golgi apparatus
Gene	SLC27A2	solute carrier family 27 (fatty acid transporter), member 2	mitochondrion, peroxisome, peroxisomal membrane, peroxisomal matrix, endoplasmic reticulum, membrane, integral to membrane
Gene	CHAT	choline acetyltransferase	nucleus, cytoplasm, cytosol, cell soma
Gene	TREH	trehalase (brush-border membrane glycoprotein)	plasma membrane, anchored to plasma membrane
Gene	CHKA	choline kinase alpha	cytoplasm
Gene	CHKB	choline kinase beta	NONE
Gene	SAT2	spermidine/spermine N1-acetyltransferase family member 2	NONE
Gene	ADC	arginine decarboxylase	cellular_component, cytosol
Gene	CMA1	chymase 1, mast cell	extracellular region, intracellular
Gene	ADSSL1	adenylosuccinate synthase like 1	cytoplasm
Gene	EARS2	glutamyl-tRNA synthetase 2, mitochondrial (putative)	cytoplasm, mitochondrion, mitochondrial matrix
Gene	CYB5D1	cytochrome b5 domain containing 1	NONE
Gene	ACOT12	acyl-CoA thioesterase 12	cytoplasm, cytosol
Gene	CPA1	carboxypeptidase A1 (pancreatic)	extracellular region, extracellular space, soluble fraction
Gene	CPA2	carboxypeptidase A2 (pancreatic)	extracellular region
Gene	CPA3	carboxypeptidase A3 (mast cell)	nucleus, secretory granule, mast cell granule
Gene	UPP2	uridine phosphorylase 2	cytoplasm, cytosol, type III intermediate filament
Gene	ADSS	adenylosuccinate synthase	cellular_component, cytoplasm
Gene	AARS	alanyl-tRNA synthetase	soluble fraction, cytoplasm
Gene	LDHAL6A	lactate dehydrogenase A-like 6A	cytoplasm
Gene	DARS	aspartyl-tRNA synthetase	soluble fraction, cytoplasm, cytosol
Gene	NAGS	N-acetylglutamate synthase	mitochondrion, mitochondrial matrix
Gene	PHOSPHO1	phosphatase, orphan 1	NONE
Gene	DDC	dopa decarboxylase (aromatic L-amino acid decarboxylase)	NONE
Gene	CLYBL	citrate lyase beta like	mitochondrion, citrate lyase complex
Gene	AGA	aspartylglucosaminidase	lysosome
Gene	SARDH	sarcosine dehydrogenase	cytoplasm, mitochondrion, mitochondrial matrix
Gene	DPYD	dihydropyrimidine dehydrogenase	cytoplasm, cytosol, cytosol
Gene	AGXT	alanine-glyoxylate aminotransferase	mitochondrion, mitochondrial matrix, peroxisome
Gene	TYMP	thymidine phosphorylase	cytosol
Gene	PAOX	polyamine oxidase (exo-N4-amino)	NONE
Gene	EPRS	glutamyl-prolyl-tRNA synthetase	soluble fraction, cytoplasm, cytosol
Gene	ALDH2	aldehyde dehydrogenase 2 family (mitochondrial)	mitochondrion, mitochondrial matrix
Gene	ALDH3A1	aldehyde dehydrogenase 3 family, memberA1	cytoplasm, endoplasmic reticulum, cytosol
Gene	ALDH1B1	aldehyde dehydrogenase 1 family, member B1	mitochondrion, mitochondrial matrix
Gene	FARSA	phenylalanyl-tRNA synthetase, alpha subunit	soluble fraction, cytoplasm, cytosol

Category	Canonical Name/ Gene Symbol	Gene Description	Gene Location
Gene	ALDH1A3	aldehyde dehydrogenase 1 family, member A3	cytoplasm
Gene	ALDH3B1	aldehyde dehydrogenase 3 family, member B1	NONE
Gene	ALDH3B2	aldehyde dehydrogenase 3 family, member B2	NONE
Gene	ALDH9A1	aldehyde dehydrogenase 9 family, member A1	nucleus, cytoplasm, cytoplasm, cytosol, cytoskeleton
Gene	ALDH3A2	aldehyde dehydrogenase 3 family, member A2	endoplasmic reticulum, membrane, integral to membrane
Gene	AKR1B1	aldo-keto reductase family 1, member B1 (aldose reductase)	extracellular space, cytoplasm, cytosol
Gene	GANAB	glucosidase, alpha; neutral AB	endoplasmic reticulum, Golgi apparatus, melanosome
Gene	LARS2	leucyl-tRNA synthetase 2, mitochondrial	cytoplasm, mitochondrion, mitochondrial matrix
Gene	TPSD1	tryptase delta 1	extracellular region
Gene	FPGS	folylpolyglutamate synthase	cytoplasm, mitochondrion, cytosol
Gene	GAA	glucosidase, alpha; acid	lysosome
Gene	GAD1	glutamate decarboxylase 1 (brain, 67kDa)	intracellular, cytoplasm, mitochondrion, vesicle membrane, axon, synapse
Gene	GAD2	glutamate decarboxylase 2 (pancreatic islets and brain, 65kDa)	cytoplasm, Golgi apparatus, cytosol, plasma membrane, cytoplasmic membrane-bounded vesicle, cell junction, axon, synaptic vesicle membrane, anchored to membrane, synapse, perinuclear region of cytoplasm
Gene	GALE	UDP-galactose-4-epimerase	cytosol
Gene	GALT	galactose-1-phosphate uridylyltransferase	soluble fraction, cytosol
Gene	IL4I1	interleukin 4 induced 1	lysosome
Gene	GANC	glucosidase, alpha; neutral C	NONE
Gene	ABP1	amiloride binding protein 1 (amine oxidase (copper-containing))	extracellular region, extracellular space, peroxisome
Gene	GGT1	gamma-glutamyltransferase 1	membrane, integral to membrane
Gene	GGT3	gamma-glutamyltransferase 3 pseudogene	membrane, integral to membrane
Gene	GGTL3	gamma-glutamyltransferase 7	membrane, integral to membrane
Gene	GGTLA1	gamma-glutamyltransferase 5	plasma membrane, integral to membrane
Gene	OPLAH	5-oxoprolinase (ATP-hydrolysing)	NONE
Gene	GLS2	glutaminase 2 (liver, mitochondrial)	mitochondrion, mitochondrial matrix
Gene	GLA	galactosidase, alpha	extracellular region, extracellular region, cytoplasm, cytoplasm, lysosome, lysosome, Golgi apparatus
Gene	GNMT	glycine N-methyltransferase	nucleus, cytoplasm, cytosol
Gene	GCLC	glutamate-cysteine ligase, catalytic subunit	cytosol, glutamate-cysteine ligase complex
Gene	GCLM	glutamate-cysteine ligase, modifier subunit	soluble fraction, cytosol, glutamate-cysteine ligase complex
Gene	GLS	glutaminase	mitochondrion, mitochondrial matrix
Gene	GLUD1	glutamate dehydrogenase 1	cytoplasm, mitochondrion, mitochondrial matrix
Gene	GLUD2	glutamate dehydrogenase 2	cytoplasm, mitochondrion, mitochondrial matrix
Gene	GLUDP5	glutamate dehydrogenase pseudogene 5	NONE
Gene	GLUL	glutamate-ammonia ligase (glutamine synthetase)	intracellular, cytoplasm, mitochondrion, Golgi apparatus, cytosol
Gene	GLYD	NULL	NONE
Gene	GOT1	glutamic-oxaloacetic transaminase 1, soluble (aspartate aminotransferase 1)	soluble fraction, cytoplasm, lysosome, cytosol, nerve terminal
Gene	GOT2	glutamic-oxaloacetic transaminase 2, mitochondrial (aspartate aminotransferase 2)	mitochondrion, mitochondrion, mitochondrial inner membrane, mitochondrial matrix, plasma membrane
Gene	GPT	glutamic-pyruvate transaminase (alanine aminotransferase)	cytoplasm, cytosol

Category	Canonical Name/ Gene Symbol	Gene Description	Gene Location
Gene	GYG1	glycogenin 1	soluble fraction, cytosol
Gene	DMGDH	dimethylglycine dehydrogenase	cytoplasm, mitochondrion, mitochondrial matrix
Gene	GYS1	glycogen synthase 1 (muscle)	soluble fraction, cytoplasm, cytosol, inclusion body
Gene	GYS2	glycogen synthase 2 (liver)	soluble fraction, insoluble fraction, cytoplasm, cytosol, cytoskeleton, cell cortex, cortical actin cytoskeleton, ectoplasm
Gene	HK1	hexokinase 1	mitochondrion, mitochondrial outer membrane, cytosol, membrane
Gene	HK2	hexokinase 2	mitochondrion, mitochondrial outer membrane, cytosol, membrane
Gene	HK3	hexokinase 3 (white cell)	cytosol, membrane, protein complex
Gene	AOC2	amine oxidase, copper containing 2 (retina-specific)	cytoplasm, plasma membrane, extrinsic to membrane
Gene	IARS	isoleucyl-tRNA synthetase	soluble fraction, cytoplasm, cytosol
Gene	IMPA1	inositol(myo)-1(or 4)-monophosphatase 1	cytoplasm
Gene	IMPA2	inositol(myo)-1(or 4)-monophosphatase 2	cytoplasm
Gene	KLK1	kallikrein 1	NONE
Gene	KLK2	kallikrein-related peptidase 2	NONE
Gene	LCT	lactase	membrane fraction, plasma membrane, integral to plasma membrane, brush border
Gene	LDHA	lactate dehydrogenase A	cellular_component, cytoplasm, cytosol, flagellum
Gene	LDHB	lactate dehydrogenase B	soluble fraction, cytoplasm
Gene	LDHC	lactate dehydrogenase C	cytoplasm
Gene	LPO	lactoperoxidase	extracellular region, extracellular space
Gene	ACHE	acetylcholinesterase (Yt blood group)	extracellular region, extracellular region, extracellular region, basal lamina, nucleus, Golgi apparatus, plasma membrane, extrinsic to membrane, cell junction, anchored to membrane, synapse, perinuclear region of cytoplasm
Gene	MPO	myeloperoxidase	extracellular space, nucleus, lysosome, secretory granule
Gene	ASNS	asparagine synthetase	soluble fraction, cytosol
Gene	ASPA	aspartoacylase (Canavan disease)	nucleus, cytoplasm
Gene	ASPH	aspartate beta-hydroxylase	endoplasmic reticulum, endoplasmic reticulum membrane, membrane, integral to membrane, integral to endoplasmic reticulum membrane
Gene	ASS1	argininosuccinate synthetase 1	cytoplasm
Gene	NP	purine nucleoside phosphorylase	intracellular, cytoplasm, cytosol, cytoskeleton
Gene	ODC1	ornithine decarboxylase 1	cellular_component, cytosol
Gene	ALDH7A1	aldehyde dehydrogenase 7 family, member A1	cellular_component, mitochondrion
Gene	OXCT1	3-oxoacid CoA transferase 1	mitochondrion, mitochondrion, mitochondrial matrix
Gene	PAFAH1B1	platelet-activating factor acetylhydrolase, isoform 1b, subunit 1 (45kDa)	astral microtubule, kinetochore, soluble fraction, insoluble fraction, nucleus, cytoplasm, centrosome, spindle, cytosol, cytosol, microtubule, microtubule associated complex, cell cortex, membrane, growth cone, cell leading edge, motile primary cilium, nonmotile primary cilium, nuclear membrane, vesicular fraction, cell soma, perinuclear region of cytoplasm
Gene	PAFAH1B2	platelet-activating factor acetylhydrolase, isoform 1b, subunit 2 (30kDa)	cytoplasm
Gene	PAFAH1B3	platelet-activating factor acetylhydrolase, isoform 1b, subunit 3 (29kDa)	cytoplasm
Gene	PAFAH2	platelet-activating factor acetylhydrolase 2, 40kDa	cytoplasm
Gene	PAH	phenylalanine hydroxylase	NONE
Gene	PIPOX	pipecolic acid oxidase	peroxisome
Gene	CSAD	cysteine sulfinic acid decarboxylase	NONE

Category	Canonical Name/ Gene Symbol	Gene Description	Gene Location
Gene	LARS	leucyl-tRNA synthetase	cytoplasm, cytosol
Gene	ENPP1	ectonucleotide pyrophosphatase/phosphodiesterase 1	extracellular space, plasma membrane, plasma membrane, cell surface, integral to membrane, basolateral plasma membrane
Gene	ENPP2	ectonucleotide pyrophosphatase/phosphodiesterase 2	extracellular region, plasma membrane, integral to plasma membrane
Gene	ENPP3	ectonucleotide pyrophosphatase/phosphodiesterase 3	extracellular region, integral to plasma membrane, membrane, perinuclear region of cytoplasm
Gene	PEPB	peptidase B	NONE
Gene	PHYH	phytanoyl-CoA 2-hydroxylase	peroxisome
Gene	PLD1	phospholipase D1, phosphatidylcholine-specific	cytoplasm, endosome, endoplasmic reticulum, microsome, Golgi apparatus, membrane, lamellipodium, vesicle, Golgi cisterna, perinuclear region of cytoplasm
Gene	PLD2	phospholipase D2	plasma membrane, extrinsic to membrane, brush border membrane
Gene	SIAE	sialic acid acetyltransferase	lysosome
Gene	PON1	paraoxonase 1	extracellular region, extracellular space, microsome, spherical high-density lipoprotein particle
Gene	PON2	paraoxonase 2	extracellular region, plasma membrane, extrinsic to membrane
Gene	PON3	paraoxonase 3	extracellular region, extracellular space, microsome
Gene	P DPR	pyruvate dehydrogenase phosphatase regulatory subunit	cytoplasm, mitochondrion, mitochondrial matrix
Gene	DARS2	aspartyl-tRNA synthetase 2, mitochondrial	cytoplasm, mitochondrion, mitochondrial matrix
Gene	CHDH	choline dehydrogenase	mitochondrion, mitochondrial inner membrane
Gene	MIOX	myo-inositol oxygenase	cytoplasm, inclusion body
Gene	HIF1AN	hypoxia inducible factor 1, alpha subunit inhibitor	nucleus
Gene	IARS2	isoleucyl-tRNA synthetase 2, mitochondrial	cytoplasm, mitochondrion, mitochondrial matrix
Gene	ACSS2	acyl-CoA synthetase short-chain family member 2	nucleus, nucleolus, cytoplasm, cytoplasm, cytosol
Gene	BDH2	3-hydroxybutyrate dehydrogenase, type 2	cytoplasm, mitochondrion
Gene	BAAT	bile acid Coenzyme A: amino acid N- acyltransferase (glycine N- choloyltransferase)	cytoplasm, peroxisome, peroxisomal matrix, cytosol
Gene	CPA6	carboxypeptidase A6	extracellular region
Gene	VAR2	valyl-tRNA synthetase 2, mitochondrial (putative)	cytoplasm, mitochondrion
Gene	AARS2	alanyl-tRNA synthetase 2, mitochondrial (putative)	cytoplasm, mitochondrion, mitochondrial matrix
Gene	ALDH18A1	aldehyde dehydrogenase 18 family, member A1	cytoplasm, mitochondrion, mitochondrial inner membrane, membrane
Gene	BCAT1	branched chain aminotransferase 1, cytosolic	cytoplasm, cytosol
Gene	BCAT2	branched chain aminotransferase 2, mitochondrial	nucleus, cytoplasm, mitochondrion
Gene	BCHE	butyrylcholinesterase	extracellular region, extracellular space, membrane fraction, nuclear envelope lumen, endoplasmic reticulum, endoplasmic reticulum lumen, membrane
Gene	AASDHPPT	aminoadipate-semialdehyde dehydrogenase-phosphopantetheinyl transferase	cytoplasm, cytosol
Gene	BDH1	3-hydroxybutyrate dehydrogenase, type 1	mitochondrion, mitochondrial inner membrane, mitochondrial matrix, mitochondrial matrix
Gene	SAT1	spermidine/spermine N1- acetyltransferase 1	intracellular, cytoplasm
Gene	SDHA	succinate dehydrogenase complex, subunit A, flavoprotein (Fp)	mitochondrion, mitochondrial inner membrane, mitochondrial inner membrane, mitochondrial respiratory chain complex II, membrane
Gene	SDHB	succinate dehydrogenase complex, subunit B, iron sulfur (Ip)	mitochondrion, mitochondrial inner membrane, membrane
Gene	SDHC	succinate dehydrogenase complex, subunit C, integral membrane protein, 15kDa	mitochondrion, mitochondrial inner membrane, membrane, integral to membrane, respiratory chain complex II
Gene	SDHD	succinate dehydrogenase complex, subunit D, integral membrane protein	mitochondrion, mitochondrial envelope, mitochondrial inner membrane, mitochondrial inner membrane, membrane, integral to membrane

Category	Canonical Name/ Gene Symbol	Gene Description	Gene Location
Gene	OXCT2	3-oxoacid CoA transferase 2	mitochondrion, microtubule-based flagellum
Gene	TPSB2	tryptase beta 2 (gene/pseudogene)	extracellular region
Gene	AGXT2	alanine-glyoxylate aminotransferase 2	mitochondrion
Gene	SRM	spermidine synthase	cytosol
Gene	TAT	tyrosine aminotransferase	cellular_component, mitochondrion
Gene	TPO	thyroid peroxidase	mitochondrion, plasma membrane, integral to plasma membrane, cell surface
Gene	TPSAB1	tryptase alpha/beta 1	extracellular region
Gene	GGT2	gamma-glutamyltransferase 2	cellular_component, membrane, integral to membrane
Gene	UGDH	UDP-glucose dehydrogenase	cytosol
Gene	UGP1	UDP-glucose pyrophosphorylase 1	NONE
Gene	UGP2	UDP-glucose pyrophosphorylase 2	cytoplasm, cytosol
Gene	UPP1	uridine phosphorylase 1	cytoplasm, cytosol
Gene	VARS	valyl-tRNA synthetase	intracellular, cytoplasm, mitochondrion, cytosol
Gene	CAD	carbamoyl-phosphate synthetase 2, aspartate transcarbamylase, and dihydroorotase	nucleus, cytoplasm, cytosol, cytosol, nuclear matrix
Gene	ALDH5A1	aldehyde dehydrogenase 5 family, member A1	soluble fraction, mitochondrion
Gene	PLA2G7	phospholipase A2, group VII (platelet-activating factor acetylhydrolase, plasma)	extracellular region, extracellular space
Gene	AGMAT	agmatine ureohydrolase (agmatinase)	mitochondrion
Gene	EPX	eosinophil peroxidase	NONE
Gene	ADPGK	ADP-dependent glucokinase	extracellular region
Gene	ACSS1	acyl-CoA synthetase short-chain family member 1	mitochondrion, mitochondrial matrix
Gene	GPT2	glutamic pyruvate transaminase (alanine aminotransferase) 2	NONE
Gene	RPUSD4	RNA pseudouridylate synthase domain containing 4	NONE
Gene	AOC3	amine oxidase, copper containing 3 (vascular adhesion protein 1)	plasma membrane, cell surface, integral to membrane
Gene	ALDH4A1	aldehyde dehydrogenase 4 family, member A1	mitochondrion, mitochondrial matrix
Gene	SUCLG2	succinate-CoA ligase, GDP-forming, beta subunit	mitochondrion, mitochondrial matrix
Gene	SUCLG1	succinate-CoA ligase, alpha subunit	mitochondrion, mitochondrial inner membrane, mitochondrial matrix, succinate-CoA ligase complex (GDP-forming)
Gene	SUCLA2	succinate-CoA ligase, ADP-forming, beta subunit	mitochondrion
Gene	CCBL1	cysteine conjugate-beta lyase, cytoplasmic	cytoplasm, cytosol
Gene	GYG2	glycogenin 2	soluble fraction, cytosol
Gene	MGAM	maltase-glucoamylase (alpha-glucosidase)	plasma membrane, integral to membrane
Gene	GGTL4	gamma-glutamyltransferase light chain 2	cellular_component
Gene	ACY3	aspartoacylase (aminocyclase) 3	membrane fraction, cytoplasm, plasma membrane, apical plasma membrane, extrinsic to membrane
Gene	LDHAL6B	lactate dehydrogenase A-like 6B	cytoplasm
Gene	GRHPR	glyoxylate reductase/hydroxypyruvate reductase	cellular_component, cytoplasm
Gene	CPA5	carboxypeptidase A5	extracellular region
Gene	ACY1	aminoacylase 1	cytoplasm, cytosol
Gene	PRDX6	peroxiredoxin 6	nucleus, cytoplasm, lysosome, cytosol, cytoplasmic membrane-bounded vesicle
Gene	ACYP1	acylphosphatase 1, erythrocyte (common) type	NONE
Gene	ACYP2	acylphosphatase 2, muscle type	NONE

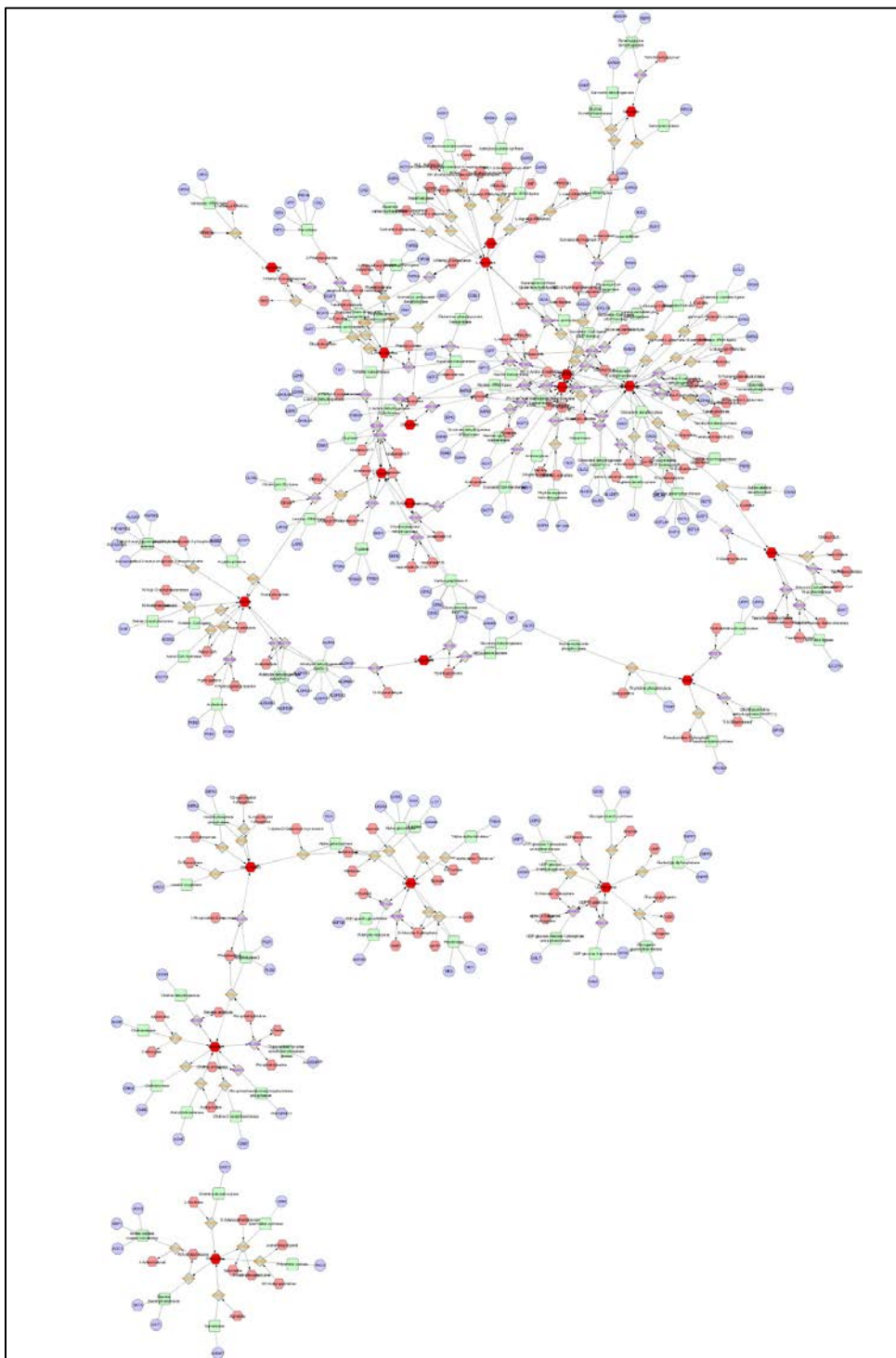


Figure 4.19. All biochemical effects of the altered metabolites identified in the Hg dosed diamondback terrapins.

The metabolites are represented by dark red octagons, the additional effected compounds are represented by pale red octagons, effected reactions, enzymes and genes are represented by grey diamonds, green squares and purple circles, respectively

4.4. Chapter Discussion

The goal of this project was to elucidate the sub-lethal, biochemical effects of mercury exposure, which are difficult to pin point, as they have no observable phenotype or behavior to guide the analysis. Generally, once an observable effect occurs the exposure has become lethal. The plasma and liver samples allowed observation of primary (increased oxidative stress) and secondary effects of mercury exposure (decreased food consumption).

The plasma samples highlight the onset of sublethal effects, before an observable behavior occurred. The OHD liver samples provide information regarding the biochemical changes taking place once the classic symptoms of mercury poisoning have set in. Using both samples, information can be gained to understand biochemical response during toxic exposures, and identify a biochemical pathway and biomarker that can be used to identify a detrimental exposure.

Biochemical significance of metabolites identified

The effects of diet are clear between the high dose and OHD terrapins since the OHD terrapins stopped eating. Many of the altered molecules between the high and OHD terrapins found in the turtle gelatin that the OHD terrapins stopped consuming. The metabolites that were not found in their food, but changed with mercury exposure were glucose, glutamate, lactate, putrescine, succinate, uracil, hypoxanthine, and aspartate. Several of these metabolites likely changed as a result of the decreased dietary molecules. In this instance, it is likely that the change in diet of the OHD terrapins lead to the downstream changes in glucose, lactate, glutamate, aspartate, and uracil, as they are drivers of energy metabolism. The decrease in glucose as a result of the lack of food

consumption is not surprising, as glucose is synthesized from food (401). Glutamate can be used as a component of flavor enhancing chemicals, but it is also synthesized by the body for use in cellular metabolism, and is an important neurotransmitter (402, 403). With glutamate decreased, pyruvate will not be synthesized and then cannot be converted to lactate. The changed molecules that are known components of the terrapin food are related to the folate cycle, and when there are deficiencies in the folate cycle uracil is erroneously incorporated into the DNA (404). Both of these relationships account for the decreases observed.

Apart from the metabolites that are related to diet changes, three molecules may provide more details about the effects of mercury exposure the OHD terrapins experienced; succinate, putrescine and hypoxanthine. Succinate is generated in the mitochondria by the tricarboxylic acid (TCA) cycle, and is important in many aspects of cellular function. Decreases in succinate can cause dysfunction of several biochemical pathways leading to inflammation, and tissue injury (405, 406). Several previous studies investigating the effects of mercury exposure on the metabolome have also identified disruptions in the TCA cycle (242, 243). Succinate is also important regulator in epigenetics and signal transduction, which may lend insight to the epigenetic results in Chapter 3 (406). The relationship between the changed dietary molecule and the behavioral changes observed in the OHD terrapins is discussed in greater detail below.

Putrescine and hypoxanthine are both indicators of oxidative stress, which is a known effect of mercury exposure (199, 244). Decreased putrescine is indicative of oxidative stress response, as putrescine is a precursor to other polyamines that aid in stress resistance (407). The increased oxidative stress the OHD terrapins experienced

would have caused putrescine to be synthesized into other polyamines to manage increased oxidative stress. Hypoxanthine is synthesized in the liver for purine degradation, and induces increased oxidative stress as a result of those reactions (408, 409). When purine metabolism is altered, like it would have been due to the changes in the TCA cycle from decreased succinate, hypoxanthine can be erroneously incorporated into DNA (410).

Many of the differences in the OHD terrapin metabolome was due to their reduced, or non-existent food consumption, but succinate, putrescine and hypoxanthine may be indicative of mercury exposure. Mercury induces oxidative stress, and alterations in putrescine and hypoxanthine indicate that oxidative stress was increased in the liver of the OHD terrapins. The mitochondrial dysfunction, implied by the reduction in succinate, has also been shown to occur under oxidative stress (411). Increased oxidative stress can cause alterations in many different biochemical processes that are discussed in greater detail below.

Metabolic changes related to mercury-induced behavioral changes

Throughout the dosing study, the most notable behavioral change was the decrease in food consumption in the high dose terrapins, and cessation of food consumption in the OHD terrapins. Many of the affected metabolites are directly related to the ingredients of the turtle gelatin the terrapins were fed during the dosing experiment.

In the high dose plasma samples, methyl malonate, acetate, myo-inositol, leucine, glycerate and glucose were significantly decreased, all of which are listed in the

ingredients list of the Mazrui turtle gelatin fed to the terrapins. As the high dose terrapins slowed their eating habits, the decrease in circulating glucose in the blood would have had an immediate effect on glucose homeostasis and metabolism, stimulating both gluconeogenesis, and glycogen degradation. The decrease in lactate in the high dose terrapins is also indicative of gluconeogenesis occurring, since it is converted to pyruvate for use in gluconeogenesis. Gluconeogenesis is only one alternative energy source, the increased ketone, 3-hydroxybutyrate in the high dose samples, indicates that stored fat is being burned for energy. The increase of n-methylhydantoin (deoxy-creatinine) suggests that creatine and muscle tissue are being degraded, which is an additional site of glycogen storage. The decreased amount of glycerol also suggests that it has been metabolized into glucose for energy. All of these molecules point to a changing biochemical energy source in the high dose terrapins, which is exacerbated in the OHD terrapins.

The OHD terrapins experienced a decrease in all molecules found in the Mazrui turtle gelatin; alanine, isoleucine, leucine, valine, methionine, phenylalanine, taurine, and choline. While the decreases in these molecules are related to their lack of food consumption, these declines could have resulted in the behavioral changes in the OHD terrapins being unable to swim or “right” themselves, which could be indicative of neurological and muscular denegation

Many of the decreased dietary molecules are related neurological function. The decrease in acetate and choline would result in less acetylcholine and acetyl-coenzyme-A forming, which are important neurotransmitters that are required for protein, carbohydrate, and lipid metabolism. Glycine and myo-inositol are derived from glucose,

and important inhibitory and secondary messengers in the body. The decrease in all of these neurotransmitters could lead to the lack of responsiveness of the OHD terrapins. Both leucine, and valine are branched chain amino acids (BCAA) that are involved in stress, energy regulation, protein synthesis, glucose metabolism, brain function and muscle metabolism (412). Taurine and phenylalanine are both dietary molecules, but are also essential to neurotransmitter synthesis and proper nervous system function (413, 414). The change in these amino acids would have played a large role in the behavioral changes observed in the OHD terrapins, as they are involved in many of the biochemical pathways that are associated with the effects of mercury poisoning (353). These effects stem from a dietary change, and deprive important biochemical pathways of the components necessary for function (Table 4.16).

Several metabolites are related to muscular function. The decrease in alanine, and glutamate in the OHD terrapins also could have had a significant impact on motor ability and altered glucose metabolism, since alanine is a precursor to glutamate in the degradation of amino acids for energy (415). Lactate is commonly observed to change in response to mercury exposure, and could be related to the lack of movement of the OHD terrapins. Without fast movement or strenuous exercise, the body can continually process lactate, and it does not build up in cells. The normal swimming, walking, and foraging behaviors of terrapins would likely cause more lactate to build up than when they are motionless for extended periods of time (353, 415). In the case of the OHD terrapins, lactate is quickly processed as a result of sedentary behavior, as well as being utilized by gluconeogenesis.

The dietary metabolites that decreased in the OHD terrapins are likely related to health declines observed by Schwenter (2007), in the following manner. When the terrapins stopped eating, taurine and phenylalanine, concentrations dropped and the onset of neurological symptoms began. The lack of food influenced the metabolism of stored energy, evident by the decrease in glycerol and lactate. The continued behavioral changes in the OHD terrapins can be attributed to the decrease in leucine, valine, alanine, and glutamate, which are all involved in brain and motor function.

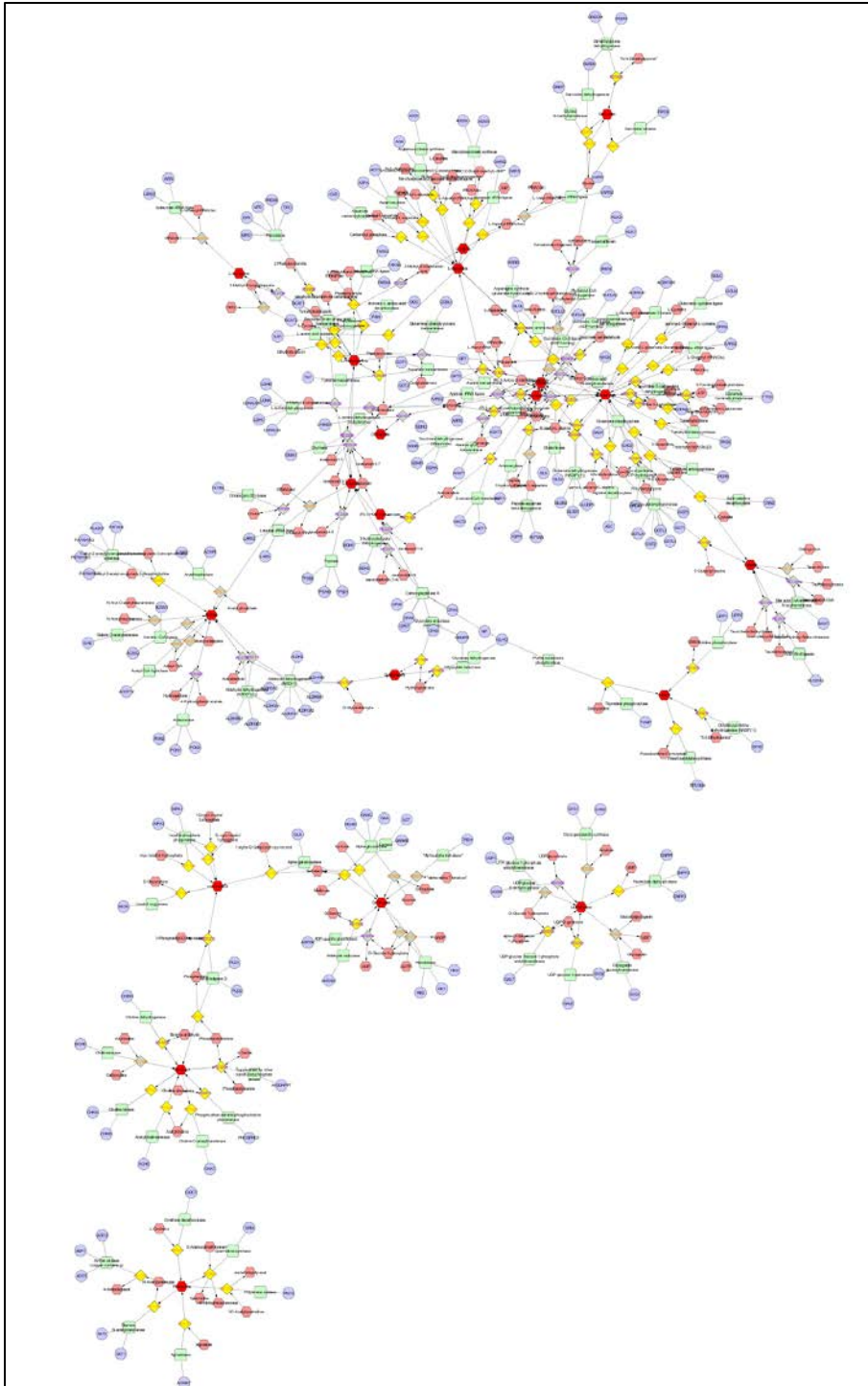


Figure 4.20. The biochemical relationships between the altered metabolites and energy metabolism. The altered metabolites are represented by dark red octagons, the additional effected compounds are represented by pale red octagons, effected reactions, enzymes and genes are represented by grey diamonds, green squares and purple circles, respectively. Biochemical constituents related to energy metabolism are highlighted in yellow.

Metabolites involved in oxidative stress management

A primary effect of mercury exposure is oxidative stress (199, 200, 244). The OHD terrapin liver samples had two significant metabolites that are indicators of oxidative stress; decreased putrescine and increased hypoxanthine (407, 408). Changes in the TCA cycle have also been shown to be the result of mercury exposure, which was observed in the OHD terrapins by decreased succinate (406). The onset of mercury induced oxidative stress is likely marked by subtle changes in oxidative stress management, which could be observed in the plasma samples.

The decrease in the dietary molecules observed would exacerbate oxidative stress by limiting the production of antioxidant response molecules, as many are components of GSH synthesis (208). Without GSH the antioxidant response to the mercury induced oxidative stress is greatly diminished, and ROS will accumulate in the cells (321, 350). GSH is also required to synthesize the glutathione peroxidases (GPX) that are responsible for the removal of the hydroxyl ions, resulting from the increased ROS. Without GPX managing the hydroxyl ions in the liver, the ions are free to cause lipid membrane damage, causing instability in the lipid membrane, and resulting in cellular damage. The drop in succinate and uracil, and increase in hypoxanthine in the OHD terrapins indicate that the increased effects oxidative stress have led to changes in DNA replication, and epigenetic modifications, as the maintenance of both processes is altered by changes in these three metabolites (405, 406).

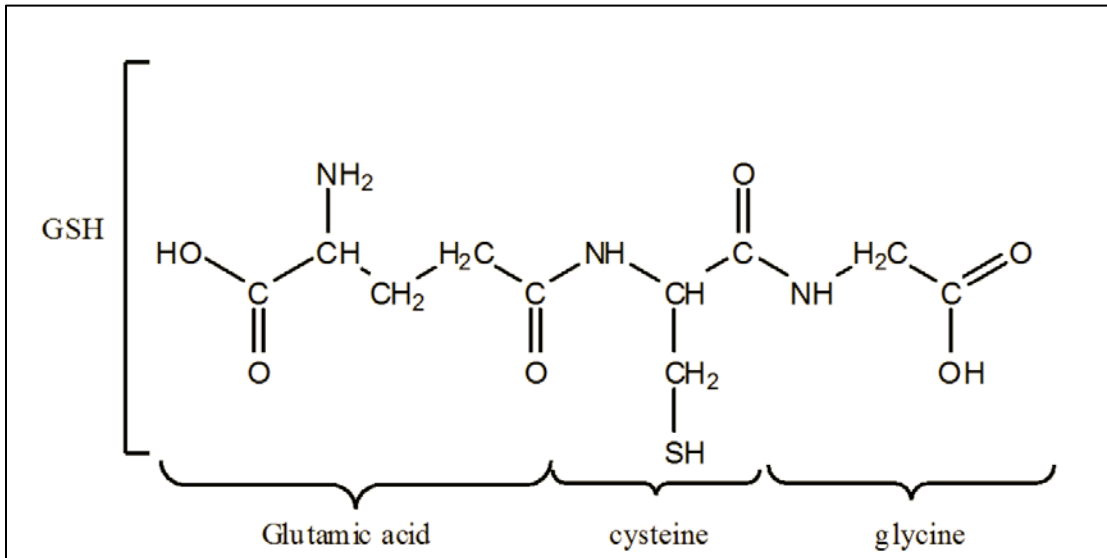


Figure 4.21. A diagram of the three components of the tripeptide glutathione (GSH), taken from Eteshola (321).

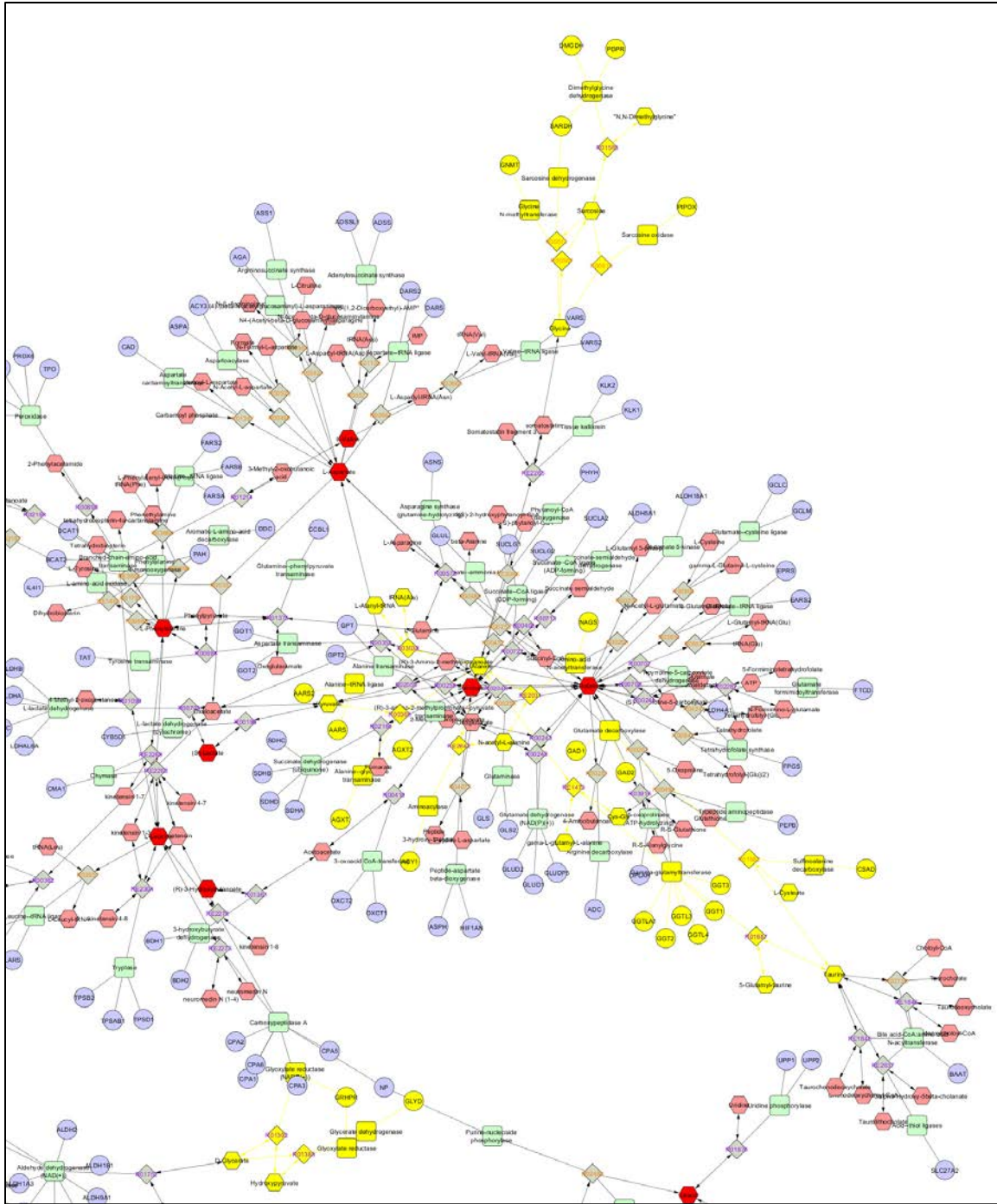


Figure 4.22. The biochemical relationships between the altered metabolites and GSH production. The altered metabolites are represented by dark red octagons, the additional effected compounds are represented by pale red octagons, effected reactions, enzymes and genes are represented by grey diamonds, green squares and purple circles, respectively. GSH and the immediately related compounds and reactions are highlighted in yellow.

Potential biochemical model for mercury exposure

A candidate pathway for monitoring the onset of mercury induced oxidative stress is the glutathione (GSH) biochemical pathway, as this pathway manages ROS and is disturbed by mercury exposure (208, 321, 322, 350). The high dose terrapin plasma samples had elevated concentrations of sarcosine compared to the other dose groups, which is an intermediate in the conversion of choline to glycine, for the synthesis of GSH. The high dose terrapins were likely experiencing oxidative stress as a result of the exposure, but since they were still consuming the turtle gelatin, they had an ample supply of choline for conversion to sarcosine, and drive the subsequent reactions of GSH synthesis, since GSH was continually being depleted by mercury. However, the OHD terrapins no longer had the necessary dietary components of GSH synthesis, and experienced increased oxidative stress, that may have led to epigenetic changes, as a result.

Since GSH synthesis is subject to dietary differences, and can aid in the detoxification of mercury, it does not make a reliable biomarker of a detrimental exposure. However, due to the increased oxidative stress caused by mercury exposure as well as mercury's utilization of GSH, the GPXs are an attractive option for a biomarker. The GPX molecules require GSH for synthesis, so when mercury is in excess GSH will be depleted, resulting in depletion of the GPXs. The GPXs are responsible for the removal of hydroxyl ions that results from increased oxidative stress. This would further deplete the available GPXs. Monitoring the concentration and activity of GPX in blood samples would be a reliable way to assess for deleterious mercury exposures, since that circumstance would deplete the GPX concentration, as it is not being synthesized from

lack of GSH, as well as the activity of GPX should be comparable to the concentration, as all available GPX would be utilized to reduce the buildup of hydroxyl ions. In situations of normal oxidative stress, GPX would be in greater concentration, and its activity should be lower than the concentration as the normal buildup of ROS can be managed by the GSH pathway.

Adverse outcome pathways

While the toxic effects of mercury exposure are well known, the biochemical underpinning of those outcomes are not. Biochemical data, like those generated here using ^1H NMR based metabolomics, can provide valuable information regarding how toxic effects begin (373). Using the data from this experiment several links can be made between the initial effect of exposure, oxidative stress, and some of the known adverse outcomes of mercury exposure.

Within the AOP paradigm, many AOs can occur based on a single CIE, which in this case is mercury binding to GSH, and causing increased oxidative stress. The KEs that link the CIE to the various AOs can also stimulate a variety of other KEs and AOs enabling a single CIE to cast a wide net of effects in the body. Here, based on the behavior changes observed in the high dose terrapins, the KE would be the decrease in food consumption, which sets off a cascade of effects in many different biochemical pathways (Figure 4.20). One of the goals of using the AOP framework is to link the known effects of a CIE, so that the missing links can be investigated by the research community (Figure 4.23) (195). Here, we identify several AOPs that are potentially related to mercury exposure, and the subsequent changed behavior of the terrapins, as altered behavior is commonly associated with high mercury exposures (113, 114). The

information gained from the metabolomics analysis in this chapter, put into the context of the AOP framework could advance the understanding of mercury exposure by detailing the missing pieces that need to be investigated further.

In this experiment, we observed that the effects of mercury exposure can be observed in a non-model organism (Figure 4.24). Several metabolites that change with the mercury induced health declines were elucidated. While related to diet, the metabolites identified in the liver samples can affect brain function, metabolization of stored energy, and muscle function. Linking these changes to the molecule altered in the plasma samples provided the ability to identify a potential biomarker of deleterious mercury exposure.

The data from this experiment has been confirmed through four combinations of scaling and bucketing techniques, and analyzed by both multivariate and univariate statistics. The persistence of the results through different analyses provides support for the proposed biomarker. However, the proposed biomarker, GPX, requires validation before it can confidently be used across species to identify problematic mercury exposures. The changes in GPX concentration and activity could be tested using a high through-put screening over a range of mercury concentrations using zebrafish. Zebrafish provide the opportunity to dose a large number of animals consistently in a small space. The small size of the zebrafish would prohibit multiple analyses being conducted on each tissue, but using different animals from the same treatment tank should circumvent this issues. Also using color-metric GPX activity kit, and an ELISA based assay to measure GPX concentration the small size of the tissues should not be a problem.

If this experiment were conducted again, circumventing the unexpected variable

that Schwenter (353) encountered; the shrimp used to feed/dose the terrapins hyper-accumulating the CH₃Hg out of solution, resulting in a higher dose than expected would be necessary (353). This could be accomplished by adding the dosing compound to the gelatin powder before mixing it with water to turn it into a gelatin. However, the high mercury concentrations that Schwenter (353) reported for the erythrocytes of the high dose terrapins are still environmentally relevant, but not for diamondback terrapins. These high concentrations would be found in an upper trophic level predator in a highly contaminated ecosystem, such as the Florida Everglades (43, 416).

Dietary differences play a large role in the ability to observe changes in the small molecule profile of organisms, and appear to mask the initial effects of mercury exposure in the terrapins. A follow up analysis could be done on more of the plasma samples taken by Schwenter (2007) to attempt to observe any metabolomic changes that took place before the health of the high dose terrapins started to decline.

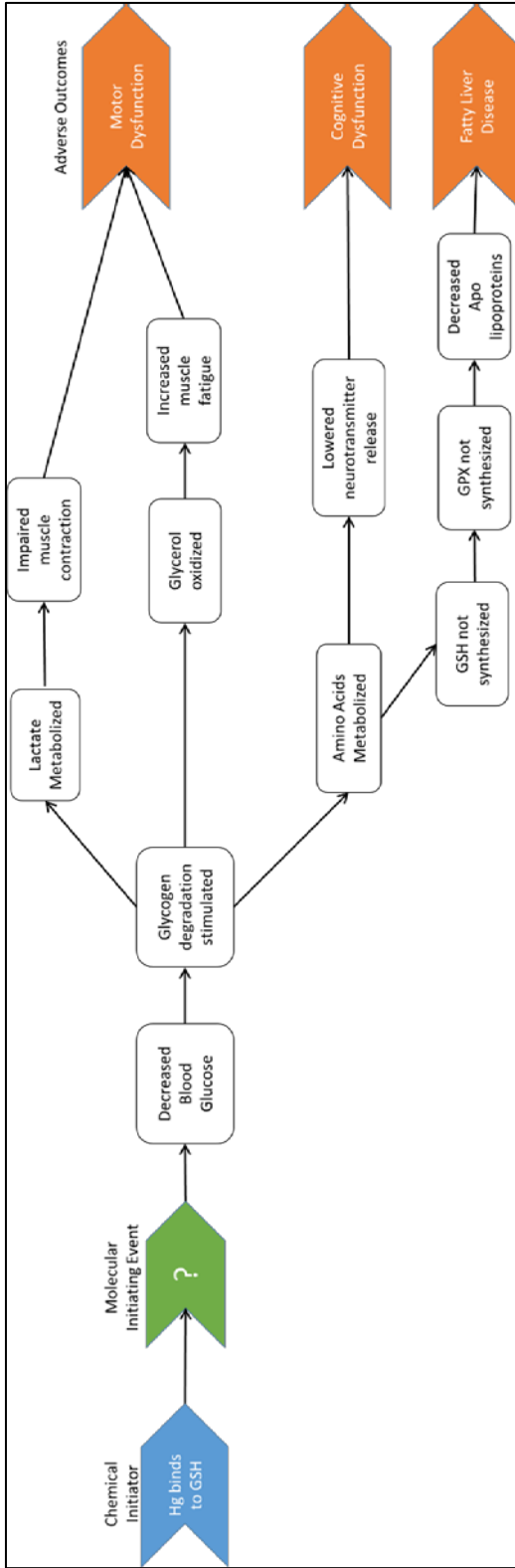


Figure 4.23. The effects of reduced blood glucose levels as a result of decreased feeding observed in the high dose and OHD terrapins within the AOP framework.



Figure 4.24. The graphical abstract of all experiments conducted relating to increased Hg exposure.

Chapter Five: Synopsis, synthesis & final comments

5.1. Major findings of specific aims & experiments

This body of work utilized important ecological species as environmental sentinels to explore the hypothesis that increased **dietary mercury exposure alters DNA methylation and small molecule profiles in American alligators and diamondback terrapins**. This work used the natural dietary mercury exposure of sentinel species, which coastal human populations are subject to, in the Southeastern United States to examine health effects of mercury exposure that can be translated to human populations. The major findings of each Specific Aims used to achieve that understanding are detailed below.

Specific Aim 1: *Evaluate American alligators as sentinels for mercury exposure.*

The six experiments used for evaluation of the alligator as a sentinel species illustrated that mercury is a contaminant of concern along the SE Atlantic Coast of the US, particularly in the Florida Everglades, despite bioremediation efforts. The body distribution of mercury in alligators is to humans, making tissue specific analyses relevant to the health of normal and subsistence diet populations. Mercury concentration in alligators was observed to change with body condition, and not seasonal behaviors. This finding elucidates the complications that arise during disease progression, as environmental contaminants could have an increasing effect as health and body condition decline. Human body condition changes drastically with pregnancy, making changing mercury concentrations problematic for embryonic development. Mercury was observed to be incorporated to alligator eggs, but the difficulty encountered while attempting to increase egg mercury concentrations in the laboratory lead to the conclusion that that

alligator is a worthy sentinel for human health issues of lifetime mercury exposure, not embryonic development.

Use of the alligator also provides the opportunity to examine the effects mercury of exposure that are difficult to observe in mammals, as reptiles are more susceptible to environmental contaminant exposures, based on their life history traits (417). The greater susceptibility of reptiles is advantageous to environmental risk assessment efforts, as some ‘missing links’ between exposure and adverse effects may be elucidated with this species.

Specific Aim 2: *Determine if mercury exposure affects DNA methylation.*

Six sites of varying mercury concentrations demonstrated that hypomethylation is associated with high mercury concentrations. The confounding factor of potentially different diets was investigated using captive juvenile alligators, and lead to the conclusion that erythrocytes have a greater methylation plasticity than internal organs, when diet is standardized. Combining varied mercury exposure and standardized diet will lead to further clarification of the observed relationship.

This experiment detailed different epigenetic responses to exposure at different locations, which could complicate risk assessment for this species using this metric, as it indicates that this effect of exposure is contingent on many variables.

Specific Aim 3: *Investigate biochemical pathways affected by mercury exposure.*

Using an NMR-based metabolomics approach, molecules involved in oxidative stress altered by mercury exposure were identified in captive diamondback terrapins. The

biochemical pathways related to the identified molecules were used to identify a potential biomarker of mercury induced oxidative stress, can be used across species.

These Specific Aims sought to contribute to the field of environmental toxicology by elucidating the effects of mercury exposure on sentinel species. Singularly, the results provide a new sentinel species for mercury exposure, demonstrate a statistically significant relationship between mercury exposure and a well-studied epigenetic modification, and identify metabolites altered in response to mercury exposure as well as a potential biomarker of exposure. Each of these results adds to the body of work investigating mercury exposure, however a significantly larger impact is made when the results are considered together.

We propose that DNA methylation changed with mercury exposure, because it is affected by the oxidative stress mercury causes. While the relationship between oxidative stress and DNA methylation was not directly tested here, it is comprehensively described in the literature, so often that wildlife studies comparing mercury and DNA methylation seldom describe details of the biochemical link. Based on these data from Chapter 3, the inverse relationship between mercury and DNA methylation is strictly correlative. However, when the results of the metabolomics investigation are also considered, a biochemical link connecting DNA methylation and mercury in the data becomes clear.

The few molecules that changed solely in response to mercury exposure are involved in oxidative stress management, further supporting the link found in the literature. Two of the molecules that changed in the high dose, and OHD terrapins were uracil and hypoxanthine, which are both tangentially related to energy metabolism.

However both of these molecules are known to be erroneously incorporated into nascent DNA when there are deficiencies in cellular metabolism (404, 410). The incorporation into nascent DNA strands, could lead to chromosome breakages, altered gene regulation, and exacerbate the inability of the DNMTs to bind to and methylate the DNA strand, initially caused only by the hydroxyl adducts as a result of oxidative stress (218, 404). Since it appears that mercury is causing errors in DNA, it may be classified as a genomic mutagen in wildlife, which has only been observed with certain genes in laboratory models, including glutamic--pyruvic transaminase, LacZ and, GPX (106, 364, 365).

The potential for mercury to be classified as a genomic mutagen, paired with the potential biomarker of exposure, provides the opportunity to examine the effects of exposure at a deeper level. Using the concentration and activity of GPX to determine if mercury exposure is detrimental, follow up studies can be done to determine DNA methylation. If the amount of DNA methylation is what is expected for the specific species, biological time point, and mercury concentration in question, then the methylation is likely the result of hydroxyl lesions, and oxidative stress. If the DNA methylation is not what is expected, the methylation changes may be occurring as a result of erroneously incorporated purines and pyrimidines into the DNA strand.

The idea that mercury causes genetic mutations, which are normally considered random, and the drivers of evolutionary adaptation, suggests that mercury causes a major change in the organisms that are exposed to it. Determination of the specific mutations caused by mercury would have to be elucidated, but if they are related to improved management of exposure, mercury could be a driving force of natural selection that influences evolutionary adaptation.

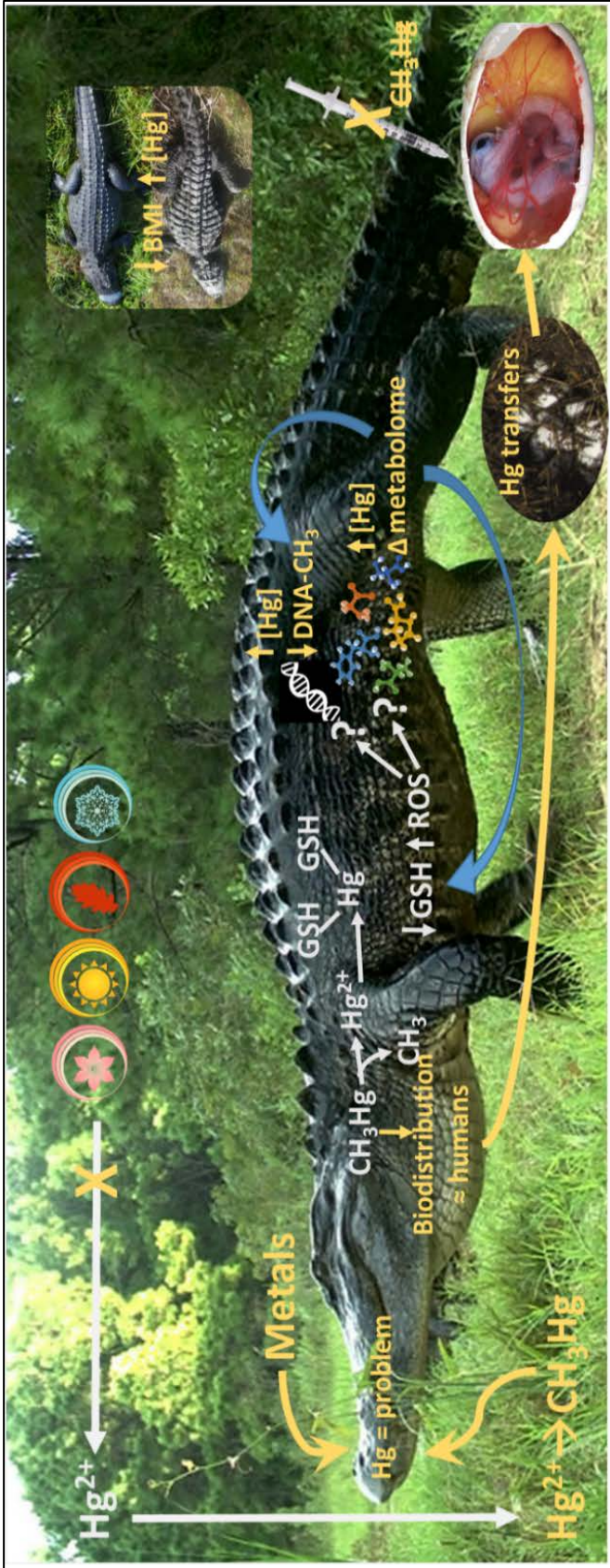


Figure 5.25. The graphical abstract depicting the results from this dissertation and how the results relate back to each other.

5.2. *Ecotoxicology risk assessment*

Much of these data discussed herein add to the greater body of work describing the effects of mercury exposure on wildlife, at both the individual, and population level. Using large sample sizes and robust statistical analyses, models were developed to aid in the identification of populations “at risk” of the deleterious effects associated with mercury exposure. However, numerous studies have been conducted demonstrating the negative impacts mercury exposure has on wildlife populations, and while the models presented here can extend previous studies measurements, and outcomes to uncharacterized populations, they can be added to more elegant methods of risk assessment that have recently been developed.

The adverse outcome pathway (AOP) framework has begun gaining ground as the most salient method of combining environmental contaminant exposures with established adverse outcomes, and emerging cellular mechanisms linking both the exposure and outcome. This framework enables the existing data to serve as a predictive tool for risk assessment (195, 196). The data presented here in can be applied to the AOP design in a bottom-up fashion, in that we began with a well-defined chemical initiating event (CIE), mercury reducing intracellular GSH, and used the information in the literature to create a putative AOP (Figure 1.4). Through the analysis presented herein, additional connections can be made within the framework and a qualitative AOP network can be developed (195).

Toxic metal exposure triggers a known Chemical Initiating Event

Mercury belongs to the group of toxic metals that elicit increased oxidative stress through GSH utilization (199). The depletion of the thiol pool of GSH within the cell and subsequent damage to the antioxidant system results in increased ROS that cause hydroxyl adducts to attach to the DNA, and lead to DNA damage, which is a molecular initiating event (MIE) (195, 199). The damage that occurs to the DNA strands limits the ability of the DNMTs to bind to the DNA strand and methylate it, which regulate gene expression (217, 218). This relationship between mercury exposures, increased oxidative stress, DNA damage, and altered DNA methylation can be found in the literature and represents a putative AOP, until specific measurements are made. These data presented herein provide both the chemical exposure and DNA methylation information.

DNA methylation as a Key Event

The damage to the DNA could be observed in a few ways: by measuring the amount of hydroxyl adducts on the DNA, the amount of DNMT activity, or the methylation on DNA, which is altered following the previous two changes. Key events (KE) are defined as measureable effects at various levels of biological organization (195). All three of these measurements represent post-translational changes to the DNA strand. Since the DNA methylation measurement represents the effects of the two other measurements, hydroxyl adducts and decreased methylation by the DNMTs, it provides the most effective KE for this AOP, whereas the other measurements could represent a key event relationship (KER).

The DNA hypomethylation observed in Chapter 3 provides support that the

exposure to mercury is causing measurable changes. However, the link between these two measurements is tenuous without specific measurement of the hydroxyl adducts or DNMT activity. Rather than explore each step of the putative AOP related to mercury exposure that is extensively described in the literature, additional relationships were explored (Figure 5.2). In the literature, measurable parameters are correlated to adverse outcomes, with the biochemical pathway linking the two never being identified. The metabolomic data described herein that describes the changes in small molecules between various treatments can potentially guide the framework through the biochemical pathways affected by mercury exposure.

Using NMR based metabolomics to aid in AOP development related to mercury exposure

These metabolomics data herein identify oxidative stress molecules affected by mercury exposure. As well as the changes in energy and lipid metabolism that result from decreased foraging, as a secondary effect of exposure (Figure 4.19, 4.20). These pathways are also related to the same chemical initiator (CIE) and key event (KE), GSH depletion, and increased ROS, but stem from a different MIE, lipid peroxidation. This data allows the identification of a second AOP, which was not originally predicted (Figure 5.2).

During lipid peroxidation, ROS damage the lipid membranes of cells, causing irreversible damage (418, 419). Most membrane lipids are glycerophospholipids, which makes the network of affected biochemical pathways from Chapter 4 relevant to this MIE (Figure 4.19) (419). As lipid peroxidation would consume the glycerophospholipids, the stored glucose and glycerol needed to produce new glycerophospholipids would become

depleted, especially if the organism was not eating. Glycerophospholipid metabolism directly affects valine, leucine and isoleucine biosynthesis and degradation, as well as serine, glycine and threonine metabolism. The altered amino acid interconversion pathway also affects acetylcholine synthesis and the citric acid cycle. Altered acetylcholine affects neurotransmitter release and cycling, which effects could be exacerbated by the changes in the citric acid cycle intermediates, which are also important for neurotransmission (420). These alterations could result in enough change in neurotransmitter maintenance to interfere with cognition and behavior (Figure 5.2)

Generally, the AOP framework suggests that a singular effect should be investigated with specific but flexible details elucidated (196). The more branched an AOP is, the more specific it becomes and the less it can be used as a guide for risk assessment of a specific class of chemical exposures, (196). However, AOPs describe complex biological processes and can become large networks that converge on a few AOs with enough information (196).

Upon constructing the second AOP that was elucidated by the data presented herein, links between the two AOPs became apparent. Many of the biochemical pathways and intermediate molecules that are altered during lipid peroxidation are involved in the precursor steps of DNA methylation (421, 422). There are also negative feedback loops that continue to cause increased ROS, since GSH and glutathione peroxidase (GPX), a molecule involved in regulating oxidized lipids within cells, are both depleted by the ROS, and their continued synthesis is impacted by the loss of other necessary metabolites (419).

The AOP network created based on the results of Specific Aims 2 and 3 illustrate

that there may not be singular mode of action for mercury exposure (Figure 5.2). Despite both MIEs initiating from increased oxidative stress, the following cascade of effects is complex, and involved in numerous biochemical pathways. Based on these data, there does not appear to be a clear solution that would remediate the effects of mercury exposure. The intertwined effects illustrated by the AOP network lend insight as to why no single effect of mercury exposure has been identified (Figure 5.2). Despite the variety of pathways affected, DNA methylation appears to be an effective measure of exposure, as it is modified by both AOPs.

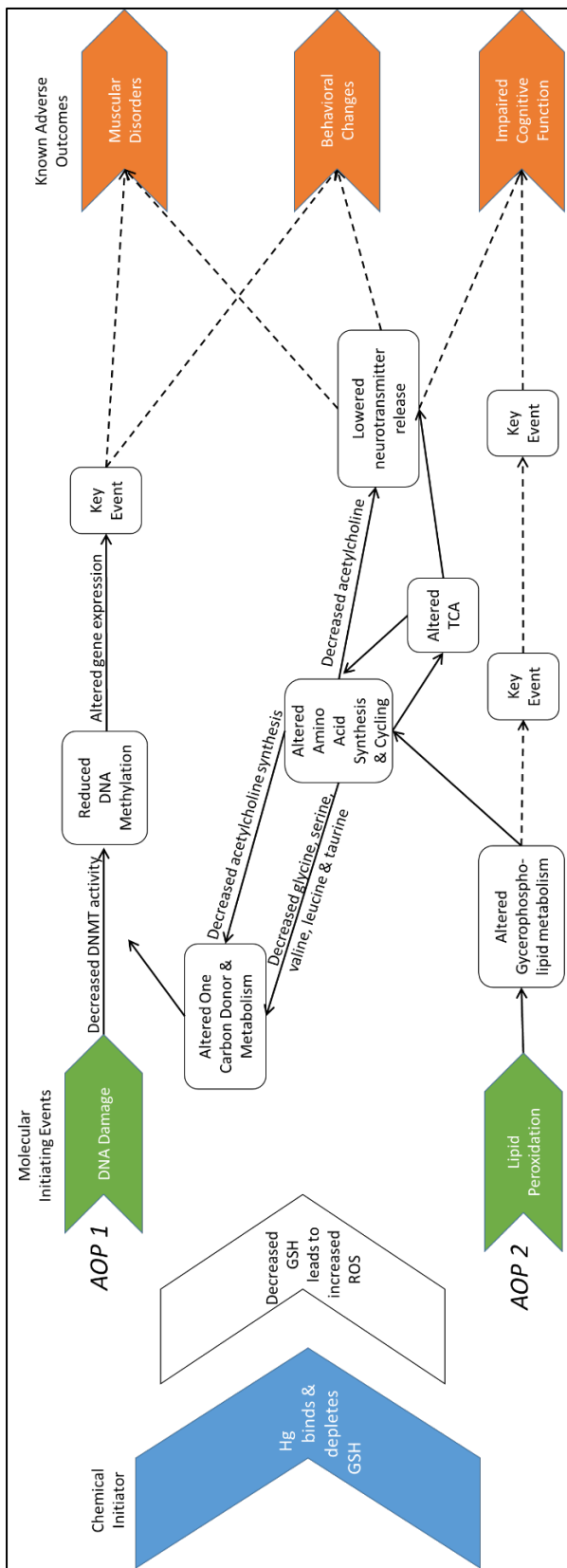


Figure 5.26. The AOP network devised using the data generated from the Specific Aims of this work. The key events are denoted by white boxes, with the key event relationships written along the solid arrows. The dotted arrows indicate relationship that these data do not provide.

5.3. *Human health implications*

The DNA methylation, and metabolomics results presented in this dissertation have several implications for human health. The fact that DNA methylation appeared to be reversed based on the high quality diet the juvenile alligators in Chapter 3 were fed, suggests that mercury induced hypomethylation could be reversed prior to the onset of toxic effects. If DNA methylation were used in tandem with the GPX measurements to assess mercury exposure, when hypomethylation is identified in a patient, their diet can be supplemented with the small molecules that aid in the reduction of oxidative stress and fuel proper cellular metabolism. While these data in Chapter 3 suggests that erythrocytes have a greater plasticity in methylation than internal organs, problematic methylation changes could potentially be reversed in organs over time as the cells regenerate.

The mercury induced oxidative stress observed in Chapter 4, indicated that lipid peroxidation was also taking place. This was likely the combined result of depleted energy stores, and increased oxidative stress in the OHD terrapin livers, but could lead to a variety of liver problems. The increased lipid peroxidation in the OHD livers could also cause swelling in the membrane and endoplasmic reticulum, which would result in the loss of ribosomes, and the unfolded protein response (UPR) signaling network (418, 423, 424). If the UPR cannot manage the oxidative stress, and restore homeostasis, it promotes apoptosis (424). The unresolved oxidative stress can lead to the dysregulation of protein synthesis in the liver, particularly synthesis of the Apo-lipoproteins (425). A major function of the Apo-lipoproteins is to transport lipids throughout the body, and without them lipids would accumulate in the liver. This has become known as non-alcoholic fatty liver disease (NAFLD), or steatosis (426-428). While this disease is generally associated

with obesity and diabetes, oxidative stress is a common trait in all symptoms associated with NAFLD, and leads to the development of nonalcoholic steatohepatitis (NASH) in the liver as well (429-431). If left untreated, NAFLD and NASH will progress to cirrhosis, and eventually liver cancer (432). Interestingly, one of the treatments for NAFLD and NASH is an improved diet including many antioxidants, to reduce the amount of oxidative stress that the liver experiences (433, 434).

The idea that liver diseases as detrimental as cirrhosis and cancer can be ameliorated by simple dietary improvements is encouraging, and supports the idea that dietary changes can offset the toxic effects of mercury exposure. While NAFLD seems to be an extreme effect of mercury exposure, sub-clinical alterations in the liver are associated with increasing mercury concentrations, and men in Japan that are exposed to high mercury concentrations through their diet, are increasingly being diagnosed with NAFLD, even when the common precursors of the disease (obesity, diabetes) are not present (435-437).

5.4. *Future directions*

To better understand the effects of mercury induced oxidative stress, high throughput laboratory models are an attractive option for determination of dose-response effects, and determining at which point the effects become irreversible. Using the zebrafish as a model many doses can be tested simultaneously to examine several different measures of effect on a single animal from a large does group. Analyzing blood GPX and DNA methylation would aid in the validation of the model suggested in Chapter 4, and using the liver to determine when oxidative stress becomes problematic

would aid in the understanding of NAFLD in humans. Liver samples could be split for histology and metabolomic analysis to provide morphological and biochemical information regarding the onset of NAFLD, which is only done by liver biopsy after NAFLD has been detected in humans. The dosing time can be extended to determine how NASH, cirrhosis and liver cancer may be related to extended mercury induced oxidative stress. Examining prevention and therapeutic options related to dietary changes could also be tested using the zebrafish. Conducting similar analyses as the treatment options are tested would enable comparison between pre- and post- treatment to determine how effective the treatment is at remediating or reversing the liver diseases.

The dosed zebrafish could also be used to investigate the relationship between oxidative stress and neurodegenerative disorders, such as Parkinson's disease (146, 322, 438). The brain tissue can be analyzed similarly to the liver tissue, determining any morphological and metabolomic changes with increasing dosage, including lipidomic analyses to investigate lipid peroxidation further. Cognitive tests could be conducted on the zebrafish prior to necropsy to determine if there is an observable behavior associated with any changes observed in the tissues (439).

In addition to the global methylation analysis on the zebrafish, specific regions of DNA that are related to the adverse outcomes being investigated, could be analyzed to determine if the methylation pattern has changed in concert with dosage and any affects observed. Several genetic variants in humans have been shown to affect susceptibility to NAFLD and Parkinson's disease (440-442). Using DNA methylation to determine the effect of mercury exposure on these variants will enable determination of populations that could be increasingly susceptible, or resistant, to these diseases as they are exposed to

mercury through their normal diet.

These zebrafish experiments would be able to connect the MIE lipid peroxidation to an additional AO, liver disease. Using histology of the tissues would provide KE leading to that AO, and the metabolomics data can provide the KERs, as well as information regarding biochemical pathways that may be affected during each stage of dosing and treatment. A large dosing experiment, such as the one proposed here, would likely elucidate many other relationships between GSH depletion leading to increased oxidative stress, and the known AOs of mercury exposure.

5.5. *Conclusions*

This body of work contributes to the larger body of knowledge elucidating the effects of environmental contaminants on wildlife, by advancing the current knowledge regarding the effect of mercury exposure and providing an additional dimension to mercury exposure studies by linking a suspected cause with a measureable effect through metabolomic data. Using the vast amount of technology that is available today, the biochemical pathways that are affected by mercury exposure can be elucidated. To the best of our knowledge, this is the first study that has linked mercury exposure with a sub-lethal effect by identifying the cellular pathways altered in a non-model reptilian species.

The use of a non-model species provides information that is directly related to the organisms in the environment that are experiencing the exposure that cannot be gained from using traditional model species. Non-model species also widen the scope of exposure research to not only provide detailed information regarding the effects of the

exposure, but could also allow faster intervention and remediation of contamination prior to the onset of lethality.

These metabolomics data presented here show that there is increased oxidative stress occurring from mercury exposure, prior to the display of the classical signs of mercury poisoning, and highlights the importance of diet in the body's ability to manage oxidative stress, and prevent the onset of deleterious symptoms. Using the proposed oxidative stress biomarker, GPX, better assessment the effects in highly exposed populations can begin, and using the information from the proposed zebrafish experiment, could potentially be treated, Since most of the human population experiences mercury exposure, this information could lend insight into the latent affects that humans experience, and should be used as cautionary information when future mercury emissions decisions are made.

5.6. Final thoughts

The data presented herein describe the effects of exposure to a toxic pollutant increasingly emitted by human activity, and highlight the biochemical effects of exposure, which can be used to better understand human health and disease. This information is particularly relevant as the current administration promises a resurgence in coal mining and coal fired power plants, which are one of the largest emission sources of mercury.

Only recently has the One Health paradigm become pervasive in environmental health literature, with any scientific disciplines agreeing that environmental and human health effects are the same issue. However, native populations have long understood that

our actions have a profound effect on the environment, and everything within it. Today, this cumulative body of knowledge that includes the beliefs handed down through generations by cultural transmission regarding the relationship of living beings, with one another and with their environment, is referred to as Traditional Ecological Knowledge (TEK) (443, 444).

For decades, scientists were resistant to utilize the cultural knowledge of indigenous people, because their interactions with their environment are closely linked to their spirituality (445). However, through the integration of native populations in ecological research, TEK has become an important tool in maintaining biodiversity and establishing conservation guidelines through location specific knowledge and increased knowledge of environmental linkages (443, 446, 447).

Only recently has modern science caught up with these ideals and come to accept the One Health paradigm, that all aspects of the ecosystem are related. Modern society would benefit from the ideals held by indigenous populations that not only integrated environmental management with their everyday life, but considered the impact of their actions on future generations.

*In our every deliberation, we must consider the impact
of our decisions on the next seven generations.*

—Iroquois maxim

Modern society could benefit greatly from the implementation of this tenant across many disciplines. Mercury emissions and exposure is no exception, as the toxic

effects are well documented, and may even be affecting how organisms adapt to their environment. The mercury released today will persist in the environment, and travel through the food web causing a wide range of toxic effects. As the climate changes, the optimal conditions for methylation in the Everglades would spread to northern wetlands, and potentially more mercury would enter the food web. Actions taken now, facing a drastically changing planet, perhaps more than ever, need to consider the Iroquois maxim and future generations.

References

1. Erickson, P. R.; Lin, V. S., Research highlights: elucidation of biogeochemical factors influencing methylmercury production. *Environmental Science: Processes & Impacts* **2015**, *17*, (10), 1708-1711.
2. Lange, T. R. R., D.A. And Royals, H.E., Long-Term Trends of Mercury Bioaccumulation in Florida's Largemouth Bass. *Abstracts of the Annual Meeting of the South Florida Mercury Science Program, Tarpon Springs, FL*. **2000**.
3. Parrott, B. B.; Bowden, J. A.; Kohno, S.; Cloy-McCoy, J. A.; Hale, M. D.; Bangma, J. T.; Rainwater, T. R.; Wilkinson, P. M.; Kucklick, J. R.; Guillette, L. J., Influence of tissue, age, and environmental quality on DNA methylation in Alligator mississippiensis. *Reproduction* **2014**, REP-13-0498.
4. Julian, P., Mercury hotspot identification in Water Conservation Area 3, Florida, USA. *Ann. GIS* **2013**, *19*, (2), 79-88.
5. King, W. D.; Ho, V.; Dodds, L.; Perkins, S. L.; Casson, R. I.; Massey, T. E., Relationships among biomarkers of one-carbon metabolism. *Molecular biology reports* **2012**, *39*, (7), 7805-7812.
6. Liu, X.; Zhang, L.; You, L.; Yu, J.; Zhao, J.; Li, L.; Wang, Q.; Li, F.; Li, C.; Liu, D., Differential toxicological effects induced by mercury in gills from three pedigrees of Manila clam *Ruditapes philippinarum* by NMR-based metabolomics. *Ecotoxicology* **2011**, *20*, (1), 177-186.
7. Harada, M., Minamata disease: methylmercury poisoning in Japan caused by environmental pollution. *CRC Critical Reviews in Toxicology* **1995**, *25*, (1), 1-24.
8. Bank, M. S.; Vignati, D. a. L.; Vigon, B., United Nations Environment Programme's Global Mercury Partnership: Science for successful implementation of the Minamata Convention. *Environmental toxicology and chemistry* **2014**, *33*, (6), 1199-1201.
9. Mason, R. P., Mercury emissions from natural processes and their importance in the global mercury cycle. In *Mercury fate and transport in the global atmosphere*, Springer: 2009; pp 173-191.
10. Pirrone, N.; Cinnirella, S.; Feng, X.; Finkelman, R.; Friedli, H.; Leaner, J.; Mason, R.; Mukherjee, A.; Stracher, G.; Streets, D., Global mercury emissions to the atmosphere from anthropogenic and natural sources. *Atmospheric Chemistry and Physics* **2010**, *10*, (13), 5951-5964.
11. Pirrone, N.; Munthe, J.; Barregård, L.; Ehrlich, H.; Petersen, G.; Fernandez, R.; Hansen, J.; Grandjean, P.; Horvat, M.; Steinnes, E., EU Ambient Air Pollution by Mercury (Hg)-Position Paper. *Office for Official Publications of the European Communities* **2001**.
12. Unep, U. N. E. P., Global Mercury Assessment 2013: Sources, Emissions, Releases and Environmental Transport. In United Nations Environment Programme Chemicals Branch, Geneva, Switzerland: 2013.
13. Streets, D. G.; Zhang, Q.; Wu, Y., Projections of global mercury emissions in 2050. *Environmental science & technology* **2009**, *43*, (8), 2983-2988.
14. Schroeder, W. H.; Munthe, J., Atmospheric mercury—an overview. *Atmospheric Environment* **1998**, *32*, (5), 809-822.

15. Shia, R. L.; Seigneur, C.; Pai, P.; Ko, M.; Sze, N. D., Global simulation of atmospheric mercury concentrations and deposition fluxes. *Journal of Geophysical Research: Atmospheres (1984–2012)* **1999**, *104*, (D19), 23747-23760.
16. Lindberg, S.; Meyers, T.; Taylor, G.; Turner, R.; Schroeder, W., Atmosphere-surface exchange of mercury in a forest: Results of modeling and gradient approaches. *Journal of Geophysical Research: Atmospheres* **1992**, *97*, (D2), 2519-2528.
17. Selin, N. E.; Jacob, D. J., Seasonal and spatial patterns of mercury wet deposition in the United States: Constraints on the contribution from North American anthropogenic sources. *Atmospheric Environment* **2008**, *42*, (21), 5193-5204.
18. Usgs, U. S. G. S. Mercury in the Environment. <http://www.usgs.gov/themes/factsheet/146-00/index.html> (Feb 15, 2016),
19. Winner, C., How does mercury get into fish? A WHOI scientist tackles the mercury cycle. *Oceanus* **2010**, *48*, (2), 23-27.
20. Ekstrom, E. B.; Morel, F. M.; Benoit, J. M., Mercury methylation independent of the acetyl-coenzyme A pathway in sulfate-reducing bacteria. *Applied and environmental microbiology* **2003**, *69*, (9), 5414-5422.
21. King, J. K.; Saunders, F. M.; Lee, R. F.; Jahnke, R. A., Coupling mercury methylation rates to sulfate reduction rates in marine sediments. *Environmental toxicology and chemistry* **1999**, *18*, (7), 1362-1369.
22. Hintelmann, H.; Keppel-Jones, K.; Evans, R. D., Constants of mercury methylation and demethylation rates in sediments and comparison of tracer and ambient mercury availability. *Environmental toxicology and chemistry* **2000**, *19*, (9), 2204-2211.
23. Zhang, T.; Kim, B.; Levard, C. M.; Reinsch, B. C.; Lowry, G. V.; Deshusses, M. A.; Hsu-Kim, H., Methylation of mercury by bacteria exposed to dissolved, nanoparticulate, and microparticulate mercuric sulfides. *Environmental science & technology* **2012**, *46*, (13), 6950-6958.
24. Kerin, E. J.; Gilmour, C.; Roden, E.; Suzuki, M.; Coates, J.; Mason, R., Mercury methylation by dissimilatory iron-reducing bacteria. *Applied and environmental microbiology* **2006**, *72*, (12), 7919-7921.
25. Hammerschmidt, C. R.; Fitzgerald, W. F., Geochemical controls on the production and distribution of methylmercury in near-shore marine sediments. *Environmental science & technology* **2004**, *38*, (5), 1487-1495.
26. Benoit, J.; Gilmour, C.; Heyes, A.; Mason, R.; Miller, C. In *Geochemical and biological controls over methylmercury production and degradation in aquatic ecosystems*, ACS symposium series, 2003; Washington, DC; American Chemical Society; 1999: 2003; pp 262-297.
27. Compeau, G.; Bartha, R., Sulfate-reducing bacteria: principal methylators of mercury in anoxic estuarine sediment. *Applied and environmental microbiology* **1985**, *50*, (2), 498-502.
28. Fitzgerald, W. F.; Lamborg, C. H.; Hammerschmidt, C. R., Marine biogeochemical cycling of mercury. *Chemical reviews* **2007**, *107*, (2), 641-662.

29. Warner, K. A.; Roden, E. E.; Bonzongo, J.-C., Microbial mercury transformation in anoxic freshwater sediments under iron-reducing and other electron-accepting conditions. *Environmental science & technology* **2003**, *37*, (10), 2159-2165.
30. Watras, C. J.; Bloom, N. S., Mercury and methylmercury, in individual zooplankton: Implications for bioaccumulation. *Limnology and Oceanography* **1992**, *37*, (6), 1313-1318.
31. Driscoll, C. T.; Yan, C.; Schofield, C. L.; Munson, R.; Holsapple, J., The mercury cycle and fish in the Adirondack lakes. *Environmental science & technology* **1994**, *28*, (3), 136A-143A.
32. Cleckner, L. B.; Garrison, P. J.; Hurley, J. P.; Olson, M. L.; Krabbenhoft, D. P., Trophic transfer of methyl mercury in the northern Florida Everglades. *Biogeochemistry* **1998**, *40*, (2-3), 347-361.
33. Abi-Ghanem, C.; Nakhlé, K.; Khalaf, G.; Cossa, D., Mercury distribution and methylmercury mobility in the sediments of three sites on the Lebanese Coast, Eastern Mediterranean. *Archives of environmental contamination and toxicology* **2011**, *60*, (3), 394-405.
34. Atwell, L.; Hobson, K. A.; Welch, H. E., Biomagnification and bioaccumulation of mercury in an arctic marine food web: insights from stable nitrogen isotope analysis. *Canadian Journal of Fisheries and Aquatic Sciences* **1998**, *55*, (5), 1114-1121.
35. Zhang, L.; Campbell, L. M.; Johnson, T. B., Seasonal variation in mercury and food web biomagnification in Lake Ontario, Canada. *Environmental Pollution* **2012**, *161*, 178-184.
36. Lavoie, R. A.; Jardine, T. D.; Chumchal, M. M.; Kidd, K. A.; Campbell, L. M., Biomagnification of mercury in aquatic food webs: a worldwide meta-analysis. *Environmental science & technology* **2013**, *47*, (23), 13385-13394.
37. Bri-Ipen, B. R. I. I., Global Mercury Hotspots: New evidence reveals mercury contamination regularly exceeds health advisory levels in humans and fish worldwide. *A publication by the Biodiversity Research Institute and IPEN* **2014**, 19.
38. Driscoll, C. T.; Han, Y.-J.; Chen, C. Y.; Evers, D. C.; Lambert, K. F.; Holsen, T. M.; Kamman, N. C.; Munson, R. K., Mercury contamination in forest and freshwater ecosystems in the northeastern United States. *BioScience* **2007**, *57*, (1), 17-28.
39. Evers, D. C.; Han, Y.-J.; Driscoll, C. T.; Kamman, N. C.; Goodale, M. W.; Lambert, K. F.; Holsen, T. M.; Chen, C. Y.; Clair, T. A.; Butler, T., Biological mercury hotspots in the northeastern United States and southeastern Canada. *BioScience* **2007**, *57*, (1), 29-43.
40. Monson, B. A.; Staples, D. F.; Bhavsar, S. P.; Holsen, T. M.; Schrank, C. S.; Moses, S. K.; Mcgoldrick, D. J.; Backus, S. M.; Williams, K. A., Spatiotemporal trends of mercury in walleye and largemouth bass from the Laurentian Great Lakes region. *Ecotoxicology* **2011**, *20*, (7), 1555-1567.
41. Friedmann, A. S.; Costain, E. K.; Maclatchy, D. L.; Stansley, W.; Washuta, E. J., Effect of mercury on general and reproductive health of largemouth bass

- (*Micropterus salmoides*) from three lakes in New Jersey. *Ecotoxicology and environmental safety* **2002**, 52, (2), 117-122.
42. Foster, E.; Drake, D.; Didomenico, G., Seasonal changes and tissue distribution of mercury in largemouth bass (*Micropterus salmoides*) from Dorena Reservoir, Oregon. *Archives of environmental contamination and toxicology* **2000**, 38, (1), 78-82.
 43. Axelrad, D. M.; Lange, T.; Gabriel, M.; Atkeson, T. D.; Pollman, C. D.; Orem, W. H.; Scheidt, D. J.; Kalla, P. I.; Frederick, P. C.; Gilmour, C. C., B: Mercury and Sulfur Monitoring, Research and Environmental Assessment in South Florida. *South Florida Environmental Report* **2009**.
 44. Lodge, T., The Everglades handbook: understanding the ecosystem. *The Everglades handbook: understanding the ecosystem* **2004**, (Ed. 2).
 45. Rea, A. W.; Keeler, G. J.; Scherbatskoy, T., The deposition of mercury in throughfall and litterfall in the Lake Champlain watershed: a short-term study. *Atmospheric Environment* **1996**, 30, (19), 3257-3263.
 46. Browder, J. A.; Gleason, P. J.; Swift, D. R., Periphyton in the Everglades: spatial variation, environmental correlates, and ecological implications. *Everglades: The ecosystem and its restoration* **1994**, 379-418.
 47. Smith, J.; Summers, G.; Wong, R., Nutrient and heavy metal content of edible seaweeds in New Zealand. *New Zealand Journal of Crop and Horticultural Science* **2010**, 38, (1), 19-28.
 48. Andersen, J.; Depledge, M., A survey of total mercury and methylmercury in edible fish and invertebrates from Azorean waters. *Marine Environmental Research* **1997**, 44, (3), 331-350.
 49. Turoczy, N. J.; Mitchell, B. D.; Levings, A. H.; Rajendram, V. S., Cadmium, copper, mercury, and zinc concentrations in tissues of the King Crab (*Pseudocarcinus gigas*) from southeast Australian waters. *Environment international* **2001**, 27, (4), 327-334.
 50. Evans, D. W.; Crumley, P. H., Mercury in Florida Bay fish: Spatial distribution of elevated concentrations and possible linkages to Everglades restoration. *Bulletin of Marine Science* **2005**, 77, (3), 321-346.
 51. Adams, D. H.; McMichael, R. H.; Henderson, G. E., Mercury Levels in Marine and Estuarine Fishes of Florida 1989–2001. revised. **2003**.
 52. Ache, B.; Boyle, J.; Morse, C., *A survey of the occurrence of mercury in the fishery resources of the Gulf of Mexico*. Gulf of Mexico Program: 2000.
 53. Strom, D. G.; Graves, G. A., A comparison of mercury in estuarine fish between Florida Bay and the Indian River Lagoon, Florida, USA. *Estuaries* **2001**, 24, (4), 597-609.
 54. Srebocan, E.; Pompe-Gotal, J.; Prevendar-Crnic, A.; Ofner, E., Mercury concentrations of captive Atlantic bluefin tuna (*Thunnus thynnus*) farmed in the Adriatic Sea. *VETERINARNI MEDICINA-PRAHA*- **2007**, 52, (4), 175.
 55. Voegborlo, R.; El-Methnani, A.; Abedin, M., Mercury, cadmium and lead content of canned tuna fish. *Food Chemistry* **1999**, 67, (4), 341-345.

56. Yamashita, Y.; Omura, Y.; Okazaki, E., Total mercury and methylmercury levels in commercially important fishes in Japan. *Fisheries Science* **2005**, *71*, (5), 1029-1035.
57. Jewett, S. C.; Duffy, L. K., Mercury in fishes of Alaska, with emphasis on subsistence species. *Science of the total environment* **2007**, *387*, (1), 3-27.
58. Hinck, J. E.; Schmitt, C. J.; Echols, K. R.; May, T. W.; Orazio, C. E.; Tillitt, D. E., Environmental contaminants in fish and their associated risk to piscivorous wildlife in the Yukon River Basin, Alaska. *Archives of environmental contamination and toxicology* **2006**, *51*, (4), 661.
59. Jewett, S. C.; Zhang, X.; Naidu, A. S.; Kelley, J. J.; Dasher, D.; Duffy, L. K., Comparison of mercury and methylmercury in northern pike and Arctic grayling from western Alaska rivers. *Chemosphere* **2003**, *50*, (3), 383-392.
60. Duffy, L. K.; Scofield, E.; Rodgers, T.; Patton, M.; Bowyer, R. T., Comparative baseline levels of mercury, Hsp 70 and Hsp 60 in subsistence fish from the Yukon-Kuskokwim delta region of Alaska. *Comparative Biochemistry and Physiology Part C: Pharmacology, Toxicology and Endocrinology* **1999**, *124*, (2), 181-186.
61. Mueller, K.; Matz, A. *Water quality, and metal and metalloid concentrations in water, sediment, and fish tissues from Innoko National Wildlife Refuge; Alaska, 1995–1997*. Tech Rep NAES-TR-02-01. US Fish and Wildlife Service, Northern Alaska Ecological Services, Fairbanks: 2002.
62. Mueller, K.; Snyder-Conn, E.; Scannell, P., Metal and metalloid contaminants in water, sediments, and fish of Kanuti National Wildlife Refuge, Alaska, 1985–1990, Ecological Services, Fairbanks, Alaska. *US Fish and Wildlife Service. Technical report NAES-TR-95-02* **1995**, *125*.
63. Mueller, K. A.; Snyder-Conn, E.; Doyle, T. J.; Fairbanks, A., *Contaminant Baseline Data for Water, Sediments, and Fish of Selawik National Wildlife Refuge, Alaska, 1987-1988*. Fish and Wildlife Service, US Department of [the] Interior: 1993.
64. Snyder-Conn, E.; Patton, T.; Bertram, M.; Scannell, P.; Anthony, C., Contaminant baseline data from water, sediments, and fish of Nowitna National Wildlife Refuge, Alaska, 1985–1988. Ecological Services, Fairbanks, Alaska. *US Fish and Wildlife Service, Technical Report NAES-TR-92-02* **1992**.
65. Gray, J.; Theodorakos, P.; Budahn, J.; O'leary, R. In *Mercury in the environment and its implications, Kuskokwim River region, southwestern Alaska*, International Journal of Rock Mechanics and Mining Sciences and Geomechanics Abstracts, 1996; 1996; p 96A.
66. Headlee, P., Mercury and selenium concentrations in fish tissue and surface waters of the northern unit of the Innoko National Wildlife Refuge (Kaiyuh Flats), west central Alaska, 1993. Tanana Chiefs Conference, Inc. Fairbanks, Alaska. *Water resources report* **1996**, 96-3.
67. Bastos, W. R.; Dórea, J. G.; Bernardi, J. V. E.; Lauthartte, L. C.; Mussy, M. H.; Hauser, M.; Dória, C. R. D. C.; Malm, O., Mercury in muscle and brain of catfish from the Madeira river, Amazon, Brazil. *Ecotoxicology and environmental safety* **2015**, *118*, 90-97.

68. Brázová, T.; Torres, J.; Eira, C.; Hanzelová, V.; Miklisová, D.; Šalamún, P., Perch and its parasites as heavy metal biomonitors in a freshwater environment: the case study of the Ružín water reservoir, Slovakia. *Sensors* **2012**, *12*, (3), 3068-3081.
69. Corsolini, S.; Ancora, S.; Bianchi, N.; Mariotti, G.; Leonzio, C.; Christiansen, J. S., Organotropism of persistent organic pollutants and heavy metals in the Greenland shark *Somniosus microcephalus* in NE Greenland. *Marine pollution bulletin* **2014**, *87*, (1), 381-387.
70. Adams, D. H.; Sonne, C., Mercury and histopathology of the vulnerable goliath grouper, *Epinephelus itajara*, in US waters: A multi-tissue approach. *Environmental research* **2013**, *126*, 254-263.
71. Burger, J.; Jeitner, C.; Donio, M.; Pittfield, T.; Gochfeld, M., Mercury and selenium levels, and selenium: mercury molar ratios of brain, muscle and other tissues in bluefish (*Pomatomus saltatrix*) from New Jersey, USA. *Science of the total environment* **2013**, *443*, 278-286.
72. Menon, J. S.; Mahajan, S. V., Mercury accumulation in different tissues of fish from Ulhas River Estuary and Thane Creek and the pattern of fish consumption among fish-eaters. **2013**.
73. Mieiro, C.; Coelho, J.; Pacheco, M.; Duarte, A.; Pereira, M., Evaluation of species-specific dissimilarities in two marine fish species: mercury accumulation as a function of metal levels in consumed prey. *Archives of environmental contamination and toxicology* **2012**, *63*, (1), 125-136.
74. Coulibaly, S.; Atse, B. C.; Koffi, K. M.; Sylla, S.; Konan, K. J., Seasonal accumulations of some heavy metal in water, sediment and tissues of black-chinned tilapia *Sarotherodon melanotheron* from Biétri Bay in Ebrié Lagoon, Ivory Coast. *Bulletin of environmental contamination and toxicology* **2012**, *88*, (4), 571-576.
75. Storelli, M. M.; Cuttone, G.; Marcotrigiano, G. O., Distribution of trace elements in the tissues of smooth hound *Mustelus mustelus* (Linnaeus, 1758) from the southern-eastern waters of Mediterranean Sea (Italy). *Environmental monitoring and assessment* **2011**, *174*, (1-4), 271-281.
76. Cardoso, T. P.; Mársico, E. T.; Medeiros, R. J.; Tortelly, R.; Sobreiro, L. G., Mercury level and histopathologic analysis of muscle, kidney and brain of largehead hairtail (*Trichiurus lepturus*) collected in Itaipu beach-Niterói, Rio de Janeiro, Brazil. *Ciência Rural* **2009**, *39*, (2), 540-546.
77. Núñez-Nogueira, G.; Botello, A.; Rendón-Von Osten, J.; Gold-Bouchot, G.; Agraz-Hernández, C., Concentration of essential and non-essential metals in two shark species commonly caught in Mexican (Gulf of Mexico) coastline. *Golfo de México Contaminación e impacto Ambiental: Diagnóstico y Tendencias. Universidad Autónoma de Campeche, Universidad Autónoma Campeche, Universidad Nacional Autónoma de México, instituto Nacional de Ecología* **2005**, 451-474.
78. Cizdziel, J.; Hinnens, T.; Cross, C.; Pollard, J., Distribution of mercury in the tissues of five species of freshwater fish from Lake Mead, USA. *Journal of Environmental Monitoring* **2003**, *5*, (5), 802-807.

79. Hoguet, J.; Keller, J. M.; Reiner, J. L.; Kucklick, J. R.; Bryan, C. E.; Moors, A. J.; Pugh, R. S.; Becker, P. R., Spatial and temporal trends of persistent organic pollutants and mercury in beluga whales (*Delphinapterus leucas*) from Alaska. *Science of the total environment* **2013**, *449*, 285-294.
80. Dehn, L.-A.; Follmann, E. H.; Rosa, C.; Duffy, L. K.; Thomas, D. L.; Bratton, G. R.; Taylor, R. J.; O'hara, T. M., Stable isotope and trace element status of subsistence-hunted bowhead and beluga whales in Alaska and gray whales in Chukotka. *Marine pollution bulletin* **2006**, *52*, (3), 301-319.
81. Joiris, C. R.; Holsbeek, L.; Bolba, D.; Gascard, C.; Stanev, T.; Komakhidze, A.; Baumgärtner, W.; Birkun, A., Total and Organic Mercury in the Black Sea Harbour Porpoise *Phocoena phocoena relicta*. *Marine pollution bulletin* **2001**, *42*, (10), 905-911.
82. Smith, T. G.; Armstrong, F., Mercury and selenium in ringed and bearded seal tissues from Arctic Canada. *Arctic* **1978**, 75-84.
83. Blanvillain, G.; Schwenter, J. A.; Day, R. D.; Point, D.; Christopher, S. J.; Roumillat, W. A.; Owens, D. W., Diamondback terrapins, *Malaclemys terrapin*, as a sentinel species for monitoring mercury pollution of estuarine systems in South Carolina and Georgia, USA. *Environmental toxicology and chemistry* **2007**, *26*, (7), 1441-1450.
84. Burger, J., Metals in tissues of diamondback terrapin from New Jersey. *Environmental monitoring and assessment* **2002**, *77*, (3), 255-263.
85. Branco, V.; Vale, C.; Canário, J.; Dos Santos, M. N., Mercury and selenium in blue shark (*Prionace glauca*, L. 1758) and swordfish (*Xiphias gladius*, L. 1758) from two areas of the Atlantic Ocean. *Environmental Pollution* **2007**, *150*, (3), 373-380.
86. Lacerda, L.; Paraquetti, H.; Marins, R.; Rezende, C.; Zalmon, I.; Gomes, M.; Farias, V., Mercury content in shark species from the south-eastern Brazilian coast. *Revista Brasileira de Biologia* **2000**, *60*, (4), 571-576.
87. Marcovecchio, J. E.; Moreno, V. J.; Perez, A., Determination of heavy metal concentrations in biota of Bahía Blanca, Argentina. *Science of the total environment* **1988**, *75*, (2-3), 181-190.
88. Marcovecchio, J. E.; Moreno, V. J.; Pérez, A., Metal accumulation in tissues of sharks from the Bahia Blanca Estuary, Argentina. *Marine Environmental Research* **1991**, *31*, (4), 263-274.
89. Scapini, E.; Andrade, S.; Marcovecchio, J. In *Total mercury distribution in two shark species from Buenos Aires province coastal waters*, Argentina. Proc. Intern. Conf. Heavy Metals in the Environment, Toronto, 1993; 1993; pp 82-85.
90. Delany, M. F.; Bell, J. U.; Sundlof, S. F., Concentrations of contaminants in muscle of the American alligator in Florida. *J. Wildl. Dis.* **1988**, *24*, (1), 62-66.
91. Burger, J.; Gochfeld, M.; Rooney, A.; Orlando, E.; Woodward, A.; Guillette Jr, L., Metals and metalloids in tissues of American alligators in three Florida lakes. *Archives of environmental contamination and toxicology* **2000**, *38*, (4), 501-508.
92. Horai, S.; Itai, T.; Noguchi, T.; Yasuda, Y.; Adachi, H.; Hyobu, Y.; Riyadi, A. S.; Boggs, A. S.; Lowers, R.; Guillette Jr, L. J., Concentrations of trace elements in

- American alligators (*Alligator mississippiensis*) from Florida, USA. *Chemosphere* **2014**, *108*, 159-167.
93. Nilsen, F. M.; Parrott, B. B.; Bowden, J. A.; Kassim, B. L.; Somerville, S. E.; Bryan, T. A.; Bryan, C. E.; Lange, T. R.; Delaney, J. P.; Brunell, A. M.; Long, S. E.; Guillette Jr, L. J., Global DNA methylation loss associated with mercury contamination and aging in the American alligator (*Alligator mississippiensis*). *Science of the total environment* **2016**, *545–546*, 389-397.
 94. Heaton-Jones, T. G.; Homer, B. L.; Heaton-Jones, D.; Sundlof, S. F., Mercury distribution in American alligators (*Alligator mississippiensis*) in Florida. *Journal of Zoo and Wildlife Medicine* **1997**, 62-70.
 95. Rumbold, D.; Fink, L.; Laine, K.; Niemczyk, S.; Chandrasekhar, T.; Wankel, S.; Kendall, C., Levels of mercury in alligators (*Alligator mississippiensis*) collected along a transect through the Florida Everglades. *Sci. Total Environ.* **2002**, *297*, (1), 239-252.
 96. Yanochko, G.; Jagoe, C.; Brisbin Jr, I., Tissue mercury concentrations in alligators (*Alligator mississippiensis*) from the Florida Everglades and the Savannah River site, South Carolina. *Archives of environmental contamination and toxicology* **1997**, *32*, (3), 323-328.
 97. Adams, D. H.; Sonne, C.; Basu, N.; Dietz, R.; Nam, D.-H.; Leifsson, P. S.; Jensen, A. L., Mercury contamination in spotted seatrout, *Cynoscion nebulosus*: An assessment of liver, kidney, blood, and nervous system health. *Science of the total environment* **2010**, *408*, (23), 5808-5816.
 98. Magalhães, M. C.; Costa, V.; Menezes, G. M.; Pinho, M. R.; Santos, R. S.; Monteiro, L. R., Intra-and inter-specific variability in total and methylmercury bioaccumulation by eight marine fish species from the Azores. *Marine pollution bulletin* **2007**, *54*, (10), 1654-1662.
 99. Pilsner, R. J.; Lazarus, A. L.; Nam, D. H.; Letcher, R. J.; Sonne, C.; Dietz, R.; Basu, N., Mercury-associated DNA hypomethylation in polar bear brains via the LUMinometric Methylation Assay: a sensitive method to study epigenetics in wildlife. *Molecular ecology* **2010**, *19*, (2), 307-314.
 100. Basu, N.; Scheuhammer, A. M.; Sonne, C.; Letcher, R. J.; Born, E. W.; Dietz, R., Is dietary mercury of neurotoxicological concern to wild polar bears (*Ursus maritimus*)? *Environmental toxicology and chemistry* **2009**, *28*, (1), 133-140.
 101. Basu, N.; Head, J.; Nam, D.-H.; Pilsner, J. R.; Carvan, M. J.; Chan, H. M.; Goetz, F. W.; Murphy, C. A.; Rouvinen-Watt, K.; Scheuhammer, A. M., Effects of methylmercury on epigenetic markers in three model species: mink, chicken and yellow perch. *Comparative Biochemistry and Physiology Part C: Toxicology & Pharmacology* **2013**, *157*, (3), 322-327.
 102. Basu, N.; Goodrich, J. M.; Head, J., Ecogenetics of mercury: From genetic polymorphisms and epigenetics to risk assessment and decision-making. *Environmental toxicology and chemistry* **2014**, *33*, (6), 1248-1258.
 103. Laporte, J.; Truchot, J.; Ribeyre, F.; Boudou, A., Combined effects of water pH and salinity on the bioaccumulation of inorganic mercury and methylmercury in the shore crab *Carcinus maenas*. *Marine pollution bulletin* **1997**, *34*, (11), 880-893.

104. Crump, K. L.; Trudeau, V. L., Mercury-induced reproductive impairment in fish. *Environ. Toxicol. Chem.* **2009**, *28*, (5), 895-907.
105. Jayasena, N.; Frederick, P. C.; Larkin, I. L., Endocrine disruption in white ibises (*Eudocimus albus*) caused by exposure to environmentally relevant levels of methylmercury. *Aquatic Toxicology* **2011**, *105*, (3), 321-327.
106. Olsvik, P. A.; Lindgren, M.; Maage, A., Mercury contamination in deep-water fish: Transcriptional responses in tusk (*Brosme brosme*) from a fjord gradient. *Aquatic Toxicology* **2013**, *144*, 172-185.
107. Ung, C. Y.; Lam, S. H.; Hlaing, M. M.; Winata, C. L.; Korzh, S.; Mathavan, S.; Gong, Z., Mercury-induced hepatotoxicity in zebrafish: in vivo mechanistic insights from transcriptome analysis, phenotype anchoring and targeted gene expression validation. *Bmc Genomics* **2010**, *11*, (1), 212.
108. Tsai, C.-L.; Jang, T.-H.; Wang, L.-H., Effects of mercury on serotonin concentration in the brain of tilapia, *Oreochromis mossambicus*. *Neuroscience Letters* **1995**, *184*, (3), 208-211.
109. Kirubakaran, R.; Joy, K., Changes in brain monoamine levels and monoamine oxidase activity in the catfish, *Clarias batrachus*, during chronic treatments with mercurials. *Bulletin of environmental contamination and toxicology* **1990**, *45*, (1), 88-93.
110. Zhou, T.; Rademacher, D. J.; Steinpreis, R. E.; Weis, J. S., Neurotransmitter levels in two populations of larval *Fundulus heteroclitus* after methylmercury exposure. *Comparative Biochemistry and Physiology Part C: Pharmacology, Toxicology and Endocrinology* **1999**, *124*, (3), 287-294.
111. Wester, P., Histopathological effects of environmental pollutants β -HCH and methyl mercury on reproductive organs in freshwater fish. *Comparative Biochemistry and Physiology Part C: Comparative Pharmacology* **1991**, *100*, (1-2), 237-239.
112. Kirubakaran, R.; Joy, K., Toxic effects of mercury on testicular activity in the freshwater teleost, *Clarias batrachus* (L.). *Journal of Fish Biology* **1992**, *41*, (2), 305-315.
113. Frederick, P.; Jayasena, N., Altered pairing behaviour and reproductive success in white ibises exposed to environmentally relevant concentrations of methylmercury. *Proceedings of the Royal Society B: Biological Sciences* **2010**, rspb20102189.
114. Heath, J. A.; Frederick, P. C.; Karasov, W., Relationships among mercury concentrations, hormones, and nesting effort of white ibises (*Eudocimus albus*) in the Florida Everglades. *The Auk* **2005**, *122*, (1), 255-267.
115. Wolfe, M. F.; Schwarzbach, S.; Sulaiman, R. A., Effects of mercury on wildlife: a comprehensive review. *Environmental toxicology and chemistry* **1998**, *17*, (2), 146-160.
116. Frederick, P.; Campbell, A.; Jayasena, N.; Borkhataria, R., Survival of White Ibises (*Eudocimus albus*) in response to chronic experimental methylmercury exposure. *Ecotoxicology* **2011**, *20*, (2), 358-364.

117. Kružíková, K.; Svobodová, Z.; Valentová, O.; Randák, T.; Velíšek, J., Mercury and methylmercury in muscle tissue of chub from the Elbe River main tributaries. *Czech J. Food Sci. Vol* **2008**, *26*, (1), 65-70.
118. Alonso, M. L.; Benedito, J.; Miranda, M.; Castillo, C.; Hernández, J.; Shore, R., Mercury concentrations in cattle from NW Spain. *Science of the total environment* **2003**, *302*, (1), 93-100.
119. Gupta, U. C.; Gupta, S. C., Trace element toxicity relationships to crop production and livestock and human health: implications for management. *Communications in Soil Science & Plant Analysis* **1998**, *29*, (11-14), 1491-1522.
120. Gray, J. E.; Meier, A. L.; O'leary, R. M.; Outwater, C.; Theodorakos, P., Environmental geochemistry of mercury deposits in southwestern Alaska: mercury contents in fish, stream-sediment, and stream-water samples. *US Geol Surv Bull* **1996**, *2152*, 17-29.
121. Horai, S.; Itai, T.; Noguchi, T.; Yasuda, Y.; Adachi, H.; Hyobu, Y.; Riyadi, A. S.; Boggs, A. S.; Lowers, R.; Guillette Jr, L. J., Concentrations of trace elements in American alligators (*Alligator mississippiensis*) from Florida, USA. *Chemosphere* **2014**, *108*, 159-167.
122. Nilsen, F.; Dorsey, J.; Lowers, R.; Guillette Jr, L.; Long, S.; Bowden, J.; Schock, T., Evaluating mercury concentrations and body condition in American alligators (*Alligator mississippiensis*) at Merritt Island National Wildlife Refuge (MINWR), Florida. *The Science of the total environment* **2017**, *607*, 1056.
123. Dey, S.; Bhattacharya, S., Ovarian damage to *Channa punctatus* after chronic exposure to low concentrations of elsan, mercury, and ammonia. *Ecotoxicology and environmental safety* **1989**, *17*, (2), 247-257.
124. Ceccatelli, S.; Daré, E.; Moors, M., Methylmercury-induced neurotoxicity and apoptosis. *Chemico-biological interactions* **2010**, *188*, (2), 301-308.
125. Devlin, E. W., Acute toxicity, uptake and histopathology of aqueous methyl mercury to fathead minnow embryos. *Ecotoxicology* **2006**, *15*, (1), 97-110.
126. Weihe, P.; Hansen, J. C.; Murata, K.; Debes, F.; Jørgensen, P. J.; Steuerwald, U.; White, R. F.; Grandjean, P., Neurobehavioral performance of Inuit children with increased prenatal exposure to methylmercury. *International journal of circumpolar health* **2002**, *61*, (1), 41-49.
127. Hrubá, F.; Strömberg, U.; Černá, M.; Chen, C.; Harari, F.; Harari, R.; Horvat, M.; Koppová, K.; Kos, A.; Krsková, A., Blood cadmium, mercury, and lead in children: an international comparison of cities in six European countries, and China, Ecuador, and Morocco. *Environment international* **2012**, *41*, 29-34.
128. Schulz, C.; Angerer, J.; Ewers, U.; Heudorf, U.; Wilhelm, M.; Agency, H. B. C. O. T. G. F. E., Revised and new reference values for environmental pollutants in urine or blood of children in Germany derived from the German environmental survey on children 2003-2006 (GerES IV). *International journal of hygiene and environmental health* **2009**, *212*, (6), 637-647.
129. Schoeters, G.; Colles, A.; Den Hond, E.; Croes, K.; Vrijens, J.; Baeyens, W.; Nelen, V.; Van De Mieroop, E.; Covaci, A.; Bruckers, L., F: The Flemish Environment and Health Study (FLEHS)–Second Survey (2007–2011):

- Establishing Reference Values for Biomarkers of Exposure in the Flemish Population. In *Biomarkers and human biomonitoring*, 2011; pp 135-165.
130. Pino, A.; Amato, A.; Alimonti, A.; Mattei, D.; Bocca, B., Human biomonitoring for metals in Italian urban adolescents: data from Latium Region. *International journal of hygiene and environmental health* **2012**, *215*, (2), 185-190.
 131. Steuerwald, U.; Weihe, P.; Jørgensen, P. J.; Bjerve, K.; Brock, J.; Heinzow, B.; Budtz-Jørgensen, E.; Grandjean, P., Maternal seafood diet, methylmercury exposure, and neonatal neurologic function. *The Journal of pediatrics* **2000**, *136*, (5), 599-605.
 132. Sorensen, N.; Murata, K.; Budtz-Jørgensen, E.; Weihe, P.; Grandjean, P., Prenatal methylmercury exposure as a cardiovascular risk factor at seven years of age. *Epidemiology* **1999**, *10*, (4), 370-375.
 133. De Burbure, C.; Buchet, J.-P.; Leroyer, A.; Nisse, C.; Haguenoer, J.-M.; Mutti, A.; Smerhovský, Z.; Cikrt, M.; Trzcinka-Ochocka, M.; Razniewska, G., Renal and neurologic effects of cadmium, lead, mercury, and arsenic in children: evidence of early effects and multiple interactions at environmental exposure levels. *Environmental Health Perspectives* **2006**, 584-590.
 134. Jarosińska, D.; Horvat, M.; Sällsten, G.; Mazzolai, B.; Dąbkowska, B.; Prokopowicz, A.; Biesiada, M.; Barregård, L., Urinary mercury and biomarkers of early renal dysfunction in environmentally and occupationally exposed adults: a three-country study. *Environmental research* **2008**, *108*, (2), 224-232.
 135. Wilhelm, M.; Ewers, U.; Schulz, C., Revised and new reference values for some trace elements in blood and urine for human biomonitoring in environmental medicine. *International journal of hygiene and environmental health* **2004**, *207*, (1), 69-73.
 136. Jenssen, M. T.; Brantsæter, A. L.; Haugen, M.; Meltzer, H. M.; Larssen, T.; Kvale, H. E.; Birgisdóttir, B. E.; Thomassen, Y.; Ellingsen, D.; Alexander, J., Dietary mercury exposure in a population with a wide range of fish consumption—Self-capture of fish and regional differences are important determinants of mercury in blood. *Science of the total environment* **2012**, *439*, 220-229.
 137. Chojnacka, K.; Zielińska, A.; Górecka, H.; Dobrzański, Z.; Górecki, H., Reference values for hair minerals of Polish students. *Environmental toxicology and pharmacology* **2010**, *29*, (3), 314-319.
 138. Pichery, C.; Bellanger, M.; Zmirou-Navier, D.; Fréry, N.; Cordier, S.; Roue-Legall, A.; Hartemann, P.; Grandjean, P., Economic evaluation of health consequences of prenatal methylmercury exposure in France. *Environmental Health* **2012**, *11*, (1), 53.
 139. Díez, S.; Montuori, P.; Pagano, A.; Sarnacchiaro, P.; Bayona, J. M.; Triassi, M., Hair mercury levels in an urban population from southern Italy: fish consumption as a determinant of exposure. *Environment international* **2008**, *34*, (2), 162-167.
 140. Salonen, J. T.; Seppänen, K.; Lakka, T. A.; Salonen, R.; Kaplan, G. A., Mercury accumulation and accelerated progression of carotid atherosclerosis: a population-based prospective 4-year follow-up study in men in eastern Finland. *Atherosclerosis* **2000**, *148*, (2), 265-273.

141. Björnberg, K. A.; Vahter, M.; Petersson-Grawe, K.; Glynn, A.; Cnattingius, S.; Darnerud, P. O.; Atuma, S.; Aune, M.; Becker, W.; Berglund, M., Methyl mercury and inorganic mercury in Swedish pregnant women and in cord blood: influence of fish consumption. *Environmental Health Perspectives* **2003**, *111*, (4), 637.
142. Guldner, L.; Monfort, C.; Rouget, F.; Garlantezec, R.; Cordier, S., Maternal fish and shellfish intake and pregnancy outcomes: a prospective cohort study in Brittany, France. *Environmental Health* **2007**, *6*, (1), 33.
143. Pouzaud, F.; Ibbou, A.; Blanchemanche, S.; Grandjean, P.; Krempf, M.; Philippe, H.-J.; Verger, P., Use of advanced cluster analysis to characterize fish consumption patterns and methylmercury dietary exposures from fish and other sea foods among pregnant women. *Journal of Exposure Science and Environmental Epidemiology* **2010**, *20*, (1), 54-68.
144. Vahter, M.; Åkesson, A.; Lind, B.; Björs, U.; Schütz, A.; Berglund, M., Longitudinal study of methylmercury and inorganic mercury in blood and urine of pregnant and lactating women, as well as in umbilical cord blood. *Environmental research* **2000**, *84*, (2), 186-194.
145. Björkman, L.; Lundekvam, B. F.; Lægreid, T.; Bertelsen, B. I.; Morild, I.; Lilleng, P.; Lind, B.; Palm, B.; Vahter, M., Mercury in human brain, blood, muscle and toenails in relation to exposure: an autopsy study. *Environ Health* **2007**, *6*, (30), 17931423.
146. Gorell, J.; Johnson, C.; Rybicki, B.; Peterson, E.; Kortsha, G.; Brown, G.; Richardson, R., Occupational exposures to metals as risk factors for Parkinson's disease. *Neurology* **1997**, *48*, (3), 650-658.
147. Oliveira, R. C.; Dórea, J. G.; Bernardi, J. V.; Bastos, W. R.; Almeida, R.; Manzatto, Â. G., Fish consumption by traditional subsistence villagers of the Rio Madeira (Amazon): impact on hair mercury. *Annals of human biology* **2010**, *37*, (5), 629-642.
148. Dewailly, E.; Ayotte, P.; Bruneau, S.; Lebel, G.; Levallois, P.; Weber, J. P., Exposure of the Inuit population of Nunavik (Arctic Quebec) to lead and mercury. *Archives of Environmental Health: An International Journal* **2001**, *56*, (4), 350-357.
149. Inoue, S.; Yorifuji, T.; Tsuda, T.; Doi, H., Short-term effect of severe exposure to methylmercury on atherosclerotic heart disease and hypertension mortality in Minamata. *Science of the total environment* **2012**, *417*, 291-293.
150. Yorifuji, T.; Tsuda, T.; Kashima, S.; Takao, S.; Harada, M., Long-term exposure to methylmercury and its effects on hypertension in Minamata. *Environmental research* **2010**, *110*, (1), 40-46.
151. Fillion, M.; Mergler, D.; Passos, C. J.; Larribe, F.; Lemire, M.; Guimarães, J. R., A preliminary study of mercury exposure and blood pressure in the Brazilian Amazon. *Environmental Health* **2006**, *5*, (1), 29.
152. Zahir, F.; Rizwi, S. J.; Haq, S. K.; Khan, R. H., Low dose mercury toxicity and human health. *Environmental toxicology and pharmacology* **2005**, *20*, (2), 351-360.

153. Chan, H. M.; Egeland, G. M., Fish consumption, mercury exposure, and heart diseases. *Nutr Rev* **2004**, *62*, (2), 68-72.
154. Virtanen, J. K.; Rissanen, T. H.; Voutilainen, S.; Tuomainen, T.-P., Mercury as a risk factor for cardiovascular diseases. *The Journal of nutritional biochemistry* **2007**, *18*, (2), 75-85.
155. Valera, B.; Muckle, G.; Poirier, P.; Jacobson, S. W.; Jacobson, J. L.; Dewailly, E., Cardiac autonomic activity and blood pressure among Inuit children exposed to mercury. *Neurotoxicology* **2012**, *33*, (5), 1067-1074.
156. Višnjevec, A. M.; Kocman, D.; Horvat, M., Human mercury exposure and effects in Europe. *Environmental toxicology and chemistry* **2014**, *33*, (6), 1259-1270.
157. Pedersen, E. B.; Jørgensen, M. E.; Pedersen, M. B.; Siggaard, C.; Sørensen, T. B.; Mulvad, G.; Hansen, J. C.; Asmund, G.; Skjoldborg, H., Relationship between mercury in blood and 24-h ambulatory blood pressure in Greenlanders and Danes. *American journal of hypertension* **2005**, *18*, (5), 612-618.
158. Counter, S. A.; Buchanan, L. H., Mercury exposure in children: a review. *Toxicology and applied pharmacology* **2004**, *198*, (2), 209-230.
159. Mahaffey, K. R.; Mergler, D., Blood levels of total and organic mercury in residents of the upper St. Lawrence River basin, Quebec: association with age, gender, and fish consumption. *Environmental research* **1998**, *77*, (2), 104-114.
160. Airey, D., Mercury in human hair due to environment and diet: a review. *Environmental Health Perspectives* **1983**, *52*, 303.
161. Berzas Nevado, J.; Rodríguez Martín-Doimeadios, R.; Guzmán Bernardo, F.; Jiménez Moreno, M.; Herculano, A.; Do Nascimento, J.; Crespo-López, M., Mercury in the Tapajós River basin, Brazilian Amazon: a review. *Environment international* **2010**, *36*, (6), 593-608.
162. Batista, B. L.; Rodrigues, J. L.; De Souza, S. S.; Oliveira Souza, V. C.; Barbosa Jr, F., Mercury speciation in seafood samples by LC-ICP-MS with a rapid ultrasound-assisted extraction procedure: Application to the determination of mercury in Brazilian seafood samples. *Food Chemistry* **2011**, *126*, (4), 2000-2004.
163. Chang, L.-F.; Jiang, S.-J.; Sahayam, A., Speciation analysis of mercury and lead in fish samples using liquid chromatography-inductively coupled plasma mass spectrometry. *Journal of chromatography A* **2007**, *1176*, (1), 143-148.
164. Burger, J.; Gochfeld, M.; Jeitner, C.; Burke, S.; Stamm, T.; Snigaroff, R.; Snigaroff, D.; Patrick, R.; Weston, J., Mercury levels and potential risk from subsistence foods from the Aleutians. *Science of the total environment* **2007**, *384*, (1), 93-105.
165. Day, R. D.; Vander Pol, S. S.; Christopher, S. J.; Davis, W. C.; Pugh, R. S.; Simac, K. S.; Roseneau, D. G.; Becker, P. R., Murre eggs (*Uria aalge* and *Uria lomvia*) as indicators of mercury contamination in the Alaskan marine environment. *Environmental science & technology* **2006**, *40*, (3), 659-665.
166. Kurland, T.; Faro, S. N.; Siedler, H., Minamata disease. The outbreak of a neurologic disorder in Minamata, Japan, and its relationship to the ingestion of seafood contaminated by mercuric compounds. *World neurology* **1960**, *1*, (5), 370-95.

167. Rustam, H.; Hamdi, T., Methyl mercury poisoning in Iraq a neurological study. *Brain* **1974**, *97*, (1), 499-510.
168. Lim, S.; Chung, H.-U.; Paek, D., Low dose mercury and heart rate variability among community residents nearby to an industrial complex in Korea. *Neurotoxicology* **2010**, *31*, (1), 10-16.
169. Salonen, J. T.; Seppänen, K.; Nyyssönen, K.; Korpela, H.; Kauhanen, J.; Kantola, M.; Tuomilehto, J.; Esterbauer, H.; Tatzber, F.; Salonen, R., Intake of mercury from fish, lipid peroxidation, and the risk of myocardial infarction and coronary, cardiovascular, and any death in eastern Finnish men. *Circulation* **1995**, *91*, (3), 645-655.
170. Milnes, M. R.; Guillette, L. J., Alligator tales: new lessons about environmental contaminants from a sentinel species. *BioScience* **2008**, *58*, (11), 1027-1036.
171. Bryan, C. E.; Christopher, S. J.; Balmer, B. C.; Wells, R. S., Establishing baseline levels of trace elements in blood and skin of bottlenose dolphins in Sarasota Bay, Florida: implications for non-invasive monitoring. *Science of the total environment* **2007**, *388*, (1), 325-342.
172. Lee, C.-S.; Lutcavage, M. E.; Chandler, E.; Madigan, D. J.; Cerrato, R. M.; Fisher, N. S., Declining Mercury Concentrations in Bluefin Tuna Reflect Reduced Emissions to the North Atlantic Ocean. *Environmental science & technology* **2016**, *50*, (23), 12825-12830.
173. Rumbold, D.; Niemczyk, S.; Fink, L.; Chandrasekhar, T.; Harkanson, B.; Laine, K., Mercury in eggs and feathers of great egrets (*Ardea albus*) from the Florida Everglades. *Archives of environmental contamination and toxicology* **2001**, *41*, (4), 501-507.
174. Kushlan, J. A., Observations on the role of the American alligator (*Alligator mississippiensis*) in the southern Florida wetlands. *Copeia* **1974**, 993-996.
175. Guillette, L. J.; Crain, D. A.; Gunderson, M. P.; Kools, S. A.; Milnes, M. R.; Orlando, E. F.; Rooney, A. A.; Woodward, A. R., Alligators and endocrine disrupting contaminants: a current perspective. *American Zoologist* **2000**, *40*, (3), 438-452.
176. Lance, V. A., Alligator physiology and life history: the importance of temperature. *Experimental gerontology* **2003**, *38*, (7), 801-805.
177. Kushlan, J. A.; Kushlan, M. S., Everglades alligator nests: nesting sites for marsh reptiles. *Copeia* **1980**, 930-932.
178. Elsey, R. M.; Trosclair Iii, P. L.; Glenn, T. C., Nest-site fidelity in American alligators in a Louisiana coastal marsh. *Southeastern Naturalist* **2008**, *7*, (4), 737-743.
179. Bossart, G., Marine mammals as sentinel species for oceans and human health. *Veterinary Pathology Online* **2011**, *48*, (3), 676-690.
180. Bangma, J. T.; Reiner, J. L.; Jones, M.; Lowers, R. H.; Nilsen, F.; Rainwater, T. R.; Somerville, S.; Guillette, L. J.; Bowden, J. A., Variation in perfluoroalkyl acids in the American alligator (*Alligator mississippiensis*) at Merritt Island National Wildlife Refuge. *Chemosphere* **2017**, *166*, 72-79.
181. Guillette Jr, L. J.; Pickford, D. B.; Crain, D. A.; Rooney, A. A.; Percival, H. F., Reduction in penis size and plasma testosterone concentrations in juvenile

- alligators living in a contaminated environment. *General and comparative endocrinology* **1996**, *101*, (1), 32-42.
182. Tuberville, T. D.; Scott, D. E.; Metts, B. S.; Finger, J. W.; Hamilton, M. T., Hepatic and renal trace element concentrations in American alligators (*Alligator mississippiensis*) following chronic dietary exposure to coal fly ash contaminated prey. *Environmental Pollution* **2016**, *214*, 680-689.
183. Lance, V.; Joanen, T.; Mcnease, L., Selenium, vitamin E, and trace elements in the plasma of wild and farm-reared alligators during the reproductive cycle. *Canadian Journal of Zoology* **1983**, *61*, (8), 1744-1751.
184. Boggs, A. S.; Lowers, R. H.; Cloy-McCoy, J. A.; Guillette Jr, L. J., Organizational Changes to Thyroid Regulation in Alligator mississippiensis: Evidence for Predictive Adaptive Responses. *PloS one* **2013**, *8*, (1), e55515.
185. Gunderson, M.; Kools, S.; Milnes, M.; Guillette Jr, L., Effect of acute stress on plasma β -corticosterone, estradiol-17 β and testosterone concentrations in juvenile American alligators collected from three sites within the Kissimmee–Everglades drainage basin in Florida (USA). *Comparative Biochemistry and Physiology Part C: Toxicology & Pharmacology* **2003**, *135*, (3), 365-374.
186. Hord, L.; Jennings, M.; Brunell, A. In *Mercury contamination of Florida alligators*, Crocodiles: Proceedings of the 10th Working Meeting of the Crocodile Specialist Group, IUCN-The World Conservation Union, Gland Switzerland, 1990; 1990; pp 1-15.
187. Jagoe, C.; Arnold-Hill, B.; Yanochko, G.; Winger, P.; Brisbin Jr, I., Mercury in alligators (*Alligator mississippiensis*) in the southeastern United States. *Science of the total environment* **1998**, *213*, (1), 255-262.
188. Campbell, J. W.; Waters, M. N.; Tarter, A.; Jackson, J., Heavy metal and selenium concentrations in liver tissue from wild American alligator (*Alligator mississippiensis*) livers near Charleston, South Carolina. *Journal of Wildlife Diseases* **2010**, *46*, (4), 1234-1241.
189. Hopkins, W. A.; Durant, S. E.; Staub, B. P.; Rowe, C. L.; Jackson, B. P., Reproduction, embryonic development, and maternal transfer of contaminants in the amphibian *Gastrophryne carolinensis*. *Environmental Health Perspectives* **2006**, 661-666.
190. Verreault, J.; Villa, R. A.; Gabrielsen, G. W.; Skaare, J. U.; Letcher, R. J., Maternal transfer of organohalogen contaminants and metabolites to eggs of Arctic-breeding glaucous gulls. *Environmental Pollution* **2006**, *144*, (3), 1053-1060.
191. Park, B.-K.; Park, G.-J.; An, Y.-R.; Choi, H.-G.; Kim, G. B.; Moon, H.-B., Organohalogen contaminants in finless porpoises (*Neophocaena phocaenoides*) from Korean coastal waters: contamination status, maternal transfer and ecotoxicological implications. *Marine pollution bulletin* **2010**, *60*, (5), 768-774.
192. Ffwcc, F. F. a. W. C. C. Statewide alligator harvest data summary. Available online at http://myfwc.com/media/1357388/alligator_annual_summaries.pdf. (Accessed March 22, 2016.),
193. Pfau, B.; Roosenburg, W. M., Diamondback terrapins in Maryland: research and conservation. In *Radiata*: 2010.

194. Frankson, R.; Hueston, W.; Christian, K.; Olson, D.; Lee, M.; Valeri, L.; Hyatt, R.; Anelli, J.; Rubin, C., One health core competency domains. *Frontiers in public health* **2016**, *4*.
195. Villeneuve, D. L.; Crump, D.; Garcia-Reyero, N.; Hecker, M.; Hutchinson, T. H.; Lalone, C. A.; Landesmann, B.; Lettieri, T.; Munn, S.; Nepelska, M., Adverse outcome pathway (AOP) development I: strategies and principles. *Toxicological Sciences* **2014**, *142*, (2), 312-320.
196. Villeneuve, D. L.; Crump, D.; Garcia-Reyero, N.; Hecker, M.; Hutchinson, T. H.; Lalone, C. A.; Landesmann, B.; Lettieri, T.; Munn, S.; Nepelska, M., Adverse outcome pathway development II: best practices. *Toxicological Sciences* **2014**, *142*, (2), 321-330.
197. Andres, S.; Laporte, J.-M.; Mason, R. P., Mercury accumulation and flux across the gills and the intestine of the blue crab (*Callinectes sapidus*). *Aquatic Toxicology* **2002**, *56*, (4), 303-320.
198. WHO, W. H. O., Environmental Health Criteria 101 Methylmercury,. *Geneva: World Health Organization* **1990**, 1-144.
199. Ercal, N.; Gurer-Orhan, H.; Aykin-Burns, N., Toxic metals and oxidative stress part I: mechanisms involved in metal-induced oxidative damage. *Current topics in medicinal chemistry* **2001**, *1*, (6), 529-539.
200. Stohs, S.; Bagchi, D., Oxidative mechanisms in the toxicity of metal ions. *Free radical biology and medicine* **1995**, *18*, (2), 321-336.
201. Raymond, L. J.; Ralston, N. V., Mercury: selenium interactions and health implications. *Seychelles Medical and Dental Journal* **2004**, *7*, (1), 72-77.
202. Carrier, G.; Bouchard, M.; Brunet, R. C.; Caza, M., A toxicokinetic model for predicting the tissue distribution and elimination of organic and inorganic mercury following exposure to methyl mercury in animals and humans. II. Application and validation of the model in humans. *Toxicology and applied pharmacology* **2001**, *171*, (1), 50-60.
203. Lieske, C. L.; Moses, S. K.; Castellini, J. M.; Klejka, J.; Hueffer, K.; O'hara, T. M., Toxicokinetics of mercury in blood compartments and hair of fish-fed sled dogs. *Acta Veterinaria Scandinavica* **2011**, *53*, (1), 1.
204. Ekstrand, J.; Nielsen, J. B.; Havarinasab, S.; Zalups, R. K.; Söderkvist, P.; Hultman, P., Mercury toxicokinetics—dependency on strain and gender. *Toxicology and applied pharmacology* **2010**, *243*, (3), 283-291.
205. Benison, G. C.; Di Lello, P.; Shokes, J. E.; Cospers, N. J.; Scott, R. A.; Legault, P.; Omichinski, J. G., A stable mercury-containing complex of the organomercurial lyase MerB: catalysis, product release, and direct transfer to MerA. *Biochemistry* **2004**, *43*, (26), 8333-8345.
206. Miller, S. M., Cleaving C-Hg bonds: two thiolates are better than one. *Nature chemical biology* **2007**, *3*, (9), 537-538.
207. Qvarnström, J.; Lambertsson, L.; Havarinasab, S.; Hultman, P.; Frech, W., Determination of methylmercury, ethylmercury, and inorganic mercury in mouse tissues, following administration of thimerosal, by species-specific isotope dilution GC-inductively coupled plasma-MS. *Analytical chemistry* **2003**, *75*, (16), 4120-4124.

208. Griffith, O. W.; Meister, A., Glutathione: interorgan translocation, turnover, and metabolism. *Proceedings of the National Academy of Sciences* **1979**, *76*, (11), 5606-5610.
209. Hayes, J. D.; Mclellan, L. I., Glutathione and glutathione-dependent enzymes represent a co-ordinately regulated defence against oxidative stress. *Free radical research* **1999**, *31*, (4), 273-300.
210. Wu, G.; Fang, Y.-Z.; Yang, S.; Lupton, J. R.; Turner, N. D., Glutathione metabolism and its implications for health. *The Journal of nutrition* **2004**, *134*, (3), 489-492.
211. El-Demerdash, F., Effects of selenium and mercury on the enzymatic activities and lipid peroxidation in brain, liver, and blood of rats. *Journal of Environmental Science and Health, Part B* **2001**, *36*, (4), 489-499.
212. Al-Ebraheem, A.; Farquharson, M.; Ryan, E., The evaluation of biologically important trace metals in liver, kidney and breast tissue. *Applied Radiation and Isotopes* **2009**, *67*, (3), 470-474.
213. Wayland, M.; Garcia-Fernandez, A.; Neugebauer, E.; Gilchrist, H., Concentrations of cadmium, mercury and selenium in blood, liver and kidney of common eider ducks from the Canadian Arctic. *Environmental monitoring and assessment* **2001**, *71*, (3), 255-267.
214. Dieguez-Acuña, F. J.; Polk, W. W.; Ellis, M. E.; Simmonds, P. L.; Kushleika, J. V.; Woods, J. S., Nuclear factor κ B activity determines the sensitivity of kidney epithelial cells to apoptosis: implications for mercury-induced renal failure. *Toxicological Sciences* **2004**, *82*, (1), 114-123.
215. Olivieri, G.; Novakovic, M.; Savaskan, E.; Meier, F.; Baysang, G.; Brockhaus, M.; Müller-Spahn, F., The effects of β -estradiol on SHSY5Y neuroblastoma cells during heavy metal induced oxidative stress, neurotoxicity and β -amyloid secretion. *Neuroscience* **2002**, *113*, (4), 849-855.
216. Cooke, M. S.; Evans, M. D.; Dizdaroglu, M.; Lunec, J., Oxidative DNA damage: mechanisms, mutation, and disease. *The FASEB Journal* **2003**, *17*, (10), 1195-1214.
217. Weitzman, S. A.; Turk, P. W.; Milkowski, D. H.; Kozlowski, K., Free radical adducts induce alterations in DNA cytosine methylation. *Proceedings of the National Academy of Sciences* **1994**, *91*, (4), 1261-1264.
218. Turk, P. W.; Laayoun, A.; Smith, S. S.; Weitzman, S. A., DNA adduct 8-hydroxyl-2'-deoxyguanosine (8-hydroxyguanine) affects function of human DNA methyltransferase. *Carcinogenesis* **1995**, *16*, (5), 1253-1255.
219. Franco, R.; Schoneveld, O.; Georgakilas, A. G.; Panayiotidis, M. I., Oxidative stress, DNA methylation and carcinogenesis. *Cancer letters* **2008**, *266*, (1), 6-11.
220. Gilmour, P. S.; Rahman, I.; Donaldson, K.; Macnee, W., Histone acetylation regulates epithelial IL-8 release mediated by oxidative stress from environmental particles. *American Journal of Physiology-Lung Cellular and Molecular Physiology* **2003**, *284*, (3), L533-L540.
221. Shimazu, T.; Hirschey, M. D.; Newman, J.; He, W.; Shirakawa, K.; Le Moan, N.; Grueter, C. A.; Lim, H.; Saunders, L. R.; Stevens, R. D., Suppression of oxidative

- stress by β -hydroxybutyrate, an endogenous histone deacetylase inhibitor. *Science* **2013**, *339*, (6116), 211-214.
222. Tsai, M.-C.; Manor, O.; Wan, Y.; Mosammamparast, N.; Wang, J. K.; Lan, F.; Shi, Y.; Segal, E.; Chang, H. Y., Long noncoding RNA as modular scaffold of histone modification complexes. *Science* **2010**, *329*, (5992), 689-693.
223. Lee, J. T., Epigenetic regulation by long noncoding RNAs. *Science* **2012**, *338*, (6113), 1435-1439.
224. Cedar, H.; Bergman, Y., Linking DNA methylation and histone modification: patterns and paradigms. *Nature Reviews Genetics* **2009**, *10*, (5), 295-304.
225. Conrad, D. F.; Keebler, J. E.; Depristo, M. A.; Lindsay, S. J.; Zhang, Y.; Cassals, F.; Idaghdour, Y.; Hartl, C. L.; Torroja, C.; Garimella, K. V., Variation in genome-wide mutation rates within and between human families. *Nature genetics* **2011**, *43*, (7), 712.
226. Kujoth, G.; Hiona, A.; Pugh, T.; Someya, S.; Panzer, K.; Wohlgemuth, S.; Hofer, T.; Seo, A.; Sullivan, R.; Jobling, W., Mitochondrial DNA mutations, oxidative stress, and apoptosis in mammalian aging. *Science* **2005**, *309*, (5733), 481-484.
227. Varriale, A.; Bernardi, G., DNA methylation and body temperature in fishes. *Gene* **2006**, *385*, 111-121.
228. Varriale, A.; Bernardi, G., DNA methylation in reptiles. *Gene* **2006**, *385*, 122-127.
229. Head, J. A.; Mittal, K.; Basu, N., Application of the LUMinometric Methylation Assay to ecological species: tissue quality requirements and a survey of DNA methylation levels in animals. *Molecular ecology resources* **2014**, *14*, (5), 943-952.
230. Barchet, G., A brief overview of metabolomics: What it means, how it is measured, and its utilization. *The Science Creative Quarterly* **2013**, *8*.
231. Locasale, J. W., Serine, glycine and one-carbon units: cancer metabolism in full circle. *Nature Reviews Cancer* **2013**, *13*, (8), 572-583.
232. Rhee, E. P.; Gerszten, R. E., Metabolomics and cardiovascular biomarker discovery. *Clinical chemistry* **2012**, *58*, (1), 139-147.
233. Mayr, M.; Grainger, D.; Mayr, U.; Leroyer, A. S.; Leseche, G.; Sidibe, A.; Herbin, O.; Yin, X.; Gomes, A.; Madhu, B., Proteomics, metabolomics, and immunomics on microparticles derived from human atherosclerotic plaques. *Circulation: Cardiovascular Genetics* **2009**, *2*, (4), 379-388.
234. Barderas, M. G.; Laborde, C. M.; Posada, M.; De La Cuesta, F.; Zubiri, I.; Vivanco, F.; Alvarez-Llamas, G., Metabolomic profiling for identification of novel potential biomarkers in cardiovascular diseases. *BioMed Research International* **2011**, *2011*.
235. Mayr, M.; Yusuf, S.; Weir, G.; Chung, Y.-L.; Mayr, U.; Yin, X.; Ladroue, C.; Madhu, B.; Roberts, N.; De Souza, A., Combined metabolomic and proteomic analysis of human atrial fibrillation. *Journal of the American College of Cardiology* **2008**, *51*, (5), 585-594.
236. Lin, C. Y.; Viant, M. R.; Tjeerdema, R. S., Metabolomics: methodologies and applications in the environmental sciences. *Journal of Pesticide Science* **2006**, *31*, (3), 245-251.

237. Bundy, J. G.; Davey, M. P.; Viant, M. R., Environmental metabolomics: a critical review and future perspectives. *Metabolomics* **2009**, *5*, (1), 3.
238. Jones, O. A.; Spurgeon, D. J.; Svendsen, C.; Griffin, J. L., A metabolomics based approach to assessing the toxicity of the polyaromatic hydrocarbon pyrene to the earthworm *Lumbricus rubellus*. *Chemosphere* **2008**, *71*, (3), 601-609.
239. Brown, S. A.; Mckelvie, J. R.; Simpson, A. J.; Simpson, M. J., ¹H NMR metabolomics of earthworm exposure to sub-lethal concentrations of phenanthrene in soil. *Environmental Pollution* **2010**, *158*, (6), 2117-2123.
240. Mckelvie, J. R.; Yuk, J.; Xu, Y.; Simpson, A. J.; Simpson, M. J., ¹H NMR and GC/MS metabolomics of earthworm responses to sub-lethal DDT and endosulfan exposure. *Metabolomics* **2009**, *5*, (1), 84-94.
241. Guo, Q.; Sidhu, J. K.; Ebbels, T. M.; Rana, F.; Spurgeon, D. J.; Svendsen, C.; Stürzenbaum, S. R.; Kille, P.; Morgan, A. J.; Bundy, J. G., Validation of metabolomics for toxic mechanism of action screening with the earthworm *Lumbricus rubellus*. *Metabolomics* **2009**, *5*, (1), 72-83.
242. Liu, X.; Zhang, L.; You, L.; Cong, M.; Zhao, J.; Wu, H.; Li, C.; Liu, D.; Yu, J., Toxicological responses to acute mercury exposure for three species of Manila clam *Ruditapes philippinarum* by NMR-based metabolomics. *Environmental toxicology and pharmacology* **2011**, *31*, (2), 323-332.
243. Liu, X.; Wu, H.; Ji, C.; Wei, L.; Zhao, J.; Yu, J., An integrated proteomic and metabolomic study on the chronic effects of mercury in *Suaeda salsa* under an environmentally relevant salinity. *PloS one* **2013**, *8*, (5), e64041.
244. Cappello, T.; Brandão, F.; Guilherme, S.; Santos, M. A.; Maisano, M.; Mauceri, A.; Canário, J.; Pacheco, M.; Pereira, P., Insights into the mechanisms underlying mercury-induced oxidative stress in gills of wild fish (*Liza aurata*) combining ¹H NMR metabolomics and conventional biochemical assays. *Science of the total environment* **2016**, *548*, 13-24.
245. Cappello, T.; Mauceri, A.; Corsaro, C.; Maisano, M.; Parrino, V.; Lo Paro, G.; Messina, G.; Fasulo, S., Impact of environmental pollution on caged mussels *Mytilus galloprovincialis* using NMR-based metabolomics. *Marine pollution bulletin* **2013**, *77*, (1), 132-139.
246. Liu, X.; Zhang, L.; You, L.; Yu, J.; Cong, M.; Wang, Q.; Li, F.; Li, L.; Zhao, J.; Li, C., Assessment of Clam *Ruditapes philippinarum* as Heavy Metal Bioindicators Using NMR-Based Metabolomics. *CLEAN–Soil, Air, Water* **2011**, *39*, (8), 759-766.
247. Wu, H.; Liu, X.; Zhao, J.; Yu, J., Toxicological responses in halophyte *Suaeda salsa* to mercury under environmentally relevant salinity. *Ecotoxicology and environmental safety* **2012**, *85*, 64-71.
248. Brandão, F.; Cappello, T.; Raimundo, J.; Santos, M. A.; Maisano, M.; Mauceri, A.; Pacheco, M.; Pereira, P., Unravelling the mechanisms of mercury hepatotoxicity in wild fish (*Liza aurata*) through a triad approach: bioaccumulation, metabolomic profiles and oxidative stress. *Metallomics* **2015**, *7*, (9), 1352-1363.

249. Chen, X.; Zhang, R.; Li, C.; Bao, Y., Mercury exposure modulates antioxidant enzymes in gill tissue and hemocytes of *Venerupis philippinarum*. *ISJ* **2014**, *11*, 298-308.
250. Van Vliet, E.; Morath, S.; Eskes, C.; Linge, J.; Rappsilber, J.; Honegger, P.; Hartung, T.; Coecke, S., A novel in vitro metabolomics approach for neurotoxicity testing, proof of principle for methyl mercury chloride and caffeine. *Neurotoxicology* **2008**, *29*, (1), 1-12.
251. Guillette Jr, L. J.; Crain, D. A.; Rooney, A. A.; Pickford, D. B., Organization versus activation: the role of endocrine-disrupting contaminants (EDCs) during embryonic development in wildlife. *Environmental Health Perspectives* **1995**, *103*, (Suppl 7), 157.
252. Crain, D. A.; Guillette, L., Reptiles as models of contaminant-induced endocrine disruption. *Animal reproduction science* **1998**, *53*, (1), 77-86.
253. Wilkinson, P. M.; Rainwater, T. R.; Woodward, A. R.; Leone, E. H.; Carter, C., Determinate Growth and Reproductive Lifespan in the American Alligator (*Alligator mississippiensis*): Evidence from Long-term Recaptures. *Copeia* **2016**, *104*, (4), 843-852.
254. Bergeron, C. M.; Husak, J. F.; Unrine, J. M.; Romanek, C. S.; Hopkins, W. A., Influence of feeding ecology on blood mercury concentrations in four species of turtles. *Environmental toxicology and chemistry* **2007**, *26*, (8), 1733-1741.
255. Rimmer, C. C.; Mcfarland, K. P.; Evers, D. C.; Miller, E. K.; Aubry, Y.; Busby, D.; Taylor, R. J., Mercury concentrations in Bicknell's thrush and other insectivorous passerines in montane forests of northeastern North America. *Ecotoxicology* **2005**, *14*, (1-2), 223-240.
256. Osenberg, C. W.; Schmitt, R. J.; Holbrook, S. J.; Abu-Saba, K. E.; Flegal, A. R., Detection of environmental impacts: natural variability, effect size, and power analysis. *Ecological applications* **1994**, *4*, (1), 16-30.
257. Nakagawa, S.; Cuthill, I. C., Effect size, confidence interval and statistical significance: a practical guide for biologists. *Biological reviews* **2007**, *82*, (4), 591-605.
258. Buhl-Mortensen, L., Type-II statistical errors in environmental science and the precautionary principle. *Marine pollution bulletin* **1996**, *32*, (7), 528-531.
259. Ellis, D. V., The precautionary principle and environmental monitoring. *Marine pollution bulletin* **2003**, *46*, (8), 933-934.
260. Gerard, P. D.; Smith, D. R.; Weerakkody, G., Limits of retrospective power analysis. *The Journal of Wildlife Management* **1998**, 801-807.
261. Cherry, S., Statistical tests in publications of The Wildlife Society. *Wildlife Society Bulletin (1973-2006)* **1998**, *26*, (4), 947-953.
262. Steidl, R. J.; Hayes, J. P.; Schaubert, E., Statistical power analysis in wildlife research. *The Journal of Wildlife Management* **1997**, 270-279.
263. Hoenig, J. M.; Heisey, D. M., The abuse of power: the pervasive fallacy of power calculations for data analysis. *The American Statistician* **2001**, *55*, (1), 19-24.
264. Nakagawa, S., A farewell to Bonferroni: the problems of low statistical power and publication bias. *Behavioral ecology* **2004**, *15*, (6), 1044-1045.

265. Cameron, J.; Abouchar, J., The precautionary principle: a fundamental principle of law and policy for the protection of the global environment. *BC Int'l & Comp. L. Rev.* **1991**, *14*, 1.
266. Hickey Jr, J. E.; Walker, V. R., Refining the precautionary principle in international environmental law. *Virginia Environmental Law Journal* **1995**, 423-454.
267. Iso, I.; Biplm, I.; Ifcc, I.; Iupap, O., Evaluation of Measurement Data—Guide to the Expression of Uncertainty in Measurement GUM 1995 with minor corrections. *Joint Committee for Guides in Metrology, JCGM* **2008**, *100*.
268. Julian, P.; Gu, B.; Redfield, G.; Weaver, K.; Lange, T.; Frederick, P.; Mccray, J. M.; Wright, A. L.; Dierberg, F. E.; Debusk, T. A.; Jerauld, M.; Debusk, W. F.; Bae, H.-S.; Ogram, A., Chapter 3B: Mercury and sulfur environmental assessment for the everglades. *South Florida Environmental Report. South Florida Water Management District, West Palm Beach, FL* **2015**.
269. Burch, J. B.; Robb, S. W.; Puett, R.; Cai, B.; Wilkerson, R.; Karmaus, W.; Vena, J.; Svendsen, E., Mercury in fish and adverse reproductive outcomes: results from South Carolina. *International journal of health geographics* **2014**, *13*, (1), 30.
270. Ralston, N. V.; Raymond, L. J., Dietary selenium's protective effects against methylmercury toxicity. *Toxicology* **2010**, *278*, (1), 112-123.
271. Cuvin-Aralar, M. L. A.; Furness, R. W., Mercury and selenium interaction: a review. *Ecotoxicology and environmental safety* **1991**, *21*, (3), 348-364.
272. Peterson, S. A.; Ralston, N. V.; Whanger, P. D.; Oldfield, J. E.; Mosher, W. D., Selenium and mercury interactions with emphasis on fish tissue. *Environmental Bioindicators* **2009**, *4*, (4), 318-334.
273. Gray, R.; Canfield, P.; Rogers, T., Trace element analysis in the serum and hair of Antarctic leopard seal, *Hydrurga leptonyx*, and Weddell seal, *Leptonychotes weddellii*. *Science of the total environment* **2008**, *399*, (1), 202-215.
274. Ikemoto, T.; Kunito, T.; Watanabe, I.; Yasunaga, G.; Baba, N.; Miyazaki, N.; Petrov, E. A.; Tanabe, S., Comparison of trace element accumulation in Baikal seals (*Pusa sibirica*), Caspian seals (*Pusa caspica*) and northern fur seals (*Callorhinus ursinus*). *Environmental Pollution* **2004**, *127*, (1), 83-97.
275. Fraga, C. G., Relevance, essentiality and toxicity of trace elements in human health. *Molecular aspects of medicine* **2005**, *26*, (4), 235-244.
276. Almlı, B.; Mwase, M.; Sivertsen, T.; M Musonda, M.; Flaoyen, A., Hepatic and renal concentrations of 10 trace elements in crocodiles (*Crocodylus niloticus*) in the Kafue and Luangwa rivers in Zambia. *Science of the total environment* **2005**, *337*, (1), 75-82.
277. Davison, R. L.; Natusch, D. F.; Wallace, J. R.; Evans Jr, C. A., Trace elements in fly ash. Dependence of concentration on particle size. *Environmental science & technology* **1974**, *8*, (13), 1107-1113.
278. Salomons, W., Environmental impact of metals derived from mining activities: processes, predictions, prevention. *Journal of Geochemical exploration* **1995**, *52*, (1), 5-23.
279. Dietz, R.; Rıget, F.; Johansen, P., Lead, cadmium, mercury and selenium in Greenland marine animals. *Science of the total environment* **1996**, *186*, (1), 67-93.

280. Keller, J. M.; Balazs, G. H.; Nilsen, F.; Rice, M.; Work, T. M.; Jensen, B. A., Investigating the potential role of persistent organic pollutants in Hawaiian green sea turtle fibropapillomatosis. *Environmental science & technology* **2014**, *48*, (14), 7807-7816.
281. Burger, J.; Gochfeld, M., Mercury and selenium levels in 19 species of saltwater fish from New Jersey as a function of species, size, and season. *Science of the total environment* **2011**, *409*, (8), 1418-1429.
282. Fang, G.; Nam, D.; Basu, N., Mercury and selenium content of Taiwanese seafood. *Food Additives and Contaminants: Part B* **2011**, *4*, (3), 212-217.
283. Storelli, M.; Ceci, E.; Marcotrigiano, G., Comparison of total mercury, methylmercury, and selenium in muscle tissues and in the liver of *Stenella coeruleoalba* (Meyen) and *Caretta caretta* (Linnaeus). *Bulletin of environmental contamination and toxicology* **1998**, *61*, (4), 541-547.
284. Mjöberg, B.; Hellquist, E.; Mallmin, H.; Lindh, U., Aluminum, Alzheimer's disease and bone fragility. *Acta Orthopaedica Scandinavica* **1997**, *68*, (6), 511-514.
285. Hopkins, W.; Roe, J.; Snodgrass, J.; Jackson, B.; Kling, D.; Rowe, C.; Congdon, J., Nondestructive indices of trace element exposure in squamate reptiles. *Environmental Pollution* **2001**, *115*, (1), 1-7.
286. Loumbourdis, N., Heavy metal contamination in a lizard, *Agama stellio stellio*, compared in urban, high altitude and agricultural, low altitude areas of North Greece. *Bulletin of environmental contamination and toxicology* **1997**, *58*, (6), 945-952.
287. Lázaro, W. L.; De Oliveira, R. F.; Dos Santos-Filho, M.; Da Silva, C. J.; Malm, O.; Ignácio, Á. R.; Díez, S., Non-lethal sampling for mercury evaluation in crocodylians. *Chemosphere* **2015**, *138*, 25-32.
288. Myburgh, J. G.; Kirberger, R. M.; Steyl, J. C.; Soley, J. T.; Booyse, D. G.; Huchzermeyer, F. W.; Lowers, R. H.; Guillette Jr, L. J., The post-occipital spinal venous sinus of the Nile crocodile (*Crocodylus niloticus*): its anatomy and use for blood sample collection and intravenous infusions: original research. *Journal of the South African Veterinary Association* **2014**, *85*, (1), 1-10.
289. Day, R. D.; Christopher, S. J.; Becker, P. R.; Whitaker, D. W., Monitoring mercury in the loggerhead sea turtle, *Caretta caretta*. *Environmental science & technology* **2005**, *39*, (2), 437-446.
290. Eggins, S.; Schneider, L.; Krikowa, F.; Vogt, R. C.; Silveira, R. D.; Maher, W., Mercury concentrations in different tissues of turtle and caiman species from the Rio Purus, Amazonas, Brazil. *Environmental toxicology and chemistry* **2015**, *34*, (12), 2771-2781.
291. Tchounwou, P. B.; Yedjou, C. G.; Patlolla, A. K.; Sutton, D. J., Heavy metal toxicity and the environment. In *Molecular, clinical and environmental toxicology*, Springer: 2012; pp 133-164.
292. Kobal, A. B.; Horvat, M.; Prezelj, M.; Briški, A. S.; Krsnik, M.; Dizdarevič, T.; Mazej, D.; Falnoga, I.; Stibilj, V.; Arnerič, N., The impact of long-term past exposure to elemental mercury on antioxidative capacity and lipid peroxidation in

- mercury miners. *Journal of Trace Elements in Medicine and Biology* **2004**, *17*, (4), 261-274.
293. Carmignani, M.; Boscolo, P.; Artese, L.; Del Rosso, G.; Porcelli, G.; Felaco, M.; Volpe, A. R.; Giuliano, G., Renal mechanisms in the cardiovascular effects of chronic exposure to inorganic mercury in rats. *British journal of industrial medicine* **1992**, *49*, (4), 226-232.
294. Born, E. W.; Renzoni, A.; Dietz, R., Total mercury in hair of polar bears (*Ursus maritimus*) from Greenland and Svalbard. *Polar research* **1991**, *9*, (2), 113-120.
295. Day, R. D. Mercury in loggerhead sea turtles, *Caretta caretta*: Developing monitoring strategies, investigating factors affecting contamination, and assessing health impacts. COLLEGE OF CHARLESTON, 2003.
296. Mazzotti, F. J.; Brandt, L. A., Ecology of the American alligator in a seasonally fluctuating environment. *Everglades: The ecosystem and its restoration* **1994**, 485-505.
297. Rainwater, T. R.; Adair, B. M.; Platt, S. G.; Anderson, T.; Cobb, G. P.; Mcmurry, S. T., Mercury in Morelet's crocodile eggs from northern Belize. *Archives of environmental contamination and toxicology* **2002**, *42*, (3), 319-324.
298. Stoneburner, D.; Kushlan, J., Heavy metal burdens in American crocodile eggs from Florida Bay, Florida, USA. *Journal of herpetology* **1984**, *18*, (2), 192-193.
299. Guentzel, J.; Landing, W.; Gill, G.; Pollman, C., Atmospheric deposition of mercury in Florida: the FAMS project (1992–1994). *Water, Air, and Soil Pollution* **1995**, *80*, (1-4), 393-402.
300. Sexauer Gustin, M.; Weiss-Penzias, P. S.; Peterson, C., Investigating sources of gaseous oxidized mercury in dry deposition at three sites across Florida, USA. *Atmospheric Chemistry and Physics* **2012**, *12*, (19), 9201-9219.
301. Jepson, P. D.; Bennett, P. M.; Deaville, R.; Allchin, C. R.; Baker, J. R.; Law, R. J., Relationships between polychlorinated biphenyls and health status in harbor porpoises (*Phocoena phocoena*) stranded in the United Kingdom. *Environmental toxicology and chemistry* **2005**, *24*, (1), 238-248.
302. Guillette Jr, L. J.; Gross, T. S.; Masson, G. R.; Matter, J. M.; Percival, H. F.; Woodward, A. R., Developmental abnormalities of the gonad and abnormal sex hormone concentrations in juvenile alligators from contaminated and control lakes in Florida. *Environmental Health Perspectives* **1994**, *102*, (8), 680.
303. Green, A. D.; Buhlmann, K. A.; Hagen, C.; Gibbons, J. W. In *Tissue distribution and maternal transfer of mercury in diamondback terrapins with implications for human health*, 2010 South Carolina Water Resources Conference, Columbia Metropolitan Convention Center, 2010; Columbia Metropolitan Convention Center, 2010.
304. Sandovici, I.; Smith, N. H.; Nitert, M. D.; Ackers-Johnson, M.; Uribe-Lewis, S.; Ito, Y.; Jones, R. H.; Marquez, V. E.; Cairns, W.; Tadayyon, M., Maternal diet and aging alter the epigenetic control of a promoter–enhancer interaction at the *Hnf4a* gene in rat pancreatic islets. *Proceedings of the National Academy of Sciences* **2011**, *108*, (13), 5449-5454.
305. Grandjean, P.; Weihe, P.; Jørgensen, P.; Clarkson, T.; Cernichiari, E.; Viderø, T., Impact of maternal seafood diet on fetal exposure to mercury, selenium, and lead.

- Archives of Environmental Health: An International Journal* **1992**, 47, (3), 185-195.
306. Roe, J. H.; Hopkins, W. A.; Baionno, J. A.; Staub, B. P.; Rowe, C. L.; Jackson, B. P., Maternal transfer of selenium in Alligator mississippiensis nesting downstream from a coal-burning power plant. *Environmental toxicology and chemistry* **2004**, 23, (8), 1969-1972.
 307. Needham, L. L.; Grandjean, P.; Heinzow, B.; Jørgensen, P. J.; Nielsen, F.; Patterson Jr, D. G.; SjöDin, A.; Turner, W. E.; Weihe, P., Partition of environmental chemicals between maternal and fetal blood and tissues. *Environmental science & technology* **2010**, 45, (3), 1121-1126.
 308. Lyons, K.; Lowe, C. G., Mechanisms of maternal transfer of organochlorine contaminants and mercury in the common thresher shark (*Alopias vulpinus*). *Canadian Journal of Fisheries and Aquatic Sciences* **2013**, 70, (12), 1667-1672.
 309. Latif, M.; Bodaly, R.; Johnston, T.; Fudge, R., Effects of environmental and maternally derived methylmercury on the embryonic and larval stages of walleye (*Stizostedion vitreum*). *Environmental Pollution* **2001**, 111, (1), 139-148.
 310. Johnston, T.; Bodaly, R.; Latif, M.; Fudge, R.; Strange, N., Intra- and interpopulation variability in maternal transfer of mercury to eggs of walleye (*Stizostedion vitreum*). *Aquatic Toxicology* **2001**, 52, (1), 73-85.
 311. Cooney, C. A.; Dave, A. A.; Wolff, G. L., Maternal methyl supplements in mice affect epigenetic variation and DNA methylation of offspring. *The Journal of nutrition* **2002**, 132, (8), 2393S-2400S.
 312. Habran, S.; Debier, C.; Crocker, D. E.; Houser, D. S.; Das, K., Blood dynamics of mercury and selenium in northern elephant seals during the lactation period. *Environmental Pollution* **2011**, 159, (10), 2523-2529.
 313. Sakamoto, M.; Chan, H. M.; Domingo, J. L.; Kubota, M.; Murata, K., Changes in body burden of mercury, lead, arsenic, cadmium and selenium in infants during early lactation in comparison with placental transfer. *Ecotoxicology and environmental safety* **2012**, 84, 179-184.
 314. Ferguson, M., Post-laying stages of embryonic development for crocodilians. *Wildlife management: crocodiles and alligators* **1987**, 427-444.
 315. Astheimer, L. B.; Manolis, S. C.; Grau, C., Egg formation in crocodiles: avian affinities in yolk deposition. *Copeia* **1989**, 1989, (1), 221-224.
 316. Muller, J. K.; Gross, T. S.; Borgert, C. J., Topical dose delivery in the reptilian egg treatment model. *Environmental toxicology and chemistry* **2007**, 26, (5), 914-919.
 317. Powell, D.; Aulerich, R.; Meadows, J.; Tillitt, D.; Giesy, J.; Stromborg, K.; Bursian, S., Effects of 3, 3', 4, 4', 5-pentachlorobiphenyl (PCB 126) and 2, 3, 7, 8-tetrachlorodibenzo-p-dioxin (TCDD) injected into the yolks of chicken (*Gallus domesticus*) eggs prior to incubation. *Archives of environmental contamination and toxicology* **1996**, 31, (3), 404-409.
 318. Roos, D. H.; Puntel, R. L.; Lugokenski, T. H.; Ineu, R. P.; Bohrer, D.; Burger, M. E.; Franco, J. L.; Farina, M.; Aschner, M.; Rocha, J. B. T., Complex methylmercury–cysteine alters mercury accumulation in different tissues of mice. *Basic & clinical pharmacology & toxicology* **2010**, 107, (4), 789-792.

319. Podreka, S.; Georges, A.; Maher, B.; Limpus, C. J., The environmental contaminant DDE fails to influence the outcome of sexual differentiation in the marine turtle *Chelonia mydas*. *Environmental Health Perspectives* **1998**, *106*, (4), 185.
320. Cruze, L.; Roark, A. M.; Rolland, G.; Younas, M.; Stacy, N.; Guillette, L. J., Endogenous and exogenous estrogens during embryonic development affect timing of hatch and growth in the American alligator (*Alligator mississippiensis*). *Comparative Biochemistry and Physiology Part B: Biochemistry and Molecular Biology* **2015**, *184*, 10-18.
321. Eteshola, E., Antioxidant Mechanisms of Glutathione against Metal-Mediated Oxidative DNA Damage. **2015**.
322. Schulz, J. B.; Lindenau, J.; Seyfried, J.; Dichgans, J., Glutathione, oxidative stress and neurodegeneration. *The FEBS Journal* **2000**, *267*, (16), 4904-4911.
323. Di Giacomo, M.; Comazzetto, S.; Saini, H.; De Fazio, S.; Carrieri, C.; Morgan, M.; Vasiliauskaite, L.; Benes, V.; Enright, A. J.; O'carroll, D., Multiple epigenetic mechanisms and the piRNA pathway enforce LINE1 silencing during adult spermatogenesis. *Mol Cell* **2013**, *50*, (4), 601-8.
324. Rodriguez, J.; Frigola, J.; Vendrell, E.; Risques, R. A.; Fraga, M. F.; Morales, C.; Moreno, V.; Esteller, M.; Capella, G.; Ribas, M.; Peinado, M. A., Chromosomal instability correlates with genome-wide DNA demethylation in human primary colorectal cancers. *Cancer research* **2006**, *66*, (17), 8462-9468.
325. Brandeis, M.; Ariel, M.; Cedar, H., Dynamics of DNA methylation during development. *Bioessays* **1993**, *15*, (11), 709-713.
326. Macdonald, W. A.; Mann, M. R., Epigenetic regulation of genomic imprinting from germ line to preimplantation. *Mol Reprod Dev* **2014**, *81*, (2), 126-40.
327. Bollati, V.; Schwartz, J.; Wright, R.; Litonjua, A.; Tarantini, L.; Suh, H.; Sparrow, D.; Vokonas, P.; Baccarelli, A., Decline in genomic DNA methylation through aging in a cohort of elderly subjects. *Mechanisms of ageing and development* **2009**, *130*, (4), 234-9.
328. Hannum, G.; Guinney, J.; Zhao, L.; Zhang, L.; Hughes, G.; Sada, S.; Klotzle, B.; Bibikova, M.; Fan, J. B.; Gao, Y.; Deconde, R.; Chen, M.; Rajapakse, I.; Friend, S.; Ideker, T.; Zhang, K., Genome-wide methylation profiles reveal quantitative views of human aging rates. *Molecular cell* **2013**, *49*, (2), 359-67.
329. Heyn, H.; Li, N.; Ferreira, H. J.; Moran, S.; Pisano, D. G.; Gomez, A.; Diez, J.; Sanchez-Mut, J. V.; Setien, F.; Carmona, F. J.; Puca, A. A.; Sayols, S.; Pujana, M. A.; Serra-Musach, J.; Iglesias-Platas, I.; Formiga, F.; Fernandez, A. F.; Fraga, M. F.; Heath, S. C.; Valencia, A.; Gut, I. G.; Wang, J.; Esteller, M., Distinct DNA methylomes of newborns and centenarians. *Proceedings of the National Academy of Sciences of the United States of America* **2012**, *109*, (26), 10522-7.
330. Fuke, C.; Shimabukuro, M.; Petronis, A.; Sugimoto, J.; Oda, T.; Miura, K.; Miyazaki, T.; Ogura, C.; Okazaki, Y.; Jinno, Y., Age related changes in 5-methylcytosine content in human peripheral leukocytes and placentas: an HPLC-based study. *Annals of human genetics* **2004**, *68*, (Pt 3), 196-204.
331. Christensen, B. C.; Houseman, E. A.; Marsit, C. J.; Zheng, S.; Wrensch, M. R.; Wiemels, J. L.; Nelson, H. H.; Karagas, M. R.; Padbury, J. F.; Bueno, R.;

- Sugarbaker, D. J.; Yeh, R. F.; Wiencke, J. K.; Kelsey, K. T., Aging and environmental exposures alter tissue-specific DNA methylation dependent upon CpG island context. *PLOS Genet.* **2009**, *5*, (8), e1000602.
332. Dolinoy, D. C.; Huang, D.; Jirtle, R. L., Maternal nutrient supplementation counteracts bisphenol A-induced DNA hypomethylation in early development. *Proceedings of the National Academy of Sciences* **2007**, *104*, (32), 13056-13061.
333. Bromer, J. G.; Zhou, Y.; Taylor, M. B.; Doherty, L.; Taylor, H. S., Bisphenol-A exposure in utero leads to epigenetic alterations in the developmental programming of uterine estrogen response. *FASEB journal : official publication of the Federation of American Societies for Experimental Biology* **2010**, *24*, (7), 2273-80.
334. Rusiecki, J. A.; Baccarelli, A.; Bollati, V.; Tarantini, L.; Moore, L. E.; Bonefeld-Jorgensen, E. C., Global DNA hypomethylation is associated with high serum-persistent organic pollutants in Greenlandic Inuit. *Environ Health Perspect* **2008**, *116*, (11), 1547-1552.
335. Guo, L.; Byun, H. M.; Zhong, J.; Motta, V.; Barupal, J.; Zheng, Y.; Dou, C.; Zhang, D.; Zhang, F.; Mccracken, J. P.; Diaz, A.; Marco, A.-G.; Colicino, S.; Schwartz, J.; Wang, S.; Hou, L.; Baccarelli, A., Effects of short-term exposure to inhalable particulate matter on DNA methylation of tandem repeats. *Environmental and Molecular Mutagenesis* **2014**, *55*, (4), 322-335.
336. Quinlivan, E. P.; Gregory, J. F., DNA methylation determination by liquid chromatography–tandem mass spectrometry using novel biosynthetic [U-15N] deoxycytidine and [U-15N] methyldeoxycytidine internal standards. *Nucleic acids research* **2008**, *36*, (18), e119-e119.
337. Hanna, C. W.; Bloom, M. S.; Robinson, W. P.; Kim, D.; Parsons, P. J.; Vom Saal, F. S.; Taylor, J. A.; Steuerwald, A. J.; Fujimoto, V. Y., DNA methylation changes in whole blood is associated with exposure to the environmental contaminants, mercury, lead, cadmium and bisphenol A, in women undergoing ovarian stimulation for IVF. *Human reproduction* **2012**, *27*, (5), 1401-1410.
338. Croes, K.; De Coster, S.; De Galan, S.; Morrens, B.; Loots, I.; Van De Mierop, E.; Nelen, V.; Sioen, I.; Bruckers, L.; Nawrot, T., Health effects in the Flemish population in relation to low levels of mercury exposure: from organ to transcriptome level. *International journal of hygiene and environmental health* **2014**, *217*, (2), 239-247.
339. Hou, L.; Zhang, X.; Wang, D.; Baccarelli, A., Environmental chemical exposures and human epigenetics. *International journal of epidemiology* **2011**, *41*, (1), 79-105.
340. Glasel, J., Validity of nucleic acid purities monitored by 260nm/280nm absorbance ratios. *Biotechniques* **1995**, *18*, (1), 62-63.
341. Quinlivan, E. P.; Gregory, J. F., DNA digestion to deoxyribonucleoside: a simplified one-step procedure. *Analytical biochemistry* **2008**, *373*, (2), 383-385.
342. Asih, A. S. O. I. a. H., Guidelines for use of live amphibians and reptiles in field and laboratory research. *Herpetological Animal Care and Use Committee of the ASIH, Washington, DC* **2004**.

343. Fdep, F. D. O. E. P. D. O. W. R. M. a. E. a. a. R. Florida Watersheds and River Basins Map. <http://www.protectingourwater.org/watersheds/map/>
344. Choi, A. L.; Weihe, P.; Budtz-Jørgensen, E.; Jørgensen, P. J.; Salonen, J. T.; Tuomainen, T.-P.; Murata, K.; Nielsen, H. P.; Petersen, M. S.; Askham, J., Methylmercury exposure and adverse cardiovascular effects in Faroese whaling men. *Environmental Health Perspectives* **2009**, *117*, (3), 367.
345. Robinet, T. T.; Feunteun, E. E., Sublethal effects of exposure to chemical compounds: a cause for the decline in Atlantic eels? *Ecotoxicology* **2002**, *11*, (4), 265-277.
346. Brasso, R. L.; Cristol, D. A., Effects of mercury exposure on the reproductive success of tree swallows (*Tachycineta bicolor*). *Ecotoxicology* **2008**, *17*, (2), 133-141.
347. Hopkins, B. C.; Willson, J. D.; Hopkins, W. A., Mercury exposure is associated with negative effects on turtle reproduction. *Environmental science & technology* **2013**, *47*, (5), 2416-2422.
348. Niculescu, M. D.; Zeisel, S. H., Diet, methyl donors and DNA methylation: interactions between dietary folate, methionine and choline. *The Journal of nutrition* **2002**, *132*, (8), 2333S-2335S.
349. Fortin, C.; Beauchamp, G.; Dansereau, M.; Lariviere, N.; Belanger, D., Spatial variation in mercury concentrations in wild mink and river otter carcasses from the James Bay Territory, Quebec, Canada. *Archives of environmental contamination and toxicology* **2001**, *40*, (1), 121-127.
350. Patrick, L., Mercury toxicity and antioxidants: part i: role of glutathione and alpha-lipoic acid in the treatment of mercury toxicity-mercury toxicity. *Toxicol Appl Pharmacol* **2002**, *7*, 456-471.
351. Chen, R. Z.; Pettersson, U.; Beard, C.; Jackson-Grusby, L.; Jaenisch, R., DNA hypomethylation leads to elevated mutation rates. *Nature* **1998**, *395*, (6697), 89-93.
352. Padmanabhan, N.; Jia, D.; Geary-Joo, C.; Wu, X.; Ferguson-Smith, A. C.; Fung, E.; Bieda, M. C.; Snyder, F. F.; Gravel, R. A.; Cross, J. C., Mutation in folate metabolism causes epigenetic instability and transgenerational effects on development. *Cell* **2013**, *155*, (1), 81-93.
353. Schwenter, J. A. Monitoring Mercury in the Diamondback Terrapin (*Malaclemys terrapin*): Kinetics and Accumulation of an Emerging Global Contaminant. The College of Charleston, 2007.
354. Head, J. A., Patterns of DNA methylation in animals: an ecotoxicological perspective. *Integrative and comparative biology* **2014**, icu025.
355. Jirtle, R. L.; Skinner, M. K., Environmental epigenomics and disease susceptibility. *Nature reviews. Genetics* **2007**, *8*, (4), 253.
356. Esteller, M., Cancer epigenomics: DNA methylomes and histone-modification maps. *Nature reviews. Genetics* **2007**, *8*, (4), 286.
357. Davis, C. D.; Uthus, E. O., DNA methylation, cancer susceptibility, and nutrient interactions. *Experimental biology and medicine* **2004**, *229*, (10), 988-995.

358. Goodrich, J. M.; Basu, N.; Franzblau, A.; Dolinoy, D. C., Mercury biomarkers and DNA methylation among Michigan dental professionals. *Environmental and Molecular Mutagenesis* **2013**, *54*, (3), 195-203.
359. Baccarelli, A.; Bollati, V., Epigenetics and environmental chemicals. *Current opinion in pediatrics* **2009**, *21*, (2), 243.
360. Sidoli, S.; Bhanu, N. V.; Karch, K. R.; Wang, X.; Garcia, B. A., Complete workflow for analysis of histone post-translational modifications using bottom-up mass spectrometry: from histone extraction to data analysis. *Journal of visualized experiments: JoVE* **2016**, (111).
361. Cortessis, V. K.; Thomas, D. C.; Levine, A. J.; Breton, C. V.; Mack, T. M.; Siegmund, K. D.; Haile, R. W.; Laird, P. W., Environmental epigenetics: prospects for studying epigenetic mediation of exposure–response relationships. *Human genetics* **2012**, *131*, (10), 1565-1589.
362. Rakyan, V.; Whitelaw, E., Transgenerational epigenetic inheritance. *Current Biology* **2003**, *13*, (1), R6.
363. Kakutani, T.; Jeddeloh, J. A.; Flowers, S. K.; Munakata, K.; Richards, E. J., Developmental abnormalities and epimutations associated with DNA hypomethylation mutations. *Proceedings of the National Academy of Sciences* **1996**, *93*, (22), 12406-12411.
364. Ariza, M. E.; Williams, M. V., Lead and mercury mutagenesis: type of mutation dependent upon metal concentration. *J BIOCHEM* **1999**, *13*, (2).
365. Schurz, F.; Sabater-Vilar, M.; Fink-Gremmels, J., Mutagenicity of mercury chloride and mechanisms of cellular defence: the role of metal-binding proteins. *Mutagenesis* **2000**, *15*, (6), 525-530.
366. Frederick, P. C.; Spalding, M. G.; Sepälveda, M. S.; Williams, G. E.; Nico, L.; Robins, R., Exposure of great egret (*Ardea albus*) nestlings to mercury through diet in the Everglades ecosystem. *Environmental toxicology and chemistry* **1999**, *18*, (9), 1940-1947.
367. Veenstra, T. D., Metabolomics: the final frontier? *Genome medicine* **2012**, *4*, (4), 40.
368. Zhang, A.; Sun, H.; Wang, P.; Han, Y.; Wang, X., Modern analytical techniques in metabolomics analysis. *Analyst* **2012**, *137*, (2), 293-300.
369. Hirai, M. Y.; Klein, M.; Fujikawa, Y.; Yano, M.; Goodenowe, D. B.; Yamazaki, Y.; Kanaya, S.; Nakamura, Y.; Kitayama, M.; Suzuki, H., Elucidation of gene-to-gene and metabolite-to-gene networks in *Arabidopsis* by integration of metabolomics and transcriptomics. *Journal of Biological Chemistry* **2005**, *280*, (27), 25590-25595.
370. Cappello, T.; Pereira, P.; Maisano, M.; Mauceri, A.; Pacheco, M.; Fasulo, S., Advances in understanding the mechanisms of mercury toxicity in wild golden grey mullet (*Liza aurata*) by ¹H NMR-based metabolomics. *Environmental Pollution* **2016**, *219*, 139-148.
371. Holmes, P.; James, K.; Levy, L., Is low-level environmental mercury exposure of concern to human health? *Science of the total environment* **2009**, *408*, (2), 171-182.

372. Clarkson, T. W.; Magos, L., The toxicology of mercury and its chemical compounds. *CRC Critical Reviews in Toxicology* **2006**, *36*, (8), 609-662.
373. Brockmeier, E. K.; Hodges, G.; Hutchinson, T. H.; Butler, E.; Hecker, M.; Tollefson, K. E.; Garcia-Reyero, N.; Kille, P.; Becker, D.; Chipman, K., The Role of Omics in the Application of Adverse Outcome Pathways for Chemical Risk Assessment. *Toxicological Sciences* **2017**, kfx097.
374. Williams, T. D.; Turan, N.; Diab, A. M.; Wu, H.; Mackenzie, C.; Bartie, K. L.; Hrydziusko, O.; Lyons, B. P.; Stentiford, G. D.; Herbert, J. M., Towards a system level understanding of non-model organisms sampled from the environment: a network biology approach. *PLoS computational biology* **2011**, *7*, (8), e1002126.
375. Roosenburg, W. M. In *The diamondback terrapin: population dynamics, habitat requirements, and opportunities for conservation*, New Perspectives in the Chesapeake System: A Research and Management Partnership. Proceedings of a Conference. CRC Publ, 1991; 1991; pp 227-234.
376. Nilsen, F. M.; Kassim, B. L.; Delaney, J. P.; Lange, T. R.; Brunell, A. M.; Guillette, L. J.; Long, S. E.; Schock, T. B., Trace element biodistribution in the American alligator (*Alligator mississippiensis*). *Chemosphere* **2017**.
377. Pedrero, Z.; Ouerdane, L.; Mounicou, S.; Lobinski, R.; Monperrus, M.; Amouroux, D., Identification of mercury and other metals complexes with metallothioneins in dolphin liver by hydrophilic interaction liquid chromatography with the parallel detection by ICP MS and electrospray hybrid linear/orbital trap MS/MS. *Metallomics* **2012**, *4*, (5), 473-479.
378. Belyaeva, E. A.; Korotkov, S. M.; Saris, N.-E., < i> In vitro</i> modulation of heavy metal-induced rat liver mitochondria dysfunction: A comparison of copper and mercury with cadmium. *Journal of Trace Elements in Medicine and Biology* **2011**, *25*, S63-S73.
379. Naz, S.; Vallejo, M.; García, A.; Barbas, C., Method validation strategies involved in non-targeted metabolomics. *Journal of chromatography A* **2014**, *1353*, 99-105.
380. Beckonert, O.; Keun, H. C.; Ebbels, T. M.; Bundy, J.; Holmes, E.; Lindon, J. C.; Nicholson, J. K., Metabolic profiling, metabolomic and metabonomic procedures for NMR spectroscopy of urine, plasma, serum and tissue extracts. *Nature protocols* **2007**, *2*, (11), 2692.
381. Weckwerth, W., *Metabolomics: methods and protocols*. Springer Science & Business Media: 2007; Vol. 358.
382. Le Gall, G., Sample collection and preparation of biofluids and extracts for NMR spectroscopy. *Metabonomics: Methods and Protocols* **2015**, 15-28.
383. Lin, C. Y.; Wu, H.; Tjeerdema, R. S.; Viant, M. R., Evaluation of metabolite extraction strategies from tissue samples using NMR metabolomics. *Metabolomics* **2007**, *3*, (1), 55-67.
384. Bligh, E. G.; Dyer, W. J., A rapid method of total lipid extraction and purification. *Canadian journal of biochemistry and physiology* **1959**, *37*, (8), 911-917.

385. McKay, R. T., How the 1D-NOESY suppresses solvent signal in metabonomics NMR spectroscopy: An examination of the pulse sequence components and evolution. *Concepts in Magnetic Resonance Part A* **2011**, 38, (5), 197-220.
386. Wu, S., 1D and 2D NMR Experiment Methods. *Emory University* **2011**.
387. Loss, S. K.; Till, *Introduction to 1- and 2-dimensional NMR Spectroscopy Version 001 Bruker*. 2005.
388. Parsons, H. M.; Ekman, D. R.; Collette, T. W.; Viant, M. R., Spectral relative standard deviation: a practical benchmark in metabolomics. *Analyst* **2009**, 134, (3), 478-485.
389. Craig, A.; Cloarec, O.; Holmes, E.; Nicholson, J. K.; Lindon, J. C., Scaling and normalization effects in NMR spectroscopic metabonomic data sets. *Analytical chemistry* **2006**, 78, (7), 2262-2267.
390. Friebolin, H.; Beconsall, J. K., *Basic one- and two-dimensional NMR spectroscopy*. VCH Weinheim: 1993.
391. Abdi, H.; Williams, L. J., Principal component analysis. *Wiley interdisciplinary reviews: computational statistics* **2010**, 2, (4), 433-459.
392. Shlens, J., A tutorial on principal component analysis. *arXiv preprint arXiv:1404.1100* **2014**.
393. Candès, E. J.; Li, X.; Ma, Y.; Wright, J., Robust principal component analysis? *Journal of the ACM (JACM)* **2011**, 58, (3), 11.
394. Benjamini, Y.; Hochberg, Y., Controlling the false discovery rate: a practical and powerful approach to multiple testing. *Journal of the royal statistical society. Series B (Methodological)* **1995**, 289-300.
395. Broadhurst, D. I.; Kell, D. B., Statistical strategies for avoiding false discoveries in metabolomics and related experiments. *Metabolomics* **2006**, 2, (4), 171-196.
396. Sumner, L. W.; Amberg, A.; Barrett, D.; Beale, M. H.; Beger, R.; Daykin, C. A.; Fan, T. W.-M.; Fiehn, O.; Goodacre, R.; Griffin, J. L., Proposed minimum reporting standards for chemical analysis. *Metabolomics* **2007**, 3, (3), 211-221.
397. Karnovsky, A.; Weymouth, T.; Hull, T.; Tarcea, V. G.; Scardoni, G.; Laudanna, C.; Sartor, M. A.; Stringer, K. A.; Jagadish, H.; Burant, C., Metscape 2 bioinformatics tool for the analysis and visualization of metabolomics and gene expression data. *Bioinformatics* **2011**, 28, (3), 373-380.
398. Shannon, P.; Markiel, A.; Ozier, O.; Baliga, N. S.; Wang, J. T.; Ramage, D.; Amin, N.; Schwikowski, B.; Ideker, T., Cytoscape: a software environment for integrated models of biomolecular interaction networks. *Genome research* **2003**, 13, (11), 2498-2504.
399. Martyn, J.; White, D.; Gronert, G.; Jaffe, R.; Ward, J., Up-and-down regulation of skeletal muscle acetylcholine receptors. Effects on neuromuscular blockers. *Anesthesiology* **1992**, 76, (5), 822-843.
400. Fertuck, H. C.; Salpeter, M. M., Quantitation of junctional and extrajunctional acetylcholine receptors by electron microscope autoradiography after (125) I- α -bungarotoxin binding at mouse neuromuscular junctions. *The Journal of Cell Biology* **1976**, 69, (1), 144.
401. Cha, S. H.; Wolfgang, M.; Tokutake, Y.; Chohnan, S.; Lane, M. D., Differential effects of central fructose and glucose on hypothalamic malonyl-CoA and food

- intake. *Proceedings of the National Academy of Sciences* **2008**, *105*, (44), 16871-16875.
402. Kurihara, K., Glutamate: from discovery as a food flavor to role as a basic taste (umami). *The American journal of clinical nutrition* **2009**, *90*, (3), 719S-722S.
403. Traynelis, S. F.; Wollmuth, L. P.; McBain, C. J.; Menniti, F. S.; Vance, K. M.; Ogden, K. K.; Hansen, K. B.; Yuan, H.; Myers, S. J.; Dingledine, R., Glutamate receptor ion channels: structure, regulation, and function. *Pharmacological reviews* **2010**, *62*, (3), 405-496.
404. Blount, B. C.; Mack, M. M.; Wehr, C. M.; Macgregor, J. T.; Hiatt, R. A.; Wang, G.; Wickramasinghe, S. N.; Everson, R. B.; Ames, B. N., Folate deficiency causes uracil misincorporation into human DNA and chromosome breakage: implications for cancer and neuronal damage. *Proceedings of the National Academy of Sciences* **1997**, *94*, (7), 3290-3295.
405. Mills, E.; O'neill, L. A., Succinate: a metabolic signal in inflammation. *Trends in cell biology* **2014**, *24*, (5), 313-320.
406. Tretter, L.; Patocs, A.; Chinopoulos, C., Succinate, an intermediate in metabolism, signal transduction, ROS, hypoxia, and tumorigenesis. *Biochimica et Biophysica Acta (BBA)-Bioenergetics* **2016**, *1857*, (8), 1086-1101.
407. Minois, N.; Carmona-Gutierrez, D.; Madeo, F., Polyamines in aging and disease. *Aging (Albany NY)* **2011**, *3*, (8), 716.
408. Rodrigues, A. F.; Roecker, R.; Junges, G. M.; Lima, D. D.; Cruz, J. G.; Wyse, A. T.; Magro, D.; Delwing, D., Hypoxanthine induces oxidative stress in kidney of rats: protective effect of vitamins E plus C and allopurinol. *Cell biochemistry and function* **2014**, *32*, (4), 387-394.
409. Örström, Å.; Örström, M.; Krebs, H. A., The formation of hypoxanthine in pigeon liver. *Biochemical Journal* **1939**, *33*, (6), 990.
410. Pang, B.; Mcfaline, J. L.; Burgis, N. E.; Dong, M.; Taghizadeh, K.; Sullivan, M. R.; Elmquist, C. E.; Cunningham, R. P.; Dedon, P. C., Defects in purine nucleotide metabolism lead to substantial incorporation of xanthine and hypoxanthine into DNA and RNA. *Proceedings of the National Academy of Sciences* **2012**, *109*, (7), 2319-2324.
411. Tretter, L.; Adam-Vizi, V., Inhibition of Krebs cycle enzymes by hydrogen peroxide: a key role of α -ketoglutarate dehydrogenase in limiting NADH production under oxidative stress. *Journal of Neuroscience* **2000**, *20*, (24), 8972-8979.
412. Monirujjaman, M.; Ferdouse, A., Metabolic and physiological roles of branched-chain amino acids. *Advances in Molecular Biology* **2014**, *2014*.
413. Albrecht, J.; Schousboe, A., Taurine interaction with neurotransmitter receptors in the CNS: an update. *Neurochemical research* **2005**, *30*, (12), 1615-1621.
414. Butler, I.; O'flynn, M.; Seifert, W.; Howell, R. R., Neurotransmitter defects and treatment of disorders of hyperphenylalaninemia. *The Journal of pediatrics* **1981**, *98*, (5), 729-733.
415. Nelson, D. L.; Lehninger, A. L.; Cox, M. M., *Lehninger principles of biochemistry*. Macmillan: 2008.

416. Rumbold, D.; Lange, T.; Axelrad, D.; Atkeson, T., Ecological risk of methylmercury in Everglades National Park, Florida, USA. *Ecotoxicology* **2008**, *17*, (7), 632-641.
417. Khan, M. Z.; Law, F. C., Adverse effects of pesticides and related chemicals on enzyme and hormone systems of fish, amphibians and reptiles: a review. *Proceedings of the Pakistan Academy of Sciences* **2005**, *42*, (4), 315-323.
418. Niki, E.; Yamamoto, Y.; Komuro, E.; Sato, K., Membrane damage due to lipid oxidation. *The American journal of clinical nutrition* **1991**, *53*, (1), 201S-205S.
419. Ayala, A.; Muñoz, M. F.; Argüelles, S., Lipid peroxidation: production, metabolism, and signaling mechanisms of malondialdehyde and 4-hydroxy-2-nonenal. *Oxidative medicine and cellular longevity* **2014**, *2014*.
420. Schousboe, A.; Westergaard, N.; Waagepetersen, H. S.; Larsson, O. M.; Bakken, I. J.; Sonnewald, U., Trafficking between glia and neurons of TCA cycle intermediates and related metabolites. *Glia* **1997**, *21*, (1), 99-105.
421. Salminen, A.; Kauppinen, A.; Hiltunen, M.; Kaarniranta, K., Krebs cycle intermediates regulate DNA and histone methylation: epigenetic impact on the aging process. *Ageing research reviews* **2014**, *16*, 45-65.
422. Salminen, A.; Kaarniranta, K.; Hiltunen, M.; Kauppinen, A., Krebs cycle dysfunction shapes epigenetic landscape of chromatin: novel insights into mitochondrial regulation of aging process. *Cellular signalling* **2014**, *26*, (7), 1598-1603.
423. Seki, S.; Kitada, T.; Yamada, T.; Sakaguchi, H.; Nakatani, K.; Wakasa, K., In situ detection of lipid peroxidation and oxidative DNA damage in non-alcoholic fatty liver diseases. *Journal of hepatology* **2002**, *37*, (1), 56-62.
424. Osowski, C. M.; Urano, F., Measuring ER stress and the unfolded protein response using mammalian tissue culture system. *Methods in enzymology* **2011**, *490*, 71.
425. Ota, T.; Gayet, C.; Ginsberg, H. N., Inhibition of apolipoprotein B100 secretion by lipid-induced hepatic endoplasmic reticulum stress in rodents. *The Journal of clinical investigation* **2008**, *118*, (1), 316.
426. Malaguarnera, L.; Madeddu, R.; Palio, E.; Arena, N.; Malaguarnera, M., Heme oxygenase-1 levels and oxidative stress-related parameters in non-alcoholic fatty liver disease patients. *Journal of hepatology* **2005**, *42*, (4), 585-591.
427. Ong, J. P.; Pitts, A.; Younossi, Z. M., Increased overall mortality and liver-related mortality in non-alcoholic fatty liver disease. *Journal of hepatology* **2008**, *49*, (4), 608-612.
428. Targher, G.; Arcaro, G., Non-alcoholic fatty liver disease and increased risk of cardiovascular disease. *Atherosclerosis* **2007**, *191*, (2), 235-240.
429. Narasimhan, S.; Gokulakrishnan, K.; Sampathkumar, R.; Farooq, S.; Ravikumar, R.; Mohan, V.; Balasubramanyam, M., Oxidative stress is independently associated with non-alcoholic fatty liver disease (NAFLD) in subjects with and without type 2 diabetes. *Clinical biochemistry* **2010**, *43*, (10), 815-821.
430. Videla, L. A.; Rodrigo, R.; Araya, J.; Poniachik, J., Oxidative stress and depletion of hepatic long-chain polyunsaturated fatty acids may contribute to nonalcoholic fatty liver disease. *Free radical biology and medicine* **2004**, *37*, (9), 1499-1507.

431. Rolo, A. P.; Teodoro, J. S.; Palmeira, C. M., Role of oxidative stress in the pathogenesis of nonalcoholic steatohepatitis. *Free radical biology and medicine* **2012**, *52*, (1), 59-69.
432. Michelotti, G. A.; Machado, M. V.; Diehl, A. M., NAFLD, NASH and liver cancer. *Nature Reviews Gastroenterology and Hepatology* **2013**, *10*, (11), 656-665.
433. Adams, L.; Angulo, P., Treatment of non-alcoholic fatty liver disease. *Postgraduate medical journal* **2006**, *82*, (967), 315-322.
434. Sozio, M. S.; Chalasani, N.; Liangpunsakul, S., What advice should be given to patients with NAFLD about the consumption of alcohol? *Nature Reviews Gastroenterology & Hepatology* **2009**, *6*, (1), 18.
435. Eguchi, Y.; Hyogo, H.; Ono, M.; Mizuta, T.; Ono, N.; Fujimoto, K.; Chayama, K.; Saibara, T., Prevalence and associated metabolic factors of nonalcoholic fatty liver disease in the general population from 2009 to 2010 in Japan: a multicenter large retrospective study. *Journal of gastroenterology* **2012**, *47*, (5), 586-595.
436. Lee, H.; Kim, Y.; Sim, C.-S.; Ham, J.-O.; Kim, N.-S.; Lee, B.-K., Associations between blood mercury levels and subclinical changes in liver enzymes among South Korean general adults: Analysis of 2008–2012 Korean national health and nutrition examination survey data. *Environmental research* **2014**, *130*, 14-19.
437. Endo, T.; Haraguchi, K., High mercury levels in hair samples from residents of Taiji, a Japanese whaling town. *Marine pollution bulletin* **2010**, *60*, (5), 743-747.
438. Dringen, R.; Gutterer, J. M.; Hirrlinger, J., Glutathione metabolism in brain. *The FEBS Journal* **2000**, *267*, (16), 4912-4916.
439. Levin, E. D., Zebrafish assessment of cognitive improvement and anxiolysis: filling the gap between in vitro and rodent models for drug development. *Reviews in the Neurosciences* **2011**, *22*, (1), 75-84.
440. Simon-Sanchez, J.; Schulte, C.; Bras, J. M.; Sharma, M.; Gibbs, J. R.; Berg, D.; Paisan-Ruiz, C.; Lichtner, P.; Scholz, S. W.; Hernandez, D. G., Genome-wide association study reveals genetic risk underlying Parkinson's disease. *Nature genetics* **2009**, *41*, (12), 1308-1312.
441. Sookoian, S.; Pirola, C. J., Meta-analysis of the influence of I148M variant of patatin-like phospholipase domain containing 3 gene (PNPLA3) on the susceptibility and histological severity of nonalcoholic fatty liver disease. *Hepatology* **2011**, *53*, (6), 1883-1894.
442. Dongiovanni, P.; M Anstee, Q.; Valenti, L., Genetic predisposition in NAFLD and NASH: impact on severity of liver disease and response to treatment. *Current pharmaceutical design* **2013**, *19*, (29), 5219-5238.
443. Gadgil, M.; Berkes, F.; Folke, C., Indigenous knowledge for biodiversity conservation. *Ambio* **1993**, 151-156.
444. Jones, J. P.; Andriamarivololona, M. M.; Hockley, N., The importance of taboos and social norms to conservation in Madagascar. *Conservation biology* **2008**, *22*, (4), 976-986.
445. Berkes, F.; Colding, J.; Folke, C., Rediscovery of traditional ecological knowledge as adaptive management. *Ecological applications* **2000**, *10*, (5), 1251-1262.

446. Drew, J. A., Use of traditional ecological knowledge in marine conservation. *Conservation biology* **2005**, *19*, (4), 1286-1293.
447. Mihesuah, D. A., Suggested guidelines for institutions with scholars who conduct research on American Indians. *American Indian Culture and Research Journal* **1993**, *17*, (3), 131-139.

Globe-trotting scientist lived remarkable life

Dawn Brazell | MUSC News Center | August 12, 2015



Provided

Dr. Louis Guillette doing research in South Africa. His local and global research with alligators and crocodiles shed light on how environmental contaminants are affecting human health. [See his photo gallery.](#)

*“Being a scientist is the four best jobs on Earth.
You are a detective, an adventurer, an artist and a storyteller.”*

Louis J. Guillette in a recent article for MUSC’s Center for Global Health

Still reeling from the news of the passing of Louis “Lou” J. Guillette, Ph.D. Aug. 6, colleagues mourned the loss of an internationally-renowned scientist described as “larger than life” and “a force of nature.” David Cole, M.D., president of the Medical University of South Carolina, called Guillette a rare individual and talented scientist. “It’s a testament to his character how well loved he was by his students,” Cole said. “As an investigator, he was highly accomplished and had prestigious global connections working at the frontiers of multiple disciplines of science, including biomedicine and the environment. His model of team science was ahead of its time and helped set MUSC in a direction in which we want to continue.”

Guillette, an endowed chair in marine genomics and director of the [Marine Biomedicine & Environmental Sciences Center](#) at MUSC, was an expert in comparative reproductive biology and developmental endocrinology. His research explored how to prevent and treat health problems caused by environmental factors. Conducting research with MUSC’s departments of Obstetrics and Gynecology and Pediatrics, he focused on how various environmental factors might lead to birth defects or other reproductive abnormalities in wildlife and humans.



Provided

Dr. Louis Guillette (center) and his team with a crocodile in South Africa

Guillette's work often took him out in the field, whether doing research on crocodiles in South Africa or alligators in local refuges. In his wildlife biology research over the past 20 years, Guillette found links between environmental contaminants and infertility and reproductive issues in alligator populations from Florida to South Carolina.

Guillette held dual appointments, which allowed him to work closely with MUSC physicians and researchers as well as scientists at the Hollings Marine Laboratory (HML). The HML is a National Oceanic and Atmospheric Administration (NOAA)-administered facility, with

activities governed by the five partner organizations that include MUSC, the National Institute of Standards and Technology (NIST) and the College of Charleston.

MUSC researcher Demetri Spyropoulos, Ph.D., said he and Guillette had a webinar presentation last Wednesday, but his friend and colleague was not feeling well from a fever related to what he called his "3-year-old" immune system, which was weakened by the effects of chemotherapy. Guillette told him not to worry, and Spyropoulos didn't since his friend always bounced back to 10 times the energy level of anyone around him.

"He assured me that I knew my stuff and he had all the confidence in me going it alone. He said, 'Demetri, remember the power of positive thinking!' I told him the difference was that the web viewers would be jumping up and down applauding in front of their computer screens if he did it. I said, 'Rest up, and I'll let you know how it went.'"

Unfortunately, Spyropoulos didn't get that chance. Guillette, 62, passed away Thursday, Aug. 6. In his passing, though, he left a wake of colleagues he had touched and many of whom he had mentored, a cause near and dear to his heart. ([Read their tributes here.](#))

Team Science

Roger Newman, M.D., professor and Maas Chair for Reproductive Sciences in MUSC's Department of Obstetrics and Gynecology, was instrumental in recruiting Guillette from the University of Florida, where he had made an international name for himself in reproductive biology [using the alligator model as a sentinel species](#). Despite his distinction and standing in that academic community, Guillette embraced the opportunity at a late stage in his career to make a change and collaborate with researchers in the medical field, he said.

"He embraced it so enthusiastically that it was invigorating," Newman said of the groundbreaking move. "He was larger than life. What impressed me the most was his contagious enthusiasm and vigorous belief in the importance of environmental exposure on human health."



Lou Guillette

One of Dr. Guillette's many wildlife images from his travels for work.

Guillette had top-tier, international connections and brought a new level of collaborative enterprise to MUSC. He opened doors to intramural and extramural research collaborations that were previously closed and his leadership contributed to significant research opportunities, including his involvement with the [Deepwater Horizon Oil Spill studies](#).

"He was an extremely prestigious person to have in our department. In just a few years after coming here, he was the recipient of the [Heinz Award](#) for his career achievement in

environmental research, which is equivalent to the environmental Nobel Prize and one of the top awards a scientist can receive,” Newman said.

Guillette was a talented teacher and mentor, Newman said. He was always looking for ways to train, protect and support his students. “He had a Pied Piper relationship with students. Lou was a tremendous teacher. They loved him and were inspired by him.”

One legacy Guillette leaves is that he sparked interest among animal-based researchers who took note of his interdisciplinary collaborations with clinical researchers and physicians. Newman said he blazed a trail in crossing traditional boundaries of how science can be performed. Though Guillette’s loss is a setback, his legacy will continue not only in the students he influenced, but also in how he worked at the frontiers of multiple scientific disciplines building bridges across those gaps.

Guillette recently discussed with Newman his dream of establishing a graduate-level marine biomedicine environmental program among MUSC, the Hollings Marine Laboratory and the College of Charleston, an idea Newman describes as “brilliant.” The program would be far-reaching, exploring how environmental contaminants may be impacting not only reproductive disorders but also a wide range of chronic diseases including obesity, cancer, diabetes, autism and immunological diseases.

Some people fear his loss will disrupt those plans. “My hope is that his passing might serve as a catalyst to make that dream become a reality. What he has done will not be lost or forgotten,” Newman said.

In the future, Newman predicts, Guillette and his colleagues will be recognized for one very important paradigm shift they accomplished. This shift already is starting to affect federal and environmental regulatory agencies, where scientists are beginning to acknowledge that the danger of certain chemicals is not just related to the exposure dosage, but also the timing of exposure, particularly if it occurs during critical windows of fetal development.

“When you lose someone of his dominating personality, it leaves a void,” Newman said.

After all, there aren’t many researchers as comfortable talking with physicians and basic scientists as they are “wrangling alligators” in the field.

An incredible [wildlife and nature photographer](#), Guillette used that talent in slide shows he tirelessly shared with community groups to raise awareness of the interactions between the environment and human health. He particularly liked a photo he shot at night, showing hundreds of glowing alligator eyes. No one left one of his lectures without being changed, better understanding the interaction between human health and the environment, Newman said.

“More and more, I wake up feeling like I’m getting old. But when you were around Lou, you didn’t feel old. There were so many ideas, so much enthusiasm, all of a sudden there was just so much to do, and you were enveloped by his zest and zeal,” Newman said.



Provided

Dr. Guillette works with Ph.D. student James Nifong, using National Geographic's Crittercams to capture video footage from alligators to get a view into their private lives.

Relationship Web

That's the experience Kathleen Ellis, director of operations for MUSC's Center for Global Health, had as well. She described Guillette as the consummate storyteller.

"Listening to Lou could transport you on a journey from his work in the remote village of Botswana where he lived with his wife, Buzzy, an anthropologist, to his environmental research on the crocodiles and fish wildlife of Kruger Park, South Africa, to his early roots in global health which went all the way back to his Ph.D. days when he was in Mexico trying to understand high altitude pregnancy and the evolution of the placenta," she said.



Dr. Lou Guillette

One of Dr. Guillette's many wildlife images from his travels for work.

"It was impossible to walk away from Lou without feeling a little in awe, a little more curious, inspired by his science to make the world a better, healthier place. How could you not?" Ellis said Guillette's [global health research](#) took him to every corner of the world - every continent except Antarctica. He worked to mentor and support students and scientists in developing countries who didn't have the technology and resources some other researchers have.

"He believed that we are all part of a global environment and that while individuals can make a difference, you can't build a community with one person. 'The minute that person is gone, the community collapses' - which is why

he worked tirelessly to provide mentorship and build networks around the world for his students and colleagues," Ellis said.

In a conversation she had with him just a few weeks ago, he told her: "My legacy to science is not just the work I did - that's just bricks and walls. Your true legacy is the people you leave behind."

Ellis said Guillette had an impact on almost everyone he met. "Lou's legacy will forever be imprinted in the hearts and minds of all those lives he touched - students, colleagues, friends and family."

Spyropoulos said his friend, who always was traveling to some exotic place or other, was supposed to go to Africa this week for more field work. "He was such a force of nature, his passing just wasn't a possibility. He was always on the move, always motivating, pushing quality science and public awareness," he said.



Theresa Cantu

Dr. Guillette in the field on Father's Day with his son Matt.

Known for a witty sense of humor and relentless optimism, Guillette's words of encouragement will always resonate with Spyropoulos. "Our Gulf grant meetings were always electrifying — we fed off of each other's excitement and energy, eagerly refining our thoughts and course of action. The scientific endeavor was paramount. What is the big question? How do we break this up into testable hypotheses? What are the priorities?" Spyropoulos said. "Ideas and words were his domain. He would say 'a good idea instilled into the minds of others will never die.' "But I find myself at a loss for words now — you can't hug or shake hands with or get a hearty pat on the back from a word. It is the man who will be missed."

Guillette is survived by his wife, Elizabeth Arnold Guillette, two sons and two daughters